Oxidative Medicine and Cellular Longevity

Molecular Mechanisms Underlying Age-Related Ocular Diseases

Lead Guest Editor: Marialaura Amadio
Guest Editors: Kai Kaarniranta, Heping Xu, Adrian Smedowski, and Deborah A. Ferrington

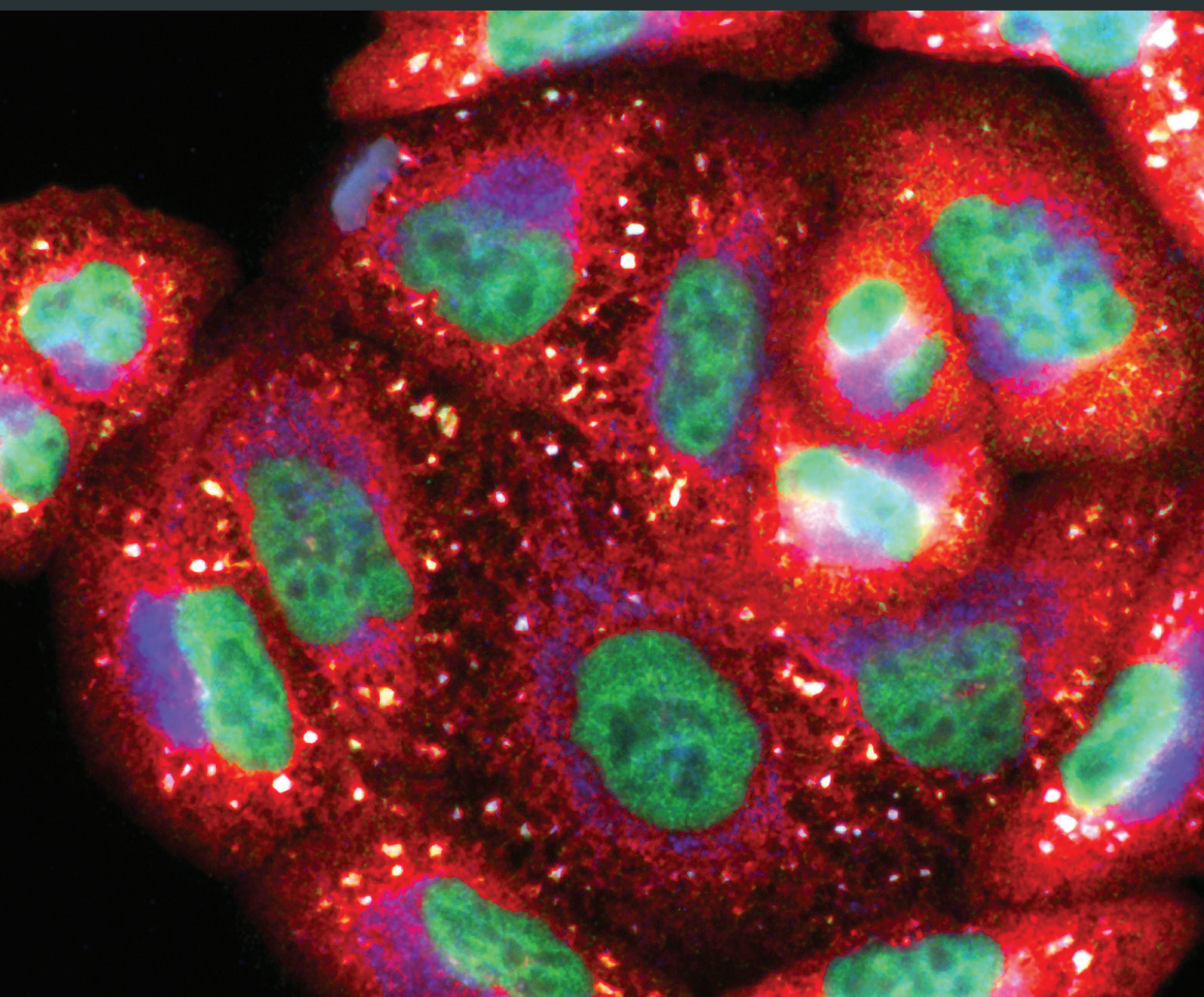

Molecular Mechanisms Underlying Age-Related Ocular Diseases

Oxidative Medicine and Cellular Longevity

Molecular Mechanisms Underlying Age-Related Ocular Diseases

Lead Guest Editor: Marialaura Amadio
Guest Editors: Kai Kaarniranta, Heping Xu, Adrian Smedowski, and Deborah A. Ferrington

Editorial Board

Contents

Hindawi
Oxidative Medicine and Cellular Longevity
Volume 2018, Article ID 8476164, 2 pages
https://doi.org/10.1155/2018/8476164

Editorial

Molecular Mechanisms Underlying Age-Related Ocular Diseases

Marialaura Amadio,[1] **Kai Kaarniranta**,[2,3] **Heping Xu**,[4] **Adrian Smedowski**,[5,6] **and Deborah A. Ferrington**[7]

[1]*Department of Drug Sciences, Section of Pharmacology, University of Pavia, Pavia, Italy*
[2]*Department of Ophthalmology, University of Eastern Finland and Kuopio University Hospital, Kuopio, Finland*
[3]*Department of Molecular Genetics, University of Lodz, Lodz, Poland*
[4]*The Wellcome-Wolfson Institute of Experimental Medicine, School of Medicine, Dentistry and Biomedical Sciences, Queen's University Belfast, Belfast, UK*
[5]*Chair and Department of Physiology, School of Medicine in Katowice, Medical University of Silesia, Katowice, Poland*
[6]*Department of Ophthalmology, School of Medicine in Katowice, Medical University of Silesia, Katowice, Poland*
[7]*Department of Ophthalmology and Visual Neurosciences, University of Minnesota, Minneapolis, MN, USA*

Correspondence should be addressed to Marialaura Amadio; marialaura.amadio@unipv.it

Received 25 December 2017; Accepted 26 December 2017; Published 21 May 2018

The guest editors of this special issue are pleased to present a compendium of original research and review articles focusing on molecular mechanisms underlying age-related ocular diseases.

According to the World Health Organization (WHO), the 65-and-over global population is predicted to almost double over the next three decades. By 2050, less than one-fifth of the world's old population will reside in more developed countries; the functional visual decline associated with the elderly thus creates a challenge to be met by the national healthcare systems of industrialized countries. The WHO has identified some irreversible diseases, such as age-related macular degeneration (AMD), diabetic retinopathy, and glaucoma, as priority eye diseases in terms of prevention of visual impairment and blindness.

The lack of effective therapies for prevention or cure of such widespread sight-threatening diseases is mainly due to the insufficient understanding of the molecular and cellular events underlying the disease onset or progression. For this reason, basic scientific studies shedding light on the molecular and cellular responses to physiological/pathological stimuli (such as oxidative stress) are of great relevance and may help to translate pioneering "bench to bedside" research into effective clinical strategies.

After the awarding of 1974 Nobel Prize to Christian De Duve, who discovered the lysosomes and coined the term autophagy, and the awarding of 2016 Nobel Prize to Yoshinori Ohsumi for his discoveries of the mechanisms of autophagy, the importance of autophagy in physiological and pathological contexts has come to the forefront. The number of peer-reviewed publications with autophagy as a keyword has doubled in the last 5 years, at the present passing 32,500 papers. Accordingly, autophagy has been object of several contributions of this special issue.

Recent observations reveal that autophagy is declined in advanced AMD. J. Blasiak et al. wrote a review article for cellular senescence in AMD, the most common cause of irreversible blindness in the elderly of industrialized countries. Increased oxidative stress, protein aggregation, and inflammation are likely contributors to AMD pathology. Authors discussed cross talk of oxidative stress, DNA damage response, autophagy, and senescence in the retinal pigment epithelium (RPE) cell. Likewise, the article by L. F. Hernandez-Zimbron et al. provided a review of some AMD-related factors and mainly focused on feasible treatments targeting autophagy, oxidative stress, VEGF, and glial cell dysfunction, emphasizing the increasing relevance of stem cell-based research as a promising area in biology.

Despite significant breakthrough in the understanding of how autophagy modulates cellular processes, the entire puzzle of autophagy-related pathways is not yet completely elucidated. In particular, the role of posttranscriptional control of gene expression in autophagy is poorly characterized. Findings of the research article entitled "Autophagy stimulus promotes early HuR protein activation and p62/SQSTM1 protein synthesis in ARPE-19 cells by triggering Erk1/2, $p38^{MAPK}$, and JNK kinase pathways" by N. Marchesi et al. focused on the early events occurring in response to a proautophagy stimulus and supported modulation of the autophagy-regulating kinases as a potential therapeutic target for AMD.

One of the factors promoting inflammation in AMD is lipid oxidation. Mao et al. provided *in vitro* and *in vivo* evidence that oxidized low-density lipoprotein (ox-LDL) promoted laser-induced choroidal neovascularization by increasing VEGF/PDGF and CYLD (tumor suppressor cylindromatosis) levels. The authors also proposed salvianolic acid A as a novel potential therapeutic reagent for exudative AMD in virtue of its beneficial antagonism on the ox-LDL-induced effects.

Many age-related ocular pathologies are multifactorial and are triggered by consecutive or overlapping insults that are hard to eliminate. The recovery of retinal health in spite of injury and the preservation (or reinforce) of its physiological defense thus represent a valuable strategy to fight factors that harm vision.

Several publications provide evidence that indicate a protective association between dietary antioxidant intake and the incidence of oxidative stress-related ocular diseases. D. Rajapakse et al. underlined the importance of physiological concentration of zinc for retina's homeostasis. In their *in vitro* study, the authors showed that zinc supplementation protects RPE cells from oxidative stress-induced death by improving mitochondrial function and preventing lysosome rupture.

The context of cytoprotection, of interest, is also the original *in vitro* study by S. Davinelli et al., showing that citicoline and homotaurine cotreatment protects primary cultured retinal cells from glutamate and high-glucose-induced neurotoxicity. Another contribution in the identification of molecules endowed with neuroprotective effects came from the *in vitro* study by Pittalà et al., who suggested the new nature-inspired NO-releasing compound VP10/39 as a promising candidate to protect RPE cells against oxidative stress, via induction of the Nrf2/Keap1/HO-1 pathway.

To this regard, one of the most comprehensive transcription systems to neutralize oxidative stress and maintain cellular homeostasis in the retina is the Keap1-Nrf2-ARE pathway, whose impairment has been associated with ageing. The review on the "Involvement of Nrf2 in Ocular Diseases" by S. Batliwala et al. provided thorough information regarding the relationship of Nrf2 and various age-related ocular pathologies, giving a perspective on possible therapeutic or preventive approaches targeting the Keap1-Nrf2-ARE pathway.

Novel cellular and animal models are needed to better understand the pathogenesis of age-related ocular diseases and to screen potential drugs. In this context, the original basic scientific study by A. Smedowski et al., on the FluoroGold-labeled organotypic retinal explant culture (FLOREC), proposed a new interesting and versatile ex vivo method to detect neurotoxicity/neurodegeneration in the retina and to test potential neuroprotective agents.

Among age-related conditions is the dry eye syndrome, which affects also young population and counts more than 300 million people worldwide suffering from this disease. The *in vivo* study by E. Y. Zernii et al. showed that the mitochondrial-targeted antioxidant SkQ1 is able to suppress oxidative stress and stimulate intrinsic antioxidant activity in the cornea and also improve the stability of the tear film.

Likewise, a contribution in the context of ocular surface inflammation came from the study entitled "Cyclodextrin enhances corneal tolerability and reduces ocular toxicity caused by diclofenac" by H. Abdelkader et al., investigating the use of cyclodextrins (CDs) to reduce ocular toxicity of NSAIDs, specifically diclofenac (Diclo). The authors provided *in vitro* and *in vivo* evidence that Diclo-γ-CD and Diclo-HP-β-CD inclusion complexes are able to reduce diclofenac-induced ocular toxicity and show fast healing rates without scar formation.

We hope the papers are informative for basic researchers, clinician scientists, and patients who are affected by age-related ocular conditions.

Acknowledgments

We would like to express our appreciation to all the authors for their informative contributions and the reviewers for their support and constructive critiques in making this special issue possible.

Marialaura Amadio
Kai Kaarniranta
Heping Xu
Adrian Smedowski
Deborah A. Ferrington

Hindawi
Oxidative Medicine and Cellular Longevity
Volume 2018, Article ID 5260976, 13 pages
https://doi.org/10.1155/2018/5260976

Research Article

Cyclodextrin Enhances Corneal Tolerability and Reduces Ocular Toxicity Caused by Diclofenac

Hamdy Abdelkader,[1] Zeinab Fathalla,[1] Hossam Moharram,[2] Taha F. S. Ali,[3] and Barbara Pierscionek[4]

[1]*Department of Pharmaceutics, Faculty of Pharmacy, Minia University, Mina, Egypt*
[2]*Department of Ophthalmology, Faculty of Medicine, Minia University, Minia, Egypt*
[3]*Department of Medicinal Chemistry, Faculty of Pharmacy, Minia University, Mina, Egypt*
[4]*School of Science and Technology, Nottingham Trent University, 50 Shakespeare Street, Nottingham NG1 4FQ, UK*

Correspondence should be addressed to Barbara Pierscionek; barbara.pierscionek@ntu.ac.uk

Received 22 July 2017; Revised 1 October 2017; Accepted 17 December 2017; Published 13 February 2018

Academic Editor: Kai Kaarniranta

With advances in refractive surgery and demand for cataract removal and lens replacement, the ocular use of nonsteroidal anti-inflammatory drugs (NSAIDs) has increased. One of the most commonly used NSAIDs is diclofenac (Diclo). In this study, cyclodextrins (CDs), α-, β-, γ-, and HP-β-CDs, were investigated with *in vitro* irritation and *in vivo* ulceration models in rabbits to reduce Diclo toxicity. Diclo-, α-, β-, γ-, and HP-β-CD inclusion complexes were prepared and characterized and Diclo-CD complexes were evaluated for corneal permeation, red blood cell (RBCs) haemolysis, corneal opacity/permeability, and toxicity. Guest- (Diclo-) host (CD) solid inclusion complexes were formed only with β-, γ-, and HP-β-CDs. Amphipathic properties for Diclo were recorded and this surfactant-like functionality might contribute to the unwanted effects of Diclo on the surface of the eye. Contact angle and spreading coefficients were used to assess Diclo-CDs in solution. Reduction of ocular toxicity 3-fold to16-fold and comparable corneal permeability to free Diclo were recorded only with Diclo-γ-CD and Diclo-HP-β-CD complexes. These two complexes showed faster healing rates without scar formation compared with exposure to the Diclo solution and to untreated groups. This study also highlighted that Diclo-γ-CD and Diclo-HP-β-CD demonstrated fast healing without scar formation.

1. Introduction

Cyclodextrins (CDs) are cyclic oligosaccharides with a hydrocarbon (water repellant) cavity and a hydrophilic outer surface composed of 6, 7, or 8 dextrose units forming the three parent cyclodextrins α-, β-, and γ-CDs. Depending on the number of dextrose units, the hydrophobic cavity varies in size and can accommodate various lipophilic moieties and form guest-host complexes. These complexes have been well-known as inclusion complexes and utilized in pharmacy and cosmetic industries to enhance water solubility and bioavailability of poorly soluble drugs and to improve palatability by reducing the bitterness of certain drugs [1, 2]. More recently, CDs have been employed to fabricate drug-loaded textiles for treatment of surface skin diseases due to psoriasis, fungal infections, and insect bites [3].

CDs have gained much popularity and are widely used in the pharmaceutical industry for systemic routes such as oral and parenteral dosage forms [4]. Orally administered CDs are considered to be nontoxic because of their lack of absorption from the gastrointestinal tract and γ- and hydroxypropyl- (HP-) β-CD having been used safely via the parenteral route [5]. It is well-known that faster onset of action and less gastrointestinal side effects are attributed to oral piroxicam-β-CD than piroxicam alone [4]. In addition, Dyloject® and Akis® are two relatively new commercially available

injectable Diclo-HP-β-CD complexes that gave rapid and effective analgesia comparable to Voltaren® IM injection not containing CDs [4].

The use of CDs in ophthalmology has been recently reported for solubilization of insoluble drugs such as corticosteroids [6], medications for treating glaucoma [7] and immunosuppressive agents [8] and for enhancing ocular permeability of drugs through the extremely lipophilic corneal epithelial membrane [9]. For example, CDs have been more successfully used to solubilize dorzolamide at physiological pH and to offer comparable ocular bioavailability at low viscosity (3 to 5 centipoises), to that found with high viscosity (100 centipoises) eye drops as well as at low pH of 5.65 to solubilize 2% of dorzolamide [7]. However, the use of eye drops containing α-CD > 4% has been found to cause superficial epithelial toxicity and microerosion in rabbit corneal tissue [10]. These effects most likely result from the ability of CD, especially α- and β-CD, to extract cholesterol and other lipid components from cell membranes [11] leading to cellular disruption and enhanced drug permeation through the corneal epithelial membrane [9]. Conversely, γ- and hydroxypropyl-β-CD are better tolerated in ocular tissues and less likely to cause disruption of the corneal epithelial barrier [8, 9]. CDs have the potential to alter drug availability at the absorption site as well as to modify the rate of drug release and hence can be applied to reduce drug irritation caused by localized high concentrations. There are no reports of research that has critically assessed the ocular irritation potential from drug-CD complexes versus free drug solutions using *in vitro* irritation models.

With the advent of modern refractive and cataract surgeries, nonsteroidal anti-inflammatory drugs (NSAIDs) have been increasingly used in ophthalmology as a safer alternative to topical corticosteroids, avoiding serious side effects such as increasing IOP, cataractogenesis, risk of infection, and stromal melting [12]. NSAIDs can effectively reduce miosis, inflammation, pain, and scleritis and, more importantly, prevent and treat cystoid macular oedema associated with cataract surgeries [13, 14]. Diclofenac eye drops (0.1% *w*/*v*) and other NSAIDs such as ketorolac tromethamine (0.5% *w*/*v*), suprofen (1% *w*/*v*), flurbiprofen (0.03% *w*/*v*), and indomethacin (1%) are commercially available and widely used for multiple indications such as reducing pain and inflammation after ocular surgery and for seasonal allergic conjunctivitis [14]. Side effects and toxicities that have been widely reported with topical application of NSAIDs can range from transient burning, stinging, and conjunctival hyperaemia to more serious effects such as superficial keratitis, corneal erosion, corneal epithelial defect, and corneal ulceration and melting [12, 15, 16].

This study aimed to investigate a possible role of CDs for reducing local irritation and corneal toxicity of the most widely used NSAID, namely, diclofenac. Previous studies have sought to investigate corneal irritation potential from Voltaren Ophtha eye drops and cyclodextrins such as hydroxypropyl-β-CD using *in vitro* models such as hen's egg test-chorioallantoic membrane (HET-CAM), cytotoxicity, and haemolysis assay [17, 18]. Both *in vitro* and *in vivo* assessments for ocular irritation potential of Diclo with four different CDs, employing bovine corneal opacity and permeability (BCOP), RBC haemolysis and MTT assay using human primary corneal epithelial cells, and *in vivo* corneal healing in rabbits have been undertaken in this study. No reported investigations to date have considered the amphipathic properties of Diclo that are assessed in this work for surface tension and contact angle measurements using drop shape analysis.

2. Materials and Methods

2.1. Materials. Diclofenac sodium was donated by PSM Healthcare Pharma, Auckland, New Zealand. α-, β-, γ-, and HP-β-CD, cellophane membrane (MW-cut off 12,000-14,000 Dalton), nitro blue tetrazolium (NBT), and 3-(4,5-dimethylthiazol-2-yl)-2,5-diphenyltetrazolium bromide (MTT) were purchased from Sigma-Aldrich, UK. All other chemicals and reagents were of analytical grade and used as received.

2.2. Preparation of Diclo-CD Physical Mixtures. Equivalent amounts in mg of 1 : 1 molar ratios of Diclo and different types of CD (α-, β-, γ-, and HP-β-CD) were separately weighed and mixed uniformly in a porcelain dish with a spatula for 5 minutes. The physical mixtures were collected in glass vials and sealed and stored in a cool dry place for further use.

2.3. Preparation of Diclo-CD Complexes Using Solvent Evaporation Method. Diclo and different types of CD (α-, β-, γ-, and HP-β-CD) were weighed in 1 : 1 molar ratios and dissolved separately in methanol (20 ml) and deionized water (10 ml), respectively. The two solutions were mixed and magnetically stirred in 100 ml capacity-evaporating basins and allowed to completely evaporate at 60°C. The resulting solid complexes were left overnight in a desiccator for removal of residual moisture and pulverized and stored in glass vials for subsequent use.

2.4. Characterization of the Prepared Cyclodextrin Complexes

2.4.1. Differential Scanning Calorimetry. Diclo-, α-, β-, γ-, and HP-β-CD and corresponding physical mixtures and complexes (amounts of 5 to 8 mg) were weighed separately in an aluminum pan; an aluminum lid was replaced and crimped using a pan press (Thermal Science, USA). The temperature of the pan was gradually raised from 25 to 300°C at a rate of 10°C/min using a differential scanning calorimeter (DSC) (Mettler Toledo DSC 822e0, Switzerland). Nitrogen gas was purged at a rate of 45 ml/min. Data were collected online using Mettler STARe software version 8.10, Switzerland.

2.4.2. Fourier Transform Infrared Spectroscopy (FT-IR). Amounts (2–4 mg) of Diclo-, α-, β-, γ-, and HP-β-CD and the physical mixtures and complexes were used to form a thin film covering a diamond window of the FT-IR spectrometer (Thermo Scientific Nicolet iS5, Thermo fisher, Madison, USA). The data were collected and analyzed using Omnic software (Omnic version 8.2, USA). The FT-IR

spectra were registered at a spectral resolution of 2 cm^{-1} with an average of 20 scans and a scanning range of 4000 cm^{-1} to 600 cm^{-1}.

2.4.3. Molecular Docking. In order to predict the orientation within the cavity and/or rim and gain more insights into the stability/binding constants of Diclo with α-CD, β-CD, γ-CD, and HP-β-CD, molecular docking studies were performed using Molecular Operating Environment (MOE) 2014.09 software (Chemical Computing Group, Montreal, QC, Canada). The crystal structures of CDs were extracted from Protein Data Bank (PDB): α-CD (PDB code: 5E6Y), β-CD (PDB code: 5E6Z), and γ-CD (PDB code: 5E70) [19]. Since no crystal structure is available for HP-β-CD, the crystal structure of β-CD (PDB code: 5E6Z) was used as a template to build the 3D structure of HP-β-CD by substituting four primary hydroxyl groups with 2-hydroxypropyl radical, as described elsewhere [20]. The 3D crystal structure of Diclo was retrieved from crystallographic data available in the Cambridge structural database (Ref. Code: LIQFUN) [21]. The docking simulations were performed using the induced fit docking protocol. All other parameters were used with the default molecular operating environment (MOE) settings. The resulting docking poses were visually inspected, and the best energy pose for each type of the four Diclo-CD complexes was selected.

2.5. Preparation of Diclo Solution (0.1% w/v) and Its Equivalent from Diclo-CD Complexes. An amount of Diclo (10 mg) or equivalent to 10 mg from the prepared Diclo-CD complexes was dissolved in 10 ml of isotonic solution of phosphate buffer saline (PBS) pH 7.4 and sterile filtered through 0.22 μm sterile syringe filters to prepare final solutions containing 0.1% *w/v* of Diclo. The prepared solutions were stored at 4°C until further use.

2.6. Evaluation of Diclo and Diclo-CD Solutions

2.6.1. Contact Angle, Surface Tension, and Spreading Coefficient Measurements. The contact angle and surface tension for Diclo (0.1% *w/v*) and its equivalent from Diclo-CD solutions in PBS were performed according to our previously published work using a drop shape analyzer (goniometer) (Kruss Drop Shape Analysis, Hamburg, Germany) [22].

2.6.2. Transcorneal Permeation Studies Using Excised Porcine Eyes. Excised porcine eyes were collected from a local abattoir (Jennings Butchery, Surbiton, UK). The cornea was dissected as previously described [22]. Franz diffusion cells were employed for ex vivo permeation, and the temperature was maintained at 35°C ± 0.5°C. The receptor chambers were filled (12 ml) with PBS, pH 7.4. The medium was constantly stirred using small magnetic bars. Volumes of 2 ml of each formulation were pipetted into the donor compartment providing a surface area of 1.7 cm^2. Samples of 1 ml were withdrawn at predetermined time points for up to 8 h and replaced with the same volume of the medium without drug. The samples were analyzed at $\lambda_{max} = 275$ nm using a UV/visible spectrophotometer (Genway 7305, Hanwell, London, UK). Negative controls (in PBS without the drug) were placed on corneae and were withdrawn at the same time points as test samples.

The permeability coefficient (P_{app}, cm/s) was calculated using [23]:

$$P_{app} = \frac{\Delta Q}{\Delta t (3600) A C_o}. \quad (1)$$

$\Delta Q/\Delta t$ is the permeability rate of Diclo across the excised porcine cornea; C_o is the initial Diclo concentration ($\mu g/cm^3$); A is the exposed surface area of the cornea (cm^2). The value of 3600 represents the conversion of hours to seconds.

2.6.3. Red Blood Cell (RBC) Haemolysis Assay. The RBC assay was based on DB-ALM protocol number 99 [24]. Fresh bovine blood samples were collected from ABP Guildford London, UK, and were mixed in a ratio of 1 in 10 with citrate buffer as anticoagulate. The citrated blood was further diluted to 4 : 10 volumes in PBS and then centrifuged at 1500 ×g, 4°C for 10 minutes. The supernatant was carefully discarded, and the pellets were washed with sterile PBS. A total of five washes were made. The final pellets were resuspended in PBS supplemented with 10 mmol/l glucose and stored in the fridge until further use. The test materials (Diclo-, α-, β-, γ-, and HP-β-CD and Diclo-, α-, β-, γ-, and HP-β-CD dispersed mixtures) were dissolved in PBS at the following final assay concentrations in mg/l (*w/v*): 1, 10, 100, 1000, and 10,000. One part of the RBC final suspension was added to 3 parts of the test material in PBS to give the aforementioned final assay concentrations. The mixtures were incubated for 60 minutes with agitation at room temperature. After incubation, the samples were centrifuged at 1500 ×g and 4°C for 1 minute and the extent of haemolysis was determined spectrophotometrically at 541 nm using a UV/visible spectrophotometer (Genway 7305, Hanwell, London, UK) and the percentage haemolysis estimated by comparison with a sample that was totally lysed with deionized water. The concentration of a test substance that induced the lysis of 50% of RBCs ($H_{50\%}$) was determined and used to evaluate the irritation potential of Diclo-CD mixtures.

2.6.4. Bovine Corneal Opacity and Permeability (BCOP) Assay. Bovine eyes were obtained from a local slaughterhouse (ABP Guilford, London, UK). Eyes with corneal damage or abnormalities were discarded. Three different controls were used for validation purposes; sodium hydroxide (0.5 M) was used as a corrosive test substance, benzalkonium chloride (BKC) 1% *w/v* in PBS was used as a strong irritant control, and propylene glycol as a slight irritant. Diclo solution (0.1% *w/v*) and Diclo-CD solutions containing an amount equivalent to 0.1% *w/v* of Diclo were tested.

The extent of corneal damage was assessed by evaluating the opacity, followed by application of sodium fluorescein solution (2% *w/v* pH 7.4) to examine the integrity of the corneal epithelium, using an examination lamp and a cobalt blue filter (Leica, GmbH, Germany). Individual numerical scores for opacity, epithelial integrity (degree of staining), and epithelial detachment were reported elsewhere [25] and in more

Table 1: Summary of the rabbit groups recruited in the study and their treatments.

Group	Left eye	Right eye
Group 1	Vigamox eye drops	Vigamox eye drops containing 0.1% *w*/*v* Diclo
Group 2		Vigamox eye drops containing Diclo-γ-CD equivalent to 0.1% *w*/*v* Diclo
Group 3		Vigamox® eye drops containing Diclo-HP-β-CD equivalent to 0.1% *w*/*v* Diclo

recently published work [26]. The sum score was estimated and the mean score for each of the three eyes was used to interpret the corneal irritation potential.

2.6.5. Cytotoxicity Evaluation (MTT Assay). Primary human corneal epithelial cells (ATCC pcs-700-010) from ATCC were seeded at approximately 2×10^4 cells/well into 96 well plates (Nunc, Netherland) using corneal epithelial cell basal medium containing apotransferrin (5 mg/ml), epinephrine (1.0 mM) extract P (0.4%), hydrocortisone hemisuccinate (100 ng/ml), L-glutamine (6 mM), rh insulin (5 mg/ml), and CE growth factor (1 ml). The cells were allowed to establish for 48 hours prior to treatment. Media were removed and fresh media containing 5 different treatments were added. The treatments were Diclo (0.1% *w*/*v*) and Diclo-, α-, β-,γ-, and HP-β-CD solutions containing equivalent concentrations of Diclo 0.1% *w*/*v*. The medium served as the negative control and benzalkonium chloride (BKC) at a concentration of 0.01% *w*/*v* was used as the positive control. After 4 hours of treatment, the media were removed and the cells were washed twice with sterile PBS at 37°C and then further incubated with 200 μl per well of 0.5 mg/ml 3-(4,5-dimethylthiazol-2-yl)-2,5-diphenyltetrazolium bromide (MTT) solution at 37°C. After incubation, the MTT solution was carefully removed and the wells were washed twice with sterile PBS. Finally, 200 μl of dimethylsulfoxide (DMSO) was added to each well to lyse the cells. The cells were then gently agitated to mix the samples and analyzed on a TECAN Infinite M200 pro plate reader (Männedorf, Switzerland) at a wavelength of 540 nm. Experiments were performed in triplicate, and the average percentage cell viability was estimated.

2.6.6. In Vivo Study (Alcohol Delamination and Corneal Epithelial Scrapping). Specified amounts of Diclo or equivalent from Diclo-γ-CD- and HP-β-CD-dispersed mixtures were dissolved in Vigamox® eye drops to form Diclo 0.1% *w*/*v* solutions. Twenty-seven white albino rabbits, weighing between 2.0 and 2.5 kg, were used in the experiments. The rabbits were fed on balanced diet pellets and maintained on 12 h/12 h light/dark cycle in an air-conditioned room, at 28°C before the experiment. The experimental procedures were approved by Minia University Animal Ethics Committee (Minia, Egypt) and conformed to ethical guidelines.

The rabbits were divided into three groups with nine animals in each. Table 1 summarizes the different types of treatment. Each treatment was initiated directly after induction of the corneal ulcer as a single drop instilled every 6 hours.

Prior to induction of ulcers, both eyes were locally anaesthetized with instillation of a single drop of Benox® eye drops (0.4% benoxinate hydrochloride) in each eye. A 6 mm ring was applied to the central corneal zone, and 20% *v*/*v* ethyl alcohol was applied inside the ring for 15 seconds to ease epithelial removal (delamination) followed by epithelial scrapping with a sterile scalpel blade. The ulcers were immediately stained with fluorescein, and the stain was visualized in a dark room using a hand-held indirect ophthalmoscope with a cobalt blue filter (Omega 500, Heine, Germany); the treatment was initiated as aforementioned.

2.6.7. Statistical Analysis. Statistical analysis was performed with GraphPad Prism 6 (2014) software, using analysis of variance (ANOVA) with a Dunnett post hoc test for confidence intervals of 95% with statistical significance set at $p < 0.05$ in order to reveal statistical significant differences among contact angle, surface tension, spreading coefficient, transcorneal permeation parameters, cumulative BCOP scores, and % cell viability.

3. Results and Discussion

3.1. Differential Scanning Colorimetry. DSC was used to study the crystallinity of Diclo and the possibility of formation of Diclo-CD inclusion complexes. Figures 1(a)-1(d) shows the thermal behavior of Diclo with different types of CDs (α-, β-, γ-, and HP-β-CD), respectively. Diclo demonstrates a strong thermal endothermic event at 290°C caused by melting of diclofenac sodium. This strong melting peak was reduced in intensity with α-CD PM and complexes, and it completely disappeared with β-, γ-, and HP-β-CDs. The complete disappearance of the drug peak with CDs strongly suggests molecular dispersion and formation of molecular inclusion complexes of Diclo with β-, γ-, and HP-β-CDs. Shifting of the melting peak to the lower end of the temperature scale and formation of a lower intensity melting peak may indicate the formation of partial/incomplete inclusion complexes of Diclo with α-CD and could be caused by poorer fitting of the relatively bulky diclofenac within the smallest cavity size of 6-sugar units α-CD, compared with the higher 7- and 8-sugar units β- and HP-β-CDs, and γ-CD, respectively. The DSC curves of the physical mixtures and the dispersed mixtures that were prepared by the solvent evaporation technique did not show any marked differences because the heat supply during the DSC procedure can provide sufficient power equivalent to that of the solvent evaporation, which brings drug molecules and CD into intimate molecular dispersion/complexation. Similar behavior with other water-soluble carriers has been reported [27].

3.2. FT-IR Spectroscopy. FT-IR spectroscopy was utilized to study any potential interactions between Diclo and different CDs, as shown in Figures 2(a)-2(d). The IR spectrum of Diclo

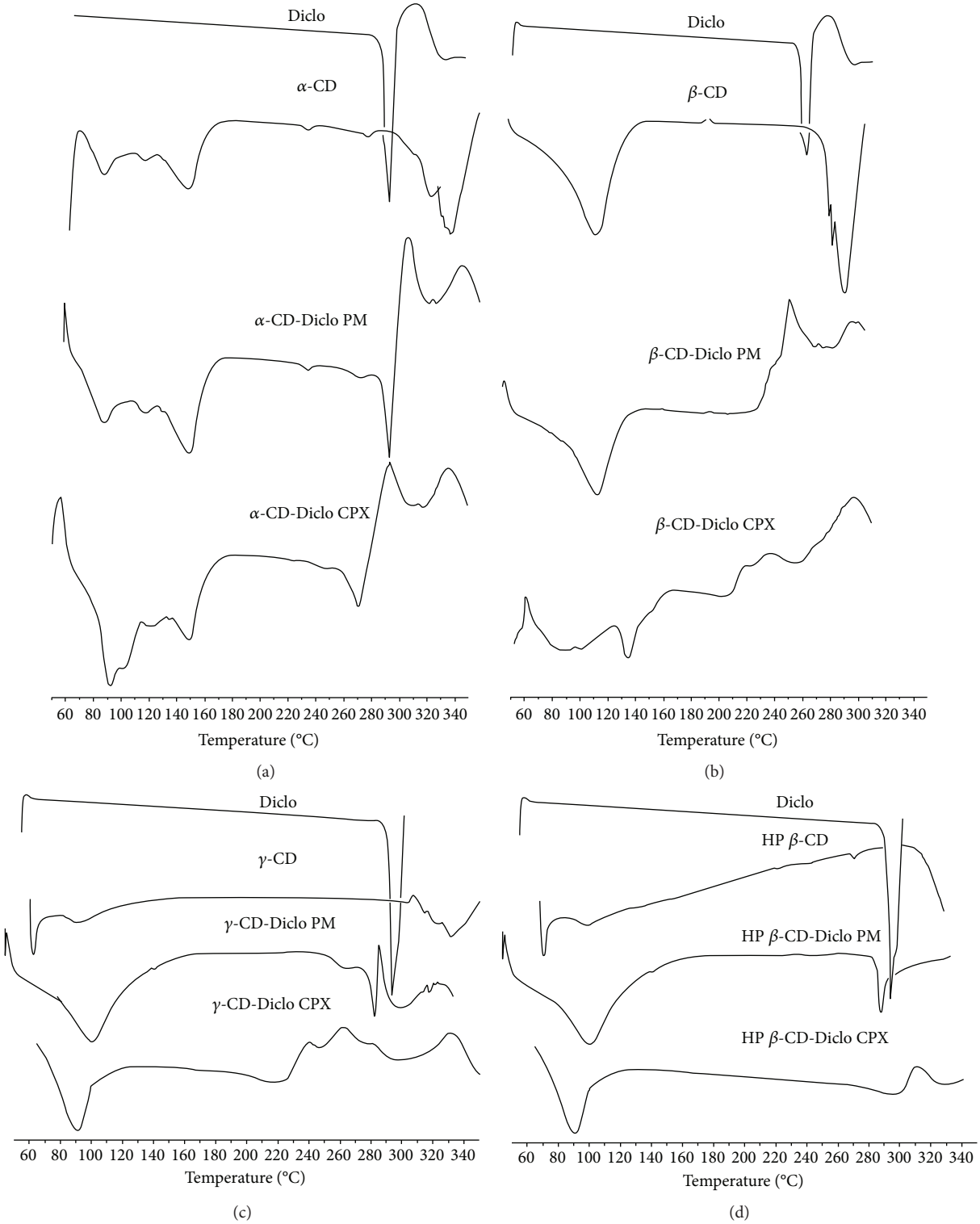

Figure 1: DSC curves for (a) Diclo, α-CD, α-CD-Diclo (PM), and dispersed (CPX); (b) Diclo, β-CD, β-CD-Diclo (PM), and dispersed (CPX); (c) Diclo, γ-CD, γ-CD-Diclo (PM), and dispersed (CPX); and (d) Diclo, HP-β-CD, and HP-β-CD physical (PM) and dispersed (CPX) mixtures.

showed a strong characteristic peak at 1600 cm^{-1} assigned for $C=O$, two IR absorption peaks resulting from secondary amine N-H, and aromatic stretching $C=C$-bands at 3400 and 3300 cm^{-1} [28]. These spectral regions are of interest for investigating the possibility of formation of inclusion complexes [29]. All CDs that showed a characteristic broad stretching absorption peak appearing at 3550 to 3200 cm^{-1} were assigned to different alcoholic O-H of the cyclic sugar

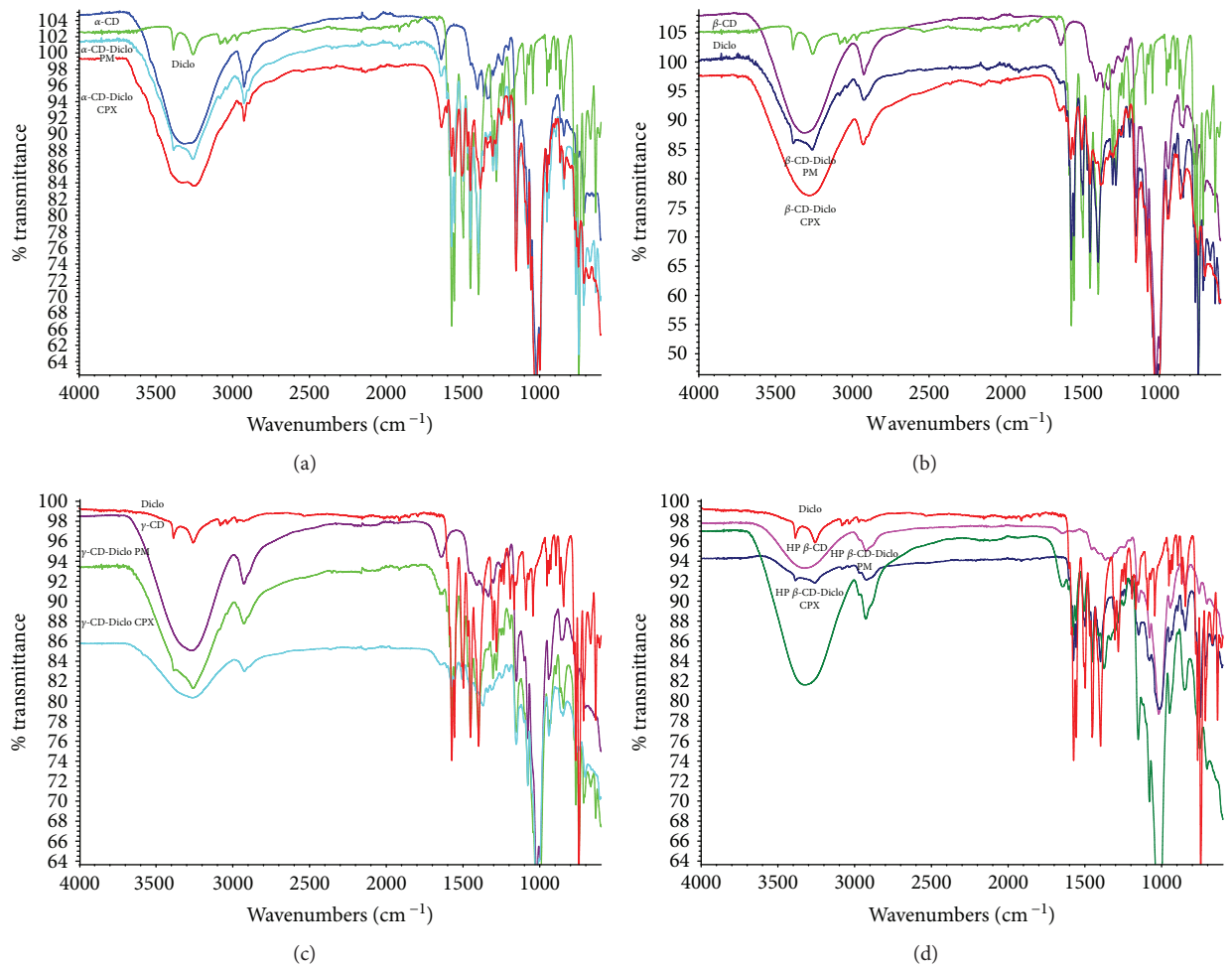

Figure 2: FT-IR spectra for (a) Diclo, α-CD, α-CD-Diclo (PM), and dispersed (CPX); (b) Diclo, β-CD, β-CD-Diclo (PM), and dispersed (CPX); (c) Diclo, γ-CD, γ-CD-Diclo (PM), and dispersed (CPX); and (d) Diclo, HP-β-CD, and HP-β-CD physical (PM), and dispersed (CPX) mixtures.

units of α-, β-, γ-, and HP-β-CDs (Figures 2(a)-2(d)). The physical mixtures (PM) were a superimposition of the two spectra of Diclo and corresponding CDs when their characteristic peaks were unchanged; this occurred with Diclo-α, β-, γ-, and HP-β-CD PM. Apart from Diclo-α-CD, significant changes in the IR region of 3550–3200 cm^{-1} were seen with Diclo-, β-, γ-, and HP-β-CD-dispersed mixtures prepared by the solvent evaporation method. Additionally, the strong absorption bands of $C=O$ group of Diclo were markedly reduced in intensity and showed a frequency shift with all CDs. These changes can be explained by characteristic guest-host interactions and formation of inclusion complexes of Diclo with β-, γ-, and HP-β-CD-dispersed mixtures. Conversely, Diclo- and α-CD complex still shows a small peak at 3300, which might be indicating the free drug, as well as incomplete complexation for α-CD. These results concurred with those obtained using DSC.

3.3. Molecular Docking. To gain more insights into the binding mode and binding constants between Diclo and individual CDs, molecular docking between Diclo and α-, β-, γ-, and HP-β-CDs was performed. Molecular docking simulation is the best method to predict drug (guest) orientations, molecular fitting and interactions into/onto the host (CDs) hydrophobic cavity, and hydrophilic rims at the molecular level [30]. Figure 3 summarizes the molecular docking results. The binding constants estimated for Diclo-, α-, β-, γ-, and HP-β-CDs complexes were −4.3 kcal/mol, −4.4 kcal/mol, −4.8 kcal/mol, and −5.2 kcal/mol, and the force of binding of Diclo with CDs was in the following order: HP-β-CD > > γ-CD > β-CD > α-CD.

Electrostatic interactions (H-bonding) between carboxylate group of Diclo and the hydrophilic rim (hydroxyl groups: OH) of α-CD Figure 3, ia and ic) were recorded. However, the size of the α-CD cavity was too small to host the dichlorophenyl ring of Diclo (the dichlorophenyl ring was completely outside the CD cavity) (Figures 1(a) and 2(a)). This led to a less stable complex with a binding constant of −4.3 kcal/mol. These results correlated well with DSC and FT-IR studies (Figures 1(a) and 2(a)) where the Diclo melting peak appeared with the processed Diclo- and α-CD mixture indicating a negligible physicochemical interaction. Conversely, both γ- and HP-β-CDs had suitable cavity sizes for hosting Diclo in their hydrophobic cavity (Figure 3, ic, iic,

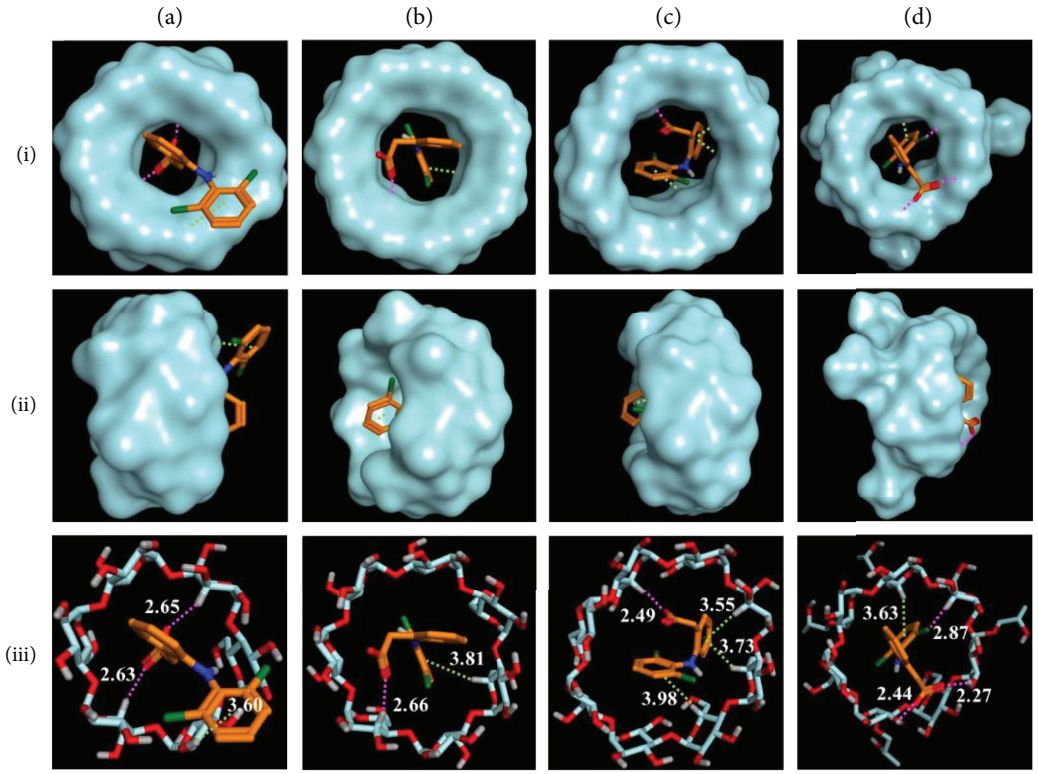

Figure 3: The predicted orientations and binding interactions of diclofenac within the cavity of four cyclodextrins (a) α-CD, (b) β-CD, (c) γ-CD, and (d) HP-β-CD from the top view of the wide edge (i), side view (ii), and as stick molecular depiction (iii). Hydrogen bonds and hydrophobic interactions are demonstrated as magenta and green dashed lines, respectively.

Table 2: Contact angle, surface tension measurements, spreading, flux, and apparent permeability coefficient of diclofenac sodium from solution and cyclodextrin complexes. Results presented as mean values ± SD, $n = 3$. $*$ denotes statistically significant differences ($p < 0.05$).

Formulation	Contact angle (θ)	Surface tension (mN/m)	Spreading coefficient	Steady-state flux (μg/h)	$P_{app} \times 10^{-6}$ (cm/s)
Diclo	$34 \pm 0.65^*$	$52.0 \pm 2.5^*$	$-8.9 \pm 2.00^*$	$53 \pm 1.5^*$	$12.0 \pm 0.5^*$
Diclo-α-CD	52 ± 0.55	65.5 ± 1.0	-25.2 ± 1.0	21 ± 0.7	5.0 ± 0.5
Diclo-β-CD	50 ± 0.45	61.5 ± 2.0	-22.0 ± 1.5	19 ± 2.8	4.3 ± 1.0
Diclo-γ-CD	52 ± 0.80	60.35 ± 2.8	-23.2 ± 1.5	41.5 ± 3.5	9.4 ± 2.0
Diclo-HP-β-CD	53 ± 0.55	61.33 ± 2.0	-24.4 ± 2.0	41 ± 4.5	9.3 ± 2.0

iiic, id, iid, and iiid) where the dichlorophenyl ring was completely buried in γ- and HP-β-CDs. The cavity size of HP-β-CDs is larger than that of α-CD, and it contains an additional extension arising from the hydroxypropyl substitution when compared with β-CD. The two hydrogen bonds as well as the halogen-hydrogen bond could also contribute to a very stable complex with binding energy of −5.2 kcal/mol. The cavity size of γ-CD is sufficiently large to host Diclo with three hydrophobic interaction sites that lead to a stable complex with binding energy of −4.8 kcal/mol (Figure 3, iiic).

While the β-CD cavity size is larger than that of α-CD, the dichlorophenyl ring could not be entirely hosted within it (Figure 3, iiib). Instead, the two aromatic rings of Diclo were bent with a torsional angle of 69 degrees [31]; the dichlorophenyl was partly outside the pocket/cavity as shown in Figure 3, ib and Figure 3, iiib. This produces a fairly stable complex with binding energy of −4.4 kcal/mol. Similar results of the crystal structures of Diclo with β-CD have been reported elsewhere [32].

3.4. Contact Angle, Surface Tension, and Spreading Coefficient. Table 2 shows the surface tension for Diclo solution (0.1% *w*/*v* in PBS) and equivalent amounts of Diclo-, α-, β-, γ-, and HP-β-CD-dispersed mixtures that constitute the Diclo solution of 0.1% *w*/*v*. The γ value recorded for Diclo solution (0.1% *w*/*v*) was 52 mN/m. This is a significant decrease in the surface tension of the Diclo solution compared with the solvent (PBS) which was 76 mN/m and suggests that Diclo in solution has a surfactant-like property. The dichloride substituted aromatic ring with the NH linker to benzoate structure can explain the amphipathic nature and surface active properties of diclofenac sodium.

Amphipathic properties have been reported with structurally similar drugs such as chlorpromazine, diphenhydramine, chlordiazepoxide, and chlorcyclizine [33].

While the exact mechanism of the onset of corneal melting remains unknown [12], the above-reported surface active properties attributed to Diclo may provide some insight into how the topical ocular administration of Diclo produces irritant/toxic effects. It could be caused by exposure of the ocular surface to relatively high local concentrations of a drug with surface active properties that can induce emulsification and/or a sloughing of the extremely lipophilic corneal epithelium.

The surface tension of Diclo-, α-, β-, γ-, and HP-β-CD solutions exhibited a significant ($p < 0.05$) increase in the surface tension values (60–65.5 mN/m). Furthermore, Diclo-CD solutions showed significant increases in contact angle (θ) and associated significant decreases in spreading coefficients (S). This supports the formation of complexes of Diclo with α-, β-, γ-, and HP-β-CDs in solution that may result in reducing the surface active properties of the drug because the hydrophobic part of Diclo is found within the cavity of CDs. These results are consistent with the docking calculations: various H-bonding and hydrophobic interactions of carboxylate group and/or dichlorophenyl ring of Diclo with the hydrophilic rims and hydrophobic cavities of CDs were recorded (Figure 3, ia, iia, iiia, ib, iib, iiib, ic, iic, iiic, id, iid, and iiid). Furthermore, the behavior of complexes of Diclo with CDs in solutions was reported to be different than their behavior in the solid state (1 : 1 molar complexation) [34, 35]. The two aromatic rings have been reported to be involved 1 : 2 CD complexation. This could explain why the contact angle and surface tension measurements for Diclo-, α-, β-, γ-, and HP-β-CD solutions did not show statistically significant differences ($p > 0.05$).

3.5. Transcorneal Permeation Study. Porcine corneal permeation profiles of Diclo from free drug solutions and different Diclo-, α-, β-, γ-, and HP-β-CD complexes are outlined in Figure 4. Permeation parameters (steady-state flux and apparent permeability coefficient (P_{app})) of the different Diclo solutions tested are given in Table 2. Both steady-state flux and P_{app} values (19–41.5 μg/h and 4–9 cm/s) for Diclo permeated from different Diclo-, α-, β-, γ-, and HP-β-CD solutions showed significant controlled/sustained permeation of Diclo from α-, β-, γ-, and HP-β-CD solutions compared with those values estimated for free Diclo solution (53 μg/h and 12 cm/s). Cyclodextrins are extremely hydrophilic and cannot permeate through lipophilic corneal barriers [1, 10] suggesting that Diclo molecules had to be liberated from the guest-host complex in order to permeate through the corneal barrier and that the P_{app} of Diclo is dependent on the binding forces of the guest-host complexes [18].

Diclo complex with β-cyclodextrin has been reported to transfer with higher rate through the cornea compared to free drug in the previous studies [36]. Valls et al. used a different device to study transcorneal permeation through rabbit's cornea. While the setup was developed in-house and to our knowledge this device is not available commercially, this setup can take into consideration tear dynamics (washings) and other ocular pharmacokinetic parameters. It is worth noting that Franz diffusion cells are a static *in vitro* permeation model that cannot perfectly mimic *in vivo* tear/ocular dynamics that represent a major factor for drug loss of topically administered eye drops on the surface of the eye. Other positive features resulting in prolonging precorneal residence and mucoadhesion cannot be taken into account while using this model. Therefore, faster permeation rates from drug solutions have consistently been reported with this model compared with many other formulations [22, 37].

More pertinently, the results showed that not all CDs used provided equally controlled Diclo permeation through

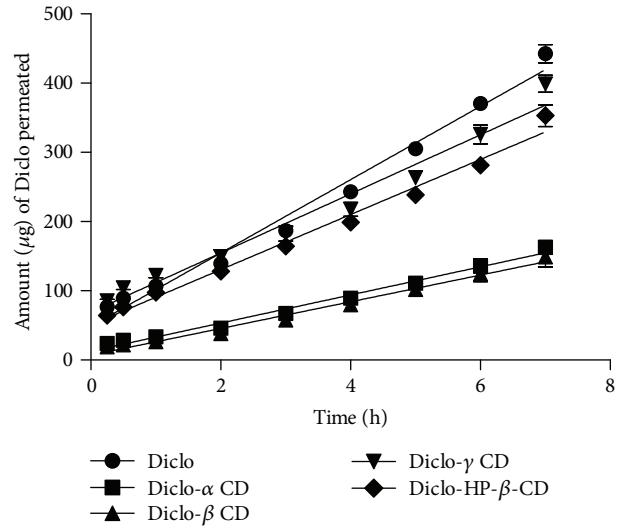

Figure 4: Transcorneal permeation profiles of Diclo form drug solution and Diclo-CD solutions. Results presented as mean values ± SD, $n = 3$.

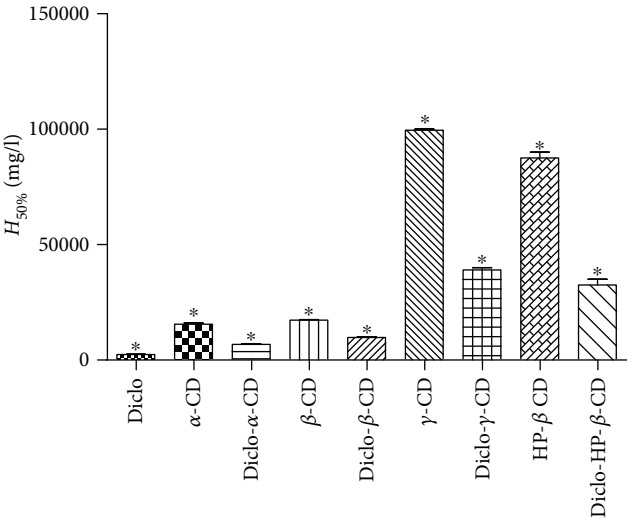

Figure 5: RBC haemolysis potential expressed in $H_{50\%}$ for Diclo solution and Diclo- α-, β-, γ-, HP-β-CD solutions. Results are expressed as mean values ± SD, $n = 3$. * denotes statistically significant differences ($p < 0.05$).

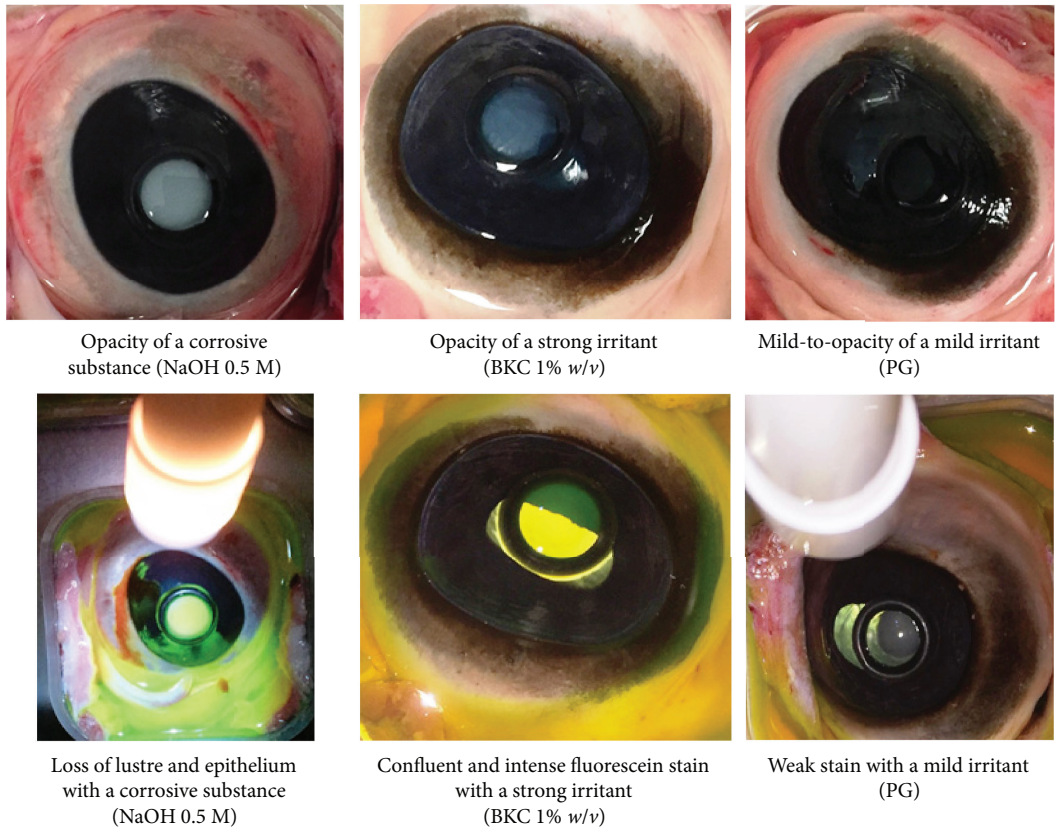

Figure 6: Degree of corneal opacity (upper) and fluorescein permeability (lower) used to score the test substances (corrosive (sodium hydroxide 0.5 M), strong irritant (benzalkonium chloride 1%), and mild irritant (propylene glycol) models).

excised porcine corneae. While Diclo-, α-, and β-CDs showed the lowest permeation rate (P_{app}) with 2.4-fold and 2.8-fold decreases compared with free Diclo solution, Diclo-, γ-, and HP-β-CD solutions showed markedly higher (P_{app}) compared with the previous two CD congers. Both Diclo-, γ-, and HP-β-CD recorded (P_{app}) 1.27-fold lower than free Diclo solution. Paradoxically, despite the docking calculations, showing that Diclo-, γ-, and HP-β-CDs were the most stable complexes; the drug transcorneal permeation from Diclo-, γ-, and HP-β-CD complexes was slightly faster than that from Diclo-, α-, and β-CD complexes. It may be that with ex vivo permeation, the binding forces are not the only factors that affect permeation rates through the cornea.

3.6. RBC Haemolysis Assay. RBC assay is an *in vitro* test that has been used widely for testing ocular irritation potential of ophthalmic pharmaceutical and cosmetic ingredients and surfactants [38, 39]. Acute cytotoxicity due to cell lysis, corneal erosion, and deepithelisation is well correlated with haemolytic activity and RBC lysis of test substances. The RBC assay has been reported to be correlated with the *in vivo* rabbit Draize test [10, 39]. Figure 5 shows the concentrations (H_{50}) of the test substance that showed an absorbance value equivalent to 50% haemolysis of RBCs. The estimated $H_{50\%}$ for Diclo was 2500 mg/l, which is equal to 2.5 times of the drug concentration in commercial eye drops (0.1% *w*/*v*). The γ- and HP-β-CDs recorded $H_{50\%}$ at extremely high concentrations and can be considered as essentially nonirritant. Nevertheless, the α- and β-CDs were deemed to cause haemolysis at lower concentrations compared with γ- and HP-β-CDs. These findings support previous results indicating that α- and β-CDs can extract cholesterol and other lipid components of cell membranes thereby contributing to cell lysis [10, 11, 40]. It is worth noting that inclusion of Diclo into the cavities of the CDs by formation of guest-host complexes may have masked the inherent RBC haemolysis potential of Diclo. For example, $H_{50\%}$ recorded for Diclo-, α-, β-, γ-, and HP-β-CDs ranged from 7000 to 40,000 mg/l compared with a much lower $H_{50\%}$ value (2500 mg/l) for Diclo alone. This was accompanied by a reduction of cell lysis and possible corneal erosion by 3 to 16 times, compared with using the free drug alone.

3.7. BCOP Assay. The use of BCOP assay has been validated and approved by the Scientific Advisory Committee of the European Centre for the Validation of Alternatives (ECVAM). The BCOP assay is widely used across the cosmetic and pharmaceutical industries to test the ocular irritation potential of surfactants, pharmaceutical ingredients, and finished products [41–43]. The BCOP assay uses the assessment of corneal opacity and fluorescence intensity as an indication of degree of the disruption of the corneal barrier after exposure to the test material (Figure 6).

Figure 7 shows the cumulative BCOP scores of corneal opacity and epithelial integrity recorded for corrosive, strong, and mild irritant control and test substance Diclo solution

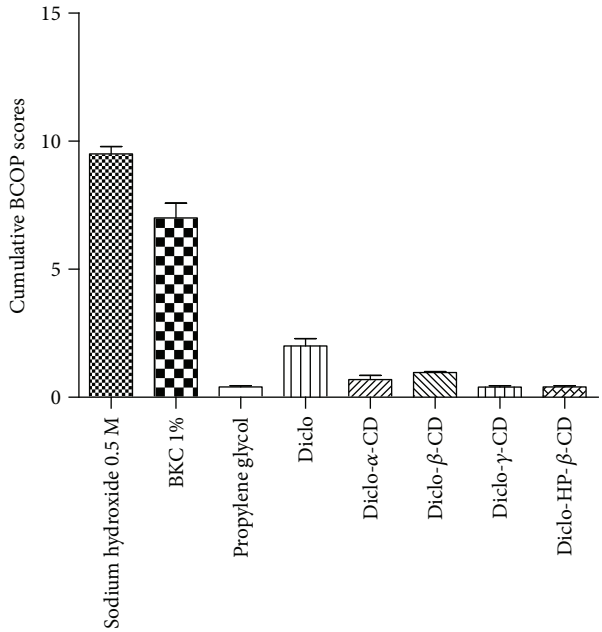

Figure 7: Cumulative BCOP scores for the three controls, Diclo, and different Diclo-CDs. Results presented as mean values ± SD, $n = 3$.

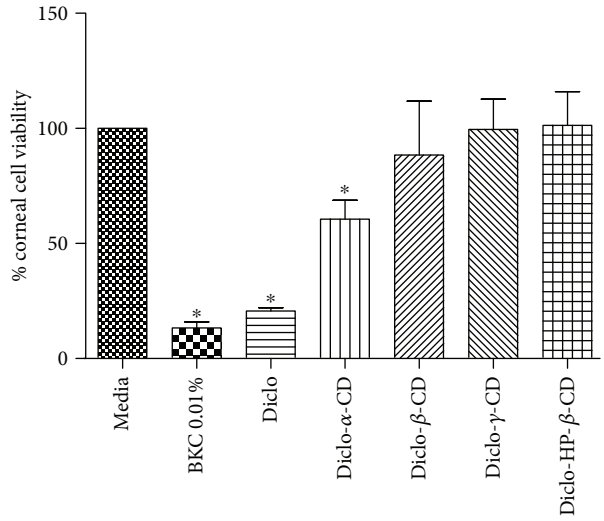

Figure 8: Percentage (%) cell viability for human primary corneal epithelial cells exposed to the test substances for 3 hours. Results are expressed as mean values ± SD, $n = 3$. ∗ denotes statistically significant differences ($p < 0.05$).

and Diclo-, α-, β-, γ-, HP-β-CD solutions. The cumulative score for Diclo solution recorded 1.5 corresponding to mild-to-moderate irritants whereas Diclo-, α-, β-, γ-, HP-β-CD solutions recorded scores 0.5 to 1 corresponding to none-to-mild irritants with Diclo-, γ-, and HP-β-CD solutions exhibited the lowest cumulative scores. These results accord with the results from the RBC haemolysis assays.

3.8. Cytotoxicity Evaluation (MTT Assay). Percentage (%) corneal epithelial cell viability after a 4-hour exposure to various treatments is shown in Figure 8. BKC was used as a positive control and showed extremely low cell viability (13%) and was deemed to be cytotoxic at the duration tested in this study [44–46]. Diclo recorded corneal cell viability of 21% indicating poor cell viability and these results concur with the other two *in vitro* ocular toxicity models (BCOP and RBC haemolysis assays) and support previous reports on the harmful effects of topical application of Diclo to the corneal epithelium [13, 14]. The % cell viability estimated for Diclo-, α-, β-, γ-, and HP-β-CDs that contained an equivalent concentration of Diclo 0.1% *w*/*v* was significantly increased from 3-fold to 5-fold ($p < 0.01$) compared with free Diclo alone. While there were slight decreases in cell viability after exposure to Diclo-, α-, and β-CDs, these were correlated with the previous results that showed α- and β-CDs are less tolerated by the ocular surface, compared with γ- and HP-β-CDs. The latter can be considered as practically nonirritant and were able to mask the acute ocular toxicity of free Diclo solution.

3.9. In Vivo Study. Induction of corneal epithelial debridement by alcohol-assisted removal of corneal epithelium was adopted in this study as clinically relevant to the type of corneal wounds created with photorefractive keratectomy [47, 48]. Figure 9 shows a range of fluorescein stained corneal ulcers and corneal healing over time. Both eyes in group I showed complete healing in four days but with a nebula/scar in the right eye that received Vigamox eye drops with the anti-inflammatory drug Diclo 0.1% *w*/*v* (the nebula, seen at 72 hours, is indicated by an arrow). Group II and group III showed markedly faster healing rates; five rabbits out of 9 demonstrated complete corneal healing in 2 days without scar formation. These results can be ascribed to the following possibilities:

(i) Diclo-CDs may have lower direct irritation potential and lower toxicity by masking the inherent surfactant-like characteristics of Diclo.

(ii) Subjecting the corneal ulcer to a transient high local concentration of free Diclo solution was avoided when Diclo was instilled as inclusion complexes with γ- and HP-β-CDs.

(iii) Diclo-CDs may prolong precorneal residence time and enhance ocular bioavailability, compared with instillation of free Diclo eye drops. The literature indicates that dorzolamide-CD eyes drops with low viscosity (3 to 5 centipoises) exhibited comparable bioavailability with commercially viscous (100 centipoises) dorzolamide eye drops (Trusopt®) [7].

4. Conclusions

Ocular toxicity due to Diclo has been well reported and attributed solely to pharmacological factors such as inhibition of cyclooxygenase and/or upregulation of metalloproteinase matrix [17]. In this study, we report for the first time the possible toxicity of Diclo due to surfactant-like functionality and a formulation approach to significantly reduce/mask these undesirable characteristics using CD inclusion complexation.

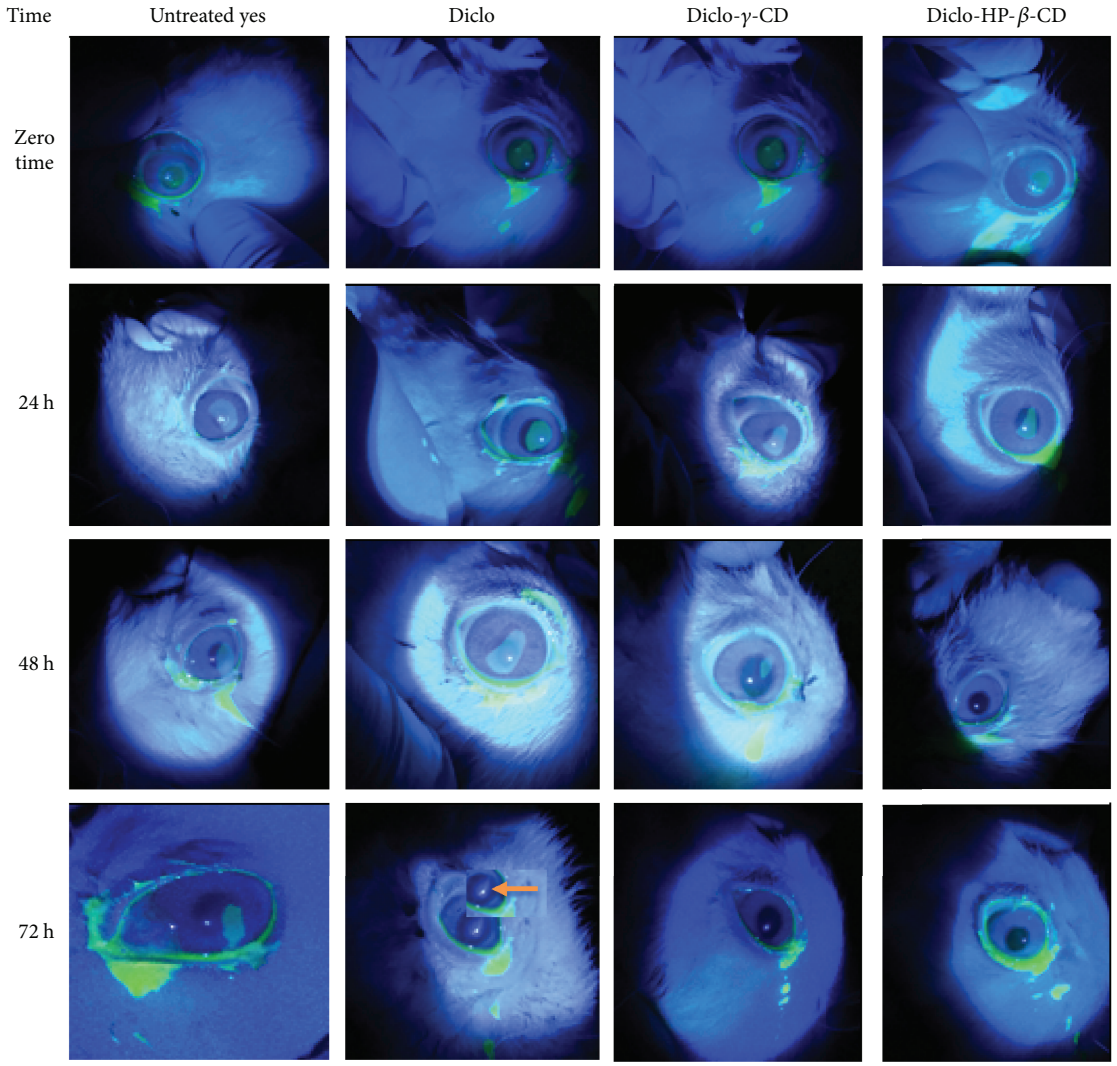

Figure 9: Progressive changes in alcohol-induced corneal ulcers in rabbit eyes where left eyes were untreated and right eyes were treated with Diclo, Diclo-γ-CD, and Diclo-HP-β-CD just after induction of ulceration. Of note is the corneal opacity (nebula) in the Diclo eye after 72 hours (as marked with an arrow).

Diclo and β-, γ-, and HP-β-CDs can form guest-host inclusion complexes with different capacities for permeating through porcine corneae. The α- and β-CDs were deemed to be less effective at reducing the ocular unwanted toxicities of Diclo resulting from inherent ability to extract cholesterol and lipid components from the lipophilic corneal cell membranes. Contact angles, surface tensions, and spreading coefficients, measured for the first time, confirmed guest-host complex formation in solutions for the amphipathic drug Diclo. *In vitro* toxicity model RBC haemolysis and BCOP assays indicated the irritation potential from CD formulations, and the results were well correlated with those from the MTT cytotoxicity assay. The γ- and HP-β-CDs offer potential as carriers for effectively diminishing Diclo ocular toxicities. These two CD complexes exhibited a marked reduction in RBC haemolysis and significant increase in cell viability compared with Diclo solution alone. Diclo-γ- and Diclo-HP-β-CDs greatly enhance corneal wound closure without scar formation, compared with delayed corneal wound repair and scar formation with Diclo solution alone.

Conflicts of Interest

The authors disclose that there is no conflict of interest or financial interest.

References

[1] T. Loftsson and M. Masson, "Cyclodextrins in topical drug formulations: theory and practice," *International Journal of Pharmaceutics*, vol. 225, no. 1-2, pp. 15–30, 2001.

[2] A. Mai, E. L.-M. MA, O. Y. Abdallah, and H. Abdelkader, "Reduction of bitterness and enhancing palatability of cetirizine oral liquid dosage forms by cyclodextrins," *Journal of Pharmaceutics & Drug Development*, vol. 1, no. 3, pp. 1–8, 2014.

[3] C. D. Radu, O. Parteni, and L. Ochiuz, "Applications of cyclodextrins in medical textiles-review," *Journal of Controlled Release*, vol. 224, pp. 146–157, 2016.

[4] C. Scavone, A. C. Bonagura, S. Fiorentino et al., "Efficacy and safety profile of diclofenac/cyclodextrin and progesterone/cyclodextrin formulations: a review of the literature data," *Drugs in R&D.*, vol. 16, no. 2, pp. 129–140, 2016.

[5] T. Irie and K. Uekama, "Pharmaceutical applications of cyclodextrins. III. Toxicological issues and safety evaluation," *Journal of Pharmaceutical Sciences*, vol. 86, no. 2, pp. 147–162, 1997.

[6] T. Loftsson and E. Stefánsson, "Cyclodextrins in eye drop formulations: enhanced topical delivery of corticosteroids to the eye," *Acta Ophthalmologica Scandinavica*, vol. 80, no. 2, pp. 144–150, 2002.

[7] H. H. Sigurdsson, E. Stefánsson, E. Gudmundsdóttir, T. Eysteinsson, M. Thorsteinsdóttir, and T. Loftsson, "Cyclodextrin formulation of dorzolamide and its distribution in the eye after topical administration," *Journal of Controlled Release*, vol. 102, no. 1, pp. 255–262, 2005.

[8] EMA, *Background Review for Cyclodextrins Used as Excipients*, pp. 1–17, 2014.

[9] P. W. Morrison, C. J. Connon, and V. Khutoryanskiy, "Cyclodextrin-mediated enhancement of riboflavin solubility and corneal permeability," *Molecular Pharmaceutics*, vol. 10, no. 2, pp. 756–762, 2013.

[10] T. Loftsson and T. Jarvinen, "Cyclodextrins in ophthalmic drug delivery," *Advanced Drug Delivery Reviews*, vol. 36, no. 1, pp. 59–79, 1999.

[11] Y. Ohtani, T. Irie, K. Uekama, K. Fukunaga, and J. Pitha, "Differential effects of α-, β- and γ-cyclodextrins on human erythrocytes," *European Journal of Biochemistry*, vol. 186, no. 1-2, pp. 17–22, 1989.

[12] A. C. Guidera, J. I. Luchs, and I. J. Udell, "Keratitis, ulceration, and perforation associated with topical nonsteroidal anti-inflammatory drugs," *Ophthalmology*, vol. 108, no. 5, pp. 936–944, 2001.

[13] M. Ahuja, A. S. Dhake, S. K. Sharma, and D. K. Majumdar, "Topical ocular delivery of NSAIDs," *The AAPS Journal*, vol. 10, no. 2, pp. 229–241, 2008.

[14] S. J. Kim, A. J. Flach, and L. M. Jampol, "Nonsteroidal anti-inflammatory drugs in ophthalmology," *Survey of Ophthalmology*, vol. 55, no. 2, pp. 108–133, 2010.

[15] N. G. Congdon, O. D. Schein, P. von Kulajta, L. H. Lubomski, D. Gilbert, and J. Katz, "Corneal complications associated with topical ophthalmic use of nonsteroidal antiinflammatory drugs," *Journal of Cataract and Refractive Surgery*, vol. 27, no. 4, pp. 622–631, 2001.

[16] A. J. Flach, "Corneal melts associated with topically applied nonsteroidal anti-inflammatory drugs," *Transactions of the American Ophthalmological Society*, vol. 99, pp. 205–210, 2001.

[17] A. Fernandez-Ferreiro, M. Santiago-Varela, M. Gil-Martínez et al., "Ocular safety comparison of non-steroidal anti-inflammatory eye drops used in pseudophakic cystoid macular edema prevention," *International Journal of Pharmaceutics*, vol. 495, no. 2, pp. 680–691, 2015.

[18] O. Reer, T. K. Bock, and B. W. Müller, "In vitro corneal permeability of diclofenac sodium in formulations containing cyclodextrins compared to the commercial product voltaren ophtha," *Journal of Pharmaceutical Sciences*, vol. 83, no. 9, pp. 1345–1349, 1994.

[19] L. Feng, R. Fawaz, S. Hovde, F. Sheng, M. Nosrati, and J. H. Geiger, "Crystal structures of *Escherichia coli* branching enzyme in complex with cyclodextrins," *Acta Crystallographica Section D Structural Biology*, vol. 72, no. 5, pp. 641–647, 2016.

[20] S. Shityakov, R. E. Salmas, S. Durdagi et al., "Characterization, in vivo evaluation, and molecular modeling of different propofol-cyclodextrin complexes to assess their drug delivery potential at the blood-brain barrier level," *Journal of Chemical Information and Modeling*, vol. 56, no. 10, pp. 1914–1922, 2016.

[21] A. Llinàs, J. C. Burley, K. J. Box, R. C. Glen, and J. M. Goodman, "Diclofenac solubility: independent determination of the intrinsic solubility of three crystal forms," *Journal of Medicinal Chemistry*, vol. 50, no. 5, pp. 979–983, 2007.

[22] H. Abdelkader, M. R. Longman, R. G. Alany, and B. Pierscionek, "Phytosome-hyaluronic acid systems for ocular delivery of L-carnosine," *International Journal of Nanomedicine*, vol. 11, pp. 2815–2827, 2016.

[23] R. D. Schoenwald and H. S. Huang, "Corneal penetration behavior of β-blocking agents I: physichochemical factors," *Journal of Pharmaceutical Sciences*, vol. 72, no. 11, pp. 1266–1272, 1983.

[24] R. W. Lewis, *Red Blood Cell (RBC)Llysis and Protein Denaturation DB-ALM Protocol No 99*, EURL ECVAM DB-ALM, 2010.

[25] P. J. Weterings and Y. H. Vanerp, Eds.A. M. Goldberg, Ed., *Validation of the Becam Assay: An Eye Irritancy Screening Test, in Alternative Methods in Toxicology*, Mary Ann Liebert, Inc, New York, 1987.

[26] H. Abdelkader, S. Ismail, A. Hussein, Z. Wu, R. al-Kassas, and R. G. Alany, "Conjunctival and corneal tolerability assessment of ocular naltrexone niosomes and their ingredients on the hen's egg chorioallantoic membrane and excised bovine cornea models," *International Journal of Pharmaceutics*, vol. 432, no. 1-2, pp. 1–10, 2012.

[27] H. Abdelkader, O. Y. Abdallah, and H. Salem, "Comparison of the effect of tromethamine and polyvinylpyrrolidone on dissolution properties and analgesic effect of nimesulide," *AAPS PharmSciTech*, vol. 8, no. 3, pp. E110–E117, 2007.

[28] M. Saravanan, K. Bhaskar, G. Maharajan, and K. S. Pillai, "Development of gelatin microspheres loaded with diclofenac sodium for intra-articular administration," *Journal of Drug Targeting*, vol. 19, no. 2, pp. 96–103, 2011.

[29] I. Bratu, A. Hernanz, J. M. Gavira, and G. H. Bora, "FT-IR spectroscopy of inclusion complexes of β-cyclodextrin with fenbufen and ibuprofen," *Romanian Journal of Physics*, vol. 50, pp. 1063–1071, 2005.

[30] J. Li, Q. Jiang, P. Deng et al., "The formation of a host-guest inclusion complex system between β-cyclodextrin and baicalin and its dissolution characteristics," *The Journal of Pharmacy and Pharmacology*, vol. 69, no. 6, pp. 663–674, 2017.

[31] A. Sallmann, *Chemical Aspects of Diclofenac, in Chronic Forms of Polyarthritis*, F. J. Wagenhäuser, Ed., International Symposium, Torremolinos, Hans Huber Berne, 1975.

[32] M. R. Caira, V. J. Griffith, L. R. Nassimbeni, and B. van Oudtshoorn, "Synthesis and X-ray crystal structure of β-cyclodextrin diclofenac sodiu undecahydrate, a β-CD complex with a unique crystal packing arrangement," *Journal of the Chemical Society, Chemical Communications*, vol. 9, no. 9, pp. 1061-1062, 1994.

[33] D. Attwood, "The mode of association of amphiphilic drugs in aquoes solution," *Advances in Colloid and Interface Science*, vol. 55, pp. 271–303, 1995.

[34] A. Mucci, L. Schenetti, M. A. Vandelli, B. Ruozi, and F. Forni, "Evidence of the existence of 2:1 guest-host complexes between diclofenac and cyclodextrins in D_2O solutions. A ^{1}H and ^{13}C NMR study on diclofenac/β-cyclodextrin and diclofenac/2-hydroxypropyl-β-cyclodextrin," *Journal of Chemical Research*, vol. S, pp. 414-415, 1999.

[35] B. Pose-Vilarnovo et al., "Interaction of diclofena sodium with β and hydroxypropyl-β-cyclodextrin in solution," *STP Pharma Sciences*, vol. 9, pp. 231–236, 1999.

[36] R. Valls, E. Vega, M. L. Garcia, M. A. Egea, and J. O. Valls, "Transcorneal permeation in a corneal device of non-steroidal anti-inflammatory drugs in drug delivery systems," *The Open Medicinal Chemistry Journal*, vol. 2, no. 1, pp. 66–71, 2008.

[37] H. Abdelkader, S. Ismail, A. Kamal, and R. G. Alany, "Design and evaluation of controlled release niosomes and discomes for naltrexone hydrochloride ocular delivery," *Journal of Pharmaceutical Sciences*, vol. 100, no. 5, pp. 1833–1846, 2011.

[38] E. N. Alves, F. Presgrave Rde, O. A. Presgrave, F. P. Sabagh, J. C. de Freitas, and A. P. Corrado, "A reassessment of the in vitro RBC haemolysis assay with defibrinated sheep blood for the determination of the ocular irritation potential of cosmetic products: comparison with the in vivo draize rabbit test," *Alternatives to Laboratory Animals*, vol. 36, no. 3, pp. 275–284, 2008.

[39] W. J. Pape and U. Hoppe, "Standardization of an in vitro red blood cell test for evaluating the acute cytotoxic potential of tensides," *Arzneimittelforschung*, vol. 40, no. 4, pp. 498–502, 1990.

[40] K. Jarvinen, T. Jarvinen, and A. Urtti, "Ocular absorption following topical delivery," *Advanced Drug Delivery Reviews*, vol. 16, no. 1, pp. 3–19, 1995.

[41] P. Gautheron, M. Dukic, D. Alix, and J. F. Sina, "Bovine corneal opacity and permeability test: an in vitro assay of ocular irritancy," *Fundamental and Applied Toxicology*, vol. 18, no. 3, pp. 442–449, 1992.

[42] P. Grover and K. Jamil, "Alternatives methods for dermal and ocular animal safety testing of chemicals," *Proceedings-Indian National Science Academy Part A*, vol. B67, pp. 1–20, 2001.

[43] C. K. Muir, "Opacity of bovine cornea in vitro induced by surfactants and industrial chemicals compared with ocular irritancy in vivo," *Toxicology Letters*, vol. 24, no. 2-3, pp. 157–162, 1985.

[44] M. Ayaki, A. Iwasawa, and Y. Inoue, "Toxicity of antiglaucoma drugs with and without benzalkonium chloride to cultured human corneal endothelial cells," *Clinical Ophthalmology*, vol. 4, pp. 1217–1222, 2010.

[45] H. Eleftheriadis, M. Cheong, S. Sandeman et al., "Corneal toxicity secondary to inadvertent use of benzalkonium chloride preserved viscoelastic material in cataract surgery," *The British Journal of Ophthalmology*, vol. 86, no. 3, pp. 299–305, 2002.

[46] R. Mencucci, D. E. Pellegrini-Giampietro, I. Paladini, E. Favuzza, U. Menchini, and T. Scartabelli, "Azithromycin: assessment of intrinsic cytotoxic effects on corneal epithelial cell cultures," *Clinical Ophthalmology*, vol. 7, pp. 965–971, 2013.

[47] G. Ghoreishi, H. Attarzadeh, M. Tavakoli et al., "Alcohol-assisted versus mechanical epithelium removal in photorefractive keratectomy," *Journal of. Ophthalmic& Vision Research.*, vol. 5, no. 4, pp. 223–227, 2010.

[48] J. C. Abad, B. An, W. J. Power, C. S. Foster, D. T. Azar, and J. H. Talamo, "A prospective evaluation of alcohol-assisted versus mechanical epithelial removal before photorefractive keratectomy," *Ophthalmology*, vol. 104, no. 10, pp. 1566–1575, 1997.

Hindawi
Oxidative Medicine and Cellular Longevity
Volume 2018, Article ID 2487473, 11 pages
https://doi.org/10.1155/2018/2487473

Research Article

FluoroGold-Labeled Organotypic Retinal Explant Culture for Neurotoxicity Screening Studies

Adrian Smedowski,[1,2] **Marita Pietrucha-Dutczak**,[1] **Ruchi Maniar**,[1] **Michael Ajeleti**,[1] **Iwona Matuszek**,[1] **and Joanna Lewin-Kowalik**[1]

[1]*Chair and Department of Physiology, School of Medicine in Katowice, Medical University of Silesia, Medykow 18, 40-752 Katowice, Poland*
[2]*Department of Ophthalmology, School of Medicine in Katowice, Medical University of Silesia, Ceglana 35, 40-514 Katowice, Poland*

Correspondence should be addressed to Adrian Smedowski; asmedowski@sum.edu.pl

Received 26 July 2017; Revised 24 November 2017; Accepted 5 December 2017; Published 13 February 2018

Academic Editor: Morishita Ryuichi

Preclinical toxicity screening of the new retinal compounds is an absolute requirement in the pathway of further drug development. Since retinal neuron cultivation and in vivo studies are relatively expensive and time consuming, we aimed to create a fast and reproducible ex vivo system for retinal toxicity screening. For this purpose, we used rat retinal explant culture that was retrogradely labeled with the FluoroGold before the isolation. Explants were exposed to a toxic concentration of gentamicin and ciliary neurotrophic factor (CNTF), a known neuroprotective agent. The measured outcomes showed the cell density in retinal ganglion cell layer (GCL) and the activity of lactate dehydrogenase (LDH) in the culture medium. Gentamicin-induced oxidative stress resulted in retinal cell damage and rapid LDH release to the culture medium ($p < 0.05$). Additional CNTF supplementation minimized the cell damage, and the increase of LDH release was insignificant when compared to LDH levels before gentamicin insult ($p > 0.05$). As well as this, the LDH activity was directly correlated with the cell count in GCL ($R = -0.84$, $p < 0.00001$), making a sensitive marker of retinal neuron damage. The FLOREC protocol could be considered as a fast, reproducible, and sensitive method to detect neurotoxicity in the screening studies of the retinal drugs.

1. Introduction

Retina and optic nerve diseases are one of the major causes of irreversible blindness worldwide, with increasing prevalence associated with aging of population [1]. Due to the development of a rapidly growing understanding of the pathomechanism of ocular disorders, novel ideas for their treatment and for drug delivery systems are being established [2]. The major reasonable route of retinal drug delivery is an intravitreal injection [2]. Although it provides the highest bioavailability of active compounds, the direct contact with the vitreoretinal compartment may result in interactions that can be either beneficial or toxic [3–5]. The beneficial success of these novel therapies cannot come at a price of safety or integrity of the tissue it is targeting; therefore, preclinical tolerability studies are performed as the first stage in the process of the evaluation of new drugs [6]. In case of the retina, the safety studies consider mostly *in vivo* intravitreal delivery of the active compound, and the histological evaluation of the retina remains the gold standard in retinal toxicity studies; however, some complementary methods examining the retinal morphology and function are also used [2]. For this purpose, rabbit, guinea pig, or rat models are the most commonly utilized as a basis for preclinical studies. In the case of bigger animals, that is, rabbits, ophthalmic examination, including funduscopy, fluorescein angiography, or optical coherence tomography can be performed [7–9]. However, there are growing evidences of applicability of optical coherence tomography in retina studies involving also small rodents [10–12]. In contrast to these methods, which evaluate only the retinal morphology, electrophysiological examination, that is, electroretinography, can provide information

about the retinal function and integrity [2, 13–16]. The more advanced methods include tracking of delivered compounds with SPECT/CT cameras (single photon emission computed tomography), MALDI-MS (matrix-assisted laser desorption and ionization-mass spectrometry), or LC-MS/MS (liquid chromatography-tandem mass spectrometry) [17, 18]. Most of these methods require recruitment of highly specialized equipment, and the size of the small animals' eyeball (i.e., rodents) can be the limiting factor. As the demand for new pharmaceutical technologies in ocular therapies is high, there is a real need for creating economical and innovative, reproducible systems for the preclinical retinal drug toxicity screening that are equally efficient and rapid in terms of delivery.

Since there is no fully reliable and successful method of the retinal neuron culture (i.e., RGC), except complicated immunopanning separation method, and the *in vivo* studies are relatively cost and time consuming, the ex vivo organotypic retinal culture could be a competitive and highly efficient method for initial drug toxicity screening [14, 19–22]. The cultivation of ex vivo retinal tissue has major advantage over dissociated primary neuron culture, since in the whole tissue, the mutual multiple neuronal interactions and connections are still preserved, allowing to observe processes more closely mimicking those in living organism [23].

Initially, cultivation of neonatal retinal explants was reserved for studying retinal synaptic organizations, cell-cell interactions, axonal growth, and retinal cell differentiation using various culture settings [24–29]. The recent modification of retinal explant culture has been introduced by Johnson et al. In their model, retinal tissue isolated from adult rats is cultivated in system of culture inserts placed in wells containing culture medium [30, 31]. The semipermeable membrane that is forming the basis of insert isolates the explant from the culture medium and allows for selective passage of supplements added to the culture medium.

In this study, we propose a novel application of insert-cultured organotypic rat retinal explants, additionally prelabeled retrogradely by FluoroGold dye, as a fast and sensitive method, for safety studies of compounds delivered to the back of the eye.

2. Methods

2.1. Animals. The study protocol has been approved by the Local Committee for an Animal Research and follows the ARVO statement for the use of Animals in Ophthalmic and Vision Research. In all experiments, we used approximately eight-week-old male Wistar rats weighing approximately 180 g (Center of Experimental Medicine, Medical University of Silesia, Katowice, Poland). For the retinal explant preparation, we used 20 animals. Twelve of them received a 3 μl injection of 3% hydroxystilbamidine (FluoroGold, FG, Biotium, Fremont, CA, US) in 10% DMSO-saline into both the superior colliculi of the midbrain seven days before animals were sacrificed (FLOREC group). The specific contents of the injection allowed us to retrogradely label the retinal ganglion cells (RGC) [32]. The FG injection was performed under the general anesthesia with an intraperitoneal injection of ketamine (50 mg/kg; VetaKetam, Vetagro, Poland) and xylazine (5 mg/kg; Xylapan, Vetoquinol Biowet, Poland). The sites of injection were localized on the rat skull using stereotactic equipment. To ensure the correct localization of injection, the online atlas of the rat brain was used (Figure 1). Other eight animals were utilized without prior FG injection (OREC group).

2.2. Explant Preparation. After seven days from the day of the initial FG injection, rats belonging to both study groups were sacrificed with an overdose of anesthetics (ketamine and xylazine) and subsequent decapitation. Immediately after euthanasia, the eyeballs were removed and collected in an ice-cold PBS solution containing 1% penicillin (Gibco, Carlsbad, CA, USA). After the anterior segments were removed, the retinas were isolated, cut into two halves through the vertical line, in the way that each explant contained half of superior and half of inferior retina and placed on culture inserts (0.4 μm Millicell tissue culture insert, Millipore, Billerica, MA, USA) with the ganglion cell layer (GCL) upwards. During the isolation procedure, special care was taken to preserve the vitreous attached to the retinal surface. Inserts were placed in a twelve-well plate containing a culture medium consisting of Neurobasal A (NA, Gibco, Carlsbad, CA, USA) supplemented with 2% B-27 supplement (Gibco, Carlsbad, CA, USA), 1% N2 supplement (Invitrogen, Carlsbad, CA, USA), 1% penicillin solution (Gibco, Carlsbad, CA, USA), and 0.4% GlutaMax (Gibco, Carlsbad, CA, USA). Using the above-detailed method, we prepared 80 explants. The experiment was divided into three steps. For the first step ("*system validation group*"), we used 32 explants—16 FLOREC explants (previously labeled with FG) and 16 OREC explants (without FG labeling). These explants were cultured in standard medium (NA with standard supplementation as described above) for seven days at 37°C and 5% CO_2. Every second day, the whole culture medium (500 μl) was exchanged and the waste medium was collected for pH measurement and lactate dehydrogenase (LDH) cytotoxicity assay. After seven days, the explants were fixed in 4% paraformaldehyde (PFA) overnight at +4°C and then processed for immunostaining and GCL cell counting. In the second step of experiment ("*FLOREC/OREC comparative safety study*"), we cultured another 32 explants—16 FLOREC and 16 OREC explants. Eight of the explants from each group were cultured with standard supplemented NA medium with addition of 10 ng/ml of ciliary neurotrophic factor (CNTF, PeproTech, Rocky Hill, NJ, US), a neuroprotective agent. Four explants from each group were additionally exposed to a 1 μg/ml concentration of gentamicin (G, Gibco, Carlsbad, CA, USA) supplemented to the condition medium on the fifth day of culture, a known inducer of oxidative stress, especially in neuron cell-expressing LDLR2 receptor. The selection of gentamicin as a neurotoxic agent is based on our previous observations involving retinal explant culture [33]. The explants were cultured for seven days at 37°C and 5% CO_2. Every second day, the culture medium (500 μl) was exchanged and the waste medium was collected for pH measurement and LDH cytotoxic assay. After seven days, the explants were fixed in 4% PFA overnight at +4°C and

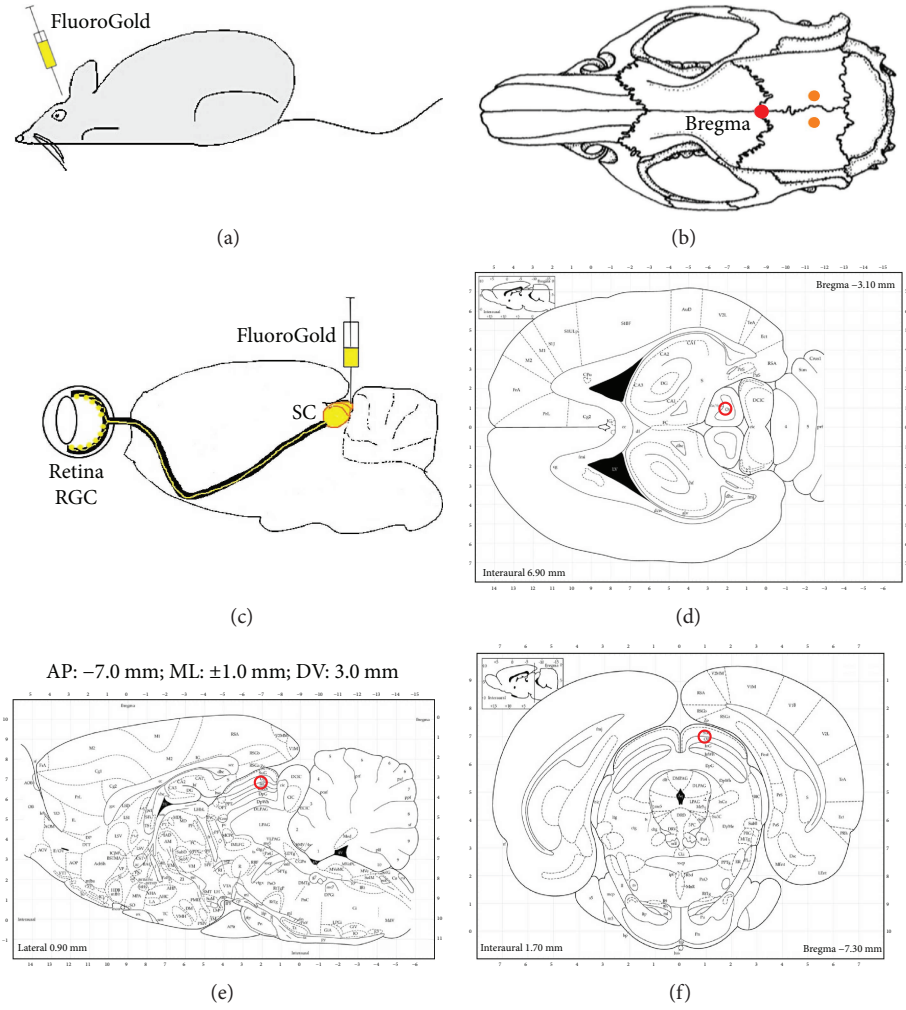

Figure 1: Stereotactic injection of the FluoroGold into optical portion of superior colliculi of the midbrain. (a–c) Principles of FG injection. (d–f) Horizontal, sagittal, and frontal section of rat brain with highlighted target of FG injection.

then processed for immunostaining and cell counting. In the third step of the experiment (*FLOREC safety study*), we used 16 FLOREC explants. Eight explants were cultured with standard supplemented NA medium with addition of 10 ng/ml CNTF. Four explants from each group (with and without CNTF) were exposed to 1 μg/ml of gentamicin added to the condition medium on the third day of culture. The explants were cultured for seven days at 37°C and 5% CO_2. Every second day, the culture medium (500 μl) was exchanged and the waste medium was collected for LDH cytotoxic assay. After seven days, the explants were fixed in 4% PFA overnight at +4°C and then processed for immunostaining and GCL cell counting (Figure 2).

2.3. Immunostaining. After fixation, the floating samples were washed in the 0.05 M TBS overnight at +4°C and incubated in 20% NGS 0.1% Triton X-100 in 0.05 M TBS for 45 min. Primary antibody incubation was performed overnight at +4°C, after which samples were washed in 0.05 M TBS, pH 7.4 and incubated for 3 h at the room temperature (RT) with an appropriate secondary antibody and washed again. To counterstain nuclei, samples were incubated with 1 : 10,000 dilution of 4′,6-diamidino-2-phenylindole (DAPI, Sigma-Aldrich, St. Louis, MO, USA) for 10 min at RT and mounted with Mowiol (Calbiochem, San Diego, CA, USA). As a primary antibody, we used rabbit β3tubulin (dilution 1 : 300, Santa Cruz Biotechnology Inc, Santa Cruz, CA, US). As a secondary antibody, AlexaFluor 488 or 594 was applied (dilution 1 : 500, Thermo Fisher Scientific, Waltham, MA, US). Visualization was performed with a fluorescent microscope Zeiss Axio Scope.A1 (Zeiss, Oberkochen, Germany) and fluorescence microscope (Nikon, Japan). The RGC were counted manually using ImageJ software with Cell Counter plugin (http://imagej.nih.gov/ij/). For cell counting purpose, from each explant, photographs of six areas under 40x magnification for β3tubulin staining and FG labeling were obtained. Cell count is expressed as RGC density per mm^2. Pictures were representing corresponding areas of peripheral (three pictures) and central (three pictures) retina. The cell count was expressed as a mean number of cells per visual field.

2.4. Colorimetric Cytotoxicity Assays. The release of LDH due to the cell membrane damage was detected by a CytoTox 96

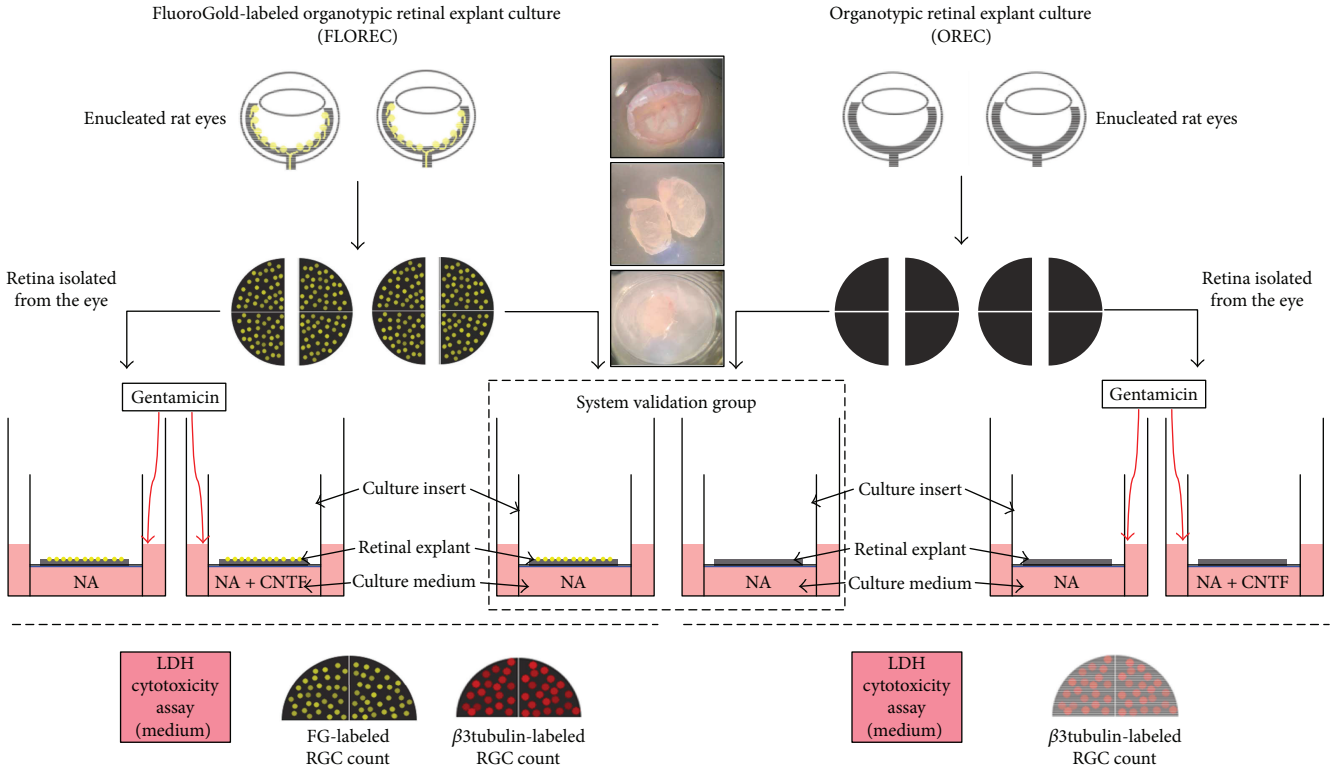

Figure 2: The layout of the experimental settings. The explants separated from 2 groups of Wistar rats—after FG injection (FLOREC) and without FG injection (OREC). System validation was used to determine whether the FG injection itself affects the retinal explant survival. Proper experiment consisted of comparable exposure of FLOREC and OREC explants to gentamicin and CNTF. The outcomes measured were RGC count for FG and β3tubulin and LDH activity in culture medium.

nonradioactive cytotoxicity assay kit (Promega, Madison, WI, USA) according to the manufacturer's instructions. LDH activity in the culture medium was quantified using a plate reader (BIO-RAD Model 550, BIO-RAD, Hercules, CA, USA) with a measurement wavelength of 490 nm and a reference wavelength of 655 nm. Results were presented as optical densities (OD) or the OD ratio.

Since pH of the culture medium indirectly reflects the metabolic activity of retinal explants, we additionally measured the pH of waste medium.

2.5. Statistics. Statistical analysis was performed with the IBM statistical software SPSS 20 (IBM, Armonk, NY, USA). Descriptive statistical results were reported as a mean ± SD (standard deviation). Comparisons between groups were performed using an independent or a paired sample t-test. Multiple comparisons were performed using ANOVA test with post hoc Bonferroni correction. For the predictive relationship analysis, we used the Spearman correlation test. p values lower than 0.05 were considered statistically significant.

3. Results

3.1. Step 1: The System Validation Group. In this part of the experiment, we aimed to evaluate an impact of FG retrograde labeling of RGC on the quality of the retinal explants and to compare FLOREC and OREC explants for pH fluctuations of culture medium, LDH release into medium after seven days of culture, RGC survival for β3tubulin cell count, and correspondence of β3tubulin and FG labeling. The pH of FLOREC culture medium was 7.69 ± 0.08, and in OREC culture medium, it was 7.61 ± 0.02 ($p = 0.2$, $n = 16$/group, independent t-test, Figure 3(a)). The measured LDH release into culture medium of FLOREC explants on day seven was 0.76 ± 0.4 OD and in OREC medium 0.75 ± 0.2 OD ($p = 0.9$, $n = 16$/group, independent t-test, Figure 3(b)) and the LDH activity changes from day 3 to day 7 were also comparable. The mean RGC count in FLOREC explants for β3tubulin was 393 ± 117 cells/mm^2 (469 ± 83 cells/mm^2 in central and 318 ± 68 cells/mm^2 in peripheral region), which was comparable with OREC explants—362 ± 106 cells/mm^2 (437 ± 60 cells/mm^2 in central and 286 ± 42 cells/mm^2 in peripheral region; $p = 0.5$, $n = 16$/group, independent t-test). We did not find a statistical difference between the number of RGC stained with β3tubulin or FG in FLOREC explants (393 ± 117–469 ± 83 cells/mm^2 in central and 318 ± 68 cells/mm^2 in peripheral region and 399 ± 89–494 ± 94 cells/mm^2 in central and 304 ± 81 cells/mm^2 in peripheral region, respectively, $p = 0.9$, $n = 16$, paired t-test; Figures 3(c)–3(i)).

3.2. Step 2: FLOREC/OREC Comparative Safety Study. After confirming that FG retrograde labeling of RGC does not negatively affect the FLOREC explants, we next aimed to compare the response of both types of explants to neuroprotective (i.e., CNTF) and neurotoxic (i.e., gentamicin) agents

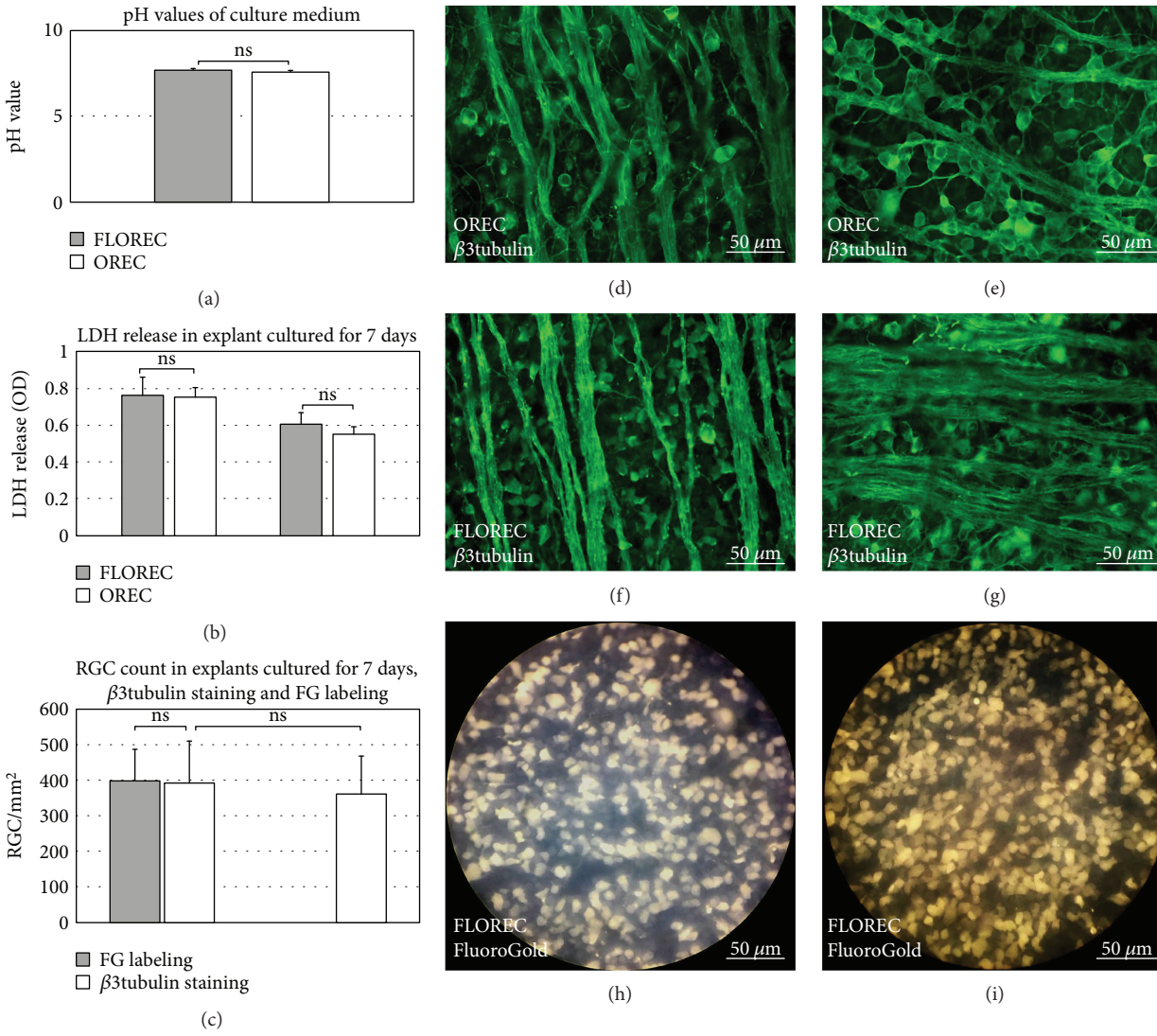

Figure 3: The system validation group. (a–c) Comparison of waste medium pH, medium LDH activity, LDH activity change between day 7 and day 3 (ΔLDH), and RGC count for FG and β3tubulin in OREC and FLOREC explants after 7 days of culture. In FLOREC explants, the difference in number of cells labeled with FG and β3tubulin was not significant, similarly as the difference in number of β3tubulin cells in FLOREC and OREC explants. nFLOREC = 16 explants, nOREC = 16 explants. (d–g) Immunofluorescent staining of whole-mounted explants for β3tubulin after 7 days of culture. (h-i) FG-labeled whole-mounted FLOREC explants after 7 days of culture.

and the possibility of detecting induced fluctuations of LDH in the culture medium. In these settings, the pH of the culture medium ranged from 7.5 to 7.8 and the differences were insignificant ($p > 0.05$, $n = 4$ explants/group, independent t-test, Figure 4(a)). The absolute values of LDH activity in culture medium for FLOREC explants were slightly higher than for explants without FG; however, the difference was not significant ($p > 0.05$, $n = 4$ explants/group, independent t-test, Figure 4(b)). In relative comparison, the exposition of explants to gentamicin on the fifth day resulted in a rapid release of LDH into culture medium starting after this day of culture (Figures 4(c)-4(d)). In multiple comparisons, there was significant difference in LDH release in time ($p = 0.0001$, ANOVA). This calculated increase of LDH activity in culture medium of explants without CNTF treatment was 44% in FLOREC explants ($p = 0.05$, $n = 4$ explants/group, independent t-test) and 57% in OREC explants ($p = 0.04$, $n = 4$ explants/group, independent t-test) at day seven when compared to the fifth day of culture (Figure 4(e)). The CNTF treatment minimized the release of LDH from the retinal cells, reducing the overall increase of LDH release to 4% in FLOREC explants and 6% in OREC explants at day seven when compared to the fifth day of culture ($p > 0.05$, $n = 4$ explants/group, independent t-test, Figure 4(f)). In both types of cultured explants, gentamicin insult was related to significant release of LDH into culture medium when compared to untreated explants at the same time point, that is, day 7 ($p = 0.01$ in OREC and $p = 0.03$ in FLOREC explants, ANOVA with post hoc Bonferroni correction, Figure 4(e)). Additional CNTF treatment prevented gentamicin-induced LDH release when compared to explants that were not treated with

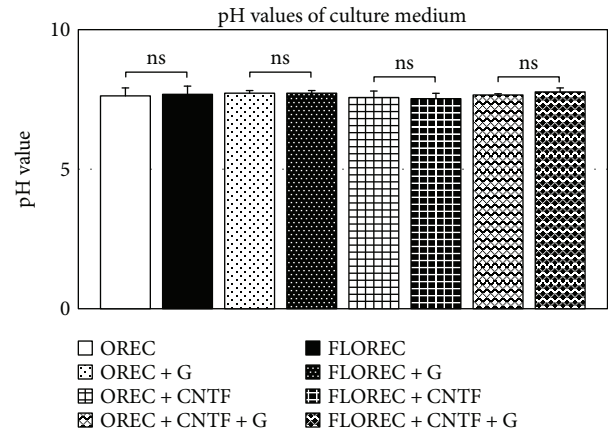

(a)

Explant		LDH in culture medium (OD MEAN ± SD)		
Group	n	Day 3	Day 5	Day 7
OREC	4	2.20 ± 0.13	1.38 ± 0.54	1.31 ± 0.55
FLOREC	4	2.21 ± 0.24	1.96 ± 0.29	1.73 ± 0.24
OREC + CNTF	4	2.07 ± 0.12	1.66 ± 0.60	1.48 ± 0.68
FLOREC + CNTF	4	2.22 ± 0.15	1.96 ± 0.50	1.81 ± 0.32
OREC + G	4	1.88 ± 0.48	1.28 ± 0.62	2.01 ± 0.15
FLOREC + G	4	2.11 ± 0.41	1.62 ± 0.36	2.33 ± 0.23
OREC + CNTF + G	4	1.91 ± 0.44	1.74 ± 0.38	1.84 ± 0.39
FLOREC + CNTF + G	4	2.09 ± 0.35	1.95 ± 0.34	2.02 ± 0.34

(b)

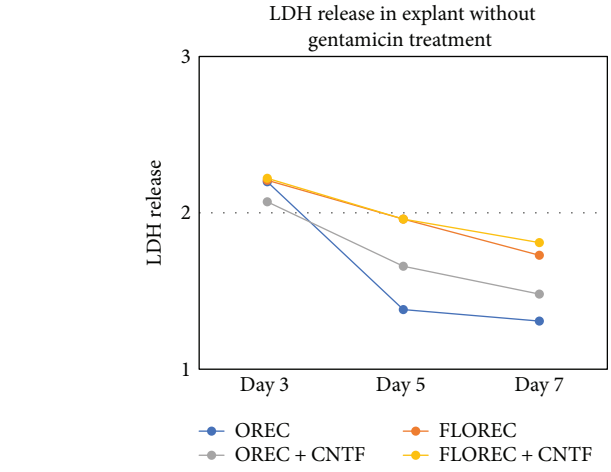

(c)

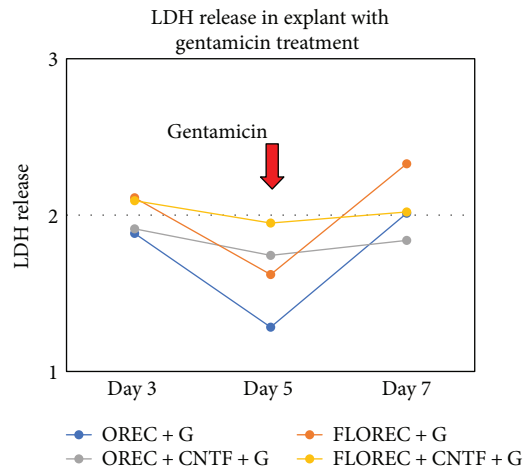

(d)

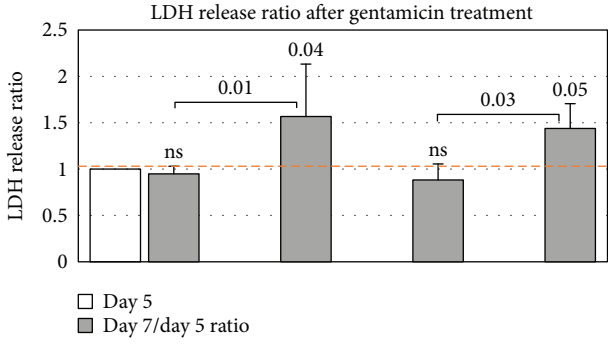

(e)

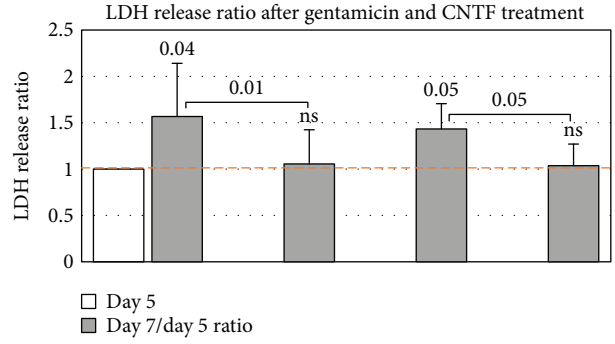

(f)

Figure 4: FLOREC/OREC comparative safety study. (a) The pH values of culture medium in OREC and FLOREC explants. (b) The absolute values of LDH activity in culture medium for FLOREC explants were slightly higher than for OREC explants without FG. (c-d) In explants without gentamicin insult (c), the LDH activity tended to decrease in time, while in case of explants after gentamicin exposure (d), there was rapid LDH outflux detected in culture medium due to cell membrane damage. The gentamicin insult was visibly alleviated by CNTF supplementation and resulted in almost 3-fold lower release of LDH. (e-f) Relative ratio comparisons of LDH activity. ANOVA p value for multiple comparisons = 0.0001. Bolded italic p values represent significance after post hoc Bonferroni correction.

CNTF at the same time point, that is, day 7 ($p = 0.01$ in OREC and $p = 0.05$ in FLOREC explants, ANOVA with post hoc Bonferroni correction, Figure 4(f)).

3.3. Step 3: FLOREC Safety Study. After we demonstrated that both types of explant reactions are similar in either neurotoxic or neuroprotective environment, in the next stage, we performed a full screening study for CNTF and gentamicin using only FLOREC explants. The gentamicin insult introduced on day three resulted in an accelerated release of LDH by 9% in explants with additional CNTF treatment ($p > 0.05$, $n = 4$ explants/group, independent t-test),

and 15% in explants without CNTF treatment ($p > 0.05$, $n = 4$ explants/group, independent t-test) on day five and by 17% ($p > 0.05$, $n = 4$ explants/group, independent t-test) and 57% ($p = 0.01$, $n = 4$ explants/group, independent t-test) on day seven, respectively. Explants cultured without gentamicin showed tendency for time-dependent decrease of LDH activity in the culture medium, as observed in the previous steps of experiment (Figures 5(a)-5(b)). These fluctuations of enzymatic activity in medium were linked with changes in RGC count for FG-labeling in GCL ($p = 0.001$, ANOVA test, Figures 5(c)–5(k)). CNTF treatment of gentamicin-induced explants resulted in higher RGC count when compared with group that was not treated with CNTF (430 ± 109 cells/mm^2 versus 246 ± 96 cells/mm^2, respectively, $p = 0.02$, ANOVA with post hoc Bonferroni correction, Figure 5(g)). In the correlation analysis, there was strong, significant negative relation between RGC count and LDH activity in culture medium ($R = -0.84$; $p = 0.00001$, $n = 4$/group, the Spearman test). The lower count of RGC, the higher activity of LDH in culture medium was observed (Figure 5(l)).

4. Discussion

In our current work, we present a new idea for the retinal drug toxicity screening method, based on organotypic ex vivo retinal explant culture. We have shown here that the retrograde labeling of the RGC with FluoroGold prior to the retinal explant isolation allows to simplify the quantitative evaluation of the retinal explants without affecting their survival. The new method we introduced includes analysis of the retinal cell membrane permeability for LDH as well as RGC quantification after the exposure to tested agents.

Attempts to create the protocol for the ex vivo retinal explant culture have been made since late 70s of the last century using goldfish models [34]. In 1981, Smalheiser et al. reported the first protocol for the fetal rodent (mouse) retinal organotypic culture [25]. Since then, the organotypic retinal cultures have become the method of growing interest as an independent setting for ocular research. Regardless of the utilized species—fish, mice, rats, rabbits, chickens, monkeys, pigs, bovines, or human, the ex vivo cultures were mostly used to observe processes associated with the degeneration of retinal neurons induced by denervation [24]. The 21st century brought significant development in retinal organotypic cultures and they started to be used as models, applied in neurodevelopmental studies as well as to seek opportunities to delay the neurodegenerative process or to replace the nonfunctional neurons [30, 31, 35–39]. Ex vivo retinal cultures have also become a substitute for disease models, that is, diabetic retinopathy or glaucoma [40, 41].

There are different approaches to prepare and maintain the retinal cultures, differing from the point of view of tissue separation, size of retinal pieces, and preferable culture medium [21, 23, 30, 38, 40–44]. In our study, we used a model based on rat retinal explants cultured in Neurobasal A medium described previously by Johnson et al., since it provides a good survival of retinal neurons after seven days [30, 45]. From our culture protocol, we excluded supplementation with streptomycin, because another aminoglycoside antibiotic (gentamicin) was applied as our tested agent. We also decided to divide retinas into 2 instead of 4 explants, to ensure more reliable representation of RGC, taking into account their asymmetric distribution in the retina. The retrograde labeling of RGC with fluorescent tracer FluoroGold is a widely used approach in eye research. Similarly, as it is shown in available *in vivo* data, and also in our ex vivo settings, the FG retrograde labeling does not seem to affect the RGC survival; however, FLOREC explants presented slightly higher initial LDH activity in culture medium which could be caused by DMSO used as a solvent for FG injection [32, 46–51]. Moreover, in our study, FG labeling did not impair the reactions of retinal explants to exposed treatment, which were comparable with those observed in unlabeled explants. Since the FG is a fluorescent dye, the only inconvenience that must be considered, special care during explant culture should be taken to avoid excess exposure of the explants to the light and to prevent fluorescence diminishing.

The cell membrane's permeability for LDH has been used widely as a method for cytotoxicity assays in different settings [52, 53]. In our study, the LDH membrane's permeability was affected by the toxic concentration of gentamicin and the protective mechanisms were activated using CNTF. Since LDH is released from the cells due to membrane damage, the initial absolute activity of this enzyme in culture medium varied due to explant preparation technique itself (the exact size of explants, time of isolation). In our reasoning, we made conclusions based on LDH activity changes after exposition to tested agents rather than on absolute values of LDH activity which could be affected by other external factors. It is known from neuro- and ototoxicity studies that aminoglycoside antibiotics can affect mitochondrial bioenergetics and induce reactive oxygen species (ROS) production in cells, which express the megalin receptor (LDLR2), like retinal neurons [33, 54, 55]. The energy failure related to aberrant mitochondrial metabolism and the ROS are affecting Bcl-2 gene, CNTF expression, activate stress kinase and the caspase family of proteases leading to subsequent neurodegeneration [56, 57]. The CNTF supplementation can alleviate the aminoglycoside-related insults, results in the overexpression of antiapoptotic Bcl-2 gene, reverses the aberrant mitochondrial bioenergetics, and reduces the ROS production [58]. Similarly, as in ototoxicity studies, in our experiment, we observed that CNTF treatment alleviated the toxicity of gentamicin in retinal explant culture. The LDH activity in culture medium appeared to be a sensitive marker of retinal cell damage (here correlated with the RGC count), which reflected the cytotoxic status of the whole retina, since gentamicin can damage also other than RGC populations of neurons [55]. In our study, the RGC cell damage (expressed in decreased cell count) was associated with an increased permeability of retinal cell membranes, leading to subsequent leakage of LDH that was then detected in the culture medium.

The screening method in its nature should be highly efficient, fast, repeatable, and low cost. The organotypic retinal explant culture as a model of neurodegeneration has been

Explant		LDH in culture medium (OD MEAN ± SD)		
Group	n	Day 3	Day 5	Day 7
NA	4	1.31 ± 0.36	1.28 ± 0.45	0.95 ± 0.49
NA + G	4	1.13 ± 0.11	1.30 ± 0.40	1.78 ± 0.34
NA + CNTF	4	1.10 ± 0.18	1.14 ± 0.11	0.99 ± 0.39
NA + CNTF + G	4	0.99 ± 0.14	1.09 ± 0.20	1.17 ± 0.29

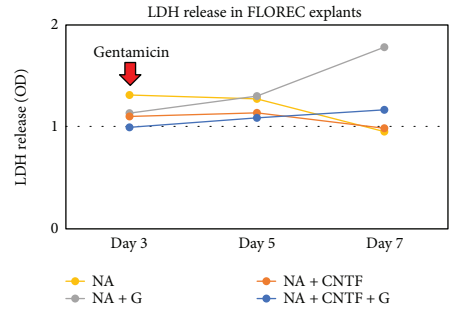

(a) (b)

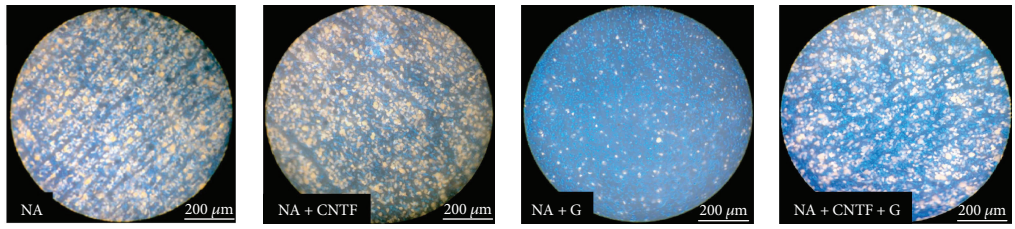

(c) (d) (e) (f)

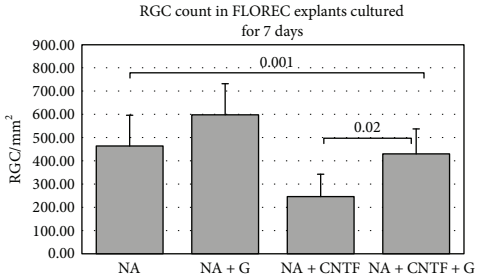

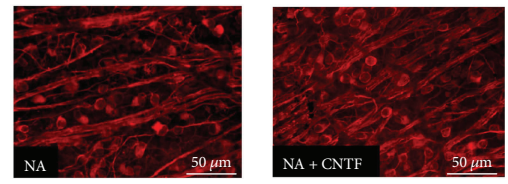

(g) (h) (i)

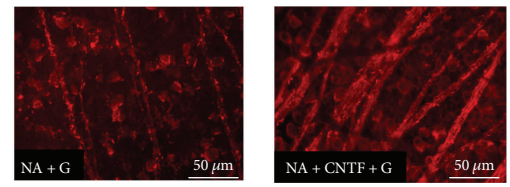

(j) (k)

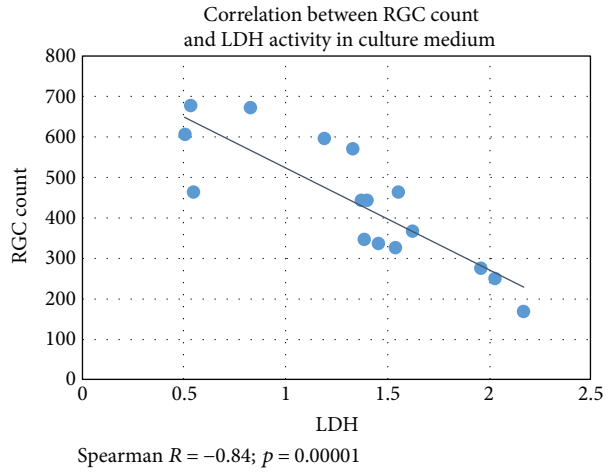

(l)

Figure 5: FLOREC safety study. (a-b) The absolute LDH activity in culture medium of FLOREC explants. The gentamicin insult introduced on the third day of culture resulted in accelerated release of LDH which was higher in explants without CNTF treatment. (c–f) FG-labeled whole-mounted explants representing study groups (after 7 days of culture). (g) RGC count in FLOREC explants after 7 days of culture. ANOVA p value for multiple comparisons = 0.001. Bolded italic p values represent significance after post hoc Bonferroni correction. (h–k) Immunofluorescent staining of whole-mounted explants for β3tubulin (after 7 days of culture). (l) The correlation between LDH activity in culture medium and RGC count after 7 days of explant culture.

applied as a supplementary method for various studies in the area of the experimental retinal neuroprotection therapies. Undoubtedly, the basic advantage of this method is a short experiment duration—only seven days (twelve days, when considering the timing of the *in vivo* FG labeling), which can lower the costs of the experiment. Moreover, we should also pay attention to the ethical aspect: the retinal explant culture does not require utilization a large number of animals, as one retina can be divided into two explants. This fact also proves to be economical, but what is very important is that it allows us to study the effects of the selected agents at different concentrations on the retinal parts from the same animal in the same culture environment, excluding intraindividual variabilities. Although there are various protocols for retinal isolation and culture, their application (except the basic science studies), is limited. Here, we propose to consider the retinal explant culture assay as an applicable method in the testing of new ocular therapeutic agents. Perhaps, the application of these methods would allow the faster selection of effective drugs and reduce the time needed to test the drug in preclinical settings.

5. Conclusions

The FluoroGold-labeled organotypic rat retinal explant culture can be considered as a fast, reproducible, and sensitive method for safety studies of compounds delivered to the back of the eye.

Disclosure

The study was partially presented during XX European Association for Vision and Eye Research Conference in Nice, 2017.

Conflicts of Interest

The authors declare that they have no conflicts of interest.

Authors' Contributions

Smedowski Adrian and Pietrucha-Dutczak Marita contributed equally to the study.

Acknowledgments

The authors thank to Mrs. Joanna Mazela for the technical help to the study. The project was supported by the research funds of Department of Physiology, Medical University of Silesia, Katowice, Poland (Grant no. KNW-1-057/K/7/0).

References

[1] W. L. Wong, X. Su, X. Li et al., "Global prevalence of age-related macular degeneration and disease burden projection for 2020 and 2040: a systematic review and meta-analysis," *The Lancet Global Health*, vol. 2, no. 2, pp. e106–e116, 2014.

[2] E. M. Del Amo, A. K. Rimpelä, E. Heikkinen et al., "Pharmacokinetic aspects of retinal drug delivery," *Progress in Retinal and Eye Research*, vol. 57, pp. 134–185, 2017.

[3] B. G. Short, "Safety evaluation of ocular drug delivery formulations: techniques and practical considerations," *Toxicologic Pathology*, vol. 36, no. 1, pp. 49–62, 2008.

[4] J. Kohn, S. Abramson, and R. Langer, "Bioresorbable and bioerodible materials," in *Biomaterials Science: An Introduction to Materials in Medicine*, B. Ratner, A. Hoffman, F. Schoen and J. Lemons, Eds., Academic Press, Cambridge, 2004.

[5] F. M. Penha, E. B. Rodrigues, M. Maia et al., "Retinal and ocular toxicity in ocular application of drugs and chemicals-part II: retinal toxicity of current and new drugs," *Ophthalmic Research*, vol. 44, no. 4, pp. 205–224, 2010.

[6] S. L. Wilson, M. Ahearne, and A. Hopkinson, "An overview of current techniques for ocular toxicity testing," *Toxicology*, vol. 327, pp. 32–46, 2015.

[7] S. Schnichels, T. Dorfi, M. Schultheiss et al., "*Ex-vivo*-examination of ultrastructural changes in organotypic retina culture using near-infrared imaging and optical coherence tomography," *Experimental Eye Research*, vol. 147, pp. 31–36, 2016.

[8] M. I. Uddin, S. M. Evans, J. R. Craft et al., "*In vivo* imaging of retinal hypoxia in a model of oxygen-induced retinopathy," *Scientific Reports*, vol. 6, no. 1, article 31011, 2016.

[9] E. A. Atzpodien, B. Jacobsen, J. Funk et al., "Advanced clinical imaging and tissue-based biomarkers of the eye for toxicology studies in minipigs," *Toxicologic Pathology*, vol. 44, no. 3, pp. 398–413, 2016.

[10] C. A. Smith and B. C. Chauhan, "Imaging retinal ganglion cells: enabling experimental technology for clinical application," *Progress in Retinal and Eye Research*, vol. 44, pp. 1–14, 2015.

[11] G. Rovere, F. M. Nadal-Nicolás, M. Agudo-Barriuso et al., "Comparison of retinal nerve fiber layer thinning and retinal ganglion cell loss after optic nerve transection in adult albino rats," *Investigative Ophthalmology & Visual Science*, vol. 56, no. 8, pp. 4487–4498, 2015.

[12] A. Ortín-Martínez, F. J. Valiente-Soriano, D. García-Ayuso et al., "A novel *in vivo* model of focal light emitting diode-induced cone-photoreceptor phototoxicity: neuroprotection afforded by brimonidine, BDNF, PEDF or bFGF," *PLoS One*, vol. 9, no. 12, article e113798, 2014.

[13] A. Koizumi, G. Zeck, Y. Ben, R. H. Masland, and T. C. Jakobs, "Organotypic culture of physiologically functional adult mammalian retinas," *PLoS One*, vol. 2, no. 2, article e221, 2007.

[14] F. M. Penha, E. B. Rodrigues, M. Maia et al., "Retinal and ocular toxicity in ocular application of drugs and chemicals-part I: animal models and toxicity assays," *Ophthalmic Research*, vol. 44, no. 2, pp. 82–104, 2010.

[15] L. Alarcón-Martínez, P. de la Villa, M. Avilés-Trigueros, R. Blanco, M. P. Villegas-Pérez, and M. Vidal-Sanz, "Short and long term axotomy-induced ERG changes in albino and pigmented rats," *Molecular Vision*, vol. 15, pp. 2373–2383, 2009.

[16] L. Alarcón-Martínez, M. Avilés-Trigueros, C. Galindo-Romero et al., "ERG changes in albino and pigmented mice after optic nerve transection," *Vision Research*, vol. 50, no. 21, pp. 2176–2187, 2010.

[17] S. Liu, "Bifunctional coupling agents for radiolabeling of biomolecules and target-specific delivery of metallic radionuclides," *Advanced Drug Delivery Reviews*, vol. 60, no. 12, pp. 1347–1370, 2008.

[18] S. Aretz, T. U. Krohne, K. Kammerer et al., "In-depth mass spectrometric mapping of the human vitreous proteome," *Proteome Science*, vol. 11, no. 1, p. 22, 2013.

[19] F. Gao, T. Li, J. Hu, X. Zhou, J. Wu, and Q. Wu, "Comparative analysis of three purification protocols for retinal ganglion cells from rat," *Molecular Vision*, vol. 22, pp. 387–400, 2016.

[20] D. Gaublomme, T. Buyens, and L. Moons, "Automated analysis of neurite outgrowth in mouse retinal explants," *Journal of Biomolecular Screening*, vol. 18, no. 5, pp. 534–543, 2013.

[21] H. Xin, J. A. Yannazzo, R. S. Duncan, E. V. Gregg, M. Singh, and P. Koulen, "A novel organotypic culture model of the postnatal mouse retina allows the study of glutamate-mediated excitotoxicity," *Journal of Neuroscience Methods*, vol. 159, no. 1, pp. 35–42, 2007.

[22] A. Feigenspan, J. Bormann, and H. Wässle, "Organotypic slice culture of the mammalian retina," *Visual Neuroscience*, vol. 10, no. 02, pp. 203–217, 1993.

[23] S. Gustmann and N. Dünker, "*In vivo*-like organotypic murine retinal wholemount culture," *Journal of Visualized Experiments*, vol. 35, p. 1634, 2010.

[24] G. M. Seigel, "The golden age of retinal cell culture," *Molecular Vision*, vol. 5, p. 4, 1999.

[25] N. R. Smalheiser, S. M. Crain, and M. B. Bornstein, "Development of ganglion cells and their axons in organized cultures of fetal mouse retinal explants," *Brain Research*, vol. 204, no. 1, pp. 159–178, 1981.

[26] J. Pérez-León, M. J. Frech, J. E. Schröder et al., "Spontaneous synaptic activity in an organotypic culture of the mouse retina," *Investigative Ophthalmology & Visual Science*, vol. 44, no. 3, pp. 1376–1387, 2003.

[27] S. Schulz-Key, H. D. Hofmann, C. Beisenherz-Huss, C. Barbisch, and M. Kirsch, "Ciliary neurotrophic factor as a transient negative regulator of rod development in rat retina," *Investigative Ophthalmology & Visual Science*, vol. 43, no. 9, pp. 3099–3108, 2002.

[28] J. M. Ogilvie, J. D. Speck, J. M. Lett, and T. T. Fleming, "A reliable method for organ culture of neonatal mouse retina with long-term survival," *Journal of Neuroscience Methods*, vol. 87, no. 1, pp. 57–65, 1999.

[29] N. Duenker, A. I. Valenciano, A. Franke et al., "Balance of pro-apoptotic transforming growth factor-beta and anti-apoptotic insulin effects in the control of cell death in the postnatal mouse retina," *The European Journal of Neuroscience*, vol. 22, no. 1, pp. 28–38, 2005.

[30] T. V. Johnson and K. R. Martin, "Development and characterization of an adult retinal explant organotypic tissue culture system as an in vitro intraocular stem cell transplantation model," *Investigative Ophthalmology & Visual Science*, vol. 49, no. 8, pp. 3503–3512, 2008.

[31] N. D. Bull, T. V. Johnson, G. Welsapar, N. W. DeKorver, S. I. Tomarev, and K. R. Martin, "Use of an adult rat retinal explant model for screening of potential retinal ganglion cell neuroprotective therapies," *Investigative Ophthalmology & Visual Science*, vol. 52, no. 6, pp. 3309–3320, 2011.

[32] F. M. Nadal-Nicolás, M. Salinas-Navarro, M. Vidal-Sanz, and M. Agudo-Barriuso, "Two methods to trace retinal ganglion cells with fluorogold: from the intact optic nerve or by stereotactic injection into the optic tract," *Experimental Eye Research*, vol. 131, pp. 12–19, 2015.

[33] M. Pietrucha-Dutczak, A. Smedowski, X. Liu, I. Matuszek, M. Varjosalo, and J. Lewin-Kowalik, "Candidate proteins from predegenerated nerve exert time-specific protection of retinal ganglion cells in glaucoma," *Scientific Reports*, vol. 7, no. 1, article 14540, 2017.

[34] G. E. Landreth and B. W. Agranoff, "Explant culture of adult goldfish retina: effect of prior optic nerve crush," *Brain Research*, vol. 118, no. 2, pp. 299–303, 1976.

[35] R. M. Ferrer-Martín, D. Martín-Oliva, A. Sierra-Martín et al., "Microglial activation promotes cell survival in organotypic cultures of postnatal mouse retinal explants," *PLoS One*, vol. 10, no. 8, article e0135238, 2015.

[36] A. J. White, J. P. Heller, J. Leung, A. Tassoni, and K. R. Martin, "Retinal ganglion cell neuroprotection by an angiotensin II blocker in an ex vivo retinal explant model," *Journal of the Renin Angiotensin Aldosterone System*, vol. 16, no. 4, pp. 1193–1201, 2015.

[37] M. Hirata, T. R. Shearer, and M. Azuma, "Hypoxia activates calpains in the nerve fiber layer of monkey retinal explants," *Investigative Ophthalmology & Visual Science*, vol. 56, no. 10, pp. 6049–6057, 2015.

[38] A. Osborne, M. Hopes, P. Wright, D. C. Broadway, and J. Sanderson, "Human organotypic retinal cultures (HORCs) as a chronic experimental model for investigation of retinal ganglion cell degeneration," *Experimental Eye Research*, vol. 143, pp. 28–38, 2016.

[39] T. V. Johnson, N. D. Bull, and K. R. Martin, "Transplantation prospects for the inner retina," *Eye*, vol. 23, no. 10, pp. 1980–1984, 2009.

[40] U. Pattamatta, Z. McPherson, and A. White, "A mouse retinal explant model for use in studying neuroprotection in glaucoma," *Experimental Eye Research*, vol. 151, pp. 38–44, 2016.

[41] J. Valdés, L. Trachsel-Moncho, A. Sahaboglu et al., "Organotypic retinal explant cultures as in vitro alternative for diabetic retinopathy studies," *ALTEX*, vol. 33, pp. 459–464, 2016.

[42] L. Taylor, D. Moran, K. Arnér, E. Warrant, and F. Ghosh, "Stretch to see: lateral tension strongly determines cell survival in long-term cultures of adult porcine retina," *Investigative Ophthalmology & Visual Science*, vol. 54, no. 3, pp. 1845–1856, 2013.

[43] M. H. Lye, T. C. Jakobs, R. H. Masland, and A. Koizumi, "Organotypic culture of adult rabbit retina," *Journal of Visualized Experiments*, vol. 190, no. 3, 2007.

[44] J. Wang, A. M. Kolomeyer, M. A. Zarbin, and E. Townes-Anderson, "Organotypic culture of full-thickness adult porcine retina," *Journal of Visualized Experiments*, vol. 49, p. 2655, 2011.

[45] A. Smedowski, X. Liu, M. Pietrucha-Dutczak, I. Matuszek, M. Varjosalo, and J. Lewin-Kowalik, "Predegenerated Schwann cells-a novel prospect for cell therapy for glaucoma: neuroprotection, neuroregeneration and neuroplasticity," *Scientific Reports*, vol. 6, no. 1, article 23187, 2016.

[46] S. I. Balendra, E. M. Normando, P. A. Bloom, and M. F. Cordeiro, "Advances in retinal ganglion cell imaging," *Eye*, vol. 29, no. 10, pp. 1260–1269, 2015.

[47] M. Vidal-Sanz, M. Salinas-Navarro, F. M. Nadal-Nicolás et al., "Understanding glaucomatous damage: anatomical and functional data from ocular hypertensive rodent retinas," *Progress in Retinal and Eye Research*, vol. 31, no. 1, pp. 1–27, 2012.

[48] M. Salinas-Navarro, S. Mayor-Torroglosa, M. Jiménez-López et al., "A computerized analysis of the entire retinal ganglion cell population and its spatial distribution in adult rats," *Vision Research*, vol. 49, no. 1, pp. 115–126, 2009.

[49] A. M. Gómez-Ramírez, M. P. Villegas-Pérez, J. Miralles de Imperial, M. Salvador-Silva, and M. Vidal-Sanz, "Effects of intramuscular injection of botulinum toxin and doxorubicin

on the survival of abducens motoneurons," *Investigative Ophthalmology & Visual Science*, vol. 40, no. 2, pp. 414–424, 1999.

[50] I. Sellés-Navarro, M. P. Villegas-Pérez, M. Salvador-Silva, J. M. Ruiz-Gómez, and M. Vidal-Sanz, "Retinal ganglion cell death after different transient periods of pressure-induced ischemia and survival intervals. A quantitative in vivo study," *Investigative Ophthalmology & Visual Science*, vol. 37, no. 10, pp. 2002–2014, 1996.

[51] J. Galvao, B. Davis, M. Tilley, E. Normando, M. R. Duchen, and M. F. Cordeiro, "Unexpected low-dose toxicity of the universal solvent DMSO," *The FASEB Journal*, vol. 28, no. 3, pp. 1317–1330, 2014.

[52] A. Smedowski, J. J. Paterno, E. Toropainen, D. Sinha, E. Wylegala, and K. Kaarniranta, "Excipients of preservative-free latanoprost induced inflammatory response and cytotoxicity in immortalized human HCE-2 corneal epithelial cells," *Journal of Biochemical and Pharmacological Research*, vol. 2, no. 4, pp. 175–184, 2014.

[53] A. Trzeciecka, J. J. Paterno, E. Toropainen et al., "Long-term topical application of preservative-free prostaglandin analogues evokes macrophage infiltration in the ocular adnexa," *European Journal of Pharmacology*, vol. 788, pp. 12–20, 2016.

[54] R. Dagil, C. O'Shea, A. Nykjær, A. M. Bonvin, and B. B. Kragelund, "Gentamicin binds to the megalin receptor as a competitive inhibitor using the common ligand binding motif of complement type repeats: insight from the nmr structure of the 10th complement type repeat domain alone and in complex with gentamicin," *Journal of Biological Chemistry*, vol. 288, no. 6, pp. 4424–4435, 2013.

[55] G. Zheng, D. R. Bachinsky, I. Stamenkovic et al., "Organ distribution in rats of two members of the low-density lipoprotein receptor gene family, gp330 and LRP/alpha 2MR, and the receptor-associated protein (RAP)," *Journal of Histochemistry and Cytochemistry*, vol. 42, no. 4, pp. 531–542, 1994.

[56] L. P. Rybak and V. Ramkumar, "Ototoxicity," *Kidney International*, vol. 72, no. 8, pp. 931–935, 2007.

[57] M. E. Huth, A. J. Ricci, and A. G. Cheng, "Mechanisms of aminoglycoside ototoxicity and targets of hair cell protection," *International Journal of Otolaryngology*, vol. 2011, Article ID 937861, 19 pages, 2011.

[58] T. Nakaizumi, K. Kawamoto, R. Minoda, and Y. Raphael, "Adenovirus-mediated expression of brain-derived neurotrophic factor protects spiral ganglion neurons from ototoxic damage," *Audiology and Neurootology*, vol. 9, no. 3, pp. 135–143, 2004.

Hindawi
Oxidative Medicine and Cellular Longevity
Volume 2018, Article ID 4956080, 15 pages
https://doi.org/10.1155/2018/4956080

Research Article

Autophagy Stimulus Promotes Early HuR Protein Activation and p62/SQSTM1 Protein Synthesis in ARPE-19 Cells by Triggering Erk1/2, p38^{MAPK}, and JNK Kinase Pathways

Nicoletta Marchesi,[1] Natthakan Thongon,[2] Alessia Pascale,[1] Alessandro Provenzani,[2] Ali Koskela,[3] Eveliina Korhonen,[4] Adrian Smedowski,[5] Stefano Govoni,[1] Anu Kauppinen,[4] Kai Kaarniranta,[3,6] and Marialaura Amadio[1]

[1]*Department of Drug Sciences, Pharmacology Section, University of Pavia, 27100 Pavia, Italy*
[2]*Laboratory of Genomic Screening, Center for Integrative Biology, University of Trento, 38123 Trento, Italy*
[3]*Department of Ophthalmology, University of Eastern Finland, 70211 Kuopio, Finland*
[4]*School of Pharmacy, Faculty of Health Sciences, University of Eastern Finland, 70211 Kuopio, Finland*
[5]*Chair and Department of Physiology, School of Medicine in Katowice, Medical University of Silesia, Katowice, Poland*
[6]*Department of Ophthalmology, Kuopio University Hospital, 70029 Kuopio, Finland*

Correspondence should be addressed to Marialaura Amadio; marialaura.amadio@unipv.it

Received 25 May 2017; Revised 3 November 2017; Accepted 5 December 2017; Published 8 February 2018

Academic Editor: Shane Thomas

RNA-binding protein dysregulation and altered expression of proteins involved in the autophagy/proteasome pathway play a role in many neurodegenerative disease onset/progression, including age-related macular degeneration (AMD). HuR/ELAVL1 is a master regulator of gene expression in human physiopathology. In ARPE-19 cells exposed to the proteasomal inhibitor MG132, HuR positively affects at posttranscriptional level p62 expression, a stress response gene involved in protein aggregate clearance with a role in AMD. Here, we studied the early effects of the proautophagy AICAR + MG132 cotreatment on the HuR-p62 pathway. We treated ARPE-19 cells with Erk1/2, AMPK, p38^{MAPK}, PKC, and JNK kinase inhibitors in the presence of AICAR + MG132 and evaluated HuR localization/phosphorylation and p62 expression. Two-hour AICAR + MG132 induces both HuR cytoplasmic translocation and threonine phosphorylation via the Erk1/2 pathway. In these conditions, p62 mRNA is loaded on polysomes and its translation in de novo protein is favored. Additionally, for the first time, we report that JNK can phosphorylate HuR, however, without modulating its localization. Our study supports HuR's role as an upstream regulator of p62 expression in ARPE-19 cells, helps to understand better the early events in response to a proautophagy stimulus, and suggests that modulation of the autophagy-regulating kinases as potential therapeutic targets for AMD may be relevant.

1. Introduction

Posttranscriptional mechanisms are key determinants in the modulation of gene expression by allowing a punctual, localized adaptation of protein levels to changing environmental conditions. In particular, RNA-binding proteins (RBPs) are predicted to regulate up to 90% of human genes, and their physiological role is critical for the maintenance of health conditions in all tissues, including the eye [1–3]. Recent evidence has shown that the dysregulation of RBPs controlling the expression of proteins involved in the autophagy/proteasome pathway has a role in the onset and the progression of many neurodegenerative diseases [4].

The RBP HuR (human antigen R or HuA) is a master regulator of gene expression in several physiological and pathological conditions. HuR (also named ELAVL1 (embryonic lethal abnormal vision-like 1)) belongs to the mammalian ELAV family, one of the most abundant and the best-known RBPs affecting the RNA fate at various levels. ELAV (or Hu) proteins interact preferentially with adenine-uracil-rich elements (ARE) mainly, but not exclusively, present in the 3′-untranslated region of a high number of mRNAs [5]. Despite the high homology in the primary sequences among the four ELAV members, certain specificity for their localization, behavior, function, and target mRNAs has been evidenced [6, 7]. The so-called neuronal ELAV proteins, namely, HuB, HuC, and HuD, are almost exclusively present in neurons and mostly localized in the cytoplasm [8]. HuR is expressed in all tissues and in basal conditions remains mainly within the nucleus [9]. Following an extracellular stimulus (such as stress), HuR protein shuttles from the nucleus to the cytoplasm, where it can increase the stability and/or the rate of translation of the bound transcripts [10, 11]. HuR's targets include mRNAs coding proteins involved in the cellular stress response and survival, inflammation, and cell cycle progression [12–17]. We previously showed that under proteasome inhibition, HuR posttranscriptionally affects the expression of p62/sequestosome 1 (SQSTM1) in a retinal pigment epithelial (RPE) cell line. p62 is a key factor to regulate protein aggregate clearance via autophagy and proteasome pathways that are involved in the pathology of age-related macular degeneration (AMD) [18].

Autophagy is a stress-responsive process playing a crucial role in the homeostasis of cells and tissues, especially in the retina, where the postmitotic RPE cells are primarily responsible for the phagocytosis of photoreceptor outer segments, thereby promoting the retina's health [19, 20]. One of the early triggering factors in the pathogenesis of AMD is the degeneration of RPE. During aging, RPE cells show increased susceptibility to oxidative stress and increased protein aggregation due to impaired autophagy and proteasome-mediated proteolysis [21, 22], which finally contributes to the RPE cell death [23].

Accumulating evidence suggests that autophagy proceeds in two phases: first, within minutes or hours of exposure to a stressful condition, a rapid activation of stress proteins and protective mechanisms takes place, and it is mainly mediated by posttranslational protein modifications. After that, a delayed and sustained stress response, relying on the activation of programs modifying gene expression at the transcriptional level, occurs [24].

With the aim to dissect the early phase of autophagy induction on the HuR-p62 pathway, we exposed ARPE-19 cells to the proautophagy AICAR and MG132 cotreatment and evaluated the p62 expression and HuR activation. The list of signaling pathways directly or indirectly involved in the nucleocytoplasmic HuR shuttling and/or HuR phosphorylation (both of the indexes of HuR activation) is long [25, 26]. Therefore, we focused on those kinases affecting the cellular localization of HuR and/or its binding to target RNAs and whose relevance in the cellular stress response and/or autophagy has been acknowledged. In particular, the involvement of extracellular signal-regulated kinase [Erk1/2, also known as p-44/42 mitogen-activated protein kinase (MAPK)], AMP-activated protein kinase (AMPK), $p38^{MAPK}$, c-Jun N-terminal kinase (JNK), and protein kinase C (PKC) was studied in ARPE-19 cells.

2. Materials and Methods

2.1. Cell Culture and Treatments. The human RPE cell line ARPE-19 was obtained from American Type Culture Collection. Cells were grown in a humidified 5% CO_2 atmosphere at 37°C in Dulbecco's Modified Eagle Medium: F12 (1 : 1; Gibco, Invitrogen, Carlsbad, CA), including 10% inactivated fetal bovine serum, 100 units/ml penicillin, 100 μg/ml streptomycin, and 2 mM L-glutamine (Sigma-Aldrich, Milan, Italy). To find out the best conditions for studying both HuR protein translocation and p62 protein expression, cells were exposed to either the solvent (DMSO, 0.1%), the proteasome inhibitor MG132 (1 μM, Calbiochem, San Diego, CA), or AICAR (2 mM 5-aminoimidazole-4-carboxy amide ribonucleoside, Toronto Research Chemical, Canada), alone or together, for 15 min, 30 min, or 2 hrs. AICAR and MG132 (A + M) cotreatment for 2 hrs was selected for all the following experiments. Protein synthesis was inhibited by 1 μM puromycin (Sigma-Aldrich). Kinase inhibitors were used at the concentrations suggested by the manufacturers or optimized in previous studies [27, 28]—PD98059 (MEK1/2 inhibitor; Cell Signaling, Danvers, MA): 50 μM; compound C (CC, AMPK inhibitor; Sigma-Aldrich): 5 μM; SB203580 ($p38^{MAPK}$ inhibitor; Cell Signaling): 50 μM; SP600125 (JNK-1,-2, and −3 inhibitor; Cell Signaling): 10 μM; and Gö6976 (Ca^{2+}-dependent PKC inhibitor; Calbiochem): 2 μM. Each inhibitor was added to the cell culture medium at least 15 min before the A + M cotreatment and maintained until the end of the experiment.

2.2. LDH Experiment. To evaluate the plasma membrane damage and the cell viability at 24 hrs, a colorimetric assay for measuring lactate dehydrogenase (LDH) was performed on ARPE-19 cell culture medium samples. The medium was tested using the LDH substrate included in a commercial kit (cytoxicity detection kit, Roche, Molecular Biochemicals, Mannheim, Germany). The absorbance values were measured at 450 nm using a microplate reader (Synergy HT Multi-Mode, Bio-Tek), and results were expressed as percentages of control (100%).

2.3. Cell Fractioning. After exposures, cells were washed twice with cold phosphate-buffered saline (PBS), scraped, and collected. Before cellular fractioning, a small volume of cell homogenate was held and analyzed as total lysate. Nuclear and cytoplasmic extracts were separated by using the Nuclear Extract kit (Active Motif, Carlsbad, CA) according to [18].

2.4. Western Blotting. Proteins of whole cell lysates and nuclear and cytoplasmic fractions were separated on 10% or 12% SDS-polyacrylamide gel electrophoresis and processed

following the standard procedures. Briefly, the nitrocellulose membrane was washed with 0.1% Tween20 in Tris-buffered saline (TTBS), incubated for 1 hr at the room temperature (RT) with 5% non-fat milk in TTBS (blocking solution), and incubated overnight at 4°C with the primary antibody diluted in milk–TTBS. Specific antibodies for HuR (1 : 1000), p62 (1 : 800), phosphothreonine (1 : 750), phosphoserine (1 : 750) (all from Santa Cruz Biotechnology Inc., Santa Cruz, CA), phospho-p-44/42 MAPK (Erk1/2) (Thr202/Tyr204) (Cell Signaling), beclin-1, α-tubulin (Sigma-Aldrich), and lamin C (Abcam, Cambridge, UK) were diluted as suggested by the manufacturers. Membranes were then washed and incubated with HRP-conjugated secondary antibodies diluted in milk–TTBS for 1 hr at RT. The immunoreactive bands were visualized by chemiluminescence. Experiments were performed in duplicate for each different cell preparation. As for loading controls, α-tubulin was used for both total homogenate and cytoplasm, while lamin C for the rough nuclear fraction, respectively. The same proteins were also used as purity controls for each cellular fraction; however, according to [18], α-tubulin was detectable also in rough nuclei when loading ~40 μg of protein extract. Statistical analysis of the Western blotting data was performed on the densitometric values obtained by quantifying the immunoblots with the Scion Image software (Scion Corporation) after the image acquisition.

2.5. Real-Time Quantitative PCR. RNA was extracted from whole cell homogenates, cytoplasmic fractions, or immunoprecipitated samples by the RNeasy-Plus Micro Kit (Qiagen, Milan, Italy) and subjected to reverse transcription following standard procedures. Real-time quantitative PCR (qPCR) amplifications were carried out using the Lightcycler instrument (Roche), with the following primers:

HuR: 5'-GAGGCTCCAGTCAAAAACCA-3′ (upstream) and 5′-GTTGGCGTCTTTGATCACCT-3′ (downstream); p62/SQSTM1: 5′-CTGGGACTGAGAAGGCTCAC-3′ (upstream) and 5′-GCAGCTGATGGTTTGGAAAT-3′ (downstream); and RPL6: 5′-AGATTACGGAGCAG CG CAAGATTG-3′ (upstream) and 5′-GCAAACACA GATCGCAGGTAGCCC-3′ (downstream). *RPL6* mRNA was the reference on which all the other values were normalized because it remained substantially stable during all the treatments.

2.6. Immunoprecipitation. Immunoprecipitation was performed at RT for 2 hrs using 1 μg of an anti-HuR antibody (Santa Cruz Biotechnology Inc.) per 50 μg of cytoplasmic proteins diluted in the immunoprecipitation buffer (50 mM Tris pH 7.4, 150 mM NaCl, 1 mM $MgCl_2$, 0.05% Igepal, 20 mM EDTA, 100 mM DTT, protease inhibitor cocktail, and RNAase inhibitor) in the presence of 50 μl protein A/G plus agarose (Santa Cruz Biotechnology Inc.), according to a previously published protocol with minor modifications [15]. The sample, representing the immunoprecipitated HuR protein, was then subjected to either Western blotting with antibodies recognizing phosphorylated residues (anti-phospho-threonine or anti-phospho-serine, resp.) or RNA extraction. For each sample, 100 μl of immunoprecipitation mix was taken and used as "input signals" to normalize the data in Western blotting or real-time qPCR. An irrelevant antibody (Santa Cruz Biotechnology Inc.) with the same isotype as the specific immunoprecipitating antibody served as a negative control.

2.7. Polysome RNA Extraction and Profile Analysis. ARPE-19 cells (3×10^6 cells) were treated with either DMSO or MG132 + AICAR as described. Two hours after treatment, cells were incubated with 10 mg/ml cycloheximide (Sigma-Aldrich) for 5 min at 37°C and washed twice with cold PBS containing 1 mg/ml cycloheximide. Cells were scraped and lysed in fresh polysome buffer (10 mM NaCl, 10 mM $MgCl_2$, 10 mM Tris–HCl pH 7.5, 1% Triton-X100, 1% Na-deoxycholate, 0.2 U/μl RiboLock RNase inhibitor, 1 mM dithiothreitol, and 0.01 mg/ml cycloheximide). Cell lysates were centrifuged at 13000g for 10 min at 4°C. The supernatants were then layered onto 15/50% sucrose gradients (prepared in 300 mM Tris–HCl, 1 M NaCl, and 100 mM $MgCl_2$) and centrifuged at 40000 rpm for 1.40 hrs at 4°C in SW41Ti Rotor. The gradients were fractionated using a Teledyne Isco gradient fractionator that continuously measured the absorbance at 260 nm. Fractions containing free RNA (pooled sample of fractions 3 and 4) subpolysomal, monosome (pooled sample of fractions 5 and 6), and polysomal RNA (pooled sample of fractions 7, 8, and 9) were prepared. Free RNA, monosome, and polysome samples were treated with proteinase K (100 μg/ml) in 1% SDS for 1 hr at 37°C followed by extraction with 250 μl volumes of phenol–chloroform and 1 mM NaCl and by precipitation in one volume of isopropanol for 30 min at 14000g and 4°C. The recovered RNA pellet was resuspended in 20 μl of RNase-free water. Synthesis of cDNA was carried out on a RevertAid RT kit (Thermo Fisher Scientific, Waltham, MA, USA). Real-time qPCR analysis was performed with triplicates using 2XqPCR SybrGreen Mix Separate-Rox PB20 (PCR Biosystems, London, United Kingdom) on a CFX96-RT-PCR Detection system (Bio-Rad Laboratories, Watford, United Kingdom). Expression levels of *HuR* and *p62* were evaluated and normalized to free RNA. *GAPDH* was used as a housekeeping gene.

2.8. Immunocytochemistry. ARPE-19 cells (7500 cells/well) were seeded onto poly-L-lysin-coated plates for 48 hrs before exposures. Cells were pretreated or not with the compound C and then exposed to either AICAR, MG132, or both, for 2 hrs. Cells were fixed using 4% paraformaldehyde for 10 min, then incubated with a permeabilizing buffer (0.02% Triton-X100 in PBS) for 15 min, and incubated with 3% albumin for 45 min. Cells were incubated with the primary HuR antibody (at dilution 1 : 200) for 1 hr, and the secondary Alexa fluor 594 goat anti-mouse IgG (Life Technology, Thermo Fisher Scientific, Waltham, MA) (at dilution 1 : 500) for 1 hr; then cells were stained with DAPI (1 : 10,000) (Life Technology). The PerkinElmer image plate reader Operetta was used for imaging and the evaluation of HuR localization. The ratio between the cytoplasmic and nuclear signals of HuR was calculated as the mean of each ratio in every single cell in every well (triplicates). For higher magnification, immunofluorescence analysis was

performed using a Zeiss Observer Z1 microscope equipped with Apotome module, with a Plan Apochromatic (63x, NA 1.4) objective. Images were acquired using Zen 1.1 (blue edition) imaging software (Zeiss, Milan, Italy) and assembled with ImageJ software.

2.9. ELISA Assay. Cells were quantitatively analyzed for phospho-SAPK/JNK using an ELISA kit (Cell Signaling) according to the manufacturer's instructions. The concentrations of phospho-SAPK/JNK were calculated from a standard curve and corrected for the protein concentration of each sample.

2.10. Statistical Analysis. Three independent experiments with 1–3 parallel samples were performed for each exposure. The statistical analyses were performed using the GraphPad InStat software. Results were analyzed by either the analysis of variance (ANOVA) or the nonparametric method followed by an appropriate post hoc test, as indicated in the figure legends. Differences were considered statistically significant when $p < 0.05$.

3. Results

3.1. AICAR and MG132 Cotreatment Leads to a Rapid HuR Protein Activation. We previously showed that in ARPE-19 cell line under 24 hr proteasomal inhibitor MG132, HuR protein binds *p62* mRNA; the specific involvement of HuR in p62 expression regulation at the posttranscriptional level was confirmed by the finding that the MG132-induced increase of p62 protein is counteracted in HuR-silenced ARPE-19 cells [18]. The addition of AICAR triggered autophagy by favoring the clearance of p62-conjugated protein aggregates, finally improving survival in 24 hr MG132-treated RPE cells [18]. In the present study, we aim to demonstrate that at early time points the AICAR + MG132 cotreatment activates HuR and upregulates p62 expression needed for the autophagy process.

ARPE-19 cells were exposed concurrently to AICAR and MG132 (A + M) for increasing times (15 min, 30 min, and 2 hrs), to study the early events of the HuR-p62 pathway under proautophagy conditions. Since both the abundance and subcellular localization of HuR protein are key determinants for its activity, we first evaluated the HuR levels in both nuclear and cytoplasmic fractions after A + M. We found that the cotreatment triggered a rapid HuR translocation from the nucleus to the cytoplasm, evident after 15 min and statistically significant in both the cellular fractions after 2 hr exposure (Figures 1(a) and 1(b)). Immunocytochemistry experiments confirmed that HuR content was elevated in the cytoplasm of ARPE-19 cells after 2 hr A + M (Figure 1(f)). At this time, a significant increase of total HuR protein level (Figure 1(c)), associated with a higher phosphorylation of HuR in threonine residues in the cytoplasm (Figure 1(d)), was also found. Conversely, at all the times considered, no significant changes in phosphorylated serine residues of HuR were detected (Figure 1(e)). For this, in the following experiments, we focused on HuR threonine phosphorylation.

We then evaluated possible changes in p62 protein levels in the nucleus, cytoplasm, and total lysate at all the times considered (15 min, 30 min, and 2 hrs) (Figures 2(a)–2(c)). We found that 2 hr A + M-treated ARPE-19 cells showed a significant increase of p62 in the cytoplasm (Figure 2(b)), together with a higher p62 total content than control cells (Figure 2(c)). In contrast, the 2 hr treatment with either MG132 or AICAR alone was not able to increase the p62 protein levels [mean ± S.E.M.; CTR: 808.4 ± 48.7; MG132: 1078.0 ± 143.3; AICAR: 894.7 ± 123.4; not significant (N.S.); A + M: 1496.0 ± 208.5; $p < 0.05$ for A + M versus CTR; $n = 7$, Dunn's multiple comparisons test]. According to these results, the 2 hr A + M cotreatment was selected for all the following experiments.

In addition, to confirm that A + M triggers autophagy, we measured the early marker of autophagy beclin-1, finding a slight but significant increase of its protein level (Supplementary Figure 1, A), coherent with the first steps of autophagy that require the synthesis of effectors to be properly induced [29]. Even the 24 hr A + M cotreatment did not affect the viability of the ARPE-19 cell, as demonstrated by the LDH assay (Supplementary Figure 1, B).

3.2. HuR Binds to p62 Transcript and Positively Affects Its New Protein Synthesis under AICAR and MG132 Cotreatment. To evaluate whether the increased cytoplasmic p62 level following the 2 hr A + M cotreatment was due to de novo protein synthesis, we measured by Western blotting p62 protein levels in total homogenates of ARPE-19 cells exposed or not to puromycin, an inhibitor of protein synthesis. We found that the A + M cotreatment led to a significant p62 protein upregulation that was prevented by puromycin (Figure 3(a)), indicating that new p62 protein synthesis occurred in this condition. Interestingly, following A + M, total homogenates of ARPE-19 cells displayed also augmented HuR protein level, an effect that was blocked by puromycin (Supplementary Figure 2, A). To investigate whether A + M also favored the *p62* transcription, we measured by real-time qPCR *p62* mRNA content in both total homogenate and the cytoplasmic fraction of ARPE-19 cells, finding no changes in the *p62* mRNA expression (Figure 3(b)). As well, total *HuR* mRNA content was not affected by the cotreatment (Supplementary Figure 2, B). Notably, A + M promoted HuR protein binding to *p62* mRNA in the cytoplasmic fraction of ARPE-19 cells (Figure 3(c)). In basal conditions, the physical association between HuR protein and *p62* mRNA was almost absent, being the content of *p62* transcript in the immunoprecipitated HuR of control cells as low as the one observed for an immunoprecipitating irrelevant antibody (Figure 3(c)). Finally, polysome profiling of *p62* mRNA during the A + M cotreatment showed a massive shift of this transcript on heavy polysomes from monosomes or free RNA fractions (Figures 3(d) and 3(e)). We found the same for *HuR* transcript (Supplementary Figure 3). Together, these data indicate that during the A + M treatment at 2 hours, both p62 and HuR proteins increase their expression levels by an exquisitely posttranscriptional mechanism inducing their de novo translation.

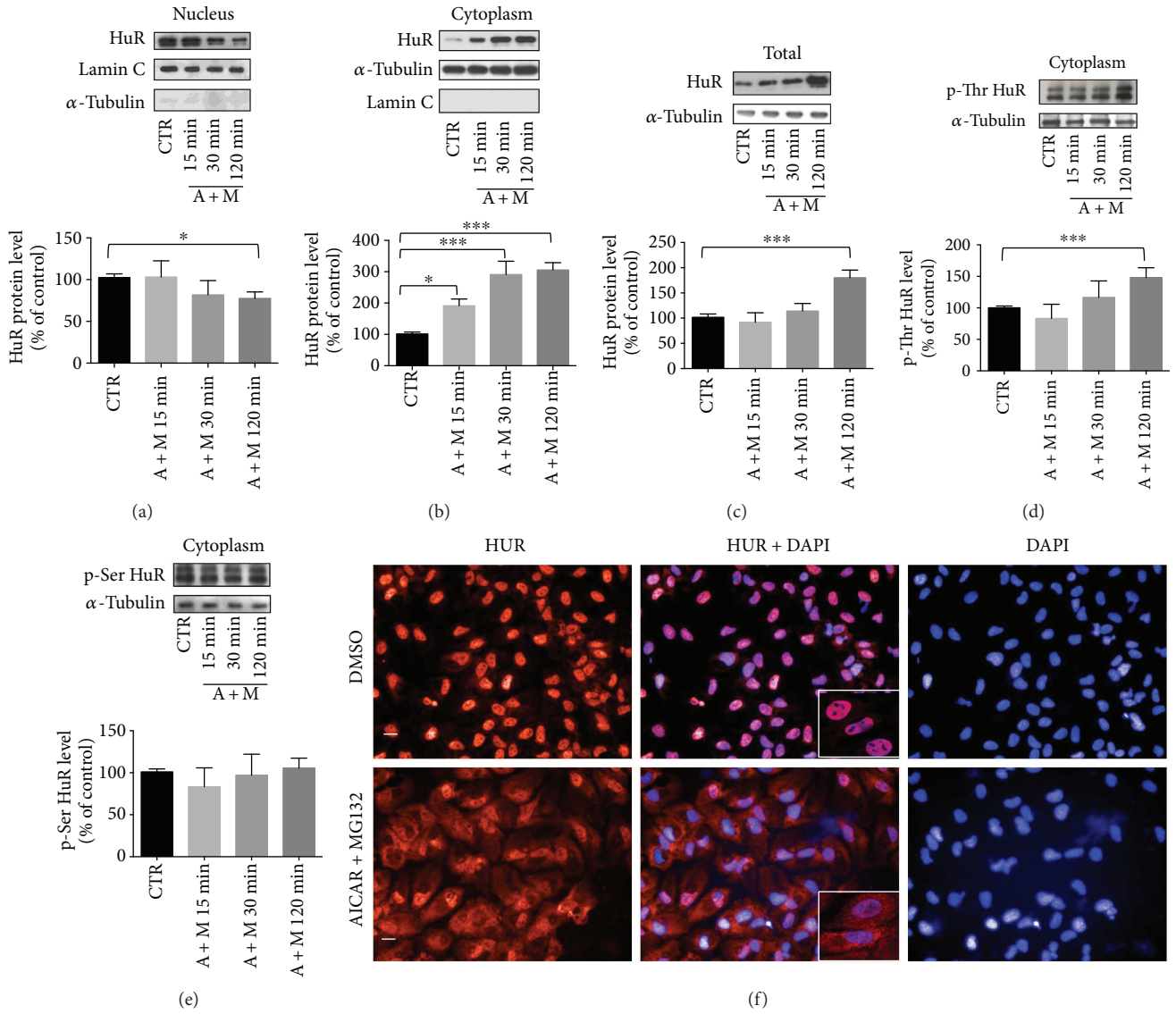

Figure 1: Translocation of HuR protein following AICAR + MG132 exposure. (a) Representative Western blotting (upper) and densitometric analysis (lower) of HuR protein levels in the nucleus (a), cytoplasm (b), and total homogenate (c) of ARPE-19 cells exposed to either solvent (CTR) or AICAR + MG132 (A + M) for increasing times (15, 30, and 120 min). Optical densities of HuR bands were normalized to lamin C for the nucleus and to α-tubulin for both the cytoplasm and total homogenate. The same proteins were also used as purity controls for each cellular fraction. The values are expressed as mean percentages + S.E.M. ($n = 3 - 6$; $^{*}p < 0.05$ and $^{***}p < 0.0001$; Dunnett's multiple comparison test). (d, e) Representative Western blotting (upper) and densitometric analyses (lower) of HuR protein phosphorylated in threonine residues (p-Thr HuR; (d)) and serine residues (p-Ser HuR; (e)) in the cytoplasm of ARPE-19 cells exposed to either solvent (CTR) or AICAR + MG132 (A + M) for increasing times (15, 30, and 120 min). Optical densities of phosphorylated HuR bands were normalized to α-tubulin (loading control detected in the input signals), and the results expressed as mean percentages + S.E.M. ($n = 3 - 6$; $^{***}p < 0.0001$; Dunnett's multiple comparison test). (f) Representative immunocytochemistry images of HuR protein in ARPE-19 cells exposed to either solvent (CTR) or AICAR + MG132 for 2 hrs. The left panels show HuR staining (red), the right panels show nuclei staining with DAPI (blue), and the middle panels merged images. Imaging (40x magnification) was made with a PerkinElmer image plate reader Operetta. Scale bar: 20 μm. Inserts: immunofluorescence analysis of HuR was performed using a Zeiss Observer Z1 microscope equipped with Apotome module, with a Plan Apochromatic (63x, NA 1.4) objective. Nuclei staining with DAPI (blue). Images were acquired using Zen 1.1 (blue edition) imaging software and assembled with ImageJ software.

3.3. AICAR and MG132 Cotreatment Activates Erk1/2 Mediating HuR Cytoplasmic Increase, HuR Phosphorylation, and p62 Protein Upregulation. It is known that phosphorylation of HuR protein can affect its cellular localization and/or activity [30]. To study in further detail the effects of the A + M cotreatment on HuR activation, we evaluated the nucleocytoplasmic shuttling of HuR protein and its phosphorylation status in the presence of some kinase inhibitors.

Literature data on different cellular models reported that MG132 determines the Erk1/2 activation [31] and that Erk1/2 regulates the cytoplasmic translocation of HuR [32]. Thus, we first investigated the possible activation of Erk1/2

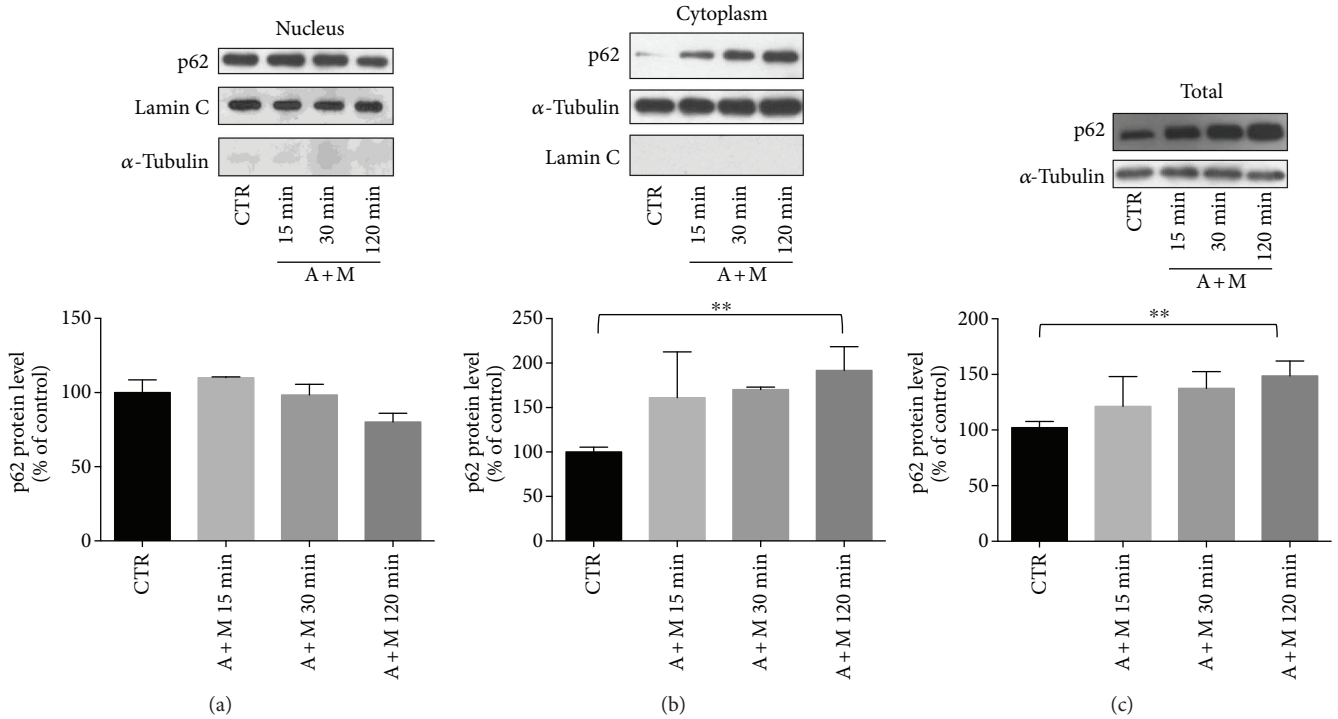

Figure 2: Evaluation of p62 protein level following AICAR + MG132 exposure. (a) Representative Western blotting (upper) and densitometric analysis (lower) of p62 protein levels in the nucleus (a), cytoplasm (b), and total homogenate (c) of ARPE-19 cells exposed to either solvent (CTR) or AICAR + MG132 (A + M) for increasing times (15, 30, and 120 min). Optical densities of p62 bands were normalized to lamin C for the nucleus and to α-tubulin for both the cytoplasm and total homogenate. The same proteins were also used as purity controls for each cellular fraction. The values are expressed as mean percentages + S.E.M. ($^{**}p < 0.005$, $n = 4$; Dunnett's multiple comparison test).

in our experimental conditions. We found a significant increase of phosphorylated Erk1/2 (p-Erk1/2) following the 2 hr A + M cotreatment in comparison to control cells (Supplementary Figure 4, A); interestingly, already at 30 min, A + M led to significantly higher p-Erk1/2 levels when compared to control (Supplementary Figure 4, B). The increase of p-Erk1/2 at 2 hrs was abolished by PD98059 (MEK-Erk inhibitor), which led downstream to a complete absence of a detectable p-Erk1/2 signal in all samples (Supplementary Figure 4, A). The cytoplasmic accumulation of HuR following the A + M exposure was compromised when the MEK/Erk1/2 pathway was inhibited (Figure 4(a)), being PD98059 responsible for HuR staying inside the nucleus (Supplementary Figure 4, C). This suggests the importance of Erk1/2 activation in the HuR translocation. The increase in phosphorylated HuR (p-HuR, in threonine residues) levels observed following A + M was not detectable when PD98059 was added (Figure 4(b)). Interestingly, PD98059 also impeded the p62 upregulation occurring under the A + M cotreatment (Figure 4(c)). ARPE-19 cells exposed to PD98059 alone showed a cytoplasmic/nuclear distribution of HuR protein mostly comparable to control (Supplementary Figure 4, C), while increased p62 protein levels were observed in the cytoplasm (Figure 4(c)).

3.4. Cytoplasmic HuR Increase and p62 Protein Upregulation Are Favored by AMPK Inhibition. Considering the well-known role of AMPK as a positive regulator of autophagy and the fact that AICAR is an AMPK activator, we evaluated on HuR and p62 the effects of the A + M cotreatment with/without AMPK inhibition. It was previously reported that AMPK favors HuR nuclear import by phosphorylating the HuR-mediating transport protein [33]. Accordingly, our Western blotting analyses showed that blocking AMPK by the compound C (CC) further potentiated the cytoplasmic accumulation of HuR triggered by A + M (Figure 4(d)), possibly explaining the trend to the increase of p-HuR observed in this compartment (Figure 4(e)). Immunocytochemistry experiments (Supplementary Figure 5) confirmed that in the presence of CC alone HuR content was unchanged in the nucleus and increased in the cytoplasm, respectively. Interestingly, the AMPK activator AICAR, alone or together with CC ± MG132, determined the HuR nuclear export and cytoplasmic accumulation. Therefore, AICAR's effect on the HuR nuclear-cytoplasmic shuttling is independent of AMPK activation. The blockade of AMPK resulted in increased cytoplasmic p62 protein level, which was even more pronounced when CC was given alone with respect to A + M (Figure 4(f)).

Some evidence from the literature shows that both the nuclear export and the phosphorylation of HuR are regulated by $p38^{MAPK}$, a kinase important for the cell stress response [34, 35]. The inhibition of $p38^{MAPK}$ by SB203580 did not affect the HuR export to the cytoplasm induced by A + M (Figure 5(a)), suggesting that, in our conditions, $p38^{MAPK}$

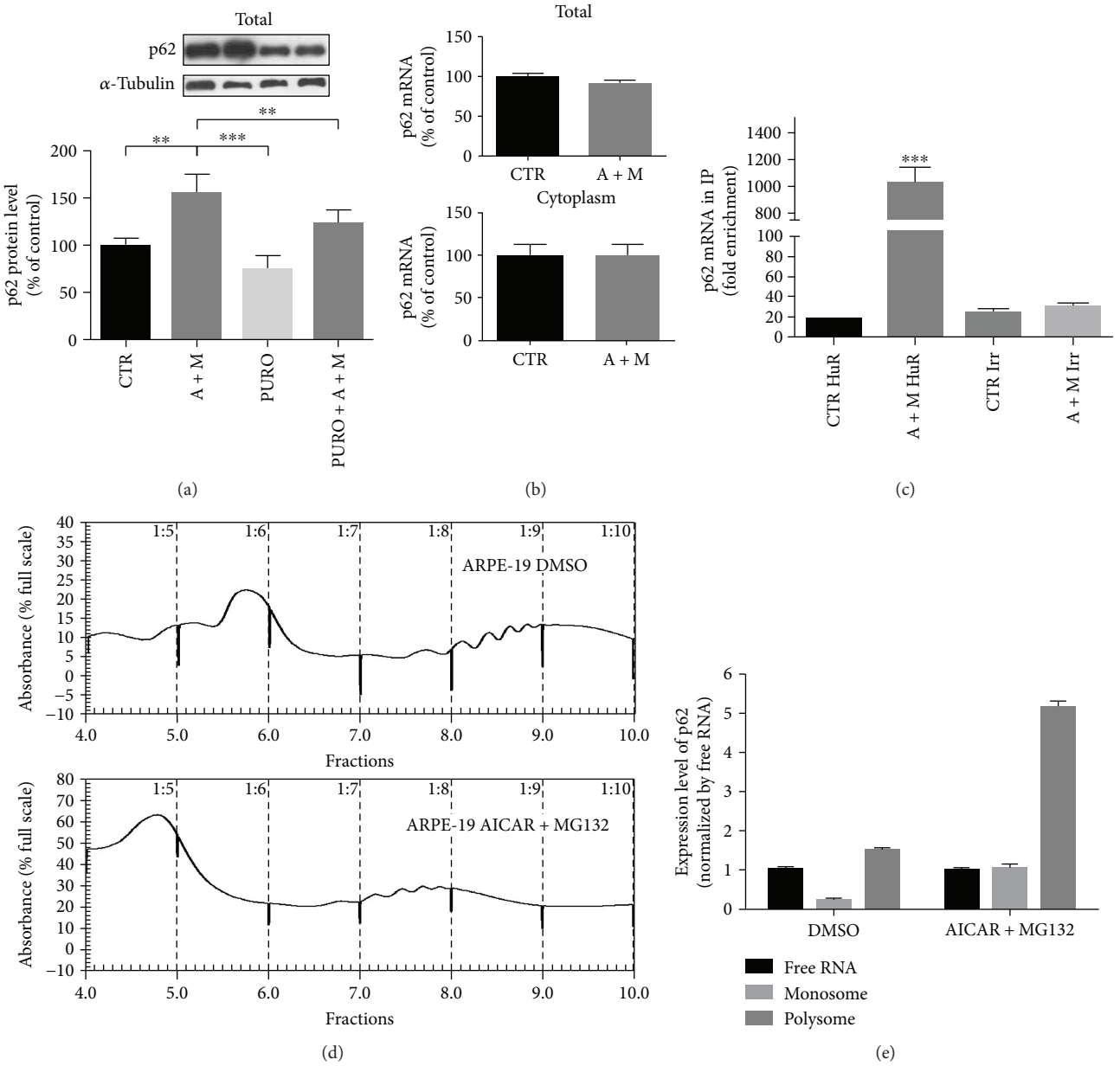

Figure 3: Levels of *p62* mRNA, its binding by HuR protein, and de novo translation following AICAR + MG132 exposure. (a) Representative Western blotting (upper) and densitometric analyses (lower) of p62 protein levels in the total homogenates of ARPE-19 cells exposed to either solvent (CTR) or AICAR + MG132 (A + M) for 2 hrs in the presence or not of puromycin (1 μM, PURO). Optical densities of p62 bands were normalized to α-tubulin, and the results expressed as mean percentages + S.E.M. ($n = 6$; $^{**}p < 0.001$ and $^{***}p < 0.0001$; Tukey's multiple comparisons test). (b) Determination by real-time qPCR of *p62* mRNA levels in the total homogenate (upper) and cytoplasm (lower) of ARPE-19 cells exposed to either solvent (CTR) or AICAR + MG132 (A + M) for 2 hrs. *p62* mRNA levels were normalized in accordance with the corresponding *RPL6* mRNA content. The values are expressed as mean percentages + S.E.M. The experiments were performed in duplicate on 4-5 independent sets of cells ($^{**}p < 0.01$, Student's t test). (c) Fold enrichment detected by real-time qPCR of *p62* mRNA following immunoprecipitation (IP) with either anti-HuR antibody or irrelevant antibody (Irr) in the cytoplasm of ARPE-19 cells exposed to either solvent (CTR) or AICAR + MG132 (A + M) for 2 hrs ($n = 3$; $^{***}p < 0.0001$; Tukey's multiple comparison test). (d) Polysome profile of *p62* mRNA was determined using 15–50% sucrose gradient sedimentation. (e) Real-time qPCR analysis and transcript level quantification for *p62* were performed in free RNA (pooled fractions 3 and 4), monosomes (pooled fractions 5 and 6), and polysome (pooled fractions 7, 8, and 9) of ARPE-19 cells treated with either solvent (DMSO) or AICAR + MG132 for 2 hrs. Relative expression of *p62* was normalized to mRNA of free RNA sample, considering the value of *GAPDH* as a housekeeping gene.

was not primarily involved in the HuR nucleocytoplasm shuttling. However, SB203580 decreased the p-HuR levels in the cytoplasm (Figure 5(b)) and also counteracted the increased levels of p62 under the A + M cotreatment, although without statistical significance (Figure 5(c); A + M + SB203580 versus A + M $p = 0.07$).

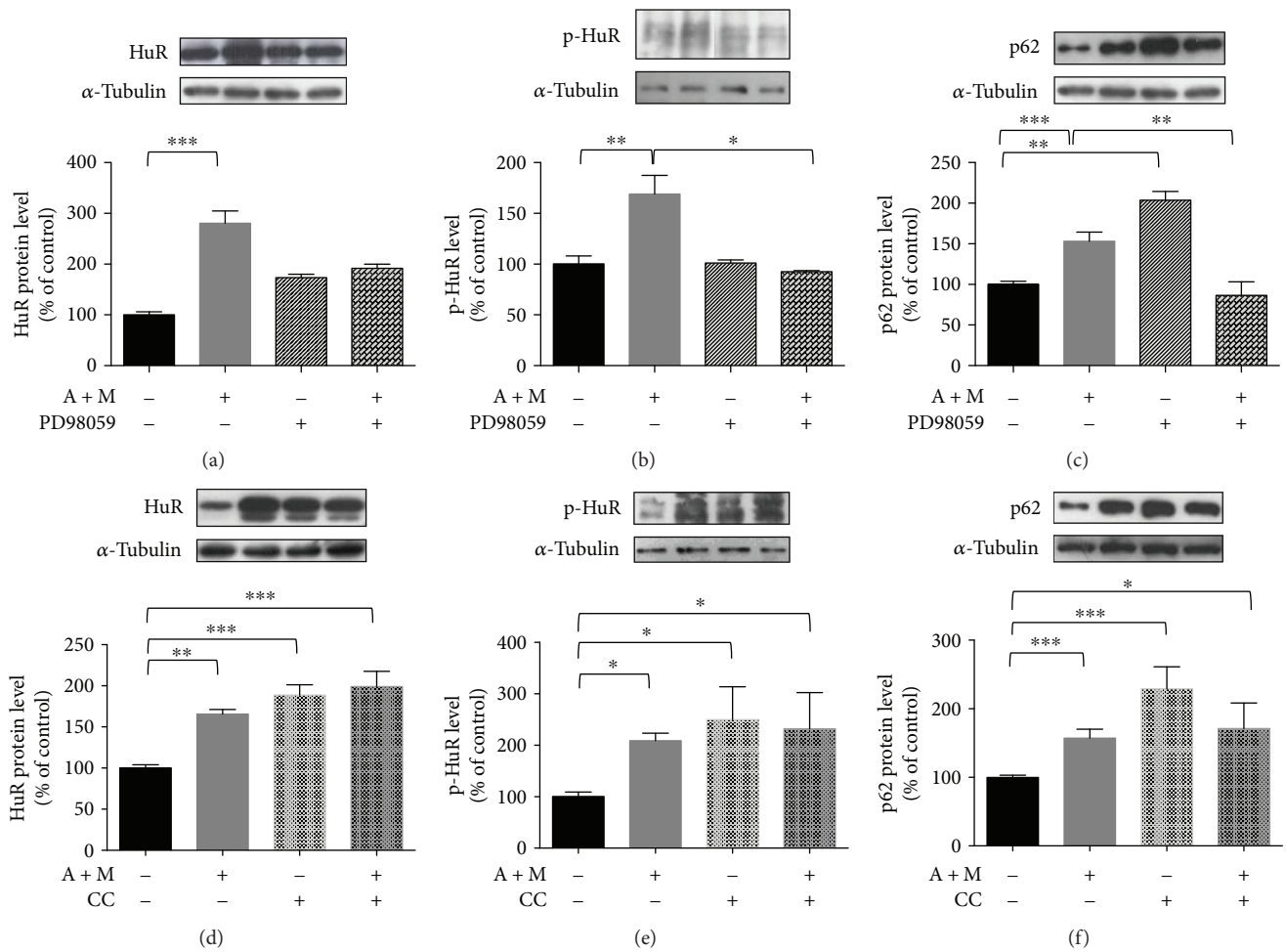

Figure 4: Effects of Erk1/2 and AMPK inhibitors on HuR translocation, its phosphorylation, and p62 expression. Representative Western blotting (upper) and densitometric analysis (lower) of levels of HuR (a, d), phospho-HuR (p-HuR, in threonine residues) (b, e), and p62 (c, f), in the cytoplasm of ARPE-19 cells exposed to either solvent or AICAR + MG132 (A + M) for 2 hrs, in the presence or not of Erk1/2 inhibitor (50 μM PD98059) (a–c) or AMPK inhibitor (5 μM compound C (CC)) (d–f). Optical densities of HuR, phospho-HuR (p-HuR, in threonine residues), and p62 bands were normalized to α-tubulin, and the results expressed as mean percentages + S.E.M. ($n = 3 - 6$; $^{*}p < 0.05$, $^{**}p < 0.001$, and $^{***}p < 0.0001$; Tukey's multiple comparison test).

3.5. Inhibition of JNK, but Not PKC, Counteracts p62 Increase under the AICAR and MG132 Cotreatment. JNK plays an important role in cellular response to a variety of stimuli. Previous studies found that JNK activation regulates the p62 expression in different contexts [31, 36, 37]. Therefore, the role of JNK in the modulation of p62 protein expression under the A + M cotreatment was examined. First, by ELISA, we found that cytoplasmic JNK is activated upon our proautophagy stimulus (Supplementary Figure 6). The phosphorylation of HuR, but not its accumulation in the cytoplasm, was affected by the JNK inhibitor SP600125 (Figures 5(d) and 5(e)), suggesting that JNK may be a new kinase regulating HuR. SP600125 alone resulted in significantly decreased p62 protein levels in the cytoplasm with respect to control ($p < 0.05$); SP600125 also prevented the increase of p62 upon the A + M cotreatment (Figure 5(f)).

Considering that HuR protein is a target of conventional PKC isoforms (cPKC) [15, 38] and that PKC is often an upstream regulator of other kinases, including Erk1/2 [27], we investigated the effects of cPKC blocking by Gö6976. Basal p-Erk1/2 was inhibited by Gö6976; in contrast, Erk1/2 activation under the A + M cotreatment seems to be PKC-independent since p-Erk1/2 remained unchanged upon the concomitant administration of Gö6976 to ARPE-19 cells (Supplementary Figure 7). As expected, the cytoplasmic increase of HuR protein was not affected by the PKC inhibition in A + M-treated ARPE-19 cells, although we observed decreased levels of p-HuR (Figures 5(g) and 5(h)). No significant alteration in the p62 protein content was observed in A + M-treated cells also exposed to Gö6976 (Figure 5(i)). These data suggest that PKC is not necessary for the A + M-induced p62 upregulation.

4. Discussion and Conclusion

Autophagy is a highly coordinated process that is regulated at several levels, including protein-protein interactions and transcriptional control, both representing the main concerns

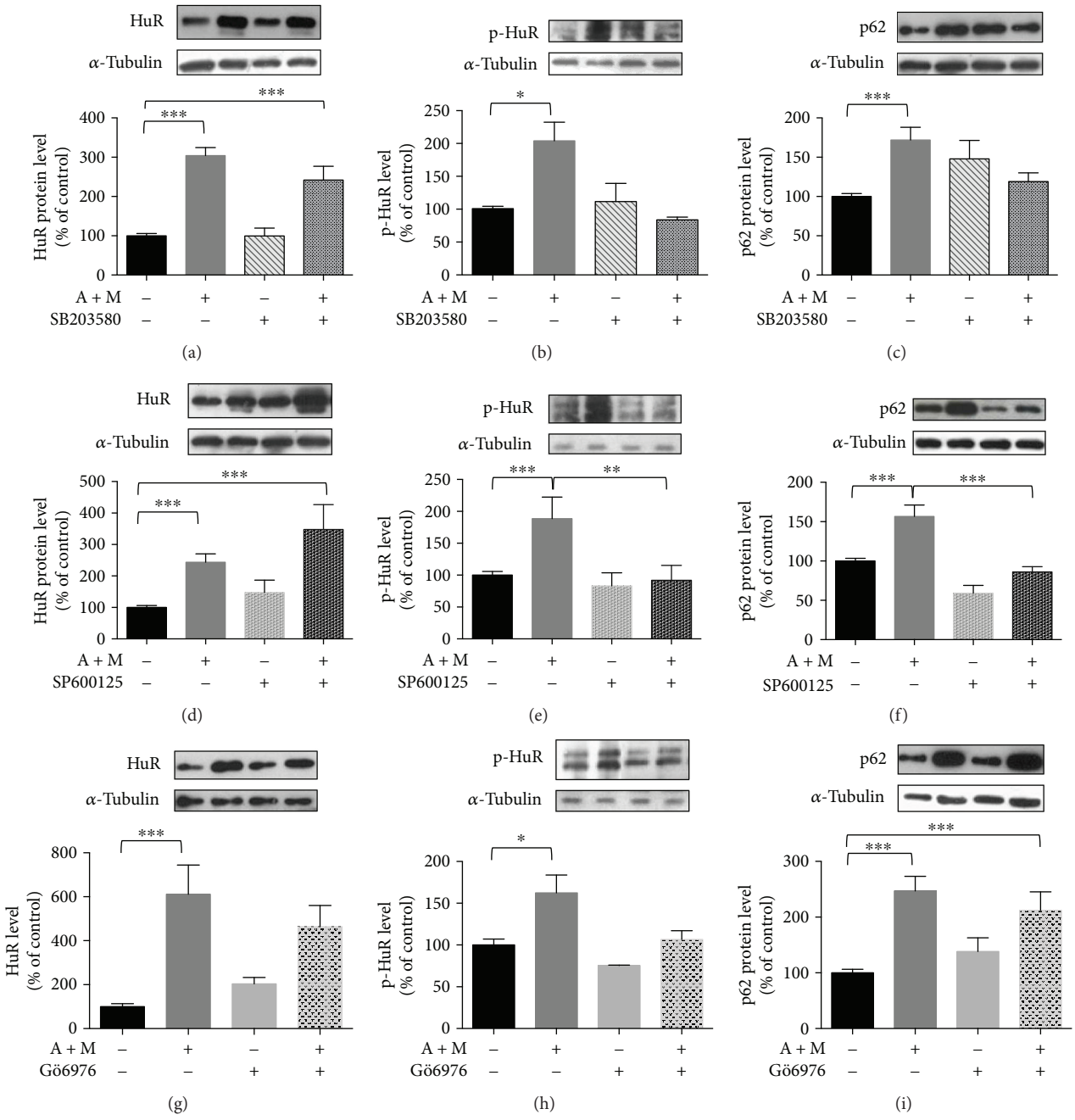

Figure 5: Effects of $p38^{MAPK}$, JNK, and cPKC inhibitors on HuR translocation, its phosphorylation, and p62 expression. Representative Western blotting (upper) and densitometric analysis (lower) of levels of HuR (a, d, g), phospho-HuR (p-HuR) (b, e, h), and p62 (c, f, i), in the cytoplasm of ARPE-19 cells exposed to either solvent or AICAR + MG132 (A + M) for 2 hrs, in the presence or not of $p38^{MAPK}$ inhibitor (50 μM SB203580) (a–c), JNK inhibitor (10 μM SP600125) (d–f), or cPKC inhibitor (2 μM Gö6976) (g–i). Optical densities of HuR, phospho-HuR (p-HuR, in threonine residues), and p62 bands were normalized to α-tubulin, and the results expressed as mean percentages + S.E.M. ($n = 3 - 6$; $^{*}p < 0.05$, $^{**}p < 0.001$, and $^{***}p < 0.0001$; Tukey's multiple comparison test).

of most studies on the regulation of autophagy. Conversely, although it is becoming clear that a "whole-cell view" of autophagy is needed to understand better the molecular basis of its regulation [39], posttranscriptional mechanisms controlling the gene expression in autophagy are mainly unknown. In this study with ARPE-19 cells, we provide information on the early effects of a proautophagy stimulus on the RNA-binding HuR protein and p62, whose mRNA we previously demonstrated to be a HuR's target [18].

As known, p62 acts as a carrier for protein degradation in the autophagy machinery and its levels change in the function of the stimuli and the autophagy phases; p62 levels increase when autophagy needs to be triggered, and they decrease when autophagy is fully activated since p62 itself is

Table 1: Effects of specific kinase inhibitors on HuR cytoplasmic accumulation, its threonine phosphorylation, and p62 increase, compared to the AICAR + MG132 cotreatment.

	Kinase targeted by inhibition	HuR cytoplasmic accumulation	HuR phosphorylation	p62 protein levels
AICAR + MG132		↑	↑	↑
	Erk1/2	↓	↓	↓
	AMPK	—	—	—
	p38^{MAPK}	—	↓	↓
	JNK	—	↓	↓
	cPKC	—	↓	—

↑: increase; ↓: decrease; —: no variation. For further details, see the text.

degraded by autophagy [40, 41]. In our previous publication [18], we showed that a long exposure (24 hours) of ARPE-19 cells to the AICAR + MG132 cotreatment activates autophagy flux, leading to a consequent decrease of p62 protein content, clearance of protein aggregates, and improvement in cell viability. In the present research, we aimed to dissect the early phases following the AICAR + MG132 cotreatment, in particular, the activation of HuR and the upregulation of p62 that is required for triggering the autophagy process.

First, we here demonstrate that the proautophagy A + M cotreatment promotes HuR protein translocation from the nucleus to the cytoplasm, which is observable already after a few minutes (15 and 30 min), and reaches statistical significance at 2 hrs. In parallel, a dramatic increase of the binding between HuR protein and *p62* mRNA in the cytoplasm is observed after the 2 hr A + M exposure, being almost absent in basal conditions. No change in the *p62* mRNA level is observed, indicating that *p62* transcription does not occur. We thought that the binding of HuR protein to *p62* mRNA could affect its translation, not its stability, as previously reported for another HuR's target transcript (*VEGF*) in human HeLa cell line [42]. Consistently, after 2 hr A + M, we found a significant increase of *p62* and *HuR* mRNAs on heavy polysomes and that both protein levels increase in the cytoplasm and whole lysate of ARPE-19 cells; this effect is prevented by inhibiting protein synthesis, further supporting that de novo p62 protein translation occurs. These effects at the polysomal level may be mediated by HuR, although future studies on HuR-*p62* mRNA association in HuR-deficient cells will be needed to confirm our hypothesis. In agreement with our results on p62, a recent study demonstrated that H_2O_2 exposure enhances the autophagic pathway together with increased p62 protein levels in RPE cells as an early prosurvival response against oxidative stress [43]. As expected in the timeframe here being considered, besides increased levels of p62 protein, after 2 hr A + M, we also found a slight upregulation of beclin-1, an early marker of autophagy activation.

The A + M-mediated nucleocytoplasmic shuttling of HuR is also accompanied by the new synthesis of HuR protein at 2 hrs, in line with the previous *in vitro* observation in human SH-SY5Y cells for the ELAV member upregulation [44]. After 2 hr A + M, an increase in cytoplasmic HuR phosphorylation status, specifically in threonine residues, also occurs. With the aim to identify the pathways potentially mediating these effects on HuR and finally affecting p62 expression, we studied the involvement of various kinases (Erk1/2, AMPK, p38^{MAPK}, JNK, and PKC). The main findings and final hypotheses are reported in Table 1 and Figure 6, respectively.

Distinct subfamilies of MAPK include Erk1/2, p38^{MAPK}, and JNK, which can be activated in response to diverse extracellular stimuli [45]. We found that A + M induces the activation of Erk1/2, which contributes to HuR nuclear export and cytoplasmic accumulation and to a parallel increase in p62 protein level; both A + M-mediated effects are prevented by PD98059. These findings are in agreement with the literature reporting that Erk1/2 regulates the HuR nucleocytoplasmic shuttling in hepatic cells [32] and it increases the p62 expression in various cell types [30]. Likewise, in hepatocytes, AICAR treatment favors the HuR binding to its target mRNA in an Erk1/2-dependent manner [46]. In our context, cytoplasmic p-HuR levels following the A + M treatment are also decreased by PD98059, suggesting that Erk1/2 is important for HuR/p62 pathway activation in ARPE-19 cells.

It was previously reported that AMPK indirectly regulates the HuR nucleocytoplasmic shuttling, promoting HuR nuclear import in intestinal epithelial cells [33]. In agreement with this, we found that inhibiting AMPK by CC (in both presence and absence of the A + M stimulus) favors HuR cytoplasmic accumulation and, therefore, p62 increase.

Erk1/2 inhibits AMPK in a tissue- and context-dependent manner [47], so we may also hypothesize that A + M triggers Erk1/2 activation, which in turn inhibits AMPK, finally leading to HuR cytoplasmic accumulation and p62 increase.

PKC is upstream of Erk1/2, and PKC activation induces the activation of the Raf/MEK/Erk1/2 pathway [27, 48, 49]. However, we have to point out that the axis PKC-Erk1/2 is not widely spread and, where it is present, functional outcomes of the PKC-induced Raf-MEK-Erk1/2 cascade activation are both cell type-specific and PKC isoform-specific [50, 51]. We found that in ARPE-19 cells, Erk1/2 activation is PKC-dependent in basal condition, but PKC-independent under the A + M exposure, since no change in p-Erk1/2 is observed when the proautophagy stimulus is coadministered with Gö6976. These findings may be explained by considering that AICAR can directly activate Erk1/2 [46], thus

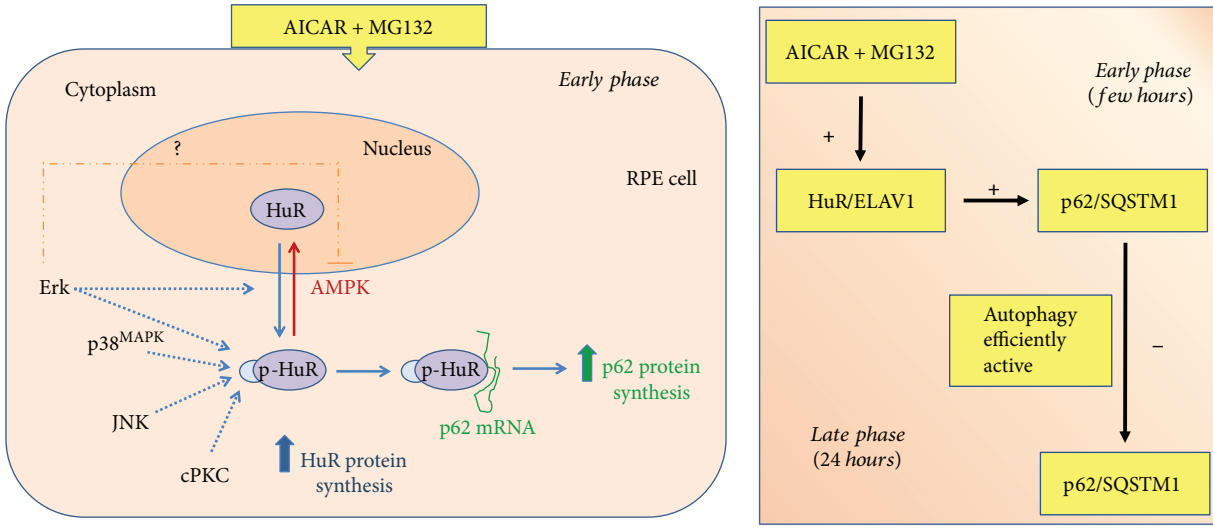

FIGURE 6: Hypothesis of the flowchart induced by AICAR + MG132 in RPE cells. (a) According to our findings, AICAR + MG132 cotreatment induces an early translocation of HuR protein from the nucleus to the cytoplasm, accompanied by an increase of its phosphorylation in threonine residues. The activated HuR protein binds to *p62* mRNA and favors its translation, upregulating p62 protein. As well, HuR protein expression is increased in this condition. Both AICAR + MG132-mediated HuR shuttling and phosphorylation are prevented by Erk inhibitor, and this possibly reverberates on p62 levels. Vice versa, AMPK is involved in HuR nucleus import, and AMPK inhibition favors both HuR permanence in the cytoplasm and p62 increase. The AICAR + MG132-induced phosphorylation of HuR is affected by inhibitors of $p38^{MAPK}$, JNK, and cPKC. $p38^{MAPK}$ and JNK inhibitors seem to contrast p62 increase under AICAR + MG132 cotreatment, while PKC inhibitor has no substantial effect. For further details, see the text. (b) The ideal temporal sequela of the events with the difference between the early and late effects induced by the AICAR + MG132 cotreatment, based on present results and our previous publication [18].

possibly bypassing the PKC inhibition. In our condition, Gö6976 affects the HuR phosphorylation but not its shuttling, which is in agreement with a previous observation on ELAV proteins [44]. Given that the PKC-γ isoform is not expressed in RPE cells [52], we hypothesize the involvement of PKC-α, or PKC-βI/II in HuR phosphorylation and/or Erk1/2 modulation. However, the increase in p62 levels under the A + M coexposure seems to be PKC-independent since it also occurs in the presence of Gö6976.

Previous studies showed that $p38^{MAPK}$ signaling is involved in the p62 expression via Nrf2 transcription and that the pharmacological inhibition of $p38^{MAPK}$ reduces p62 levels in fibroblasts exposed to oxidative stress [53]. In other cellular models, it was reported that the $p38^{MAPK}$ activation leads to HuR phosphorylation, cytoplasmic accumulation, and enhanced binding to its target mRNAs [34, 35]. We observed that, when SB203580 is added to A + M, impaired phosphorylation of HuR, but not HuR cytoplasmic increase, is observed. This may reveal that $p38^{MAPK}$ is more involved in the HuR phosphorylation than in its nucleocytoplasm shuttling. We also found that blocking $p38^{MAPK}$ prevents the p62 increase, by possibly acting on its posttranscriptional control via HuR.

Finally, we evaluated the involvement of another MAPK, JNK, that has been suggested to regulate p62 expression via Nrf2 in human hepatoma cells [54]. We found that JNK is activated under A + M and that SP600125 causes suppressed levels of both p62 and p-HuR, suggesting that JNK may promote the accumulation of p62 also at posttranscriptional level through HuR. Interestingly, to our knowledge, there is no evidence in the literature on a possible link between JNK and HuR. Our findings represent the first clue on this topic.

Based on literature and our present findings, we hypothesize the involvement of Erk1/2, $p38^{MAPK}$, and JNK kinases in HuR activation and p62 expression, and we suggest that alterations in these pathways may be relevant for AMD. Future studies evaluating in more detail the effects of these kinase modulators on HuR-p62 binding and p62 translational efficiency will be of interest to confirm the relevance of these cascades in RPE.

A growing body of literature indicates that autophagy impairment plays a role in the AMD pathogenesis and that the modulation of autophagy and related signaling pathways may provide novel therapeutic strategies for human disease prevention or treatment, including ocular diseases [23, 55–61]. Due to the complexity of mechanisms regulating this process, the modulation of autophagy is a challenging field of research. Interestingly, no molecules directly targeting the autophagy machinery are currently in clinical trials; the majority of the compounds under such studies indeed affect the regulation of autophagy [61]. Autophagy-regulating kinases have been proposed as potential therapeutic targets for AMD [62]. For instance, a key role for Erk1/2, as well as AMPK, in AMD has been suggested [63]. Moreover, recent studies have confirmed the importance of HuR in various ocular pathologies [64, 65] and laid the foundation for the

druggability assessment of HuR protein [66]; compounds able to directly act on the HuR protein and *p62* mRNA complex formation may thus represent new potential tools regulating p62 content.

In conclusion, our study supports the importance of the HuR-p62 pathway and the autophagy-regulating kinases as potential therapeutic targets for AMD.

Conflicts of Interest

The authors have declared that no competing interests exist.

Acknowledgments

This work was supported by the Finnish Eye Foundation and the University of Eastern Finland strategy support (Kai Kaarniranta) and by Fondazione Cariplo (no. 40102636 to Alessandro Provenzani). The authors acknowledge Fondazione Banca del Monte di Lombardia for supporting Nicoletta Marchesi during her training. The authors are grateful to Anne Seppänen and Chiara Zucal for technical support.

Supplementary Materials

Supplementary 1. Effects on beclin-1 expression and cell viability following AICAR + MG132 exposure. (A) Representative Western blotting (upper) and densitometric analysis (lower) of beclin-1 protein levels in the cytoplasm of ARPE-19 cells exposed to either solvent (CTR) or AICAR and MG132 (A + M) for 2 hrs. Optical densities of beclin-1 bands were normalized to α-tubulin, and the results expressed as mean percentages + S.E.M. ($n = 6$; $^{**}p < 0.001$; $n = 7$; Student's t-test). (B) Absorbance values relative to cell viability measured by LDH assay in ARPE-19 cells exposed to either solvent (CTR) or AICAR and MG132 (A + M) for 24 hrs. Results expressed as mean percentages + S.E.M. versus control (100%) ($n = 6$; N.S.).

Supplementary 2. Evaluation of HuR protein and mRNA levels following AICAR + MG132 exposure. (A) Representative Western blotting (upper) and densitometric analyses (lower) of HuR protein levels in the total homogenates of ARPE-19 cells exposed to either solvent (CTR) or AICAR + MG132 (A + M) for 2 hrs in the presence or not of puromycin (1 μM, PURO). Optical densities of HuR bands were normalized to α-tubulin, and the results expressed as mean percentages + S.E.M. ($n = 3$; $^{*}p < 0.05$; $^{***}p < 0.0001$; Tukey's multiple comparison test). (B) Determination by real-time qPCR of *HuR* mRNA levels in the total homogenate of ARPE-19 cells exposed to either solvent (CTR) or AICAR + MG132 (A + M) for 2 hrs. *HuR* mRNA levels were normalized in accordance with the corresponding *RPL6* mRNA content. The values are expressed as mean percentages + S.E.M. The experiments were performed in duplicate on 4-5 independent sets of cells.

Supplementary 3. AICAR + MG132 induces de novo translation of *HuR* mRNA. ARPE-19 cells were treated with either solvent (DMSO) or AICAR + MG132 for 2 hrs followed by polysome separation and Real-time qPCR analysis. *HuR* transcript level quantification was performed in free RNA, monosomes, and polysome of ARPE-19 cells. Relative expression of *HuR* was normalized to mRNA of free RNA sample, considering the value of *GAPDH* as a housekeeping gene.

Supplementary 4. Effects on Erk1/2 activation following AICAR + MG132 exposure in the presence of Erk1/2 inhibitor. (A) Representative Western blotting (upper) and densitometric analyses (lower) of phospho-Erk1/2 (p-Erk) protein levels in the cytoplasm of ARPE-19 cells exposed to either solvent or AICAR + MG132 (A + M), in the presence or not of Erk1/2 inhibitor (50 μM PD98059) for 2 hrs. Optical densities of p-Erk bands were normalized to α-tubulin, and the results are expressed as mean percentages + S.E.M. ($n = 4$; $^{***}p < 0.0001$; Tukey's multiple comparison test). (B) Representative Western blotting (upper) and densitometric analyses (lower) of phospho-Erk1/2 (p-Erk) protein levels in the cytoplasm of ARPE-19 cells exposed to either solvent or AICAR + MG132 (A + M) for 30 min. Optical densities of p-Erk bands were normalized to α-tubulin, and the results are expressed as mean percentages + S.E.M. ($n = 4$; $^{***}p < 0.0001$; Student's t-tests). (C) The mean ratio + S.E.M. between the cytoplasmic and nuclear signals of HuR protein in the cytoplasm of ARPE-19 cells exposed to either solvent or AICAR + MG132 (A + M), in the presence or not of Erk1/2 inhibitor (50 μM PD98059) for 2 hrs ($n = 3$; $^{*}p < 0.05$; Dunnett's multiple comparisons test).

Supplementary 5. Effects of AMPK inhibitor on HuR translocation. (A) Immunocytochemistry of ARPE-19 cells exposed to either solvent (CTR) or AICAR + MG132 alone or together, in the presence or not of AMPK inhibitor (5 μM CC) for 2 hrs. The left panels of immunocytochemistry show HuR staining (red), the right panels show nuclei staining with DAPI (blue), and the middle panels show merged images. Scale bar: 20 μm. Inserts: immunofluorescence analysis of HuR was performed using a Zeiss Observer Z1 microscope equipped with Apotome module, with a Plan Apochromatic (63x, NA 1.4) objective. Nuclei staining with DAPI (blue). Images were acquired using Zen 1.1 (blue edition) imaging software and assembled with ImageJ software. (B) The ratio between the cytoplasmic and nuclear signals of HuR is calculated as the mean of each ratio in each single cell in every well ($n = 3$; $^{*}p < 0.05$ and $^{**}p < 0.005$; Dunnett's multiple comparison test). Imaging (40x magnification) and evaluation of HuR localization were made with the PerkinElmer image plate reader Operetta.

Supplementary 6. Effects on JNK activation following AICAR + MG132 exposure. Levels of phosphorylated JNK in the cytoplasm of ARPE-19 cells exposed for 2 hrs to either solvent (CTR) or AICAR (A + M) measured by ELISA ($n = 4$; $^{***}p < 0.0001$; Student's t-test).

Supplementary 7. Effects of cPKC inhibitor on Erk activation. Representative Western blotting (upper) and densitometric analyses (lower) of phospho-Erk1/2 (p-Erk) protein levels in the cytoplasm of ARPE-19 cells exposed to either solvent or AICAR (A + M), in the presence or not of cPKC inhibitor (2 μM Gö6976) for 2 hrs. Optical densities of p-Erk bands

were normalized to α-tubulin, and the results are expressed as mean percentages + S.E.M. ($^{**}p < 0.005$; $n = 4$; Tukey's multiple comparison test).

References

[1] A. Pascale and S. Govoni, "The complex world of post-transcriptional mechanisms: is their deregulation a common link for diseases? Focus on ELAV-like RNA-binding proteins," *Cellular and Molecular Life Sciences*, vol. 69, no. 4, pp. 501–517, 2012.

[2] A. E. Brinegar and T. A. Cooper, "Roles for RNA-binding proteins in development and disease," *Brain Research*, vol. 1647, pp. 1–8, 1647.

[3] S. Dash, A. D. Siddam, C. E. Barnum, S. C. Janga, and S. A. Lachke, "RNA-binding proteins in eye development and disease: implication of conserved RNA granule components," *WIREs RNA*, vol. 7, no. 4, pp. 527–557, 2016.

[4] L. De Conti, M. Baralle, and E. Buratti, "Neurodegeneration and RNA-binding proteins," *WIREs RNA*, vol. 8, no. 2, 2017.

[5] L. B. Nabors, G. Y. Gillespie, L. Harkins, and P. H. King, "HuR, a RNA stability factor, is expressed in malignant brain tumors and binds to adenine- and uridine-rich elements within the 3′ untranslated regions of cytokine and angiogenic factor mRNAs," *Cancer Research*, vol. 61, no. 5, pp. 2154–2161, 2001.

[6] M. N. Hinman and H. Lou, "Diverse molecular functions of Hu proteins," *Cellular and Molecular Life Sciences*, vol. 65, no. 20, pp. 3168–3181, 2008.

[7] C. Colombrita, V. Silani, and A. Ratti, "ELAV proteins along evolution: back to the nucleus?," *Molecular and Cellular Neurosciences*, vol. 56, pp. 447–455, 2013.

[8] A. Pascale, M. Amadio, and A. Quattrone, "Defining a neuron: neuronal ELAV proteins," *Cellular and Molecular Life Sciences*, vol. 65, no. 1, pp. 128–140, 2008.

[9] P. J. Good, "A conserved family of ELAV-like genes in vertebrates," *Proceedings of the National Academy of Sciences of the United States of America*, vol. 92, no. 10, pp. 4557–4561, 1995.

[10] C. M. Brennan and J. A. Steitz, "HuR and mRNA stability," *Cellular and Molecular Life Sciences*, vol. 58, no. 2, pp. 266–277, 2001.

[11] C. Zucal, V. D'Agostino, R. Loffredo et al., "Targeting the multifaceted HuR protein, benefits and caveats," *Current Drug Targets*, vol. 16, no. 5, pp. 499–515, 2015.

[12] V. Katsanou, M. Dimitriou, and D. L. Kontoyiannis, "Post-transcriptional regulators in inflammation: exploring new avenues in biological therapeutics," *Ernst Schering Foundation Symposium Proceedings*, vol. 1, no. 4, pp. 37–57, 2006.

[13] K. Abdelmohsen, A. Lal, H. H. Kim, and M. Gorospe, "Post-transcriptional orchestration of an anti-apoptotic program by HuR," *Cell Cycle*, vol. 6, no. 11, pp. 1288–1292, 2007.

[14] F. Bolognani and N. I. Perrone-Bizzozero, "RNA–protein interactions and control of mRNA stability in neurons," *Journal of Neuroscience Research*, vol. 86, no. 3, pp. 481–489, 2008.

[15] M. Amadio, G. Scapagnini, U. Laforenza et al., "Post-transcriptional regulation of HSP70 expression following oxidative stress in SH-SY5Y cells: the potential involvement of the RNA-binding protein HuR," *Current Pharmaceutical Design*, vol. 14, no. 26, pp. 2651–2658, 2008.

[16] Z. Yuan, A. J. Sanders, L. Ye, and W. G. Jiang, "HuR, a key post-transcriptional regulator, and its implication in progression of breast cancer," *Histology and Histopathology*, vol. 25, no. 10, pp. 1331–1340, 2010.

[17] P. Milani, M. Amadio, U. Laforenza et al., "Posttranscriptional regulation of *SOD1* gene expression under oxidative stress: potential role of ELAV proteins in sporadic ALS," *Neurobiology of Disease*, vol. 60, pp. 51–60, 2013.

[18] J. Viiri, M. Amadio, N. Marchesi et al., "Autophagy activation clears ELAVL1/HuR-mediated accumulation of SQSTM1/p62 during proteasomal inhibition in human retinal pigment epithelial cells," *PLoS One*, vol. 8, no. 7, article e69563, 2013.

[19] O. Strauss, "The retinal pigment epithelium in visual function," *Physiological Reviews*, vol. 85, no. 3, pp. 845–881, 2005.

[20] J. M. Hyttinen, M. Amadio, J. Viiri, A. Pascale, A. Salminen, and K. Kaarniranta, "Clearance of misfolded and aggregated proteins by aggrephagy and implications for aggregation diseases," *Ageing Research Reviews*, vol. 18, pp. 16–28, 2014.

[21] D. A. Ferrington, D. Sinha, and K. Kaarniranta, "Defects in retinal pigment epithelial cell proteolysis and the pathology associated with age-related macular degeneration," *Progress in Retinal and Eye Research*, vol. 51, pp. 69–89, 2016.

[22] A. Kauppinen, J. J. Paterno, J. Blasiak, A. Salminen, and K. Kaarniranta, "Inflammation and its role in age-related macular degeneration," *Cellular and Molecular Life Sciences*, vol. 73, no. 9, pp. 1765–1786, 2016.

[23] K. Kaarniranta, P. Tokarz, A. Koskela, J. Paterno, and J. Blasiak, "Autophagy regulates death of retinal pigment epithelium cells in age-related macular degeneration," *Cell Biology and Toxicology*, vol. 33, no. 2, pp. 113–128, 2017.

[24] F. Pietrocola, V. Izzo, M. Niso-Santano et al., "Regulation of autophagy by stress-responsive transcription factors," *Seminars in Cancer Biology*, vol. 23, no. 5, pp. 310–322, 2013.

[25] W. Eberhardt, A. Doller, and J. Pfeilschifter, "Regulation of the mRNA-binding protein HuR by posttranslational modification: spotlight on phosphorylation," *Current Protein & Peptide Science*, vol. 13, no. 4, pp. 380–390, 2012.

[26] I. Grammatikakis, K. Abdelmohsen, and M. Gorospe, "Post-translational control of HuR function," *WIREs RNA*, vol. 8, no. 1, p. e1372, 2017.

[27] V. Talman, M. Amadio, C. Osera et al., "The C1 domain-targeted isophthalate derivative HMI-1b11 promotes neurite outgrowth and GAP-43 expression through PKCα activation in SH-SY5Y cells," *Pharmacological Research*, vol. 73, pp. 44–54, 2013.

[28] M. Hytti, N. Piippo, E. Korhonen, P. Honkakoski, K. Kaarniranta, and A. Kauppinen, "Fisetin and luteolin protect human retinal pigment epithelial cells from oxidative stress-induced cell death and regulate inflammation," *Scientific Reports*, vol. 5, no. 1, p. 17645, 2015.

[29] R. Kang, H. J. Zeh, M. T. Lotze, and D. Tang, "The Beclin 1 network regulates autophagy and apoptosis," *Cell Death & Differentiation*, vol. 18, no. 4, pp. 571–580, 2011.

[30] U. Bräuer, E. Zaharieva, and M. Soller, "Regulation of ELAV/Hu RNA-binding proteins by phosphorylation," *Biochemical Society Transactions*, vol. 42, no. 4, pp. 1147–1151, 2014.

[31] J. H. Kim, S. K. Hong, P. K. Wu, A. L. Richards, W. T. Jackson, and J. I. Park, "Raf/MEK/Erk can regulate cellular levels of LC3B and SQSTM1/p62 at expression levels," *Experimental Cell Research*, vol. 327, no. 2, pp. 340–352, 2014.

[32] A. Woodhoo, M. Iruarrizaga-Lejarreta, N. Beraza et al., "Human antigen R contributes to hepatic stellate cell activation and liver fibrosis," *Hepatology*, vol. 56, no. 5, pp. 1870–1882, 2012.

[33] T. Zou, L. Liu, J. N. Rao et al., "Polyamines modulate the subcellular localization of RNA-binding protein HuR through AMP-activated protein kinase-regulated phosphorylation and acetylation of importin α1," *The Biochemical Journal*, vol. 409, no. 2, pp. 389–398, 2008.

[34] F. Farooq, S. Balabanian, X. Liu, M. Holcik, and A. MacKenzie, "p38 mitogen-activated protein kinase stabilizes SMN mRNA through RNA binding protein HuR," *Human Molecular Genetics*, vol. 18, no. 21, pp. 4035–4045, 2009.

[35] V. Lafarga, A. Cuadrado, I. Lopez de Silanes, R. Bengoechea, O. Fernandez-Capetillo, and A. R. Nebreda, "p38 mitogen-activated protein kinase- and HuR-dependent stabilization of $p21^{Cip1}$ mRNA mediates the G_1/S checkpoint," *Molecular and Cellular Biology*, vol. 29, no. 16, pp. 4341–4351, 2009.

[36] X. Zou, Z. Feng, Y. Li et al., "Stimulation of GSH synthesis to prevent oxidative stress-induced apoptosis by hydroxytyrosol in human retinal pigment epithelial cells: activation of Nrf2 and JNK-p62/SQSTM1 pathways," *The Journal of Nutritional Biochemistry*, vol. 23, no. 8, pp. 994–1006, 2012.

[37] R. Vegliante, E. Desideri, L. Di Leo, and M. R. Ciriolo, "Dehydroepiandrosterone triggers autophagic cell death in human hepatoma cell line HepG2 via JNK-mediated p62/SQSTM1 expression," *Carcinogenesis*, vol. 37, no. 3, pp. 233–244, 2016.

[38] M. Amadio, G. Scapagnini, G. Lupo, F. Drago, S. Govoni, and A. Pascale, "PKCβII/HuR/VEGF: a new molecular cascade in retinal pericytes for the regulation of VEGF gene expression," *Pharmacological Research*, vol. 57, no. 1, pp. 60–66, 2008.

[39] S. H. Baek and K. I. Kim, "Epigenetic control of autophagy: nuclear events gain more attention," *Molecular Cell*, vol. 65, no. 5, pp. 781–785, 2017.

[40] Y. Ichimura, E. Kominami, K. Tanaka, and M. Komatsu, "Selective turnover of p62/A170/SQSTM1 by autophagy," *Autophagy*, vol. 4, no. 8, pp. 1063–1066, 2008.

[41] A. Jain, T. Lamark, E. Sjøttem et al., "*p62/SQSTM1* is a target gene for transcription factor NRF2 and creates a positive feedback loop by inducing antioxidant response element-driven gene transcription," *Journal of Biological Chemistry*, vol. 285, no. 29, pp. 22576–22591, 2010.

[42] C. Osera, J. L. Martindale, M. Amadio et al., "Induction of *VEGFA* mRNA translation by $CoCl_2$ mediated by HuR," *RNA Biology*, vol. 12, no. 10, pp. 1121–1130, 2015.

[43] C. Song, S. K. Mitter, X. Qi et al., "Oxidative stress-mediated NFκB phosphorylation upregulates p62/SQSTM1 and promotes retinal pigmented epithelial cell survival through increased autophagy," *PLoS One*, vol. 12, no. 2, article e0171940, 2017.

[44] A. Pascale, M. Amadio, G. Scapagnini et al., "Neuronal ELAV proteins enhance mRNA stability by a PKCα-dependent pathway," *Proceedings of the National Academy of Sciences of the United States of America*, vol. 102, no. 34, pp. 12065–12070, 2005.

[45] L. Chang and M. Karin, "Mammalian MAP kinase signalling cascades," *Nature*, vol. 410, pp. 37–40, 2001.

[46] T. Yashiro, M. Nanmoku, M. Shimizu, J. Inoue, and R. Sato, "5-Aminoimidazole-4-carboxamide ribonucleoside stabilizes low density lipoprotein receptor mRNA in hepatocytes via ERK-dependent HuR binding to an AU-rich element," *Atherosclerosis*, vol. 226, no. 1, pp. 95–101, 2013.

[47] A. Salminen, K. Kaarniranta, and A. Kauppinen, "Age-related changes in AMPK activation: role for AMPK phosphatases and inhibitory phosphorylation by upstream signaling pathways," *Ageing Research Reviews*, vol. 28, pp. 15–26, 2016.

[48] D. C. Schönwasser, R. M. Marais, C. J. Marshall, and P. J. Parker, "Activation of the mitogen-activated protein kinase/extracellular signal-regulated kinase pathway by conventional, novel, and atypical protein kinase C isotypes," *Molecular and Cellular Biology*, vol. 18, no. 2, pp. 790–798, 1998.

[49] S. Zisopoulou, O. Asimaki, G. Leondaritis et al., "PKC-epsilon activation is required for recognition memory in the rat," *Behavioural Brain Research*, vol. 253, pp. 280–289, 2013.

[50] C. Yang and M. G. Kazanietz, "Divergence and complexities in DAG signaling: looking beyond PKC," *Trends in Pharmacological Sciences*, vol. 24, no. 11, pp. 602–608, 2003.

[51] Y. Guo and P. Feng, "OX2R activation induces PKC-mediated ERK and CREB phosphorylation," *Experimental Cell Research*, vol. 318, no. 16, pp. 2004–2013, 2012.

[52] K. Yu, P. Ma, J. Ge et al., "Expression of protein kinase C isoforms in cultured human retinal pigment epithelial cells," *Graefe's Archive for Clinical and Experimental Ophthalmology*, vol. 245, no. 7, pp. 993–999, 2007.

[53] N. Rubio, J. Verrax, M. Dewaele et al., "$p38^{MAPK}$-regulated induction of p62 and NBR1 after photodynamic therapy promotes autophagic clearance of ubiquitin aggregates and reduces reactive oxygen species levels by supporting Nrf2-antioxidant signaling," *Free Radical Biology & Medicine*, vol. 67, pp. 292–303, 2014.

[54] C. Su, Q. Shi, X. Song et al., "Tetrachlorobenzoquinone induces Nrf2 activation *via* rapid Bach1 nuclear export/ubiquitination and JNK-P62 signaling," *Toxicology*, vol. 363-364, pp. 48–57, 2016.

[55] Y. Cheng, X. Ren, W. N. Hait, and J. M. Yang, "Therapeutic targeting of autophagy in disease: biology and pharmacology," *Pharmacological Reviews*, vol. 65, no. 4, pp. 1162–1197, 2013.

[56] N. Marchesi, C. Osera, L. Fassina et al., "Autophagy is modulated in human neuroblastoma cells through direct exposition to low frequency electromagnetic fields," *Journal of Cellular Physiology*, vol. 229, no. 11, pp. 1776–1786, 2014.

[57] Y. J. Li, Q. Jiang, G. F. Cao, J. Yao, and B. Yan, "Repertoires of autophagy in the pathogenesis of ocular diseases," *Cellular Physiology and Biochemistry*, vol. 35, no. 5, pp. 1663–1676, 2015.

[58] P. Boya, L. Esteban-Martínez, A. Serrano-Puebla, R. Gómez-Sintes, and B. Villarejo-Zori, "Autophagy in the eye: development, degeneration, and aging," *Progress in Retinal and Eye Research*, vol. 55, pp. 206–245, 2016.

[59] M. Amadio, S. Govoni, and A. Pascale, "Targeting VEGF in eye neovascularization: what's new?: a comprehensive review on current therapies and oligonucleotide-based interventions under development," *Pharmacological Research*, vol. 103, pp. 253–269, 2016.

[60] N. Golestaneh, Y. Chu, Y. Y. Xiao, G. L. Stoleru, and A. C. Theos, "Dysfunctional autophagy in RPE, a contributing factor in age-related macular degeneration," *Cell Death & Disease*, vol. 8, no. 1, article e2537, 2017.

[61] E. Morel, M. Mehrpour, J. Botti et al., "Autophagy: a druggable process," *Annual Review of Pharmacology and Toxicology*, vol. 57, no. 1, pp. 375–398, 2017.

[62] K. Kaarniranta, A. Kauppinen, J. Blasiak, and A. Salminen, "Autophagy regulating kinases as potential therapeutic targets for age-related macular degeneration," *Future Medicinal Chemistry*, vol. 4, no. 17, pp. 2153–2161, 2012.

[63] S. V. Kyosseva, "Targeting MAPK signaling in age-related macular degeneration," *Ophthalmology and Eye Diseases*, vol. 8, article OED.S32200, 2016.

[64] M. Amadio, A. Pascale, S. Cupri et al., "Nanosystems based on siRNA silencing HuR expression counteract diabetic retinopathy in rat," *Pharmacological Research*, vol. 111, pp. 713–720, 2016.

[65] A. Smedowski, X. Liu, L. Podracka et al., "Increased intraocular pressure alters the cellular distribution of HuR protein in retinal ganglion cells – a possible sign of endogenous neuroprotection failure," *Biochimica et Biophysica Acta (BBA) - Molecular Basis of Disease*, vol. 1864, no. 1, pp. 296–306, 2018.

[66] R. Nasti, D. Rossi, M. Amadio et al., "Compounds interfering with embryonic lethal abnormal vision (ELAV) protein-RNA complexes: an avenue for discovering new drugs," *Journal of Medicinal Chemistry*, vol. 60, no. 20, pp. 8257–8267, 2017.

Hindawi
Oxidative Medicine and Cellular Longevity
Volume 2018, Article ID 8374647, 14 pages
https://doi.org/10.1155/2018/8374647

Review Article

Age-Related Macular Degeneration: New Paradigms for Treatment and Management of AMD

Luis Fernando Hernández-Zimbrón,[1] **Ruben Zamora-Alvarado**,[1] **Lenin Ochoa-De la Paz**,[1,2] **Raul Velez-Montoya**,[1,3] **Edgar Zenteno**,[2] **Rosario Gulias-Cañizo**,[1] **Hugo Quiroz-Mercado**,[1] **and Roberto Gonzalez-Salinas**[1]

[1]*Research Department, Asociación Para Evitar la Ceguera, México City, Mexico*
[2]*Biochemistry Department, School of Medicine, UNAM, 04510 México City, Mexico*
[3]*Retina Department, Asociación Para Evitar la Ceguera, México City, Mexico*

Correspondence should be addressed to Luis Fernando Hernández-Zimbrón; lfhernandez@unam.mx

Received 29 July 2017; Accepted 6 December 2017; Published 1 February 2018

Academic Editor: Kai Kaarniranta

Age-related macular degeneration (AMD) is a well-characterized and extensively studied disease. It is currently considered the leading cause of visual disability among patients over 60 years. The hallmark of early AMD is the formation of drusen, pigmentary changes at the macula, and mild to moderate vision loss. There are two forms of AMD: the "dry" and the "wet" form that is less frequent but is responsible for 90% of acute blindness due to AMD. Risk factors have been associated with AMD progression, and they are taking relevance to understand how AMD develops: (1) advanced age and the exposition to environmental factors inducing high levels of oxidative stress damaging the macula and (2) this damage, which causes inflammation inducing a vicious cycle, altogether causing central vision loss. There is neither a cure nor treatment to prevent AMD. However, there are some treatments available for the wet form of AMD. This article will review some molecular and cellular mechanisms associated with the onset of AMD focusing on feasible treatments for each related factor in the development of this pathology such as vascular endothelial growth factor, oxidative stress, failure of the clearance of proteins and organelles, and glial cell dysfunction in AMD.

1. Introduction

The hallmark of early AMD is the formation of drusen, pigmentary changes at the macula, and mild to moderate vision loss (Figure 1). There are two major advanced forms of the disease: the "dry" or atrophic form is the most prevalent and is characterized by slow progressive dysfunction of the retinal pigment epithelium (RPE), photoreceptor loss, and retinal degeneration [1, 2] (Figure 2(a)). The "wet" or neovascular form is less frequent but is responsible for 90% of acute blindness due to AMD. It is characterized by choroidal neovascularization (CNV) with intraretinal or subretinal leakage, hemorrhage, and RPE detachments [1, 2] (Figure 2(b)). Both forms are not mutually exclusive. It is known that the dry form can eventually develop CNV and patients with CNV may display some degree of atrophy after a few years [3].

The treatment of the wet form had a major breakthrough due to the introduction of antiangiogenic drugs; suddenly, the functional prognosis changed from almost-certain blindness to more than 90% chance of three-line visual improvement after two years of treatment [1, 4]. Nevertheless, even after this progress, therapy is far from being perfect and there is still ample room for improvement.

There are three main drugs that provide indirect antiangiogenesis by blocking vascular endothelial growth factor (VEGF) in the retina. Ranibizumab (Lucentis, Genentech Inc., South San Francisco CA; commercialized worldwide by Novartis) was approved by the Food and Drug Administration (FDA) in 2006 for the treatment of neovascular

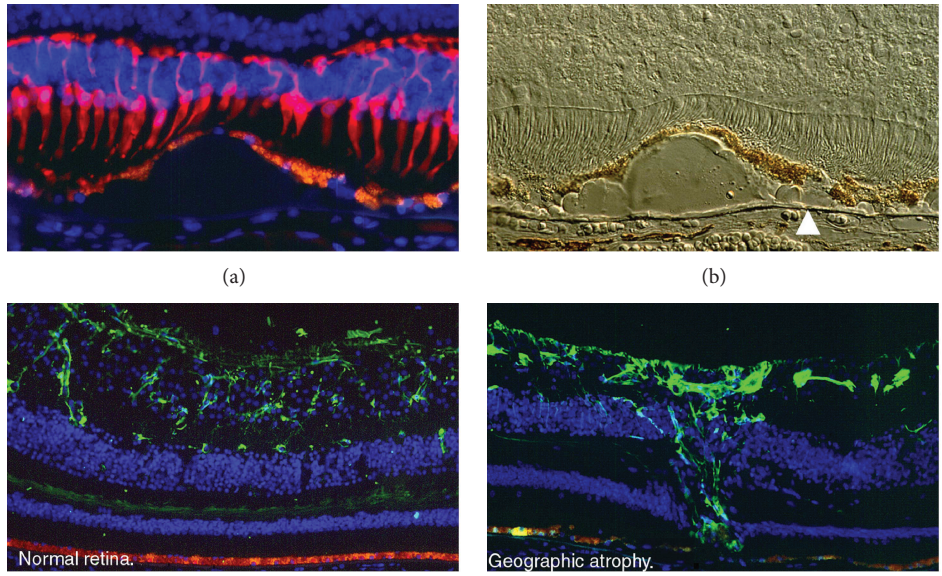

Figure 1: (a) Representative immunofluorescence image of the macula with geographic atrophy and loss of cones (red cells, mAb 7G6) over drusen. The RPE (orange) is thinned over drusen. Cell nuclei are blue (DAPI). 40x objective. (b) Nomarski image of the previous image. Note refractile drusen on Brunch's membrane (arrowhead). 40x objective. (c) Representative immunofluorescence image of the macula in a normal retina. Orange (RPE) and green (GFP) in astrocytes (anti-GFAP). (d) Representative immunofluorescence image of the macula with geographic atrophy. Orange (RPE) and green (GFP) in Müller cell scar (anti-GFAP). Photo credit: "The Human Retina in Health and Disease" Teaching Set by Ann H. Milam Ph.D., University of Pennsylvania.

AMD [1]. It is a recombinant humanized Immunoglobulin (Ig) G1 kappa isotype monoclonal antigen-binding fragment (Fab) that targets and binds VEGF-A with high affinity. Several clinical trials have proven that a monthly intravitreal dose of 0.5 mg ranibizumab results in the stabilization and improvement of visual acuity in 95% of the patients with neovascular AMD [1]. Aflibercept (Regeneron, Tarrytown, NY; commercialized worldwide by Bayer AG) was approved by the FDA in 2011. It is a fusion protein that combines two key binding domains of human VEGF receptors 1 and 2 and a fragment crystallizable (Fc) region of a human IgG1 [3]. This specially designed protein has a higher affinity for VEGF-A than its natural receptor. In addition, it is capable to bind and effectively block VEGF-B and placental growth factor 1 (PGF1) [1, 3]. Because of its greater half-life, the drug can be used in a bimonthly regimen, which greatly reduces the number of necessary intravitreal injections without losing efficacy [3]. Finally, bevacizumab (Genentech Inc., South San Francisco, CA; commercialized worldwide by Roche) is a full-length humanized antibody that binds and blocks all VEGF isoforms. Despite being an off-label drug for the treatment of AMD, it is the most used ocular antiangiogenic and the 7th best-selling drug in the world with revenues over 6.5 billion US dollars in 2016 [1].

The antiangiogenic treatment is aimed at treating the consequences of long-lasting cellular damage (vascular endothelial growth factor (VEGF) production) but adds nothing to the prevention and prophylaxis of AMD development. In reality, this therapy is not modifying the course of the disease at all but merely resisting its impact through time and delaying its progression. Moreover, there is no proven treatment available for the dry form of AMD. This is in part because until now, the results of research on AMD are just beginning to unravel the intricate relationship between genetic predisposition, environmental factors, and the normal aging process that take place as part of the disease mechanisms. A better understanding of these relationships will help us to identify better potential treatment targets for both wet and dry forms of AMD.

Therefore, the aim of the current manuscript is to review some of the principal molecular mechanisms associated with the pathogenesis of AMD such as the principal mechanism associated with neovascularization through VEGF signaling, oxidative stress, dysregulation of the mechanisms of clearance of proteins and organelles in AMD (autophagy), the pathophysiology of glial cells in the retina on AMD, and closing each subject of this review explaining some of the new potential treatment alternatives for AMD. We have divided the review into two big major subjects: molecular mechanisms and cellular mechanisms, for a better understanding of this work.

2. Molecular Mechanisms

2.1. Associated Factors with Neovascularization in Age-Related Macular Degeneration. The AMD process starts with atrophic formation, called dry AMD, characterized by decreased vision principally caused by retinal dysfunction,

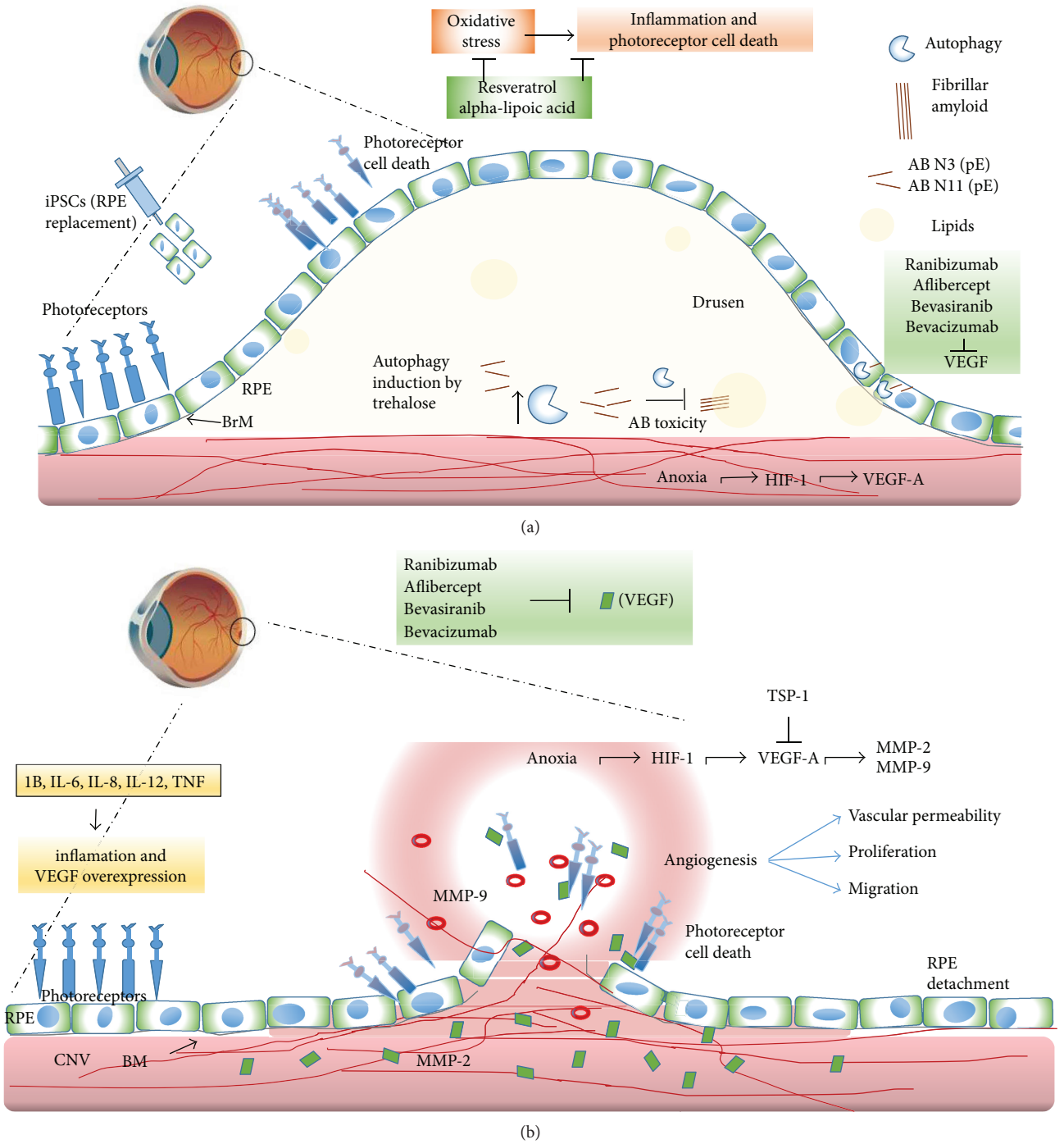

Figure 2: A diagram illustrating the anatomical differences between RPE and BM on dry AMD (a) and wet AMD (b). Early AMD involves the accumulation of drusen and beta-amyloid peptides in the subretinal space. This might progress to dry AMD (a), which is characterized by inflammation and photoreceptor degeneration, caused in part by oxidative stress; resveratrol and alpha-lipoic acid prevent these effects. Autophagy induction by trehalose might help to eliminate intracellular components that abnormally accumulate intracellularly avoiding the following extracellular accumulation of toxic peptides, like beta-amyloid and lipids. Another strategy for the physiological recovery in AMD is the administration of induced pluripotent stem cells (iPSCs). Wet AMD (b) in which neovascularization from invading choroid vessels and the Bruch's membrane (BM) rupture cause photoreceptor damage. Besides, neovascularization of the retina ruptures the Bruch's membrane, which damages the macula and results in blurry or spotty vision. Anoxia and hypoxia-inducible factor 1 (HIF-1) induce the expression of VEGF-A, and as a possible treatment, thrombospondin-1 (TSP-1) protein might be used to block VEGF-A and metalloproteinases 2 and 9 (MMP-2 and MMP-9). Additionally, ranibizumab, aflibercept, bevacizumab, and bevasiranib could be used to block the angiogenic effects of VEGF on both cases.

subsequently, developing to a wet condition. The latter occurs when abnormal blood vessels behind the retina start to grow under the macula; these new blood vessels are very fragile and often have blood and fluid leaks [5, 6]. The blood and fluid raise the macula from its normal position in the back of the eye, and the macula is damaged quickly favoring the loss of central vision.

The most studied factor related to ocular neovascularization is the vascular endothelial growth factor (VEGF) [7]. VEGF was first identified as a signal protein of vascular permeability. The VGEF gene encodes a family of glycoproteins generated by alternative splicing, whose primary function is the formation of blood vessels de novo (embryonic development) and angiogenesis (formation of new blood vessels from preexisting vessels) by activating cellular signal pathways.

Members of the VEGF family (VEGF-A, VEGF-B, VEGF-C, VEGF-D, and VEGF-E and the placental growth factor (PGF)) are proteins of approximately 40 kDa. The VEGF-A's biological activity is dependent on proteolytic processes; the products obtained from this degradation interact differentially with VEGF-R1 and VEGF-R2 receptors [8].

Within this group of proteins, it has been reported that the VEGF-A protein induces vascular proliferation and migration of endothelial cells and is essential for both physiological and pathological angiogeneses.

In several diseases, such as rheumatoid arthritis, cardiac ischemia, psoriasis, growth tumor, and diabetic retinopathy, as well as in AMD, the activity of the VEGF-A protein plays an important role. However, the VEGF released in these diseases is due to different factors. The best-studied mechanism of VEGF-A release is associated with the lack of available oxygen; thus, the production of VEGF can be induced in hypoxic cells. When cells are in a low-oxygen microenvironment, they produce the transcription of the hypoxia-inducible factor 1 (HIF-1) inducing the release of VEGF-A (Figure 2(a)). VEGF-A is a heparin-binding homodimeric glycoprotein that acts via endothelial-specific receptor tyrosine kinases, VEGFR1 (Flt1), VEGFR2 (KDR/Flk1), and VEGFR3 (Flt4), located in endothelial cells and in other cell types, and it is known that the most important for angiogenesis is the VEGFR-2 receptor [9].

Once VEGF-A binds to the receptor, several signaling pathways are activated. These pathways are the following: (1) the Mitogen-activated protein kinase- (MAPK-) p38 signaling pathway, where the effector protein (the heat shock protein HSP27) acts by reorganizing actin, (2) the phosphatidylinositol 3-kinase- (PI3K-) AKT protein kinase B pathway, promoting the formation of nitric oxide (ON), and (3) the phospholipase C-gamma (PLCγ) triggering the intracellular calcium release, promoting prostaglandin production, and increasing vascular permeability. The three pathways promote angiogenesis [10].

2.1.1. Other Signaling Pathways Involved in Angiogenesis. Currently, other proteins associated with VEGF-A signaling are involved in corneal neovascularization. The best-described proteins related to these processes are metalloproteinases 2 and 9 (MMP-2 and MMP-9). These proteins have acidic properties, are rich in cysteine, and promote angiogenesis as they act to degrade the extracellular matrix, increasing the filtering of molecules that modify the microenvironment finally promoting the formation of new blood vessels [11] (Figure 2(b)).

During the development of AMD, there is a balance between angiogenic and antiangiogenic factors and the loss of this balance favors the development of blood vessels de novo.

Another factor associated with an antiangiogenesis function in AMD is thrombospondin-1 (TSP-1). TSP-1 is a glycoprotein of 450 kDa, a major component of platelet alpha-granules, produced in various cell types such as endothelial cells, monocytes, macrophages, and retinal pigment epithelium (RPE). One function of this glycoprotein in *in vivo* and *in vitro* studies is the inhibition of angiogenesis. In addition, it has been demonstrated that its expression is dependent on the localization. In fact, it is mainly located in the basal lamina of RPE, Bruch's membrane (BM), choriocapillaris, the retinal wall, and the choroidal blood vessels in normal eyes, but in AMD, its expression is significantly decreased, especially in Bruch's membrane and choriocapillaris at the submacular region [12, 13]. These data support the hypothesis that the decrease in the expression and activity of antiangiogenic factors promotes neovascularization. Therefore, we can suggest that the activity of the angiogenic factor VEGF would not be enough to increase vascularization but requires abatement of the activity of antagonist factors.

In another way, the role of cytokines in AMD progression has been controversial. Elevated serum levels of interleukin-6 (IL-6) are associated with an increased incidence and progression of AMD, whereas the presence of interleukin-8 (IL-8) decreases the development of neovascularization and apparently confers a protective effect. However, this topic is not discussed in this review. For a better understanding of inflammation and its role in age-related macular degeneration, authors refer to Kauppinen et al.'s work [14].

2.1.2. Novel Molecular Anti-VEGF Therapies for AMD. Several specific drugs have been developed that inhibit the angiogenic effect or activity of VEGF. In addition to conventional drugs that have been approved so far, currently, progress has been made in the development of small interfering RNAs (siRNAs) as therapeutic agents. These siRNAs are small strands of about 21 nucleotides of RNA that bind specifically to the target mRNA to regulate its expression. Within this group of therapeutic agents, the effect of the siRNA anti-VEGF, named bevasiranib, has been studied [15, 16]. Although, in the clinical trial phases I and II, positive effects in patients were demonstrated, the results in clinical phase III in 2010 were inconclusive and the clinical study was stopped.

A second alternative is the use of siRNA AGN211745 that targets the VEGF receptor 1 (VEGFR-1). The preclinical studies in animal models have shown encouraging results [16]. However, researchers are still working in the development of another specific siRNAs, to provide more

advantages in the use of siRNAs and decrease the adverse effects in patients.

2.1.3. Anti-Integrin Therapies. The integrin family of cell adhesion molecules mediates host defense, homeostasis, signal transduction, and various other interactions between the cell and the extracellular matrix. Integrins are type-1 transmembrane glycoproteins expressed on the cell surface widely expressed in choroidal cells and RPE cells and play an important role in the angiogenic pathway.

Three classes of integrin inhibitors are in preclinical or clinical trials: monoclonal antibodies that target the extracellular domain of the integrin heterodimer, synthetic tri-amino acid sequence, arginine-glycine-aspartate (RGD) motif-containing peptides, and peptidomimetics, which are orally bioavailable nonpeptidic molecules that mimic the RGD sequence [17]. A study in a mouse oxygen-induced retinopathy (OIR) model evaluated the in vitro and in vivo pharmacological activity of a novel nonpeptidic integrin alpha v beta 3 (avb3) antagonist, 3-[3-(6-guanidino-1-oxoisoindolin-2-yl) propanamido]-3-(pyridin-3-yl) propanoic acid dihydrochloride (GOPPP), which was shown to inhibit retinal neovascularization. The major results were that GOPPP reduced pathologic but not developmental angiogenesis in neonatal mice. GOPPP effectively reduced pathologic angiogenesis, adhesion, proliferation, and migration, through the inhibition of ERK1/2 and Akt phosphorylation in a model of ischemic retinopathy and its beneficial effects likely involved in the inhibition of retinal VEGF [17].

2.2. Oxidative Stress: Implications for AMD. The association between oxidative stress with age-related pathologies, like Alzheimer's disease (AD), Parkinson's disease, atherosclerosis, certain types of cancer, and AMD, is a common finding and has been extensively documented [18–20]. Despite being a disease of unknown etiology, there is strong evidence suggesting that oxidative stress has a major role in the development and progression of AMD [20, 21]. The retina and RPE are extremely susceptible to oxidative stress damage: they both have high metabolic demands and require large amounts of adenosine triphosphate (ATP) to support their functions [22]. The retina has the highest consumption of oxygen per gram of tissue in the human body. Reactive oxygen species (ROS), like hydrogen peroxide, superoxide anions, hydroxyl free radicals, and hydroperoxyl radicals, among others, are readily created as a by-product of increased oxidative phosphorylation in mitochondria [22–24]. In addition, the constant exposure of both structures to UV radiation from white bright light, especially UVA, which is able to excite ocular chromophores and induce DNA damage by secondary photoreactions and indirect photosensitizing reactions, is also a constant source of ROS like hydrogen peroxide (Figure 2(a)) [25–27]. The damage induced by the latter may be enhanced with age due to increased deposits of lipofuscin within the RPE [28]. Moreover, cataract surgery may worsen UV-mediated retinal damage due to the loss of the lens' natural protection, despite implantation of an intraocular lens with a blue-light filter [29].

Environmental insults like cigarette smoking, which is a known inducer of oxidative stress, have been identified as the strongest risk factor for AMD, second only to age (OR 4.5) [26, 30]. When these factors are combined in time, the oxidative burden can build up quickly and eventually surpass the eye's antioxidant capacity. Evidence of this disequilibrium is the finding of many oxidative-modified proteins, lipids, and inflammation-related factors as part of drusen constituents [31]. The dry advanced form of AMD has also been associated with high levels of iron, a prooxidant factor, in RPE and Bruch's membrane [32].

The process of photoreceptors' outer segment shedding and its heterophagy by the RPE is a constant source of polyunsaturated fatty acids like phosphatidylcholine [33]. An environment rich in ROS may induce oxidative modification of excessive phospholipids. In another way, ROS interact with double-bound lipids, inducing their breakdown and giving rise to oxidized forms, like pentosidine, 1-palmitoyl-2-(5′-oxo-valeroyl)-sn-glycero-3-phosphocholine, malondialdehyde, malondialdehyde-acetaldehyde, oxidized phosphocholine, and oxysterols such as 7-ketocholesterol and 25-hydroxycholesterol, among others [33–35]. Most of them can be found as drusen constituents. These newly modified lipoproteins are very reactive and can easily interact with other molecules to form adducts and molecular moieties, which can promote a wide array of effects, mainly the change of nonreactive molecules into epitope-like structures, inducing immune recognition and inflammatory damage via complement cascade activation [34, 36]. This effect can be potentiated further in case of concomitant genetic defects that predispose the patient to the dysregulation of the complement pathway like the H402Y variant or mutations in complement factors H and B [21, 35–37].

Other cellular damages induced by ROS associated with AMD pathogenesis include nuclear and mitochondrial DNA damage, autophagy decline, and induction of programmed cell death of photoreceptors and RPE cells by upregulating the mitogen-activated protein kinase (MAPK), which leads to chronic inflammation and the upregulation of the production of VEGF via ERK1/2 activation [29, 38–42]. They can also act as chemoattractants for systemic macrophages and perpetuate inflammation. Finally, oxidative stress triggers the expression of proinflammatory cytokines, such as IL-1β, IL-6, IL-8, IL-12, and TNF-α, and depending on which of them is increased, the effect will be either a development or an inhibition of AMD [14]. However, as we mentioned before, we have recommended Kauppinen et al.'s review [14].

2.2.1. Antioxidant Therapies for AMD. In order to restore the balance previously described, antioxidant supplements and ROS scavengers have been proposed as potential therapies for prophylaxis and to decrease AMD's progression (Figure 2(a)).

One of these studies has been entitled "Age-Related Eye Disease Study (AREDS) 1 and 2" and proved, despite their limitations, that nutritional supplementation with antioxidants and micronutrients can effectively reduce the progression toward advanced forms of AMD by 28% over a 5-year

period (OR = 0.72; 99% CI = 0.52–0.98), in patients over 55 years of age [43]. It also demonstrated that supplementation of the original formula with lutein, zeaxanthin, and polyunsaturated fatty acids (docosahexaenoic acid (DHA) and eicosapentaenoic acid (EPA)) is safe, although no additional benefit was detected [44, 45].

In another way, resveratrol (3,4,5-trihydroxystilbene) could help for AMD treatment. This molecule is a polyphenolic antioxidant that belongs to the stilbene family, commonly found in grape skin and seeds [29, 46]. It has been recently studied as a potential therapeutic target since it has antioxidant effects against peroxide-induced oxidative stress, reduces the UVA-induced ERK1/2 activation in RPE cells, and reduces MAPK activation and the expression of cyclooxygenase-2 in RPE cells *in vitro* [29, 45–47]. Small case series, using commercially available over-the-counter resveratrol, have shown improvement in retinal structure and function [47]. The use of resveratrol for exudative age-related macular degeneration (AGED) is a phase I/II interventional, prospective, randomized clinical trial (NCT02625376) that will compare the incidence of advanced neovascular AMD between a 250 mg resveratrol bid group and placebo after 24 months of follow-up. The study started in August of 2015 and has a completion date set for 2019. It is currently enrolling, and no results have been released so far.

Another option for AMD treatment is alpha-lipoic acid, which is a cofactor of mitochondrial dehydrogenase. It acts as a free radical scavenger, chelating transition metals, and promotes the regeneration of endogenous antioxidant systems like superoxide dismutase [48]. The use of alpha-lipoic acid in geographic atrophy (GA) is a phase I/II clinical trial, sponsored by the University of Pennsylvania (NCT02613572), which aims to assess the safety and tolerability of 800 mg and 1200 mg alpha-lipoic acid, as well as the change over time in the area of GA in the studied eyes. The study entered phase 2 in May of 2016 and has a completion date set for May 2018. It is currently enrolling, and no results have been released so far.

As we have mentioned before, UV light induces the increase of oxidative damage to the RPE in AMD. The principal associated mechanism to RPE damage has not been clearly described, but oxidative stress has been associated with the overproduction and accumulation of lipofuscin, beta-amyloid peptides, and different proteins, and the accumulation of these molecules is toxic for RPE cells. In AMD, the formation of these aggregates has been related to failures in the normal clearance mechanisms of the cells. One of these processes is called autophagy, and next, we will describe it and its participation in AMD progression.

2.3. Autophagy in AMD: Is Cellular Recycling Affected in AMD? As seen previously in the text, the etiology of AMD is not fully understood yet. Recent information has proposed that failures in autophagy might be a key factor in the development and progression of AMD. We could define autophagy as a normal catabolic process, evolutionarily conserved, that regulates the degradation of dysfunctional cellular and unnecessary components through the formation of a double-vesicle structure, called autophagosome, and its subsequent fusion with lysosomes.

There are three different mechanisms of autophagy: macroautophagy, microautophagy, and chaperone-mediated autophagy. We will focus, here, in an extensive description of this process.

Cellular homeostasis depends on the proteostasis network, and under normal conditions, this can sense and rectify disturbances in the proteome to restore homeostasis in cells. Two of the principal players in proteostasis maintenance are two proteolytic systems, the ubiquitin-proteasome and the autophagy systems. Although there are some differences in these systems, while substrates of the ubiquitin-proteasomal pathway are predominantly short-lived proteins and misfolded or damaged proteins, autophagy substrates are long-lived proteins, damaged organelles, and multiple proteins organized into oligomeric complex or aggregates that cannot be degraded by other systems [49].

In this sense, autophagy has been characterized as a catabolic process that "eats" aberrant organelles, misfolded proteins, and protein aggregates into double-membrane autophagosomes and delivers it to lysosomes [50]. The correct function of this process is important because it is the only known mechanism that eukaryotic cells possess to degrade protein aggregates and the only one by which entire organelles, such as mitochondria and peroxisomes, are recycled [51]. Cell survival is highly dependent on autophagy. In this regard, loss of autophagy particularly causes accumulation of ubiquitin-positive inclusion bodies and triggers degeneration processes [52].

Autophagy is a very complex process and requires a series of coordinated steps. The first step is the formation of an isolation vesicle called phagophore. After the phagophore formation, it elongates around the cytoplasmatic components selected for degradation. The recognition of the components for degradation and the closing of the vesicle are dependent on the lipidated form of LC3 protein (a microtubule-associated protein light chain 3). Then, the lipidated form of LC3 is associated with the outer and the inner membranes of the autophagosome [53, 54]. These autophagosomes are formed by a particular pathway that requires at least twenty proteins called "atg" (autophagy-related proteins) [54]. Finally, the late stage of autophagy (maturation) depends on the fusion of autophagosome and lysosome. This allows contact of autophagosome cargo with lysosomal hydrolases and consequently the degradation of the components that could be recycled (Figure 2(b)). These steps are fundamental for the autophagic flux (the continuous series of events since the cargo is engulfed until it is degraded). Any event that could alter this flux also alters the degradation process and consequently leads to accumulation of autophagosomes. At the end, the cargo degradation is dependent on the interplay between lysosomes and autophagosomes and this is called the autolysosome. In the eye, all cells present autophagy in order to maintain the normal function contributing to healthy vision. These cells express differential autophagy-related proteins, and when there are mutations in these genes, the stress-induced autophagic

pathways can be activated inducing the development of ocular diseases [55].

This part of the review summarizes the current knowledge about the role of autophagy in eye health and AMD as potential molecules that could be used as a protective therapy against AMD progression. Many factors activate autophagy in stress conditions similar to those involved in AMD: inflammation, oxidative stress, and hypoxia, and these conditions have been explained before in this review.

Autophagy is especially useful to eliminate or reutilize proteins with a high aggregation propensity. Regarding prone-aggregation proteins or peptides, the beta-amyloid 1–42 peptide (the major toxic peptide observed in Alzheimer's disease) and lipofuscin have been characterized like two of the most prone-aggregation polypeptides in AMD recently. Both polypeptides have gained relevance in AMD because the burden of both increases with age, in RPE-Bruch's region, photoreceptor outer segments (POS), and retinal ganglion cells (RGCs) [56, 57].

We know now that drusen observed in AMD are deposits composed of different intracellular originated proteins and some of them regulate proteolytic processes [1, 58, 59]. In these deposits, the presence of beta-amyloid peptides correlates with age as well as the extent of druse loads observed in AMD [60, 61]. It has been shown that autophagy reduces the toxicity caused by protein aggregates that accumulate in different age-related diseases [58]. Similarly, patients with AMD have shown accumulation of autophagosomes and decreased lysosomes [60, 62].

The presence of such peptides may serve as indicators of an impaired autophagy process in RPE cells that could involve AMD development [57, 62]. Therefore, preservation of the autophagic activity has been related to a lower intracellular accumulation of damaged proteins, improving RPE cell function and retarding the aging process.

Autophagy induction to clear drusen and beta-amyloid peptides from the macula can be induced by different molecules, and some of them have been proven. It has been reported that autophagy could be involved in the degradation of beta-amyloid peptides through the internalization in clathrin-positive endosomes. However, these mechanisms have not been totally elucidated and current research is being performed in order to probe it in the eye [59, 61, 62].

Among the compounds that induce autophagy, we can find trehalose, metformin, and rapamycin. Trehalose is a disaccharide of glucose, a food constituent produced by different organisms, but it is not present in mammals and it is produced under stress conditions. Its production helps to restore cellular integrity, especially cell membranes. More specifically, in the cornea, this sugar suppresses inflammation and neovascularization. In dry eye, it helps to decrease cell death as well as inflammation. Trehalose has been extensively studied to prevent neurodegenerative disorders, principally by promoting autophagy, reducing the presence of toxic proteins or peptides. Besides, it is not toxic and it could be administrated to humans [63, 64]. In fact, there are trehalose-based eye droops that help to preserve viability and the correct function of cultured human corneal epithelial cells during desiccation [64]. However, its participation in autophagy activation and the mechanisms involved in AMD has not been proven. Another potential use of trehalose is the capability to rescue glial cell dysfunction in mice and to induce autophagy in microglial cells, which degrades beta-amyloid peptides and regulates inflammation in mice [63–65]. For these reasons, we propose that stimulation of autophagy might be a potential therapeutic treatment to decrease the drusen burden, the presence of toxic amyloid peptides, and inflammation. It could be a target for the development of new drugs to retain degeneration processes and prevent AMD development. The pathologies associated with autophagy and AMD are intriguing in their many similarities. Whether one contributes to the other remains to be determined, but now that the reagents are available, experiments can be performed to address this question. This opens up a new area of discovery for AMD.

3. Cellular Mechanisms

3.1. Pathophysiology of Glial Cells in the Retina and Their Potential as Endogenous Stem Cells. In the central nervous system (CNS), the responses to any pathogenic insult include a prominent participation of glial cells [66]. Glia populations in the CNS consist primarily of microglia, the main resident immune cells, and macroglia, which include astrocytes and oligodendrocytes. These nonneuronal cell populations are intimately integrated into a healthy neuronal function, play important homeostatic roles maintaining the CNS environment, and play a key role in tissue responses to diseases, inflammation, and injury [67–70].

3.1.1. Microglia and Macroglia in the Retina. In the retina, microglia and macroglia are similarly represented. Retinal microglia are found distributed throughout the inner retina in a laminated pattern [71]. Retinal macroglia, consisting of astrocytes and Müller cells (MC), provide support to neuronal functions [72, 73]. As in the CNS and in the retina, both glial cell populations are involved in retinal responses to pathological conditions [74, 75].

While the astrocytic and microglial responses, in an injury context, have been thought to involve cross-talk between these two cell populations, the mechanisms and functional significance underlying these interactions are incompletely understood [76, 77]. MC as well as retinal microglia, similarly, depict marked cellular changes in different retinal pathologies, like AMD [78]. The responses of Müller and microglial cells to injury in the retina have been described as beneficial and deleterious processes [79, 80]. Nevertheless, it is not well known how these types of cells interact in the aftermath of retinal injury and how they shape in adaptive or nonadaptive overall response to the insult.

In healthy retinas, MC cells and microglia are in a constant two-way communication process, where MC signals inform microglia of neural activity and are then integrated to drive a behavioral response in microglia, according to their functions of regulation, synapse modulation, activity, and source of trophic factor release. For instance, neurotransmission between them is a candidate factor for regulating microglial behavior [81, 82]. Current evidence indicates

that microglial process motility is sensitive to excitatory and inhibitory forms of neurotransmission. The neural activity induces ATP release, which constitutes the direct signal to regulate the dynamic behavior of microglia [83]. In addition to the release of ATP induced by the activation of metabotropic glutamate receptor [84–86], Müller cells also release ATP by membrane stretch induced by osmotic perturbation as it occurs during neuronal activation [87–89]. In both cases, the ATP release from Müller glia is a Ca^{2+}-independent process. This was supported by experimental data which suggest that ATP is released from Müller cells in a SNARE-independent manner, probably via hemichannels [90–94].

Under pathological conditions, microglia react rapidly activating different processes, promoting an activated state in these cells [95, 96]. This microglia condition is the first step of injury response that precedes macroglial responses [97, 98]. The MG responses involve cellular hypertrophy, proliferation, and down- or upregulation of different genes and proteins suggesting that MG respond to microglial activation with an increase in cell-cell contacts and chemokine secretion, which facilitates and guides the radial migration of microglial cell in inflammatory responses in the retina [99]. This Müller glia-microglia response may underlie a mechanism in which an initial detection of injury in a particular locus by microglia may be augmented in magnitude and spatial scale to broaden the adaptive injury response, involving both cell types, to restore homeostasis.

3.1.2. Müller Glia-Like Stem Cells. MC are remarkably resilient to damage and respond to retinal injury and disease by changing their morphology, biochemistry, and physiology [100]. Depending on the severity of the damage, this response may include proliferative events. However, the triggers for proliferative gliosis are not well understood yet. Both proliferative and nonproliferative processes of injury include changes in the gene and protein expression pattern and are often associated with MC hypertrophy.

The nature of the Müller glia is clearly defined by structure, function, and gene expression patterns, providing the neuronal cells with structural, metabolic, and ion homeostasis and synaptic support.

However, it should be noted that normal MC have significant transcriptome overlap with retinal progenitors, and there seems to be a gradual transition in phenotype from neural progenitor to mature MC during early postnatal retinal development [101, 102]. Nevertheless, MC should not be referred to as stem cells, given that these glial cells do not function as stem cells in the retina under physiological conditions. Furthermore, MC have also been characterized as the "radial glia" of the retina based, at least in part, on their morphology and radially oriented processes that span the retina from outer to inner limiting membranes. Radial glia in the developing brain has been shown to function as a progenitor and to provide structural guides for the functions of migrating and differentiating neurons that MG do not provide during development, but can provide in a regenerating retina [103].

In the last two decades, MC cells have been considered a source of stem cells of retinal regeneration in fish, chicks, and rodents. The neurogenic potential of MC was first identified in a chicken retina [104] and thereafter in a rodent retina [105]. There is also evidence that MC from the primate retina can become progenitor-like cells in vitro [105] but the potential of these glial cells to regenerate neurons in an intact primate retina remains unexplored. In addition, mammalian MC can respond to injury, proliferate, and express genes associated with retinal stem cells but they do not function as retinal progenitors *in vivo* [106, 107]. Nonetheless, these characteristics suggest that, under the right conditions, MC might be induced to adopt the characteristics of a retinal progenitor that could be used for retinal neuron repair. Indeed, MC cell culture from humans has the capacity to generate both neurons and glial cells [108, 109] suggesting that human MC are capable of generating neurons under appropriate conditions and they could be able to participate in retinal repair and could be used for AMD treatment.

Experimental data showed the expression of neurogenic genes, such as Notch and Wnt, in MG culture that induce photoreceptor progenitors [110]. On the other hand, activation of FGF, Notch, Wnt, and Sonic-hedgehog signaling events induces a significant number of MC cells to reenter the cell cycle and display properties of retinal progenitors in the injured mammalian retina [111–115]. These results indicate that some part of the regenerative cellular program may be induced for retinal repair in patients with retinal degeneration, suggesting that overexpression of Achaete-Scute complex-like 1 (Ascl1) in MC culture induces a neurogenic state of MC, proliferation, and bipolar neuron generation. This has led to propose Ascl1 as a potential target for neurodegenerative therapy after disease or injury [116].

Apparently, microglia lack the neurogenic capacity observed in macroglia stimulated *in vitro* [117]. Nevertheless, it seems that activation of microglial reactivity is an important step in stimulating MC to dedifferentiate, proliferate, and become progenitor-like. It is likely that reactive microglia provide signals to modulate the reentry into the cell cycle [118]. Alternatively, the reactive microglia could suppress inhibitory signals that prevent the formation of MG progenitor-like cells [119]. The identity of the signals provided by reactive microglia to stimulate the formation of progenitor-like MG remains uncertain, but the participation of proinflammatory cytokines and components of the complement system is possible [118]. Another important factor for the neurogenic potential of MG might be the age of the organisms. Experimental studies have shown that MG from the mouse retina ex vivo express neurogenic factors and generate progeny expressing neuronal and glial markers in response to growth factor stimulation; nevertheless, the potential regenerative capacity of MG becomes limited with increasing mouse age [120].

In conclusion, the concept that the adult mammalian central nervous system contains populations of resident neural stem/progenitor cells was accepted two decades ago. Emerging evidence suggests that MG are dormant stem-like cells found throughout the retina and serve as a source of progenitor cells to regenerate retinal neurons after injury,

although barriers to regenerative cell survival, migration, integration, and safety concerns remain to overcome. Endogenous retinal repair is progressing rapidly, and the turn of the endogenous stem cells approach into viable therapy might be soon.

3.2. Cell Transplantation for Dry AMD, Functional RPE Cells, and Stem Cells. In the past decades, stem cell-based research has become a very promising area in biology. It has been acknowledged that terminally differentiated cells can be successfully reprogrammed [121, 122]. Furthermore, both systemic and local stem cell-based therapies have been used in various diseases with positive results.

While the wet AMD could be treated and fairly controlled by the use of drugs that target the VEGF receptor, the application of laser photocoagulation, and vitrectomy, among other surgical procedures, the dry AMD commonly demonstrates poor outcomes with conventional therapeutic approaches. Damage in dry AMD is mostly attributed to the accumulation of reactive oxygen species and peroxide, in addition to chronic inflammation in the retina that leads to apoptosis of the retinal pigment epithelial (RPE) cells, which gradually damage the photoreceptors [123, 124]. At the present, no treatment can reverse dry AMD; therefore, RPE replacement and retinal microenvironmental regulation represent potential new approaches for dry AMD (Figure 2(a)). [124, 125].

RPE cells can be divided into stem cell-derived RPE cells, fetal or adult RPE cells, iris pigment epithelial cells, and autologous RPE cells [126]. Autologous RPE transplantation as an alternative surgical approach has been extensively studied, generally performed by collecting the healthy RPE in the peripheral retina and transplanting them into the subretinal space at the diseased macula [125, 126]. Fully functional RPE cells can be generated from stem cells or somatic cells by spontaneous differentiation or cell reprogramming [125]. Moreover, RPE cells can be differentiated from human embryonic stem cells (hESCs) or human induced pluripotent stem cells (hiPSCs) [127, 128]. Both the hESC- and the iPSC-derived RPE cells display RPE-like morphology, express typical RPE markers, and have the ability to phagocytose photoreceptor segments [129].

Takahashi and Yamanaka and Yu et al. recently described the iPSCs, which consist of a line of cells reprogrammed by the use of Thomson factors or Yamanaka factors, showing morphological characteristics and differentiation abilities similar to those of the hESCs [130, 131].

In addition, in a study by Carr et al., human RPE cells could be generated from iPSCs by spontaneous differentiation or directed differentiation, as described by Kokkinaki et al. and Kamao et al. in their respective reports [129, 132, 133]. Similarly, Vaajasaari et al. successfully differentiated RPE-like cells from several human pluripotent stem cell lines without the use of animal cells or serum during the differentiation, demonstrating that the appearance of the first pigmented cells was relatively fast, both in hESC and hiPSC lines, varying from 10 to 21 days [134].

Transplantation of intact primary RPE cells has been previously attempted for the treatment of AMD. However, there are several advantages to the use of progeny obtained from hESCs as a source of replacement tissue for clinical studies (Figure 2(a)) [123]. These include *in vitro* differentiation that can be controlled to ensure optimum safety, purity, and potency before transplantation into the selected population of patients [123, 134].

Based on the preclinical data reported, the initial clinical trials, evaluating the performance of the transplantation of hESC-derived RPE cells to subretinal space, were phase I trials designed to test the safety and tolerability of grafted hESC-derived RPE cells in patients with either dry AMD or Stargardt's macular dystrophy [135]. The first data obtained from two of these clinical trials reported no signs of rejection, evident hyperproliferation, or tumorigenesis [136]. Moreover, Schwartz et al. [124] reported recently that within the confines of these phase 1 trials, the transplanted hESC-RPE cells appear to be well tolerated, without the presence of adverse intraocular or systemic events related to the cells [124]. There are, at this time, two other clinical trials using hESC-RPE cells, and both are designed to evaluate safety and tolerability of the injection and/or transplantation of MA09-RPE cells in the subretinal space of patients with dry AMD, recruiting patients aged 55 years and older, who will be receiving between 50,000 and 200,000 MA09-hRPE cells [137].

Conversely, stem cell generation may present challenges as well. Abnormal gene expression has been reported in some iPSCs, in which the T-cell-mediated immune response can be elicited even in syngeneic hosts [138]. In addition, another pending challenge would be the immunosenescence, a process that results in the progressive decline of the fine control in the immune system, including the loss of the CD28 receptor, increased interleukin-17 production, and an increase in the IL-6 receptor. All of these changes could not only annul the immune privilege but could also create an environment appropriate for cell death [139, 140].

Stem cell-based therapies have been the object of an extensive research, and great advances have recently been made towards the generation of stem cell transplantation techniques for the functional replacement of RPE cells and photoreceptors. However, it is crucial to assess the long-term safety and efficacy of the current hESC- or iPSC-based RPE transplantation approach in human patients. Adverse events related to the surgery have to be further studied, and large numbers of patients with microperimetry assessments in conjunction with optical coherence tomography (OCT) and autofluorescence estimation should be evaluated to provide more rigorous structure-function correlations.

Recent promising developments in the functional replacement of retinal RPE cells give rise to the expectation that clinical replacement of damaged retinal cells may be able to improve the outcomes of patients with retinal degenerative disease in the near future.

4. Conclusions

As we have seen, there are many factors that influence the origin and progression of AMD and the more relevant pathways associated with chronic retinal degeneration. This

opens new windows to provide multiple therapeutic targets for disease treatment. However, the design of new treatments must be very carefully done because most of the altered pathways in AMD are broadly redundant and may induce negative effects. Therefore, the new treatments should be carefully designed to cover different altered mechanisms at the same time. Looking towards the future of AMD therapy, there is an emerging paradigm that diverges from the normal approach of preventing retinal dysfunction and death. We should try to recover retinal health in spite of injury, rather than avoid and eliminate numerous overlapping insults. This kind of research should not be discarded in order to improve AMD prevention and treatment. Some experimental ideas are already being performed in our laboratory.

Finally, it is totally necessary to consider the financial burden that AMD represents due to its progressive nature, for example, loss of productivity, and related expenses like nursing homes, caretakers, and comorbidities, and currently available treatment is a significant challenge to any health system. Currently, it represents an excessive direct annual medical cost and, as the incidence raises with the passing of time, the annual cost will increase; for this reason, the finding of a new functional treatment for AMD becomes totally needful.

Disclosure

The funding organization had no role in the review design, data collection and analysis, decision to publish, or preparation of the manuscript. The authors state that they have full control of all primary data.

Conflicts of Interest

The authors have declared no conflict of interest.

Acknowledgments

This work was supported by generous funding from Asociación Para Evitar la Ceguera en México IAP. The authors thank Ann H. Milam Ph.D. for the permission to use their images shown in Figure 1.

References

[1] R. Velez-Montoya, S. C. N. Oliver, J. L. Olson, S. L. Fine, N. Mandava, and H. Quiroz-Mercado, "Current knowledge and trends in age-related macular degeneration: today's and future treatments," *Retina*, vol. 33, no. 8, pp. 1487–1502, 2013.

[2] S. M. Salvi, S. Akhtar, and Z. Currie, "Ageing changes in the eye," *Postgraduate Medical Journal*, vol. 82, no. 971, pp. 581–587, 2006.

[3] M. Ashraf and A. A. R. Souka, "Aflibercept in age-related macular degeneration: evaluating its role as a primary therapeutic option," *Eye*, vol. 31, no. 11, pp. 1523–1536, 2017.

[4] R. Velez-Montoya, S. C. N. Oliver, J. L. Olson, S. L. Fine, H. Quiroz-Mercado, and Naresh Mandava, "Current knowledge and trends in age-related macular degeneration: genetics, epidemiology, and prevention," *Retina*, vol. 34, no. 3, pp. 423–441, 2014.

[5] S. G. Jarrett and M. E. Boulton, "Consequences of oxidative stress in age-related macular degeneration," *Molecular Aspects of Medicine*, vol. 33, no. 4, pp. 399–417, 2012.

[6] S. M. Whitcup, A. Sodhi, J. P. Atkinson et al., "The role of the immune response in age-related macular degeneration," *International Journal of Inflammation*, vol. 2013, Article ID 348092, 10 pages, 2013.

[7] A. G. Marneros, J. Fan, Y. Yokoyama et al., "Vascular endothelial growth factor expression in the retinal pigment epithelium is essential for choriocapillaris development and visual function," *The American Journal of Pathology*, vol. 167, no. 5, pp. 1451–1459, 2005.

[8] A. K. Olsson, A. Dimberg, J. Kreuger, and L. Claesson-Welsh, "VEGF receptor signalling? In control of vascular function," *Nature Reviews Molecular Cell Biology*, vol. 7, no. 5, pp. 359–371, 2006.

[9] S. Koch, S. Tugues, X. Li, L. Gualandi, and L. Claesson-Welsh, "Signal transduction by vascular endothelial growth factor receptors," *Biochemical Journal*, vol. 437, no. 2, pp. 169–183, 2011.

[10] S. H. Byeon, S. C. Lee, S. H. Choi et al., "Vascular endothelial growth factor as an autocrine survival factor for retinal pigment epithelial cells under oxidative stress via the VEGF-R2/PI3K/Akt," *Investigative Ophthalmology & Visual Science*, vol. 51, no. 2, pp. 1190–1197, 2010.

[11] Y. Gu, G. Ke, L. Wang et al., "Silencing matrix metalloproteinases 9 and 2 inhibits human retinal microvascular endothelial cell invasion and migration," *Ophthalmic Research*, vol. 55, no. 2, pp. 70–75, 2015.

[12] K. Uno, I. A. Bhutto, D. S. McLeod, C. Merges, and G. A. Lutty, "Impaired expression of thrombospondin-1 in eyes with age related macular degeneration," *British Journal of Ophthalmology*, vol. 90, no. 1, pp. 48–54, 2006.

[13] I. A. Bhutto, K. Uno, C. Merges, L. Zhang, D. S. McLeod, and G. A. Lutty, "Reduction of endogenous angiogenesis inhibitors in Bruch's membrane of the submacular region in eyes with age-related macular degeneration," *Archives of Ophthalmology*, vol. 126, no. 5, pp. 670–678, 2008.

[14] A. Kauppinen, J. J. Paterno, J. Blasiak, A. Salminen, and K. Kaarniranta, "Inflammation and its role in age-related macular degeneration," *Cellular and Molecular Life Sciences*, vol. 73, no. 9, pp. 1765–1786, 2016.

[15] A. O. Garba and S. A. Mousa, "Bevasiranib for the treatment of wet, age-related macular degeneration," *Ophthalmology and Eye Diseases*, vol. 2, pp. 75–83, 2010.

[16] M. E. Kleinman, K. Yamada, A. Takeda et al., "Sequence- and target-independent angiogenesis suppression by siRNA via TLR3," *Nature*, vol. 452, no. 7187, pp. 591–597, 2008.

[17] G. C. Alghisi and C. Ruegg, "Vascular integrins in tumor angiogenesis: mediators and therapeutic targets," *Endothelium*, vol. 13, no. 2, pp. 113–135, 2006.

[18] A. Dong, B. Xie, J. Shen et al., "Oxidative stress promotes ocular neovascularization," *Journal of Cellular Physiology*, vol. 219, no. 3, pp. 544–552, 2009.

[19] T. Dentchev, A. H. Milam, V. M. Lee, J. Q. Trojanowski, and J. L. Dunaief, "Amyloid-β is found in drusen from some age-related macular degeneration retinas, but not in drusen from normal retinas," *Molecular Vision*, vol. 9, pp. 184–190, 2003.

[20] J. G. Hollyfield, V. L. Bonilha, M. E. Rayborn et al., "Oxidative damage-induced inflammation initiates age-related macular degeneration," *Nature Medicine*, vol. 14, no. 2, pp. 194–198, 2008.

[21] P. X. Shaw, T. Stiles, C. Douglas et al., "Oxidative stress, innate immunity, and age-related macular degeneration," *AIMS Molecular Science*, vol. 3, no. 2, pp. 196–221, 2016.

[22] B. Halliwell, "Reactive oxygen species in living systems: source, biochemistry, and role in human disease," *The American Journal of Medicine*, vol. 91, no. 3, pp. S14–S22, 1991.

[23] J. Iacovelli, G. C. Rowe, A. Khadka et al., "PGC-1α induces human RPE oxidative metabolism and antioxidant capacity," *Investigative Ophthalmology & Visual Science*, vol. 57, no. 3, pp. 1038–1051, 2016.

[24] D. Schmidl, G. Garhofer, and L. Schmetterer, "Nutritional supplements in age-related macular degeneration," *Acta Ophthalmologica*, vol. 93, no. 2, pp. 105–121, 2015.

[25] J. K. Leach, G. Van Tuyle, P. S. Lin, R. Schmidt-Ullrich, and R. B. Mikkelsen, "Ionizing radiation-induced, mitochondria-dependent generation of reactive oxygen/nitrogen," *Cancer Research*, vol. 61, no. 10, pp. 3894–3901, 2001.

[26] Y. Chen, J. Zeng, C. Zhao et al., "Assessing susceptibility to age-related macular degeneration with genetic markers and environmental factors," *Archives of Ophthalmology*, vol. 129, no. 3, pp. 344–351, 2011.

[27] Y. Saitoh, A. Miyanishi, H. Mizuno et al., "Super-highly hydroxylated fullerene derivative protects human keratinocytes from UV-induced cell injuries together with the decreases in intracellular ROS generation and DNA damages," *Journal of Photochemistry and Photobiology B: Biology*, vol. 102, no. 1, pp. 69–76, 2011.

[28] J. T. Handa, "How does the macula protect itself from oxidative stress?," *Molecular Aspects of Medicine*, vol. 33, no. 4, pp. 418–435, 2012.

[29] C. M. Chan, C. H. Huang, H. J. Li et al., "Protective effects of resveratrol against UVA-induced damage in ARPE19 cells," *International Journal of Molecular Sciences*, vol. 16, no. 3, pp. 5789–5802, 2015.

[30] K. Renganathan, Q. Ebrahem, A. Vasanji et al., "Carboxyethylpyrrole adducts, age-related macular degeneration and neovascularization," *Advances in Experimental Medicine and Biology*, vol. 613, pp. 261–267, 2008.

[31] J. Blasiak, J. Szaflik, and J. P. Szaflik, "Implications of altered iron homeostasis for age-related macular degeneration," *Frontiers in Bioscience*, vol. 16, no. 1, pp. 1551–1559, 2011.

[32] P. Hahn, A. H. Milam, and J. L. Dunaief, "Maculas affected by age-related macular degeneration contain increased chelatable iron in the retinal pigment epithelium and Bruch's membrane," *Archives of Ophthalmology*, vol. 121, no. 8, pp. 1099–1105, 2003.

[33] A. Catala, "Lipid peroxidation of membrane phospholipids in the vertebrate retina," *Frontiers in Bioscience*, vol. 3, pp. 52–60, 2011.

[34] P. X. Shaw, L. Zhang, M. Zhang et al., "Complement factor H genotypes impact risk of age-related macular degeneration by interaction with oxidized phospholipids," *Proceedings of the National Academy of Sciences of the United States of America*, vol. 109, no. 34, pp. 13757–13762, 2012.

[35] T. M. Jeitner, I. Voloshyna, and A. B. Reiss, "Oxysterol derivatives of cholesterol in neurodegenerative disorders," *Current Medicinal Chemistry*, vol. 18, no. 10, pp. 1515–1525, 2011.

[36] P. X. Shaw, S. Hörkkö, M. K. Chang et al., "Natural antibodies with the T15 idiotype may act in atherosclerosis, apoptotic clearance, and protective immunity," *The Journal of Clinical Investigation*, vol. 105, no. 12, pp. 1731–1740, 2000.

[37] L. V. Johnson, S. Ozaki, M. K. Staples, P. A. Erickson, and D. H. Anderson, "A potential role for immune complex pathogenesis in drusen formation," *Experimental Eye Research*, vol. 70, no. 4, pp. 441–449, 2000.

[38] P. P. Karunadharma, C. L. Nordgaard, T. W. Olsen, and D. A. Ferrington, "Mitochondrial DNA damage as a potential mechanism for age-related macular degeneration," *Investigative Ophthalmology & Visual Science*, vol. 51, no. 11, pp. 5470–5479, 2010.

[39] S. K. Mitter, C. Song, X. Qi et al., "Dysregulated autophagy in the RPE is associated with increased susceptibility to oxidative stress and AMD," *Autophagy*, vol. 10, no. 11, pp. 1989–2005, 2014.

[40] T. C. Ho, Y. C. Yang, H. C. Cheng et al., "Activation of mitogen-activated protein kinases is essential for hydrogen peroxide -induced apoptosis in retinal pigment epithelial cells," *Apoptosis*, vol. 11, no. 11, pp. 1899–1908, 2006.

[41] N. L. Wu, J. Y. Fang, M. Chen, C. J. Wu, C. C. Huang, and C. F. Hung, "Chrysin protects epidermal keratinocytes from UVA- and UVB-induced damage," *Journal of Agricultural and Food Chemistry*, vol. 59, no. 15, pp. 8391–8400, 2011.

[42] N. B. Javitt and J. C. Javitt, "The retinal oxysterol pathway: a unifying hypothesis for the cause of age-related macular degeneration," *Current Opinion in Ophthalmology*, vol. 20, no. 3, pp. 151–157, 2009.

[43] Age-Related Eye Disease Study Research Group, J. P. SanGiovanni, E. Y. Chew et al., "The relationship of dietary carotenoid and vitamin A, E, and C intake with age-related macular degeneration in a case-control study: AREDS report no. 22," *Archives of Ophthalmology*, vol. 125, no. 9, pp. 1225–1232, 2007.

[44] Writing Group for the AREDS2 Research Group, D. E. Bonds, M. Harrington et al., "Effect of long-chain ω-3 fatty acids and lutein + zeaxanthin supplements on cardiovascular outcomes: results of the age-related eye disease study 2 (AREDS2) randomized clinical trial," *JAMA Internal Medicine*, vol. 174, no. 5, pp. 763–771, 2014.

[45] N. Nagai, S. Kubota, K. Tsubota, and Y. Ozawa, "Resveratrol prevents the development of choroidal neovascularization by modulating AMP-activated protein kinase in macrophages and other cell types," *The Journal of Nutritional Biochemistry*, vol. 25, no. 11, pp. 1218–1225, 2014.

[46] C. Bola, H. Bartlett, and F. Eperjesi, "Resveratrol and the eye: activity and molecular mechanisms," *Graefe's Archive for Clinical and Experimental Ophthalmology*, vol. 252, no. 5, pp. 699–713, 2014.

[47] S. Richer, S. Patel, S. Sockanathan, L. J. Ulanski 2nd, L. Miller, and C. Podella, "Resveratrol based oral nutritional supplement produces long-term beneficial effects on structure and visual function in human patients," *Nutrients*, vol. 6, no. 10, pp. 4404–4420, 2014.

[48] Y. D. Sun, Y. D. Dong, R. Fan, L. L. Zhai, Y. L. Bai, and L. H. Jia, "Effect of (R)-α-lipoic acid supplementation on serum lipids and antioxidative ability in patients with age-related

macular degeneration," *Annals of Nutrition & Metabolism*, vol. 60, no. 4, pp. 293–297, 2012.

[49] F. M. Menzies and A. Fleming, "Compromised autophagy and neurodegenerative diseases," *Nature Reviews Neuroscience*, vol. 16, no. 6, pp. 345–357, 2015.

[50] I. Milisav, D. Suput, and S. Ribaric, "Unfolded protein response and macroautophagy in Alzheimer's, Parkinson's and prion diseases," *Molecules*, vol. 20, no. 12, pp. 22718–22756, 2015.

[51] K. E. Larsen and D. Sulzer, "Autophagy in neurons: a review," *Histology and Histopathology*, vol. 17, no. 3, pp. 897–908, 2002.

[52] M. Komatsu, S. Waguri, T. Chiba et al., "Loss of autophagy in the central nervous system causes neurodegeneration in mice," *Nature*, vol. 441, no. 7095, pp. 880–884, 2006.

[53] M. Mehrpour, A. Esclatine, I. Beau, and P. Codogno, "Overview of macroautophagy regulation in mammalian cells," *Cell Research*, vol. 20, no. 7, pp. 748–762, 2010.

[54] L. Galluzzi, J. M. Bravo-San Pedro, K. Blomgren, and G. Kroemer, "Autophagy in acute brain injury," *Nature Reviews Neuroscience*, vol. 17, no. 8, pp. 467–484, 2016.

[55] G. Petrovski, R. Albert, K. Kaarniranta et al., "Autophagy in the eye: a double-edged sword," in *Autophagy: Principles, Regulation and Roles in Disease, Chapter: 8*pp. 157–180, Nova Publishers, Hauppauge, New York.

[56] J. Liu, D. A. Copland, S. Theodoropoulou et al., "Impairing autophagy in retinal pigment epithelium leads to inflammasome activation and enhanced macrophage-mediated angiogenesis," *Scientific Reports*, vol. 6, article 20639, 2016.

[57] L. F. Hernández-Zimbrón, E. Gorostieta-Salas, M. L. Díaz-Hung, R. Pérez-Garmendia, G. Gevorkian, and H. Quiroz-Mercado, "Beta Amyloid Peptides: Extracellular and Intracellular Mechanisms of Clearance in Alzheimer's Disease," in *Update on Dementia*, D. Moretti, Ed., 2016.

[58] J. A. Ratnayaka, L. C. Serpell, and A. J. Lotery, "Dementia of the eye: the role of amyloid beta in retinal degeneration," *Eye*, vol. 29, no. 8, pp. 1013–1026, 2015.

[59] Y. Yonekawa, J. Miller, and I. Kim, "Age-related macular degeneration: advances in management and diagnosis," *Journal of Clinical Medicine*, vol. 4, no. 2, pp. 343–359, 2015.

[60] V. Soura, M. Stewart-Parker, T. L. Williams et al., "Visualization of co localizationin Aβ42-administered neuroblastoma cells reveals lysosome damage and autophagosome accumulationrelated to cell death," *Biochemical Journal*, vol. 441, no. 2, pp. 579–590, 2012.

[61] A. Salminen, K. Kaarniranta, A. Kauppinen et al., "Impaired autophagy and APP processing in Alzheimer's disease: the potential role of Beclin 1 interactome," *Progress in Neurobiology*, vol. 106–107, pp. 33–54, 2013.

[62] S. K. Mitter, H. V. Rao, X. Qi et al., "Autophagy in the retina: a potential role in age-related macular degeneration," in *Retinal Degenerative Diseases. Advances in Experimental Medicine and Biology*, M. LaVail, J. Ash, R. Anderson, J. Hollyfield and C. Grimm, Eds., vol. 723, Springer, Boston, MA, USA, 2012.

[63] J. Du, Y. Liang, F. Xu, B. Sun, and Z. Wang, "Trehalose rescues Alzheimer's disease phenotypes in APP/PS1 transgenic mice," *Journal of Pharmacy and Pharmacology*, vol. 65, no. 12, pp. 1753–1756, 2013.

[64] A. Hill-Bator, M. Misuik-Hojlo, K. Marycz, and J. Grzesiak, "Trehalose based eye drops preserve viability and functionality of cultured human corneal epithelial cells during dessication," *BioMed Research International*, vol. 2014, Article ID 292139, 8 pages, 2014.

[65] J. Cejkova and C. Cejka, "Trehalose–current applications in ophthalmology and future perspectives," *Global Journal For Research Analysis*, vol. 4, no. 8, 2015.

[66] A. Buffo, C. Rolando, and S. Ceruti, "Astrocytes in the damaged brain: molecular and cellular insights into their reactive response and healing potential," *Biochemical Pharmacology*, vol. 79, no. 2, pp. 77–89, 2010.

[67] U. K. Hanisch and H. Kettenmann, "Microglia: active sensor and versatile effector cells in the normal and pathologic brain," *Nature Neuroscience*, vol. 10, no. 11, pp. 1387–1394, 2007.

[68] H. Wake, A. J. Moorhouse, and J. Nabekura, "Functions of microglia in the central nervous system - beyond the immune response," *Neuron Glia Biology*, vol. 7, no. 01, pp. 47–53, 2011.

[69] R. M. Ransohoff and A. E. Cardona, "The myeloid cells of the central nervous system parenchyma," *Nature*, vol. 468, pp. 253–262, 2011.

[70] A. M. Santos, R. Calvente, M. Tassi et al., "Embryonic and postnatal development of microglial cells in the mouse retina," *The Journal of Comparative Neurology*, vol. 506, no. 2, pp. 224–239, 2008.

[71] A. Bringmann, T. Pannicke, J. Grosche et al., "Müller cells in the healthy and diseased retina," *Progress in Retinal and Eye Research*, vol. 25, no. 4, pp. 397–424, 2006.

[72] A. Bringmann, I. Iandiev, T. Pannicke et al., "Cellular signaling and factors involved in Müller cell gliosis: neuroprotective and detrimental effects," *Progress in Retinal and Eye Research*, vol. 28, no. 6, pp. 423–451, 2009.

[73] E. A. Newman and K. R. Zahs, "Modulation of neuronal activity by glial cells in the retina," *Journal of Neuroscience*, vol. 18, no. 11, pp. 4022–4028, 1998.

[74] A. Bringmann and P. Wiedemann, "Müller glial cells in retinal disease," *Ophthalmologica*, vol. 227, no. 1, pp. 1–19, 2012.

[75] D. Zhang, X. Hu, L. Qian, J. P. O'Callaghan, and J. S. Hong, "Astrogliosis in CNS pathologies: is there a role for microglia?," *Molecular Neurobiology*, vol. 41, no. 2-3, pp. 232–241, 2010.

[76] W. Liu, Y. Tang, and J. Feng, "Cross talk between activation of microglia and astrocytes in pathological conditions in the central nervous system," *Life Sciences*, vol. 89, no. 5-6, pp. 141–146, 2011.

[77] T. Langmann, "Microglia activation in retinal degeneration," *Journal of Leukocyte Biology*, vol. 81, no. 6, pp. 1345–1351, 2007.

[78] H. Xu, M. Chen, and J. V. Forrester, "Para-inflammation in the aging retina," *Progress in Retinal and Eye Research*, vol. 28, no. 5, pp. 348–368, 2009.

[79] M. Karlstetter, S. Ebert, and T. Langman, "Microglia in the healthy and degenerating retina: insights from novel mouse models," *Immunobiology*, vol. 215, no. 9-10, pp. 685–691, 2010.

[80] A. M. Fontainhas, M. Wang, K. J. Liang et al., "Microglial morphology and dynamic behavior is regulated by ionotropic glutamatergic and GABAergic neurotransmission," *PLoS One*, vol. 6, no. 1, article e15973, 2011.

[81] T. Weissman, S. C. Noctor, B. K. Clinton, L. S. Honig, and A. R. Kriegstein, "Neurogenic radial glial cells in reptile, rodent and human: from mitosis to migration," *Cerebral Cortex*, vol. 13, no. 6, pp. 550–559, 2003.

[82] Y. Li, X. F. Du, C. S. Liu, Z. L. Wen, and J. L. Du, "Reciprocal regulation between resting microglial dynamics and neuronal activity in vivo," *Developmental Cell*, vol. 23, no. 6, pp. 1189–1202, 2012.

[83] D. Davalos, J. Grutzendler, G. Yang et al., "ATP mediates rapid microglial response to local brain injury *in vivo*," *Nature Neuroscience*, vol. 8, no. 6, pp. 752–758, 2005.

[84] O. Uckermann, A. Wolf, F. Kutzera et al., "Glutamate release by neurons evokes a purinergic inhibitory mechanism of osmotic glial cell swelling in the rat retina: activation by neuropeptide Y," *Journal of Neuroscience Research*, vol. 83, no. 4, pp. 538–550, 2006.

[85] A. Wurm, T. Pannicke, I. Iandiev, P. Wiedemann, A. Reichenbach, and A. Bringmann, "The developmental expression of K^+ channels in retinal glial cells is associated with a decrease of osmotic cell swelling," *Glia*, vol. 54, no. 5, pp. 411–423, 2006.

[86] A. Wurm, T. Pannicke, P. Wiedemann, A. Reichenbach, and A. Bringmann, "Glial cell-derived glutamate mediates autocrine cell volume regulation in the retina: activation by VEGF," *Journal of Neurochemistry*, vol. 104, pp. 386–399, 2008.

[87] E. A. Newman, "Propagation of intercellular calcium waves in retinal astrocytes and Müller cells," *The Journal of Neuroscience*, vol. 21, no. 7, pp. 2215–2223, 2001.

[88] E. A. Newman, "Glial cell inhibition of neurons by release of ATP," *The Journal of Neuroscience*, vol. 23, no. 5, pp. 1659–1666, 2003.

[89] A. V. Dmitriev, V. I. Govardovskii, H. N. Schwahn, and R. H. Steinberg, "Light-induced changes of extracellular ions and volume in the isolated chick retina-pigment epithelium preparation," *Visual Neuroscience*, vol. 16, no. 6, pp. 1157–1167, 1999.

[90] L. Wagner, T. Pannicke, V. Rupprecht et al., "Suppression of SNARE-dependent exocytosis in retinal glial cells and its effect on ischemia-induced neurodegeneration," *Glia*, vol. 65, no. 7, pp. 1059–1071, 2017.

[91] C. E. Stout, J. L. Costantin, C. C. G. Naus, and A. C. Charles, "Intercellular calcium signaling in astrocytes via ATP release through connexin hemichannels," *The Journal of Biological Chemistry*, vol. 277, no. 12, pp. 10482–10488, 2002.

[92] Y. Pankratov, U. Lalo, A. Verkhratsky, and R. A. North, "Vesicular release of ATP at central synapses," *Pflügers Archiv*, vol. 452, no. 5, pp. 589–597, 2006.

[93] G. Dahl and S. Locovei, "Pannexin: to gap or not to gap, is that a question?," *IUBMB Life*, vol. 58, no. 7, pp. 409–419, 2006.

[94] R. Iglesias, G. Dahl, F. Qiu, D. C. Spray, and E. Scemes, "Pannexin 1: the molecular substrate of astrocyte "hemichannels"," *The Journal of Neuroscience*, vol. 29, no. 21, pp. 7092–7097, 2009.

[95] A. Nimmerjahn, F. Kirchhoff, and F. Helmchen, "Resting microglial cells are highly dynamic surveillants of brain parenchyma in vivo," *Science*, vol. 308, no. 5726, pp. 1314–1318, 2005.

[96] J. E. Lee, K. J. Liang, R. N. Fariss, and W. T. Wong, "Ex vivo dynamic imaging of retinal microglia using time-lapse confocal microscopy," *Investigative Ophthalmology & Visual Science*, vol. 49, no. 9, pp. 4169–4176, 2008.

[97] M. B. Graeber and G. W. Kreutzberg, "Delayed astrocyte reaction following facial nerve axotomy," *Journal of Neurocytology*, vol. 17, no. 2, pp. 209–220, 1988.

[98] M. Sawada, A. Suzumura, and T. Marunouchi, "Cytokine network in the central nervous system and its roles in growth and differentiation of glial and neuronal cells," *International Journal of Developmental Neuroscience*, vol. 13, no. 3-4, pp. 253–264, 1995.

[99] V. Balasingam, K. Dickson, A. Brade, and V. W. Yong, "Astrocyte reactivity in neonatal mice: apparent dependence on the presence of reactive microglia/macrophages," *Glia*, vol. 18, no. 1, pp. 11–26, 1996.

[100] M. Wang, W. Ma, L. Zhao, R. N. Fariss, and W. T. Wong, "Adaptive Müller cell responses to microglial activation mediate neuroprotection and coordinate inflammation in the retina," *Journal of Neuroinflammation*, vol. 8, no. 1, p. 173, 2011.

[101] T. Gohdo, H. Ueda, S. Ohno, H. Iijima, and S. Tsukahara, "Heat shock protein 70 expression increased in rabbit Müller cells in the ischemia-reperfusion model," *Ophthalmic Research*, vol. 33, no. 5, pp. 298–302, 2001.

[102] S. Blackshaw, S. Harpavat, J. Trimarchi et al., "Genomic analysis of mouse retinal development," *PLoS Biology*, vol. 2, no. 9, article E247, 2004.

[103] K. Roesch, A. P. Jadhav, J. M. Trimarchi et al., "The transcriptome of retinal Müller glial cells," *The Journal of Comparative Neurology*, vol. 509, no. 2, pp. 225–238, 2008.

[104] T. Wissman, S. C. Noctor, B. K. Clinton, L. S. Honig, and A. R. Kriegstein, "Neurogenic radial glial cells in reptile, rodent and human: from mitosis to migration," *Cerebral Cortex*, vol. 13, no. 6, pp. 550–559, 2003.

[105] A. J. Fischer and T. A. Reh, "Müller glia are a potential source of neural regeneration in the postnatal chicken retina," *Nature Neuroscience*, vol. 4, no. 3, pp. 247–252, 2001.

[106] S. Ooto, T. Akagi, R. Kageyama et al., "Potential for neural regeneration after neurotoxic injury in the adult mammalian retina," *Proceedings of the National Academy of Sciences of the United States of America*, vol. 101, no. 37, pp. 13654–13659, 2004.

[107] J. M. Lawrence, S. Singhal, B. Bhatia et al., "MIO-M1 cells and similar Müller glial cell lines derived from adult human retina exhibit neural stem cell characteristics," *Stem Cells*, vol. 25, no. 8, pp. 2033–2043, 2007.

[108] A. P. Jadhav, K. Roesch, and C. L. Cepko, "Development and neurogenic potential of Müller glial cells in the vertebrate retina," *Progress in Retinal and Eye Research*, vol. 28, no. 4, pp. 249–262, 2009.

[109] H. Jayaram, M. F. Jones, K. Eastlake et al., "Transplantation of photoreceptors derived from human Müller glia restore rod function in the P23H rat," *Stem Cells Translational Medicine*, vol. 3, no. 3, pp. 323–333, 2014.

[110] S. G. Giannelli, G. C. Demontis, G. Pertile, P. Rama, and V. Broccoli, "Adult human Müller glia cells are a highly efficient source of rod photoreceptors," *Stem Cells*, vol. 29, no. 2, pp. 344–356, 2011.

[111] S. Hayes, B. R. Nelson, B. Buckingham, and T. A. Reh, "Notch signaling regulates regeneration in the avian retina," *Developmental Biology*, vol. 312, no. 1, pp. 300–311, 2007.

[112] J. Wan, H. Zheng, H. L. Xiao, Z. J. She, and G. M. Zhou, "Sonic hedgehog promotes stem-cell potential of Müller glia in the mammalian retina," *Biochemical and Biophysical Research Communications*, vol. 363, no. 2, pp. 347–354, 2007.

[113] C. B. Del Debbio, S. Balasubramanian, S. Parameswaran, A. Chaudhuri, F. Qiu, and I. Ahmad, "Notch and Wnt signaling mediated rod photoreceptor regeneration by Müller cells in adult mammalian retina," *PLoS One*, vol. 5, no. 8, article e12425, 2010.

[114] F. Osakada and M. Takahashi, "Drug development targeting the glycogen synthase kinase-3β (GSK-3β)-mediated signal transduction pathway: targeting the Wnt pathway and transplantation therapy as strategies for retinal repair," *Journal of Pharmacological Sciences*, vol. 109, no. 2, pp. 168–173, 2009.

[115] D. Sanges, N. Romo, G. Simonte et al., "Wnt/β-catenin signaling triggers neuron reprogramming and regeneration in the mouse retina," *Cell Reports*, vol. 4, no. 2, pp. 271–286, 2013.

[116] J. Pollak, M. S. Wilken, Y. Ueki et al., "ASCL1 reprograms mouse Müller glia into neurogenic retinal progenitors," *Development*, vol. 140, no. 12, pp. 2619–2631, 2013.

[117] A. V. Das, K. B. Mallya, X. Zhao et al., "Neural stem cell properties of Müller glia in the mammalian retina: regulation by Notch and Wnt signaling," *Developmental Biology*, vol. 299, no. 1, pp. 283–302, 2006.

[118] A. J. Fischer, C. Zelinka, D. Gallina, M. A. Scott, and L. Todd, "Reactive microglia and macrophage facilitate the formation of Müller glia-derived retinal progenitors," *Glia*, vol. 62, no. 10, pp. 1608–1628, 2014.

[119] C. P. Zelinka, M. A. Scott, L. Volkov, and A. J. Fischer, "The reactivity, distribution and abundance of non-astrocytic inner retinal glial (NIRG) cells are regulated by microglia, acute damage, and IGF1," *PLoS One*, vol. 7, no. 9, article e44477, 2012.

[120] K. Loffler, P. Schafer, M. Volkner, T. Holdt, and M. O. Karl, "Age-dependent müller glia neurogenic competence in the mouse retina," *Glia*, vol. 63, no. 10, pp. 1809–1824, 2015.

[121] F. Parmeggiani, M. R. Romano, C. Costagliola et al., "Mechanism of inflammation in age-related macular degeneration," *Mediators of Inflammation*, vol. 2012, Article ID 546786, 16 pages, 2012.

[122] Y. Mu, M. Zhao, and G. Su, "Stem cell-based therapies for age-related macular degeneration: current status and prospects," *International Journal of Clinical and Experimental Medicine*, vol. 7, no. 11, pp. 3843–3852, 2014.

[123] S. D. Schwartz, J. P. Hubschman, G. Heilwell et al., "Embryonic stem cell trials for macular degeneration: a preliminary report," *The Lancet*, vol. 379, no. 9817, pp. 713–720, 2012.

[124] S. D. Schwartz, G. Tan, and H. Hosseini, "Subretinal transplantation of embryonic stem cell–derived retinal pigment epithelium for the treatment of macular degeneration: an assessment at 4 years," *Investigative Opthalmology & Visual Science*, vol. 57, no. 5, pp. ORSFc1–ORSFc9, 2016.

[125] Y. Dang, C. Zhang, and Y. Zhu, "Stem cell therapies for age-related macular degeneration: the past, present, and future," *Clinical Interventions in Aging*, vol. 10, pp. 255–264, 2015.

[126] C. I. Falkner-Radler, I. Krebs, C. Glittenberg et al., "Human retinal pigment epithelium (RPE) transplantation: outcome after autologous RPE-choroid sheet and RPE cell-suspension in a randomised clinical study," *British Journal of Ophthalmology*, vol. 95, no. 3, pp. 370–375, 2011.

[127] M. S. Cho, S. J. Kim, S. Y. Ku et al., "Generation of retinal pigment epithelial cells from human embryonic stem cell-derived spherical neural masses," *Stem Cell Research*, vol. 9, no. 2, pp. 101–109, 2012.

[128] D. E. Buchholz, S. T. Hikita, T. J. Rowland et al., "Derivation of Functional Retinal Pigmented Epithelium from Induced Pluripotent Stem Cells," *Stem Cells*, vol. 27, no. 10, pp. 2427–2434, 2009.

[129] M. Kokkinaki, N. Sahibzada, and N. Golestaneh, "Human induced pluripotent stem-derived retinal pigment epithelium (RPE) cells exhibit ion transport, membrane potential, polarized vascular endothelial growth factor secretion, and gene expression pattern similar to native RPE," *Stem Cells*, vol. 29, no. 5, pp. 825–835, 2011.

[130] K. Takahashi and S. Yamanaka, "Induction of pluripotent stem cells from mouse embryonic and adult fibroblast cultures by defined factors," *Cell*, vol. 126, no. 4, pp. 663–676, 2006.

[131] J. Yu, M. A. Vodyanik, K. Smuga-Otto et al., "Induced pluripotent stem cell lines derived from human somatic cells," *Science*, vol. 318, no. 5858, pp. 1917–1920, 2007.

[132] A. J. Carr, A. A. Vugler, S. T. Hikita et al., "Protective effects of human iPS-derived retinal pigment epithelium cell transplantation in the retinal dystrophic rat," *PLoS One*, vol. 4, no. 12, article e8152, 2009.

[133] H. Kamao, M. Mandai, S. Okamoto et al., "Characterization of human induced pluripotent stem cell-derived retinal pigment epithelium cell sheets aiming for clinical application," *Stem Cell Reports*, vol. 2, no. 2, pp. 205–218, 2014.

[134] H. Vaajasaari, T. Ilmarinen, K. Juuti-Uusitalo et al., "Toward the defined and xeno-free differentiation of functional human pluripotent stem cell-derived retinal pigment epithelial cells," *Molecular Vision*, vol. 17, pp. 558–575, 2011.

[135] S. Becker, H. Jayaram, and G. A. Limb, "Recent advances towards the clinical application of stem cells for retinal regeneration," *Cells*, vol. 1, no. 4, pp. 851–873, 2012.

[136] S. D. Schwartz, C. D. Regillo, B. L. Lam et al., "Human embryonic stem cell-derived retinal pigment epithelium in patients with age-related macular degeneration and Stargardt's macular dystrophy: follow-up of two open-label phase 1/2 studies," *The Lancet*, vol. 385, no. 9967, pp. 509–516, 2015.

[137] J. Hanus, F. Zhao, and S. Wang, "Current therapeutic developments in atrophic age-related macular degeneration," *British Journal of Ophthalmology*, vol. 100, no. 1, pp. 122–127, 2016.

[138] T. Zhao, Z. N. Zhang, Z. Rong, and Y. Xu, "Immunogenicity of induced pluripotent stem cells," *Nature*, vol. 474, no. 7350, pp. 212–215, 2011.

[139] L. Wei, B. Liu, J. Tuo et al., "Hypomethylation of the *IL17RC* promoter associates with age-related macular degeneration," *Cell Reports*, vol. 2, no. 5, pp. 1151–1158, 2012.

[140] X. Cao, D. Shen, M. M. Patel et al., "Macrophage polarization in the maculae of age-related macular degeneration: a pilot study," *Pathology International*, vol. 61, no. 9, pp. 528–535, 2011.

Hindawi
Oxidative Medicine and Cellular Longevity
Volume 2017, Article ID 6926485, 12 pages
https://doi.org/10.1155/2017/6926485

Research Article

Zinc Protects Oxidative Stress-Induced RPE Death by Reducing Mitochondrial Damage and Preventing Lysosome Rupture

Dinusha Rajapakse, Tim Curtis, Mei Chen, and Heping Xu

Centre for Experimental Medicine, School of Medicine, Dentistry & Biomedical Sciences, Queen's University Belfast, 97 Lisburn Road, Belfast BT9 7BL, UK

Correspondence should be addressed to Heping Xu; heping.xu@qub.ac.uk

Received 21 July 2017; Revised 2 October 2017; Accepted 3 October 2017; Published 14 November 2017

Academic Editor: Liang-Jun Yan

Zinc deficiency is known to increase the risk of the development of age-related macular degeneration (AMD), although the underlying mechanism remains poorly defined. In this study, we investigated the effect of zinc on retinal pigment epithelium (RPE) survival and function under oxidative conditions. Zinc level was 5.4 μM in normal culture conditions (DMEM/F12 with 10% FCS) and 1.5 μM in serum-free medium (DMEM/F12). Under serum-free culture conditions, the treatment of RPE cells with oxidized photoreceptor outer segment (oxPOS) significantly increased intracellular ROS production, reduced ATP production, and promoted RPE death compared to oxPOS-treated RPE under normal culture condition. Serum deprivation also reduced RPE phagocytosis of oxPOS and exacerbated oxidative insult-induced cathepsin B release from lysosome, an indicator of lysosome rupture. The addition of zinc in the serum-free culture system dose dependently reduced ROS production, recovered ATP production, and reduced oxidative stress- (oxPOS- or 4-HNE) induced cell death. Zinc supplementation also reduced oxidative stress-mediated cathepsin B release in RPE cells. Our results suggest that zinc deficiency sensitizes RPE cells to oxidative damage, and zinc supplementation protects RPE cells from oxidative stress-induced death by improving mitochondrial function and preventing lysosome rupture.

1. Introduction

Zinc is the second most prominent trace element in the human body with the majority stored in skeletal muscle and the rest distributed between the bone, liver, skin, and other tissues [1]. In the circulation, around 80% of zinc is loosely bound to albumin. When circulating levels drop, gastrointestinal absorption of dietary zinc increases to maintain systemic homeostasis. In cells, zinc is distributed within the cytoplasm, nucleus, and membrane. The majority of cellular zinc is bound with proteins and sequestered into organelles resulting in low levels of labile or free zinc. Labile zinc, defined as zinc not bound to proteins, varies among different cellular compartments with 0.14 pM in the mitochondria, 0.9 pM in the endoplasmic reticulum (ER), and 0.2 pM in the Golgi [1]. Zinc plays an important structural role in proteins by the formation of the zinc finger motif [2]. It can also be released extracellularly and functions as a signaling molecule by binding to cell surface receptors to trigger second messenger responses [3]. In addition, intracellular zinc can modulate cell signaling by targeting various kinase-dependent pathways, including the MAPK and PKC pathways [4].

Zinc is the most abundant trace metal present in the retina [5] and is found mainly in the retinal pigment epithelium (RPE) and photoreceptor layers as well as in organelles including Golgi apparatus, melanosomes, and lysosomes [6–8]. Apart from its role as a cofactor for several antioxidant enzymes [9], zinc is also involved in the visual cycle through regulation of retinol dehydrogenase and rhodopsin regeneration [10] and can metabolize ingested photoreceptor outer segments (POS) in RPE cells [11]. In normal conditions, cellular zinc concentration is tightly regulated within a concentration range that is nontoxic. Cells maintain zinc homeostasis by regulating zinc-sequestering proteins such as metallothioneins and/or altering the expression of zinc

transporter proteins which transport zinc between extracellular and intracellular regions and within intracellular compartments [12]. Zinc deficiency occurs in a number of pathologies, including epilepsy, Alzheimer's disease, and age-related macular degeneration (AMD) [13]. This is thought to arise due to the failure of regulating proteins that are important for zinc homeostasis or underlying dietary zinc deficiency [13]. Inadequate levels of serum zinc have been frequently observed in patients with age-related disease [14]. With regard to AMD, ageing RPE cells display abundant lipofuscin accumulation, while the content of zinc-containing melanosomes decreases [15]. Melanosomes are the primary zinc reservoir in pigmented tissues, and it is reported that zinc deficit is most common in elderly populations who are prone to AMD pathogenesis [16]. Erie et al. [17] demonstrated a 24% reduction in the zinc level of the RPE-choroid complex in donors with AMD compared with non-AMD donors, suggesting that zinc homeostasis may be implicated in AMD and retinal health. Indeed, zinc supplementation in AMD patients has demonstrated a beneficial effect in terms of AMD progression [18]. At a mechanistic level, zinc deficiency has been shown to promote lipid peroxidation which subsequently impairs RPE cell phagocytic and lysosomal activity [19]. Such changes may be linked to the accumulation of lipofuscin in RPE cells seen during aging. Zinc-deficient animals, for example, exhibit increased formation of lipofuscin through a pathway involving elevated oxidative stress and incomplete digestion of POS in the lysosomes of the RPE [16]. Failure to control zinc homeostasis has also been suggested to contribute to the aggregation of immunoproteins such as complement factor H (CFH) found in sub-RPE deposits in patients with AMD [20]. The mechanism by which zinc deficiency may contribute to the development of AMD, however, has yet to be fully elucidated.

Although zinc deficiency is a potential contributing factor to the progression of AMD, excessive intracellular zinc can also result in RPE cytotoxicity [21], for example, Wood and Osborne showed that 18 μM zinc decreased human RPE viability by 50%, which was reversed following supplementation with metabolic substrates and antioxidants. These findings are of interest because the in vivo level of zinc in RPE is usually high under normal conditions, and the cells do not appear to undergo significant oxidative damage. Tate et al. [22] showed that RPE cells cultured under low-zinc conditions are more susceptible to oxidative insults and that SOD activity increased in low-zinc medium in response to oxidative stressors. Other studies have also shown that zinc treatment can limit RPE cell oxidative stress induced by cadmium, a metal ion in cigarette smoke [23, 24]. Clearly, the role of zinc in RPE biology and function warrants further exploration.

We have shown previously that continuous exposure of POS and oxidized POS (oxPOS) results in a buildup of ROS in RPE cells, yet cells remained healthy and functional [25], suggesting that there are components within RPE enabling homeostasis despite this insult. The aim of this study was to determine the role of zinc in maintaining RPE cell homeostasis in cultures when exposed to low levels of oxidative insults similar to those seen with aging and age-related diseases (e.g., oxPOS or a low concentration of 4-HNE).

2. Materials and Methods

2.1. In Vitro RPE Cell Culture. ARPE19 cells were purchased from ATCC (CRL-2302, Middlesex, UK). RPE cells were cultured in complete Dulbecco's Modified Eagle Medium/F12 (DMEM/F12) medium containing 10% fetal calf serum (FCS) (Gibco Life Technology, UK) and 100 μg/mL Primocin (Invitrogen, San Diego, California, USA). Cells were maintained in an incubator at 37°C with 5% CO_2 using T25 and T75 tissue culture flasks or tissue culture plates (Nunc™ Surface, Leicestershire, UK). The phenotype of RPE cells was confirmed by pancytokeratin staining. Passages 5–10 cells were used in the study.

2.2. Preparation of Photoreceptor Outer Segments. POS were isolated from bovine eyes using the method described previously by Chen et al. [26]. In brief, 20 bovine retinas were placed in 20 ml homogenizing solution made up of 20% *w*/*v* sucrose, 20 mM Tris-acetate pH 7.2, 2 mM MgCl2, 10 mM glucose, and 5 mM taurine. The suspension was shaken for 1 min and filtered through a 100 mm cell strainer (BD, Oxford, UK) to remove tissue debris. The suspension was then carefully layered on 25–60% *w*/*v* continuous sucrose gradients containing 20 mM Tris-acetate pH 7.2, 10 mM glucose, and 5 mM taurine and centrifuged at 25,000 rpm for 45 min at 4°C. The pink band containing POS was collected and washed with storage buffer comprising of 10 mM sodium phosphate pH 7.2, 0.1 M NaCl, and 2.5% sucrose. Isolated POS aliquots were stored at −80°C at a concentration of 10^8 POS/ml.

2.3. Oxidized POS (oxPOS) Generation. The isolated POS aliquots were transferred to 9 cm petri dishes and exposed to 302 nm ultraviolet light (Ultraviolet Products, Cambridge, UK) in a laminar airflow box for 12 h to produce oxPOS. Samples were then collected and washed with distilled water. The irradiated POS were pelleted by centrifugation at 12,000*g* for 20 min and resuspended in storage buffer, and lipid oxidation was confirmed by the thiobarbituric acid reactive substance assay kit (Alexis; Axxora Ltd, Nottingham, UK). When treating RPE cells with oxPOS, a ratio of 1 : 10 RPE and oxPOS was used.

2.4. Zinc Depletion by Serum Starvation. Total zinc level in the complete medium (10% serum) is 5.4 μM [27]. To deplete total zinc in culture to 1.5 μM (Ref: http://www.thermofisher.com/us/en/home/technical-resources/media-formulation.55.html), culture media was removed and the cells were washed once with serum-free medium (SFM) before reincubating in SFM and DMEM/F12 with 100 μg/mL Primocin for 48 h. For supplementation with zinc, $ZnCl_2$ was prepared in a 15 μM concentration in SFM and filtered through a 0.22 μg filter and added to cells after 24 h.

2.5. Immunofluorescence Staining. ARPE19 cells were cultured on cover slips under different treatment conditions, including oxPOS and zinc depleted and zinc supplemented

for 48 h. Cells were washed with cold PBS and fixed with 1% paraformaldehyde (PFA) for 10 min, followed by permeabilization with 0.1% Triton-X for 5 min. The samples were then blocked with 5% BSA for 30 min at room temperature and incubated with anti-human cathepsin B (1 : 100, Life Technologies, UK) antibody for 2 h. After washing with PBS, samples were incubated with anti-mouse IgG 488 secondary antibody at a dilution of 1 : 100 with PBS and nuclei stained with DAPI at a dilution of 1 : 500 (Life Technologies, UK) in the dark for 1 h. Following thorough washing, coverslips were mounted with mounting medium (Vector Laboratories, Peterborough, UK) and examined by confocal microscopy (Eclipse TE2000-U, Nikon, Surrey, UK) at 40x magnification and numerical aperture at 0.65.

Dye-conjugated molecular probes used for staining intracellular organelles or other molecules used in this study are listed in Table 1. The dyes were added to live cells overnight in the dark at 37°C according to the manufacturers' instructions. After washing, fresh media was added and the samples were imaged by confocal microscopy.

2.6. Detection of Reactive Oxygen Species (ROS) Using CellROX Green. ARPE19 cells cultured on coverslips or 96-F fluorescence microplates (black) with/without oxPOS, under control and zinc depleted and zinc-supplemented conditions, were treated with 5 μM per well CellROX green (Life Technologies) for 30 min at 37°C.

The fluorescence intensity of CellROX green in cells was quantified using a fluorescent plate reader with an excitation filter of 485 nm and an emission filter of 520 nm. The background fluorescence intensity/autofluorescence was subtracted from the CellROX green intensity of cells for data analysis. For confocal microscopy, cells were further stained with MitoTracker Red (Life Technologies) and Hoechst 33342 (Thermo Fisher Scientific Loughborough, UK) for a further 30 min.

2.7. In Situ Cell Death Detection Terminal Deoxynucleotidyl Transferase (TdT) dUTP Nick-End Labeling (TUNEL) Assay. RPE cell death was detected using a *TUNEL* assay kit (Sigma-Aldrich, UK) according to the manufacturer's instructions. In brief, RPE cells plated for experiments with oxPOS or 4-HNE were washed with cold PBS and then fixed with 4% paraformaldehyde (PFA) for 1 h at 15–25°C before washing with PBS. The samples were then permeabilized with 0.1% Triton-X for 2 min on ice (2–8°C). As a negative control, one well contained labelling solution only. As a positive control, 3 U/ml recombinant DNASE1 was added to one group of cells to induce DNA strand breaks prior to labelling. The complete TUNEL reaction mixture was added to all experimental wells and incubated at 37°C for 1 h. The cells were washed with PBS before imaging under a confocal microscope. A series of 4-HNE concentrations were tested to choose a concentration that induced 50% or less cell death in 48 h treatment (data not shown). Therefore, apart from oxPOS, 5 μM 4-HNE for 24 h was used as an alternative oxidative insult to induce RPE cell death.

Table 1: Dye-conjugated probes for intracellular organelle or molecule staining.

Dye-conjugated molecular probes used in this study		
LysoTracker	1 : 100	Thermo Fisher
MitoTracker Red	1 : 100	Thermo Fisher
FluoZin-3 AM	5 μM	Life Technologies
CellROX® green	5 μM	Life Technologies

2.8. ToxGlo Assay to Measure Mitochondria ATP Production. RPE cells were plated on 96-well plates with clear or solid bottoms ensuring even dispersion and incubated at 37°C. Each treatment group (control untreated RPE cells, oxPOS treated, 1.5 μM zinc, 1.5 μM zinc + oxPOS treated, 15 μM zinc supplemented + oxPOS treated, and 15 μM zinc supplemented) was plated in 6 experimental wells. Five hours later and following cell attachment, zinc depleted media and oxPOS treatments were added to experiment wells. At 24 h, 15 μM zinc-supplemented media was added to the relevant experiment well for another 24 h. The cells were then washed with PBS, followed by incubation with cytotoxicity reagent (provided with assay kit) for 30 min. Fluorescence was measured at 485 nm/520–530 nm using a microplate reader (BMG Labtech, Germany). The assay plate was left to equilibrate at room temperature for 5–10 min, and 100 μl of ATP detection reagent was added to each well. The plate was mixed by orbital shaking 500–700 rpm for 1–5 min. Luminescence was measured using a microplate reader (BMG Labtech, Germany).

2.9. Western Blot. ARPE19 cells were washed with 1X phosphate-buffered saline and lysed in RIPA buffer with protease inhibitors (Sigma-Aldrich, UK). The protein concentrations were measured using a BCA protein assay kit (PIERCE, Cramlington, UK). 20 μg of the total protein was loaded onto 10% SDS-PAGE gel. Gels were run at 80 V for 30 min followed by 150 V for 60 min. Proteins were transferred to the Immobilon-FL polyvinylidene difluoride (PVDF) membrane (Millipore, Watford, UK) at 350 mA for 50 min. Blots were blocked with 5% bovine serum albumin (BSA) in tris-buffered saline with Tween-20 (TBS/T) for 1 h at room temperature then rinsed once in TBS/T. Next, the blots were incubated with rabbit polyclonal anti-Beclin-1 (Abcam) and β-actin (Santa Cruz) primary antibodies diluted 1 : 1000 with TBS/T overnight at 4°C. After thorough washes, the membranes were incubated with conjugated secondary antibodies at 1 : 1000 dilutions for 2 h in the dark at room temperature. The secondary antibodies used were goat anti-rabbit IRDye 680 (1 : 5000) and goat anti-mouse IRDye 800 (1 : 5000); (LI-COR; Lincoln).

The membrane was then washed in TBS/T 3 times before scanning using Odyssey infrared imaging system (Li-COR Biotechnology, Cambridge, UK). Quantitative Western blotting was performed using ImageJ software (version 1.45). The blots shown are representative of at least three biologic repeats of each experiment. The β-actin level was used to normalize the signal.

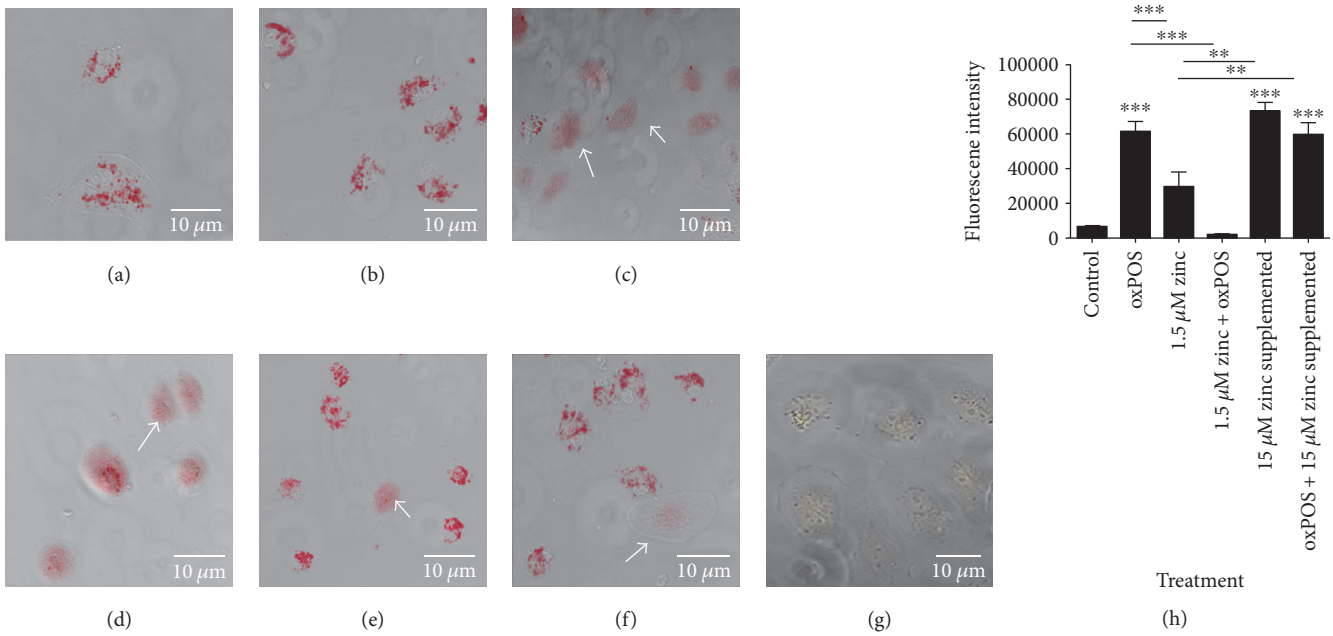

Figure 1: Confocal images of intracellular zinc using FluoZin-3 AM live cell staining. RPE cells treated under different conditions were incubated with 5 μM FluoZin-3 AM for 30 min at 37°C in the dark. The cells were then washed and further incubated for 30 min before imaging using a confocal microscope. (a) Control RPE cells cultured in 10% serum. (b) oxPOS-treated RPE cells in 10% serum. (c) RPE cells cultured in serum-free 1.5 μM zinc. (d) RPE cells cultured in serum-free 1.5 μM zinc + oxPOS. (e) RPE cells cultured in serum-free 15 μM zinc supplement + oxPOS. (f) RPE cells cultured in serum-free 15 μM zinc supplement. (g) Control RPE cells showing autofluorescence of oxPOS. Arrows show cells with decreased intracellular zinc staining. (h) Histogram showing fluorescence intensity of FluoZin-3 AM in different treatment groups of cells, $^{**}P < 0.01$ and $^{***}P < 0.001$. Data were analyzed by one-way ANOVA followed by Tukey's multiple comparison test. $N = 50$.

2.10. Data and Statistical Analysis. All experiments were performed in biological triplicate for statistical analysis. The data are expressed as mean ± SEM with $P < 0.05$ deemed statistically significant. Differences between groups were assessed using either an independent t-test or one-way analysis of variance with Dunnett's or Tukey's post hoc tests.

3. Results

3.1. Serum Starvation in Culture Reduces Intracellular Labile Zinc in ARPE19 Cells. The zinc concentration in control culture conditions with DMEM/F12+ 10% FCS is maintained at 5.4 μM, and in serum-free DMEM/F12 medium is 1.5 μM. In serum, 80% of zinc is loosely bound to albumin and the remaining 20% are present as labile zinc [1], therefore when culture media is supplemented with 15 μM zinc, there is approximately twofold increase in zinc bioavailability.

Under normal culture conditions, RPE cells contain a significant amount of intracellular labile zinc and levels were further increased following oxPOS incubation (Figures 1(a) and 1(b)). After 48 h culture in serum-free DMEM/F12 condition, the intracellular levels of zinc in RPE cells decreased significantly compared to that of cells (DMEM/F12+ 10%FCS) with/without oxPOS (Figures 1(a), 1(d), and 1(h)). However, after supplementation with 15 μM zinc for 24 h, the levels of intracellular zinc improved significantly (Figures 1(e), 1(f), and 1(h)). Figure 1(g) shows control RPE cells without FluoZin-3 AM showing autofluorescence of oxPOS which confirms there is minimal background fluorescence. Our results therefore substantiated the serum deprivation protocol resulted in intracellular zinc depletion, and the decrease in intracellular zinc is due to the reduced zinc in extracellular regions.

3.2. Zinc Depletion Induces Cellular Oxidative Stress. To determine the effects of zinc depletion on the buildup of ROS in RPE cells after exposure to oxPOS, intracellular ROS was measured using CellROX green. oxPOS treatment alone significantly increased oxidant generation in RPE cells (Figures 2(a), 2(b), and 2(g)); however, there was a greater increase in CellROX staining in the cells cultured in DMEM/F12 serum-free medium (1.5 μM Zinc, Figures 2(c) and 2(g)). The combination of low zinc + oxPOS treatment further increased CellROX staining (Figures 2(c), 2(d), and 2(g)). After supplementation with 15 μM zinc, there was a significant decrease in the intensity of CellROX staining in both groups that were cultured in serum-free condition (i.e., low zinc and low zinc + oxPOS) (Figures 2(e), 2(f), and 2(g)). The results suggest that zinc has an antioxidant role in RPE cells.

3.3. Zinc Depletion Induces Mitochondria Morphology Disorganization and Functional Changes. RPE cells cultured under control complete medium with/without oxPOS demonstrate normal mitochondrial morphology (Figures 3(a) and 3(b)), whereas cells cultured under serum-free conditions

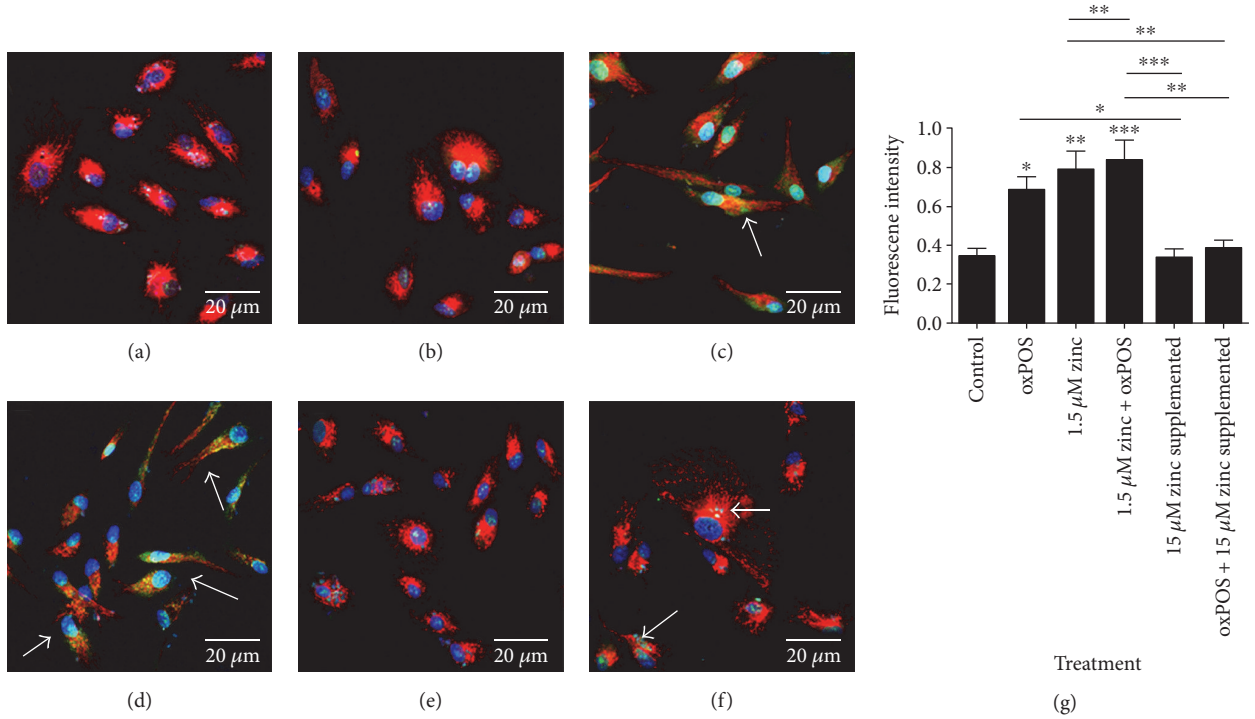

Figure 2: CellROX staining of oxidant generation in RPE following oxidative stress and zinc depletion. RPE cells under different treatment conditions were incubated with 5 μM per well concentration of CellROX for 30 min at 37°C, followed by MitoTracker and Hoechst 33,342. Cells were washed and fresh medium was added to the wells and imaged by confocal microscopy (a–f) or analyzed by a fluorescent plate reader (g). (a) Control RPE cells in 10% serum. (b) oxPOS-treated RPE cells in 10% serum. (c) Serum-free RPE cells in 1.5 μM zinc. (d) Serum-free RPE cells in 1.5 μM zinc + oxPOS. (e) 15 μM zinc-supplemented RPE cells. (f) oxPOS + 15 μM zinc-supplemented RPE cells. Red: MitoTracker; blue: nuclei Hoechst 33,342; and green: oxidant DNA in CellROX. (g) Histogram showing fluorescence intensity of CellROX green in different treatment groups of cells analyzed by a fluorescent plate reader. Mean ± SEM is plotted for 6 replicates for each condition. $^{*}P < 0.05$, $^{**}P < 0.01$, and $^{***}P < 0.001$. Data analyzed by one-way ANOVA followed by Tukey's multiple comparison test.

(1.5 μM zinc and 1.5 μM zinc + oxPOS) exhibit fragmented to elongated string-like mitochondrial morphology (Figures 3(c) and 3(d)). This change in morphology is known to be related to mitochondrial fission and fusion, which often occur when cells are under metabolic or environmental stress conditions [27]. When cells were treated with 15 μM zinc supplementation for 24 h, the changes observed in mitochondrial morphology was reversed (Figure 3(e)).

The mitochondrial ATP production was also partially but significantly decreased after serum deprivation (1.5 μM zinc). Interestingly, the addition of oxPOS did not further decrease ATP production. However, when 15 μM zinc was supplemented, ATP production returned to a level comparable to control RPE cells (Figure 3(f)). Our results suggest that zinc plays a role in maintaining mitochondrial function and ATP production.

3.4. Zinc Depletion Sensitizes ARPE19 Cells to Additional Oxidative Insults. Under normal culture conditions, 3% TUNEL^{+} cells were detected (Figures 4(a) and 4(g)). The addition of oxPOS did not significantly increase the percentage of TUNEL^{+} cells after 48 h (Figures 4(b) and 4(g)). When RPE cells were cultured in serum-free conditions (1.5 μM zinc), the percentage of TUNEL^{+} cells were significantly increased (Figures 4(c) and 4(g)). The addition of oxPOS further increased the percentage of TUNEL positive cells (Figures 4(d) and 4(g)). Supplementation of 15 μM zinc for 24 h to serum-free RPE cells significantly reduced the percentage of TUNEL^{+} cells (Figures 4(e) and 4(f)).

To further investigate the effect of zinc on oxidative stress-induced RPE cell death, ARPE19 cells in normal (DMEM/F12 with 10% FCS) or serum-free (DMEM/F12 only) culture conditions were subjected to 5 μM 4-HNE for 24 h. Under normal culture conditions, there was 3% cell death (Figures 5(a) and 5(f)). 5 μM 4-HNE treatment resulted in 10% cell death (Figures 5(b) and 5(f)), which increased to approximately 45% under serum-free conditions (Figures 5(c) and 5(f)). Zinc supplementation (5 μM and 15 μM zinc) dose dependently suppressed 4-HNE (5 μM)-induced RPE death (Figures 5(d), 5(e), and 5(f)).

Taken together, our results suggest that serum deprivation sensitizes RPE cells to oxidative insult-induced death, and zinc supplementation can protect RPE cells from oxidative stress-induced death under serum-free conditions.

3.5. Zinc Depletion Partially Decreases ARPE19 Cell Phagocytosis Function. Zinc has been previously been implicated in various RPE functions, and zinc deficiency is

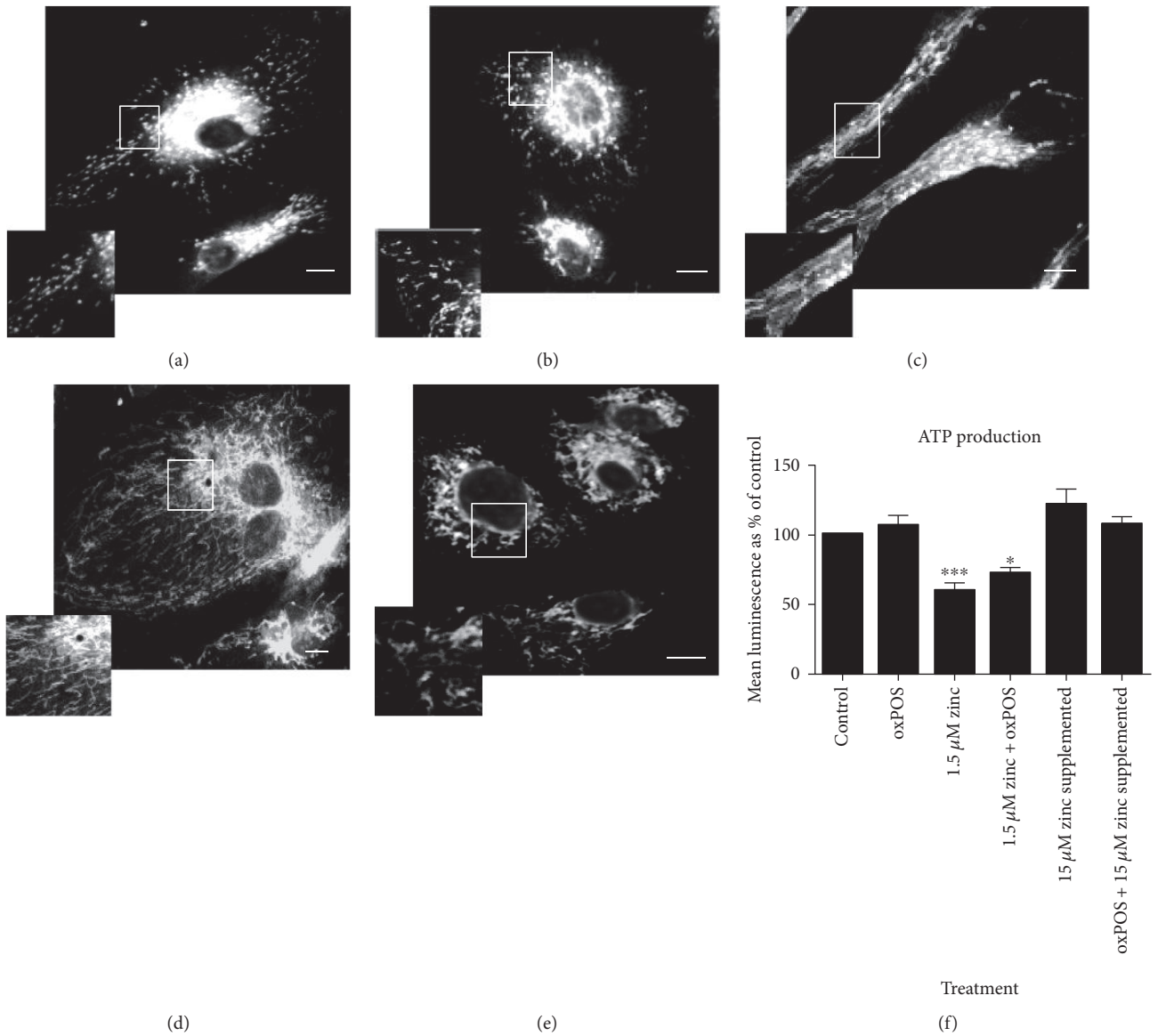

Figure 3: Changes in mitochondria morphology staining and function in a stressed environment. RPE was subjected to treatments with 1.5 μM zinc, 1.5 μM zinc + oxPOS treated, oxPOS treated + 15 μM zinc supplemented, and oxPOS-treated untreated control for 48 h. MitoTracker was added for 30 min at 37°C before imaging the cells living under the confocal microscope at 60x magnification or samples were processed for Mitochondrial ToxGlo assay to measure ATP production. (a) Control-untreated RPE cells. (b) oxPOS-treated RPE cells. (c) 1.5 μM zinc RPE cells. (d) 1.5 μM zinc + oxPOS-treated RPE cells. (e) 15 μM zinc-supplemented RPE cells. (f) Quantitative data of mitochondria ATP production in different treatment groups, $^{*}P < 0.05$ and $^{***}P < 0.001$, compared to untreated control with data analyzed using a one-way ANOVA followed by Dunnett's multiple comparison test. $N = 5$.

associated with disease condition such as AMD [23]. Phagocytosis of photoreceptor outer segments by RPE cells is important and essential to maintain visual function. Under serum-free conditions (1.5 μM zinc), RPE cells phagocytosed significantly fewer oxPOS particles compared to cells in normal culture conditions at 2 h (Figures 6(a), 6(b), and 6(d)). 15 μM zinc supplementation completely rescued the phagocytosis capacity of the RPE (Figures 6(c) and 6(d)). Phagocytosis assay at 24 h showed similar results (data not shown). Our data, therefore suggests that zinc is critically involved in RPE phagocytosis and zinc deficiency impairs this function.

3.6. Zinc Depletion Causes Lysosome Rupture Which Is Prevented by Zn Supplementation. To better understand the mechanism by which zinc deficiency mediates RPE cell dysfunction, we investigated RPE lysosome integrity. Loss of lysosomal integrity is implicated in impaired phagocytosis, autophagy, and various forms of cell death including apoptosis [28]. Cathepsins are major enzymes enclosed in lysosomes and help to maintain cell homeostasis by contributing to the degradation of heterophagic and autophagic material [29]. Lysosomal rupture and cathepsin B release to the cytosol are a characteristic of apoptosis induced by oxidative insult [30]. Immunostaining for cathepsin B in cells with

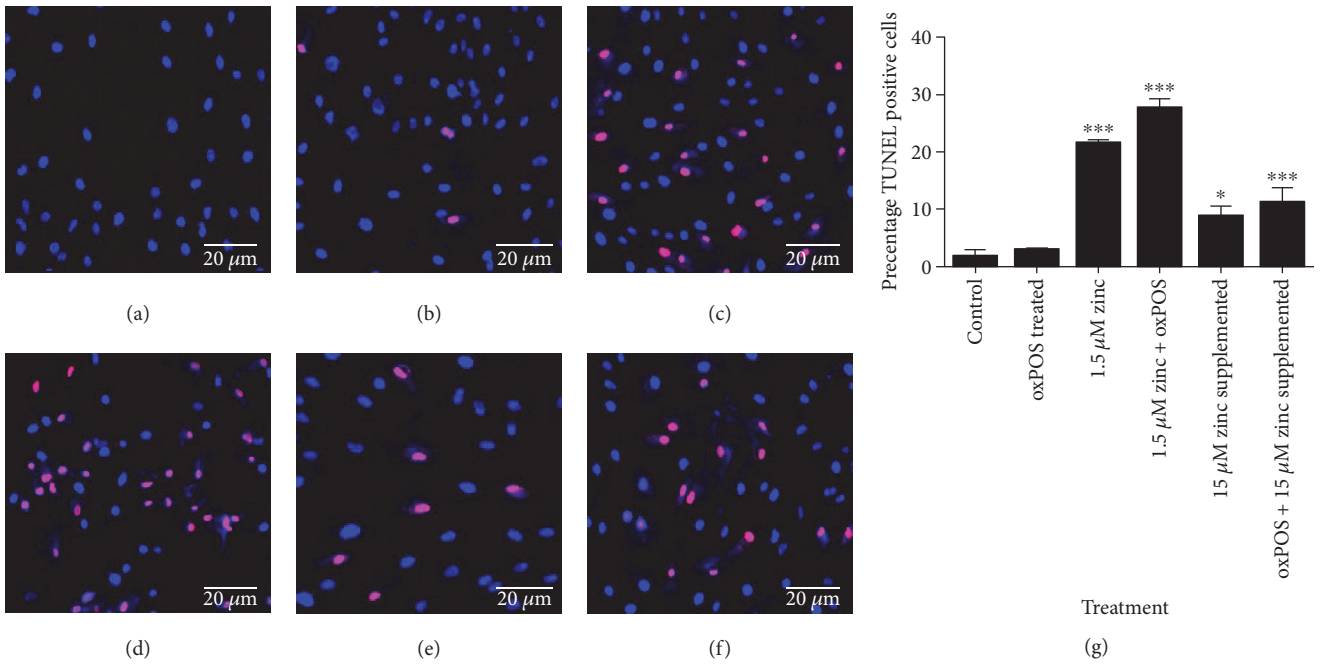

Figure 4: In situ cell death staining to detect RPE cell apoptosis in oxPOS treated and zinc depletion. RPE cells were subjected to treatments with1.5 μM zinc, 1.5 μM zinc + oxPOS treated, oxPOS treated + 15 μM zinc supplemented, and oxPOS-treated and untreated control for 48 h were fixed and processed for TUNEL assay. (a) Control-untreated RPE cells. (b) oxPOS-treated RPE cells. (c) 1.5 μM zinc RPE cells. (d) 1.5 μM zinc + oxPOS-treated RPE cells. (e) 15 μM zinc-supplemented RPE cells. (f) oxPOS + 15 μM zinc-supplemented RPE cells. The cell nucleus is stained with DAPI (blue). Red staining indicates TUNEL positive cells. (g) Histogram showing the percentage of TUNEL positive cells in each treatment groups, $^{*}P < 0.05$ and $^{***}P < 0.001$, compared to each group with the data analyzed by one-way ANOVA followed by Tukey's multiple comparison test. 200 cells were counted for each well. $N = 3$.

lysosomal rupture is known to exhibit stronger and more diffuse cytoplasmic staining when compared to healthy cells with intact lysosomal membranes. Figures 7(a), 7(b), and 7(f) show that, under serum deprivation (1.5 μM zinc) only, there is an increase in cathepsin B immunoreactivity compared to control (DMEM/F12+ 10% FCS), and this was further enhanced when cells were treated with 5 μM 4-HNE (Figure 7(c)). Zinc supplementation dose dependently reduced cathepsin B expression in serum-free +4-HNE-treated cells (Figures 7(d) and 7(e)). These findings suggest that serum deprivation and oxidative stress induce lysosomal rupture and supplementation with zinc and can maintain RPE lysosomal integrity under oxidative stress conditions.

3.7. Zinc Depletion Reduces Beclin-1 Expression in ARPE19 Cells. Lysosome is essential for the formation of autophagolysosome. To understand the role of zinc depletion in RPE autophagy, we measured the expression of Beclin-1 in RPE cells cultured under different conditions using Western blot. Under normal culture conditions, the addition of oxPOS increased the expression of Beclin-1 (Figures 8(a) and 8(b)). Serum depletion significantly reduced Beclin-1 expression, even with oxPOS, compared to controls (Figures 8(a) and 8(b)). When supplemented with 15 μM zinc to the serum-free medium, the expression of Beclin-1 returned to levels comparable to control cells. The combination of 15 μM zinc and oxPOS further increased Beclin-1 expression (Figures 8(a) and 8(b)). This result suggests that zinc deficiency may lead to autophagy dysfunction in RPE during oxidative insult.

4. Discussion

Under normal physiological conditions, the RPE-choroid complex contains high levels of zinc, and zinc is recognized to be important in RPE functions such as antioxidation, phagocytosis, and regulating enzymes involved in the retinal cycle as well as protein kinase activity [31, 32]. Zinc deficiency has been shown to associate with progression of diseases such as cataract and AMD [33–35]. It has been demonstrated that zinc depletion may increase oxidative stress in RPE cells, probably by decreasing the activity of antioxidant enzymes such as catalase and glutathione peroxidase [36]. Tate et al. [22] showed that zinc protected cultured RPE from H_2O_2 and paraquat toxicity and RPE cells in 0.55 μM zinc medium contained higher levels of oxidative stress markers such as thiobarbituric acid reactive substances (TBARS), conjugated dienes, and protein carbonyls. In this study, we show that serum deprivation depleted the intracellular zinc in RPE cells, which sensitized RPE to oxidative damage and impaired RPE cell phagocytosis. We further show that zinc supplementation concentration dependently rescued oxidative stress-induced RPE damage and recovered RPE phagocytosis.

Serum contains not only zinc but also many other growth factors essential for cell survival. The increased sensitivity to oxidative damage and reduced phagocytosis of RPE cells

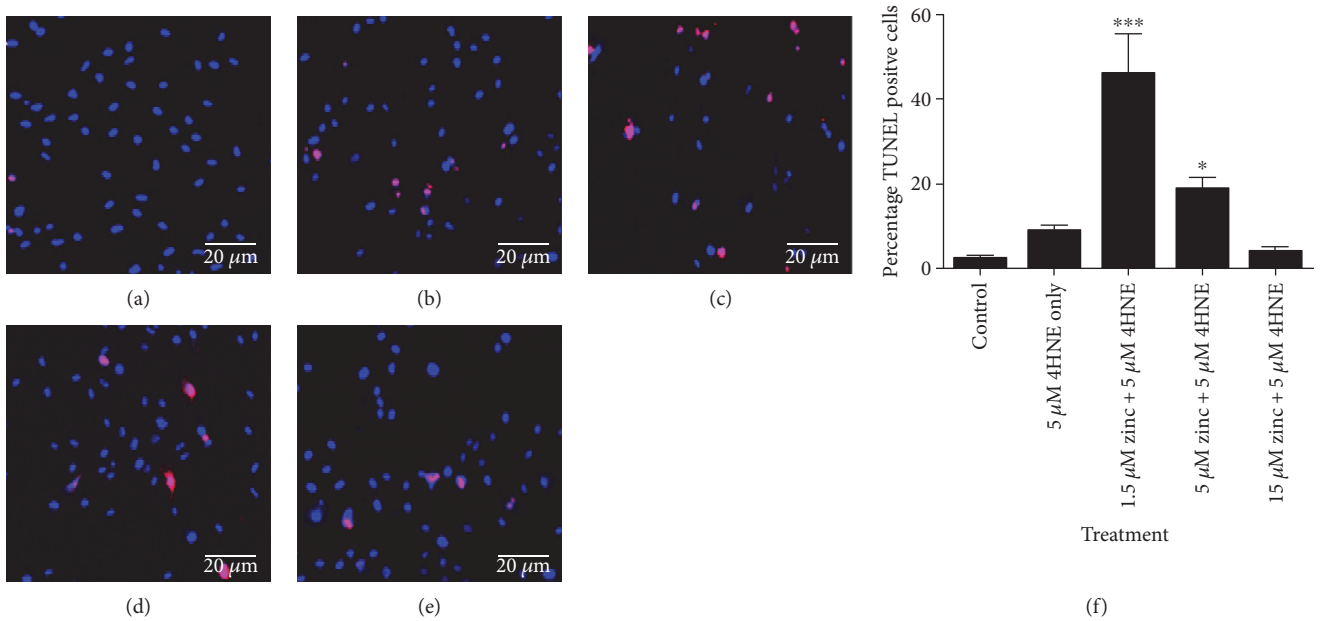

Figure 5: Dose-dependent effect of zinc on 4-HNE-induced RPE cell death. RPE cells subjected to different treatments were fixed and processed for TUNEL assay. (a) Control RPE cells. (b) 5 μM 4-HNE only-treated RPE cells. (c) 1.5 μM zinc + 4-HNE-treated RPE cells. (d) 5 μM zinc + 4-HNE-treated RPE cells. (e) 15 μM zinc + 4-HNE-treated RPE cells. Red nuclei staining indicates TUNEL positive cells. (f) Histogram showing the percentage of TUNEL positive cells in each treatment groups, $^{*}P < 0.05$ and $^{***}P < 0.001$, compared to control with data analyzed by one-way ANOVA followed by Dunnett's multiple comparison test. 100 cells were counted for each well. $N = 3$.

under serum-free conditions could be caused by multiple mechanisms. However, we show that supplementation of zinc alone is sufficient to rescue RPE cells from oxidative damage during serum starvation. Our observations are in agreement with a previous study by Hyun et al. [37] where it was shown that depletion of intracellular zinc with TPEN resulted in apoptosis of cultured human RPE cells.

Exactly how zinc protects RPE cells from oxidative damage under serum-free conditions remains unknown. We found that zinc supplementation improves mitochondrial morphology and increases ATP production. Mitochondria are the main source of intracellular ROS under oxidative conditions [38]. Under serum-free and oxidative (oxPOS or 4-HNE) conditions, RPE cells expressed higher levels of intracellular ROS (e.g., higher levels of CellROX staining) and presented fragmented mitochondrial morphology and reduced ATP production. The results suggest that mitochondrial damage is critically involved in oxidative stress-induced RPE death and dysfunction under serum-free conditions. Interestingly, the addition of zinc (15 μM) reduced ROS production and improved mitochondrial morphology and ATP production, suggesting that zinc can protect mitochondria from oxidative damage. A previous study has shown that zinc has a protective effect against tubular cell apoptosis following ATP depletion *in vitro* [39]. How zinc may protect mitochondria from oxidative damage and the role of zinc in mitochondrial function, biogenesis, and fusion/fission warrant further investigation.

The lysosome is the waste processing and waste disposal machinery of a cell. It not only digests materials phagocytized from exogenous sources (e.g., the formation of phagolysosome) but also plays an important role in the removal of damaged intracellular molecules and organelles (e.g., the formation of autophagosome of the autophagy pathways) [40]. In RPE cells, the lysosome is critically involved in the processing and recycling of phagocytized POS, and dysfunction of lysosomal activity may be related to the development of lipofuscin [41]. The integrity of the lysosome is essential to its function. It has been shown that lysosomal membrane destabilization may lead to the release of cathepsins into the cytosol, which may initiate the lysosomal pathway of apoptosis [42]. In addition, the released cathepsins can also amplify apoptotic signaling [43]. In the current study, we found that when RPE cells were subjected to serum-free conditions (1.5 μM zinc) and the release of cathepsin B in the cytosol was significantly increased. Additional oxidative insult (5 μM 4-HNE) further promoted cathepsin B release, indicative of lysosome membrane destabilization. Interestingly, zinc dose dependently prevented serum deprivation +4-HNE-induced cathepsin B release in RPE cells. Although the mechanisms related to lysosome membrane destabilization in our model system are likely to be complex and are currently unknown, our results suggest that zinc can stabilize the lysosomal membrane and maintain function.

Impaired phagocytosis of POS by RPE cells was observed in our culture system (i.e., serum deprivation). The link between zinc deficiency and decreased RPE phagocytic and lysosomal function has been suggested although not well-characterized [19]. Increased lipofuscin accumulation has been observed in zinc-deficient rats, and this phenomenon is believed to be related to elevated oxidative stress and incomplete digestion of photoreceptor outer segments in the lysosomes of the RPE [44]. The reduced phagocytosis of oxPOS by RPE cells under serum deprivation conditions

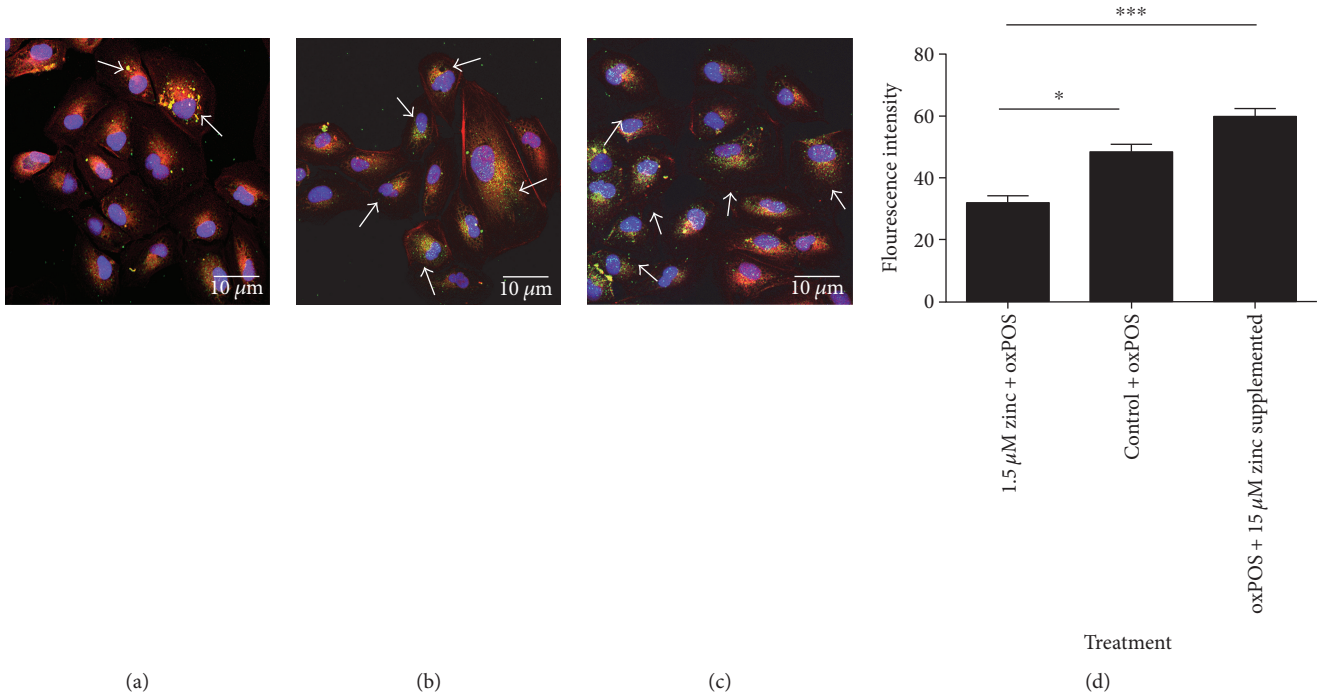

Figure 6: Changes in oxPOS phagocytosis in zinc-depleted RPE. The following zinc was depleted in RPE for 48 h; the cells were exposed to FITC-conjugated oxPOS particles (RPE: oxPOS = 1:10) for 2 h. Cells were then washed, fixed, and processed for imaging under the confocal microscope. The phagocytosis function was quantified by measuring the fluorescent intensity of the phagocytosed particles per cell. (a) 1.5 μM zinc RPE cells + oxPOS-treated. (b) Control RPE cells + oxPOS-treated. (c) oxPOS + 15 μM zinc-supplemented RPE cells. Arrows show phagocytosed oxPOS particles in cells. Cell nuclei are stained with DAPI (blue), actin with phalloidin (red), and oxPOS particles conjugated with FITC (green). (d) Histogram showing fluorescence intensity of the phagocytosed oxPOS particles in the different groups, $^{*}P < 0.05$ and $^{***}P < 0.001$. Data analyzed by one-way ANOVA followed by Tukey's multiple comparison test. 30 cells were counted for each well.

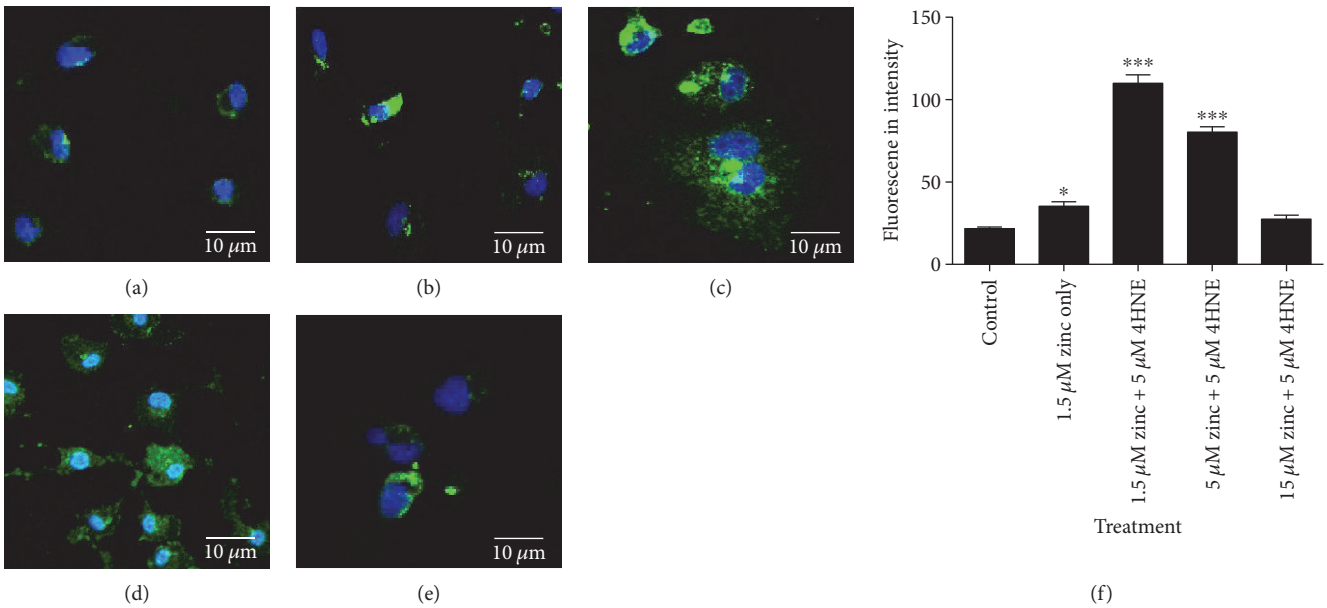

Figure 7: Cathepsin B staining indicating lysosomal rupture in zinc-depleted and oxidative-stressed RPE cells. RPE cells were treated with 5 M 4-HNE at 1.5 μM, 5 μM, and 15 μM zinc concentrations as well as an untreated control and 1.5 μM zinc only for 24 h before fixing the cells and immunostaining for cathepsin B. (a) Control RPE cells. (b) 1.5 μM zinc only. (c) 1.5 μM zinc + 4-HNE-treated RPE cells. (d) 5 μM zinc + 4-HNE-treated RPE cells. (e) 15 μM zinc + 4-HNE-treated RPE cells. Cell nuclei are stained with DAPI (blue) and cathepsin B (green). (f) Histogram showing the fluorescence intensity of cathepsin B staining in the different treatment groups, $^{*}P < 0.05$ and $^{***}P < 0.001$, compared to the control. One-way ANOVA followed by Dunnett's multiple comparison test. Fluorescence intensity of 30 cells per well was measured with three treatment replicate wells for each treatment.

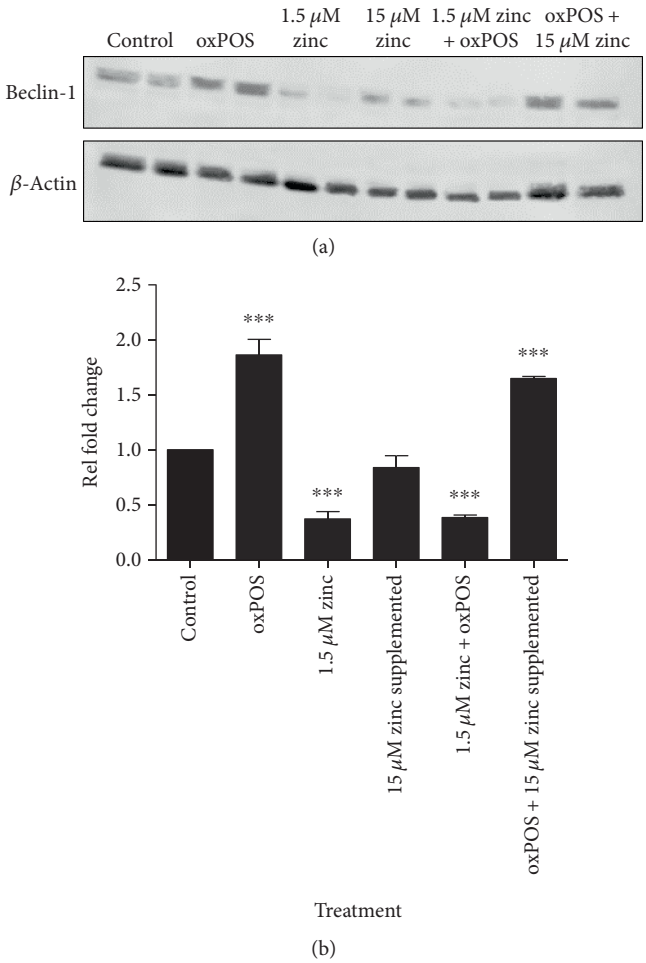

Figure 8: Expression of autophagy marker Beclin-1 following zinc supplementation.(a) Representative Western blot from untreated control, oxPOS treated, 1.5 μM zinc, 15 μM zinc, 1.5 μM zinc + oxPOS treated, and oxPOS treated + 15 μM zinc-supplemented RPE cells. Bands were detected for Beclin-1 at 55 KDa and β-actin at 40 KDa. (b) Quantification of Beclin-1 protein expression by RPE cells in the different treatment groups. Signals from Western blots were visualised by Odyssey infrared imaging system and quantified using ImageJ analysis software (version 1.45). Signals for control were set to one and the data are represented as relative fold change, $^{***}P < 0.001$, compared to the untreated control group. One-way ANOVA followed by Dunnett's multiple comparison test. $N = 3$.

may be related, at least partially, to low-zinc-mediated lysosome dysfunction.

Zinc deprivation also impaired autophagy in RPE cells evidenced by reduced Beclin-1 expression. Autophagy involves the seizing of cellular components in double-membrane vesicles known as autophagosomes and consequent delivery to lysosomes for degradation [41]. In some conditions, autophagy is considered as a physiologic prosurvival mechanism and dysregulated autophagy in RPE is associated with increased susceptibility to oxidative stress and AMD [45].

Based on the results from this study and the existing literature, it is apparent that zinc plays a key role in the regulation of apoptosis; however, the role of zinc in RPE cell autophagy remains unclear. In a recent review, Liuzzi and Cousins [46] discussed the ability of excess zinc to potentiate autophagy induced by tamoxifen, alcohol, H_2O_2, and dopamine as well as the suppressive effect of zinc depletion on early and late autophagy. In this study, a model with moderate zinc supplementation was used to determine the role of zinc in autophagy. There was a decreased expression of autophagy marker Beclin-1 at 1.5 μM conditions, was restored when supplemented with 15 μM zinc, and was significantly increased when RPE was exposed to oxPOS. This indicates that zinc depletion may lead to impaired autophagy function of RPE which could be detrimental for RPE health, but supplementation of zinc at nontoxic concentrations could be beneficial.

5. Conclusions

Overall, the data presented in this paper suggests that RPE cells depend upon zinc to protect against the constant insults associated with POS uptake and to maintain normal cellular function. Zinc deficiency may lead to malfunction of many intracellular organelles such as mitochondria and lysosomes, which may contribute to reduced function and increased death of RPE cells under stress conditions. The decreases in available zinc in ageing RPE and AMD could be a factor associated with decreased clearance of POS by RPE and cell death *in vivo*. Further understanding the molecular mechanisms related to zinc metabolism and homeostasis in RPE cells under aging and other pathophysiological conditions may shed light on the pathogenesis and provide crucial information on the management of various age-related retinal diseases.

Conflicts of Interest

The authors declare that they have no conflicts of interest.

Authors' Contributions

Dinusha Rajapakse performed the experiments, interpreted the results, and wrote the manuscript. Heping Xu, Mei Chen, and Tim Curtis helped with study design, data interpretation, and manuscript editing.

Acknowledgments

The study was funded by the Queen's University Belfast International Postgraduate Training programme.

References

[1] T. Kambe, T. Tsuji, A. Hashimoto, and N. Itsumura, "The physiological, biochemical, and molecular roles of zinc transporters in zinc homeostasis and metabolism," *Physiology Review*, vol. 95, no. 3, pp. 749–784, 2015.

[2] C. Andreini, I. Bertini, and G. Cavallaro, "Minimal functional sites allow a classification of zinc sites in proteins," *PLoS One*, vol. 6, no. 10, article e26325, 2015.

[3] A. Müller, G. Kleinau, C. L. Piechowski et al., "G-protein coupled receptor 83 (GPR83) signaling determined by

constitutive and zinc(II)-induced activity," *PLoS One*, vol. 8, no. 1, article e53347, 2013.

[4] P. Csermely, M. Szamel, K. Resch, and J. Somogyi, "Zinc can increase the activity of protein kinase C and contributes to its binding to plasma membranes in T lymphocytes," *Journal of Biological Chemistry*, vol. 263, no. 14, pp. 6487–6490, 1988.

[5] M. Ugarte and N. N. Osborne, "Recent advances in the understanding of the role of zinc in ocular tissues," *Metallomics*, vol. 6, no. 2, pp. 189–200, 2014.

[6] M. Ugarte and N. N. Osborne, "Zinc in the retina," *Progress in Neurobiology*, vol. 64, no. 3, pp. 219–249, 2001.

[7] M. Ugarte, G. W. Grime, G. Lord et al., "Concentration of various trace elements in the rat retina and their distribution in different structures," *Metallomics*, vol. 4, no. 12, pp. 1245–1254, 2012.

[8] L. Huang, Y. Y. Yu, C. P. Kirschke, E. R. Gertz, and K. K. Lloyd, "*Znt7* (*Slc30a7*)-deficient mice display reduced body zinc status and body fat accumulation," *The Journal of Biological Chemistry*, vol. 282, no. 51, pp. 37053–37063, 2007.

[9] K. Murakami, T. Kondo, M. Kawase et al., "Mitochondrial susceptibility to oxidative stress exacerbates cerebral infarction that follows permanent focal cerebral ischemia in mutant mice with manganese superoxide dismutase deficiency," *Journal of Neuroscience*, vol. 18, no. 1, pp. 205–213, 1998.

[10] U. Schraermeyer, S. Peters, G. Thumann, N. Kociok, and K. Heimann, "Melanin granules of retinal pigment epithelium are connected with the lysosomal degradation pathway," *Experimental Eye Research*, vol. 68, no. 2, pp. 237–245, 1999.

[11] M. V. Miceli, D. J. Tate, N. W. Alcock, and D. A. Newsome, "Zinc deficiency and oxidative stress in the retina of pigmented rats," *Investigative Ophthalmology & Visual Science*, vol. 40, no. 6, pp. 1238–1244, 1999.

[12] I. Sekler, S. L. Sensi, M. Hershfinkel, and W. F. Silverman, "Mechanism and regulation of cellular zinc transport," *Molecular Medicine*, vol. 13, no. 7-8, pp. 337–343, 2007.

[13] M. C. McCord and E. Aizenman, "The role of intracellular zinc release in aging, oxidative stress, and Alzheimer's disease," *Frontiers in Aging Neuroscience*, vol. 6, p. 77, 2014.

[14] J. Osredkar and N. Sustar, "Copper and zinc, biological role and significance of copper/zinc imbalance," *Journal of Clinical Toxicology*, vol. s3, no. 1, pp. 2161–2195, 2011.

[15] V. L. Bonilha, "Age and disease-related structural changes in the retinal pigment epithelium," *Clinical Ophthalmology*, vol. 2, no. 2, pp. 413–424, 2008.

[16] S. Julien, A. Biesemeier, D. Kokkinou, O. Eibl, and U. Schraermeyer, "Zinc deficiency leads to lipofuscin accumulation in the retinal pigment epithelium of pigmented rats," *PLoS One*, vol. 6, no. 12, article e29245, 2011.

[17] J. C. Erie, J. A. Good, J. A. Butz, and J. S. Pulido, "Reduced zinc and copper in the retinal pigment epithelium and choroid in age-related macular degeneration," *American Journal of Ophthalmology*, vol. 147, no. 2, pp. 276–282.e1, 2008.

[18] D. Smailhodzic, F. van Asten, A. M. Blom et al., "Zinc supplementation inhibits complement activation in age-related macular degeneration," *PLoS One*, vol. 9, no. 11, article e112682, 2014.

[19] P. Tokarz, K. Kaarniranta, and J. Blasiak, "Role of antioxidant enzymes and small molecular weight antioxidants in the pathogenesis of age-related macular degeneration (AMD)," *Biogerontology*, vol. 14, no. 5, pp. 461–482, 2013.

[20] R. Nan, J. Gor, I. Lengyel, and S. J. Perkins, "Uncontrolled zinc- and copper-induced oligomerisation of the human complement regulator factor H and its possible implications for function and disease," *Journal of Molecular Biology*, vol. 384, no. 5, pp. 1341–1352, 2008.

[21] J. P. Wood and N. N. Osborne, "Zinc and energy requirements in induction of oxidative stress to retinal pigmented epithelial cells," *Neurochemical Research*, vol. 28, no. 10, pp. 1525–1533, 2003.

[22] D. J. Tate, M. V. Miceli, and D. A. Newsome, "Zinc protects against oxidative damage in cultured human retinal pigment epithelial cells," *Free Radical Biology & Medicine*, vol. 26, no. 5-6, pp. 704–713, 1999.

[23] T. E. Clemons, R. C. Milton, R. Klein, J. M. Seddon, F. L. Ferris 3rd, and Age-Related Eye Disease Study Research Group, "Risk factors for the incidence of advanced age-related macular degeneration in the age-related eye disease study (AREDS): AREDS report no. 19," *Ophthalmology*, vol. 112, no. 4, pp. 533–539, 2005.

[24] K. Girijashanker, L. He, M. Soleimani et al., "*Slc39a14* gene encodes ZIP_{14}, a metal/biocarbonate symporter: similarities to the ZIP8 transporter," *Molecular Pharmacology*, vol. 73, no. 5, pp. 1413–1423, 2008.

[25] M. Chen, D. Rajapakse, M. Fraczek, C. Luo, J. V. Forester, and H. Xu, "Retinal pigment epithelial cell multinucleation in the ageing eye – a mechanism to repair damage and maintain homoeostasis," *Aging Cell*, vol. 15, no. 3, pp. 436–445, 2016.

[26] M. Chen, J. V. Forrester, and H. Xu, "Synthesis of complement factor H by retinal pigment epithelial cells is down-regulated by oxidized photoreceptor outer segments," *Experimental Eye Research*, vol. 84, no. 4, pp. 635–645, 2007.

[27] Y. E. Cho, R. A. Lomeda, S. H. Ryu, J. H. Lee, J. H. Beattie, and I. S. Kwun, "Cellular Zn depletion by metal ion chelators (TPEN, DTPA and chelex resin) and its application to osteoblastic MC3T3-E1 cells," *Nutrition Research and Practice*, vol. 1, no. 1, pp. 29–35, 2007.

[28] R. J. Youle and A. M. van der Bliek, "Mitochondrial fission, fusion, and stress," *Science*, vol. 337, no. 6098, pp. 1062–1065, 2012.

[29] C. Paquet, A. T. Sane, M. Beauchemin, and R. Bertrand, "Caspase- and mitochondrial dysfunction-dependent mechanisms of lysosomal leakage and cathepsin B activation in DNA damage-induced apoptosis," *Leukemia*, vol. 19, pp. 784–791, 2005.

[30] H. Wu, H. Niu, C. Wu et al., "The autophagy-lysosomal system in subarachnoid haemorrhage," *Journal of Cellular and Molecular Medicine*, vol. 20, no. 9, pp. 1770–1778, 2016.

[31] U. Repnik, V. Stoka, V. Turk, and B. Turk, "Lysosomes and lysosomal cathepsins in cell death," *Biochimica et Biophysica Acta (BBA) - Proteins and Proteomics*, vol. 1824, no. 1, pp. 22–33, 2012.

[32] S. Gleim, A. Stojanovic, E. Arehart, D. Byington, and J. Hwa, "Conserved rhodopsin intradiscal structural motifs mediate stabilization: effects of zinc," *Biochemistry*, vol. 48, no. 8, pp. 1793–1800, 2009.

[33] K. A. Rezaei, Y. Chen, J. Cai, and P. Sternberg, "Modulation of Nrf2-dependent antioxidant functions in the RPE by Zip2, a zinc transporter protein," *Investigative Ophthalmology & Visual Science*, vol. 49, no. 4, pp. 1665–1670, 2008.

[34] D. A. Newsome, M. V. Miceli, D. Tate, N. W. Alcock, and P. Oliver, "Zinc content of human retinal pigment epithelium

decreases with age and macular degeneration, but superoxide dismutase activity increases," *The Journal of Trace Elements in Experimental Medicine*, vol. 8, no. 4, pp. 193–199, 1996.

[35] N. L. Richardson, D. A. Higgs, R. M. Beames, and J. R. Mcbride, "Influence of dietary calcium, phosphorus, zinc and sodium phytate level on cataract incidence, growth and histopathology in juvenile chinook salmon (*Oncorhynchus tshawytscha*)," *The Journal of Nutrition*, vol. 115, no. 5, pp. 553–567, 1985.

[36] B. H. Grahn, P. G. Paterson, K. T. Gottschall-Pass, and Z. Zhang, "Zinc and the eye," *Journal of the American College of Nutrition*, vol. 20, no. 2, pp. 106–118, 2001.

[37] H. J. Hyun, J. H. Sohn, D. W. Ha, Y. H. Ahn, J. Y. Koh, and Y. H. Yoon, "Depletion of intracellular zinc and copper with TPEN results in apoptosis of cultured human retinal pigment epithelial cells," *Retinal Cell Biology*, vol. 42, no. 2, pp. 460–465, 2001.

[38] A. A. Starkov, "The role of mitochondria in reactive oxygen species metabolism and signaling," *Annals of the New York Academy of Sciences*, vol. 1147, pp. 37–52, 2008.

[39] Q. Wei, J. Wang, M. H. Wang, F. Yu, and Z. Dong, "Inhibition of apoptosis by Zn^{2+} in renal tubular cells following ATP depletion," *American Journal of Physiology - Renal Physiology*, vol. 287, no. 3, pp. F492–F500, 2004.

[40] D. Glick, S. Barth, and K. F. Macleod, "Autophagy: cellular and molecular mechanisms," *The Journal of Pathology*, vol. 221, no. 1, pp. 3–12, 2010.

[41] S. Guha, J. Liu, G. Baltazar, A. M. Laties, and C. H. Mitchell, "Rescue of compromised lysosomes enhances degradation of photoreceptor outer segments and reduces lipofuscin-like autofluorescence in retinal pigmented epithelial cells," *Advances in Experimental Medicine and Biology*, vol. 801, pp. 105–111, 2014.

[42] A. C. Johansson, H. Appelqvist, C. Nilsson, K. Kågedal, K. Roberg, and K. Ollinger, "Regulation of apoptosis-associated lysosomal membrane permeabilization," *Apoptosis*, vol. 15, no. 5, pp. 527–540, 2010.

[43] B. Turk and V. Stoka, "Protease signalling in cell death: caspases versus cysteine cathepsins," *FEBS Letters*, vol. 581, no. 15, pp. 2761–2767, 2007.

[44] C. J. Kennedy, P. E. Rakoczy, T. A. Robertson, J. M. Papadimitriou, and I. J. Constable, "Kinetic studies on phagocytosis and lysosomal digestion of rod outer segments by human retinal pigment epithelial cells *in vitro*," *Experimental Cell Research*, vol. 210, no. 2, pp. 209–214, 1994.

[45] S. K. Mitter, C. Song, X. Qi et al., "Dysregulated autophagy in the RPE is associated with increased susceptibility to oxidative stress and AMD," *Autophagy*, vol. 10, no. 11, pp. 1989–2005, 2014.

[46] J. P. Liuzzi and R. J. Cousins, "Mammalian zinc transporters," *Annual Review of Nutrition*, vol. 24, pp. 151–172, 2014.

Hindawi
Oxidative Medicine and Cellular Longevity
Volume 2017, Article ID 5293258, 15 pages
https://doi.org/10.1155/2017/5293258

Review Article

Cellular Senescence in Age-Related Macular Degeneration: Can Autophagy and DNA Damage Response Play a Role?

Janusz Blasiak,[1] Malgorzata Piechota,[2] Elzbieta Pawlowska,[3] Magdalena Szatkowska,[1] Ewa Sikora,[4] and Kai Kaarniranta[5,6]

[1]*Department of Molecular Genetics, University of Lodz, Pomorska 141/143, 90-236 Lodz, Poland*
[2]*Laboratory of Molecular Basis of Behavior, Nencki Institute of Experimental Biology, Polish Academy of Sciences, Pasteura 3, 02-093 Warsaw, Poland*
[3]*Department of Orthodontics, Medical University of Lodz, Pomorska 251, 92-216 Lodz, Poland*
[4]*Laboratory of Molecular Bases of Aging, Nencki Institute of Experimental Biology, Polish Academy of Sciences, Pasteura 3, 02-093 Warsaw, Poland*
[5]*Department of Ophthalmology, University of Eastern Finland, 70211 Kuopio, Finland*
[6]*Department of Ophthalmology, Kuopio University Hospital, 70029 Kuopio, Finland*

Correspondence should be addressed to Janusz Blasiak; janusz.blasiak@biol.uni.lodz.pl

Received 24 April 2017; Revised 29 May 2017; Accepted 28 June 2017; Published 1 November 2017

Academic Editor: Domenico D'Arca

Age-related macular degeneration (AMD) is the main reason of blindness in developed countries. Aging is the main AMD risk factor. Oxidative stress, inflammation and some genetic factors play a role in AMD pathogenesis. AMD is associated with the degradation of retinal pigment epithelium (RPE) cells, photoreceptors, and choriocapillaris. Lost RPE cells in the central retina can be replaced by their peripheral counterparts. However, if they are senescent, degenerated regions in the macula cannot be regenerated. Oxidative stress, a main factor of AMD pathogenesis, can induce DNA damage response (DDR), autophagy, and cell senescence. Moreover, cell senescence is involved in the pathogenesis of many age-related diseases. Cell senescence is the state of permanent cellular division arrest and concerns only mitotic cells. RPE cells, although quiescent in the retina, can proliferate *in vitro*. They can also undergo oxidative stress-induced senescence. Therefore, cellular senescence can be considered as an important molecular pathway of AMD pathology, resulting in an inability of the macula to regenerate after degeneration of RPE cells caused by a factor inducing DDR and autophagy. It is too early to speculate about the role of the mutual interplay between cell senescence, autophagy, and DDR, but this subject is worth further studies.

1. Introduction

Age-related macular degeneration affects the macula, a specific structure in the central retina, leading to worsening of visual acuity. It is the major cause of blindness in the elderly in developed countries. Its global pooled prevalence is estimated to be more than 8%. It is an emerging problem, as it is estimated that the number of people affected by AMD in 2020 will be about 200 million, increasing to almost 300 million in 2040 [1, 2]. Medical cost of care about AMD patients is high reaching over 2 billion dollars in the USA and Australia and about a hundred million euros in some European countries [3]. Therefore, AMD is an emerging element of the global issue of vision loss and medical care.

AMD is a complex disease in which both genetic and environmental factors play a role, but the exact mechanism of its pathogenesis is unknown. The disease occurs in two forms: dry and wet. Molecular studies addressing AMD are impeded by inaccessibility of the live retina tissue from AMD patients. No effective treatment for the more common, dry form of AMD has been established yet.

AMD affects mainly elderly people, and it is a major reason for blindness among individuals over 65 years in

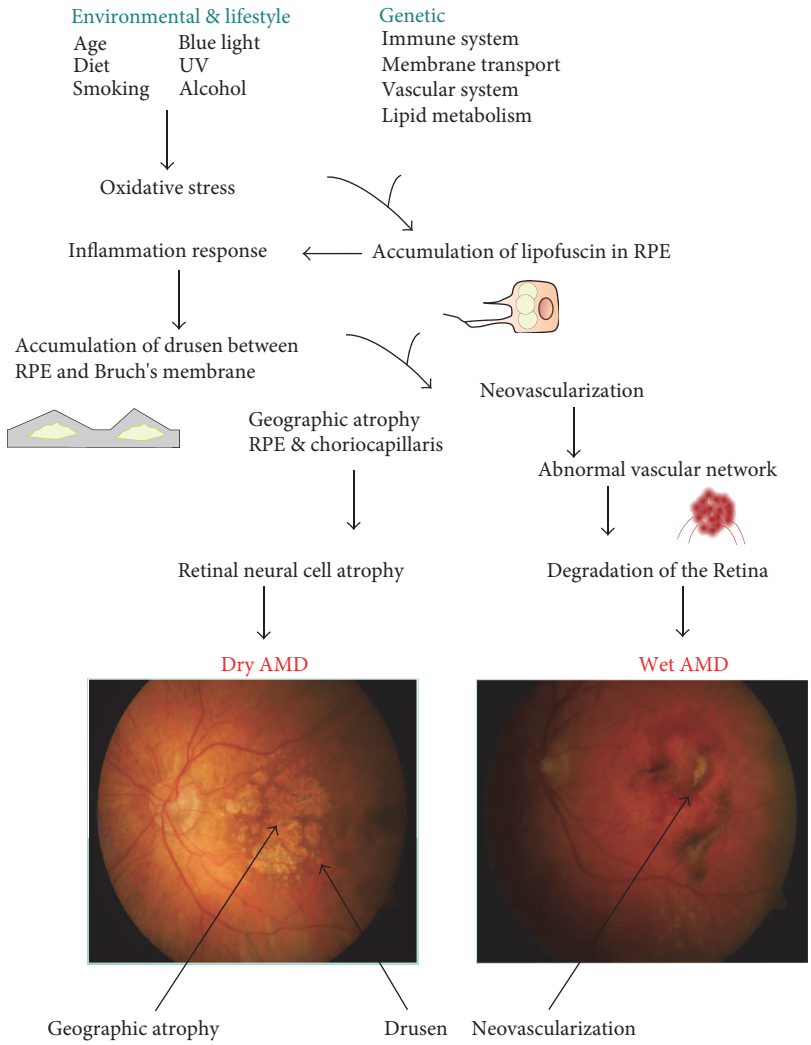

Figure 1: The exact mechanism of AMD pathogenesis is not known, but several factors can be implicated with a distinct role of aging. Besides aging, various oxidative stress-related environmental and lifestyle influences can be involved. The complement gene mutations play a major role in AMD. Oxidative stress and presumably other factors lead to accumulation of heterogenous lysosomal lipofuscin in retinal pigment epithelium (RPE), which induces a proinflammatory response. This, in turn, can lead to accumulation of extracellular drusen. Lipofuscin contains proangiogenic factors, such as A2E, that may develop choroidal neovascularization typical for wet AMD.

developed countries [4]. Aging is the most important risk factor for AMD. Although the exact mechanism of AMD pathogenesis is not known, oxidative stress, protein aggregation, and inflammation as well as some genetic factors play a central role in AMD development (Figure 1) [5]. Early dry AMD is hardly detectable and usually asymptomatic. Its advanced form, called geographic atrophy (GA), is associated with a massive loss of photoreceptors that evokes central visual loss [6]. A clinical hallmark of wet AMD is the presence of neovascular vessels sprouting from the choriocapillaris into the retina.

Progression of AMD ultimately leads to RPE and photoreceptors death via several mechanisms, including apoptosis, pyroptosis, necroptosis, and necrosis [7]. Autophagy may be involved in the regulation of the cell death mode in AMD [8] (Figure 2).

2. Cell Senescence and Aging in AMD

Kozlowski proposed that cellular senescence of RPE cells played a role in the etiology of AMD [9]. It seems that many studies on the role of cell senescence in organismal aging and age-related pathologies support this idea.

Senescence of human fibroblasts, described for the first time by Hayflick and Moorehead [10, 11] as a cell division limit in culture, affects not only fibroblasts but also other proliferating somatic human cells, such as keratinocytes and melanocytes [12], lymphocytes [13], epithelial [14] and endothelial [15] cells, vascular smooth muscle [16, 17], mesothelial cells [18], mesenchymal stem cells [19], and even cancer cells [20, 21].

Many studies suggest involvement or even a causative role of cell senescence in aging and age-related diseases [22–25]. Indeed, using different set of markers, senescent

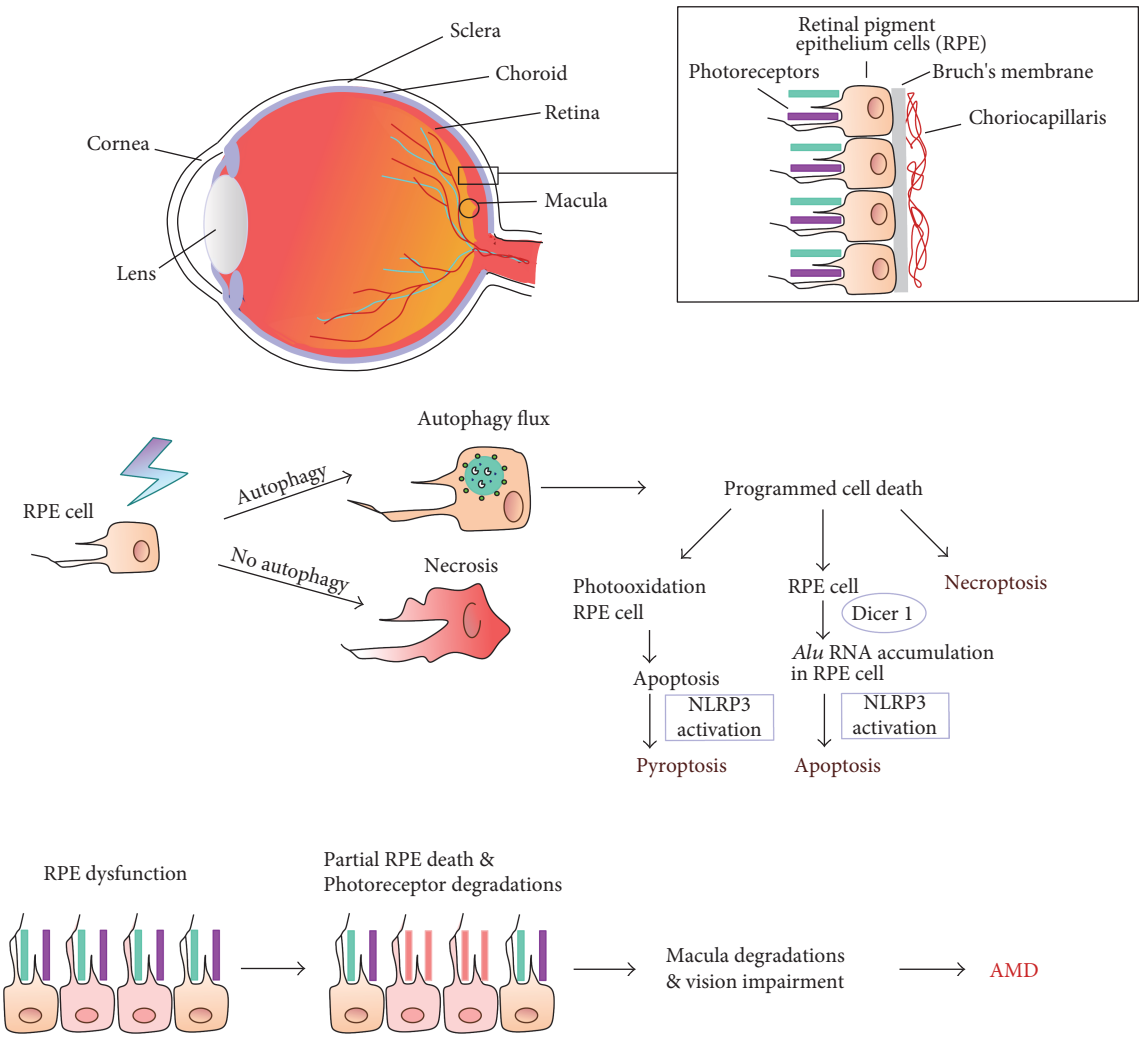

Figure 2: Cell death and autophagy in AMD progression. AMD affects the macula, a part in the central retina, and is associated with degradation of retinal pigment epithelium (RPE) cells, photoreceptors, and choriocapillaris. Autophagy can be decisive in switching between programmed and nonprogrammed cell death mode. Apoptosis of RPE cells can be linked to blue light exposure (photooxidation), oxidative stress, accumulation of *Alu* transposons due to impaired functioning of the DICER1 endonuclease, and the activation of the NLRP3 inflammasome. Pyroptosis can also result from photooxidation and activation of the NLRP3 inflammasome. Oxidative stress and other factors can induce necroptosis, a programmed version of necrosis.

cells were found *in vivo* in human, baboon, and mouse skin, human and rodent vascular endothelium, smooth and skeletal muscles, fat tissue and liver [26], skeletal muscle of rodents and primates [27], and human T cells [13]. There is emerging experimental evidence of the accumulation of senescent cells at sites of pathology, such as type 2 diabetes, atherosclerosis, hypertension, chronic pulmonary disease, cataracts, and glaucoma [28]. Senescent cells were also found in RPE of primates [29].

It was postulated that the exposure of cells to recurrent or chronic nonlethal stress might contribute to an increase in the accumulation of stress-induced senescent cells, thereby accelerating tissue aging [30]. Although we believe that senescent cells accumulate with age partially due to their resistance to apoptosis [31], one cannot exclude that at least some of them are cleared by the immune system, as recently reported [32] or that in certain circumstances they can die. Eradication of senescent cells by forcing them to undergo apoptosis is a subject of genetic manipulation [33, 34] or pharmacological interventions by using senolytic agents and can prolong health span [35]. On the other hand, age-dependent apoptosis of muscle cells (sarcopenia) is an undesirable hallmark of the process of organismal senescence, which can be more common than expected [36].

From a mechanistic point of view, a growing body of evidence proves that persistent DNA damage, especially double-strand breaks (DSBs) and DNA damage response (DDR), are closely associated with cell senescence [37]. Number of DSB sensor, γ-H2AX *foci*, a marker of DSBs, increased in both mouse and human senescent primary cells in tissue culture [38] and in the skin of old primates [39]. Senescence-associated galactosidase- (SA-β-gal-) positive cells and γ-H2AX-positive cells colocalize in old mice [40], and the number of γ-H2AX *foci* in lymphocytes in humans

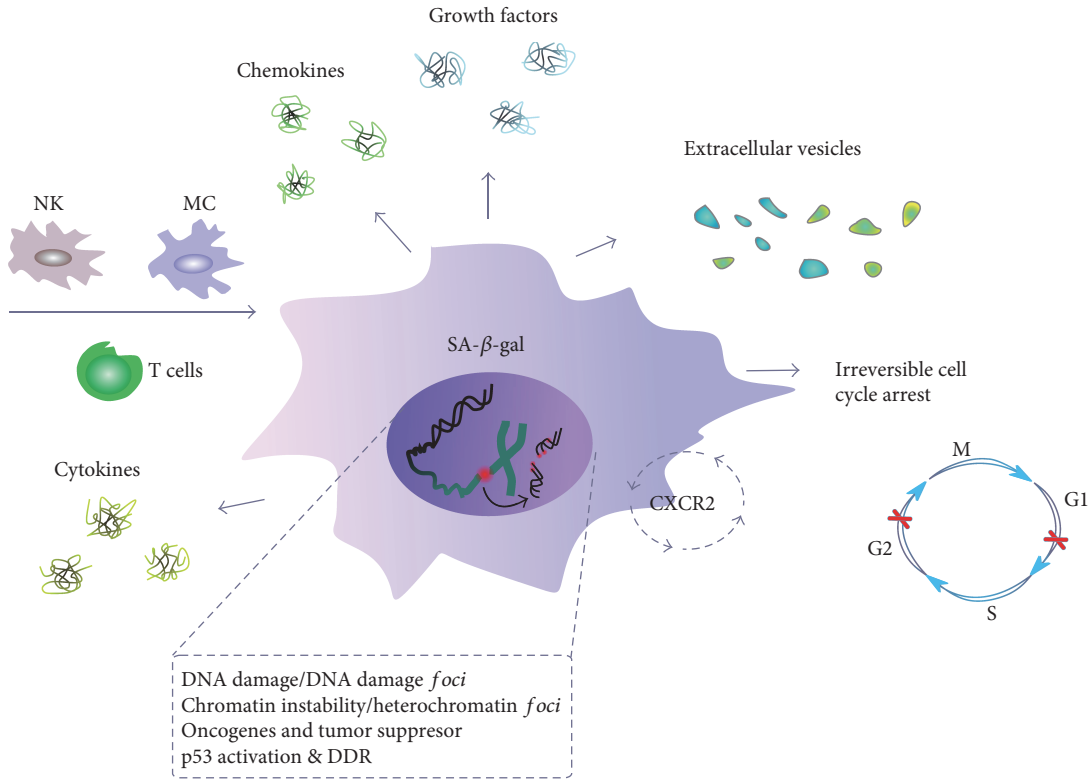

Figure 3: Senescent cells and senescence-associated secretory phenotype (SASP). A cell undergoing senescence is permanently arrested in the G1 or G2 phase of the cell cycle and has changed morphology. It is featured by an increased activity of senescence-associated-β-galactosidase (SA-β-gal) and can be targeted by the immunological system, with natural killer (NK) cells, macrophages (MS), and T-lymphocytes involved. Released various soluble agents, including cytokines, chemokines, growth factors, and extracellular vesicles, are main determinants of SASP. A senescent cell is characterized by an elevated level of DNA damage and chromosomes aberrations, which are also signs of genomic and chromosomal instability, typical for cancer cells. Chemokine signaling through the CXCR2 protein increases senescence.

increases with age [41, 42]. Fibroblasts from individuals suffering from progeria (Hutchinson-Gilford syndrome) persistently displayed many markers of increased basal DDR [43]. Recently, it has been shown that a controlled induction of DSBs in mouse liver induces features of tissue aging [44].

All senescent cells display common features, such as arrest in the G1 or G2 phase of the cell cycle, increased cell size, granularity, and increased activity of SA-β-gal (Figure 3) [24]. Senescent cells stay alive and are metabolically active and secrete a lot of factors [45] that can be classified into inflammatory chemokines and cytokines, matrix-remodeling proteases, and growth factors [46]. SASP can not only influence tissue surveillance in a way which can promote tissue repair, prevent fibrosis, and signal to the innate immune system to clear the senescent cells but also induce cancer development and other age-related diseases [47]. It also promotes a low-grade inflammation, which can drive organismal aging (inflammaging) [48].

There is a growing body of evidence linking DNA damage with inflammation and disease, particularly age-dependent diseases [49]. This is sort of a vicious cycle as DNA damage-dependent senescence can lead to secretion of molecules, which can reinforce senescence [50] and can induce DNA damage and DNA damage-dependent bystander senescence [51].

Initiation and maintenance of the SASP requires the DDR proteins ATM, NBS1, and CHK2, but not p53 and pRb. NF-κB signaling is another pathway involved in generating SASP that can be linked with DDR [52]. Recently, it has been shown that the GATA4 protein is directly involved in SASP. GATA4 is normally degraded, but it is stabilized in cells undergoing senescence. GATA4 is activated by DNA damage response regulators, ATM and ATR, but not by p53 or p16. This transcription factor activates NF-κB to initiate SASP and facilitate senescence [53]. However, NF-κB can be also activated by p38MAPK independently of DDR [54]. Also, mTOR can be involved in SASP as its inhibition by rapamycin substantially reduces the level of secreted cytokines [55, 56].

Although the causative role of reactive oxygen species (ROS) in aging is disputable, the paradigm assuming that oxidative stress and ROS produced by mitochondria play an important role in cell senescence has been supported [57, 58]. Hydrogen peroxide was the first factor used to show oxidative stress-induced senescence [59]. We also used this compound to show a canonical signaling pathway involved in cell senescence [60]. Oxidative stress, which can induce

cellular damage, has been closely connected with the pathogenesis of AMD as the retina is particularly susceptible to the stress because of its high consumption of oxygen, high proportion of polyunsaturated fatty acids, and exposure to visible light [61]. Therefore, retinal cells can be prone to stress-induced senescence. The retina is built of three layers of neural cells and one layer of RPE cells, which are quiescent.

Although cell senescence per definition denotes a permanent growth arrest of proliferation competent cells, recently, Jurk and others have shown that some features of cell senescence, including DDR, also apply to postmitotic neurons *in vivo* [62]. However, we showed that the SA-β-gal phenotype in neurons could not be attributed uniquely to cell senescence either *in vitro* or *in vivo* [63].

Although epithelial cells stay quiescent in the retina, they are proliferation-prone and vulnerable to oxidative stress-induced senescence. Indeed, in several studies using proliferating human RPE-derived ARPE-19 cells, which proliferate *in vitro*, the cell senescence process was documented upon oxidative stress. In several studies, senescence was induced by hydroxyl peroxide in nontoxic concentrations [64–67]. In other studies, *tert*-butyl hydroperoxide [68] or cigarette smoke [69] was applied. Arend et al. observed a significant increase in cell viability and reduced SA-β-gal activity, ROS amount, and DNA damage *foci* in ARPE-19 cells induced to senescence with H_2O_2 and pretreated with idebenone, which is a derivative of coenzyme Q10, but with a tenfold higher antioxidant capacity than its parental compound [64]. Similarly, fullerenol, a ROS scavenger and antioxidant, protected ARPE-19 cells from H_2O_2-induced senescence. Interestingly, fullerenol activated SIRT1, which belongs to the family of "proteins of youth"—sirtuins [70].

The use of ARPE-19 cells in senescence studies have some limitations. ARPE-19 population can contain a substantial, if not the major, fraction of cells which are able to double their population to over 270 times, so they can be considered as immortal [23]. Unlike cells with limited number of divisions, immortal cells do not undergo replicative senescence. However, it was shown that they are prone to stress-induced senescence [71, 72].

3. Autophagy and DDR-Dependent or DDR-Independent Players in AMD Pathogenesis

Autophagy controls cellular homeostasis by degrading in lysosomes damaged, nonfunctional or no longer needed cellular components, including organelles. Autophagic degradation provides energy, and lysosomal machinery can deliver amino acids and other degradation products back to the cytoplasm, where they can be reused as building blocks in cellular metabolism ("recycling") [73]. This process can be carried out through at least three distinguished pathways: macroautophagy (further referred to as autophagy), chaperone-mediated autophagy (CMA), and microautophagy. Many proteins are involved in autophagy, including autophagy-related proteins (ATGs), mammalian target of rapamycin (mTOR), the serine/threonine kinase (ULK1), FIP-200, p62 (SQSTM1), and microtubule-associated protein light chain 3 (LC3) [74]. The hallmark of autophagy and its critical stage is the formation of a double-membraned vesicle enclosing materials for degradation (cargo), called the autophagosome (Figure 4). It then fuses with the lysosome forming autolysosome, in which the cargo is degraded [75].

Impaired autophagy was observed in serious human disorders, such as cancer and neurodegenerative diseases including AMD [76]. In general, autophagy plays an important role in the functioning of RPE cells [77–79]. Drusen are a clinical hallmark of AMD and an important element of its pathogenesis [5, 80, 81]. They are yellowish deposits between RPE cells and Bruch's membrane. Consequently, impaired autophagy can lead to drusen accumulation contributing to AMD development [82]. However, the relationship between autophagy and aging is not fully known and the activity of this process changes during lifetime. In addition, detailed autophagic pathways involved in the development of AMD have not been identified as different mechanisms of autophagy can function in normal and pathological retinas [83].

There is an emerging body of experimental evidence on the involvement of autophagy in AMD pathogenesis. These experiments are performed mainly on animal model of AMD and retinas obtained postmortem from AMD donors [78]. Autophagy is closely associated with cellular response to oxidative stress with the involvement of the p62/Keap1/Nrf2 pathway [84, 85]. Moreover, autophagy can be considered as an element of DDR, in which DNA repair is a major component, being a major constituent of cellular antioxidant defense [86–88]. We and others showed that AMD could be associated with disturbed DNA repair [49, 89–91].

Oxidative stress, a main factor in AMD pathogenesis, results in various DNA lesions, and 8-oxo-7,8-dihydroguanine (8-oxoG) is a hallmark of oxidative DNA damage and a major mutagenic intermediate of oxidative stress [92]. In most cases, the repair of 8-oxoG is initiated by the hOGG1 glycosylase via the base excision repair (BER) pathway. If 8-oxoG escapes this process and replicative DNA polymerase misinserts adenine instead of cytosine opposite to 8-oxoG, an alternative pathway of BER can be activated with the hMYH (MUTYH) glycosylase, which removes that adenine. Our observations revealed that genetic variability in the *hOGG1* and *hMYH* genes may be associated with AMD occurrence and progression [93]. It was reported that the level of 8-oxoG was higher in patients with exudative AMD than in control individuals. This led to the conclusion that DNA damage may underline the role of oxidative stress in AMD pathology.

Our earlier data indicated that lymphocytes isolated from AMD patients displayed a higher level of endogenous DNA damage than lymphocytes from control individuals [89]. Also, oxidative DNA damage was higher in AMD patients than in controls and cells from the patients were more sensitive to hydrogen peroxide and UV radiation, which allowed us to speculate that the combination of impaired DNA repair and elevated sensitivity to UV radiation can be important for AMD pathogenesis.

Not only nuclear DNA (nDNA) but also its mitochondrial counterpart (mtDNA) was reported to have elevated extent of damage in AMD (Figure 5) [90, 94–96]. Moreover, in those studies, performed on macular and peripheral RPE

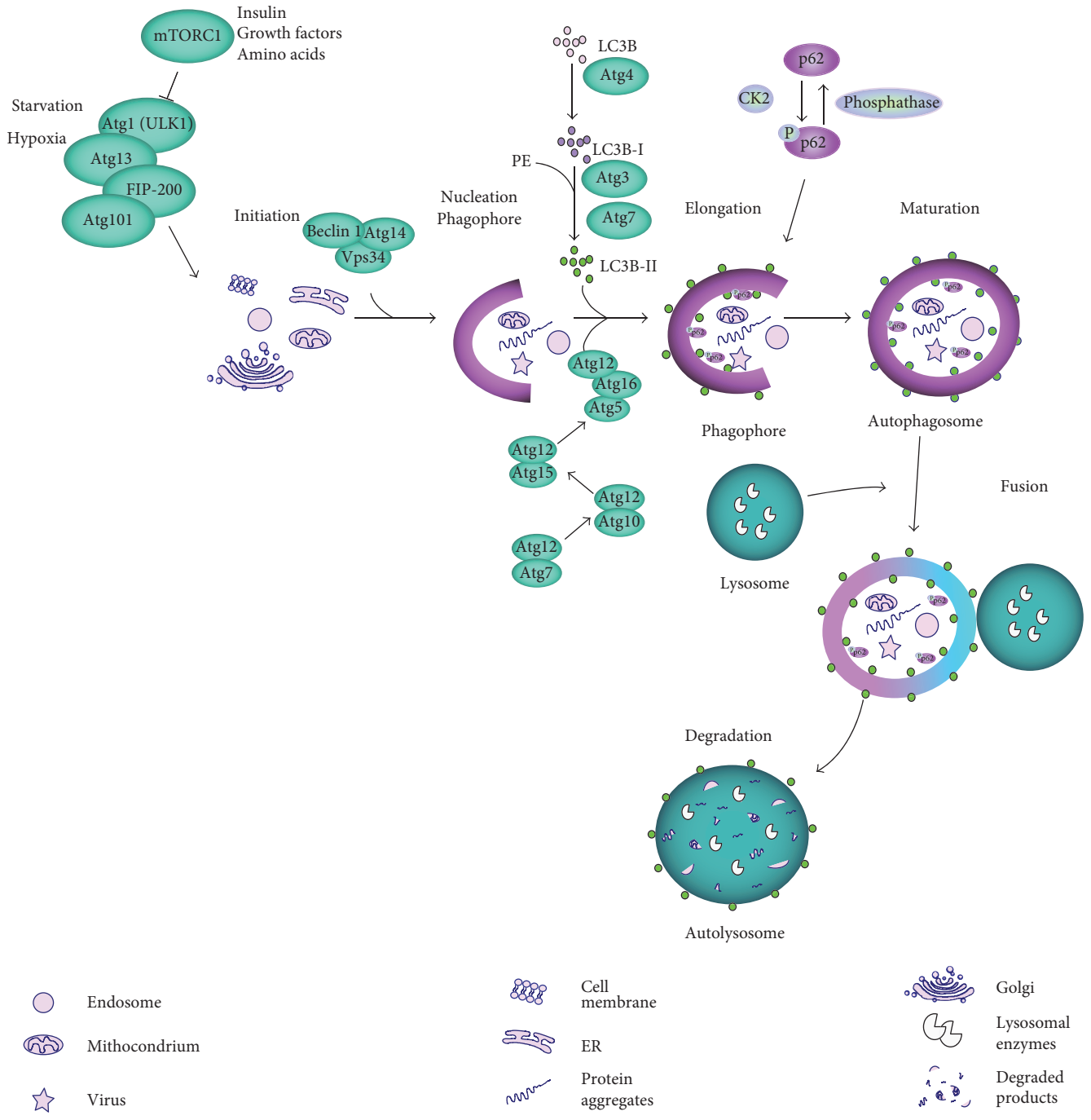

Figure 4: Autophagy dependent on mTOR. In normal nutrient conditions, the mTOR complex 1 (mTORC1) inhibits the ULK1 complex, consisting of ULK1, Atg13, Atg101, and FIP200, which can activate autophagy in stress conditions, including starvation and hypoxia or when the inhibitory effect of mTORC1 is abolished by growth factors, insulin, amino acids, or other agents. The material to be degraded (cargo) is then enclosed by a nucleating phagophore, which requires a translocation of ULK1 to endoplasmic reticulum (ER). ER membrane is used to form the phagophore, but other sources are also possible. The phagophore membrane is elongated, which leads to the formation of autophagosome, a vesicle with the enclosed cargo. This process is assisted by LC3 lipidated by phosphatidylethanolamine (PE) and many individual proteins, including Beclin 1, Vps34, and autophagy-related proteins (Atgs). The p62 protein functions as a selective autophagy receptor for degradation of ubiqutinated substrates, but it is itself a specific substrate for autophagy after its phosphorylation and can be selectively incorporated into the autophagosome and degraded. Fusion of autophagosome with lysosome creates autolysosome in which the cargo is degraded by lysosomal enzymes. Autophagy can be also activated by mTOR-independent pathways.

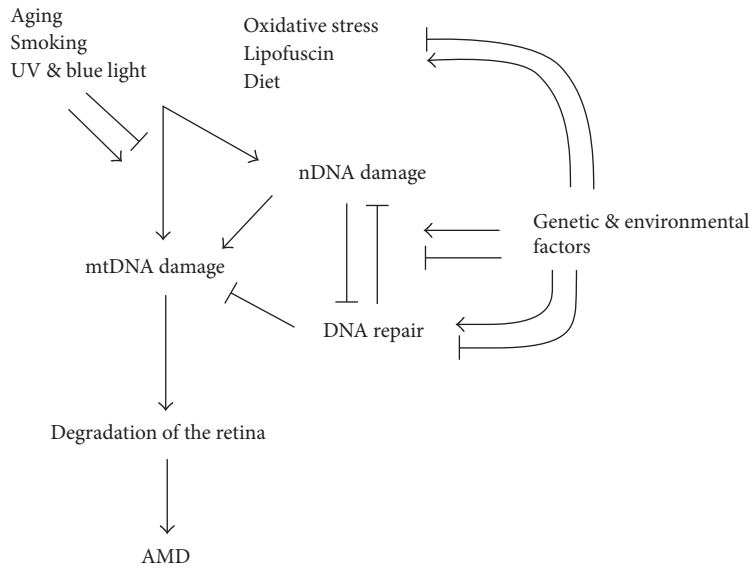

Figure 5: Nuclear and mitochondrial DNA (nDNA and mtDNA) can be damaged by AMD risk factors, which can also affect proteins, including DNA repair proteins. Nonrepaired or misrepaired DNA can contribute to retinal cell death occurring in AMD [89].

cells obtained from AMD patients and rodents, an increase in heteroplasmic mutations and a decrease in the efficacy of mtDNA repair were observed. In fact, there are reports showing that mtDNA in cultured RPE cells is more prone to DNA damage, at least induced by certain agents, than nDNA [91, 97–101]. Although the efficacy of DNA repair declines with age for both kinds of DNA, mtDNA from the retina was shown to have more potentially detrimental changes, than mtDNA from blood, for both normal and AMD samples [102]. These changes are potentially detrimental, if not repaired, as mtDNA contains almost exclusively coding sequences. The repair of mtDNA is generally considered as poorer than in the nucleus. All DNA repair proteins are encoded in nDNA, so its damage can affect protection from damage in mtDNA. Therefore, DNA damage can be associated with AMD occurrence and progression, suggesting that DDR can play a role in the pathogenesis of this disease.

4. Relationship between Senescence, Autophagy, and DNA Damage Response in RPE Cells

Many reports link oxidative stress with autophagy showing that this association is regulated in a highly coordinated pathway [103]. It is clearly illustrated by the activation of Nrf2, a transcription factor crucial for cellular antioxidant defense, by p62, a key regulator of autophagy [104]. Likely, the most direct association between oxidative stress and autophagy is expressed by mitophagy, when mitochondria with highly damaged DNA are degraded [105]. This is a specific feature of DDR in mitochondria, as in the nucleus heavily damaged DNA can induce a programmed death or in certain circumstances can be tolerated, which usually results in mutations [106]. Although ROS can induce autophagy in starvation conditions, it is not known which species are responsible for this effect [107] and both superoxide radical ($O_2^{\bullet -}$) and hydrogen peroxide were considered to trigger autophagy in starvation [108–111]. In general, ROS are inducers of autophagy [112, 113]. Moreover, some data suggest that mitochondria are the main source of ROS needed for the induction of autophagy [109, 110, 114].

Several DDR pathways prevent or cope with DNA damage. However, if DNA is highly damaged, cells remain quiescent or undergo programmed cell death. Persistent, unrepaired DNA damage is typical for cell senescence. Autophagy acts as both a prosurvival mechanism and a kind of cell death, making a critical contribution to cell fate after DNA damage. Some reports suggest that autophagy delays apoptosis induced by DNA damage, providing energy required for DNA repair [1]. In general, autophagy participates in DDR by elimination of toxic aggregates, which can be a source of ROS and in this way indirectly decrease DNA damage [115, 116].

Several DDR proteins are involved in the regulation of autophagy. PolyADP-ribose polymerase 1 (PARP1), which is essential for DNA single-strand break repair, catalyzes polyribosylation of nuclear proteins converting NAD^+ into polymers of polyADP-ribose. This leads to NAD^+ utilization and ATP depletion, resulting in an energetic imbalance, which activates autophagy via the AMPK pathway, to recycle metabolic precursors for ATP and provide energy needed for DDR [117]. ATM, a crucial protein for DDR signaling, is another protein linking DDR to autophagy. It can activate TSC2, a tumor suppressor, to inhibit mTORC1 and induce autophagy [118]. The p53 protein, a key DDR regulator, and members of its family were shown to affect expression of several genes encoding autophagic proteins [119, 120].

It is generally accepted that autophagy declines with aging of model organism, resulting in the accumulation of cellular debris and turning the cell brown. Decreased autophagy is often associated with accelerated aging, whereas

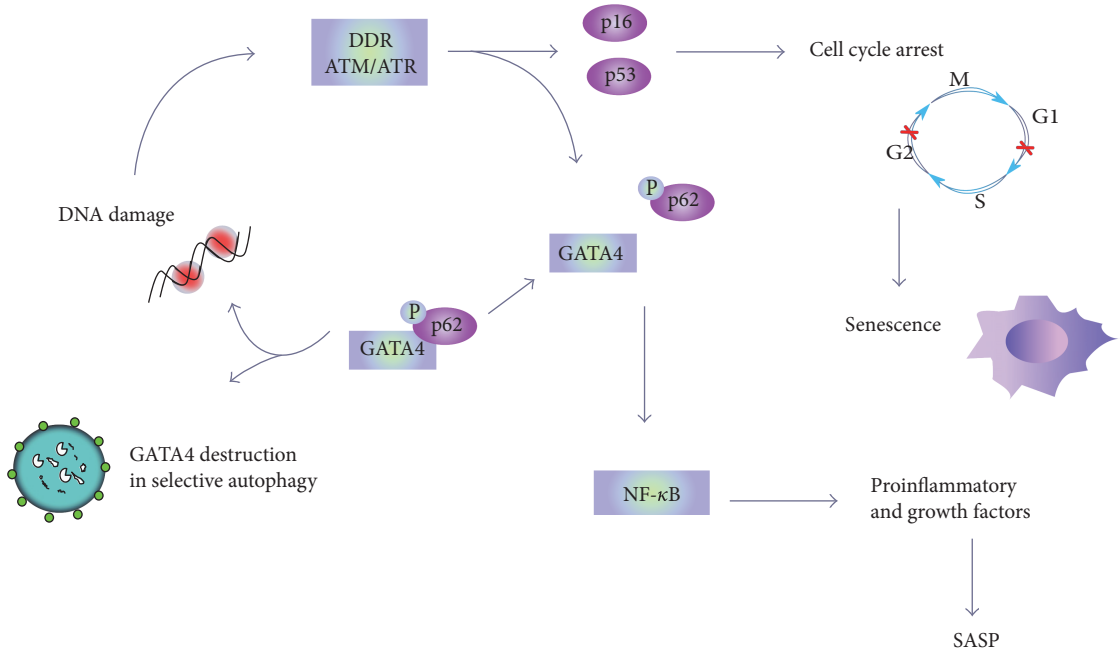

Figure 6: GATA4 can be involved in autophagy, senescence, and DNA damage response (DDR). The level of GATA4 is normally regulated by p62-dependent selective autophagy, but DNA damage and resulting DDR can release GATA4 from p62 control by its ATM-induced phosphorylation. If DNA damage cannot be repaired, DDR effectors induce permanent and irreversible cell cycle arrest, which is a hallmark of senescence with senescence-associated phenotype (SASP). GATA4 released from autophagic degradation can transactivate several genes that activate NF-κB, resulting in the release of growth factors, chemokines, cytokines, and other molecules typical for SASP.

stimulated autophagy can exert a potent antiaging effect [121]. It is associated with reduced expression of proteins important for autophagy induction, including ATGs, Sirtuin 1, Beclin 1, ULK1, and LC3 [122].

DNA damage, with the key proteins ATM and ATR is a causative signal to cellular senescence. DNA damage-dependent senescence was shown in human and murine fibroblasts upon different stimuli [37]. The role of mitochondrial homeostasis and ROS generation in the process of aging has been subject of debate. Free-radical and mitochondrial theories of aging speculate that cumulative damage to mitochondria and mitochondrial DNA induced by ROS is one of the causes of aging. Oxidative damage affects replication and transcription of mtDNA and results in a decline in mitochondrial functions, which in turn leads to enhanced ROS production and further damage to mtDNA [58]. However, we showed that a decreased ROS level did not protect cells against senescence [21, 123]. Correia-Melo et al. observed that senescent cells had an increased mitochondrial mass driven by mitochondrial biogenesis, which resulted in increased cellular oxygen consumption. They have also uncovered a novel senescence regulatory pathway, in which the activation of the ATM, AKT, and mTOR phosphorylation cascades downstream of DNA damage triggered PGC-1α- (peroxisome proliferator-activated receptor-gamma coactivator 1 alpha-) dependent mitochondrial biogenesis [57]. However, other recent studies have highlighted mTOR as a SASP regulator by alternative mechanisms emphasizing mTOR rather as an antisenescence target [55]. Therefore, the role of mitochondrial biogenesis, ROS, and mTOR in cell senescence and SASP is still an open question.

The interplay between cell senescence and autophagy is yet unclear. Young et al. have shown that autophagy is activated upon an induction of cell senescence and contributes to the establishment of senescence [124], but there are contradictory data showing that inhibition of autophagy can favor cell senescence and that autophagy is necessary for senescence [21, 123]. We showed an impaired autophagy in RPE upon chronic oxidative stress, but senescence was not induced in that study [125]. Senescence of RPE cells may be associated with alterations in PGC-1α function. In neurons as well as in RPE cells, PGC-1α was shown to regulate lysosomal activity by TFEB protein, which might be important for improvement of autophagy flux and removal of cell damage [126, 127]. It was also demonstrated in that work that PGC-1α deficient mice developed some abnormalities in RPE, which were associated with their accelerated senescence. Next, PGC-1α alpha silencing in ARPE-19 cells aggravated H_2O_2-induced senescence. These cells displayed a significantly higher SA-β-gal activity than control cells. Senescence of RPE cells has been associated with an altered mTOR signaling [128, 129].

GATA4 is a member of GATA transcription factors, and Kang and coworkers identified this protein as a key regulator of cellular senescence [53, 130]. GATA4 is also important for DDR and is regulated by autophagy, so it can be at the crossroad of these three cellular phenomena: senescence, autophagy, and DDR (Figure 6). It is also important that GATA4 is involved in the mechanisms inducing SASP phenotype, which can promote chronic inflammation associated with most age-related diseases, including AMD [5, 53, 131].

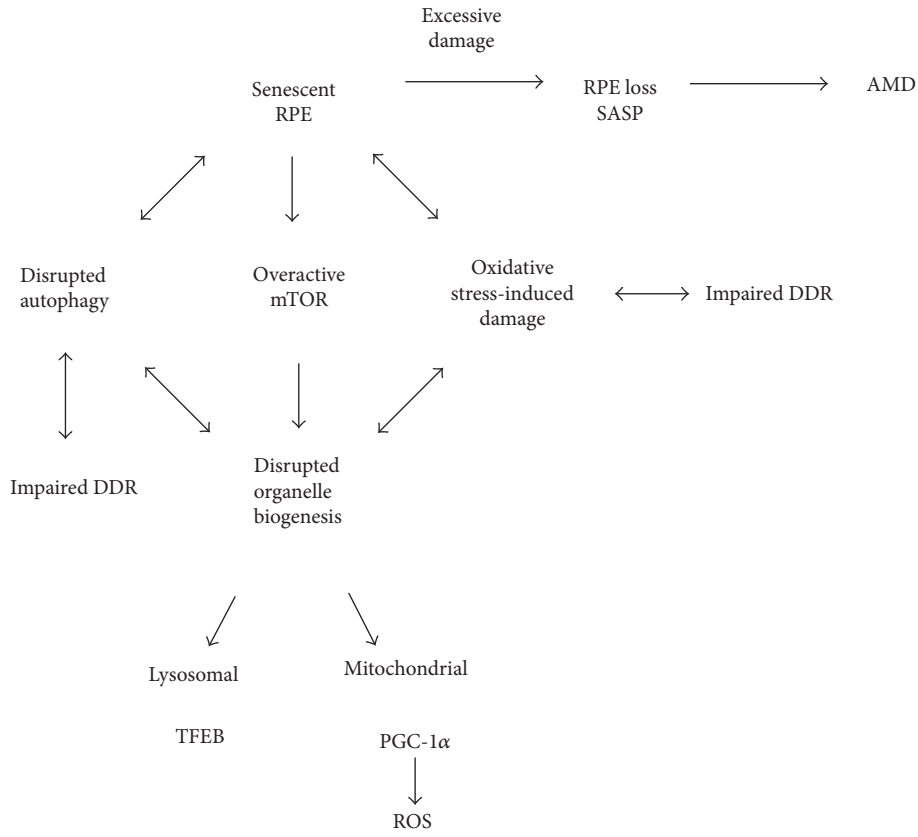

Figure 7: Senescence as a critical factor in AMD pathogenesis. In certain stress conditions, which can be induced by environmental or/and lifestyle factors in aging retina, a major fraction of RPE cells become senescent and are no longer able to regenerate damaged RPE cells, which leads to AMD. The senescence of RPE cells can result from an interplay between aging, autophagy, and DDR in stress conditions. This interplay is a kind of vicious cycle as impaired DNA damage response (DDR) can lead to an increased damage to biomolecules by ROS. Damage to biomolecules induces the degradation of organelles via mTOR-dependent autophagy. This may lead to aggravation of oxidative stress and cellular damage as well as continue to impair autophagy and antioxidant defense by altered TFEB (transcription factor E-box binding) and PGC-1α signaling and increased ROS generation.

GATA4 is normally degraded by p62-mediated autophagy and it was shown to be stabilized in cells undergoing senescence, possibly due to a decreased association with p62 [53]. As GATA4 activation depends on the key DDR signaling proteins, ATM and ATR and it is accumulated in some aging tissues, it is a good candidate to orchestrate interplay between senescence, autophagy, and DDR. Kang and coworkers postulated that the GATA4-mediated relationship between autophagy and senescence is different for different modes of autophagy [53]. GATA4 can be a positive regulator of senescence and selective autophagy, but a signal inducing senescence can stimulate GATA4 to avoid selective autophagy.

In searching for a mechanism by which GATA4 regulates senescence, Kang et al. observed that it upregulated (mostly) and downregulated genes important for senescence [53]. Therefore, GATA4 could be involved in the stimulation of a considerable fraction of genes, including the SASP genes, whose expression determines the senescence phenotype. GATA4 was shown to act upstream of NF-κB during senescence induction and depletion of RelA (p65), a component of NF-κB [53]. This effect was associated with the repression of almost all genes involved in SASP, except IL1A. Subsequent experiments showed that GATA4 regulated senescence response independently of the p53 and p16INK4a/Rb pathways.

When key DDR regulators ATM and ATR were inhibited, the GATA4 pathway was inhibited during senescence, suggesting that it is a new independent branch of DDR. The role of DDR in inhibition of autophagy-mediated degradation of GATA4 is not known yet. GATA4 was observed to accumulate in organs of 22-month-old mice as compared to their 6-month-old counterparts, which correlates with the accumulation of senescent cells in aging organism [26, 53, 132–134].

In summary, GATA4 can be involved in DDR and this involvement is independent of p53 and $p16^{INK4a}$/Rb pathways. GATA4 is closely associated with senescence and SASP and is controlled by selective autophagy, but can also stimulate general autophagy [53]. Therefore, it is justified to consider a role of GATA4 in coordinating senescence, autophagy, and DDR. In addition, as GATA4 associates with inflammation, studies on its role in AMD pathogenesis are justified.

5. Senescence-Based Pathogenesis of AMD with the Contribution of Autophagy and DDR

RPE cells in the central retina are quiescent due to spatial constraints and contact with neuroretina, and when damaged, they can be replaced by their proliferating counterparts at RPE periphery in an endogenous compensatory mechanism [135]. This endogenous regenerative mechanism is activated in pathological conditions, which can increase with age [136]. Oxidative stress can induce senescence in RPE cells if they are prone to and result in inability of peripheral RPE cells to rescue their central RPE counterparts, which can lead to a massive loss of RPE cells observed in clinically detected AMD. If most of macular peripheral RPE cells are affected by senescence, this mechanism can fail leading to AMD. Senescent RPE will be the source of pathology and have a detrimental impact on surrounding tissue through SASP.

We hypothesize that under some circumstances, RPE senescence may contribute to or/and precede irreversible pathological events in the retina specific for AMD, such as RPE loss and inflammation. Senescent RPE cells may be excessively damaged, dysfunctional, and capable of overexpression of SASP. Figure 7 illustrates this novel concept of RPE senescence as a critical contributor to AMD induction and progression.

We believe that senescence associates with autophagy and DDR. As mentioned, cell senescence can be causative for aging and age-dependent diseases. All these three effects, senescence, autophagy, and DDR, can be provoked by oxidative stress, which is a major factor in AMD pathogenesis. Moreover, aging is the main risk factor of pathogenesis of AMD and can be related to oxidative stress [46]. Inflammation associates with oxidative stress, aging (inflammaging), and AMD [5, 137, 138]. Therefore, it is logical and justified to hypothesize that senescence can play a role in AMD and this process can be influenced or regulated by autophagy and DDR. Consequently, GATA4, as an identified factor to be involved in cell senescence, autophagy, DDR, and inflammation, seems to be a natural candidate to play a major role in the proposed mechanism of AMD pathogenesis. However, this is only a hypothesis, which should be verified, but we tried to show some arguments that this subject is worth further study and development.

6. Conclusions and Perspectives

Molecular studies on AMD pathogenesis in humans are limited. Therefore, choosing an optimal experimental model for these studies is essential. ARPE-19 cell line is commonly used in molecular research on AMD, even though it is a heterogeneous cell population, including dividing and nondividing cells. However, as AMD is an age-related disease, the process of cell senescence should be included in *in vitro* models. As oxidative stress is a main AMD pathogenesis factor, cellular antioxidant defense is important in the disease prevention. That is why one can use RPE cells from mice knockout of genes essential for antioxidant defense. To include aging in that study, animals at different ages can be used. As the main AMD genetic risk factor are mutations in the gene encoding complement factor H, one can use RPE cells derived from induced pluripotent stem cells (iPSCs) obtained from AMD patients having such mutations.

It seems that the relationship between DDR and autophagy in mitochondria can be especially important for AMD pathogenesis due to many reasons [139]. First, mitochondrial DDR is different from DDR in the nucleus [140]. Second, autophagic mtDNA degradation can be considered as a DDR pathway dealing with heavily damaged molecules of mtDNA [141]. Third, mitochondrial mutagenesis was reported to play a role in AMD pathogenesis [89–91]. Furthermore, the role of mTOR, a crucial autophagy protein, in lysosomal and mitochondrial biogenesis has been recently appreciated [57, 142]. Therefore, studies of DDR and autophagy in mitochondria in the context of AMD are warranted.

To summarize, cellular senescence and SASP can be related to age-related chronic diseases [137, 143]; chronic inflammation (inflammaging) is also involved in age-related chronic diseases [137]; autophagy and senescence seem to be closely related [144]; and lastly the GATA4 protein can be involved in DDR, senescence, and autophagy as well as in inflammation and aging [53, 130].

Work to determine the relationship between aging (senescence), autophagy, and DDR and relate it to AMD can bring information important for AMD clinic and basic molecular biology as there are many essential unanswered questions and problems concerning mutual relationships between aging, autophagy, and cellular reaction to DNA damage.

Conflicts of Interest

The authors declare that they have no conflicts of interest.

References

[1] W. L. Wong, X. Su, X. Li et al., "Global prevalence of age-related macular degeneration and disease burden projection for 2020 and 2040: a systematic review and meta-analysis," *The Lancet Global Health*, vol. 2, no. 2, pp. e106–e116, 2014.

[2] J. B. Jonas, "Global prevalence of age-related macular degeneration," *The Lancet Global Health*, vol. 2, no. 2, pp. e65–e66, 2014.

[3] A. Gordois, H. Cutler, L. Pezzullo et al., "An estimation of the worldwide economic and health burden of visual impairment," *Global Public Health*, vol. 7, no. 5, pp. 465–481, 2012.

[4] M. Reibaldi, A. Longo, A. Pulvirenti et al., "Geo-epidemiology of age-related macular degeneration: new clues into the pathogenesis," *American Journal of Ophthalmology*, vol. 161, pp. 78.e1–93.e2, 2016.

[5] A. Kauppinen, J. J. Paterno, J. Blasiak, A. Salminen, and K. Kaarniranta, "Inflammation and its role in age-related macular degeneration," *Cellular and Molecular Life Sciences*, vol. 73, no. 9, pp. 1765–1786, 2016.

[6] R. Klein, B. E. Klein, M. D. Knudtson, S. M. Meuer, M. Swift, and R. E. Gangnon, "Fifteen-year cumulative incidence of age-related macular degeneration: the Beaver Dam Eye Study," *Ophthalmology*, vol. 114, no. 2, pp. 253–262, 2007.

[7] K. Kaarniranta, P. Tokarz, A. Koskela, J. Paterno, and J. Blasiak, "Autophagy regulates death of retinal pigment

epithelium cells in age-related macular degeneration," *Cell Biology and Toxicology*, vol. 33, no. 2, pp. 113–128, 2017.

[8] A. Klettner, A. Kauppinen, J. Blasiak, J. Roider, A. Salminen, and K. Kaarniranta, "Cellular and molecular mechanisms of age-related macular degeneration: from impaired autophagy to neovascularization," *The International Journal of Biochemistry & Cell Biology*, vol. 45, no. 7, pp. 1457–1467, 2013.

[9] M. R. Kozlowski, "RPE cell senescence: a key contributor to age-related macular degeneration," *Medical Hypotheses*, vol. 78, no. 4, pp. 505–510, 2012.

[10] L. Hayflick and P. S. Moorhead, "The serial cultivation of human diploid cell strains," *Experimental Cell Research*, vol. 25, pp. 585–621, 1961.

[11] P. S. Moorhead, W. W. Nicholls, F. T. Perkins, and L. Hayflick, "Standards of karyology for human diploid cells," *Journal of Biological Standardization*, vol. 2, no. 2, pp. 95–101, 1974.

[12] D. Bandyopadhyay, N. Timchenko, T. Suwa, P. J. Hornsby, J. Campisi, and E. E. Medrano, "The human melanocyte: a model system to study the complexity of cellular aging and transformation in non-fibroblastic cells," *Experimental Gerontology*, vol. 36, no. 8, pp. 1265–1275, 2001.

[13] A. Brzezinska, A. Magalska, A. Szybinska, and E. Sikora, "Proliferation and apoptosis of human $CD8^+CD28^+$ and $CD8^+CD28^-$ lymphocytes during aging," *Experimental Gerontology*, vol. 39, no. 4, pp. 539–544, 2004.

[14] S. R. Romanov, B. K. Kozakiewicz, C. R. Holst, M. R. Stampfer, L. M. Haupt, and T. D. Tlsty, "Normal human mammary epithelial cells spontaneously escape senescence and acquire genomic changes," *Nature*, vol. 409, no. 6820, pp. 633–637, 2001.

[15] J. D. Erusalimsky and D. J. Kurz, "Endothelial cell senescence," *Handbook of Experimental Pharmacology*, vol. 176, Part 2, pp. 213–248, 2006.

[16] A. Bielak-Zmijewska, M. Wnuk, D. Przybylska et al., "A comparison of replicative senescence and doxorubicin-induced premature senescence of vascular smooth muscle cells isolated from human aorta," *Biogerontology*, vol. 15, no. 1, pp. 47–64, 2014.

[17] I. Gorenne, M. Kavurma, S. Scott, and M. Bennett, "Vascular smooth muscle cell senescence in atherosclerosis," *Cardiovascular Research*, vol. 72, no. 1, pp. 9–17, 2006.

[18] K. Ksiazek, K. Piwocka, A. Brzezinska et al., "Early loss of proliferative potential of human peritoneal mesothelial cells in culture: the role of p16INK4a-mediated premature senescence," *Journal of Applied Physiology*, vol. 100, no. 3, pp. 988–995, 2006.

[19] K. R. Shibata, T. Aoyama, Y. Shima et al., "Expression of the p16INK4A gene is associated closely with senescence of human mesenchymal stem cells and is potentially silenced by DNA methylation during in vitro expansion," *Stem Cells*, vol. 25, no. 9, pp. 2371–2382, 2007.

[20] I. B. Roninson, E. V. Broude, and B. D. Chang, "If not apoptosis, then what? Treatment-induced senescence and mitotic catastrophe in tumor cells," *Drug Resistance Updates*, vol. 4, no. 5, pp. 303–313, 2001.

[21] E. Sikora, G. Mosieniak, and M. A. Sliwinska, "Morphological and functional characteristic of senescent cancer cells," *Current Drug Targets*, vol. 17, no. 4, pp. 377–387, 2016.

[22] B. G. Childs, M. Durik, D. J. Baker, and J. M. van Deursen, "Cellular senescence in aging and age-related disease: from mechanisms to therapy," *Nature Medicine*, vol. 21, no. 12, pp. 1424–1435, 2015.

[23] E. Sikora, "Rejuvenation of senescent cells-the road to postponing human aging and age-related disease?," *Experimental Gerontology*, vol. 48, no. 7, pp. 661–666, 2013.

[24] E. Sikora, T. Arendt, M. Bennett, and M. Narita, "Impact of cellular senescence signature on ageing research," *Ageing Research Reviews*, vol. 10, no. 1, pp. 146–152, 2011.

[25] E. Sikora, A. Bielak-Zmijewska, and G. Mosieniak, "Cellular senescence in ageing, age-related disease and longevity," *Current Vascular Pharmacology*, vol. 12, no. 5, pp. 698–706, 2014.

[26] J. C. Jeyapalan and J. M. Sedivy, "Cellular senescence and organismal aging," *Mechanisms of Ageing and Development*, vol. 129, no. 7-8, pp. 467–474, 2008.

[27] J. A. Kreiling, M. Tamamori-Adachi, A. N. Sexton et al., "Age-associated increase in heterochromatic marks in murine and primate tissues," *Aging Cell*, vol. 10, no. 2, pp. 292–304, 2011.

[28] R. M. Naylor, D. J. Baker, and J. M. van Deursen, "Senescent cells: a novel therapeutic target for aging and age-related diseases," *Clinical Pharmacology and Therapeutics*, vol. 93, no. 1, pp. 105–116, 2013.

[29] K. Mishima, J. T. Handa, A. Aotaki-Keen, G. A. Lutty, L. S. Morse, and L. M. Hjelmeland, "Senescence-associated beta-galactosidase histochemistry for the primate eye," *Investigative Ophthalmology & Visual Science*, vol. 40, no. 7, pp. 1590–1593, 1999.

[30] O. Toussaint, P. Dumont, J. F. Dierick et al., "Stress-induced premature senescence. Essence of life, evolution, stress, and aging," *Annals of the New York Academy of Sciences*, vol. 908, pp. 85–98, 2000.

[31] J. Campisi, "Cancer and ageing: rival demons?," *Nature Reviews Cancer*, vol. 3, no. 5, pp. 339–349, 2003.

[32] A. Sagiv and V. Krizhanovsky, "Immunosurveillance of senescent cells: the bright side of the senescence program," *Biogerontology*, vol. 14, no. 6, pp. 617–628, 2013.

[33] D. J. Baker, B. G. Childs, M. Durik et al., "Naturally occurring p16(Ink4a)-positive cells shorten healthy lifespan," *Nature*, vol. 530, no. 7589, pp. 184–189, 2016.

[34] D. J. Baker, T. Wijshake, T. Tchkonia et al., "Clearance of p16Ink4a-positive senescent cells delays ageing-associated disorders," *Nature*, vol. 479, no. 7372, pp. 232–236, 2011.

[35] Y. Ovadya and V. Krizhanovsky, "Senescent cells: SASPected drivers of age-related pathologies," *Biogerontology*, vol. 15, no. 6, pp. 627–642, 2014.

[36] E. Marzetti, G. Privitera, V. Simili et al., "Multiple pathways to the same end: mechanisms of myonuclear apoptosis in sarcopenia of aging," *Scientific World Journal*, vol. 10, pp. 340–349, 2010.

[37] F. d'Adda di Fagagna, "Living on a break: cellular senescence as a DNA-damage response," *Nature Reviews Cancer*, vol. 8, no. 7, pp. 512–522, 2008.

[38] A. J. Nakamura, Y. J. Chiang, K. S. Hathcock et al., "Both telomeric and non-telomeric DNA damage are determinants of mammalian cellular senescence," *Epigenetics & Chromatin*, vol. 1, no. 1, p. 6, 2008.

[39] U. Herbig, M. Ferreira, L. Condel, D. Carey, and J. M. Sedivy, "Cellular senescence in aging primates," *Science*, vol. 311, no. 5765, p. 1257, 2006.

[40] C. Wang, D. Jurk, M. Maddick, G. Nelson, C. Martin-Ruiz, and T. von Zglinicki, "DNA damage response and cellular

senescence in tissues of aging mice," *Aging Cell*, vol. 8, no. 3, pp. 311–323, 2009.

[41] O. A. Sedelnikova, I. Horikawa, C. Redon et al., "Delayed kinetics of DNA double-strand break processing in normal and pathological aging," *Aging Cell*, vol. 7, no. 1, pp. 89–100, 2008.

[42] O. A. Sedelnikova, I. Horikawa, D. B. Zimonjic, N. C. Popescu, W. M. Bonner, and J. C. Barrett, "Senescing human cells and ageing mice accumulate DNA lesions with unrepairable double-strand breaks," *Nature Cell Biology*, vol. 6, no. 2, pp. 168–170, 2004.

[43] C. R. Burtner and B. K. Kennedy, "Progeria syndromes and ageing: what is the connection?," *Nature Reviews Molecular Cell Biology*, vol. 11, no. 8, pp. 567–578, 2012.

[44] R. R. White, B. Milholland, A. de Bruin et al., "Controlled induction of DNA double-strand breaks in the mouse liver induces features of tissue ageing," *Nature Communications*, vol. 6, p. 6790, 2015.

[45] A. Freund, A. V. Orjalo, P. Y. Desprez, and J. Campisi, "Inflammatory networks during cellular senescence: causes and consequences," *Trends in Molecular Medicine*, vol. 16, no. 5, pp. 238–246, 2010.

[46] J. M. van Deursen, "The role of senescent cells in ageing," *Nature*, vol. 509, no. 7501, pp. 439–446, 2014.

[47] M. Hoare and M. Narita, "Transmitting senescence to the cell neighbourhood," *Nature Cell Biology*, vol. 15, no. 8, pp. 887–889, 2013.

[48] C. Franceschi, M. Bonafe, S. Valensin et al., "Inflamm-aging. An evolutionary perspective on immunosenescence," *Annals of the New York Academy of Sciences*, vol. 908, pp. 244–254, 2000.

[49] A. Ioannidou, E. Goulielmaki, and G. A. Garinis, "DNA damage: from chronic inflammation to age-related deterioration," *Frontiers in Genetics*, vol. 7, p. 187, 2016.

[50] T. Kuilman, C. Michaloglou, L. C. Vredeveld et al., "Oncogene-induced senescence relayed by an interleukin-dependent inflammatory network," *Cell*, vol. 133, no. 6, pp. 1019–1031, 2008.

[51] S. Hubackova, K. Krejcikova, J. Bartek, and Z. Hodny, "IL1- and TGFβ-Nox4 signaling, oxidative stress and DNA damage response are shared features of replicative, oncogene-induced, and drug-induced paracrine 'bystander senescence'," *Aging*, vol. 4, no. 12, pp. 932–951, 2012.

[52] A. Salminen, A. Kauppinen, and K. Kaarniranta, "Emerging role of NF-κB signaling in the induction of senescence-associated secretory phenotype (SASP)," *Cellular Signalling*, vol. 24, no. 4, pp. 835–845, 2012.

[53] C. Kang, Q. Xu, T. D. Martin et al., "The DNA damage response induces inflammation and senescence by inhibiting autophagy of GATA4," *Science*, vol. 349, no. 6255, article aaa5612, 2015.

[54] A. Freund, C. K. Patil, and J. Campisi, "p38MAPK is a novel DNA damage response-independent regulator of the senescence-associated secretory phenotype," *The EMBO Journal*, vol. 30, no. 8, pp. 1536–1548, 2011.

[55] N. Herranz, S. Gallage, M. Mellone et al., "mTOR regulates MAPKAPK2 translation to control the senescence-associated secretory phenotype," *Nature Cell Biology*, vol. 17, no. 9, pp. 1205–1217, 2015.

[56] R. M. Laberge, Y. Sun, A. V. Orjalo et al., "MTOR regulates the pro-tumorigenic senescence-associated secretory phenotype by promoting IL1A translation," *Nature Cell Biology*, vol. 17, no. 8, pp. 1049–1061, 2015.

[57] C. Correia-Melo, F. D. Marques, R. Anderson et al., "Mitochondria are required for pro-ageing features of the senescent phenotype," *The EMBO Journal*, vol. 35, no. 7, pp. 724–742, 2016.

[58] C. Correia-Melo and J. F. Passos, "Mitochondria: are they causal players in cellular senescence?," *Biochimica et Biophysica Acta (BBA) - Bioenergetics*, vol. 1847, no. 11, pp. 1373–1379, 2015.

[59] Q. Chen and B. N. Ames, "Senescence-like growth arrest induced by hydrogen peroxide in human diploid fibroblast F65 cells," *Proceedings of the National Academy of Sciences of the United States of America*, vol. 91, no. 10, pp. 4130–4134, 1994.

[60] D. Przybylska, D. Janiszewska, A. Gozdzik et al., "NOX4 downregulation leads to senescence of human vascular smooth muscle cells," *Oncotarget*, vol. 7, no. 41, pp. 66429–66443, 2016.

[61] S. Beatty, H. Koh, M. Phil, D. Henson, and M. Boulton, "The role of oxidative stress in the pathogenesis of age-related macular degeneration," *Survey of Ophthalmology*, vol. 45, no. 2, pp. 115–134, 2000.

[62] D. Jurk, C. Wang, S. Miwa et al., "Postmitotic neurons develop a p21-dependent senescence-like phenotype driven by a DNA damage response," *Aging Cell*, vol. 11, no. 6, pp. 996–1004, 2012.

[63] M. Piechota, P. Sunderland, A. Wysocka et al., "Is senescence-associated β-galactosidase a marker of neuronal senescence?," *Oncotarget*, vol. 7, no. 49, pp. 81099–81109, 2016.

[64] N. Arend, C. Wertheimer, P. Laubichler, A. Wolf, A. Kampik, and M. Kernt, "Idebenone prevents oxidative stress, cell death and senescence of retinal pigment epithelium cells by stabilizing BAX/Bcl-2 ratio," *Ophthalmologica*, vol. 234, no. 2, pp. 73–82, 2015.

[65] N. Aryan, B. S. Betts-Obregon, G. Perry, and A. T. Tsin, "Oxidative stress induces senescence in cultured RPE cells," *The Open Neurology Journal*, vol. 10, pp. 83–87, 2016.

[66] Supanji, M. Shimomachi, M. Z. Hasan, M. Kawaichi, and C. Oka, "HtrA1 is induced by oxidative stress and enhances cell senescence through p38 MAPK pathway," *Experimental Eye Research*, vol. 112, pp. 79–92, 2013.

[67] C. C. Zhuge, J. Y. Xu, J. Zhang et al., "Fullerenol protects retinal pigment epithelial cells from oxidative stress-induced premature senescence via activating SIRT1," *Investigative Ophthalmology & Visual Science*, vol. 55, no. 7, pp. 4628–4638, 2014.

[68] A. L. Glotin, F. Debacq-Chainiaux, J. Y. Brossas et al., "Prematurely senescent ARPE-19 cells display features of age-related macular degeneration," *Free Radical Biology & Medicine*, vol. 44, no. 7, pp. 1348–1361, 2008.

[69] M. C. Marazita, A. Dugour, M. D. Marquioni-Ramella, J. M. Figueroa, and A. M. Suburo, "Oxidative stress-induced premature senescence dysregulates VEGF and CFH expression in retinal pigment epithelial cells: implications for age-related macular degeneration," *Redox Biology*, vol. 7, pp. 78–87, 2016.

[70] W. Grabowska, E. Sikora, and A. Bielak-Zmijewska, "Sirtuins, a promising target in slowing down the ageing process," *Biogerontology*, vol. 18, no. 4, pp. 447–476, 2017.

[71] O. Alster, A. Bielak-Zmijewska, G. Mosieniak et al., "The role of nibrin in doxorubicin-induced apoptosis and cell

senescence in Nijmegen breakage syndrome patients lymphocytes," *PLoS One*, vol. 9, no. 8, article e104964, 2014.

[72] T. V. Pospelova, Z. N. Demidenko, E. I. Bukreeva, V. A. Pospelov, A. V. Gudkov, and M. V. Blagosklonny, "Pseudo-DNA damage response in senescent cells," *Cell Cycle*, vol. 8, no. 24, pp. 4112–4118, 2009.

[73] N. Mizushima and M. Komatsu, "Autophagy: renovation of cells and tissues," *Cell*, vol. 147, no. 4, pp. 728–741, 2011.

[74] L. E. Gallagher, L. E. Williamson, and E. Y. Chan, "Advances in autophagy regulatory mechanisms," *Cell*, vol. 5, no. 2, 2016.

[75] T. Johansen and T. Lamark, "Selective autophagy mediated by autophagic adapter proteins," *Autophagy*, vol. 7, no. 3, pp. 279–296, 2011.

[76] L. C. Li, D. L. Wang, Y. Z. Wu et al., "Gastric tumor-initiating CD44+ cells and epithelial-mesenchymal transition are inhibited by γ-secretase inhibitor DAPT," *Oncology Letters*, vol. 10, no. 5, pp. 3293–3299, 2015.

[77] Y. C. Chang, M. C. Hsieh, H. J. Wu, W. C. Wu, and Y. H. Kao, "Methylglyoxal, a reactive glucose metabolite, enhances autophagy flux and suppresses proliferation of human retinal pigment epithelial ARPE-19 cells," *Toxicology In Vitro*, vol. 29, no. 7, pp. 1358–1368, 2015.

[78] S. K. Mitter, C. Song, X. Qi et al., "Dysregulated autophagy in the RPE is associated with increased susceptibility to oxidative stress and AMD," *Autophagy*, vol. 10, no. 11, pp. 1989–2005, 2014.

[79] Y. Zhu, K. K. Zhao, Y. Tong et al., "Exogenous NAD^+ decreases oxidative stress and protects H_2O_2-treated RPE cells against necrotic death through the up-regulation of autophagy," *Scientific Reports*, vol. 6, article 26322, 2016.

[80] P. V. Algvere, A. Kvanta, and S. Seregard, "Drusen maculopathy: a risk factor for visual deterioration," *Acta Ophthalmologica*, vol. 94, no. 5, pp. 427–433, 2016.

[81] J. T. Handa, M. Cano, L. Wang, S. Datta, and T. Liu, "Lipids, oxidized lipids, oxidation-specific epitopes, and age-related macular degeneration," *Biochimica et Biophysica Acta (BBA) - Molecular and Cell Biology of Lipids*, vol. 1862, no. 4, pp. 430–440, 2017.

[82] K. Kaarniranta, D. Sinha, J. Blasiak et al., "Autophagy and heterophagy dysregulation leads to retinal pigment epithelium dysfunction and development of age-related macular degeneration," *Autophagy*, vol. 9, no. 7, pp. 973–984, 2013.

[83] N. Rodriguez-Muela, H. Koga, L. Garcia-Ledo et al., "Balance between autophagic pathways preserves retinal homeostasis," *Aging Cell*, vol. 12, no. 3, pp. 478–488, 2013.

[84] I. Johansson, V. T. Monsen, K. Pettersen et al., "The marine n-3 PUFA DHA evokes cytoprotection against oxidative stress and protein misfolding by inducing autophagy and NFE2L2 in human retinal pigment epithelial cells," *Autophagy*, vol. 11, no. 9, pp. 1636–1651, 2015.

[85] L. Wang, M. Cano, and J. T. Handa, "p62 provides dual cytoprotection against oxidative stress in the retinal pigment epithelium," *Biochimica et Biophysica Acta (BBA) - Molecular Cell Research*, vol. 1843, no. 7, pp. 1248–1258, 2014.

[86] A. G. Eliopoulos, S. Havaki, and V. G. Gorgoulis, "DNA damage response and autophagy: a meaningful partnership," *Frontiers in Genetics*, vol. 7, p. 204, 2016.

[87] G. Hewitt and V. I. Korolchuk, "Repair, reuse, recycle: the expanding role of autophagy in genome maintenance," *Trends in Cell Biology*, vol. 27, no. 5, pp. 340–351, 2017.

[88] A. Sample and Y. Y. He, "Autophagy in UV damage response," *Photochemistry and Photobiology*, vol. 93, no. 4, pp. 943–955, 2016.

[89] J. Blasiak, S. Glowacki, A. Kauppinen, and K. Kaarniranta, "Mitochondrial and nuclear DNA damage and repair in age-related macular degeneration," *International Journal of Molecular Sciences*, vol. 14, no. 2, pp. 2996–3010, 2013.

[90] S. G. Jarrett, H. Lin, B. F. Godley, and M. E. Boulton, "Mitochondrial DNA damage and its potential role in retinal degeneration," *Progress in Retinal and Eye Research*, vol. 27, no. 6, pp. 596–607, 2008.

[91] S. G. Jarrett, B. Rohrer, N. R. Perron, C. Beeson, and M. E. Boulton, "Assessment of mitochondrial damage in retinal cells and tissues using quantitative polymerase chain reaction for mitochondrial DNA damage and extracellular flux assay for mitochondrial respiration activity," *Methods in Molecular Biology*, vol. 935, pp. 227–243, 2013.

[92] U. Testa, C. Labbaye, G. Castelli, and E. Pelosi, "Oxidative stress and hypoxia in normal and leukemic stem cells," *Experimental Hematology*, vol. 44, no. 7, pp. 540–560, 2016.

[93] E. Synowiec, J. Blasiak, M. Zaras, J. Szaflik, and J. P. Szaflik, "Association between polymorphisms of the DNA base excision repair genes MUTYH and hOGG1 and age-related macular degeneration," *Experimental Eye Research*, vol. 98, pp. 58–66, 2012.

[94] F. Q. Liang and B. F. Godley, "Oxidative stress-induced mitochondrial DNA damage in human retinal pigment epithelial cells: a possible mechanism for RPE aging and age-related macular degeneration," *Experimental Eye Research*, vol. 76, no. 4, pp. 397–403, 2003.

[95] H. Lin, H. Xu, F. Q. Liang et al., "Mitochondrial DNA damage and repair in RPE associated with aging and age-related macular degeneration," *Investigative Ophthalmology & Visual Science*, vol. 52, no. 6, pp. 3521–3529, 2011.

[96] A. L. Wang, T. J. Lukas, M. Yuan, and A. H. Neufeld, "Increased mitochondrial DNA damage and down-regulation of DNA repair enzymes in aged rodent retinal pigment epithelium and choroid," *Molecular Vision*, vol. 14, pp. 644–651, 2008.

[97] S. W. Ballinger, B. Van Houten, G. F. Jin, C. A. Conklin, and B. F. Godley, "Hydrogen peroxide causes significant mitochondrial DNA damage in human RPE cells," *Experimental Eye Research*, vol. 68, no. 6, pp. 765–772, 1999.

[98] D. A. Ferrington, R. J. Kapphahn, M. M. Leary et al., "Increased retinal mtDNA damage in the CFH variant associated with age-related macular degeneration," *Experimental Eye Research*, vol. 145, pp. 269–277, 2016.

[99] A. L. Gramajo, L. C. Zacharias, A. Neekhra et al., "Mitochondrial DNA damage induced by 7-ketocholesterol in human retinal pigment epithelial cells in vitro," *Investigative Ophthalmology & Visual Science*, vol. 51, no. 2, pp. 1164–1170, 2010.

[100] S. G. Jarrett and M. E. Boulton, "Poly(ADP-ribose) polymerase offers protection against oxidative and alkylation damage to the nuclear and mitochondrial genomes of the retinal pigment epithelium," *Ophthalmic Research*, vol. 39, no. 4, pp. 213–223, 2007.

[101] S. G. Jarrett and M. E. Boulton, "Consequences of oxidative stress in age-related macular degeneration," *Molecular Aspects of Medicine*, vol. 33, no. 4, pp. 399–417, 2012.

[102] M. C. Kenney, S. R. Atilano, D. Boyer et al., "Characterization of retinal and blood mitochondrial DNA from age-related

macular degeneration patients," *Investigative Ophthalmology & Visual Science*, vol. 51, no. 8, pp. 4289–4297, 2010.

[103] G. Filomeni, D. De Zio, and F. Cecconi, "Oxidative stress and autophagy: the clash between damage and metabolic needs," *Cell Death and Differentiation*, vol. 22, no. 3, pp. 377–388, 2015.

[104] M. Komatsu, H. Kurokawa, S. Waguri et al., "The selective autophagy substrate p62 activates the stress responsive transcription factor Nrf2 through inactivation of Keap1," *Nature Cell Biology*, vol. 12, no. 3, pp. 213–223, 2010.

[105] Y. Kurihara, T. Kanki, Y. Aoki et al., "Mitophagy plays an essential role in reducing mitochondrial production of reactive oxygen species and mutation of mitochondrial DNA by maintaining mitochondrial quantity and quality in yeast," *The Journal of Biological Chemistry*, vol. 287, no. 5, pp. 3265–3272, 2012.

[106] S. Sharma, C. M. Helchowski, and C. E. Canman, "The roles of DNA polymerase zeta and the Y family DNA polymerases in promoting or preventing genome instability," *Mutation Research*, vol. 743-744, pp. 97–110, 2013.

[107] G. Filomeni, E. Desideri, S. Cardaci, G. Rotilio, and M. R. Ciriolo, "Under the ROS...thiol network is the principal suspect for autophagy commitment," *Autophagy*, vol. 6, no. 7, pp. 999–1005, 2010.

[108] Y. Chen, M. B. Azad, and S. B. Gibson, "Superoxide is the major reactive oxygen species regulating autophagy," *Cell Death and Differentiation*, vol. 16, no. 7, pp. 1040–1052, 2009.

[109] R. Scherz-Shouval, E. Shvets, and Z. Elazar, "Oxidation as a post-translational modification that regulates autophagy," *Autophagy*, vol. 3, no. 4, pp. 371–373, 2007.

[110] R. Scherz-Shouval, E. Shvets, E. Fass, H. Shorer, L. Gil, and Z. Elazar, "Reactive oxygen species are essential for autophagy and specifically regulate the activity of Atg4," *The EMBO Journal*, vol. 26, no. 7, pp. 1749–1760, 2007.

[111] C. Zhang, L. Yang, X. B. Wang et al., "Calyxin Y induces hydrogen peroxide-dependent autophagy and apoptosis via JNK activation in human non-small cell lung cancer NCI-H460 cells," *Cancer Letters*, vol. 340, no. 1, pp. 51–62, 2013.

[112] M. B. Azad, Y. Chen, and S. B. Gibson, "Regulation of autophagy by reactive oxygen species (ROS): implications for cancer progression and treatment," *Antioxidants & Redox Signaling*, vol. 11, no. 4, pp. 777–790, 2009.

[113] A. L. Levonen, B. G. Hill, E. Kansanen, J. Zhang, and V. M. Darley-Usmar, "Redox regulation of antioxidants, autophagy, and the response to stress: implications for electrophile therapeutics," *Free Radical Biology & Medicine*, vol. 71, pp. 196–207, 2014.

[114] R. Scherz-Shouval and Z. Elazar, "ROS, mitochondria and the regulation of autophagy," *Trends in Cell Biology*, vol. 17, no. 9, pp. 422–427, 2007.

[115] R. Mathew, C. M. Karp, B. Beaudoin et al., "Autophagy suppresses tumorigenesis through elimination of p62," *Cell*, vol. 137, no. 6, pp. 1062–1075, 2009.

[116] R. Mathew, S. Kongara, B. Beaudoin et al., "Autophagy suppresses tumor progression by limiting chromosomal instability," *Genes & Development*, vol. 21, no. 11, pp. 1367–1381, 2007.

[117] J. A. Munoz-Gamez, J. M. Rodriguez-Vargas, R. Quiles-Perez et al., "PARP-1 is involved in autophagy induced by DNA damage," *Autophagy*, vol. 5, no. 1, pp. 61–74, 2009.

[118] A. Alexander, S. L. Cai, J. Kim et al., "ATM signals to TSC2 in the cytoplasm to regulate mTORC1 in response to ROS," *Proceedings of the National Academy of Sciences of the United States of America*, vol. 107, no. 9, pp. 4153–4158, 2010.

[119] D. Kenzelmann Broz, S. Spano Mello, K. T. Bieging et al., "Global genomic profiling reveals an extensive p53-regulated autophagy program contributing to key p53 responses," *Genes & Development*, vol. 27, no. 9, pp. 1016–1031, 2013.

[120] M. C. Maiuri, L. Galluzzi, E. Morselli, O. Kepp, S. A. Malik, and G. Kroemer, "Autophagy regulation by p53," *Current Opinion in Cell Biology*, vol. 22, no. 2, pp. 181–185, 2010.

[121] F. Madeo, N. Tavernarakis, and G. Kroemer, "Can autophagy promote longevity?," *Nature Cell Biology*, vol. 12, no. 9, pp. 842–846, 2010.

[122] D. C. Rubinsztein, G. Marino, and G. Kroemer, "Autophagy and aging," *Cell*, vol. 146, no. 5, pp. 682–695, 2011.

[123] G. Mosieniak, M. A. Sliwinska, O. Alster et al., "Polyploidy formation in doxorubicin-treated cancer cells can favor escape from senescence," *Neoplasia*, vol. 17, no. 12, pp. 882–893, 2015.

[124] A. R. Young, M. Narita, M. Ferreira et al., "Autophagy mediates the mitotic senescence transition," *Genes & Development*, vol. 23, no. 7, pp. 798–803, 2009.

[125] P. Tokarz, K. Kaarniranta, and J. Blasiak, "Inhibition of DNA methyltransferase or histone deacetylase protects retinal pigment epithelial cells from DNA damage induced by oxidative stress by the stimulation of antioxidant enzymes," *European Journal of Pharmacology*, vol. 776, pp. 167–175, 2016.

[126] M. F. Roggia and T. Ueta, "$\alpha v\beta 5$ integrin/FAK/PGC-1α pathway confers protective effects on retinal pigment epithelium," *PLoS One*, vol. 10, no. 8, article e0134870, 2015.

[127] T. Tsunemi, T. D. Ashe, B. E. Morrison et al., "PGC-1α rescues Huntington's disease proteotoxicity by preventing oxidative stress and promoting TFEB function," *Science Translational Medicine*, vol. 4, no. 142, article 142ra97, 2012.

[128] Y. Chen, J. Wang, J. Cai, and P. Sternberg, "Altered mTOR signaling in senescent retinal pigment epithelium," *Investigative Ophthalmology & Visual Science*, vol. 51, no. 10, pp. 5314–5319, 2010.

[129] B. Yu, P. Xu, Z. Zhao, J. Cai, P. Sternberg, and Y. Chen, "Subcellular distribution and activity of mechanistic target of rapamycin in aged retinal pigment epithelium," *Investigative Ophthalmology & Visual Science*, vol. 55, no. 12, pp. 8638–8650, 2014.

[130] C. Kang and S. J. Elledge, "How autophagy both activates and inhibits cellular senescence," *Autophagy*, vol. 12, no. 5, pp. 898-899, 2016.

[131] J. P. Coppe, P. Y. Desprez, A. Krtolica, and J. Campisi, "The senescence-associated secretory phenotype: the dark side of tumor suppression," *Annual Review of Pathology*, vol. 5, pp. 99–118, 2010.

[132] J. Campisi and F. d'Adda di Fagagna, "Cellular senescence: when bad things happen to good cells," *Nature Reviews Molecular Cell Biology*, vol. 8, no. 9, pp. 729–740, 2007.

[133] J. C. Jeyapalan, M. Ferreira, J. M. Sedivy, and U. Herbig, "Accumulation of senescent cells in mitotic tissue of aging primates," *Mechanisms of Ageing and Development*, vol. 128, no. 1, pp. 36–44, 2007.

[134] C. Lopez-Otin, M. A. Blasco, L. Partridge, M. Serrano, and G. Kroemer, "The hallmarks of aging," *Cell*, vol. 153, no. 6, pp. 1194–1217, 2013.

[135] H. Al-Hussaini, J. H. Kam, A. Vugler, M. Semo, and G. Jeffery, "Mature retinal pigment epithelium cells are retained in the cell cycle and proliferate in vivo," *Molecular Vision*, vol. 14, pp. 1784–1791, 2008.

[136] H. Xia, M. P. Krebs, S. Kaushal, and E. W. Scott, "Enhanced retinal pigment epithelium regeneration after injury in MRL/MpJ mice," *Experimental Eye Research*, vol. 93, no. 6, pp. 862–872, 2011.

[137] C. Franceschi and J. Campisi, "Chronic inflammation (inflammaging) and its potential contribution to age-associated diseases," *The Journals of Gerontology. Series A, Biological Sciences and Medical Sciences*, vol. 69, Supplement 1, pp. S4–S9, 2014.

[138] N. Khansari, Y. Shakiba, and M. Mahmoudi, "Chronic inflammation and oxidative stress as a major cause of age-related diseases and cancer," *Recent Patents on Inflammation & Allergy Drug Discovery*, vol. 3, no. 1, pp. 73–80, 2009.

[139] J. M. Hyttinen, J. Blasiak, M. Niittykoski et al., "DNA damage response and autophagy in the degeneration of retinal pigment epithelial cells-implications for age-related macular degeneration (AMD)," *Ageing Research Reviews*, vol. 36, pp. 64–77, 2017.

[140] B. Van Houten, S. E. Hunter, and J. N. Meyer, "Mitochondrial DNA damage induced autophagy, cell death, and disease," *Frontiers in Bioscience*, vol. 21, pp. 42–54, 2016.

[141] K. Labbe, A. Murley, and J. Nunnari, "Determinants and functions of mitochondrial behavior," *Annual Review of Cell and Developmental Biology*, vol. 30, pp. 357–391, 2014.

[142] A. Roczniak-Ferguson, C. S. Petit, F. Froehlich et al., "The transcription factor TFEB links mTORC1 signaling to transcriptional control of lysosome homeostasis," *Science Signaling*, vol. 5, no. 228, article ra42, 2012.

[143] Y. Zhu, J. L. Armstrong, T. Tchkonia, and J. L. Kirkland, "Cellular senescence and the senescent secretory phenotype in age-related chronic diseases," *Current Opinion in Clinical Nutrition and Metabolic Care*, vol. 17, no. 4, pp. 324–328, 2014.

[144] D. A. Gewirtz, "Autophagy and senescence: a partnership in search of definition," *Autophagy*, vol. 9, no. 5, pp. 808–812, 2013.

Hindawi
Oxidative Medicine and Cellular Longevity
Volume 2017, Article ID 2825703, 7 pages
https://doi.org/10.1155/2017/2825703

Research Article

Cytoprotective Effects of Citicoline and Homotaurine against Glutamate and High Glucose Neurotoxicity in Primary Cultured Retinal Cells

Sergio Davinelli, Flavia Chiosi, Roberto Di Marco, Ciro Costagliola, and Giovanni Scapagnini

Department of Medicine and Health Sciences "V. Tiberio", University of Molise, Campobasso, Italy

Correspondence should be addressed to Sergio Davinelli; sergio.davinelli@unimol.it

Received 7 July 2017; Accepted 27 September 2017; Published 15 October 2017

Academic Editor: Deborah A. Ferrington

Citicoline and homotaurine are renowned compounds that exhibit potent neuroprotective activities through distinct molecular mechanisms. The present study was undertaken to demonstrate whether cotreatment with citicoline and homotaurine affects cell survival in primary retinal cultures under experimental conditions simulating retinal neurodegeneration. Primary cultures were obtained from the retina of fetal rats and exposed to citicoline plus homotaurine (100 μM). Subsequently, neurotoxicity was induced using excitotoxic levels of glutamate and high glucose concentrations. The effects on retinal cultures were assessed by cell viability and immunodetection of apoptotic oligonucleosomes. The results showed that a combination of citicoline and homotaurine synergistically decreases proapoptotic effects associated with glutamate- and high glucose-treated retinal cultures. This study provides an insight into the potential application of citicoline and homotaurine as a valuable tool to exert neuroprotective effects against retinal damage.

1. Introduction

Visual impairment is a worldwide health problem affecting about 285 million people [1]. Recently, it was estimated that with aging populations in high-income regions of Central/Eastern Europe, diabetic retinopathy and glaucoma will become the most important causes of vision loss [2]. The key cell type implicated in the development of glaucoma and diabetic retinopathy is the retinal ganglion cell (RGC), and apoptosis of RGC is the final event leading to visual loss [3, 4]. The cause of apoptosis is excitotoxicity due to excessive synaptic glutamate activity. Glutamate is one of the major excitatory neurotransmitters in the brain and exists in high concentrations in the retina. It is thought that exposure to moderately elevated levels of glutamate can trigger cellular processes in neurons that eventually lead to apoptosis [5, 6]. In addition, increasing evidence shows that several neuronal cell types in the retina are highly susceptible to hyperglycemia-mediated apoptosis [7]. Cell culture models have substantially contributed to the characterization of the pathophysiology of retinal neurodegeneration, providing a simplified tool to investigate in an isolated context the detrimental effects of high glucose (HG) concentrations and an excessive amount of glutamate [8, 9]. In recent years, research efforts have been made to identify neuroprotective drugs able to prevent visual field loss and preserve visual function. However, the failure of recent clinical trials raised several doubts regarding the strategies to achieve neuroprotection in retinal degeneration [10]. Based on the results of the latest investigations, it is reasonable to assert that a single constituent that affects one target has limited efficacy in preventing the progression of multifactorial diseases. A large body of research revealed that the use of a combination of compounds with synergistic multitarget effects may offer a more powerful approach for disease prevention, including retinal neurodegeneration [11–15]. This study investigated whether cotreatment of citicoline and homotaurine exhibits synergistic neuroprotective effects in experimental conditions associated with neuroretinal degeneration such as glutamate-induced excitotoxicity and HG-induced neurotoxicity. Citicoline (cytidine-5′-diphosphocholine) is an intermediate in the synthesis of phosphatidylcholine, a component of cell

membranes. It has been shown that citicoline produces neuroprotective effects in a variety of central nervous system (CNS) injury models, particularly cerebral ischemia [16]. At the experimental level, it has been reported that citicoline is a neuroprotective molecule acting through mechanisms relevant to glaucoma and diabetic retinopathy. The effects proposed to explain the neuroprotective actions of citicoline have been thoroughly reviewed and include antiapoptotic effects, neurotrophic properties, protection after partial optic nerve crush, reduction of excitotoxicity, effects on nonglutamatergic neurotransmitter systems, and effects on remyelination [17]. In recent human studies, citicoline appears to be a promising agent to improve cognitive impairment [18]. Homotaurine (3-aminopropanesulfonate), an analogue of 4-aminobutyrate (γ-aminobutyric acid, GABA), is a small natural aminosulfonate compound identified in different species of marine red algae and then chemically synthesized and introduced into clinical use under the name of tramiprosate [19]. It has been shown that homotaurine may interfere with several cellular pathways, both *in vitro* and *in vivo* experimental models, and exert neuroprotective and neurotropic activities through different mechanisms including effects against the oxidative damage to DNA, antifibrillogenic activity, and antinociceptive and analgesic activities. More interestingly, beyond its neuroprotective and neurotropic effects related to the activation of GABA type A receptors, it has been observed that homotaurine prevents the neurotoxicity of Aβ peptide by reducing amyloid aggregation [20, 21]. Considering the distinct chemical properties of citicoline and homotaurine, the purpose of this study was to assess whether cotreatment of these compounds may exert synergistic neuroprotective effects on primary retinal cultures.

2. Materials and Methods

2.1. Retinal Cultures. The study has been approved by the appropriate ethics committee and has therefore been performed in accordance with the ethical standards laid down in the 1964 Declaration of Helsinki and its later amendments. Primary cultures were obtained from the retinas of fetal Wistar rats (18-19 days' gestation), following a procedure described elsewhere [22]. Briefly, retinal tissues were mechanically dissociated, and the cell suspensions were plated into 60 mm dish ($0.8–1.0 \times 10^6$ cells/mL) (Corning, Acton, MA). Retinal cultures were incubated in Eagle's minimal essential medium (MEM) containing 2 mM glutamine, penicillin-streptomycin (100 U/ml, 50 μg/mL), and 25 mM N-(2-hydroxyethyl) piperadine-N$'$-(2-ethanesulfonic acid) (HEPES) under an atmosphere of 5% CO_2 in the air. The medium was supplemented with 10% heat-inactivated fetal bovine serum during the 1st week and with 10% horse serum for the remaining 8–11 days. To eliminate nonneuronal cells, 10 μM cytosine arabinoside (Sigma, St. Louis, MO) was added to the culture. Only those cultures maintained for 9–11 days *in vitro* and only isolated cells were used in this study. Previous studies using cultured rat retinal cells demonstrated that cell viability was reduced by exposure to glutamate (1 mM) for 10 min. Followed by postincubation in a glutamate-free medium for more than 1 hour [23, 24]. It was also showed that there was no significant difference between the values of reduction in cell viability between 1-hour and 24-hour incubations [25]. In the present study, glutamate neurotoxicity was assessed using a 25 min exposure to 100 μM glutamate followed by a 24-hour incubation in the glutamate-free medium. In the second series of experiments, the cells were treated with HG concentrations to mimic the diabetic condition and produce a hyperglycemic insult. When cells reached 80% confluence, the culture medium was supplemented with glucose, reaching a final concentration of 30 mM. Retinal cells were exposed to HG for 96 hours. The concentration of glucose in control conditions was 5 mM. Media were changed every 24 hours in all groups.

2.2. Cell Viability. The assay used to assess cell viability in retinal cells was the (3,4,5-dimethylthiazol-2-yl)-2,5-diphenyltetrazolium bromide (MTT) reduction assay modified from that of Mosmann [26]. To evaluate the effect of citicoline and homotaurine on cell survival, the cells were subdivided into three groups and treated for 24 hours with 1 μM, 10 μM, and 100 μM of citicoline (Kyowa Hakko Bio Co. Ltd., Tokyo, Japan) and with 1 μM, 10 μM, and 100 μM of homotaurine (Truffini e Reggè Farmaceutici, Milan, Italy). To evaluate the neuroprotective effects of citicoline and homotaurine, cells were treated with citicoline 100 μM, homotaurine 100 μM, or citicoline + homotaurine 100 μM, 24 hours before glutamate treatment and 30 min before HG treatment. MTT was added to wells at a final concentration of 0.5 mg/mL for 1 hour at 37°C. After this time, the medium was removed and reduced MTT (blue formazan product) was solubilized by adding 100 μL dimethyl sulfoxide to each well. After agitation of plates for 15 min, the optical density of the solubilized formazan product in each well was measured using an automatic microplate reader (Molecular Devices, Crawley, UK) with a 570 nm test wavelength and a 690 nm reference wavelength.

2.3. Apoptotic Cell Death Detection. Apoptosis was determined by using a Cell Death Detection ELISA^{PLUS} kit (Roche Applied Science, Indianapolis, IN). This photometric enzyme immunoassay provides the quantitative determination of oligonucleosomes generated from the apoptotic cells. After the treatments, cells were washed, harvested, lysed, and centrifuged to remove nuclei, and supernatants were collected. An aliquot of the supernatant from each sample was incubated with immunoreagents in 96-well streptavidin-coated plates on a shaker. After three washes with incubation buffer, the substrate solution was added to each well, and absorbance was read at 405 nm in a microplate reader. The enrichment of oligonucleosomes released into the cytoplasm was calculated as absorbance of sample cells/absorbance of control cells.

2.4. Statistical Analysis. Data are expressed as the mean ± standard error of the mean (SEM) of three independent experiments. Statistical significance was determined using one-way analysis of variance (ANOVA), followed

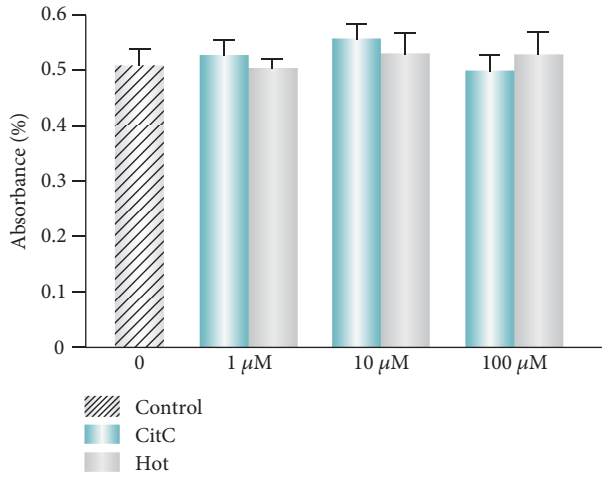

Figure 1: Effects of citicoline and homotaurine on cell viability. MTT assay shows that retinal cells were well preserved in citicoline- or homotaurine-treated cultures, with no evidence of toxicity after treatment at 1, 10, or 100 μM. All data are represented as the mean ± SEM of three independent experiments. CitC: citicoline; Hot: homotaurine.

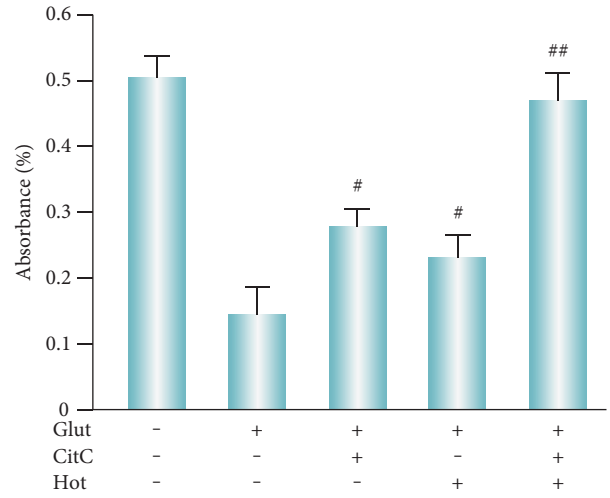

Figure 2: Cotreatment of citicoline and homotaurine protects retinal cells against glutamate-induced cytotoxicity. MTT assay was performed to detect cell viability after treatment with CitC and Hot against glutamate-induced cytotoxicity in retinal cells. The combined administration of citcoline and homotaurine demonstrated a significant synergistic cytoprotective effect. The results represent the mean ± SEM of three independent experiments. ANOVA followed by Tukey's post hoc test was carried out to determine the level of significance. $^{\#}p < 0.001$ versus glutamate. $^{\#\#}p < 0.001$ versus citicoline and homotaurine alone. CitC: citicoline; Hot: homotaurine; Glut: glutamate.

by Tukey's post hoc test. The p value < 0.05 was considered statistically significant.

3. Results

3.1. Viability of Primary Retinal Cultures Is Not Affected by Treatment with Citicoline or Homotaurine. To determine the potential neuroprotective activity of citicoline and homotaurine, we firstly treated retinal cells with increasing concentrations of citicoline or homotaurine for 24 hours. We investigated whether 1 μM, 10 μM, and 100 μM of citicoline or homotaurine may contribute to a reduced cell viability in retinal cells. As shown in Figure 1, retinal cells were well preserved in citicoline- or homotaurine-treated cultures, with no evidence of toxicity or significant loss of viability after treatments. Moreover, it has been previously shown that 100 μM of citicoline is not harmful to retinal neuroglial cells *in vitro* and 100 μM of homotaurine is an effective concentration to enhance neuroprotection in a model of experimental glaucoma [27, 28]. Therefore, this concentration of citicoline and homotaurine was used for all subsequent experiments.

3.2. Cotreatment of Citicoline and Homotaurine Exerts Synergistic Effects against Excitotoxic Cell Damage. To evaluate whether cotreatment with citicoline and homotaurine was able to induce a synergistic neuroprotective effect against glutamate excitotoxicity, retinal cell cultures were exposed to citicoline 100 μM, homotaurine 100 μM, and citicoline + homotaurine 100 μM, 24 hours before glutamate treatment. In the presence of 100 μM citicoline, a significant increase in cell viability was observed (Figure 2). Although less effective than citicoline in terms of increased cell viability, significant neuroprotection was also observed following treatment with 100 μM homotaurine (Figure 2). These data are consistent with previous studies, suggesting the neuroprotective activities of these compounds when used alone [28, 29]. However, the combination between citicoline and homotaurine significantly increased the viability of retinal cells after glutamate exposure (Figure 2). These results showed that combined administration of citicoline and homotaurine possesses a cytoprotective activity greater than the response achieved by the single compounds.

3.3. Cotreatment of Citicoline and Homotaurine Reduces Apoptosis Induced by Administration of Glutamate and HG. Next, we determined whether the synergistic effect of citicoline and homotaurine is associated with cytoprotection against glutamate-induced apoptosis. Apoptosis, measured by the number of oligonucleosomes released, was significantly decreased in cells incubated only with 100 μM of citicoline 24 hours before glutamate treatment (Figure 3). Homotaurine 100 μM also was able to decrease the neurotoxic effect glutamate in terms of reduction in apoptotic rate (Figure 3). However, as shown in Figure 3, reduction of retinal cell apoptosis induced by these compounds in combination was higher than the groups of either citicoline or homotaurine treated alone. These data suggest that citicoline or homotaurine in combination synergistically reduces apoptosis in glutamate-treated retinal cells. In addition, a neuroprotective effect was also observed against apoptosis induced by HG treatment. Primary retinal cell cultures, exposed to HG treatment, showed an increase in apoptosis, which was reduced in the presence of 100 μM citicoline (Figure 4). Significant neuroprotective effects on apoptosis induced by HG treatment were also reported following treatment with homotaurine 100 μM (Figure 4). Again in the

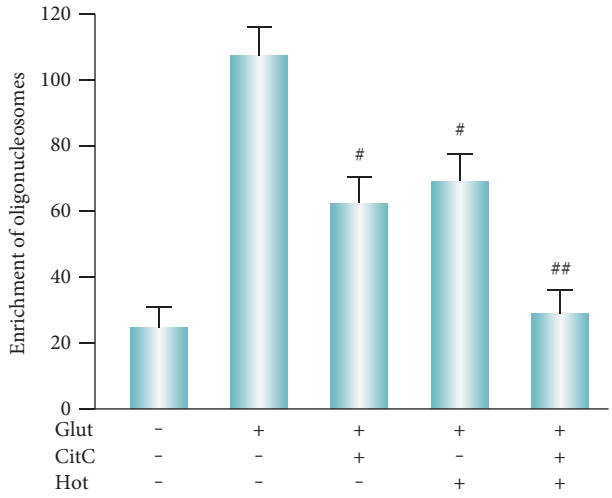

Figure 3: Cotreatment of citicoline and homotaurine significantly reduces the apoptotic rate in glutamate-treated cells. A cell death detection ELISA kit was used to determine cytoplasmic DNA oligonucleosome fragments associated with apoptotic cell death. The enrichment of oligonucleosomes released into the cytoplasm was calculated as absorbance of sample cells/absorbance of control cells. The administration of citicoline plus homotaurine demonstrated a synergistic effect in terms of apoptosis reduction. The results represent the mean ± SEM of three independent experiments. ANOVA followed by Tukey's post hoc test was carried out to determine the level of significance. $^{\#}p < 0.001$ versus glutamate. $^{\#\#}p < 0.001$ versus citicoline and homotaurine alone. CitC: citicoline; Hot: homotaurine; Glut: glutamate.

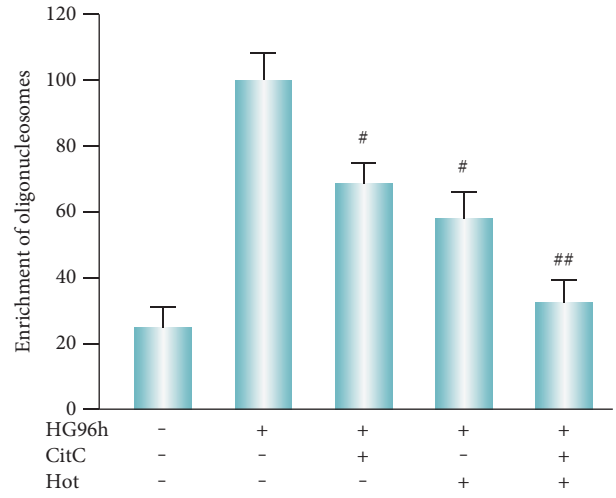

Figure 4: Combined administration of citicoline and homotaurine significantly reduces the apoptotic rate in high glucose-treated cells. Oligonucleosome fragments associated with apoptosis were quantified by cell death detection ELISA. As compared to the untreated cells, the administration of citicoline plus homotaurine demonstrated a statistically significant effect in terms of reduction of oligonucleosome levels. Data of three independent experiments are expressed as mean ± SEM of the absorbance from treated cells relative to absorbance of untreated cells. Comparison between data sets was performed using ANOVA followed by Tukey's post hoc test. $^{\#}p < 0.001$ versus high glucose 96 hours. $^{\#\#}p < 0.001$ versus citicoline and homotaurine alone. CitC: citicoline; Hot: homotaurine; HG: high glucose.

presence of cotreatment with citicoline and homotaurine, apoptosis was significantly reduced in retinal cell cultures exposed to HG toxicity (Figure 4). Collectively, these results suggested that the enhanced reduction of apoptosis by combination treatment with citicoline and homotaurine may be a useful approach to exert a neuroprotective activity under conditions inducing retinal neurodegeneration.

4. Discussion

In this study, we tested synergistic neuroprotective effects of citicoline and homotaurine in combination on primary retinal cells exposed to glutamate toxicity and HG levels. The data demonstrated that cotreatment of citicoline and homotaurine has a direct neuroprotective effect in an experimental model of retinal neurodegeneration. Glutamate-induced excitotoxicity is implicated in the pathophysiology of several degenerative diseases of the retina, including glaucoma. Moreover, HG-induced neurotoxicity is a characteristic of diabetic retinopathy [30, 31]. Thus, the results of our study provide a rationale for the use of citicoline and homotaurine as potential therapeutic compounds in acute and chronic neurodegenerative diseases of the retina. To our knowledge, this is the first report demonstrating that the neurotoxic effect of glutamate and HG is greatly reduced by simultaneous application of citicoline and homotaurine. Therefore, the neuroprotective activity observed here provides also evidence that combinatorial treatment with these compounds may be a promising strategy to support retinal health. Indeed, an emerging therapeutic approach to counteract neuronal vulnerability associated with aging involves the mixture of distinct compounds, in order to improve the neuroprotective efficacy and pharmacokinetic-pharmacodynamic properties [32, 33]. Although the neuroprotective mechanisms of citicoline have been shown in various experimental models of retinal degeneration [34], the presence of homotaurine may increase the neuroprotective effects exerted by this compound. Moreover, it should be highlighted that recent studies have associated the neuroprotective activity of citicoline to its ability in activating sirtuin-1 (SIRT1), a member of the mammalian sirtuins important for neuronal plasticity, cognitive functions, as well as protection against aging-associated neuronal degeneration, and cognitive decline [17, 18]. The clinical efficacy of homotaurine has been extensively studied in several randomized, double-blind, placebo-controlled phase I, II, and III clinical trials, showing significant positive effects on secondary endpoints in patients with Alzheimer's disease [35, 36]. More interestingly, the association of homotaurine, carnosine, and forskolin (*Coleus forskohlii* root extract) has shown synergistic neuroprotective effects on RGC both *in vitro* and *in vivo* in a mouse model of hypertensive retinal ischemia [23, 37]. Although more than one mechanism might account these synergistic properties, this neuroprotection was associated with reduced calpain activity, upregulation of the phosphoinositide 3-kinase (PI3K)/Akt pathway, and inhibition of

glycogen synthase kinase-3β (GSK-3β). Moreover, a recent pilot study demonstrated that oral administration of homotaurine, forskolin, carnosine, and folic acid improves intraocular pressure in patients with primary open-angle glaucoma [38]. Therefore, a multitarget approach by using a combination of molecules may be a more promising strategy to prevent retinal degeneration or slow down glaucomatous progression. In several experimental models of glaucoma, abundant evidence has been provided in which that RGC apoptosis is the earliest form of cell loss of the disease [39, 40]. Our results show that, following exposure to toxic levels of glutamate and glucose, cotreatment of citicoline and homotaurine reduced apoptosis of primary retinal cells (Figures 3 and 4). Although the neuroprotective mechanism of action of citicoline and homotaurine is not clear at this time, other authors have observed that particularly citicoline may reduce the retinal neuronal apoptosis induced by HG, increasing the expression of endogenous trophic factors such as brain-derived neurotrophic factor (BDNF) and ciliary neurotrophic factor (CNTF) that are transiently upregulated as part of the retinal defense responses. In addition, these effects were associated with the reduction of the expression of active forms of caspase-9 and caspase-3 [41, 42]. Alternatively, considering that toxic levels of glutamate and glucose induce an oxidative stress, by increasing reactive oxygen species (ROS), our findings may be also correlated with citicoline and homotaurine antioxidant activities [43, 44]. It should be also mentioned that taurine (2-aminoethanesulfonate), homotaurine analogue and one of the most abundant free amino acids in the brain, has been shown to attenuate retinal glial apoptosis in diabetic rats, suggesting an antiapoptotic action. It has also been suggested that taurine prevents glutamate excitotoxicity by increasing glutamate transporter expression, thereby decreasing glutamate levels. In diabetic patients, taurine depletion may be responsible for glaucomatous optic neuropathy, since RGCs are highly dependent on taurine for survival [45–48]. Altogether, the data presented here strongly suggest that citicoline and homotaurine in combination could be a potential new strategy for the prevention and treatment of neurodegenerative diseases, including glaucomatous retinopathy.

5. Conclusions

In conclusion, the present study demonstrated that cotreatment of citicoline and homotaurine exhibited synergistic neuroprotective effects on well-known experimental conditions of retinal neurodegeneration. Further studies are needed to clarify the mechanisms responsible for the observed neuroprotective properties, although our data suggest a reduction of apoptosis. Finally, these findings also suggest that cotreatment of citicoline and homotaurine may represent an interesting strategy to achieve neuroprotection in retinal neurodegeneration.

Conflicts of Interest

The authors have nothing to declare.

Acknowledgments

The authors would like to express their appreciation to the FB VISION s.r.l. group for excellent technical assistance.

References

[1] D. Pascolini and S. P. Mariotti, *Global Data on Visual Impairments 2010*, World Health Organization, Switzerland, Geneva, 2012, http://www.who.int/blindness/GLOBALDATAFINALforweb.pdf.

[2] R. R. Bourne, J. B. Jonas, S. R. Flaxman et al., "Prevalence and causes of vision loss in high-income countries and in Eastern and Central Europe: 1990-2010," *British Journal of Ophthalmology*, vol. 98, no. 5, pp. 629–638, 2014.

[3] H. Levkovitch-Verbin, "Retinal ganglion cell apoptotic pathway in glaucoma: initiating and downstream mechanisms," *Progress in Brain Research*, vol. 220, pp. 37–57, 2015.

[4] T. S. Kern and A. J. Barber, "Retinal ganglion cells in diabetes," *Journal of Physiology*, vol. 586, no. 18, pp. 4401–4408, 2008.

[5] M. Ankarcrona, J. M. Dypbukt, E. Bonfoco et al., "Glutamate-induced neuronal death: a succession of necrosis or apoptosis depending on mitochondrial function," *Neuron*, vol. 15, no. 4, pp. 961–973, 1995.

[6] X. X. Dong, Y. Wang, and Z. H. Qin, "Molecular mechanisms of excitotoxicity and their relevance to pathogenesis of neurodegenerative diseases," *Acta Pharmacologica Sinica*, vol. 30, no. 4, pp. 379–387, 2009.

[7] R. Simó, C. Hernández, and European Consortium for the Early Treatment of Diabetic Retinopathy (EUROCONDOR), "Neurodegeneration in the diabetic eye: new insights and therapeutic perspectives," *Trends in Endocrinology and Metabolism*, vol. 25, no. 1, pp. 23–33, 2014.

[8] D. R. Tomlinson and N. J. Gardiner, "Glucose neurotoxicity," *Nature Reviews Neuroscience*, vol. 9, no. 1, pp. 36–45, 2008.

[9] N. G. Hattangady and M. S. Rajadhyaksha, "A brief review of in vitro models of diabetic neuropathy," *International Journal of Diabetes in Developing Countries*, vol. 29, no. 4, pp. 143–149, 2009.

[10] N. N. Osborne, "Recent clinical findings with memantine should not mean that the idea of neuroprotection in glaucoma is abandoned," *Acta Ophthalmologica*, vol. 87, no. 4, pp. 450–4, 2009.

[11] S. Davinelli, N. Sapere, M. Visentin, D. Zella, and G. Scapagnini, "Enhancement of mitochondrial biogenesis with polyphenols: combined effects of resveratrol and equol in human endothelial cells," *Immunity & Ageing*, vol. 10, no. 1, p. 28, 2012.

[12] S. Davinelli, V. Calabrese, D. Zella, and G. Scapagnini, "Epigenetic nutraceutical diets in Alzheimer's disease," *Journal of Nutrition, Health & Aging*, vol. 18, no. 9, pp. 800–805, 2014.

[13] S. Davinelli, M. Maes, G. Corbi, A. Zarrelli, D. C. Willcox, and G. Scapagnini, "Dietary phytochemicals and neuro-inflammaging: from mechanistic insights to translational challenges," *Immunity & Ageing*, vol. 13, no. 1, p. 16, 2016.

[14] S. Davinelli, G. Scapagnini, F. Marzatico, V. Nobile, N. Ferrara, and G. Corbi, "Influence of equol and resveratrol supplementation on health-related quality of life in menopausal women: a randomized, placebo-controlled study," *Maturitas*, vol. 96, pp. 77–83, 2017.

[15] N. Pescosolido and A. Librando, "Oral administration of an association of forskolin, rutin and vitamins B1 and B2 potentiates the hypotonising effects of pharmacological treatments in POAG patients," *Clinica Terapeutica*, vol. 161, no. 3, pp. e81–e85, 2010.

[16] K. Diederich, K. Frauenknecht, J. Minnerup et al., "Citicoline enhances neuroregenerative processes after experimental stroke in rats," *Stroke*, vol. 43, no. 7, pp. 1931–1940, 2012.

[17] P. Grieb, "Neuroprotective properties of citicoline: facts, doubts and unresolved issues," *CNS Drugs*, vol. 28, no. 3, pp. 185–193, 2014.

[18] P. Gareri, A. Castagna, A. M. Cotroneo, S. Putignano, G. De Sarro, and A. C. Bruni, "The role of citicoline in cognitive impairment: pharmacological characteristics, possible advantages, and doubts for an old drug with new perspectives," *Clinical Interventions in Aging*, vol. 10, pp. 1421–1429, 2015.

[19] T. M. Wright, "Tramiprosate," *Drugs of Today*, vol. 42, no. 5, pp. 291–298, 2006.

[20] P. Kocis, M. Tolar, J. Yu et al., "Elucidating the Aβ42 anti-aggregation mechanism of action of tramiprosate in Alzheimer's disease: integrating molecular analytical methods, pharmacokinetic and clinical data," *CNS Drugs*, vol. 31, no. 6, pp. 495–509, 2017.

[21] R. Ward, T. Cirkovic-Vellichovia, F. Ledeque et al., "Neuroprotection by taurine and taurine analogues," *Advances in Experimental Medicine and Biology*, vol. 583, pp. 299–306, 2006.

[22] H. Yasuyoshi, S. Kashii, S. Zhang et al., "Protective effect of bradykinin against glutamate neurotoxicity in cultured rat retinal neurons," *Investigative Ophthalmology & Visual Science*, vol. 41, no. 8, pp. 2273–8, 2000.

[23] S. Kashii, M. Mandai, M. Kikuchi et al., "Dual actions of nitric oxide in N-methyl-D-aspartate receptor-mediated neurotoxicity in cultured retinal neurons," *Brain Research*, vol. 711, no. 1-2, pp. 93–101, 1996.

[24] S. Kashii, M. Takahashi, M. Mandai et al., "Protective action of dopamine against glutamate neurotoxicity in the retina," *Investigative Ophthalmology & Visual Science*, vol. 35, no. 2, pp. 685–695, 1994.

[25] M. Kikuchi, S. Kashii, Y. Honda et al., "Protective action of zinc against glutamate neurotoxicity in cultured retinal neurons," *Investigative Ophthalmology & Visual Science*, vol. 36, no. 10, pp. 2048–2053, 1995.

[26] T. Mosmann, "Rapid colorimetric assay for cellular growth and survival: application to proliferation and cytotoxicity assays," *Journal of Immunological Methods*, vol. 65, no. 1-2, pp. 55–63, 1993.

[27] A. Matteucci, M. Varano, L. Gaddini et al., "Neuroprotective effects of citicoline in in vitro models of retinal neurodegeneration," *International Journal of Molecular Sciences*, vol. 15, no. 4, pp. 6286–6297, 2014.

[28] R. Russo, A. Adornetto, F. Cavaliere et al., "Intravitreal injection of forskolin, homotaurine, and L-carnosine affords neuroprotection to retinal ganglion cells following retinal ischemic injury," *Molecular Vision*, vol. 21, pp. 718–729, 2015.

[29] O. Hurtado, I. Lizasoain, and M. Á. Moro, "Neuroprotection and recovery: recent data at the bench on citicoline," *Stroke*, vol. 42, no. 1, Supplement 1, pp. S33–S35, 2011.

[30] A. J. Barber, "A new view of diabetic retinopathy: a neurodegenerative disease of the eye," *Progress in Neuro-Psychopharmacology and Biological Psychiatry*, vol. 27, no. 2, pp. 283–290, 2003.

[31] C. Nucci, R. Russo, A. Martucci et al., "New strategies for neuroprotection in glaucoma, a disease that affects the central nervous system," *European Journal of Pharmacology*, vol. 787, pp. 119–126, 2016.

[32] S. Davinelli, R. Di Marco, R. Bracale, A. Quattrone, D. Zella, and G. Scapagnini, "Synergistic effect of L-carnosine and EGCG in the prevention of physiological brain aging," *Current Pharmaceutical Design*, vol. 19, no. 15, pp. 2722–2727, 2013.

[33] R. J. Williams, K. P. Mohanakumar, and P. M. Beart, "Neuronutraceuticals: the path to brain health via nourishment is not so distant," *Neurochemistry International*, vol. 89, pp. 1–6, 2015.

[34] P. Grieb, A. Jünemann, M. Rekas, and R. Rejdak, "Citicoline: a food beneficial for patients suffering from or threated with glaucoma," *Frontiers in Aging Neuroscience*, vol. 8, p. 73, 2016.

[35] C. Caltagirone, L. Ferrannini, N. Marchionni, G. Nappi, G. Scapagnini, and M. Trabucchi, "The potential protective effect of tramiprosate (homotaurine) against Alzheimer's disease: a review," *Aging Clinical and Experimental Research*, vol. 24, no. 6, pp. 580–587, 2012.

[36] P. S. Aisen, S. Gauthier, S. H. Ferris et al., "Tramiprosate in mild-to-moderate Alzheimer's disease - a randomized, double-blind, placebo-controlled, multi-centre study (the Alphase study)," *Archives of Medical Science*, vol. 7, no. 1, pp. 102–111, 2011.

[37] J. I. Dan and N. N. Osborne, "Attivita` neuroprotettiva di una associazione di forskolin, omotaurina e carnosina su cellule ganglionari retiniche in vitro sottoposte a stress ossidativo," *Ottica Fisiopatologia*, vol. 17, pp. 173–182, 2012.

[38] M. G. Mutolo, G. Albanese, D. Rusciano, and N. Pescosolido, "Oral administration of forskolin, homotaurine, carnosine, and folic acid in patients with primary open angle glaucoma: changes in intraocular pressure, pattern electroretinogram amplitude, and foveal sensitivity," *Journal of Ocular Pharmacology and Therapeutics*, vol. 32, no. 3, pp. 178–183, 2016.

[39] J. Qu, D. Wang, and C. L. Grosskreutz, "Mechanisms of retinal ganglion cell injury and defense in glaucoma," *Experimental Eye Research*, vol. 91, no. 1, pp. 48–53, 2010.

[40] F. Schuettauf, R. Rejdak, M. Walski et al., "Retinal neurodegeneration in the DBA/2J mouse-a model for ocular hypertension," *Acta Neuropathologica*, vol. 107, no. 4, pp. 352–358, 2004.

[41] T. Oshitari, N. Yoshida-Hata, and S. Yamamoto, "Effect of neurotrophic factors on neuronal apoptosis and neurite regeneration in cultured rat retinas exposed to high glucose," *Brain Research*, vol. 1346, pp. 43–51, 2010.

[42] M. Fiedorowicz, D. Makarewicz, K. I. Stańczak-Mrozek, and P. Grieb, "CDP-choline (citicoline) attenuates brain damage in a rat model of birth asphyxia," *Acta Neurobiologiae Experimentalis*, vol. 68, no. 3, pp. 389–397, 2008.

[43] R. M. Adibhatla, J. F. Hatcher, and R. J. Dempsey, "Citicoline: neuroprotective mechanisms in cerebral ischemia," *Journal of Neurochemistry*, vol. 80, no. 1, pp. 12–23, 2002.

[44] S. A. Messina and R. Dawson Jr., "Attenuation of oxidative damage to DNA by taurine and taurine analogs," *Advances in Experimental Medicine and Biology*, vol. 483, pp. 355–367, 2000.

[45] K. Zeng, H. Xu, M. Mi et al., "Effects of taurine on glial cells apoptosis and taurine transporter expression in retina under

diabetic conditions," *Neurochemical Research*, vol. 35, no. 10, pp. 1566–1574, 2010.

[46] X. Yu, Z. Xu, M. Mi et al., "Dietary taurine supplementation ameliorates diabetic retinopathy via anti-excitotoxicity of glutamate in streptozotocin-induced Sprague-Dawley rats," *Neurochemical Research*, vol. 33, no. 3, pp. 500–507, 2008.

[47] F. Franconi, F. Bennardini, A. Mattana et al., "Plasma and platelet taurine are reduced in subjects with insulin-dependent diabetes mellitus: effects of taurine supplementation," *American Journal of Clinical Nutrition*, vol. 61, no. 5, pp. 1115–1119, 1995.

[48] M. Merheb, R. T. Daher, M. Nasrallah, R. Sabra, F. N. Ziyadeh, and K. Barada, "Taurine intestinal absorption and renal excretion test in diabetic patients: a pilot study," *Diabetes Care*, vol. 30, no. 10, pp. 2652–2654, 2007.

Hindawi
Oxidative Medicine and Cellular Longevity
Volume 2017, Article ID 1420892, 11 pages
https://doi.org/10.1155/2017/1420892

Research Article

Effects of Novel Nitric Oxide-Releasing Molecules against Oxidative Stress on Retinal Pigmented Epithelial Cells

Valeria Pittalà,[1] Annamaria Fidilio,[2] Francesca Lazzara,[2] Chiara Bianca Maria Platania,[2] Loredana Salerno,[1] Roberta Foresti,[3,4] Filippo Drago,[2,5] and Claudio Bucolo[2,5]

[1]*Department of Drug Sciences, University of Catania, Catania, Italy*
[2]*Department of Biomedical and Biotechnological Sciences, Section of Pharmacology, School of Medicine, University of Catania, Catania, Italy*
[3]*Inserm U955, Equipe 12, 94000 Créteil, France*
[4]*Université Paris Est, Faculté de Médecine, 94000 Créteil, France*
[5]*Center for Research in Ocular Pharmacology – CERFO, University of Catania, Catania, Italy*

Correspondence should be addressed to Claudio Bucolo; claudio.bucolo@unict.it

Received 29 June 2017; Accepted 27 August 2017; Published 12 October 2017

Academic Editor: Adrian Smedowski

Oxidative stress is a hallmark of retinal degenerations such as age-related macular degeneration and diabetic retinopathy. Enhancement of heme oxygenase-1 (HO-1) activity in the retina would exert beneficial effects by protecting cells from oxidative stress, therefore promoting cell survival. Because a crosstalk exists between nitric oxide (NO) and HO-1 in promotion of cell survival under oxidative stress, we designed novel NO-releasing molecules also capable to induce HO-1. Starting from curcumin and caffeic acid phenethyl ester (CAPE), two known HO-1 inducers, the molecules were chemically modified by acylation with 4-bromo-butanoyl chloride and 2-chloro-propanoyl chloride, respectively, and then treated in the dark with $AgNO_3$ to obtain the nitrate derivatives VP10/12 and VP10/39. Human retinal pigment epithelial cells (ARPE-19) subjected to H_2O_2-mediated oxidative stress were treated with the described NO-releasing compounds. VP10/39 showed significant ($p < 0.05$) antioxidant and protecting activity against oxidative damage, in comparison to VP10/12, which in turn showed at 100 μM concentration a slight but significant cell toxicity. Only VP10/39 significantly ($p < 0.05$) induced HO-1 in ARPE-19, most likely through covalent bond formation at Cys151 of the Keap1-BTB domain, as revealed from molecular docking analysis. In conclusion, the present data indicate VP10/39 as a promising candidate to protect ARPE-19 cells against oxidative stress.

1. Introduction

Oxidative stress plays a key role in the pathogenesis of several eye disorders, such as, age-related macular degeneration (AMD) and diabetic retinopathy (DR) [1–5]. Heme oxygenase-1 (HO-1), also known as heat shock protein 32 (HSP32), is one of the components of cellular defense mechanisms against oxidative stress-mediated injury. The transcription of HO-1 is mediated by the nuclear transcription factor Nrf2, whose protein levels are in turn regulated by the Kelch-like ECH-associated protein 1 (Keap1) [6].

Regarding AMD, the role of HO-1 in disease pathogenesis has been highlighted by genetic association of the 19G>C HO-1 gene variant with incidence and progression of AMD. Furthermore, the gene variant 25129A>C of Nfr2, activator of HO-1 expression, was associated to AMD. $Nfr2^{-/-}$ mice developed age-dependent degeneration of the RPE and choriocapillaris function, along with spontaneous choroidal neovascularization and deposits of inflammatory proteins in the subretinal space [7]. In this perspective, activation of the Nrf2-HO1 axis would be beneficial for the treatment of AMD.

The inducible HO isoform, HO-1, is highly expressed in the retina of diabetic rats [8], and increased levels of HO-1 may be a response to oxidative stress in diabetes [9, 10]. However, it was found that long-term diabetes led to reduced

HO-1 mRNA levels in the retinal pigmented epithelium (RPE) [11]. Therefore, induction of HO-1 would be beneficial also for the treatment of diabetic retinopathy.

Curcumin and caffeic acid phenethyl ester (CAPE) are nutraceutical substances able to induce the upregulation of HO-1. Studies have shown that curcumin has a wide range of beneficial properties, including anti-inflammatory and antioxidant activities [12, 13]. The pleiotropic action of curcumin is related to regulation of multiple survival and cytoprotective signaling pathways, including anti-inflammatory pathways and those regulated by NFκB, AKT, growth factors, and Nrf2 transcription factor [14–23].

Specifically, low concentrations of curcumin induced HO-1 expression in RPE cells and decreased reactive oxygen species (ROS) in RPE cells, challenged with hydrogen peroxide [24]. Additionally, curcumin modulated retinal oxidative stress in a rat model of streptozotocin- (STZ-) induced diabetic retinopathy [25]. CAPE exhibited antioxidant [26] and anti-inflammatory properties [27] that can be exploited for treatment of several conditions such as ischemia/reperfusion injury [28, 29], atherosclerosis [30] and diabetes [31]. The cytoprotective effect of CAPE against oxidant stress is due to upregulation of HO-1 mRNA [32], through induction of transcription of the ARE-related (antioxidant response element) gene [33]. The mechanism of action of CAPE was confirmed in several *in vitro* studies [32, 34], showing that CAPE significantly increase HO-1 protein expression through inactivation of Nrf2-Keap1 complex and consequent Nrf2 activation [22].

Paeng et al. [35] showed that CAPE inhibits VEGF production in an *in vitro* model of retinal hypoxia (ARPE-19 cells under hypoxic conditions). Thus, CAPE would reduce retinal neovascularization through inhibition of ROS synthesis and reduction of HIF-1α and VEGF expression [35].

Another molecule that influences the regulation of HO-1 production is nitric oxide (NO) [36]. This diatomic molecule is recognized as an important intercellular messenger in biological systems, for example, the cardiovascular system and the nervous system, including the retina. NO is synthesized by NO synthase isoforms, expressed by endothelial cells and efferent nitrergic neurons. NO is an important modulator of homeostatic processes in the eye, such as regulation of aqueous humor dynamics, blood flow, retinal neurotransmission, and phototransduction. An imbalance in NO production is associated with pathological states such as inflammatory diseases (uveitis, retinitis) or degenerative diseases (glaucoma, retinal degeneration) [37]. The reduction of the bioavailability of NO, caused, for example, by endothelial dysfunction, increases the production of ROS. However, overproduction of NO could be harmful, such as the sustained NO synthesis by inducible NOS (iNOS), which is expressed in response to an inflammatory event. Therefore, it is difficult to design an effective therapeutic strategy with NO supplementation or NOS inhibition, due to the dual action of NO [38]. However, latanoprostene bunod, a NO-releasing prostaglandin analog, is expected to be approved by FDA in the near future for clinical use in glaucoma [39].

The HO and NOS systems show numerous and several interactions. For instance, both are activated by ROS and cytokines [40] and can activate guanylyl cyclase [41]. On the other hand, NO can upregulate HO expression by means of a cGMP-dependent pathway [42]. Datta et al. demonstrated that NO induces HO-1 and showed that there are interactions between the iNOS and HO-1 pathways [43]. Furthermore, Chen and Maines demonstrated that exposure of HeLa cells to the NO donor, sodium nitroprusside (SNP), induced a concentration and time-dependent increase of HO-1 mRNA and activation of mitogen-activated protein kinases (MAPKs): the ERK (ERK1 and ERK2) and p38 pathways [44].

In this perspective, we designed and synthesized the novel NO-releasing molecules VP10/12 and VP10/39, bearing curcumin and CAPE scaffolds, respectively (Figure 1). These compounds decreased significantly oxidative stress and increased cell viability of ARPE-19 challenged with hydrogen peroxide. VP10/39, the CAPE-NO derivative, was more effective than VP10/12, most likely due to its capability to induce HO-1 in ARPE-19 cells.

2. Materials and Methods

2.1. Chemistry, Drugs, Chemicals, and Reagents. Melting points of newly synthesized derivatives were determined with an Electrothermal IA9200 using glass capillary tubes. Infrared spectra were recorded on a Perkin–Elmer FT IR 1600 spectrometer in KBr disks. Elemental analyses for C, H, and N were within 70.4% of theoretical values and were performed on a Carlo Erba Elemental Analyzer Mod. 1108 apparatus. ^{1}H NMR spectra were recorded at 200 MHz on a Varian Inova Unity 200 spectrometer in DMSO-d_6 or chloroform-*d* solution. Chemical shifts are given in δ values (ppm), using tetramethylsilane as the internal standard; coupling constants (*J*) are given in hertz (Hz). Signal multiplicities are characterized as s (singlet), d (doublet), t (triplet), q (quartet), m (multiplet), and br (broad signal). All the synthesized compounds were tested for purity on TLC (aluminum sheet coated with silica gel F254, Merck) and visualized by UV (λ 254 and 366 nm).

2.1.1. Synthesis of bis-4-[4-(Nitrooxy)-1-Butoxy]-Caffeic Acid Phenethyl Ester (VP10/39). A solution of 4-bromobutanoyl chloride (2.5 mmol) and *N*,*N*-diisopropylethylamine (2.5 mmol) in 1 mL of anhydrous THF was slowly added to a solution of CAPE (1 mmol) in 5 mL of anhydrous THF, cooled at 0°C, and under a nitrogen atmosphere. Following the addition, the reaction mixture was left stirring at room temperature for 1 h. The obtained solution was diluted with 70 mL of EtOAc and the organic layer was washed with water (2×50 mL) and brine (1×50 mL), dried over anhydrous Na_2SO_4, filtered, and evaporated. The crude material was dissolved in 7 mL of CH_3CN, 2.5 mmol of $AgNO_3$ was added, and the mixture was left stirring at reflux for 3 h, in the dark. The obtained suspension was filtered and evaporated (Figure 2). The residue was purified by flash chromatography on silica gel 60 using a mixture of cyclohexane/EtOAc (7/3, *v*/*v*) as an eluent. Homogeneous fractions were combined and

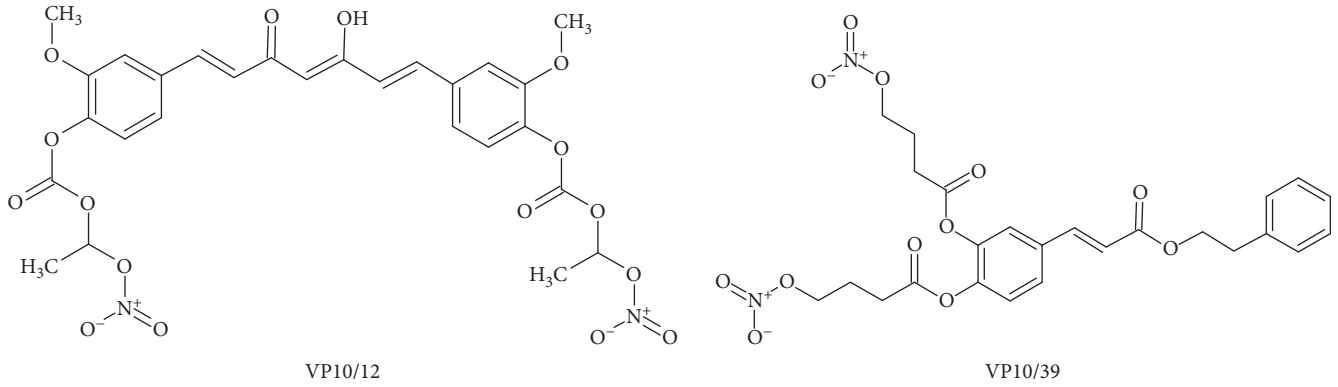

Figure 1: Chemical structure of the synthesized NO-releasing caffeic acid phenethyl ester (VP10/39) and NO-releasing curcumin (VP10/12).

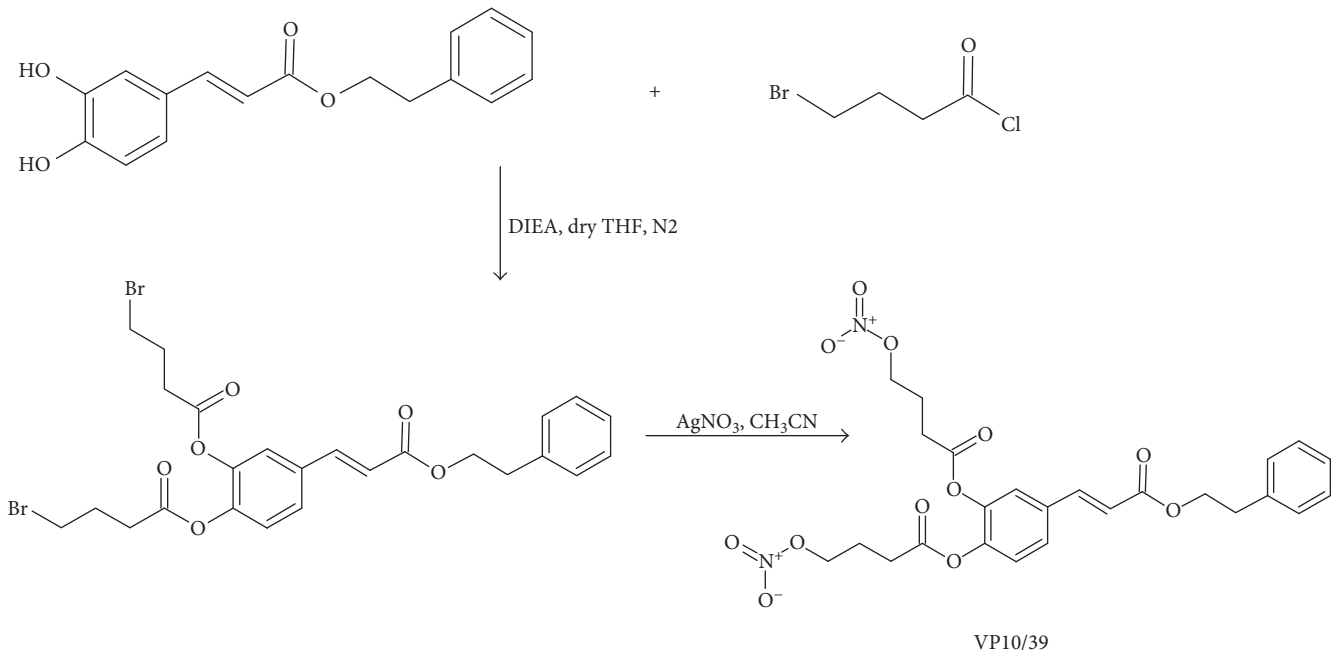

Figure 2: Synthesis of NO-releasing CAPE (VP10/39).

evaporated under reduced pressure to give the title compound (0.38 g, yield 70%) as a pure light-yellow oil: IR (KBr) cm^{-1} 2959, 1770, 1712, 1635, 1505, 1280, 1172, 1112, 869; ^{1}H NMR (DMSO-d_6): δ 7.79–7.57 (m, 2H + 1H, aromatic + C*H* = CHCOO), 7.39–7.18 (m, 6H, aromatic), 6.63 (d, J = 16 Hz, 1H, CH = C*H*COO), 4.64 (t, J = 6.4 Hz, 2H, $CH_2CH_2CH_2ONO_2$), 4.60 (t, J = 6.4 Hz, 2H, $CH_2CH_2CH_2ONO_2$),4.37 (t, J = 6.8 Hz, 2H, $COOCH_2CH_2$), 2.97 (t, J = 6.8 Hz, 2H, $COOCH_2CH_2$), 2.80–2.67 (m, 2H + 2H, $CH_2CH_2CH_2ONO_2$), 2.12–1.94 (m, 2H + 2H, $CH_2CH_2CH_2ONO_2$). Anal. ($C_{25}H_{26}N_2O_{12}$) C, H, N.

2.1.2. Synthesis of [(1E,6E)-3,5-Dioxohepta-1,6-Diene-1,7-Diyl]bis-2-Methoxy-4,1-Phenylene bis[1-(Nitrooxy)Ethyl] Biscarbonate (VP10/12). (1*E*,6*E*)-1,7-bis(4-[[[1-(chloro) ethoxy]carbonyl]oxy]-3-methoxyphenyl)hepta-1,6-diene-3,5-dione (0.5 mmol) was dissolved in 3 mL of CH_3CN; 1.0 mmol of $AgNO_3$ was added; and the mixture was left stirring at reflux for 3 h, in the dark (Figure 3). The obtained suspension was filtered and evaporated. The residue was purified by flash chromatography on silica gel 60 using a mixture of cyclohexane/EtOAc (7/3, *v*/*v*) as an eluent. Homogeneous fractions were combined and evaporated under reduced pressure to give the title compound (0.20 g, yield 62%) as a pure yellow-orange oil: IR (KBr) cm^{-1} 2953, 2929, 2880, 1635, 1621, 1510, 1438, 1257, 1027, 870; ^{1}H NMR ($CDCl_3$): δ 7.62 (d, J = 16 Hz, 1H + 1H, ArCH = C*H*), 7.27–7.10 (m, 6H, aromatic), 7.02 (q, J = 5.6 Hz, 1H + 1H, C*H*CH_3), 6.58 (d, J = 16 Hz, 1H + 1H, ArC*H* = CH), 5.87 (s, 1H, COC*H* = COH), 3.91 (s, 3H + 3H, OCH_3), 1.68 (d, J = 5.6 Hz, 3H + 3H, CHCH_3). Anal. ($C_{27}H_{26}N_2O_{16}$) C, H, N.

2.1.3. Synthesis of bis(1-Chloroethyl)[(1E,6E)-3,5-Dioxohepta-1,6-Diene-1,7-Diyl]bis-2-Methoxy-4,1-Phenylene Biscarbonate. Curcumin (2 mmol) was dissolved in 20 mL of ice-cooled

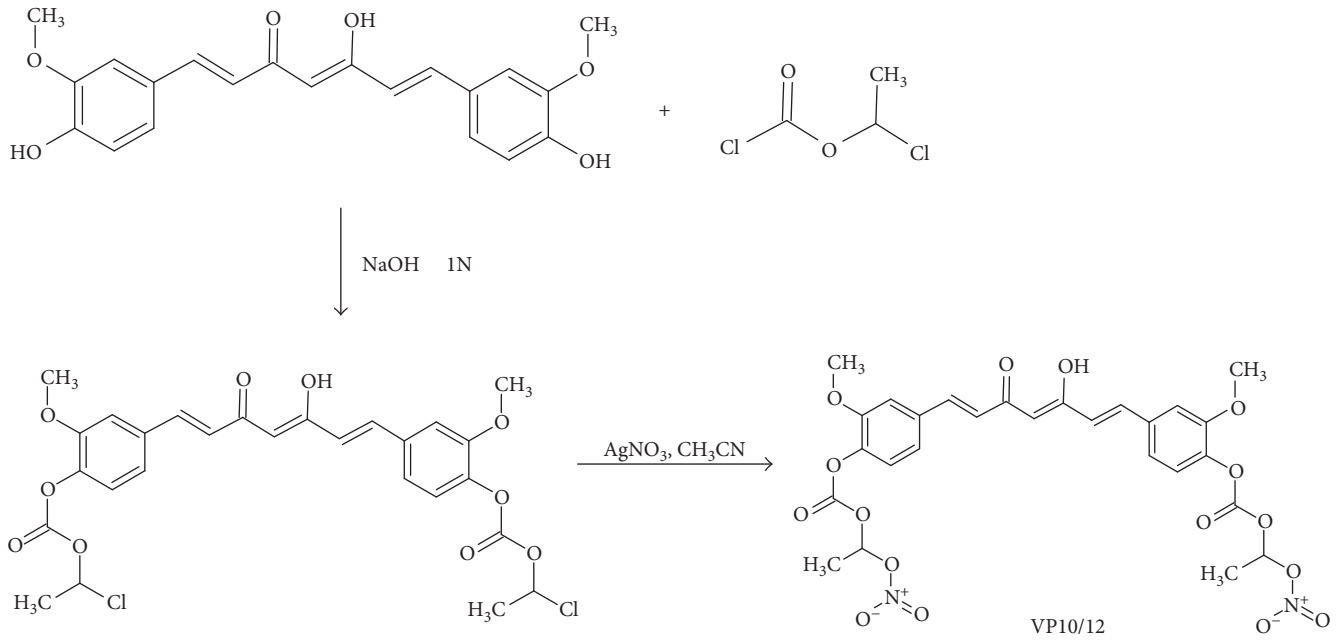

Figure 3: Synthesis of NO-releasing curcumin (VP10/12).

NaOH 1N, and 2-chloro-propanoyl chloride (8 mmol) was added (Figure 3). Following the addition, the reaction mixture was left stirring at room temperature for 15 min and filtered. The obtained crude material was purified by flash chromatography on silica gel 60 using a mixture of cyclohexane/EtOAc (5/5, *v*/*v*) as an eluent. Homogeneous fractions were combined and evaporated under reduced pressure to give the title compound (0.32 g, yield 28%) as a pure yellow solid: mp 104-105°C. IR (KBr) cm^{-1} 3003, 2955, 2870, 1620, 1597, 1581, 1508, 1422, 1250, 1120, 770 ^{1}H NMR ($CDCl_3$): δ 7.70 (d, $J = 16$ Hz, 1H + 1H, ArCH = C*H*), 7.38–7.20 (m, 6H, aromatic), 6.37–7.19 (m, 1H + 1H + 1H + 1H, ArC*H* = CH + C*H*CH_3), 5.95 (s, 1H, COC*H* = COH), 3.99 (s, 3H + 3H, OCH_3), 2.00 (d, $J = 6$ Hz, 3H + 3H, CHCH_3). Anal. ($C_{27}H_{26}Cl_2O_{10}$) C, H.

2.2. In Vitro Studies. ARPE-19 (human retinal pigment epithelial) cells were purchased from ATCC®. The cell line was cultured at 37°C (humidified atmosphere with 5% CO2), in ATCC-formulated DMEM:F12 medium (ATCC number 30-2006) with 100 U/mL penicillin, 100 μg/mL streptomycin, and 10% fetal bovine serum.

ROS were measured with the DCFDA—Cellular Reactive Oxygen Species Detection Assay Kit (ab113851)—according to manufacturer's protocol. DCFDA, a cell permeable fluorogenic dye, is deacetylated by cellular esterases to a nonfluorescent compound and later oxidized by ROS into highly fluorescent 2′,7′-dichlorofluorescein (DCF); fluorescence intensity is proportional to cell ROS concentration. ARPE-19 cells were plated into 96-well black plates ($2 \times 10E^4$ cells per well), and confluence was reached within 24 h. After confluence, cells were washed twice with phosphate-buffered saline (PBS pH 7.4) and incubated with 25 μM DCFDA in buffer solution (provided with the kit) at 37°C for 45 minutes. After two washes with PBS, cells were treated with increasing concentrations of VP10/39 and VP10/12 (1–10–20–100 μM) for 60 minutes, then oxidative stress was induced with 500 μM H_2O_2 treatment for 120 minutes. ROS concentration was measured by detection of DCF fluorescence ($\lambda_{ex} = 495$ nm, $\lambda_{em} = 529$ nm) with a Varioskan™ Flash Multimode Reader.

Lactate dehydrogenase (LDH) cell release was measured using the Cytotoxicity Detection KitPLUS (LDH) (ROCHE 04744934001) according to manufacturer's protocol. LDH is released into the medium when the integrity of the cell membrane is lost; therefore, high levels of LDH are indices of cell death. ARPE-19 cells were plated into 96-well plates ($1.5 \times 10E^4$ cells per well). After cell confluence was reached (24 h), cells were treated with increasing concentrations of VP10/39 and VP10/12 (1–10–20–100 μM) for 60 minutes and cell damage was induced by 2 mM H_2O_2 for 60 minutes. Cell-free culture supernatant was collected in empty plates and incubated with the enzymatic reaction mixture for 30 minutes. LDH was quantified by measuring absorbance at 490 nm with the Varioskan Flash Multimode Reader.

ATP is present in metabolically active cells and its concentration declines when cell necrosis and apoptosis occur. After oxidative stress induction by treatment with H_2O_2, ATP production was measured using the ATPlite 1 step kit (Perkin Elmer 6016731), according to manufacturer's protocol. ATP concentration is proportional to luminescence intensity related to ATP reaction with luciferase and D-luciferin. ARPE-19 cells were plated into 96-well white plates ($1.5 \times 10E^4$ cells per well). Cells were treated with increased concentrations of VP10/39 and VP10/12 (1–10–20–100 μM) for 60 minutes, then oxidative stress was induced with 1.5 mM H_2O_2 for 180 minutes. After that, the plate was equilibrated at room temperature (20–22°C), before addition of the reaction solution; therefore, luminescence was measured with Varioskan Flash Multimode Reader.

2.3. Heme Oxygenase Activity Assay. ARPE-19 cells were cultured in 100 mm diameter petri dishes and were collected 6 hours after incubation with VP10/12 and VP10/39 at 10 μM and 20 μM concentrations. The heme oxygenase activity assay was then carried out on the basis of the spectrophotometric determination of bilirubin as the final product of heme degradation by heme oxygenase as described previously by Foresti et al. [45]. Collected cells were incubated with hemin, NADPH, and liver cytosol (a source of biliverdin reductase); the reaction was carried out at 37°C in the dark and was stopped after 1 h with an addition of chloroform, used in order to extract the produced bilirubin. Heme oxygenase activity is expressed as picomoles of bilirubin/mg protein/60 min.

2.4. Statistical Analysis. All results were reported as mean ± SD. Statistical analysis was carried out using 1-way ANOVA followed by Tukey-Kramer multiple comparison test. Differences between two groups were considered as significant given a p value < 0.05. Graphs were done using GraphPad Prism 5 software (GraphPad Inc., San Diego, CA) that was also used for statistical analysis.

2.5. Molecular Modeling. Activation of the Nrf2 pathway occurs with inhibition of the KEAP1/Nrf2 protein-protein interaction or Keap1 dimerization. Therefore, Nrf2 inducers act by

(i) disrupting the Keap1-DC domain/Nfr2 interaction [46];

(ii) covalent binding to cysteine residues of the Keap1-BTB domain [47].

We investigated the binding of VP10/12 and VP10/39 at Keap1-DC and Keap1-BTB with a molecular modeling approach. The whole human Keap1 dimer was built with the advanced molecular modeling task of Maestro© and subjected to loop optimization and two energy minimization steps: rigid body energy and all-atom energy minimization using the VSGB 2.0 solvation model [48]. BTB and IVR domains of Keap1 were modeled on the basis of BTB and BACK (IVR) domains of Keltch11 (PDB:3I3N); the DC domain of Keap1 was modeled using the PDB:1X2R X-ray structure as template. The quality of the model was assessed by determination of protein Ramachandran plots before and after energy minimization; the two energy minimization steps led to a significant decrease of residue dihedral violations (Figure 1S supplemental material available online at https://doi.org/10.1155/2017/1420892). Superimposition between the model of human Keap1 dimer with the electron microscopy reconstruction map (24 Å) of murine Keap1 dimer [49] was carried out with Chimera 1.11.2 (Figure 2S supplemental material). RMSD between human Keap1 dimer model and electron microscopy map of murine Keap1 was 4.5 Å. VP10/12 and VP10/39.sdf files were built with the web server "Online SMILES Translator and Structure File Generator" https://cactus.nci.nih.gov/translate/. Tridimensional structures of these two ligands, tautomerization and ionization at pH 7.4, were obtained by launching the LigPrep task of Schrodinger© Maestro. Molecular docking of curcumin and CAPE was carried out in order to compare binding of novel synthetized compounds with other known Nrf2 inducers. We used the following docking protocol on the Keap1-DC domain [46]: (i) grid generation on the centroid of the binding pocket; (ii) standard precision (SP) docking (Schrodinger©) performed with Glide (Schrodinger©). At first, docking was carried out with ring conformation sampling, followed by a 500-step conjugate gradient minimization by Glide (dielectric = 1). Covalent docking of VP10/12 and VP10/39 was carried out at the BTB domain of Keap1 as follows: Cys 151 was set as reactive residue and the Michael's addition reaction was simulated [47] with CovDock task of Schrodinger© Maestro [50]. MMGBSA rescoring of semiflexible docking at the DC domain and covalent docking at BTB was carried out with Schrodinger© Maestro: the VSGB 2.0 model was used and all residues within 10 Å from ligand were allowed to move.

3. Results

3.1. Chemical Synthesis of NO-Releasing Curcumin (VP10/12) and NO-Releasing CAPE (VP10/39). Hybrid NO-releasing molecules were obtained in high yield by using an efficient synthetic route (Figures 2 and 3). The alcoholic-free groups of CAPE and curcumin were firstly acylated with 4-bromobutanoyl chloride or 2-chloro-propanoyl chloride, respectively. In a subsequent step, the intermediates were converted into the corresponding nitrate derivatives by the treatment with $AgNO_3$ at reflux into the dark. The desired final products, VP10/12 and VP10/39, were easily obtained by flash chromatography purification. VP10/12 was obtained in a high overall yield, 70% two steps; on the contrary, VP10/39 was obtained in poor yield because it is easily hydrolyzed under purification conditions.

3.2. VP10/12 and VP10/39 Protected ARPE-19 Cells from Oxidative Stress. We tested the antioxidant properties of VP10/12 and VP10/39 in ARPE-19 cells, challenged with H_2O_2. Treatment with H_2O_2 induced oxidative stress by increasing ROS concentration ([ROS]) in ARPE-19 cells (Figures 4(a) and 4(b)). While, pretreatment (60 min) with VP10/12 and VP10/39 decreased significantly ($p < 0.05$) [ROS] in ARPE-19 subjected to oxidative stress (Figures 4(a) and 4(b)). The CAPE-NO derivative, VP10/39, at 1 μM concentration induced a 1.5-fold decrease of [ROS]. Furthermore, 10 μM VP10/39 decreased ROS concentration to values of negative control cells (CTRL−), 8.7 ± 0.8 FU and 2.9 ± 0.4 FU, respectively (FU = fluorescent units, Figure 4(b)). The curcumin-NO derivative VP10/12 induced at 1 μM concentration a significant 2-fold decrease of [ROS] in ARPE-19 cells treated with H_2O_2. Additionally, VP10/12 inhibited ROS formation in a dose-dependent manner. VP10/12 did not decrease [ROS] to levels of negative control cells, in contrast to data obtained for VP10/39.

We analyzed the LDH release in medium of ARPE-19 challenged with H_2O_2, in order to assess the protective effects of tested compounds on cell death induced by oxidative stress. VP10/12 and VP10/39 significantly ($p < 0.05$) induced

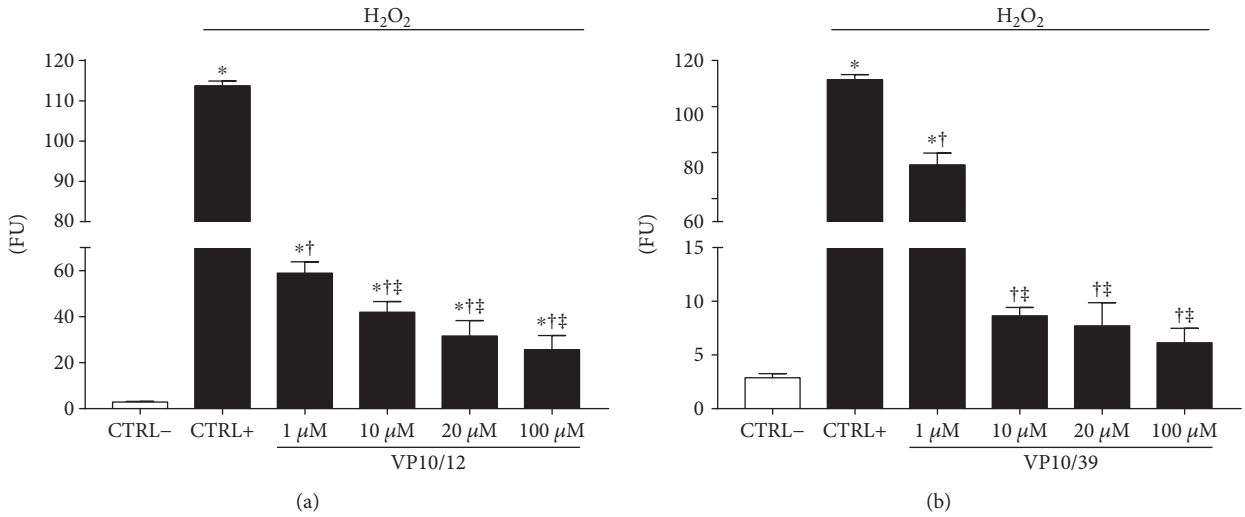

Figure 4: VP10/12 and VP10/39 decreased ROS concentration in ARPE-19 cells challenged with H_2O_2. $^*p < 0.05$ versus CTRL− cells (cells that were not treated with H_2O_2), $^\dagger p < 0.05$ versus CTRL+ cells (cells that were treated with H_2O_2), $^\ddagger p < 0.05$ versus 1 μM VP10/12 or VP10/39 treatment.

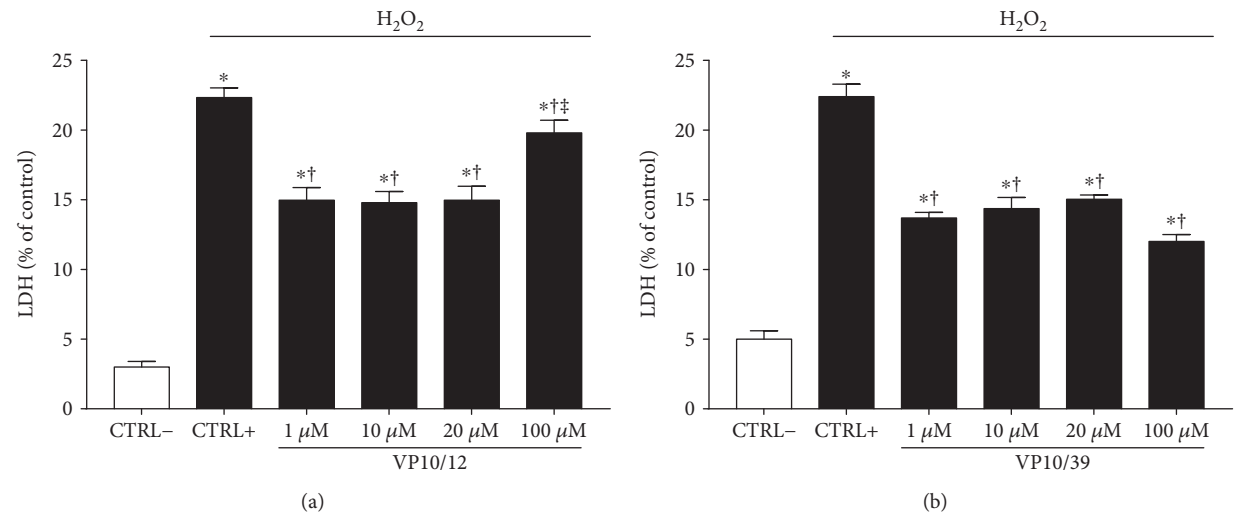

Figure 5: VP10/12 and VP10/39 decreased LDH release from ARPE-19 cells challenged with H_2O_2. $^*p < 0.05$ versus CTRL− cells (cells that were not treated with H_2O_2), $^\dagger p < 0.05$ versus CTRL+ cells (cells that were treated with H_2O_2), $^\ddagger p < 0.05$ versus 1 μM VP10/12 or VP10/39 treatment.

a 1.5-fold decrease in LDH release, in comparison to positive control cells (CTRL+, ARPE-19 treated with H_2O_2, Figures 5(a) and 5(b)). However, 100 μM VP10/12 increased LDH levels (19.80 ± 0.90) to values reported for CTRL+ cells (22.33 ± 0.70); thus curcumin-NO might exert toxic effects at high concentrations.

Oxidative damage affected cellular viability of ARPE-19 cells, given a significant ($p < 0.05$) decrease of ATP levels in CTRL+ cells, in comparison to CTRL− cells (Figures 6(a) and 6(b)). Treatment with VP10/12 and VP10/39 increased significantly ATP levels in ARPE-19 cells challenged with H_2O_2 (Figures 6(a) and 6(b)). Interestingly, VP10/39 treatment increased ARPE-19 cell viability in a dose-dependent manner.

Overall, these data indicated that both VP10/12 and VP10/39 are capable to protect ARPE-19 cells from oxidative damage; however, VP10/39 was more effective in decreasing ROS formation and LDH release than VP10/12, which at highest concentration (100 μM) exerted a slight, still significant, toxic effect on ARPE-19 cells.

3.3. VP10/39 Induced HO-1. Resistance to oxidative stress of cells treated with VP10/12 and VP10/39 can be accounted not only to ROS-scavenging capability but also to induction of HO-1. We tested the capability of VP10/12 and VP10/39 to induce HO-1 in ARPE-19 by means of a HO-1 activity assay, which was previously set for ARPE-19 cells [45]. Only VP10/39 induced significantly ($p < 0.05$) HO-1 in ARPE-19 at both tested concentrations, 10 μM and 20 μM. VP10/12 at 10 μM and 20 μM concentrations did not alter HO-1 activity in ARPE-19 cells, because no substantial differences were

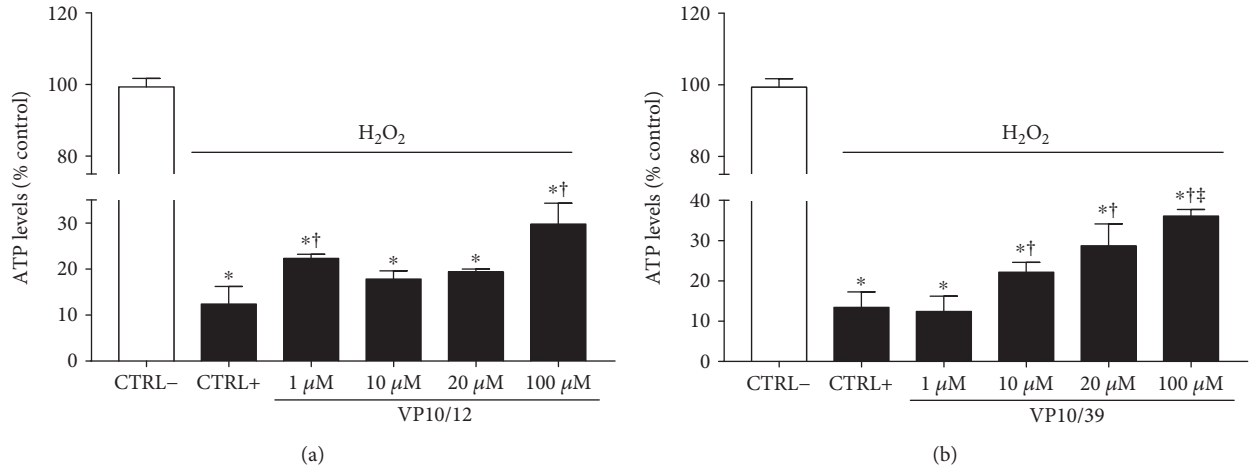

Figure 6: VP10/12 and VP10/39 viability of ARPE-19 cells challenged with H_2O_2. $^*p < 0.05$ versus CTRL− cells (cells that were not treated with H_2O_2), $^\dagger p < 0.05$ versus CTRL+ cells (cells that were treated with H_2O_2), $^\ddagger p < 0.05$ versus 1 μM VP10/12 or VP10/39 treatment.

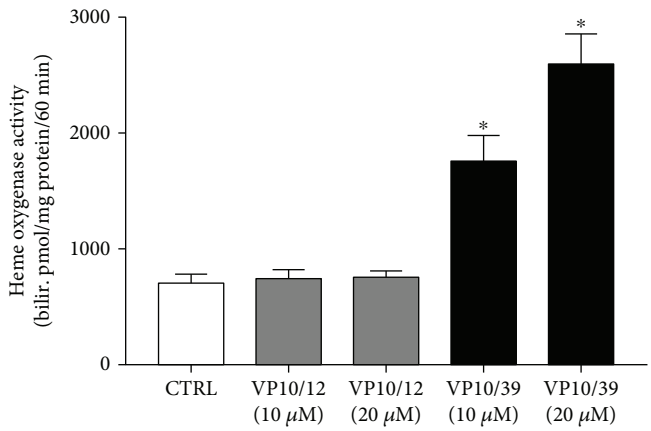

Figure 7: HO-1 induction by VP10/12 and VP10/39. $^*p < 0.05$ versus CTRL control cells.

found between control and VP10/12-treated cells (Figure 7). This result would explain the significant greater antioxidant activity of VP10/39, compared to VP10/12 (Figure 4).

In order to rationalize the capability of VP10/39 to induce HO-1, we built the model of Keap1 dimer, which, through association in a multiprotein complex, regulates the degradation of the nuclear factor Nrf2. In fact, under oxidative condition, Keap1 dimer dissociates and is not able to keep Nrf2 immobilized for ubiquitination by the E2 ubiquitin [51]. HO-1 induction can be promoted by stabilization of Nrf2 protein levels, therefore, by either inhibiting interaction between Keap1-DC/Nrf2 [46] or destabilizing the Keap1 dimer at the BTB domain [47]. In this perspective, we carried out semiflexible docking of VP10/12, VP10/39, curcumin, and CAPE at DC. Furthermore, we simulated Michael addition reaction (covalent docking) of ligands at the dimeric BTB domain of Keap1. Semiflexible docking of VP10/12 and VP10/39 at the DC domain of Keap1 was characterized by better docking scores (more negative) in comparison to

Table 1: Docking scores, covalent affinity, and $\Delta G_{binding}$ of docked ligands. Glide scores and covalent affinities are reported as arbitrary units; $\Delta G_{binding}$ are expressed in Kcal/mol.

Ligand	Semiflexible docking at DC domain		Covalent docking at BTB domain	
	Glide score	$\Delta G_{binding}$	Covalent affinity	$\Delta G_{binding}$
VP10/12	−7.66	−90.05	−5.63	−50.42
VP10/39	−7.22	−86.70	−7.06	−68.04
Curcumin	−5.74	−67.50	−4.07	−47.38
CAPE	−4.08	−62.50	−3.33	−41.67

both curcumin and CAPE. VP10/12 showed a slightly better docking score at the DC domain (Glide score = −7.66), if compared to VP10/39 (Glide score = −7.22). However, poses (binding modes) of VP10/12 and VP10/39 are not similar to poses of known ligands of Keap1-DC. This trend was confirmed by MMGBSA rescoring (Table 1). On the contrary, curcumin (Glide score = −5.74) complexed at Keap1-DC alike a crystallized Keap1-DC/ligand complex (PDB:4ZY3) [46] (Figure 8(a)). Docking score differences between VP10/12 and VP10/39 at the Keap1 DC domain did not explain the capability of VP10/39 to induce HO-1. Worthy of note, MMGBSA binding energy was more negative for binding of ligands at the DC domain than binding of ligands at the BTB domain. However, MMGBSA rescoring for docking at DC and BTB cannot be compared, because of significant differences in simulated complex formation: noncovalent binding versus covalent binding. Covalent docking of the tested compounds at the Keap1-BTB domain revealed that VP10/39 covalently bound to Cys 151 of Keap1-BTB showed better affinity (−7.06) than VP10/12 (−5.63), curcumin (−4.07), and CAPE (−3.33) (Figures 8(b), 8(c), and 8(d)). MMGBSA covalent docking rescoring confirmed that VP10/39 bound covalently to BTB domain with the lowest binding-free energy than other ligands.

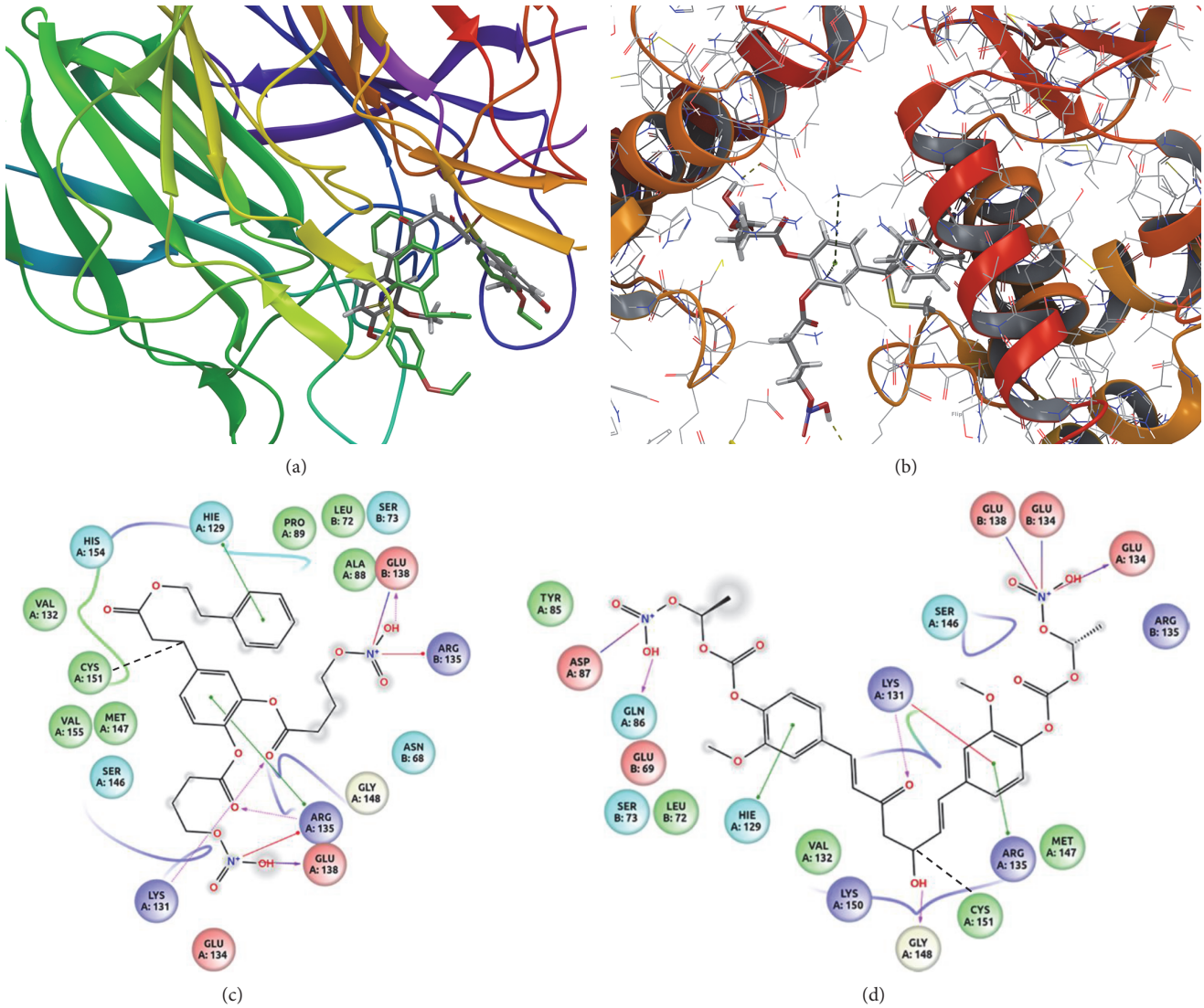

Figure 8: Molecular docking into Keap1 domains. (a) Semiflexible docking at the Keap1-DC domain of curcumin (grey stick) and K67 (PDB:4ZY3, green stick). (b) Covalent docking—Michael addition at the Cys151 of the BTB domain of Keap1. (c) 2D pose representation of VP10/39 covalent bound (black hatched line) to Cys151 of the Keap1-BTB domain. (d) 2D pose representation of VP10/12 covalent bound (black hatched line) to Cys151 of the Keap1-BTB domain.

Indeed, VP10/39 can induce HO-1 by means of a covalent bound to Cys151 of Keap1-BTB, inhibiting Keap1 dimerization at the BTB domain.

4. Discussion

This study was aimed at designing new NO-releasing molecules to be potentially used for the treatment of AMD and DR. Oxidative stress, along with inflammation, is a hallmark of age-related retinal diseases such as AMD and DR, that lead to irreversible sight loss, if not correctly managed [52, 53]. Currently, there are no approved drugs for the treatment of early phases of AMD and DR. Besides that, antiangiogenic and anti-inflammatory drugs are approved for treatment of diabetic macular edema and wet form of AMD, which are clinical forms of AMD and DR progression. Dysregulation of the HO-1 defense system against oxidative cell damage has been linked to AMD and DR progression. Antioxidant supplementation has been explored as a therapeutic strategy for diabetic retinopathy (clinicaltrial.gov "antioxidant AND diabetic retinopathy") and AMD (clinicaltrial.gov "antioxidant AND age related macular degeneration"). Furthermore, there are clinical trials about improvement of visual function in patients with diabetic retinopathy treated with curcumin supplementation (NCT02984813, NCT01646047). Besides preclinical promising results [24, 25, 35], no clinical studies have been reported about either curcumin as a treatment of AMD or CAPE as treatment of both DR and AMD. We hereby hypothesized that a HO-1 inducer with a NO-releasing moiety would be promising for protection of retinal pigmented epithelium against oxidative stress, because NO can also induce HO-1. Both VP10/12 (curcumin-NO-releasing derivative) and VP10/39 (CAPE-NO-releasing derivative) were able to decrease ROS concentration and LDH

release. Furthermore, both compounds increased cell viability in ARPE-19 cells, challenged with H_2O_2. However, VP10/39 was more effective in decreasing ROS and LDH in retinal pigmented epithelial cells treated with H_2O_2, in comparison to VP10/12.

Moreover, VP10/12 showed significant cell toxicity effects ($p < 0.05$) at the highest tested concentration (100 μM); this result can be related either to a toxic dose of curcumin from hydrolyzed VP10/12 or to rapid and sustained release of NO by VP10/12.

The better activity of VP10/39, in comparison to VP10/12, can be explained by its capability to induce HO-1, as well as other CAPE derivatives [54], likely by means of covalent binding to Cys 151 of the Keap1-BTB domain, which is involved in the dimerization of Keap1. In fact, dimerization of Keap1 is a necessary condition for ubiquitination and degradation of Nrf2; therefore, oligomerization of Keap1 is a good strategy for stabilizing Nrf2 and consequently to induce HO-1 [47].

5. Conclusions

In conclusion, VP10/39 is a promising compound capable of protective activity against oxidative damage on retinal pigmented epithelium. Therefore, this compound could be further developed as adjuvant antioxidant treatment of AMD and diabetic retinopathy.

Conflicts of Interest

The authors declare that they have no conflicts of interest.

Acknowledgments

This work was supported by the National Grant PRIN 2015JXE7E8 from the Ministry of Education, University and Research (MIUR).

References

[1] J. G. Hollyfield, V. L. Bonilha, M. E. Rayborn et al., "Oxidative damage-induced inflammation initiates age-related macular degeneration," *Nature Medicine*, vol. 14, no. 2, pp. 194–198, 2008.

[2] L. A. Donoso, D. Kim, A. Frost, A. Callahan, and G. Hageman, "The role of inflammation in the pathogenesis of age-related macular degeneration," *Survey of Ophthalmology*, vol. 51, no. 2, pp. 137–152, 2006.

[3] J. K. Shen, A. Dong, S. F. Hackett, W. R. Bell, W. R. Green, and P. A. Campochiaro, "Oxidative damage in age-related macular degeneration," *Histology and Histopathology*, vol. 22, no. 12, pp. 1301–1308, 2007.

[4] S. A. Madsen-Bouterse and R. A. Kowluru, "Oxidative stress and diabetic retinopathy: pathophysiological mechanisms and treatment perspectives," *Reviews in Endocrine and Metabolic Disorders*, vol. 9, no. 4, pp. 315–327, 2008.

[5] T. S. Kern, "Contributions of inflammatory processes to the development of the early stages of diabetic retinopathy," *Experimental Diabetes Research*, vol. 2007, Article ID 95103, 14 pages, 2007.

[6] A. Loboda, M. Damulewicz, E. Pyza, A. Jozkowicz, and J. Dulak, "Role of Nrf2/HO-1 system in development, oxidative stress response and diseases: an evolutionarily conserved mechanism," *Cellular and Molecular Life Sciences*, vol. 73, no. 17, pp. 3221–3247, 2016.

[7] Z. Zhao, Y. Chen, J. Wang et al., "Age-related retinopathy in Nrf2-deficient mice," *PLoS One*, vol. 6, no. 4, article e19456, 2011.

[8] M. Cukiernik, S. Mukherjee, D. Downey, and S. Chakabarti, "Heme oxygenase in the retina in diabetes," *Current Eye Research*, vol. 27, no. 5, pp. 301–308, 2003.

[9] R. Stocker, "Induction of haem oxygenase as a defense against oxidative stress," *Free Radical Research Communications*, vol. 9, no. 2, pp. 101–112, 1990.

[10] L. Cosso, E. P. Maineri, N. Traverso et al., "Induction of heme oxygenase 1 in liver of spontaneously diabetic rats," *Free Radical Research*, vol. 34, no. 2, pp. 189–191, 2001.

[11] J. L. da Silva, R. A. Stoltz, M. W. Dunn, N. G. Abraham, and S. Shibahara, "Diminished heme oxygenase-1 mRNA expression in RPE cells from diabetic donors as quantitated by competitive RT/PCR," *Current Eye Research*, vol. 16, no. 4, pp. 380–386, 1997.

[12] H. Hatcher, R. Planalp, J. Cho, F. M. Torti, and S. V. Torti, "Curcumin: from ancient medicine to current clinical trials," *Cellular and Molecular Life Sciences*, vol. 65, no. 11, pp. 1631–1652, 2008.

[13] A. Goel, A. B. Kunnumakkara, and B. B. Aggarwal, "Curcumin as "curecumin": from kitchen to clinic," *Biochemical Pharmacology*, vol. 75, no. 4, pp. 787–809, 2008.

[14] S. Shishodia, H. M. Amin, R. Lai, and B. B. Aggarwal, "Curcumin (diferuloylmethane) inhibits constitutive NF-κB activation, induces G1/S arrest, suppresses proliferation, and induces apoptosis in mantle cell lymphoma," *Biochemical Pharmacology*, vol. 70, no. 5, pp. 700–713, 2005.

[15] Y. Abe, S. Hashimoto, and T. Horie, "Curcumin inhibition of inflammatory cytokine production by human peripheral blood monocytes and alveolar macrophages," *Pharmacological Research*, vol. 39, no. 1, pp. 41–47, 1999.

[16] A. C. Reddy and B. R. Lokesh, "Studies on spice principles as antioxidants in the inhibition of lipid peroxidation of rat liver microsomes," *Molecular and Cellular Biochemistry*, vol. 111, no. 1-2, pp. 117–124, 1992.

[17] M. T. Huang, T. Lysz, T. Ferraro, T. F. Abidi, J. D. Laskin, and A. H. Conney, "Inhibitory effects of curcumin on in vitro lipoxygenase and cyclooxygenase activities in mouse epidermis," *Cancer Research*, vol. 51, no. 3, pp. 813–819, 1991.

[18] S. Singh and B. B. Aggarwal, "Activation of transcription factor NF-κB is suppressed by curcumin (diferuloylmethane)," *Journal of Biological Chemistry*, vol. 270, no. 50, pp. 24995–25000, 1995.

[19] J. H. Woo, Y. H. Kim, Y. J. Choi et al., "Molecular mechanisms of curcumin-induced cytotoxicity: induction of apoptosis through generation of reactive oxygen species, down-regulation of Bcl-XL and IAP, the release of cytochrome c and inhibition of Akt," *Carcinogenesis*, vol. 24, no. 7, pp. 1199–1208, 2003.

[20] M. Susan and M. N. Rao, "Induction of glutathione S-transferase activity by curcumin in mice," *Arzneimittel-Forschung*, vol. 42, no. 7, pp. 962–964, 1992.

[21] G. Scapagnini, C. Colombrita, M. Amadio et al., "Curcumin activates defensive genes and protects neurons against

oxidative stress," *Antioxidants & Redox Signaling*, vol. 8, no. 3-4, pp. 395–403, 2006.

[22] E. Balogun, M. Hoque, P. Gong et al., "Curcumin activates the haem oxygenase-1 gene via regulation of Nrf2 and the antioxidant-responsive element," *The Biochemical Journal*, vol. 371, Part 3, pp. 887–895, 2003.

[23] V. Pittala, L. Vanella, L. Salerno et al., "Effects of polyphenolic derivatives on heme oxygenase-system in metabolic dysfunctions," *Current Medicinal Chemistry*, vol. 24, 2017.

[24] J. M. Woo, D. Y. Shin, S. J. Lee et al., "Curcumin protects retinal pigment epithelial cells against oxidative stress via induction of heme oxygenase-1 expression and reduction of reactive oxygen," *Molecular Vision*, vol. 18, pp. 901–908, 2012.

[25] R. A. Kowluru and M. Kanwar, "Effects of curcumin on retinal oxidative stress and inflammation in diabetes," *Nutrition & Metabolism*, vol. 4, p. 8, 2007.

[26] S. Son and B. A. Lewis, "Free radical scavenging and antioxidative activity of caffeic acid amide and ester analogues: structure-activity relationship," *Journal of Agricultural and Food Chemistry*, vol. 50, no. 3, pp. 468–472, 2002.

[27] P. Michaluart, J. L. Masferrer, A. M. Carothers et al., "Inhibitory effects of caffeic acid phenethyl ester on the activity and expression of cyclooxygenase-2 in human oral epithelial cells and in a rat model of inflammation," *Cancer Research*, vol. 59, no. 10, pp. 2347–2352, 1999.

[28] J. Tan, Z. Ma, L. Han et al., "Caffeic acid phenethyl ester possesses potent cardioprotective effects in a rabbit model of acute myocardial ischemia-reperfusion injury," *American Journal of Physiology - Heart and Circulatory Physiology*, vol. 289, no. 5, pp. H2265–H2271, 2005.

[29] X. Wei, L. Zhao, Z. Ma et al., "Caffeic acid phenethyl ester prevents neonatal hypoxic-ischaemic brain injury," *Brain*, vol. 127, Part 12, pp. 2629–2635, 2004.

[30] K. Hishikawa, T. Nakaki, and T. Fujita, "Oral flavonoid supplementation attenuates atherosclerosis development in apolipoprotein E-deficient mice," *Arteriosclerosis, Thrombosis, and Vascular Biology*, vol. 25, no. 2, pp. 442–446, 2005.

[31] V. Pittala, L. Salerno, G. Romeo, R. Acquaviva, C. Di Giacomo, and V. Sorrenti, "Therapeutic potential of caffeic acid phenethyl ester (CAPE) in diabetes," *Current Medicinal Chemistry*, 2016.

[32] X. Wang, S. Stavchansky, B. Zhao, J. A. Bynum, S. M. Kerwin, and P. D. Bowman, "Cytoprotection of human endothelial cells from menadione cytotoxicity by caffeic acid phenethyl ester: the role of heme oxygenase-1," *European Journal of Pharmacology*, vol. 591, no. 1–3, pp. 28–35, 2008.

[33] J. K. Kim and H. D. Jang, "Nrf2-mediated HO-1 induction coupled with the ERK signaling pathway contributes to indirect antioxidant capacity of caffeic acid phenethyl ester in HepG2 cells," *International Journal of Molecular Sciences*, vol. 15, no. 7, pp. 12149–12165, 2014.

[34] X. Wang, S. Stavchansky, S. M. Kerwin, and P. D. Bowman, "Structure-activity relationships in the cytoprotective effect of caffeic acid phenethyl ester (CAPE) and fluorinated derivatives: effects on heme oxygenase-1 induction and antioxidant activities," *European Journal of Pharmacology*, vol. 635, no. 1–3, pp. 16–22, 2010.

[35] S. H. Paeng, W. K. Jung, W. S. Park et al., "Caffeic acid phenethyl ester reduces the secretion of vascular endothelial growth factor through the inhibition of the ROS, PI3K and HIF-1α signaling pathways in human retinal pigment epithelial cells under hypoxic conditions," *International Journal of Molecular Medicine*, vol. 35, no. 5, pp. 1419–1426, 2015.

[36] R. Foresti, J. E. Clark, C. J. Green, and R. Motterlini, "Thiol compounds interact with nitric oxide in regulating heme oxygenase-1 induction in endothelial cells. Involvement of superoxide and peroxynitrite anions," *The Journal of Biological Chemistry*, vol. 272, no. 29, pp. 18411–18417, 1997.

[37] I. M. Goldstein, P. Ostwald, and S. Roth, "Nitric oxide: a review of its role in retinal function and disease," *Vision Research*, vol. 36, no. 18, pp. 2979–2994, 1996.

[38] N. Toda and M. Nakanishi-Toda, "Nitric oxide: ocular blood flow, glaucoma, and diabetic retinopathy," *Progress in Retinal and Eye Research*, vol. 26, no. 3, pp. 205–238, 2007.

[39] G. A. Garcia, P. Ngai, S. Mosaed, and K. Y. Lin, "Critical evaluation of latanoprostene bunod in the treatment of glaucoma," *Clinical Ophthalmology*, vol. 10, pp. 2035–2050, 2016.

[40] R. Foresti and R. Motterlini, "The heme oxygenase pathway and its interaction with nitric oxide in the control of cellular homeostasis," *Free Radical Research*, vol. 31, no. 6, pp. 459–475, 1999.

[41] K. S. Ramos, H. Lin, and J. J. McGrath, "Modulation of cyclic guanosine monophosphate levels in cultured aortic smooth muscle cells by carbon monoxide," *Biochemical Pharmacology*, vol. 38, no. 8, pp. 1368–1370, 1989.

[42] C. L. Hartsfield, J. Alam, J. L. Cook, and A. M. Choi, "Regulation of heme oxygenase-1 gene expression in vascular smooth muscle cells by nitric oxide," *The American Journal of Physiology*, vol. 273, no. 5, Part 1, pp. L980–L988, 1997.

[43] P. K. Datta and E. A. Lianos, "Nitric oxide induces heme oxygenase-1 gene expression in mesangial cells," *Kidney International*, vol. 55, no. 5, pp. 1734–1739, 1999.

[44] K. Chen and M. D. Maines, "Nitric oxide induces heme oxygenase-1 via mitogen-activated protein kinases ERK and p38," *Cellular and Molecular Biology*, vol. 46, no. 3, pp. 609–617, 2000.

[45] R. Foresti, C. Bucolo, C. M. Platania, F. Drago, J. L. Dubois-Rande, and R. Motterlini, "Nrf2 activators modulate oxidative stress responses and bioenergetic profiles of human retinal epithelial cells cultured in normal or high glucose conditions," *Pharmacological Research*, vol. 99, pp. 296–307, 2015.

[46] T. G. Davies, W. E. Wixted, J. E. Coyle et al., "Monoacidic inhibitors of the Kelch-like ECH-associated protein 1: nuclear factor erythroid 2-related factor 2 (Keap1:Nrf2) protein-protein interaction with high cell potency identified by fragment-based discovery," *Journal of Medicinal Chemistry*, vol. 59, no. 8, pp. 3991–4006, 2016.

[47] C. Huerta, X. Jiang, I. Trevino et al., "Characterization of novel small-molecule Nrf2 activators: structural and biochemical validation of stereospecific Keap1 binding," *Biochimica et Biophysica Acta (BBA) - General Subjects*, vol. 1860, no. 11, Part A, pp. 2537–2552, 2016.

[48] J. Li, R. Abel, K. Zhu, Y. Cao, S. Zhao, and R. A. Friesner, "The VSGB 2.0 model: a next generation energy model for high resolution protein structure modeling," *Proteins*, vol. 79, no. 10, pp. 2794–2812, 2011.

[49] T. Ogura, K. I. Tong, K. Mio et al., "Keap1 is a forked-stem dimer structure with two large spheres enclosing the intervening, double glycine repeat, and c-terminal domains," *Proceedings of the National Academy of Sciences of the United States of America*, vol. 107, no. 7, pp. 2842–2847, 2010.

[50] K. Zhu, K. W. Bonelli, J. R. Greenwood et al., "Docking covalent inhibitors: a parameter free approach to pose prediction

and scoring," *Journal of Chemical Information and Modeling*, vol. 54, no. 7, pp. 1932–1940, 2014.

[51] P. Canning, F. J. Sorrell, and A. N. Bullock, "Structural basis of keap1 interactions with Nrf2," *Free Radical Biology and Medicine*, vol. 88, pp. 101–107, 2015.

[52] T. Matsuura, K. Takayama, H. Kaneko et al., "Nutritional supplementation inhibits the increase in serum malondialdehyde in patients with wet age-related macular degeneration," *Oxidative Medicine and Cellular Longevity*, vol. 2017, Article ID 9548767, 9 pages, 2017.

[53] C. Li, X. Miao, F. S. Li et al., "Oxidative stress-related mechanisms and antioxidant therapy in diabetic retinopathy," *Oxidative Medicine and Cellular Longevity*, vol. 2017, Article ID 9702820, 15 pages, 2017.

[54] V. Pittala, L. Vanella, L. Salerno et al., "Novel caffeic acid phenethyl ester (CAPE) analogues as inducers of heme oxygenase-1," *Current Pharmaceutical Design*, vol. 23, 2017.

Hindawi
Oxidative Medicine and Cellular Longevity
Volume 2017, Article ID 9281519, 17 pages
https://doi.org/10.1155/2017/9281519

Research Article

Mitochondria-Targeted Antioxidant SkQ1 Prevents Anesthesia-Induced Dry Eye Syndrome

Evgeni Yu. Zernii,[1] Olga S. Gancharova,[1] Viktoriia E. Baksheeva,[1] Marina O. Golovastova,[1] Ekaterina I. Kabanova,[1,2] Marina S. Savchenko,[1] Veronika V. Tiulina,[1,2] Larisa F. Sotnikova,[2] Andrey A. Zamyatnin Jr.,[1,3] Pavel P. Philippov,[1] and Ivan I. Senin[1]

[1]*Department of Cell Signaling, Belozersky Institute of Physico-Chemical Biology, Lomonosov Moscow State University, Moscow 119992, Russia*
[2]*Department of Biology and Pathology of Domestic, Laboratory and Exotic Animals, Skryabin Moscow State Academy of Veterinary Medicine and Biotechnology, Moscow 109472, Russia*
[3]*Institute of Molecular Medicine, Sechenov First Moscow State Medical University, Moscow 119991, Russia*

Correspondence should be addressed to Evgeni Yu. Zernii; zerni@belozersky.msu.ru and Ivan I. Senin; senin@belozersky.msu.ru

Received 29 May 2017; Accepted 14 August 2017; Published 12 October 2017

Academic Editor: Deborah A. Ferrington

Dry eye syndrome (DES) is an age-related condition increasingly detected in younger people of risk groups, including patients who underwent ocular surgery or long-term general anesthesia. Being a multifactorial disease, it is characterized by oxidative stress in the cornea and commonly complicated by ocular surface inflammation. Polyetiologic DES is responsive to SkQ1, a mitochondria-targeted antioxidant suppressing age-related changes in the ocular tissues. Here, we demonstrate safety and efficacy of topical administration of SkQ1 at a dosage of 7.5 μM for the prevention of general anesthesia-induced DES in rabbits. The protective action of SkQ1 improves clinical state of the ocular surface by inhibiting apoptotic and prenecrotic changes in the corneal epithelium. The underlying mechanism involves the suppression of the oxidative stress supported by the stimulation of intrinsic antioxidant activity and the activity of antioxidant enzymes, foremost glutathione peroxidase and glutathione reductase, in the cornea. Furthermore, SkQ1 increases antioxidant activity and stability of the tear film and produces anti-inflammatory effect exhibited as downregulation of TNF-α and IL-6 and pronounced upregulation of IL-10 in tears. Our data suggest novel features of SkQ1 and point to its feasibility in patients with DES and individuals at risk for the disease including those subjected to general anesthesia.

1. Introduction

Dry eye syndrome (DES) is a multifactorial ocular pathology characterized by corneal epithelium lesions, inflammation of ocular surface, and symptoms of discomfort including irritation, itching, and burning eyes [1, 2]. According to the epidemiological studies, DES affects more than 300 million people worldwide and represents the major reason for seeking eye care in developed countries [3]. Ageing, prolonged eye strain, environmental factors, medication intake, and refractive surgery are the major contributors to DES development [4]. General anesthesia is another risk factor for DES, which is becoming more prominent with wider use of surgical interventions in modern medicine [5, 6].

DES is commonly associated with reduced tear production and/or alterations in the tear composition, resulting in the loss of protective and nourishing qualities of tears [1]. The integrity of the outermost layers of the ocular surface is highly dependent on hydration and lubrication, provided by the tear film, as well as on the tear cytokines and growth factors, which promote wound healing and containment of inflammatory responses in the corneal epithelium and stroma. Consistently, current treatment of DES involves usage of lubricating eye drops and ointments or, in more

severe cases, anti-inflammatory medication [7]. Unfortunately, therapeutic strategies relying on the moisturization and lubrication of eye surface only provide temporary relief from DES symptoms and have no effect on the pathogenic processes underlying the disease. Treatment with anti-inflammatory drugs, such as steroids, cyclosporine A, and tetracycline, significantly improves clinical state of DES patients. However, prolonged use of corticosteroid eye drops may cause complications, namely, elevated intraocular pressure and cataract, which place restrictions on the duration of such treatment. Cyclosporine instillations cause burning eye sensation, which is a major factor limiting its employment in DES. Antibiotics, such as tetracycline and azithromycin, are applied successfully for the treatment of the disease, but it is strongly recommended to avoid using them at high doses because they are known to cause a number of side effects [8]. Lately, therapeutic application of proteins and peptides has been suggested as a prospective approach to the treatment of DES-associated corneal defects. Yet, such medications are generally based on cytokines, growth factors, hormones, and other naturally occurring tear components and, as such, could produce multifaceted and often contradictory effects on the corneal homeostasis. In addition, the majority of protein-based medications are not yet approved for clinical use [9]. All things considered, the demand for novel approaches to treating DES remains a highly relevant problem in current ophthalmology.

Growing evidence indicates that oxidative stress plays an important role in the pathogenesis of DES [10]. Normally, the tear film provides effective antioxidant protection for the ocular surface. It is enriched in both low molecular weight antioxidants (glutathione, ascorbic acid, and others) and enzymes involved in the replenishment of glutathione pool and first-hand scavenging of reactive oxygen species (ROS) (glutathione reductase, glutathione peroxidase, superoxide dismutase, etc.) [11, 12]. In DES, acute elevation in ROS levels affects corneal epithelial cells directly, by causing irreversible oxidative modifications of nuclear acids, lipids, and proteins, and indirectly, via the increased expression of proinflammatory cytokines. Thus, oxidative stress is known to induce and prolong local inflammatory responses leading to corneal injury [13]. With this in mind, antioxidant preparations to compensate for the loss of intrinsic antioxidant activity might be regarded as a feasible approach to the treatment of DES.

To date, a promising outlook on applying antioxidant therapy for the treatment of DES was demonstrated in experimental and clinical research. Thus, it has been shown that certain antioxidants can suppress inflammation of corneal epithelium and improve lacrimation [14–19]. The positive effect of this therapy could potentially be explained by its ability to balance redox status of tears and corneal epithelium. However, the most potent antioxidants are expected to be those targeting ROS directly in their intracellular sources such as mitochondria [20]. Indeed, intramitochondrial oxidative stress is associated with processes, governing cell survival, such as mitochondrial plasticity, apoptosis, and autophagy [21, 22]. Since the mitochondria are impenetrable to conventional antioxidants, the latter have low effectiveness against ROS formation in these organelles. Thus, a necessity for mitochondria-targeted antioxidants emerged. In the last 15 years, several antioxidants of this class were synthesized, including SkQ1, MitoQ, and SS31 [23–25]. These molecules are able to bypass plasma membrane and outer mitochondrial membrane and accumulate in the mitochondria, thereby displaying exceptional antioxidant activity even in nanomolar concentrations [20, 26]. As a result, they massively outperform all the conventional antioxidants in terms of specificity and activity levels. The employment of this new class of antioxidants represents an attractive pharmacological approach to the therapy of pathologies associated with oxidative stress and peroxidation of proteins and lipids of the inner membrane of mitochondria [20, 26].

Recent studies have demonstrated that administration of mitochondria-targeted antioxidant SkQ1 improves the tear film stability and regeneration of corneal epithelium in polyetiological DES [27, 28]. Furthermore, SkQ1 was found to reduce age-related alterations in lacrimal gland in animals [29]. However, detailed effects of SkQ1 on corneal state and morphology as well as the biochemical mechanisms underlying therapeutic effect of the antioxidant in DES remain scarce. These questions could be addressed using animal models of the disease such as recently characterized rabbit model of anesthesia-induced DES. Indeed, the decline in tear production and tear film stability under general anesthesia leads to erosive processes involving all layers of corneal epithelium, which are highly reminiscent of DES-associated corneal lesions [5]. Furthermore, under these conditions, significant alterations in biochemical and antioxidant properties of tears are observed, similar to those in DES patients [6, 10]. All these features make the rabbit model of anesthesia-induced DES highly convenient for investigating therapeutic strategies for the disease, including antioxidant treatment using SkQ1.

In this work, we employed the experimental model of anesthesia-induced DES to investigate the effect of mitochondria-targeted antioxidant SkQ1 on clinical status, morphology, and biochemical properties of the cornea as well as on the secretion, stability, and protective qualities of the precorneal tear film. It was demonstrated for the first time that the application of SkQ1 results in a prominent improvement of clinical state of the ocular surface by inhibiting apoptotic and necrotic changes in the corneal epithelium. Unexpectedly, this effect was produced not only via suppressing oxidative stress in the cornea but also by stimulating the intrinsic antioxidant defense of this tissue, accelerating the recovery of redox status and integrity of the tear film and dampening the local proinflammatory response. Our data suggest novel mechanisms of SkQ1 action and point to its feasibility in patients with DES and individuals at high risk for the disease including those subjected to general anesthesia.

2. Material and Methods

2.1. Materials. Anesthetic preparation containing 50 mg/ml tiletamine and 50 mg/ml zolazepam was purchased from Virbac (France). Xylazine hydrochloride was bought from

Bioveta (Czech Republic). Fluorescein sodium solution was from Novartis (Switzerland). Ultragrade Tris was purchased from Amresco (USA). Molecular biology grade phosphate buffer saline (PBS) was bought from Gibco. Hemoglobin, luminol, hydrogen peroxide solution, and Trolox (6-hydroxy-2,5,7,8-tetramethylchroman-2-carboxylic acid) were from Sigma-Aldrich (USA). Other chemicals used in this study were from Sigma-Aldrich, Amresco, or Serva (Germany) and were at least of reagent grade. All buffers and other solutions were prepared using ultrapure water. The Schirmer test tear strips were from Contacare Ophthalmics & Diagnostics (India). SkQ1 (10-(6′-plastoquinonyl)-decyltriphenylphosphonium) was synthesized and provided by the Institute of Mitoengineering of Moscow State University (Moscow, Russia).

2.2. Experimental Animals and Ethics Statement. The study involved a total of 182 healthy pigmented rabbits (6 months old, weight of 2.3 to 3 kg) purchased from a certified farm (Krolinfo, Russian Federation). The rabbits were housed at a 12 h light-dark cycle at a temperature of 22–25°C and humidity of 55–60% with free access to food and water. The animals' treatment was performed according to the 8th edition "Guide for the Care and Use of Laboratory Animals" of the National Research Council and "Statement for the Use of Animals in Ophthalmic and Visual Research" of The Association for Research in Vision and Ophthalmology (ARVO). The protocol was approved by the Belozersky Institute of Physico-chemical Biology Animal Care and Use Committee (Protocol number 1/2016).

The experiments were performed using a single-blind method. The rabbits were divided into 29 (22 experimental and 7 control) groups of 6–8 animals (see supplementary Table S1 available online at https://doi.org/10.1155/2017/9281519) and treated as described in Results. To assess safety of SkQ1 administration in a form of eye drops, the animals were medicated by conjunctival instillations of 50 μl of either vehicle solution (7 mM NaH_2PO_4, 2.6 mM $Na_2HPO_4 \cdot 12H_2O$, containing 150 mM NaCl, 0.0001% benzalkonium chloride) or the same solution containing 0.25, 2.5, 7.5, or 25 μM SkQ1 (SkQ1 eye drops) in each eye 3 times a day for 7–30 days. To induce general anesthesia, the animals were placed in prone position in a restraining device and subjected to intramuscular injection of anesthetic preparation containing 50 mg/ml tiletamine and 50 mg/ml zolazepam. The injections were repeated pro re nata to achieve continuous narcotic sleep of the required duration (see supplementary Table S1). Antioxidant premedication was performed as follows. On the day before anesthesia, the animals received conjunctival instillations of either vehicle solution or the same solution containing 0.25 μM, 2.5 μM, or 7.5 μM SkQ1, 1 drop 3 times a day. On the next day, an additional instillation of the vehicle/total solution was carried out, and the animals were exposed to general anesthesia. For the antioxidant therapy, the animals were firstly exposed to general anesthesia and then they received conjunctival instillations of the vehicle solution or the same solution containing 0.25 μM, 2.5 μM, or 7.5 μM SkQ1, 1 drop 3 times a day, for 30 days, starting from the moment of recovery from the narcosis. In the course of all experiments, the animals were kept under normal conditions described above. After the characterization of corneal state and/or tear collection, the animals were rehabilitated for 3 days and returned to the farm. For biochemical and histological studies of the cornea, the rabbits were humanely euthanized by introduction into general anesthesia and subsequent intracardiac injection of the 1 ml of 20 mg/ml xylazine hydrochloride. Enucleating of the eyeballs and corneal excision were performed postmortem.

2.3. Clinical Examination of the Cornea. The development of corneal injury was monitored by fluorescein staining of the ocular surface [30]. Briefly, 2 μl of 1% sodium fluorescein was instilled under the lower eyelid of the animal and distributed over the cornea by 2-3 movements imitating eye blinking. The corneal status was then examined under the slit-lamp microscope with or without cobalt blue filter. The registered corneal injuries were assigned with clinical scores (CS) of 0–4 depending on the size of the affected corneal surface (fluorescein rating scale): no fluorescein staining (CS = 0), staining of 0–12.5% of the corneal surface (CS = 1), staining of 12.5–25% of the corneal surface (CS = 2), staining of 25–50% of the corneal surface (CS = 3), and staining of >50% of the corneal surface (CS = 4). Mean clinical scores (MCS) were derived by adding the clinical scores for all eyes of the animals in a group and dividing by the number of eyes ± standard deviation (SD). Incidence of DES was determined as percent of eyes with diagnosed corneal injury regardless of its score.

2.4. Histological Analysis. The animals were sacrificed after fluorescein staining of the cornea given that the fluorescein exposure does not impact tissue morphology [31, 32]. The eyeballs were enucleated immediately postmortem and fixed in 10% neutral buffered formalin in phosphate buffer (pH 7.4) for 24 hours at room temperature or in Carnoy's solution (60% ethanol, 30% chloroform, and 10% glacial acetic acid) for 3 hours at room temperature. The corneas and irises were trimmed out of the fixed eyeballs along the corneal limbus, dehydrated by incubation in absolute isopropanol for 5 h and embedded in Histomix paraffin medium. Ten four-micron thick nasotemporal cross-sections of the cornea with iris were prepared and mounted on glass slides. The sections were then deparaffinized (xylene, 5 minutes, two times), placed to absolute isopropanol (5 minutes, two times), hydrated, and stained with Carazzi's hematoxylin and 0.5% eosin Y in water or with periodic acid and Schiff (PAS) reagent [33]. Stained sections were dehydrated by 96% ethanol and xylene, cleared in BioClear tissue clearing agent, mounted into BioMount synthetic medium, and examined using an Axio Scope.A1 microscope (Carl Zeiss, Germany). Lesions in the cornea were assigned with severity scores of 0–5, representing unremarkable, slight, mild, moderate, marked, and severe, respectively. Mean severity scores (MSS) were derived by adding the severity scores for all animals (eyes) in each treated group and by dividing by the number of animals (eyes) in the group [34]. Incidence of the lesions was determined as a percent of eyes with diagnosed lesion regardless of its score. Microphotographs were

obtained by an AxioCam MRc 5 megapixel color camera (Carl Zeiss, Germany) and processed using AxioVision v.3.0 (Carl Zeiss, Germany) and Photoshop CS3 software (Adobe Systems, USA). For the safety study, the lens and optic nerve were histologically processed and microscopically examined as described above. The retina was analyzed as described previously [35].

2.5. Schirmer's Test. Tear secretion was measured by means of standardized the Schirmer test [36]. Briefly, gauged Schirmer's test paper strips were placed under the lower eyelid and removed after 5 minutes of soaking, and the length of the moistened paper (in mm) was recorded. The procedure was repeated at least three times, and the average values were considered.

2.6. BUT Test. Stability of the tear film was examined using standard tear film breakup time (BUT) test [37]. The instillations of fluorescein into the rabbit eye were performed exactly as for clinical examination of the cornea (see above). After each instillation, the time of appearance of the first dry spot in the central cornea seen under a slit-lamp microscope was measured.

2.7. Corneal and Tear Samples. To obtain corneal homogenates, the full-size rabbit corneas were excised, placed into 400 μl of PBS, and frozen at −70°C. After thawing, the homogenate was sonicated for 10 min on ice. Corneal extracts for biochemical evaluations were obtained by centrifugation of the homogenates (15000g, 10 min) at +4°C. The tear samples were collected using gauged Schirmer's test strips. To this end, the length of the moistened strip was allowed to reach exactly 20 mm and its 15 mm fragments were cut off and extracted with 150 μl of PBS.

2.8. Malondialdehyde Assay. MDA concentration was measured in corneal extracts using commercially available kits (Sigma-Aldrich, USA) following the manufacturer's instructions. Intensity of colorimetric reaction was determined using MR-96A Microplate Reader (Mindray, China). The data were analyzed using SigmaPlot 11 (SYSTAT Software).

2.9. Total Protein Concentration. Protein concentration in corneal extracts and tear samples was measured by the bicinchoninic acid (BCA) method using a BCA protein assay kit (Thermo Fisher Scientific, USA) in accordance with the manufacturer's instructions.

2.10. Total Antioxidant Activity. The corneal and tear samples were analyzed using hemoglobin-H_2O_2-luminol model system [38]. Standard solutions, containing 1–8 μM Trolox in PBS, were used as a reference. Thirty microliters of standard solution or tear samples diluted 1 : 4 by PBS was added to 0.44 ml of reaction mixture, containing 0.01 mM luminol and 0.5 mM hemoglobin in PBS. Luminol oxidation reaction was stimulated by the addition of hydrogen peroxide to reach 6 μM. Chemiluminescence of the sample was registered each 1 second for 10 minutes using Glomax-Multi Detection System luminometer (Promega, USA). The data were analyzed using SigmaPlot 11 (SYSTAT Software, USA), and total antioxidant activity (AOA) was expressed in Trolox equivalent.

2.11. Antioxidant Enzyme Activity. The activity of tear enzymes involved in antioxidant protection (superoxide dismutase (SOD), glutathione peroxidase (GPx), glutathione reductase (GR), and glutathione-SH transferase (GST)) was evaluated in the corneal and tear samples, using commercially available kits (Sigma-Aldrich, USA) in accordance with the manufacturer's instructions. Intensity of colorimetric reactions was determined using MR-96A Microplate Reader (Mindray, China). The acquired data were analyzed using SigmaPlot 11 (SYSTAT Software). The activity of the enzymes in corneal extracts was normalized to 1 mg of the total protein.

2.12. Inflammatory Cytokine Content. The content of tumor necrosis factor alpha (TNF-α) and interleukins 4 (IL-4), 6 (IL-6), and 10 (IL-10) was examined in the tear samples using Rabbit ELISA kits (Cusabio Biotech, China) according to the protocols provided by the manufacturer. The colorimetric reaction was digitalized using MR-96A Microplate Reader (Mindray).

2.13. Statistics. The data were analyzed by the mean standard deviation method, using SigmaPlot 11 Software (SYSTAT Software). The bars in the figures represent standard deviation (SD). Mean scores, SD, and statistical significance were calculated using SigmaPlot 11 Software or BioStat 2009 version 5.8.3.0 software (AnalystSoft, USA). Statistical significance was assessed using paired t-test (for safety evaluations) or unpaired two-tailed t-test. The probability of 0.05 was considered significant.

3. Results

3.1. Safety of SkQ1 Eye Drop Administration. Since SkQ1 is a nonnatural antioxidant, we firstly studied whether repetitive conjunctival instillations of SkQ1 eye drops can induce ocular toxicity in rabbits. To this end, the animals were medicated with the solution containing 0.25, 2.5, 7.5, or 25 μM SkQ1 during one week and their eyes/eye tissues were examined visually (lids, lacrimal apparatus, and conjunctiva), ophthalmoscopically (cornea, anterior chamber, lens, iris, and vitreous humor), and histologically (cornea, lens, iris, retina, and optic nerve). It was found that administration of SkQ1 eye drops was generally well tolerated at a dosage of 0.25, 2.5, and 7.5 μM SkQ1. Instillations of 25 μM SkQ1 induced conjunctival redness in one animal. Thus, the dose of 0.25, 2.5, and 7.5 μM SkQ1 was considered safe for the further applications. Given that the main hallmark of DES is the altered tear secretion, we assessed this parameter in animals before and after the instillation of 0.25, 2.5, or 7.5 μM SkQ1 3 times a day for 1 month. The divergence of the results of the Schirmer test did not exceed 15% ($p > 0.05$) in all cases, indicating almost no effect of the drug on the tear secretion (Table 1).

3.2. Experimental Model of General Anesthesia-Induced DES for Trialing of SkQ1 Treatment. A rabbit model of

Table 1: Tear secretion in healthy rabbits medicated with SkQ1 eye drops.

SkQ1, μM	Length, mm*			
	Control		Medication	
	0 day	30 days	0 day	30 days
0.25	20.4 ± 0.92	22.11 ± 1.07	20.7 ± 1.18	23.2 ± 0.92 ($p = 0.112^{\#}$)
2.5	18.0 ± 1.4	17.0 ± 2.4	18.8 ± 0.9	21.4 ± 1.4 ($p = 0.175^{\#}$)
7.5	19.2 ± 0.4	18.4 ± 1.7	18.4 ± 2.1	19.1 ± 1.6 ($p = 0.700^{\#}$)

*Length of the moistened Schirmer's test paper strip. #Compared with the values measured prior to medication.

anesthesia-induced DES developed in our previous studies [6, 39] was selected for further trialing of the antioxidant therapy using SkQ1 eye drops. In order to characterize the basic parameters of the model, we determined the incidence of DES symptoms in rabbits depending on the duration of general anesthesia. To this end, the animals were exposed to general anesthesia for 0.5-6 h and their corneas were subjected to clinical and morphological examination immediately after the narcosis. The results of fluorescein test indicated anesthesia time-dependent accumulation of corneal epithelium injury in accordance with our previous findings [39]. Statistical analysis revealed that the incidence of the corneal damage rose with the duration of the narcotic sleep reaching 100% of animals after 5-6 h of the anesthesia (Figure 1(a)). Similar observations were made upon histopathological examination of corneal samples obtained from animals exposed to 1 h, 3 h, and 6 h of anesthesia (Figure 1(b), Table 2), while in control rabbits, the cornea displayed normal structure (Figure 1(b), A, E), and in 1 h anesthetized animals, it exhibited a loss of superficial epithelial layer as well as coagulation, desquamation, and shedding of the squamous cells (Figure 1(b), B, F). Exposure to 3 h anesthesia resulted in focally more extensive corneal injuries such as degenerative and necrobiotic alterations in outer wing cells denuded after superficial cell loss (Figure 1(b), C, G). These multifocal epithelial defects included cytoplasmic changes (swelling and lightening) and nuclear changes (enlargement and lightening) (Figure 1(b), G, arrows), that corresponded to typical hydropic degeneration [40]. In some cases, the injured wing cells were separated from the inner layers with only one layer of degenerating basal cells remaining at the damaged locus (Figure 1(b), H, asterisk). After 6 h of anesthesia, the corneal injuries became much more severe and diffused (Figure 1(b), D). Hydropic cell degeneration was more pronounced and detected in both wing and basal cells (Figure 1(b), I). Furthermore, progressive cell loss was accompanied by signs of apoptosis that include cell shrinkage, chromatin condensation, nuclear changes (pyknosis or karyorrhexis), dense staining, and the formation of apoptotic bodies (Figure 1(b), I-J, arrows). In addition, separated cells at different morphological stages of necrotic (Figure 1(b), L, asterisk) or apoptotic (Figure 1(b), M, arrows) cell death were found. Full-thickness epithelial damage resulted in the disruption of basal cell adhesion to the basal lamina, total loss of epithelial layer, and denudation of underlying stroma (Figure 1(b), N). The most pronounced areas of denudation in 6 h treated animals were more than 1 mm in diameter (Figure 1(b), D). Overall, by the end of 3–6 h general anesthesia, the full-scaled pathomorphological picture of DES was developed in the majority of the animals. Considering that exposure to anesthesia of similar duration reduces tear secretion significantly [6], the condition developed after 6 h narcosis was recognized as a model of severe DES, which is feasible for the proper trialing of the proposed antioxidant therapy.

3.3. Efficacy, Dosage, and Administration Scheme for SkQ1 in Treatment of General Anesthesia-Induced DES. To assess the efficacy of SkQ1 eye drops for the treatment of anesthesia-induced DES, the experimental animals were treated according to the following alternative schemes. The animals were either premedicated using instillations of SkQ1 at a concentration of 0.25, 2.5, or 7.5 μM prior to induction of DES or medicated with the same dosage of the antioxidant starting immediately after narcosis and continuing during one month after the induction of the disease. In both cases, the clinical state of the cornea was examined by fluorescein test immediately after the narcosis and on the 1st, 3rd, 7th, 14th, and 30th days of the subsequent time period. In addition, some of the animals were withdrawn right after the anesthesia (for premedicated groups) or on the 14th day of the postanesthetic period (for treated groups) for histological and biochemical studies of the cornea. As it can be seen from Figure 2(a), SkQ1 premedication had a pronounced protective effect on the cornea that was enhanced with an increase of the drug dosage. Thus, 7.5 μM SkQ1 prevented pathological changes in the cornea after recovering from the narcosis and completely neutralized clinical signs of DES as early as the first day of the postanesthetic period. By contrast, the treatment by the antioxidant after the induction of DES was less effective and less dose-dependent, although a complete recovery of the corneal injuries was also accelerated becoming reduced to one week (Figure 2(b)). These observations are generally in accord with the results of histological examination of the corneas (Figure 2(c)). Thus, in contrast to the untreated animals (Figure 2(b), B-C), the animals premedicated with eye drops containing different concentrations of SkQ1 exhibited no foci of total destruction of the epithelium by the end of the anesthesia (Figure 2(c), D–I). Moreover, no prenecrotic and necrotic changes and no cells with enlarged and enlightened cytoplasm were found in such animals. The minor changes in this case included the presence of single apoptotic cells (Figure 2(c), C–F) and consequent reduction of corneal epithelium thickness in some areas (Figure 2(c)). The least decrease of the epithelium thickness was found following administration of 7.5 μM SkQ1

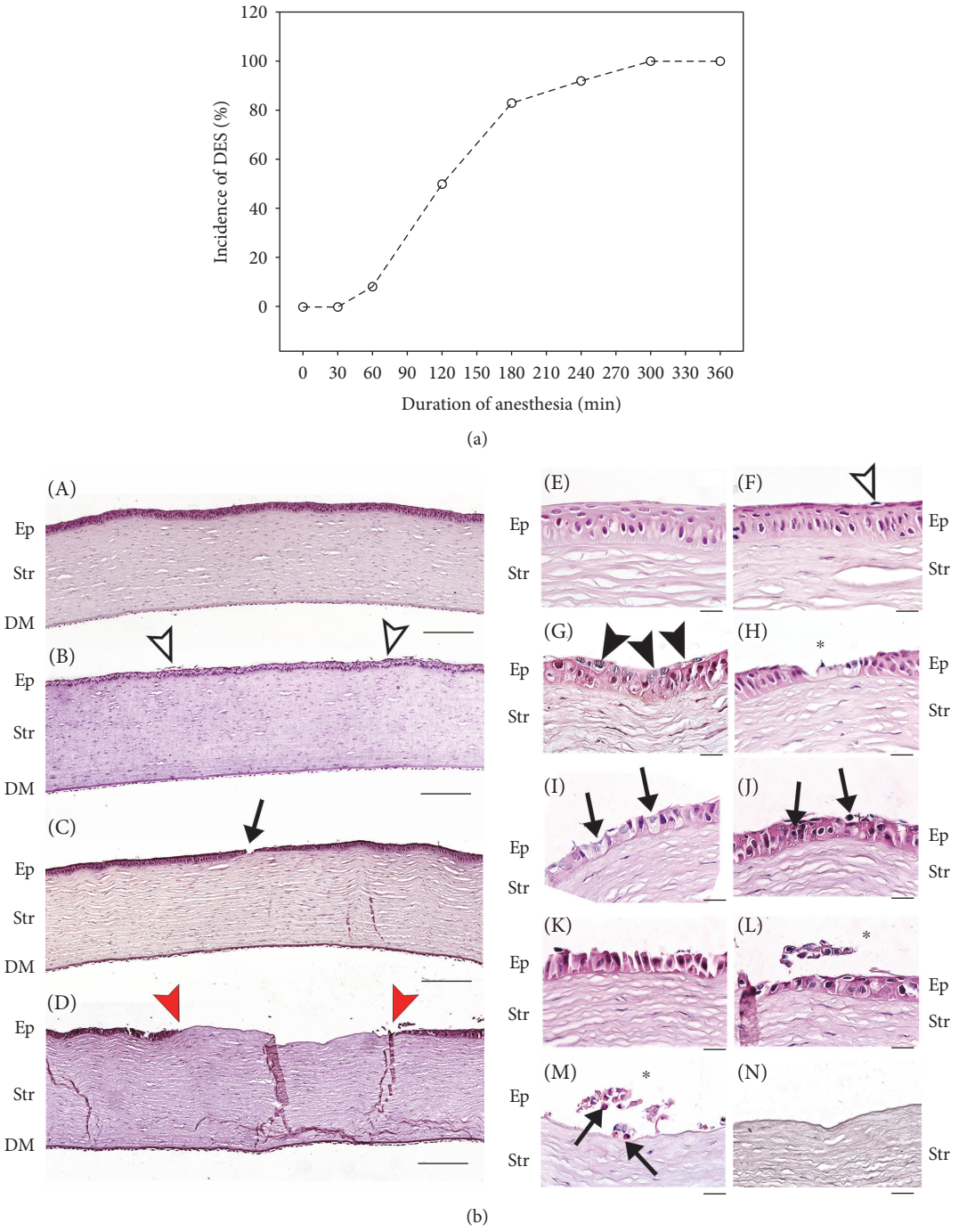

Figure 1: Clinical state and morphology of the cornea during general anesthesia. (a) Incidence of DES in the rabbits exposed to 1–6 h of general anesthesia calculated as a percent of eyes with fluorescein-stained corneal injury regardless of its score. (b) Representative microscopic images of hematoxylin and eosin staining of rabbit corneas from different experimental groups. Control animals: normal cornea (A, E). Animals after 1 h of general anesthesia: desquamation of superficial epithelial cells is indicated by white arrowhead (B, F). Animals after 3 h of general anesthesia: degeneration of epithelial cells is shown by black arrowheads (G), destruction of epithelial layer is indicated by an arrow (C), and the same locus is shown at higher magnification by an asterisk (H). Animals after 6 h of general anesthesia: prenecrotic (I) and apoptotic (J) changes are indicated by black arrows, desquamated cornea epithelial cells onto partially or fully thickness-denuded area are shown by asterisks (L-M), apoptotic degeneration of some cells is shown by arrows (M), and locus of total denudation is shown by arrowheads at lower (D) and higher (N) magnification (margins of cornea erosion are shown by red arrowheads). Ep: epithelium; Str: stroma; DM: Descemet's membrane and corneal endothelium. Magnification: ×100 (A–D) and ×1000 (E–N); scale bars: 200 μm (A–D) and 20 μm (E–N).

Table 2: Pathomorphological characteristics of the cornea in general anesthesia-induced DES.

Corneal compartment	Diagnosis	Parameter	Anesthesia time, h			
			Control	1	3	6
Epithelium	Superficial cell desquamation	Incidence, %	0	100	100	100
		MSS	0	2.3 ± 0.5*	3.6 ± 0.6*	4.3 ± 0.5*
	Deep layer cell loss (erosion)	Incidence, %	0	0	100	100
		MSS	0	0	2.0 ± 0.9	4.3 ± 0.6
	Denudation	Incidence, %	0	0	66	100
		MSS	0	0	2.0 ± 1.5*	4.0 ± 0.9*
	Cell degeneration	Incidence, %	0	0	100	100
		MSS	0	0	3.3 ± 0.6*	3.7 ± 0.5*
	Signs of apoptosis	Incidence, %	0	0	33	100
		MSS	0	0	0.6 ± 0.9	3.6 ± 0.5*
Stroma	Reepithelization	Incidence, %	0	0	0	0
		MSS	0	0	0	0
	Edema	Incidence, %	0	0	0	0
		MSS	0	0	0	0
	Inflammatory infiltration	Incidence, %	0	0	0	0
		MSS	0	0	0	0
	Neovascularization	Incidence, %	0	0	0	0
		MSS	0	0	0	0
Endothelium	Vacuolization	Incidence, %	0	0	0	0
		MSS	0	0	0	0
	Cell loss	Incidence, %	0	0	0	0
		MSS	0	0	0	0

Incidence and mean severity scores (MSS) were determined as described in Materials and Methods. *$p < 0.05$ compared with control.

(Figure 2(c), H-I). By contrast, in the animals medicated with the same dosage of SkQ1 after anesthesia, the morphology of the corneal epithelium returned to the normal state only at the fourteenth day of the postanesthetic period (Figure 2(d), K-L). It should be added that by that time the signs of active reepithelialization were absent, assuming that this process was already completed.

We concluded that SkQ1 possesses a positive effect on corneal state and that this effect is more pronounced when the drug is administrated prior to anesthesia-induced DES. Thus, SkQ1 more likely exhibits protective action on healthy corneal epithelium, rather than participate in the corneal wound healing. Since the most prominent protective effect was observed in the case of premedication using 7.5 μM SkQ1, this dosage and administration scheme was considered optimal for reproducing in subsequent experiments.

3.4. Oxidative and Antioxidant State of the Cornea in General Anesthesia-Induced DES with or without SkQ1 Premedication. The simple explanation of the revealed positive effect of SkQ1 premedication in anesthesia-induced DES was its direct antioxidant action on corneal epithelial cells. With that in mind, we compared oxidative stress and intrinsic antioxidant activity in the corneas of the control and SkQ1-premedicated animals. Without premedication, the concentration of malondialdehyde (MDA) in corneal homogenates increased noticeably with the duration of anesthesia reaching more than 10-fold excess by the 6th hour of the narcosis (Figure 3). By contrast, the antioxidant premedication using 7.5 μM SkQ1 attenuated the increase in the MDA concentration after 6 h anesthesia by 50%. This effect can be partially associated with an increase in the antioxidant protection in the cornea due to its amelioration by the drug action. Indeed, without antioxidant treatment, the animals with anesthesia-induced DES exhibited no noticeable changes in AOA, SOD activity, and glutathione-metabolizing enzymes (GR and GPx) in corneal extracts (Figures 3(b), 3(c), 3(d), and 3(e)). An exception was the growth of GST activity that may be related to the detoxification of the injected anesthetic (Figure 3(f)). By contrast, the animals premedicated with 7.5 μM SkQ1 demonstrated a significant increase in activities of GR and GPx, which were higher than the respective values registered both in the animals with untreated DES (Figures 3(d) and 3(e)). In the case of GPx, the effect was the most pronounced reaching a 5–10-fold excess of the baseline control value (Figure 3(e)). Finally, the increase in GST activity was attenuated in the cornea of SkQ1-treated animals (Figure 3(f)). Thus, the anesthesia-induced DES was associated with oxidative stress of the corneal cells without a compensatory increase in their own antioxidant protection. Under these conditions, SkQ1 possessed prominent

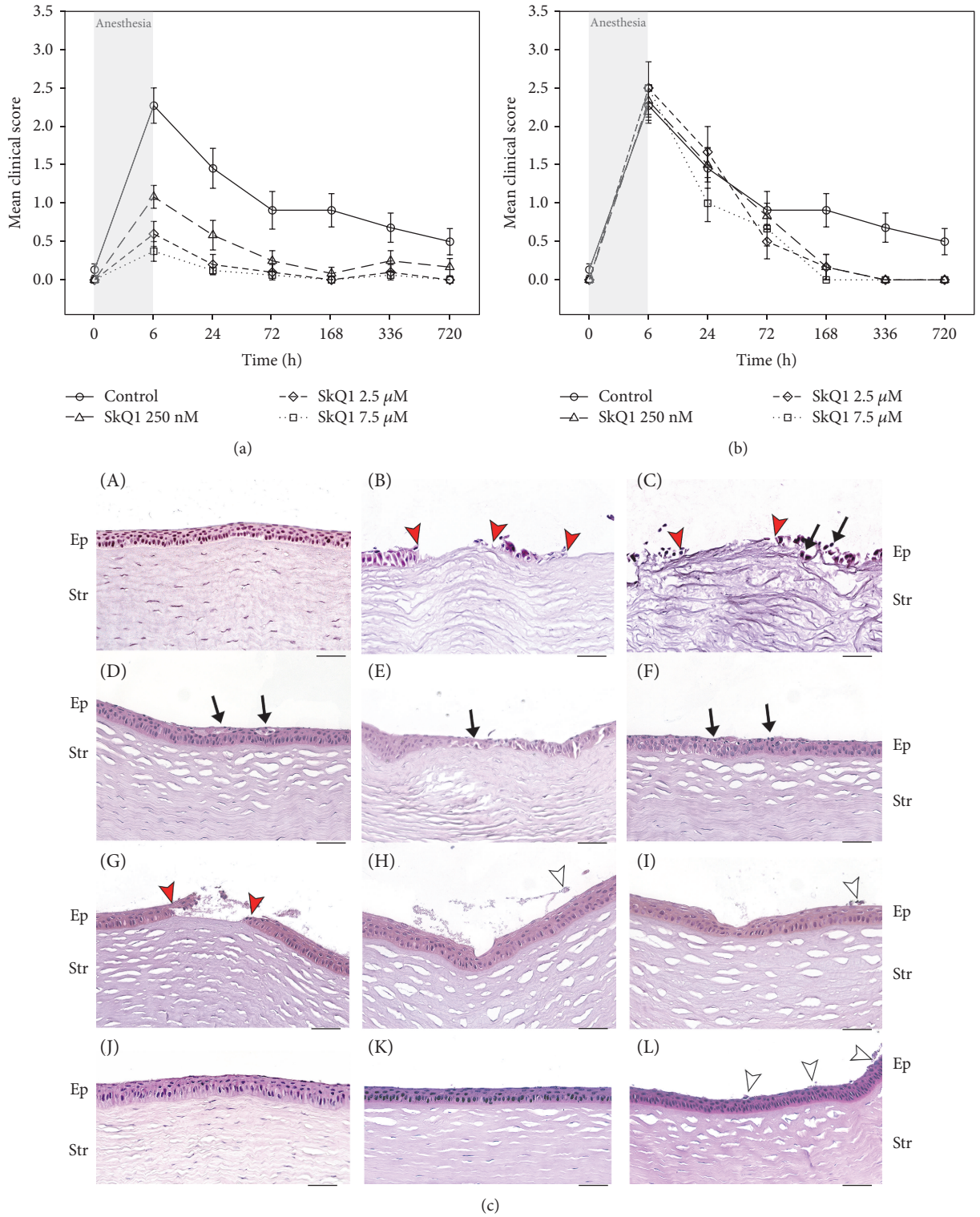

Figure 2: Clinical state and morphology of the cornea in general anesthesia-induced DES upon premedication or treatment with SkQ1. Corneal status in the rabbits with anesthesia-induced DES premedicated (a) or treated (b) with SkQ1 eye drops. $p < 0.05$ for all values measured in all premedication groups and in 7.5 μM SkQ1 treatment group compared with the values obtained for the control group. (c) Representative microscopic images of hematoxylin and eosin staining of rabbit corneas from different experimental groups. Control animals: normal cornea (A, J). Cornea immediately after 6 h general anesthesia: without premedication (B, C) and after premedication with 0.25 (D, E), 2.5 (F, G), or 7.5 μM (H, I) SkQ1. Cornea after 6 h of general anesthesia on the fourteenth day of treatment with 7.5 μM SkQ1 (K, L). Margins of cornea erosion are shown by red arrowheads; desquamation of superficial epithelial cells is indicated by white arrowheads; prenecrotic and apoptotic changes are indicated by black arrows. For abbreviations see Figure 1. Magnification: ×400; scale bar 50 μm.

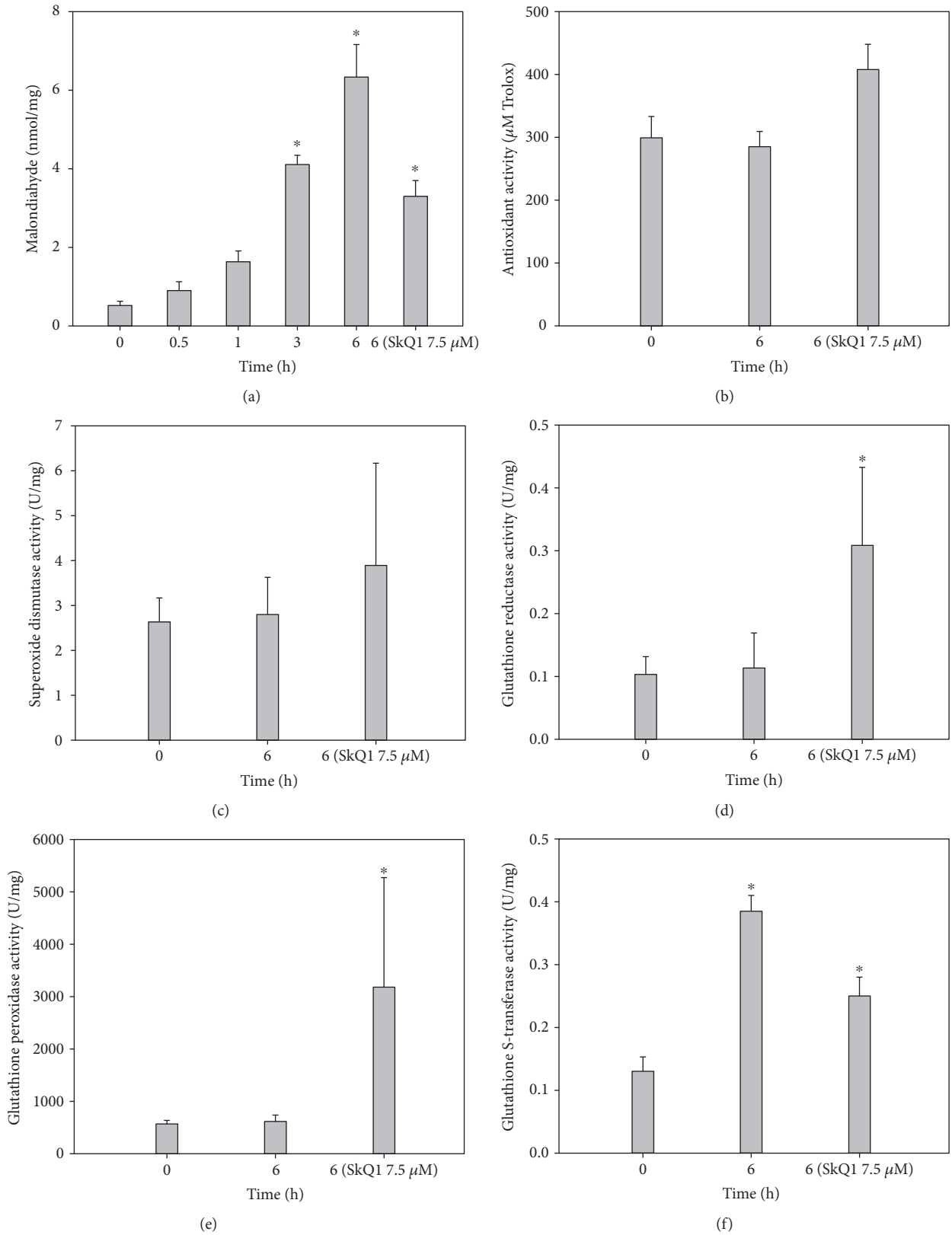

Figure 3: Oxidative stress and antioxidant activity in the cornea in general anesthesia-induced DES upon premedication with SkQ1. (a) Concentration of MDA in rabbit corneal homogenates after 1–6 h of general anesthesia with or without premedication using 7.5 μM SkQ1. (b)–(f) Total antioxidant activity (b) and activity of SOD (c), GR (d), GPx (e), and GST (f) in corneal extracts after 6 h of general anesthesia with or without premedication using 7.5 μM SkQ1. $^*p < 0.05$ compared with the values measured in control group before general anesthesia.

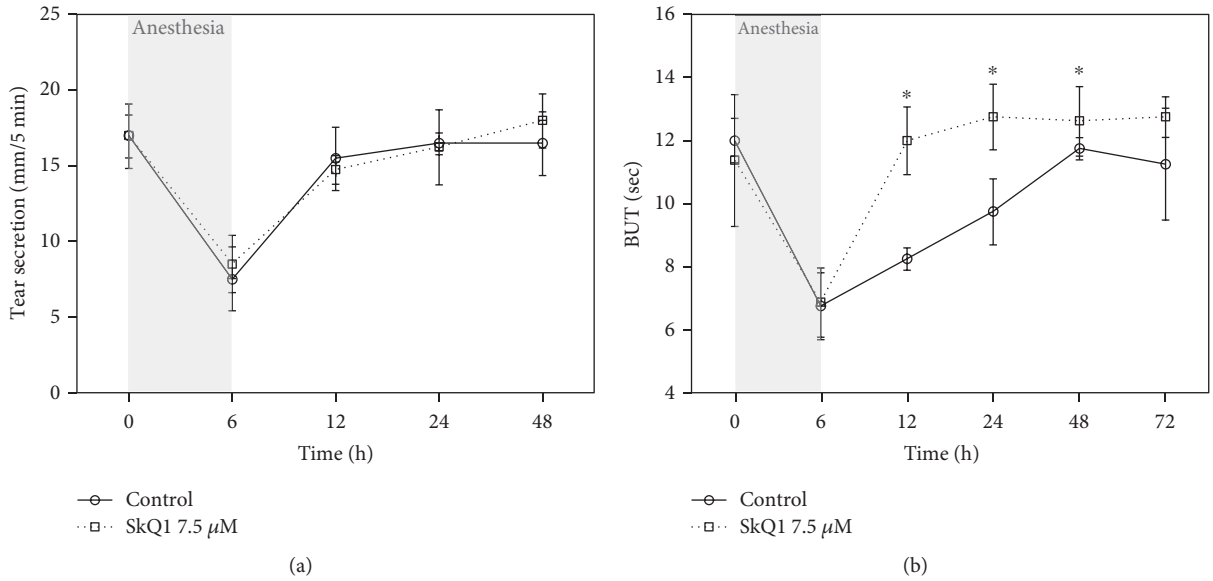

Figure 4: Secretion and stability of the tear film in general anesthesia-induced DES upon premedication with SkQ1. Results of standardized Schirmer's (a) and BUT (b) tests performed in the rabbits exposed to 6 h of general anesthesia with or without premedication using 7.5 μM SkQ1. $^{*}p < 0.05$ compared with the values measured in control group.

protective activity both by inhibiting oxidative stress in the cornea and upregulating its intrinsic antioxidant defense enzymes, foremost GPx and GR.

3.5. Tear Secretion and Stability in General Anesthesia-Induced DES with or without SkQ1 Premedication. In addition to the direct effect on the corneal cells, SkQ1 may positively affect tear-producing ocular tissues and improve tear quantity and/or quality thereby producing the revealed protective effect on the cornea. To test this suggestion, we further examined the effect of premedication using 7.5 μM SkQ1 on the tear secretion and stability in rabbits with anesthesia-induced DES by means of standardized Schirmer's and BUT tests, respectively. Exposure of the animals to general anesthesia for 6 h resulted in 2.3-fold reduction of their tear secretion, which returned to the normal values by 12 h of the postanesthetic period regardless of SkQ1 administration (Figure 4(a)). Meanwhile, the decrease in tear stability in the control animals recovered much slower (48 h), whereas the antioxidant premedication significantly accelerated the recovery (Figure 4(b)). Thus, SkQ1 had no effect on the tear secretion, but may alter tear composition thereby increasing stability and protective features of the tear film.

3.6. Antioxidant Activity of the Tear Fluid in General Anesthesia-Induced DES with or without SkQ1 Premedication. As the next step, we monitored the effect of SkQ1 on antioxidant properties of the tear in the animals with anesthesia-induced DES. Tear samples were collected from control and 7.5 μM SkQ1-premedicated rabbits prior to 6-hour general anesthesia, immediately after the recovery from narcosis or following 1 hour, 24 hours, 3 days, 1 week, or 2 weeks of the postanesthetic period. It was found that the development of the corneal injury in the control animals was associated with a pronounced decrease in AOA and the activity of antioxidant enzymes in their tear fluid. In such self-limited DES, these parameters restored only in 1-2 weeks after the narcosis (Figure 5). The premedication using SkQ1-containing eye drops had no effect on the total protein concentration in tears (data not shown), but it accelerated significantly the normalization of AOA and SOD activities (Figures 5(a) and 5(b)). Indeed, in the SkQ1-treated animals, these parameters returned to their baseline values as early as the first day of the post-anesthetic period. Thus, the revealed therapeutic action of SkQ1 in anesthesia-induced DES may include protection of the tear-producing tissues and associated improvement of the antioxidant activity of the tear film.

3.7. Inflammatory Cytokines of Tear Fluid in General Anesthesia-Induced DES with or without SkQ1 Premedication. It is widely regarded that DES pathogenesis involves inflammatory component [9, 39]. The oxidative stress of the cornea detected in our DES model can induce inflammatory responses of the ocular surface tissues [41] that may be sensitive to SkQ1 action. To test this assumption, we examined profiles of the common tear cytokines in the 6 h anesthetized rabbits with or without premedication using 7.5 μM SkQ1 (Figure 6). Approximately a 2-fold increase in proinflammatory cytokines was observed in the control animals with DES, namely, the fast growth of TNF-α concentration (within 6 hours) followed by the delayed growth in IL-6 (Figures 6(a) and 6(b)). These effects were associated with a prominent reduction in anti-inflammatory cytokines IL-4 and IL-10 (Figures 6(c) and 6(d)). Without treatment, TNF-α and IL-4 restored to their normal levels within 1 h and 1 day, respectively (Figures 6(a) and 6(b)). In contrast, premedication using 7.5 μM SkQ1 considerably suppressed the release of both

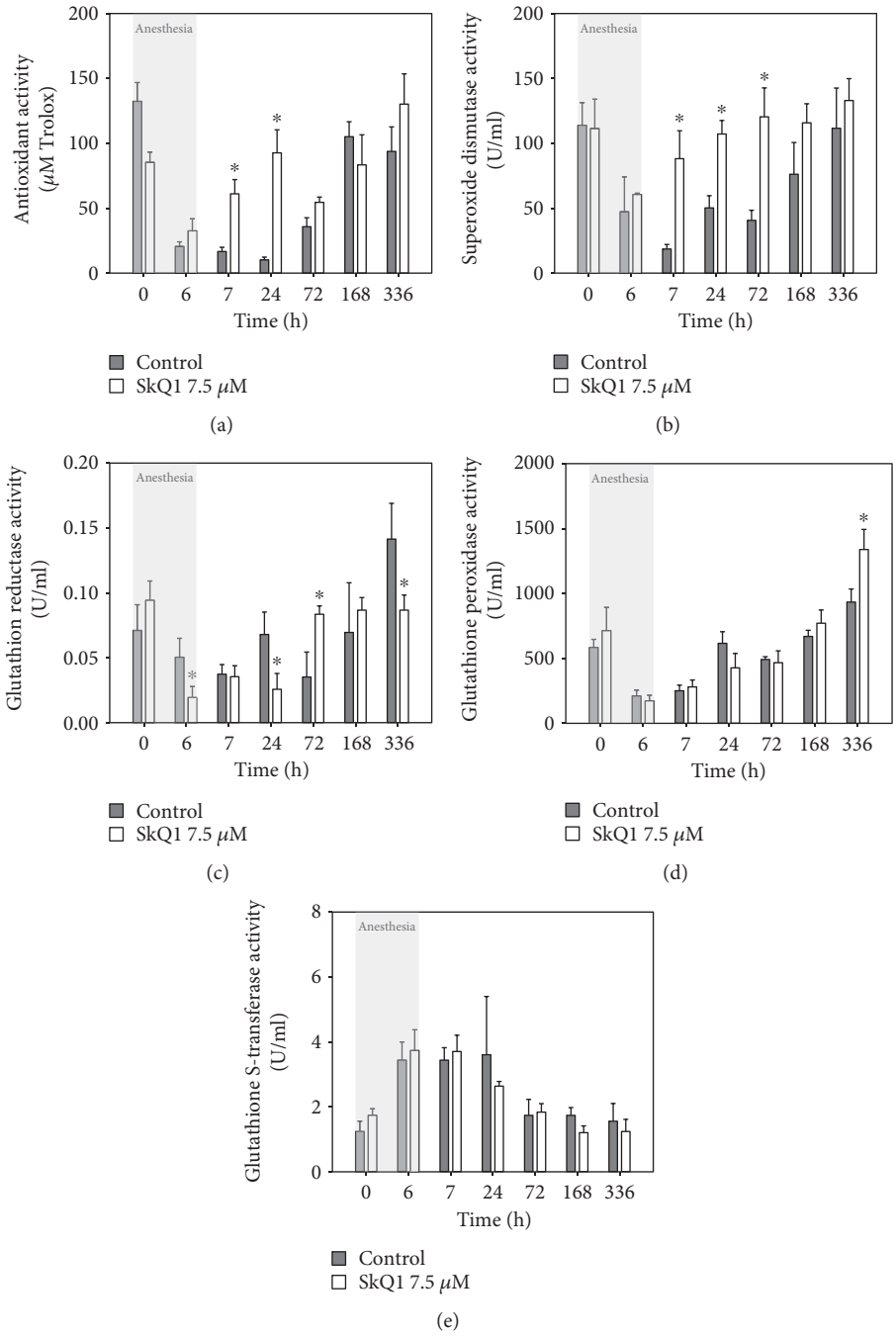

Figure 5: Antioxidant activity of the tear fluid in general anesthesia-induced DES upon premedication with SkQ1. Total antioxidant activity (a) and activity of SOD (b), GR (c), GPx (d), and GST (e) rabbit tear samples after 6 h of general anesthesia with or without premedication using 7.5 μM SkQ1. $^{*}p < 0.05$ compared with the values measured in control group.

proinflammatory cytokines and accelerated the recovery of IL-4. Interestingly, it produced a pronounced stimulatory effect on the secretion of IL-10, the concentration of which reached ~550% of the normal value within an hour after anesthesia (Figure 6(d)). Overall, the protective effect of SkQ1 may involve the inhibition of inflammatory responses of the ocular surface via suppression of the preceding oxidative stress and/or by specific overstimulation of secretion of anti-inflammatory cytokine IL-10.

4. Discussion

The goal of this study was to determine the safety, efficacy, and optimal dosage regimen of administration of mitochondria-targeted antioxidant SkQ1 for prevention and treatment of DES and to suggest cellular and biochemical mechanisms underlying therapeutic action of SkQ1. To this end, it was necessary to monitor alterations in morphological and biochemical properties of the cornea, as well as biochemical

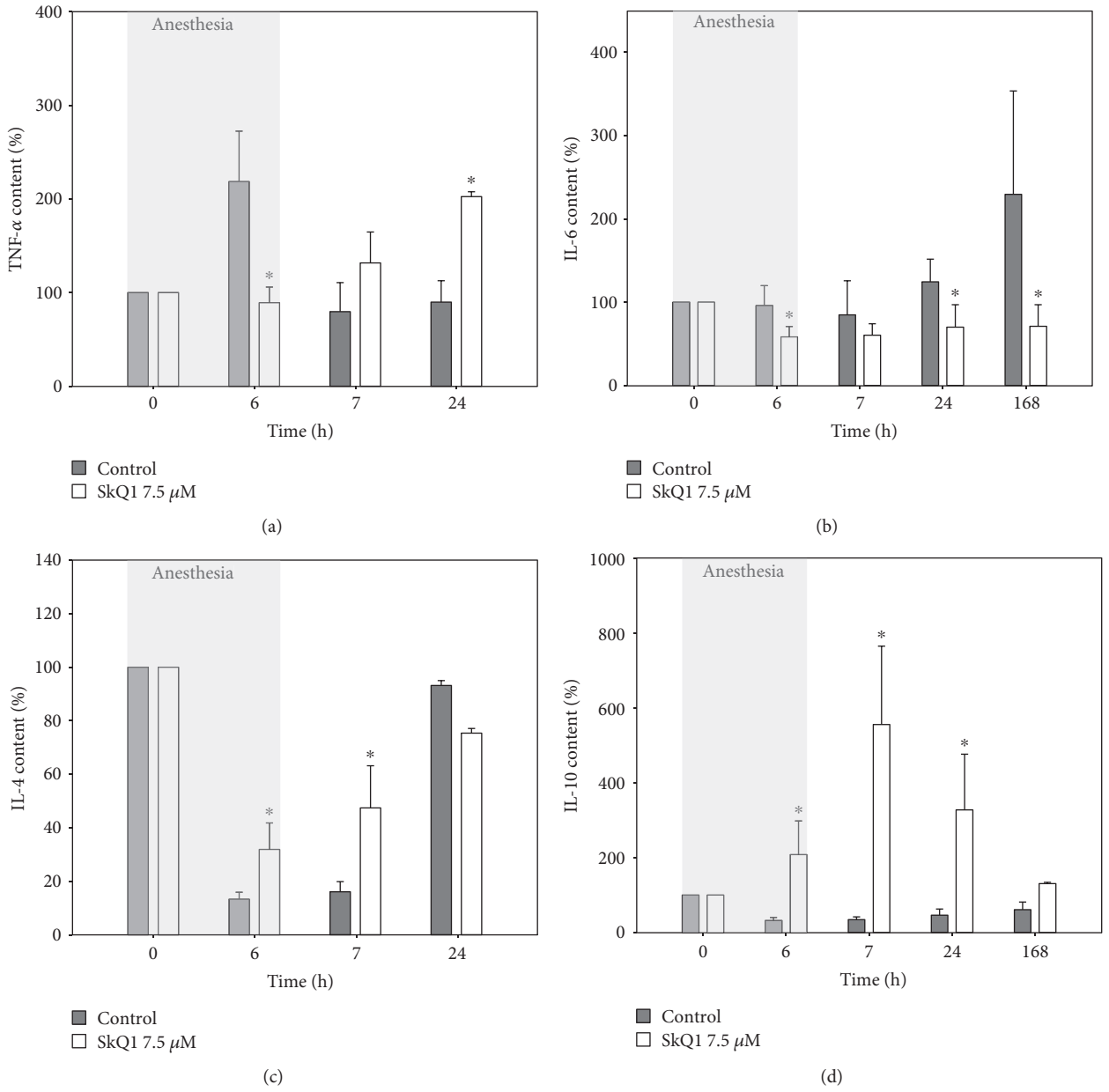

Figure 6: Inflammatory cytokines in the tear fluid in general anesthesia-induced DES upon premedication with SkQ1. Concentration of TNF-α (a), IL-6 (b), IL-4 (c), and IL-10 (d) rabbit tear samples after 6 h of general anesthesia with or without premedication using 7.5 μM SkQ1. $^{*}p < 0.05$ compared with the values measured in control group.

and biomechanical parameters of tears, under the course of the disease. However, performing these experiments in humans was hindered by limited availability of the patients for ophthalmological examination and by impossibility of obtaining the required tissue samples. Considering these limitations, we employed the rabbit model of the disease since these species share many features of ocular anatomy with humans including eyeball size, its internal structure, and optical system as well as biomechanical and biochemical features [42]. DES was simulated in rabbits by their exposure to general anesthesia [6, 39, 41]. Indeed, anesthetic injections are known to inhibit lacrimal gland innervations and suppress tear production [43]. These complications are often observed in humans during and after surgery, leading to manifestation of iatrogenic corneal lesions or so-called perioperative DES. Yet, the exposure of rabbits to general anesthesia resulted in the development of the majority of symptoms characteristic of common age-related DES, which makes such a model appropriate for testing general approaches to treatment of this disorder [5].

To optimize and characterize the selected model, we monitored time-dependent development of corneal epithelium injury on both clinical and histological levels. Fluorescein-stained point lesions became prominent as early as 1 h postinjection of the anesthetic, whereas after 5-6 h of general anesthesia the corneal injuries developed in all

animals. According to the histological study, they were caused generally by cell desquamation or degeneration, cell death (necrotic and apoptotic variants), and separation of the dying cells from the basement membrane. The injuries exhibited as marked attenuation or thinning of epithelium or its total loss (denudation) [34]. However, they did not extend into the stroma thereby representing corneal abrasion (erosion), but not corneal ulcer [44]. The signs of apoptotic and necrotic cell death were detected in middle and deep layers of corneal epithelium most commonly after 6 h of general anesthesia. By this time, the animals additionally exhibited alterations in biochemical properties of tears, in particular, decline of redox status and anti-inflammatory qualities of the tear film and loss of its stability. Thus, after 6 h of general anesthesia, the full-scale picture of DES, similar to the one found in patients [45], can be observed in experimental animals. These results provided the rationale for using this model in the treatment studies.

Like most age-related disorders, DES is associated with development of oxidative stress, which makes antioxidant therapy a favorable approach to its treatment. The feasibility of such strategy was demonstrated previously in both experimental models and clinical studies with a wide range of antioxidants, including alpha-lipoic acid, blueberry components, essential omega-3 fatty acids, L-carnitine, and selenium compounds [14–19]. However, despite their therapeutical efficiency, these chemicals have a common limitation, namely, their inability to suppress ROS formation in mitochondria [22]. In addition to providing cells with energy, the mitochondria take part in the regulation of many signaling cascades, triggered by the oxidative stress, and remain as the major source of ROS [46]. Correspondingly, in many disorders and pathological syndromes, the mitochondria are viewed as attractive targets for therapy [47–49]. Since mitochondria are impermeable to natural (conventional) antioxidants, two novel approaches to their targeting were developed recently [23–25]. Firstly, specific peptide structures were designed to penetrate into mitochondria thereby delivering protein-based antioxidants. Secondly, membrane-permeable cations were created to transport low molecular weight antioxidants to these organelles. The latter compounds demonstrated their efficacy in, for instance, preventing ROS-induced modifications of cardiolipin, the key phospholipid component of mitochondria and a common target of oxidation [50, 51]. In the current study, we used mitochondria-targeted antioxidant SkQ1 (10-(6′-plastoquinonyl)decyltriphenylphosphonium), which was designed previously using the second approach. It is comprised of naturally occurring antioxidant plastoquinone, conjugated with transport molecule triphenylphosphonium, which ensures the penetration of the drug into the cell and its accumulation in the mitochondria [23].

All mitochondria-targeted antioxidants developed so far, including SkQ1, are purely synthetic with no natural analogues. As such, it is important to examine thoroughly their toxicological properties before administering them to the patients. It is known that topical application of pharmaceuticals typically excludes unwanted systemic effects on the organism. In ophthalmology, this can be achieved by using eye drops. Our safety tests reveal that 3 instillations of SkQ1 per day are well tolerated in animals when concentration of the antioxidant did not exceed 7.5 μM, which was recognized as the maximum admissible dose. We further demonstrated protective activity of SkQ1 towards the cornea in anesthesia-induced DES on clinical and morphological levels. The premedication with SkQ1 produced dose-dependent effects in the 0.25–7.5 μM range. Consistently, dose-dependence of SkQ1 action was demonstrated in patients with polyetiological DES [27, 28]. It is noteworthy that SkQ1 had poor dose-dependency when used in treatment after anesthesia. Apparently, premedication with higher dose of the antioxidant results in its faster and more effective accumulation in the cornea, which is less essential in the case of continuous long-term treatment. Overall, regular prophylactic instillations of 7.5 μM SkQ1 can be considered as safe and effective preventive care strategy for DES.

As the next step, we attempted to specify cellular and biochemical mechanisms underlying therapeutic action of SkQ1 in DES. Our histological studies demonstrated that premedication with the antioxidant prevented corneal injury by inhibiting necrotic, prenecrotic, and apoptotic changes in the corneal epithelium. The similar protective activity of SkQ1 was demonstrated for a number of tissues. For instance, it exhibited a noticeable protective effect on heart and kidney infarction caused by ischemia/reperfusion, as well as on ischemic stroke or renal failure [52, 53]. In addition, antiapoptotic activity of SkQ1 towards neurons was demonstrated in the models of Alzheimer's disease and age-related retinopathy [54–57]. The simplest possible explanation of the protective effect of SkQ1 on the cornea is that its accumulation in the mitochondria of corneal epitheliocytes suppresses generation of ROS and propagation of oxidative stress. Indeed, the application of SkQ1 reduced the amount of malondialdehyde in corneal homogenates indicating decrease of oxidative stress in the cornea. Unexpectedly, SkQ1 also stimulated intrinsic antioxidant defense of this tissue. Two major antioxidant systems are distinguished in the cornea and other tissues. Nonenzymatic antioxidants (e.g., vitamins C and E) can provide direct protection from oxidative damage and enhance endogenous antioxidant enzyme activity via synergic scavenging of free radicals [58]. Enzymatic antioxidant system is comprised of superoxide dismutases (cytoplasmic Cu/Zn-SOD (SOD1) and mitochondrial Mn-SOD (SOD2)), catalase, glutathione peroxidases (GPx), and glutathione reductase (GR) [59]. SOD reduces superoxide radicals to hydrogen peroxide, which is decomposed into oxygen and water by catalase or (with oxidation of glutathione) by GPx. Inactivation of these enzymes leads to accumulation of peroxide and its eventual conversion into highly toxic hydroxyl radical. Finally, GR is able to reduce oxidized glutathione, replenishing its necessary pool [60–63]. We have found that premedication with SkQ1 increases GPx and GR levels in the cornea, while having almost no effect on low molecular antioxidant activity (AOA) and SOD activity in this tissue. It should be mentioned that anesthetic conditions by themselves did not cause alterations in GPx and GR activity and the observed trends might be attributed to SkQ1 treatment. The obtained data agree with the effect of another

mitochondria-targeted antioxidant MitoQ, which was demonstrated to induce GPx1 expression *in vitro* in leukocytes isolated from the second-type diabetic patients [64]. Yet, our data is the first demonstration of such effect of mitochondria-targeted antioxidant *in vivo*. Overall, application of SkQ1 provides dual action on corneal state in DES by both neutralizing ROS directly and enforcing the key elements of the antioxidant defense.

Normal maintenance of the ocular surface relies on the tear film, which prevents the cornea from desiccative stress and infection and provides it with nourishing and antioxidant compounds [65]. Consistently, in our previous studies, we have shown that development of anesthesia-induced DES in experimental animals is accompanied by a decline in tear film stability as well as by reduction in its antioxidant and anti-inflammatory activity [6]. Such alterations were found in patients with DES and suggested to play the key role in its pathogenesis [10]. Remarkably, administration of SkQ1 in general anesthesia-induced DES not only affected cornea state but also improved tear qualities. In particular, it attenuated a decline in total AOA and SOD. Meanwhile, no substantial change in GPx and GR activities was observed, in contrast to the alterations observed in the cornea. This divergence can be tied to the fact that the antioxidant components accumulate in corneal tissue and tear fluid via distinct mechanisms. In particular, SOD and low molecular antioxidants are secretable compounds therefore entering tear fluid [58]. It is known that DES can be induced by denervation of the lacrimal glands, which resembles the effect of anesthetic on their activity [66, 67]. Thus, exposure to anesthesia likely results in fast suppression of lacrimal gland function, consequent alteration of tear biochemistry, and development of DES symptoms. Consistently, SOD content in tears and intrinsic antioxidant activity of the tear fluid would be highly sensitive to protective action of SkQ1 on tear-producing glands. On the other hand, GPx and GR are predominantly intracellular proteins [68, 69] and their alterations in tears as a result of antioxidant premedication would be less noticeable, which agrees with our results. As for the cornea, the activities GPx and GR have been found in both corneal epithelium and endothelium [68, 69], and in our records, these enzymes become specifically upregulated within these cells under the SkQ1 action via a mechanism that is yet to be specified.

Apart from the improvement of tear antioxidant status, SkQ1 suppressed the development of proinflammatory reactions of the eye surface detectable in tears. In particular, the premedication averted completely acute elevation of TNF-α and delayed growth in IL-6 content, as well as promoted accumulation of anti-inflammatory IL-4 and IL-10 in tear fluid. Interestingly, the concentration of IL-10 increased more than 5-fold indicating a specific effect of SkQ1 on its expression/secretion. The revealed anti-inflammatory potential of SkQ1 agrees with its ability to prevent TNF-α-induced ICAM-1 overexpression in endothelium *in vitro* and *in vivo* and with its therapeutic effect in the case of various inflammatory disorders. Furthermore, similar antioxidant MitoQ mitigated symptoms of experimental colitis, which is governed, at least partially, by the prevention of IL-1β and IL-18 release [70]. In our case, anti-inflammatory effect may be associated with the upregulation of IL-10 by SkQ1. Indeed, overexpression of IL-10 was beneficial in treatment of ocular inflammatory diseases such as herpetic keratitis [71]. Furthermore, IL-10 is known to antagonize proinflammatory cytokines including TNF-α [72]. The latter is widely regarded as a master cytokine, downregulating of which would generally inhibit proinflammatory signaling [73].

The described increase in antioxidant and anti-inflammatory activity in the presence of SkQ1 agrees with our observations that premedication accelerates substantially tear film recovery. Given the fact that SkQ1 does not affect tear production, it can be suggested that the premedication generally improved biochemical properties of the tear film. Since the latter is produced by lacrimal and meibomian glands, as well as goblet cells of conjunctiva [65], it is possible that SkQ1 protects these tissues from the oxidative stress. Consistently, our preliminary results indicated positive effect of SkQ1 on clinical condition of conjunctiva of rabbits with anesthesia-associated DES (data not shown).

Taken together, our results demonstrate safety and efficacy of 7.5 μM SkQ1 eye drop administration for prevention and treatment of DES. Such medication can be recommended for the patients and individuals at risk for the disease, including elderly people and those who were subjected to general anesthesia. In addition, our findings provide better understanding of pathophysiological mechanisms that are susceptible to antioxidant treatment in DES. These mechanisms include oxidative stress and inflammation that manifested in the cornea and tear film and resulted in apoptotic and necrotic changes in the corneal epithelium. SkQ1 and probably other mitochondria-targeted antioxidants can be used to suppress effectively these degenerative processes. Finally, we described novel qualities of SkQ1, such as its ability to upregulate antioxidant enzymes and anti-inflammatory cytokines. These data point to the feasibility of SkQ1 for treatment of various ocular surface pathologies different from DES, such as trauma, corneal erosions, and ulcers, as well as inflammatory disorders of the cornea and other eye tissues.

Conflicts of Interest

The authors have no conflicts of interest to declare.

Acknowledgments

This study was supported by the Russian Science Foundation (Project no. 16-15-00255).

References

[1] "The definition and classification of dry eye disease: report of the definition and classification subcommittee of the international dry eye workshop (2007)," *The Ocular Surface*, vol. 5, no. 2, pp. 75–92, 2007.

[2] R. G. Fiscella, "Understanding dry eye disease: a managed care perspective," *The American Journal of Managed Care*, vol. 17, Supplement 16, pp. S432–S439, 2011.

[3] "The epidemiology of dry eye disease: report of the epidemiology subcommittee of the international dry eye workshop (2007)," *The Ocular Surface*, vol. 5, no. 2, pp. 93–107, 2007.

[4] A. Yagci and C. Gurdal, "The role and treatment of inflammation in dry eye disease," *International Ophthalmology*, vol. 34, no. 6, pp. 1291–1301, 2014.

[5] M. M. Malafa, J. E. Coleman, R. W. Bowman, and R. J. Rohrich, "Perioperative corneal abrasion: updated guidelines for prevention and management," *Plastic and Reconstructive Surgery*, vol. 137, no. 5, pp. 790e–798e, 2016.

[6] E. Y. Zernii, M. O. Golovastova, V. E. Baksheeva et al., "Alterations in tear biochemistry associated with postanesthetic chronic dry eye syndrome," *Biochemistry (Moscow)*, vol. 81, no. 12, pp. 1549–1557, 2016.

[7] S. E. Skalicky, C. Petsoglou, A. Gurbaxani, C. L. Fraser, and P. McCluskey, "New agents for treating dry eye syndrome," *Current Allergy and Asthma Reports*, vol. 13, no. 3, pp. 322–328, 2013.

[8] E. M. Messmer, "The pathophysiology, diagnosis, and treatment of dry eye disease," *Deutsches Ärzteblatt International*, vol. 112, no. 5, pp. 71–81; quiz 82, 2015.

[9] E. Y. Zernii, V. E. Baksheeva, E. V. Yani, P. P. Philippov, and I. I. Senin, "Therapeutic proteins for treatment of corneal epithelial defects," *Current Medicinal Chemistry*, vol. 24, 2017.

[10] J. Kruk, K. Kubasik-Kladna, and H. Y. Aboul-Enein, "The role oxidative stress in the pathogenesis of eye diseases: current status and a dual role of physical activity," *Mini Reviews in Medicinal Chemistry*, vol. 16, no. 3, pp. 241–257, 2015.

[11] R. K. Crouch, P. Goletz, A. Snyder, and W. H. Coles, "Antioxidant enzymes in human tears," *Journal of Ocular Pharmacology*, vol. 7, no. 3, pp. 253–258, 1991.

[12] A. V. Saijyothi, J. Fowjana, S. Madhumathi et al., "Tear fluid small molecular antioxidants profiling shows lowered glutathione in keratoconus," *Experimental Eye Research*, vol. 103, pp. 41–46, 2012.

[13] T. H. Wakamatsu, M. Dogru, and K. Tsubota, "Tearful relations: oxidative stress, inflammation and eye diseases," *Arquivos Brasileiros de Oftalmologia*, vol. 71, 6 Supplement, pp. 72–79, 2008.

[14] A. S. Andrade, T. B. Salomon, C. S. Behling et al., "Alpha-lipoic acid restores tear production in an animal model of dry eye," *Experimental Eye Research*, vol. 120, pp. 1–9, 2014.

[15] A. Higuchi, H. Inoue, Y. Kaneko, E. Oonishi, and K. Tsubota, "Selenium-binding lactoferrin is taken into corneal epithelial cells by a receptor and prevents corneal damage in dry eye model animals," *Scientific Reports*, vol. 6, p. 36903, 2016.

[16] A. Higuchi, H. Inoue, T. Kawakita, T. Ogishima, and K. Tsubota, "Selenium compound protects corneal epithelium against oxidative stress," *PLoS One*, vol. 7, no. 9, article e45612, 2012.

[17] A. Higuchi, K. Takahashi, M. Hirashima, T. Kawakita, and K. Tsubota, "Selenoprotein P controls oxidative stress in cornea," *PLoS One*, vol. 5, no. 3, article e9911, 2010.

[18] X. Hua, R. Deng, J. Li et al., "Protective effects of L-carnitine against oxidative injury by hyperosmolarity in human corneal epithelial cells," *Investigative Ophthalmology & Visual Science*, vol. 56, no. 9, pp. 5503–5511, 2015.

[19] Z. Li, J. H. Choi, H. J. Oh, S. H. Park, J. B. Lee, and K. C. Yoon, "Effects of eye drops containing a mixture of omega-3 essential fatty acids and hyaluronic acid on the ocular surface in desiccating stress-induced murine dry eye," *Current Eye Research*, vol. 39, no. 9, pp. 871–878, 2014.

[20] V. P. Skulachev, V. N. Anisimov, Y. N. Antonenko et al., "An attempt to prevent senescence: a mitochondrial approach," *Biochimica et Biophysica Acta (BBA) - Bioenergetics*, vol. 1787, no. 5, pp. 437–461, 2009.

[21] J. L. Gollihue and A. G. Rabchevsky, "Prospects for therapeutic mitochondrial transplantation," *Mitochondrion*, vol. 35, pp. 70–79, 2017.

[22] M. V. Blagosklonny, J. Campisi, D. A. Sinclair et al., "Impact papers on aging in 2009," *Aging*, vol. 2, no. 3, pp. 111–121, 2010.

[23] Y. N. Antonenko, A. V. Avetisyan, L. E. Bakeeva et al., "Mitochondria-targeted plastoquinone derivatives as tools to interrupt execution of the aging program. 1. Cationic plastoquinone derivatives: synthesis and in vitro studies," *Biochemistry (Moscow)*, vol. 73, no. 12, pp. 1273–1287, 2008.

[24] K. Zhao, G. Luo, S. Giannelli, and H. H. Szeto, "Mitochondria-targeted peptide prevents mitochondrial depolarization and apoptosis induced by tert-butyl hydroperoxide in neuronal cell lines," *Biochemical Pharmacology*, vol. 70, no. 12, pp. 1796–1806, 2005.

[25] R. A. Smith, C. M. Porteous, C. V. Coulter, and M. P. Murphy, "Selective targeting of an antioxidant to mitochondria," *European Journal of Biochemistry*, vol. 263, no. 3, pp. 709–716, 1999.

[26] T. A. Ajith and T. G. Jayakumar, "Mitochondria-targeted agents: future perspectives of mitochondrial pharmaceutics in cardiovascular diseases," *World Journal of Cardiology*, vol. 6, no. 10, pp. 1091–1099, 2014.

[27] A. Petrov, N. Perekhvatova, M. Skulachev, L. Stein, and G. Ousler, "SkQ1 ophthalmic solution for dry eye treatment: results of a phase 2 safety and efficacy clinical study in the environment and during challenge in the controlled adverse environment model," *Advances in Therapy*, vol. 33, no. 1, pp. 96–115, 2016.

[28] V. V. Brzheskiy, E. L. Efimova, T. N. Vorontsova et al., "Results of a multicenter, randomized, double-masked, placebo-controlled clinical study of the efficacy and safety of Visomitin eye drops in patients with dry eye syndrome," *Advances in Therapy*, vol. 32, no. 12, pp. 1263–1279, 2015.

[29] L. E. Bakeeva, C. M. Eldarov, I. M. Vangely, N. G. Kolosova, and V. B. Vays, "Mitochondria-targeted antioxidant SkQ1 reduces age-related alterations in the ultrastructure of the lacrimal gland," *Oncotarget*, vol. 7, no. 49, pp. 80208–80222, 2016.

[30] J. L. Wipperman and J. N. Dorsch, "Evaluation and management of corneal abrasions," *American Family Physician*, vol. 87, no. 2, pp. 114–120, 2013.

[31] K. C. Cater and J. W. Harbell, "Prediction of eye irritation potential of liquid and granular laundry detergent formulas using the bovine corneal opacity and permeability (BCOP) assay," *Cutaneous and Ocular Toxicology*, vol. 32, no. 3, pp. 210–221, 2013.

[32] F. R. Notice, Ed., *Public Comment Prepared by the Institute for In Vitro Sciences*, vol. 69, no. 212, pp. 64081-64082, 2004.

[33] J. A. Kiernan, *Histological and Histochemical Methods: Theory and Practice*, Scion Publishing, Oxford, 4th edition, 2008.

[34] J. K. Maurer and R. D. Parker, "Light microscopic comparison of surfactant-induced eye irritation in rabbits and rats at three hours and recovery/day 35," *Toxicologic Pathology*, vol. 24, no. 4, pp. 403–411, 1996.

[35] E. Y. Zernii, A. A. Nazipova, O. S. Gancharova et al., "Light-induced disulfide dimerization of recoverin under ex vivo and in vivo conditions," *Free Radical Biology & Medicine*, vol. 83, pp. 283–295, 2015.

[36] D. Bhattacharya, Y. Ning, F. Zhao et al., "Tear production after bilateral main lacrimal gland resection in rabbits," *Investigative Ophthalmology & Visual Science*, vol. 56, no. 13, pp. 7774–7783, 2015.

[37] P. D. Gautheron, V. J. Lotti, and J. C. Le Douarec, "Tear film breakup time prolonged with unmedicated cellulose polymer inserts," *Archives of Ophthalmology*, vol. 97, no. 10, pp. 1944–1947, 1979.

[38] O. V. Gulidova, O. B. Liubitskii, G. I. Klebanov, and N. B. Chesnokova, "Changes in the antioxidative activity of tears during experimental eye burns," *Biulleten' Eksperimental'noĭ Biologii i Meditsiny*, vol. 128, no. 11, pp. 571–574, 1999.

[39] E. Y. Zernii, O. S. Gancharova, I. E. Ishutina et al., "Mechanisms of perioperative corneal abrasions: alterations in tear film proteome," *Biochemistry (Moscow), Supplement Series B: Biomedical Chemistry*, vol. 11, no. 2, pp. 186–193, 2017.

[40] I. G. Sommers, "Chapter IV - general pathology in relation to the eye," in *Histology and Histopathology of the Eye and its Adnexa*, pp. 57–129, Butterworth-Heinemann, Oxford, UK, 2013.

[41] C. T. Lai, W. C. Yao, S. Y. Lin et al., "Changes of ocular surface and the inflammatory response in a rabbit model of short-term exposure keratopathy," *PLoS One*, vol. 10, no. 9, article e0137186, 2015.

[42] E. Y. Zernii, V. E. Baksheeva, E. N. Iomdina et al., "Rabbit models of ocular diseases: new relevance for classical approaches," *CNS & Neurological Disorders Drug Targets*, vol. 15, no. 3, pp. 267–291, 2016.

[43] E. White and M. M. Crosse, "The aetiology and prevention of peri-operative corneal abrasions," *Anaesthesia*, vol. 53, no. 2, pp. 157–161, 1998.

[44] L. Hua and T. Doll, "A series of 3 cases of corneal abrasion with multiple etiologies," *Optometry*, vol. 81, no. 2, pp. 83–85, 2010.

[45] Y. K. Batra and I. M. Bali, "Corneal abrasions during general anesthesia," *Anesthesia and Analgesia*, vol. 56, no. 3, pp. 363–365, 1977.

[46] D. Munro and J. R. Treberg, "A radical shift in perspective: mitochondria as regulators of reactive oxygen species," *The Journal of Experimental Biology*, vol. 220, Part 7, pp. 1170–1180, 2017.

[47] E. N. Iomdina, I. P. Khoroshilova-Maslova, O. V. Robustova et al., "Mitochondria-targeted antioxidant SkQ1 reverses glaucomatous lesions in rabbits," *Frontiers in Bioscience (Landmark Edition)*, vol. 20, pp. 892–901, 2015.

[48] V. P. Skulachev, "Cationic antioxidants as a powerful tool against mitochondrial oxidative stress," *Biochemical and Biophysical Research Communications*, vol. 441, no. 2, pp. 275–279, 2013.

[49] V. V. Neroev, M. M. Archipova, L. E. Bakeeva et al., "Mitochondria-targeted plastoquinone derivatives as tools to interrupt execution of the aging program. 4. Age-related eye disease. SkQ1 returns vision to blind animals," *Biochemistry (Moscow)*, vol. 73, no. 12, pp. 1317–1328, 2008.

[50] G. Fouret, E. Tolika, J. Lecomte et al., "The mitochondrial-targeted antioxidant, MitoQ, increases liver mitochondrial cardiolipin content in obesogenic diet-fed rats," *Biochimica et Biophysica Acta (BBA) - Bioenergetics*, vol. 1847, no. 10, pp. 1025–1035, 2015.

[51] V. P. Skulachev, Y. N. Antonenko, D. A. Cherepanov et al., "Prevention of cardiolipin oxidation and fatty acid cycling as two antioxidant mechanisms of cationic derivatives of plastoquinone (SkQs)," *Elsevier Biochimica et Biophysica Acta (BBA) - Bioenergetics*, vol. 1797, no. 6-7, pp. 878–889, 2010.

[52] S. S. Jankauskas, E. Y. Plotnikov, M. A. Morosanova et al., "Mitochondria-targeted antioxidant SkQR1 ameliorates gentamycin-induced renal failure and hearing loss," *Biochemistry (Moscow)*, vol. 77, no. 6, pp. 666–670, 2012.

[53] L. E. Bakeeva, I. V. Barskov, M. V. Egorov et al., "Mitochondria-targeted plastoquinone derivatives as tools to interrupt execution of the aging program. 2. Treatment of some ROS- and age-related diseases (heart arrhythmia, heart infarctions, kidney ischemia, and stroke)," *Biochemistry (Moscow)*, vol. 73, no. 12, pp. 1288–1299, 2008.

[54] N. A. Stefanova, N. A. Muraleva, V. P. Skulachev, and N. G. Kolosova, "Alzheimer's disease-like pathology in senescence-accelerated OXYS rats can be partially retarded with mitochondria-targeted antioxidant SkQ1," *Journal of Alzheimer's Disease*, vol. 38, no. 3, pp. 681–694, 2014.

[55] V. B. Saprunova, M. A. Lelekova, N. G. Kolosova, and L. E. Bakeeva, "SkQ1 slows development of age-dependent destructive processes in retina and vascular layer of eyes of Wistar and OXYS rats," *Biochemistry (Moscow)*, vol. 77, no. 6, pp. 648–658, 2012.

[56] V. P. Skulachev, "Mitochondria-targeted antioxidants as promising drugs for treatment of age-related brain diseases," *Journal of Alzheimer's Disease*, vol. 28, no. 2, pp. 283–289, 2012.

[57] U. M. Sarmiento, J. I. Sarmiento, and R. Storb, "Allelic variation in the DR subregion of the canine major histocompatibility complex," *Immunogenetics*, vol. 32, no. 1, pp. 13–19, 1990.

[58] Y. Chen, G. Mehta, and V. Vasiliou, "Antioxidant defenses in the ocular surface," *The Ocular Surface*, vol. 7, no. 4, pp. 176–185, 2009.

[59] J. Cejkova, S. Stipek, J. Crkovska et al., "UV rays, the prooxidant/antioxidant imbalance in the cornea and oxidative eye damage," *Physiological Research*, vol. 53, no. 1, pp. 1–10, 2004.

[60] R. Brigelius-Flohe, "Glutathione peroxidases and redox-regulated transcription factors," *Biological Chemistry*, vol. 387, no. 10-11, pp. 1329–1335, 2006.

[61] J. Kovaceva, J. Platenik, M. Vejrazka et al., "Differences in activities of antioxidant superoxide dismutase, glutathione peroxidase and prooxidant xanthine oxidoreductase/xanthine oxidase in the normal corneal epithelium of various mammals," *Physiological Research*, vol. 56, no. 1, pp. 105–112, 2007.

[62] A. Behndig, K. Karlsson, B. O. Johansson, T. Brannstrom, and S. L. Marklund, "Superoxide dismutase isoenzymes in the normal and diseased human cornea," *Investigative Ophthalmology & Visual Science*, vol. 42, no. 10, pp. 2293–2296, 2001.

[63] I. Fridovich, "Superoxide radical and superoxide dismutases," *Annual Review of Biochemistry*, vol. 64, pp. 97–112, 1995.

[64] I. Escribano-Lopez, N. Diaz-Morales, S. Rovira-Llopis et al., "The mitochondria-targeted antioxidant MitoQ modulates oxidative stress, inflammation and leukocyte-endothelium interactions in leukocytes isolated from type 2 diabetic patients," *Redox Biology*, vol. 10, pp. 200–205, 2016.

[65] M. S. Milner, K. A. Beckman, J. I. Luchs et al., "Dysfunctional tear syndrome: dry eye disease and associated tear film disorders - new strategies for diagnosis and treatment," *Current Opinion in Ophthalmology*, vol. 27, Supplement 1, pp. 3–47, 2017.

[66] H. Toshida, D. H. Nguyen, R. W. Beuerman, and A. Murakami, "Evaluation of novel dry eye model: preganglionic parasympathetic denervation in rabbit," *Investigative Ophthalmology & Visual Science*, vol. 48, no. 10, pp. 4468–4475, 2007.

[67] S. A. Aicher, S. M. Hermes, and D. M. Hegarty, "Denervation of the lacrimal gland leads to corneal hypoalgesia in a novel rat model of aqueous dry eye disease," *Investigative Ophthalmology & Visual Science*, vol. 56, no. 11, pp. 6981–6989, 2015.

[68] K. C. Bhuyan and D. K. Bhuyan, "Regulation of hydrogen peroxide in eye humors. Effect of 3-amino-1H-1,2,4-triazole on catalase and glutathione peroxidase of rabbit eye," *Elsevier Biochimica et Biophysica Acta (BBA) - General Subjects*, vol. 497, no. 3, pp. 641–651, 1977.

[69] M. V. Riley, "A role for glutathione and glutathione reductase in control of corneal hydration," *Experimental Eye Research*, vol. 39, no. 6, pp. 751–758, 1984.

[70] A. N. Lukashev, M. V. Skulachev, V. Ostapenko, A. Y. Savchenko, V. V. Pavshintsev, and V. P. Skulachev, "Advances in development of rechargeable mitochondrial antioxidants," *Progress in Molecular Biology and Translational Science*, vol. 127, pp. 251–265, 2014.

[71] M. Daheshia, N. Kuklin, S. Kanangat, E. Manickan, and B. T. Rouse, "Suppression of ongoing ocular inflammatory disease by topical administration of plasmid DNA encoding IL-10," *Journal of Immunology*, vol. 159, no. 4, pp. 1945–1952, 1997.

[72] R. de Waal Malefyt, J. Abrams, B. Bennett, C. G. Figdor, and J. E. de Vries, "Interleukin 10(IL-10) inhibits cytokine synthesis by human monocytes: an autoregulatory role of IL-10 produced by monocytes," *The Journal of Experimental Medicine*, vol. 174, no. 5, pp. 1209–1220, 1991.

[73] E. W. Lindstedt, G. S. Baarsma, R. W. Kuijpers, and P. M. van Hagen, "Anti-TNF-α therapy for sight threatening uveitis," *The British Journal of Ophthalmology*, vol. 89, no. 5, pp. 533–536, 2005.

Hindawi
Oxidative Medicine and Cellular Longevity
Volume 2017, Article ID 6210694, 14 pages
https://doi.org/10.1155/2017/6210694

Research Article

Salvianolic Acid A Inhibits OX-LDL Effects on Exacerbating Choroidal Neovascularization via Downregulating CYLD

Ke Mao, Wanting Shu, Libin Liu, Qing Gu, Qinghua Qiu, and XingWei Wu

Department of Ophthalmology, Affiliated First People's Hospital, Shanghai Jiao Tong University, Shanghai, China

Correspondence should be addressed to XingWei Wu; wxweye@sina.com

Received 17 January 2017; Revised 28 February 2017; Accepted 8 March 2017; Published 1 September 2017

Academic Editor: Heping Xu

Backgrounds. Age-related macular degeneration is closely related to lipid oxidation, while relationship between OX-LDL and choroidal neovascularization is unclear. Recently, cylindromatosis is proved to regulate angiogenesis. However, its role in CNV progression remained unclear. Salvianolic acid A is widely used in vascular diseases. We investigated the relationship between OX-LDL and CNV and explore antineovascularization mechanism of Sal A. *Methods*. C57BL6/J mice were randomized into four groups and injected with PBS or OX-LDL, together with Sal A for one week. CNV was induced by laser; CNV severity was analyzed by fundus fluorescein angiography, H&E staining, and choroid flat mount after 1 week. In in vitro experiments, ARPE-19 and HUVECs were cultured with OX-LDL (with or without Sal A) for 48 hours. Angiogenic proteins, cell junction integrity, and tube formation were measured. *CYLD* siRNA and specific inhibitors were used to explore mechanisms of CYLD in promoting OX-LDL-induced CNV progression. *Results*. OX-LDL promoted laser-induced CNV volume by increasing VEGF, PDGF, and CYLD levels. Sal A antagonized OX-LDL effects and restrained CNV progression by decreasing VEGF/PDGF/CYLD, increasing antiangiostatin levels, and promoting P62-CYLD-TRAF6 interaction. *Conclusions*. We demonstrated oxidation damage exacerbates CNV progression, and Sal A could be a clinical therapeutic reagent to exudative AMD.

1. Introduction

Choroidal neovascularization (CNV), the hallmark of exudative age-related macular degeneration (AMD), is responsible for approximately 90% of cases of severe vision loss caused by AMD [1].

CNV is a pathological angiogenesis arising from choriocapillaris, resulting in the accumulation of fluid within the retina and subretinal space [2]. Pharmacotherapy by intravitreous administration of VEGF inhibitors has been used regularly while the curative effect is unstable [3]. The pathology of exudative AMD is complicated and associated with multiple pathologic factors including photooxidative stress, complement activation, cellular senescence, and microbial assault [4]. Among all the proposed factors, oxidative stress has multieffects and plays a critical role in cardiovascular diseases and AMD [5]. Carbohydrates, membrane lipids, proteins, and nucleic acids are all vulnerable to oxidative damage and contribute to AMD progression [6].

Changes in lipid profile in terms of total cholesterol (TC), triglycerides (TG), low-density lipoprotein (LDL), and high-density lipoprotein (HDL) have been reported in AMD progression [7]. LDL is susceptible to oxidation, resulting in the formation of oxidized low-density lipoprotein (OX-LDL) [8]. Oxidized lipoproteins have been detected in CNV membranes from AMD patients [9]. Our previous studies established an animal model to study the biological effects of high circulating serum LDL on retinal pigment epithelium (RPE) and demonstrated that OX-LDL leads to RPE cell apoptosis and inflammation, which indicated the mechanism of nonexudative AMD [10, 11]. However, it remained unclear whether OX-LDL affects CNV progression and is worth studying.

Salvianolic acid A (Sal A) is the active monomer extracted from *Salvia miltiorrhiza* Bunge (Danshen), which

is a traditional Chinese medicine and has been administrated in AMD clinically [12]. Sal A is a phenolic carboxylic acid derivative which presents a variety of pharmacological functions including anti-inflammation, antioxidation, and antiplatelet effects [13]. We found that Sal A protects RPE cells from OX-LDL-induced inflammation, while it remains largely unknown whether Sal A could repress CNV progression.

Cylindromatosis (CYLD) is a tumor suppressor that regulates signaling pathways by acting as a deubiquitinating enzyme [14]. CYLD regulates diverse biological processes including cell proliferation, survival, migration, immune responses, osteoclastogenesis, and spermatogenesis [15]. Recently, CYLD was identified as a potential modulator of vascular formation [16]. However, whether CYLD involves in the pathological process of CNV has not been studied before.

Therefore, this study was undertaken to assess the biological importance of OX-LDL and its relationship with CYLD in modulating CNV progression, meanwhile proved the potential therapeutic value of Sal A.

2. Materials and Methods

2.1. Animals and Reagents. Male wild-type C57BL/6J mice (75–100 g) were purchased from the Shanghai Laboratory Animal Center of the Chinese Academy of Sciences and used for a pathologic study. Animals were kept under a 12-hour dark/light circle. This study was approved by the Institutional Animal Care and Use Committee (IACUC) at the medical academy of Shanghai Jiao Tong University. All animal experiments were performed in accordance with the guidelines of the ARVO Statement for the Use of Animals in Ophthalmic and Vision Research. Human OX-LDL was purchased from AppliChem (Darmstadt, Germany), and OX-LDL quality was detected by electrophoretic methods. Sal A was purchased from Nanjing Guangrun Biochemical Company (Nanjing, China). Forty mice were randomized into 4 groups: PBS, OX-LDL (3 mg/kg body weight), Sal A (10 mg/kg body weight), and OX-LDL (3 mg/kg) + Sal A (10 mg/kg) ($n = 10$ per group). Each group was injected with PBS or OX-LDL in the vein for 7 days; Sal A was intraperitoneally injected 3 hours before OX-LDL or PBS administration once per day.

2.2. Serum Lipid Analyses. The serum of mice in each group was collected, and we measured serum lipoprotein levels after consecutive injections of OX-LDL for 7 days. Concentrations of serum total cholesterol and OX-LDL cholesterol were measured with the commercial ELISA kits (Kmaels, Shanghai, China) and an automated biochemistry platereader (Olympus AU600, Tokyo, Japan).

2.3. Induction of Choroidal Neovascularization (CNV). CNV was induced by laser photocoagulation as described previously [17–19]. To assess CNV volumes, 3-4 spots of laser photocoagulations (parameters: 532 nm laser; power, 130 mW; duration, 100 ms; diameter, 50 μm; Novus Verdi, Coherent Inc., Santa Clara, CA, USA) were placed in the fundus of each eye. The laser spots were created around the optic nerve using a slit-lamp delivery system, a coverslip was used to allow viewing of the posterior pole of the eye. The morphologic endpoint of the laser injury was the appearance of a cavitation bubble, which is a sign of Bruch's membrane disruption.

2.4. Fundus Fluorescein Angiography (FFA) Imaging and Grading. Fundus fluorescein angiography was performed 7 days postlaser by intraperitoneal injection of 50 μL of 25% fluorescein sodium (Alcon, Fort Worth, TX, USA). Fundus images were taken using a digital fundus camera (Model TRC 50 IA; Topcon, Paramus, Japan). FFA was qualitatively and quantitatively evaluated by two blind groups of observers. The laser-induced lesions were graded based on the observed fluorescein leakage and then divided into the following four categories as described by Semkova [20]. Volumes of grade 4 laser spots were evaluated by image J software.

2.5. CNV Volume Analysis. Choroidal flat mount preparation, staining, and imaging were undertaken as previously described [21]. Briefly, eyes were enucleated at 7 day after laser injury and immediately fixed for 1 h in a solution of 4% paraformaldehyde in phosphate-buffered saline (PBS; 9 g/L NaCl, 0.232 g/L KH_2PO4, and 0.703 g/L Na^2HPO4; pH 7.3). The anterior segment and crystalline lens were removed, and the retinas were detached and separated from the optic nerve head with a pair of fine-curved scissors. The remaining eye cups were washed with cold ICC buffer (0.5% BSA, 0.2% Tween 20, and 0.05% sodium azide) in PBS. Next, a 1 : 500 dilution of isolectin B4 (Sigma-Aldrich, USA) and 1 : 1000 dilution of CD31 (Abcam, Cambridge, UK) were incubated at 4°C overnight and then washed with cold PBS buffer. A 1 : 1000 dilution of fluorescence-conjugated secondary antibody (Abcam, Cambridge, UK) was incubated for 1 hour and then washed with cold PBS buffer. Radial cuts were made toward the optic nerve head, and the sclera-choroidal/RPE complexes were flat mounted, covered, and sealed. Image J software was used to analyze fluorescence images. The summation of the whole stained area in each section multiplied by the distance between sections (1 μm) was used as an index for the CNV lesion volume. The volumes of the all lesions in each eye were averaged and considered as an $n = 1$ for statistical analysis.

2.6. Hematoxylin and Eosin (HE) Staining and Immunofluorescence. Histopathological analysis was performed as described previously [22]. Mice were killed, eyes were enucleated 7 days after laser injury, and eyecups were fixed in paraformaldehyde at 4°C for 24 h. The fixed tissues were embedded in paraffin, serially sectioned at 3 μm, and stained with hematoxylin and eosin (HE). Serial slices of each CNV were examined and digitized using a light microscope (Olympus Corporation, Tokyo, Japan). CNV thickness was measured vertically from the adjacent RPE layer to the top of the CNV, and CNV length was measured horizontally maximizing the distance of CNV using Image J software, which was expressed in μm. For CYLD immunofluorescence,

CNV sections were incubated overnight at 4°C in rabbit anti-human CYLD monoclonal antibody (Abcam, Cambridge, UK). Secondary antibodies were conjugated to Alexa-Fluor488 (Abcam, Cambridge, UK). The fluorescence intensity of CYLD was measured by Image J software.

2.7. Cell Culture. The human RPE cell line (ARPE-19) and human umbilical vein endothelial cells (HUVECs) were cultured as previously described [11]. ARPE-19 cells were grown to 70–80% confluence and placed in a serum-free medium (SFM) for 24 hours before treatments. Cells were then randomized into SFM, OX-LDL (100 mg/L), and OX-LDL + Sal A (5/50 μM) for 48 hours. Cells were pretreated with Sal A 3 hours before OX-LDL stimulation. For ERK and PI3K/mTOR inhibitor treatment, ARPE-19 cells were pretreated with FR 180204 (10 μM, Selleck, USA), LY294002 (1 mM, Darmstadt, Germany), or rapamycin (100 nM, Sigma-Aldrich, USA) for 1 hour, followed by Sal A (50 μM) for 3 hours, then stimulated with OX-LDL (100 mg/L) for 72 hours.

2.8. CYLD RNAi. To silence *CYLD* gene in ARPE-19 and HUVEC cells, the specific mixture of three preselected siRNA duplexes to target different sequences of the human *CYLD* gene was utilized according to the manufacturer's instructions. The siRNA was mixed with Opti-MEM (Invitrogen, Carlsbad, CA) and Lipofectamine®3000(ThermoFisher Scientific, USA) to form the transfection complex, prior to addition to culture medium. Nonsilencing siRNA (SI03650325, Qiagen) with the same concentration was used as a negative control. The efficiency of gene silencing was determined by western blot 24 hours after the treatments.

2.9. Western Blot and Immunoprecipitation. Western blot was accomplished as described before [11]. Vascular endothelial growth factor (VEGF), platelet-derived growth factor (PDGF), pigment epithelium -derived factor (PEDF), P62, and antiangiostatin monoclonal antibodies were purchased from Abcam (Cambridge, UK). TRAF6 and CYLD monoclonal antibodies were purchased from CST (Boston, USA). β-actin was used as a loading control for each lane. Each indicated band was quantified and normalized to the corresponding loading control through Image J software. Immunoprecipitation was performed as follows: Antibodies against TRAF6 were used to precipitate proteins from cell lysis in the presence of 20 μL protein A/G beads (Santa Cruz Biotechnology, Santa Cruz, CA, USA) overnight at 4°C. Protein complexes were washed 4 times with lysis buffer and then incubated at 95°C for 5 minutes. P62, CYLD, and ubiquitin proteins were resolved by western blot analysis.

3. Immunocytochemistry

As previously described [23], ARPE-19 cells were cultured on a 16-well glass slide. After treatment, cells were fixed for 20 minutes with 4% paraformaldehyde and permeabilized for one hour at room temperature with 10% goat serum and 0.1% Triton X-100 in PBS. ARPE-19 cells were then incubated with rabbit anti-human monoclonal antibodies directed against ZO-1 and CYLD (Abcam, Cambridge, UK) at 4°C overnight. The slides were then washed with PBS. Secondary antibodies were added to the slides for 1 hour. Slides were then rinsed with PBS, coated with mounting media containing DAPI, covered, and examined by fluorescent microscopy (Olympus, Japan).

Table 1: Serum lipid levels in mouse.

Group	TC (mmol/L)	OX-LDL-C (mmol/L)
PBS	1.56 ± 0.19	0.258 ± 0.17
Sal A	1.47 ± 0.20	0.306 ± 0.11
OX-LDL	$2.59 \pm 0.26^{*}$	$0.594 \pm 0.08^{*}$
OX-LDL + Sal A	$2.24 \pm 0.17^{\#}$	$0.414 \pm 0.01^{\#}$

Values are mean ± SD; $n = 10$. $^{*}P < 0.05$ versus the control (PBS) group; $^{\#}P < 0.05$ versus OX-LDL group. TC: Total cholesterol; OX-LDL-C: Oxidized low-density lipoprotein-cholesterol.

3.1. ELISA. VEGF measurement after silencing *CYLD* gene was performed as described previously [24]. In brief, VEGF concentrations in ARPE-19 cell culture mediums were measured using a related human ELISA kit (R&D Systems, Minneapolis, USA) following the manufacturer's instructions. Serial dilutions of recombinant human VEGF were included in all assays to serve as standards. Triplicate evaluations were performed for each sample.

3.2. Real-Time PCR. Total RNA from the choroid of C57 mice were isolated using TRIzol reagent (Life Technologies, USA). cDNA synthesis was accomplished with First-Strand Synthesis System (TaKaRa Bio, Shiga, Japan). cDNA was amplified using the SYBR® Green PCR Master Mix Reagent (BIOTNT, Shanghai, China) on viia™ 7 Real-time PCR System (ABI, USA) as follows: 95°C, 5 min; followed by 35 amplification cycles (95°C for 5 s; 60°C for 30s). Primer sequences used were the following: β-actin, forward 5′-CCT CTA TGC CAA CAC AGT 3′ and reverse 5′-AGC CAC CAA TCC ACA CAG 3′; CYLD, forward 5′-AAT GTG TCC CTG CCC TAC CTA 3′ and reverse 5′-CTC GTC CCT ACT CTG CCA CTT 3′; PEDF, forward 5′-GAG GAC AGG ACC GTG AGA GT 3′ and reverse 5′-GGG CAG GAA GAA GAT GAT G 3′;VEGF, forward 5′-GCA AGA GAA GAC ACG GTG GT 3′ and reverse 5′-CAG GAG GTG GGG TAA GGA G 3′; PDGF, forward 5′-CAG TGT CCG TTT GTT CAG TG 3′ and reverse 5′-TGG TTT TGT TTT CGC TCT CT 3′; and angiostatin, forward 5′-CCT TGG TGC TAC ACT ACA GA 3′ and reverse 5′-GGA GAT TTT GCC CTC ATA C 3′. mRNA expression was normalized to the endogenous reference gene β-actin. Specific primers were produced by BIOTNT Company (Shanghai, China), and relative quantification was achieved by the comparative $2^{-\Delta\Delta ct}$ method as described [25].

3.3. Statistical Analysis. The experimental data are expressed as mean ± SEM in figures and mean ± SD in tables. Group means were compared by a one-way analysis of variance with the use of the GraphPad Prism 4.0 software system (GraphPad, San Diego, CA), and the statistical software program

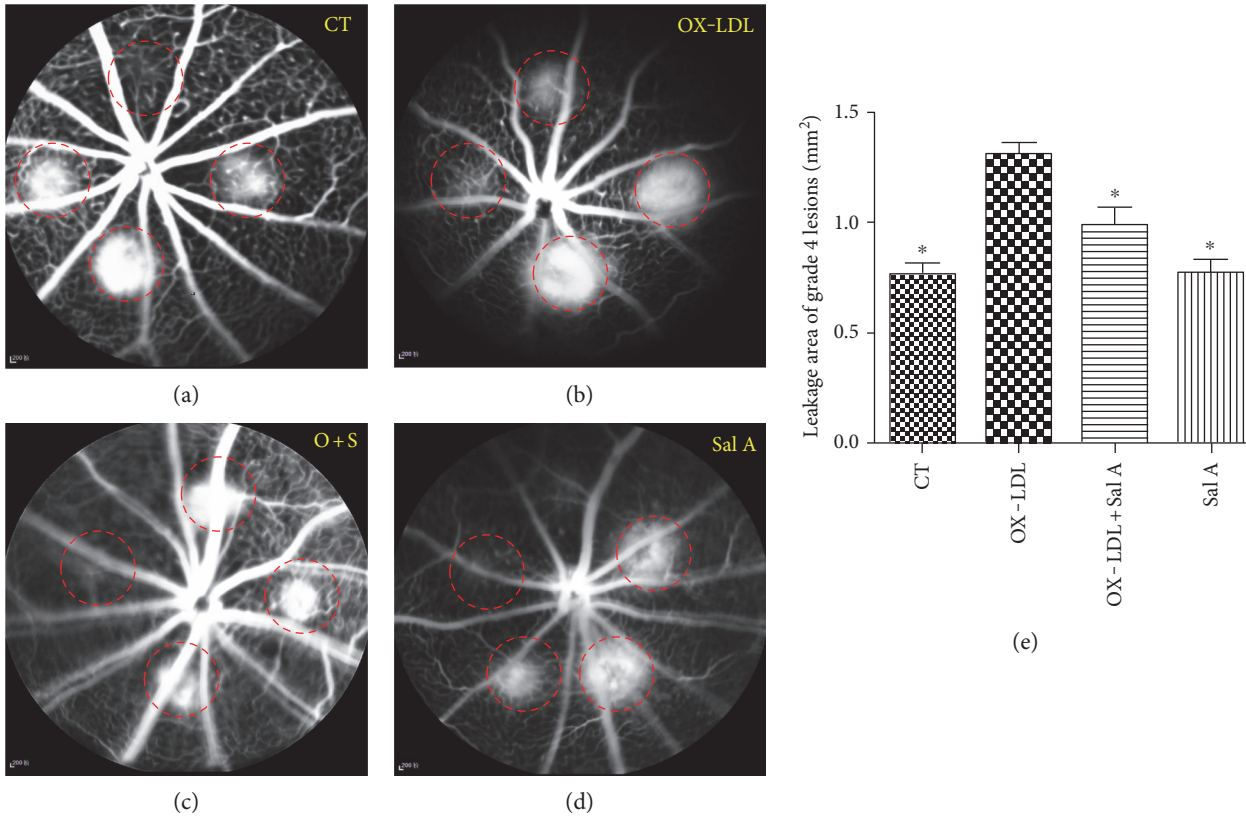

Figure 1: OX-LDL increases laser-induced CNV volume and leakage areas, and Sal A pretreatment antagonizes effects of OX-LDL. C57 mice were divided into PBS, OX-LDL, Sal A, and OX-LDL + Sal A groups. Each group was injected with PBS or OX-LDL or PBS administration. (a–d) Representative fluorescein angiograms 7 days postphotocoagulation showing late-phase leakages beyond borders. (a) Control group; (b) OX-LDL-injected group; (c) OX-LDL + Sal A-injected group; (d) Sal A-injected group. (e) Leakage areas of grade 4 lesions on the late phase of flourescein angiograms in each group. Leakage areas of grade 4 CNV lesions were measured by tracing the borders of fluorescein leakage using Image J software. Data were expressed as mean ± SEM. OX-LDL injection significantly increased a leakage area compared with the PBS group, and the OX-LDL + Sal A group had a smaller leakage area than the OX-LDL group ($^*P < 0.05$ versus the OX-LDL group).

Table 2: Percentages of grade 4 lesions in each group.

Groups	PBS	Sal A	OX-LDL	OX-LDL + Sal A
Rates (%)	56.25 ± 8.01	43.49 ± 3.54*	66.44 ± 9.47*	58.49 ± 4.47$^\#$

Values are mean ± SD; $n = 10$. $^*P < 0.05$ significant difference when compared with the PBS group; $^\#P < 0.05$ significant difference when compared with the OX-LDL group.

SigmaPlot v.10.0 software. P value less than 0.05 is considered to be significant.

4. Results

4.1. OX-LDL Increases Serum Lipoprotein Levels and Sal A Pretreatment Significantly Decreases Lipoprotein Levels. To investigate the effects of OX-LDL and Sal A injection on circulating lipoprotein level, we examined serum OX-LDL cholesterol and total cholesterol concentrations in C57 mice. Both OX-LDL and total cholesterol levels were significantly increased in the OX-LDL group compared with PBS group. And these OX-LDL-induced increases were significantly inhibited when pretreated with Sal A (see Table 1).

4.2. OX-LDL Increases Laser-CNV Volumes in C57 Mice, and Sal A Significantly Decreases CNV Volumes. Next, we studied the effect of OX-LDL and Sal A on CNV volume in vivo. FFA examination revealed CNV leakage in each group. Results in Figures 1(a)–1(e) showed that OX-LDL treatment significantly increased incidence and leakage areas of grade 4 lesion compared with the PBS group, while fluorescence leakage severity was significantly reduced in the Sal A + OX-LDL group when compared with the OX-LDL group. The grading of laser lesions in all groups is shown in Table 2.

In morphologic cross sections, CNV in the OX-LDL group was significantly longer and higher than those in the Sal A + OX-LDL group and PBS group (length: OX-LDL 765 ± 47.1 (μm) versus OX-LDL + Sal A 432.59 ± 35.1 (μm)

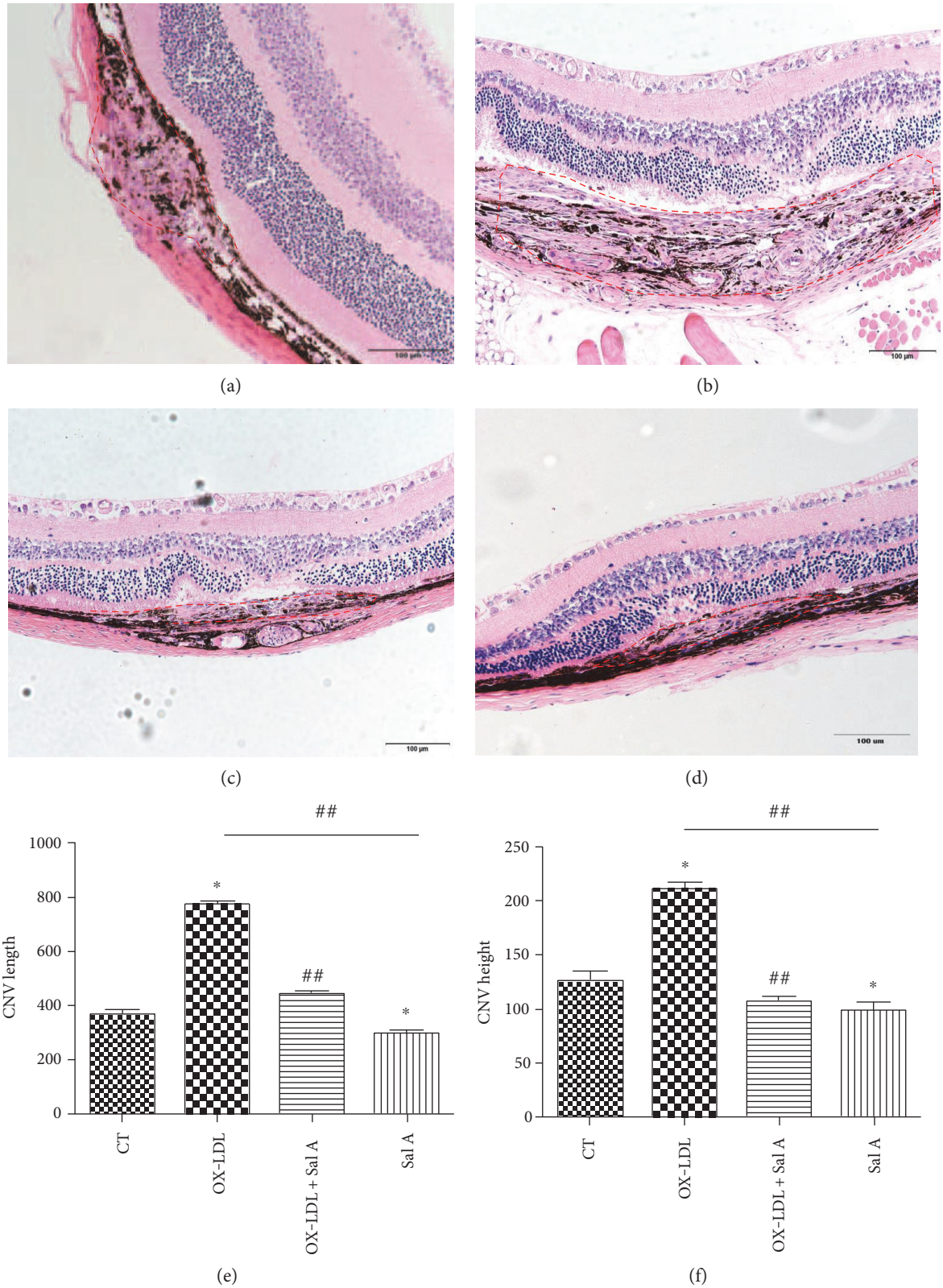

Figure 2: Continued.

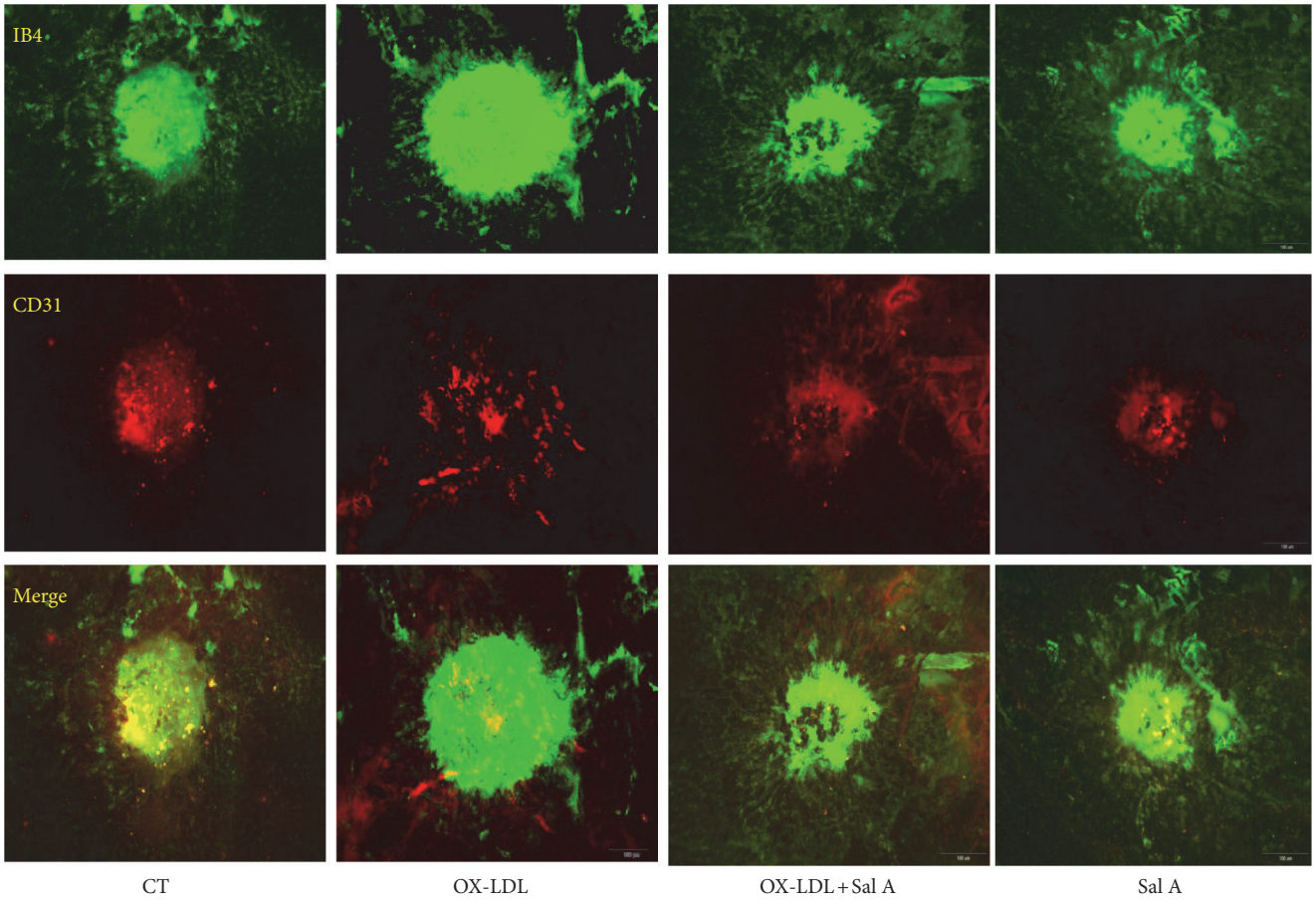

Figure 2: Representative images of hematoxylin and eosin staining of cross sections through choroidal neovascular lesions 7 days after photocoagulation were shown. CNV maximum thickness and length of the groups in cross sections represent as indicated: (a) control group; (b) OX-LDL group; (c) OX-LDL + Sal A group; (d) Sal A group. (e, f) CNV length and height of four groups in cross sections represent as indicated. ($^{*}P < 0.05$ versus the control group. $^{\#\#}P < 0.05$ versus the OX-LDL group).

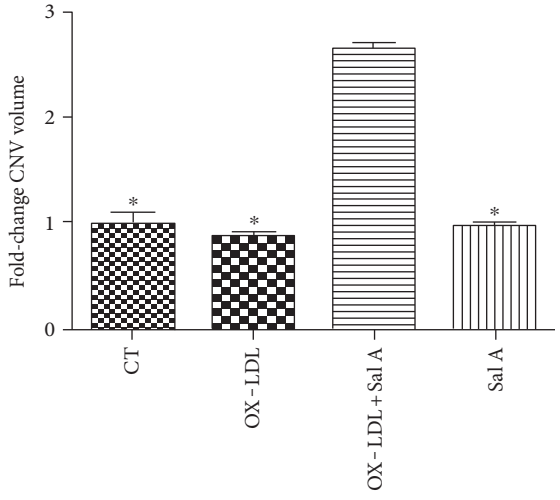

Figure 3: Representative images of laser CNV 7 days after photocoagulation. OX-LDL injection increased laser-induced CNV volume compared with PBS while OX-LDL + Sal A treatment reduced CNV volume compared with the OX-LDL group. Data were expressed as mean ± SEM ($n = 20$ eyes/group). $^{*}P < 0.05$ versus the OX-LDL group. Scale bar = 100 μm.

versus control 368.2 ± 27.1 (μm); $P < 0.05$; height: OX-LDL 195.69 ± 16.47 (μm) versus OX-LDL + Sal A 118.7 ± 16.1 (μm) versus control 128.5 ± 16.9 (μm); $P < 0.05$, $n = 20$ eyes/group); longer and higher CNV was also identified in the PBS group than the Sal A group (PBS length: 288.63 ± 14.1(μm); height:108.97 ± 18.1(μm); $P < 0.05$, $n = 20$ eyes/group) (Figure 2).

Choroidal flat mount examination showed significantly larger laser CNV volumes in the OX-LDL group compared with the PBS and OX-LDL + Sal A group, respectively ($P < 0.01$, $n = 20$ eyes/group; Figure 3). Treatment with Sal A decreased laser CNV volumes compared with the PBS group, but the difference was insignificant ($n = 20$ eyes/group; Figure 3).

4.3. Effects of OX-LDL and Sal A on Angiogenesis Gene Expression In Vivo. The angiogenesis gene expression in RPE-choroid tissue was examined by quantitative RT-PCR 7 days after laser injury. VEGF and PDGF mRNA expression was increased in the OX-LDL-injected group when compared with the PBS group ($P < 0.01$, $n = 10$; Figures 4(a) and 4(b)), meanwhile angiostatin mRNA expression was

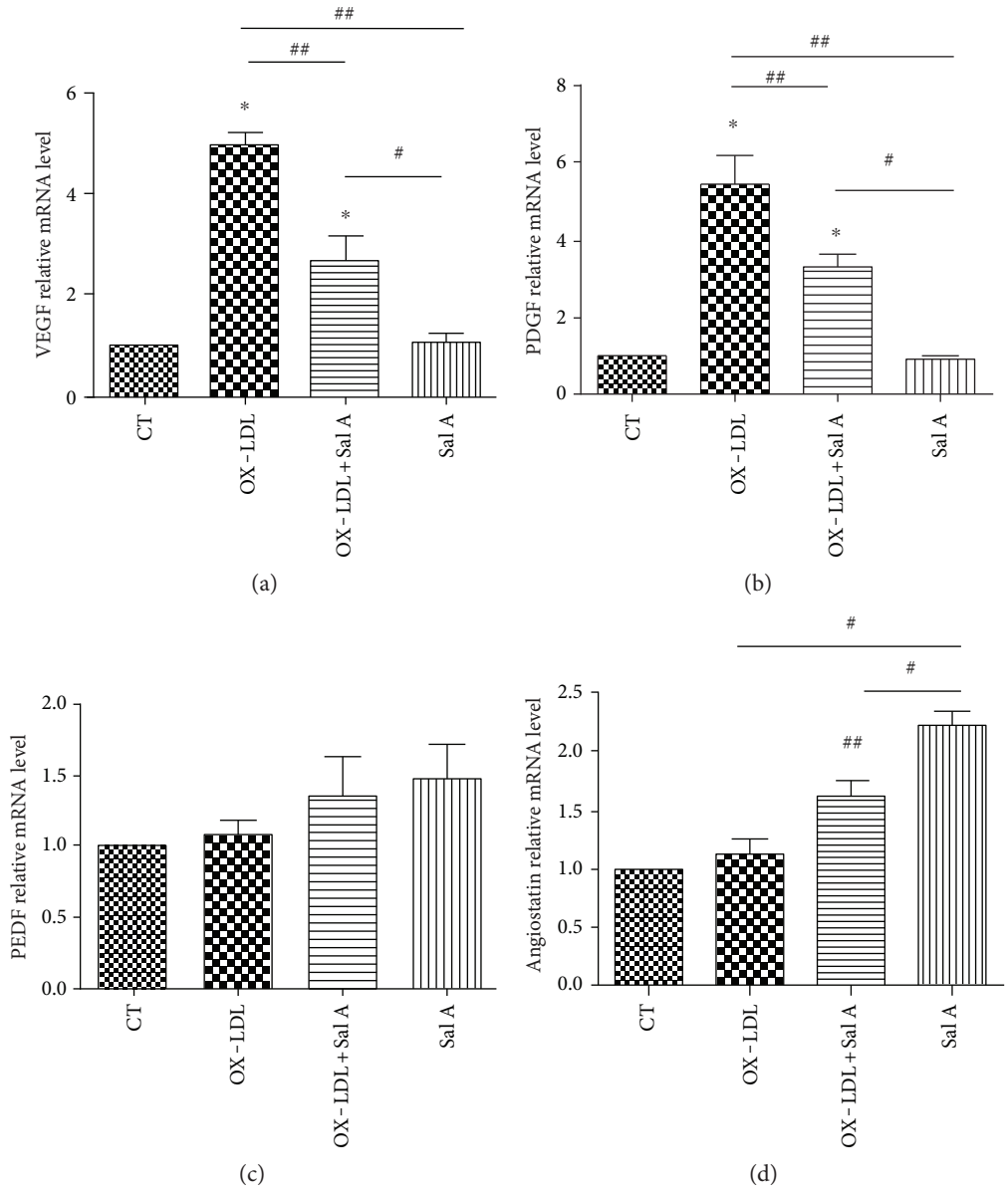

Figure 4: Real-time PCR analysis of VEGE, PDGF, PEDF, and angiostatin mRNA expression in four groups 7 days after laser. (a, b) OX-LDL injection increased both VEGF and PDGF mRNA expression compared with the PBS group, while OX-LDL + Sal A group reduced VEGF and PDGF mRNA expression compared with the OX-LDL group. (c) There was no difference between each group in PEDF gene expression. (d) The OX-LDL + Sal A group and Sal A group increased angiostatin gene expression compared with the PBS and OX-LDL groups. Data were expressed as mean ± SEM ($n = 10$ eyes/group). $^{*}P < 0.05$ versus the control group. $^{\#\#}P < 0.05$ versus the OX-LDL group. $^{\#}P < 0.05$ versus the Sal A group.

increased in the Sal A-pretreated group ($P < 0.05$, $n = 10$; Figure 4(d)). VEGF/PDGF mRNA lvels were decreased, and angiostatin was increased in the Sal A + OX-LDL group when compared with the OX-LDL group ($P < 0.01$, $n = 10$; Figure 4(d)).There was no significant difference in PEDF mRNA level between each group (Figure 4(c)).

4.4. Effects of OX-LDL and Sal A on Modulating Angiogenesis Proteins In Vitro. In order to further explore the possible relationship between CNV progression and OX-LDL, we analyzed angiogenesis protein levels secreted by ARPE-19 cells after OX-LDL and Sal A stimulation. Western blot and ELISA were performed to evaluate VEGF, PDGF, PEDF, and angiostatin concentrations 24 and 48 hours after OX-LDL (with or without Sal A) stimulation. No significant change in any of these proteins has been detected in any of these groups at 24 hours. Comparing with the control, VEGF and PDGF were increased in the OX-LDL group, while VEGF/PDGF were decreased and antiangiostatin level was sligtly increased in the OX-LDL + Sal A (50 μM) group than the OX-LDL group at 48 hours poststimulation ($P < 0.01$, Figures 5(a)–5(c) and 5(e)). There was no significant change in the PEDF level among the three groups (Figure 5(d)).

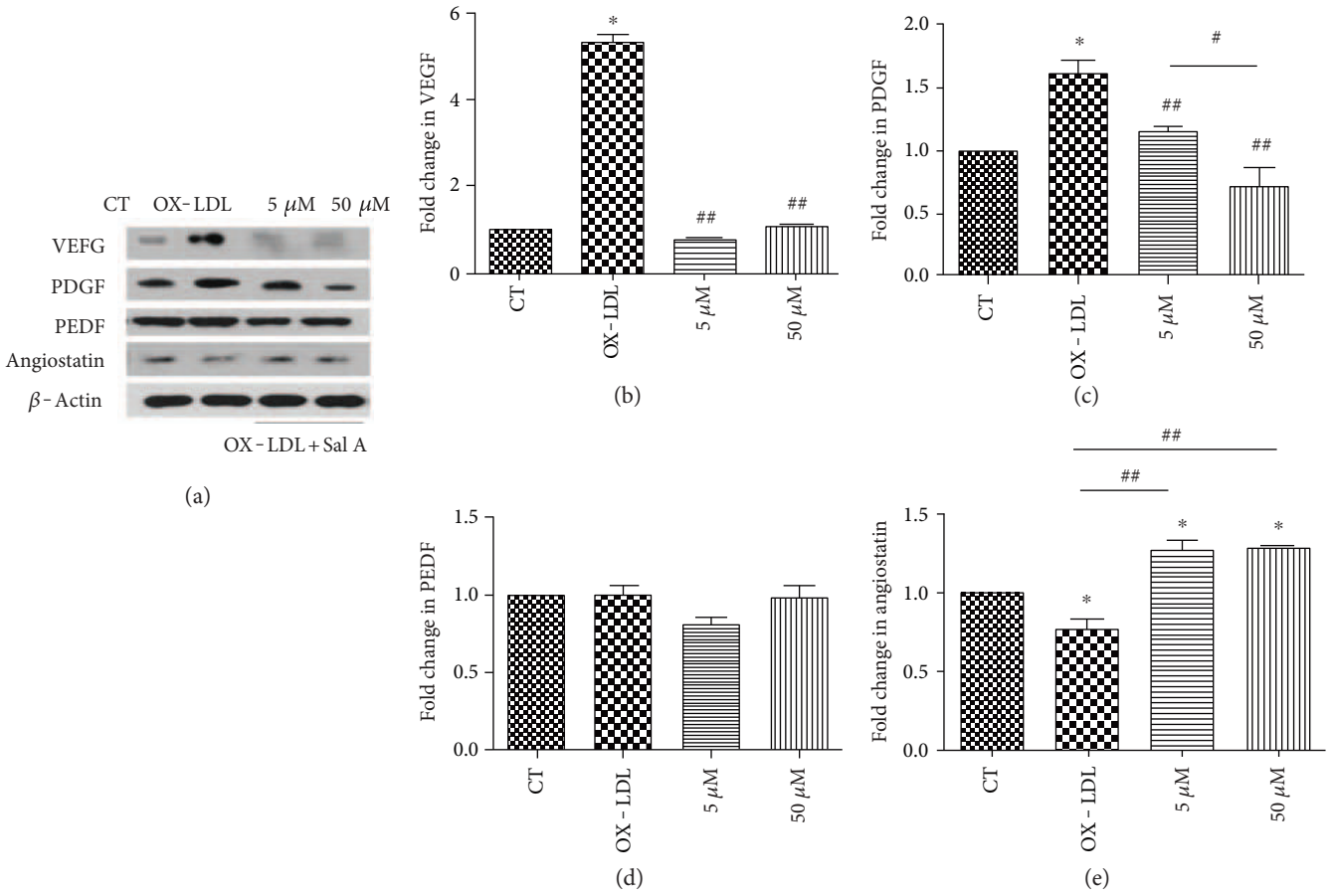

Figure 5: Angiogenesis proteins expression in ARPE-19 cells after OX-LDL and Sal A treatment. ARPE-19 cells were divided into control, OX-LDL(100 mg/L), and OX-LDL (100 mg/L) + Sal A (5 μM/50 μM) groups and cultured for 48 hours. (a) Western blot showing changes in VEGF, PDGF, PEDF, and antiangiostatin in ARPE-19 cells 48 hours after treatment. (b–e) Quantitative densitometry results showing that OX-LDL increased VEGF and PDGF levels compared with the control group, while the OX-LDL + Sal A group decreased VEGF/PDGF and slightly increased antiangiostatin level compared with the OX-LDL group. There was no significant difference between each group in PEDF level. Data were expressed as mean ± SEM. $^{*}P < 0.05$ versus the control group. $^{\#\#}P < 0.05$ versus the OX-LDL group. $^{\#}P < 0.05$ versus the Sal A group.

4.5. Effects of OX-LDL and Sal A on Tube Formation and RPE Cell Junctions. We also investigated the effects of OX-LDL and Sal A on angiogenesis process by examining vascular endothelial tube formation in vitro. Human umbilical vein endothelial cells (HUVECs) were divided into three groups: control, OX-LDL(100 mg/L), and OX-LDL + Sal A (50 μM) groups. We observed capillary/tube-like structures as early as 3 hours after plating cells onto matrigel, and the structures were more evident 6 hours after plating. The tube formation was promoted in the OX-LDL group when compared with the control. This promoted tube formation induced by OX-LDL was remarkably impaired in the OX-LDL + Sal A group. By measuring the cumulative tube length, we found that OX-LDL promotes tube formation by 43% and 63%, compared with the control and OX-LDL + Sal A groups 6 hours after plating, respectively (Figures 6(a) and 6(b)).

Additionally, to visualize the integrity of the RPE structure, zonula occludens-1 (ZO-1) staining was performed. Immunocytochemistry analysis revealed the more disturbed structures of RPE junctions in the OX-LDL group than the control, while Sal A pretreatment protected RPE junctions from disruption (Figure 7), suggesting that continuous treatment of OX-LDL adversely affects cell adhesion and Sal A can protect RPE cells against degeneration.

4.6. CYLD Involves in OX-LDL-Induced Proangiogenic Process. Based on a previous study showing that CYLD regulates vascular endothelial cell migration and angiogenesis in HUVECs [16], we hypothesized that CYLD may also promote angiogenesis in a CNV model. Hence, we first examined CYLD in cross sections of CNV lesions by immunofluorescence. Prominent CYLD fluorescence was visualized in the retina and choroid, which was enhanced in CNV focus 7 days after laser injury (Figure 8(a)). Interestingly, fluorescence intensity in the OX-LDL + Sal A group was lower than that in the OX-LDL group, while no difference was found between the PBS and Sal A group ($P < 0.05$, $n = 10$ eyes/group, Figure 8(e)). Consistent with findings in animal experiments, immunocytochemistry and western blot results in ARPE-19 cells also showed higher CYLD expression in the OX-LDL group than control. The CYLD staining and protein expression were lower in the

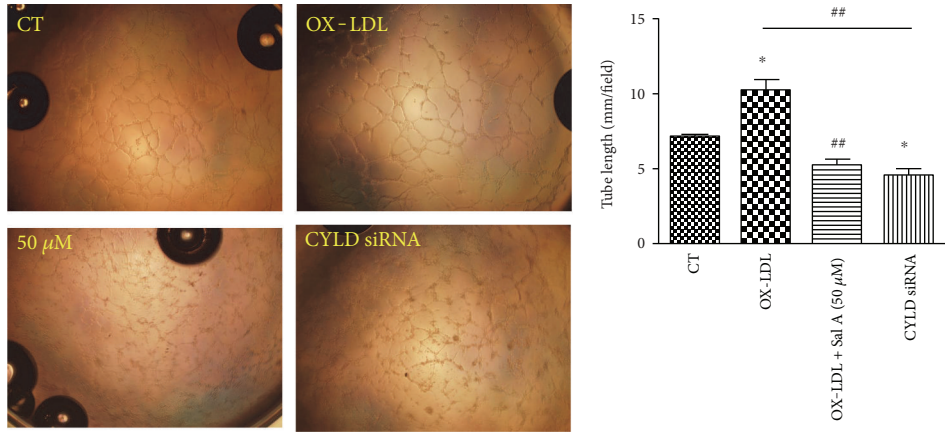

Figure 6: OX-LDL promotes endothelial tube formation and Sal A impairs this process. (a) HUVEC cells were plated onto matrigel and treated with SFM, OX-LDL (100 mg/L), and OX-LDL + Sal A (50 μM); photographs were taken 6 hours later. Objective lens used was A-Plan 10x/0.25 NA dry (Carl Zeiss Inc.). Experiments were performed as in panel (b), and the cumulative tube length was measured. Data are expressed as the mean ± SEM; each experiments was performed in triplicate ($^{*}P < 0.05$ versus the control; $^{\#\#}P < 0.05$ versus the OX-LDL group).

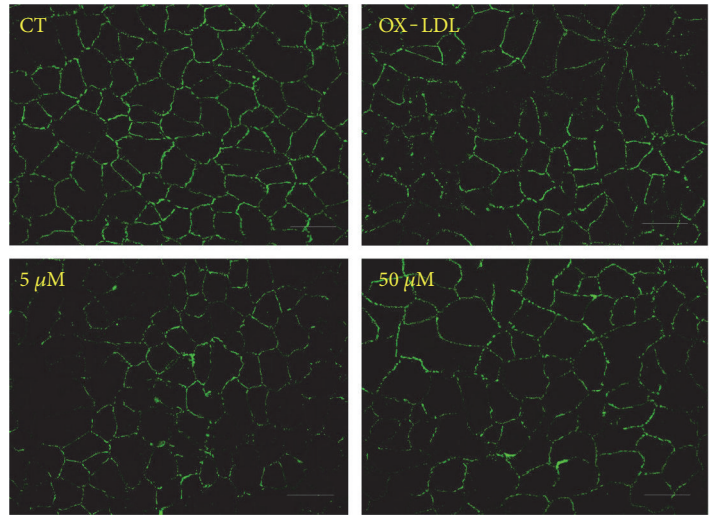

Figure 7: Effects of OX-LDL and Sal A on RPE cell junctions. ARPE-19 cells were classified and treated as before. ZO-1 was stained after treatment with SFM, OX-LDL (100 mg/L), and OX-LDL (100 mg/L) + Sal A (5 μM/50 μM) for 48 hours. Representative images of ZO-1 fluorescence showing that OX-LDL induced RPE cell junction disruption and Sal A pretreatment protected cell junction integrity. Scale bar = 50 μm.

OX-LDL + Sal A group than OX-LDL group after culturing for 48 hours ($P < 0.01$, Figures 8(b)–8(d) and 8(f)), revealing that OX-LDL increases CYLD level and Sal A antagonizes OX-LDL by downregulating CYLD.

Next, we investigated whether CYLD involves in modulating OX-LDL-induced angiogenesis process by using CYLD siRNA. As shown in Figure 9, silencing CYLD by siRNA remarkably blocked OX-LDL-induced VEGF secretion compared with the control. Tube formation experiment also proved that silencing CYLD mRNA decreased the tube length of HUVECs after OX-LDL stimulation (Figure 6(a)).

4.7. Sal A Modulates CYLD via PI3K/Akt/mTOR Pathway. Our prior study demonstrated Sal A pretreatment promoted ERK and PI3K/Akt/mTOR activation in RPE cells after OX-LDL stimulation (see also data in Figure 10(a)). Thus, we tested if Sal A modulates CYLD through ERK or PI3K/Akt/mTOR pathway. As shown in Figures 10(b) and 10(c), there was no significant change of CYLD expression after the pretreatment with ERK inhibitor, but pretreatments with PI3K and mTOR inhibitor LY294002 and rapamycin markedly blocked the inhibition effect in CYLD level by Sal A, suggesting that Sal A regulates CYLD via PI3K/Akt/mTOR pathway.

4.8. Sal A Restrains Angiogenesis by Promoting P62-CYLD-TRAF6 Interactions. CYLD is a deubiquitinating enzyme (DUB) and recently found to physically interact with P62

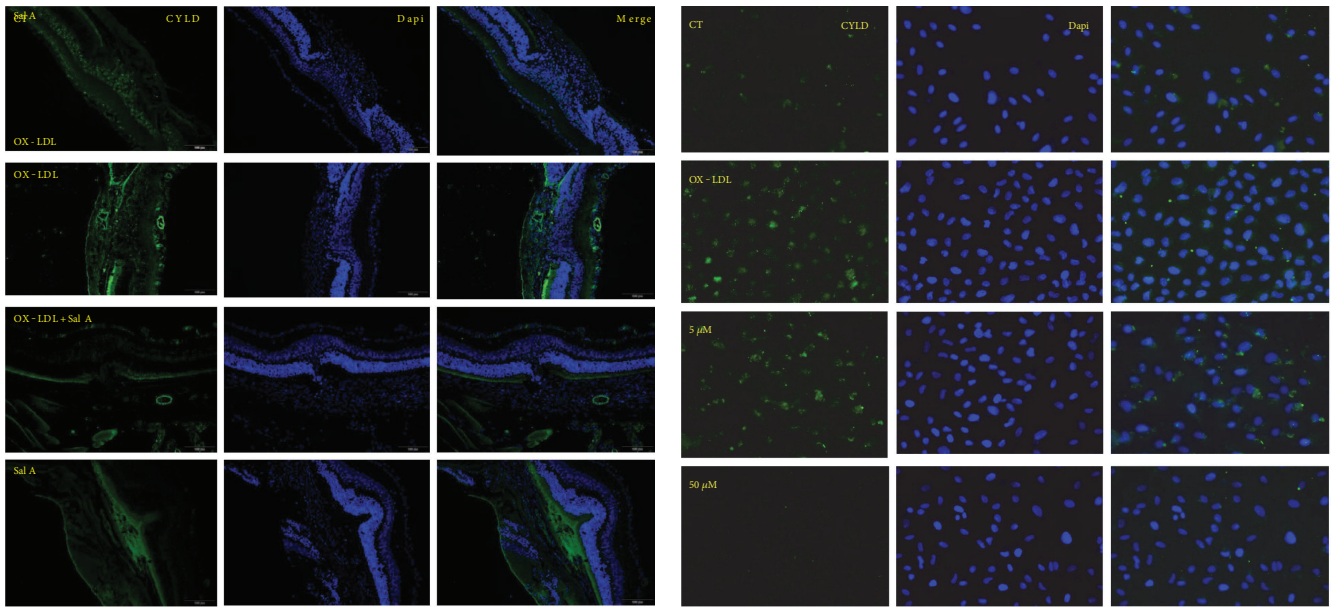

(a) (b)

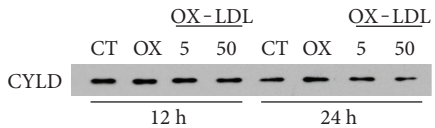

(c)

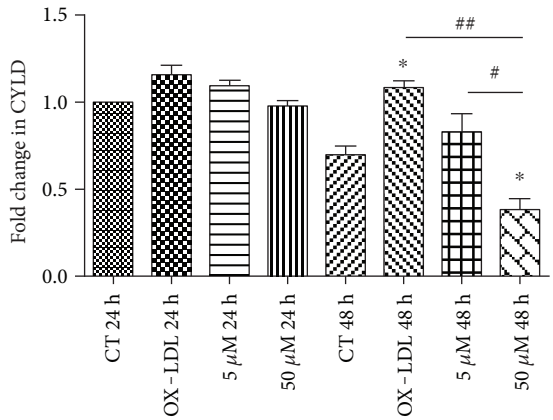

(d)

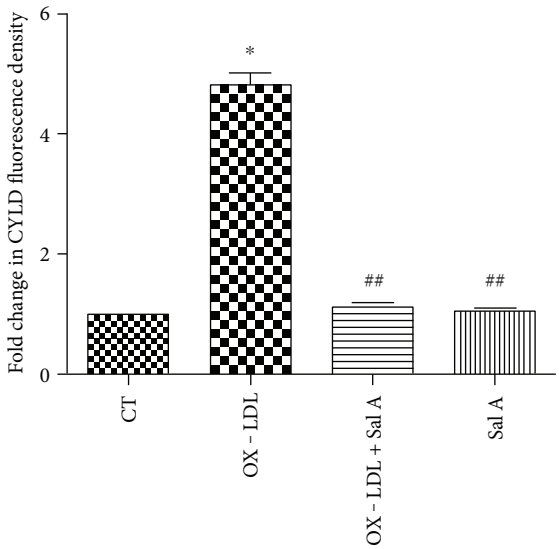

(e)

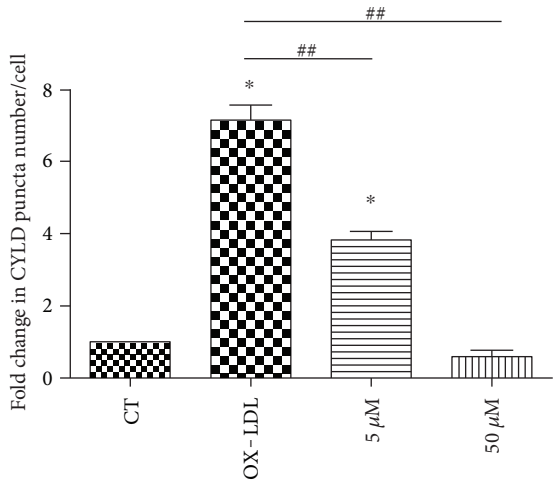

(f)

Figure 8: Continued.

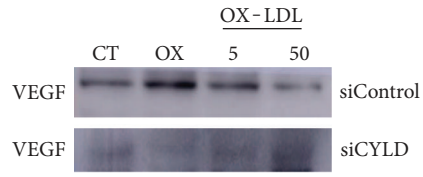

(g)

Figure 8: CYLD involves in OX-LDL-induced angiogenic process. C57 mice and ARPE-19 cells were treated as before. (a) Representative immunofluorescence images of CYLD in RPE/choroid of animal 7 days after laser. (b) Representative immunocytochemistry images of CYLD in ARPE-19 cells 48 hours after treatment with SFM, OX-LDL (100 mg/L), and OX-LDL (100 mg/L) + Sal A (50 μM). (c, d) Western blot result of ARPE-19 cells showing that CYLD was increased in the OX-LDL group compared with the control and decreased in the OX-LDL + Sal A group compared with the OX-LDL group. (e, f) Quantitative fluorescence density results showing that CYLD fluorescence was prominent in CNV focus and higher density was found in the OX-LDL group than the control and OX-LDL + Sal A groups. (g) ARPE-19 cells were transfected with CYLD siRNA or siControl and then cultured as before for 24 hours. Western blot results showing that CYLD knockdown inhibited OX-LDL VEGF secretion. Data are expressed as the mean ± SEM ($n = 10$ eyes/group; $n = 40$ cells/group). $^{*}P < 0.05$ versus the control group. $^{\#}P < .05$ versus OX-LDL + Sal A (5 μM) group after 48 hours. $^{\#\#}P < 0.05$ versus the OX-LDL group.

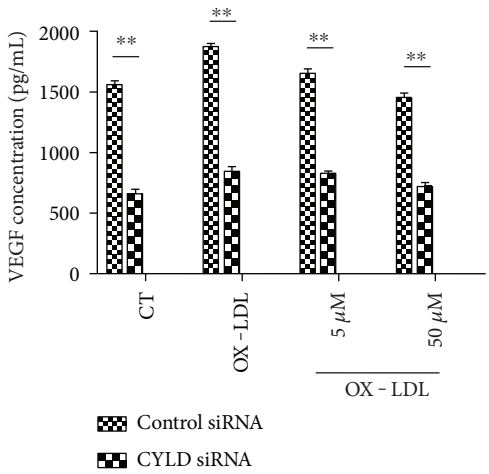

Figure 9: CYLD modulates VEGF level in RPE cells. ARPE-19 cells were transfected with CYLD siRNA or Control siRNA and then cultured as before for 24 hours. ELISA results showing VEGF concentrations in different groups. Data are expressed as mean ± SEM ($n = 4$). $^{**}P < 0.01$ versus control siRNA.

and TRAF6, then negatively regulates TRAF6 function [26]. TRAF6 is a master signaling molecule controlling multiple downstream pathways. Ubiquitination of TRAF6 plays an important role in its signaling function [27]. TRAF6 ubiquitination has been demonstrated to mediate human microvascular endothelial cell sprouting [28] and cancer angiogenesis [29]. Considering that TRAF6 induces angiogenesis and TRAF6 function is regulated by CYLD, we hypothesized that Sal A may also inhibit angiogenesis by promoting CYLD-TRAF6 interaction. Coimmunoprecipitation result (Figures 11(a)–11(c)) reveals apparent P62-CYLD-TRAF6 interaction in the Sal A + OX-LDL group than that in the OX-LDL group. Sal A pretreatment inhibited ubiquitination of TRAF6, which on the on the other side is activated by OX-LDL stimulation. Collectively, the above data demonstrate that Sal A antagonizes the proangiogenesis effect of OX-LDL by decreasing CYLD level and promoting P62-CYLD-TRAF6 interaction in RPE cells.

5. Discussion

Previous studies have shown that oxidative stress contributes to AMD progression [30, 31]. We have demonstrated that OX-LDL induces chronic RPE cell inflammation, which is the pathogenesis of nonexudative AMD. Studies described here reveal that OX-LDL injection deteriorates laser-induced CNV progression in a mouse model. Meanwhile, OX-LDL stimulation disrupts RPE barrier and induces VEGF/PDGF secretion in ARPE-19 cells, which further indicates the pathogenic mechanism of lipid oxidation to exudative AMD. Clinical trials have revealed the association between serum lipid levels and AMD [32]. However, little is known about oxidative damage of OX-LDL to CNV pathology in vivo. We developed an animal model with high circulating serum lipoprotein level by injecting OX-LDL intravenously and verified its availability in monitoring its chronic oxidative damage to the RPE layer [10]. To our knowledge, this is the first study investigating CNV pathology using OX-LDL in animals.

Sal A is extracted from Chinese medicine *Salvia miltiorrhiza* Bunge (Danshen), which has been widely used in treating vascular diseases. Sal A scavenges free radicals and inhibits lipid and thiol peroxidation in rat liver mitochondria [33]. Hui Zhang et al. demonstrated that Sal A protects RPE cells from H_2O_2-induced damage by activating Nrf2/Ho-1 [34]. In our study, Sal A has been proven to antagonize OX-LDL by reducing CNV volume and VEGF/PDGF levels. Sal A also increases antiangiostatin level, protects RPE cell junction integrity, and inhibits tube formation in HUVECs, which are inversely influenced after OX-LDL stimulation. All above evidences the inhibiting mechanism of Sal A on CNV progression.

We also demonstrated that Sal A modulates angiogenesis process by decreasing CYLD level and promoting P62-CYLD-TRAF6 interaction. CYLD is mechanistically linked to vascular endothelial barrier function [35] and anti-VEGF therapy in cancer [14]. Liu et al. [36] proved the contribution of CYLD to vascular diseases. TRAF6 also functions in promoting tumor angiogenesis [37]. Choi et al. [38] found that IL-33 induces angiogenesis and vascular leakage through TRAF6. In this research, *CYLD* gene knockdown abolished

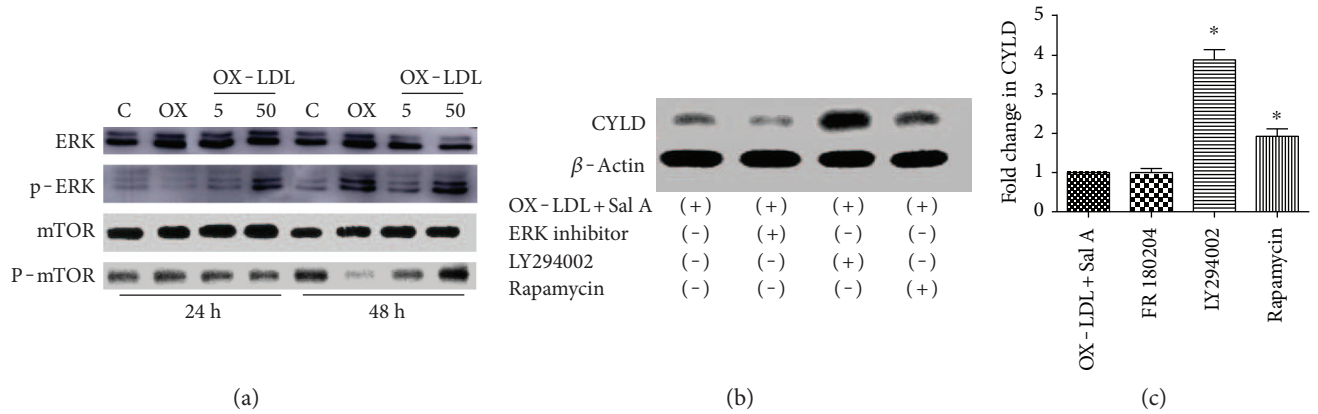

Figure 10: Sal A modulates CYLD via PI3K/AKT/mTOR pathway. (a) Our former study proved that Sal A promoted ERK and PI3K/AKT/mTOR phosphorylation in ARPE-19 cells after 48 hours. (b) Western blot results of CYLD showing that PI3k and mTOR inhibitor abolished Sal A-induced CYLD downregulation. (c) Quantitative densitometry results of western blot. Data are expressed as means ± ESM. $^*P < 0.05$ versus the control and OX-LDL + Sal A group.

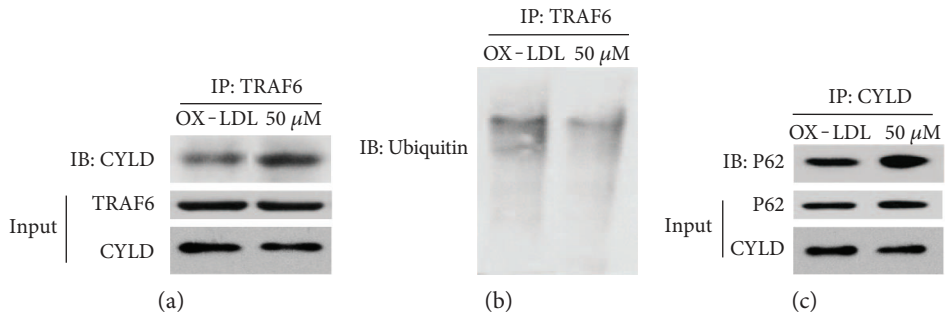

Figure 11: Sal A promotes P62-CYLD-TRAF6 interaction. (a) ARPE-19 cells were classified and treated as before. Coimmunoprecipitation assay was to determine P62-CYLD-TRAF6 interaction 48 hours after Sal A and/or OX-LDL stimulation. (a) TRAF6 was isolated by IP followed by detection of the associated CYLD by IB. The cell lysates were subjected to IB to monitor the expression of CYLD and TRAF6. (b)TRAF6 was isolated by IP, and its ubiquitination form was detected by IB. (c) Endogenous CYLD was isolated by IP followed by IB to detect the associated P62. P62 and CYLD protein expressions in cell lysates were monitored by direct IB. Compared to the OX-LDL group, the OX-LDL + Sal A group induced P62-CYLD TRAF6 interaction and promoted deubiquitination of TRAF6.

OX-LDL-induced tube formation in HUVECs and VEGF secretion in ARPE-19 cells. Sal A pretreatment inhibited OX-LDL-induced CYLD upregulation. Furthermore, the downregulation of CYLD by Sal A may be dependent on PI3K/Akt/mTOR, but not ERK. Specifically, as suggested by Jin et al. [26], deubiquitinating enzyme CYLD negatively regulated TRAF6 ubiquitination by interacting with P62 and subsequently inhibited proangiogenesis function of TRAF6. Co-IP results in our study presented that Sal A remarkably promotes P62-CYLD-TRAF6 interaction. Thus, CYLD appears to play dual roles in angiogenesis pathology: facilitating tube formation and promoting VEGF expression, meanwhile negatively regulating TRAF6 function via P62-CYLD-TRAF6 interaction.

Although our study reveals strong evidence for the pathogenic roles of OX-LDL and therapeutical effects of Sal A in age-related macular degeneration, there are still some limitations that must be addressed. First, there is a lack of direct data showing serum LDL concentration in AMD patients, especially after Sal A treatment. Moreover, further research is needed to elucidate how TRAF6 alters CNV progression and its relationship with Sal A.

In summary, our study demonstrated that increased OX-LDL level in serum has significant effects on CNV progression. Our findings also indicate pharmaceutical effects of Sal A against CNV progression. The mechanistic insights described here lay the foundation for an exciting opportunity to explore a specific concept for drug repurposing, with application to the field of exudative AMD.

Abbreviations

AMD: Age-related macular degeneration
CNV: Choroidal neovascularization
CYLD: Cylindromatosis
FFA: Fundus fluorescein angiography
HUVECs: Human umbilical vein endothelial cells
OX-LDL: Oxidized low-density lipoprotein
PDGF: Platelet-derived growth factor
PEDF: Pigment epithelium-derived factors

ROS: Reactive oxygen species
RPE: Retinal pigment epithelium
Sal A: Salvianolic acid A
SFM: Serum-free medium
VEGF: Vascular endothelial growth factor
ZO-1: Zonula occludens-1.

Conflicts of Interest

The authors declare that they have no financial or personal relationships with other people or organizations that can inappropriately influence their work. There is no professional or other personal interest of any nature or kind in any product, service, and/or company that could be construed as influencing the position presented in, or the review of, the Manuscript entitled "Salvianolic Acid A Inhibits OX-LDL Effects on Exacerbating Choroidal Neovascularization via Down-regulating CYLD."

Authors' Contributions

Professor XingWei Wu conceived of the study and participated in its design and coordination and helped to draft the manuscript. Dr. Ke Mao participated in the design and operation of this experiment, drafted the manuscript, and performed the statistical analysis and interpretation of data. All authors read and approved the final manuscript.

Acknowledgments

This work was supported by a grant from Shanghai Natural Science Foundation (14401972600). The authors would like to thank Qing Gu for excellent technical support.

References

[1] N. Sengupta, A. Afzal, S. Caballero, K. H. Chang, L. C. Shaw, and J. J. Pang, "Paracrine modulation of CXCR4 by IGF-1 and VEGF: implications for choroidal neovascularization," *Investigative Ophthalmology & Visual Science*, vol. 51, no. 5, pp. 2697–2704, 2010.

[2] J. Liu, D. A. Copland, S. Theodoropoulou et al., "Impairing autophagy in retinal pigment epithelium leads to inflammasome activation and enhancedmacrophage-mediated angiogenesis," *Scientific Reports*, vol. 6, article 20639, 2016.

[3] K. Kim, S. W. Park, J. H. Kim et al., "Genome surgery using Cas9 ribonucleoproteins for the treatment of age-related macular degeneration," *Genome Research*, vol. 27, no. 3, pp. 419–426, 2017.

[4] H. Du, X. Xiao, T. Stiles, C. Douglas, D. Ho, and P. X. Shaw, "Novel mechanistic interplay between products of oxidative stress and components of the complement system in AMD pathogenesis," *Open Journal of Ophthalmology*, vol. 6, no. 1, pp. 43–50, 2016.

[5] S. G. Jarrett and M. E. Boulton, "Consequences of oxidative stress in age-related macular degeneration," *Molecular Aspects of Medicine*, vol. 33, no. 4, pp. 399–417, 2012.

[6] M. H. Davari, H. Gheitasi, G. Yaghobi, and B. Heydari, "Correlation between serum lipids and age-related macular degeneration: a case-control study," *Journal of Research in Health Sciences*, vol. 13, no. 1, pp. 98–101, 2013.

[7] K. J. A. Davis, *Oxidative Damage and Repair: Chemical, Biological and Medical Aspects*, pp. 99–109, Pergamon Press, Oxford/New York, 1991.

[8] S. Capra, J. Bauer, W. Davidson, and S. Ash, "Nutritional therapy for cancer-induced weight loss," *Nutrition in Clinical Practice*, vol. 17, no. 4, pp. 210–213, 2002.

[9] M. Kamei, K. Yoneda, N. Kume et al., "Scavenger receptors for oxidized lipoprotein in age-related macular degeneration," *Investigative Ophthalmology & Visual Science*, vol. 48, no. 4, pp. 1801–1807, 2007.

[10] L. Yin, Y. Shi, X. Liu et al., "A rat model for the study of the biological effects of circulating LDL in the choriocapillaris–BrM–RPE complex," *The American Journal of Pathology*, vol. 180, no. 2, pp. 541–549, 2012.

[11] Q. Yating, Y. Yuan, Z. Wei et al., "Oxidized LDL induces apoptosis of human retinal pigment epithelium through activation of ERK-Bax/Bcl-2 signaling pathways," *Current Eye Research*, vol. 40, no. 4, pp. 415–422, 2015.

[12] R. A. Qin, X. X. Yao, and Z. Y. Huang, "Effects of compound danshen tablets on spatial cognition and expression of brain beta-amyloid precursor protein in a rat model of Alzheimer's disease," *Journal of Traditional Chinese Medicine*, vol. 32, no. 1, pp. 63–66, 2012.

[13] K. S. Oh, B. K. Oh, J. Mun, H. W. Seo, and B. H. Lee, "Salvianolic acid a suppress lipopolysaccharide-induced NF-kappaB signaling pathway by targeting IKKβ," *International Immunopharmacology*, vol. 11, no. 11, pp. 1901–1906, 2011.

[14] J. Guo, S. Shinriki, Y. Su et al., "Hypoxia suppresses cylindromatosis (CYLD) expression to promote inflammation in glioblastoma: possiblelink to acquired resistance to anti-VEGF therapy," *Oncotarget*, vol. 5, no. 15, pp. 6353–6364, 2014.

[15] S. C. Sun, "CYLD: a tumor suppressor deubiquitinase regulating NF-kappaB activation and diverse biological processes," *Cell Death and Differentiation*, vol. 17, no. 1, pp. 25–34, 2010.

[16] J. Gao, L. Sun, L. Huo, M. Liu, D. Li, and J. Zhou, "CYLD regulates angiogenesis by mediating vascular endothelial cell migration," *Blood*, vol. 115, no. 20, pp. 4130–4137, 2010.

[17] F. Ye, H. Kaneko, Y. Nagasaka et al., "Plasma-activated medium suppresses choroidal neovascularization in mice: a new therapeutic concept for age-related macular degeneration," *Scientific Reports*, vol. 5, article 7705, 2015.

[18] J. Guo, X. Luo, J. Liang, M. Xiao, and X. Sun, "Antiangiogenic effects of doxazosin on experimental choroidal neovascularization in mice," *Journal of Ocular Pharmacology and Therapeutics*, vol. 33, no. 1, pp. 50–56, 2017.

[19] D. Tomida, K. M. Nishiguchi, K. Kataoka, T. R. Yasuma, E. Iwata, and R. Uetani, "Suppression of choroidal neovascularization and quantitative and qualitative inhibition of VEGF and CCL2 byheparin," *Investigative Ophthalmology & Visual Science*, vol. 52, no. 6, pp. 3193–3199, 2011.

[20] Y. J. Yu, B. Mo, L. Liu, Y. K. Yue, C. L. Yue, and W. Liu, "Inhibition of choroidal neovascularization by lentivirus-mediated PEDF gene transfer in rats," *International Journal of Ophthalmology*, vol. 9, no. 8, pp. 1112–1120, 2016.

[21] R. S. Sulaiman, S. Merrigan, J. Quigley et al., "A novel small molecule ameliorates ocular neovascularisation and synergises with anti-VEGF therapy," *Scientific Reports*, vol. 6, article 25509, 2016.

[22] Y. Y. Shi, Y. S. Wang, Z. X. Zhang et al., "Monocyte/macrophages promote vasculogenesis in choroidal neovascularization

in mice by stimulating SDF-1expression in RPE cells," *Graefe's Archive for Clinical and Experimental Ophthalmology*, vol. 249, no. 11, pp. 1667–1679, 2011.

[23] G. Velez, A. R. Weingarden, B. A. Tucker, H. Lei, A. Kazlauskas, and M. J. Young, "Retinal pigment epithelium and Müller progenitor cell interaction increase Müller progenitor cell expression of PDGFRα and ability to induce proliferative vitreoretinopathy in a rabbit model," *Stem Cells International*, vol. 2012, Article ID 106486, 6 pages, 2012.

[24] M. Bergmann, F. Holz, and J. Kopitz, "Lysosomal stress and lipid peroxidation products induce VEGF-121 and VEGF-165 expression in ARPE-19 cells," *Graefe's Archive for Clinical and Experimental Ophthalmology*, vol. 249, no. 10, pp. 1477–1483, 2011.

[25] S. G. Jarrett, H. Lin, B. F. Godley, and M. E. Boulton, "Mitochondrial DNA damage and its potential role in retinal degeneration," *Progress in Retinal and Eye Research*, vol. 27, no. 6, pp. 596–607, 2008.

[26] W. Jin, M. Chang, E. M. Paul et al., "Deubiquitinating enzyme CYLD negatively regulates RANK signaling and osteoclastogenesis in mice," *The Journal of Clinical Investigation*, vol. 118, no. 5, pp. 1858–1866, 2008.

[27] B. Lamothe, W. K. Webster, A. Gopinathan, A. Besse, A. D. Campos, and B. G. Darnay, "TRAF6 ubiquitin ligase is essential for RANKL signaling and osteoclast differentiation," *Biochemical and Biophysical Research Communications*, vol. 359, no. 4, pp. 1044–1049, 2007.

[28] I. Pollet, C. J. Opina, C. Zimmerman, K. G. Leong, F. Wong, and A. Karsan, "Bacterial lipopolysaccharide directly induces angiogenesis through TRAF6-mediated activation of NF-kappaB and c-Jun N-terminal kinase," *Blood*, vol. 102, no. 5, pp. 1740–1742, 2003.

[29] H. Sun, X. B. Li, Y. Meng, L. Fan, and M. Li, "Fang J.TRAF6 upregulates expression of HIF-1α and promotes tumor angiogenesis," *Cancer Research*, vol. 73, no. 15, pp. 4950–4959, 2013.

[30] N. Golestaneh, Y. Chu, S. K. Cheng, H. Cao, E. Poliakov, and D. M. Berinstein, "Repressed SIRT1/PGC-1α pathway and mitochondrial disintegration in iPSC-derived RPE disease model of age-related macular degeneration," *Journal of Translational Medicine*, vol. 14, no. 1, p. 344, 2016.

[31] W. J. Chen, C. Wu, Z. Xu, Y. Kuse, H. Hara, and E. J. Duh, "Nrf2 protects photoreceptor cells from photo-oxidative stress induced by blue light," *Experimental Eye Research*, vol. 154, pp. 151–158, 2017.

[32] Y. Wang, M. Wang, X. Zhang et al., "The association between the lipids levels in blood and risk of age-related macular degeneration," *Nutrients*, vol. 8, no. 10, 2016.

[33] X. J. Wang, Z. B. Wang, and J. X. Xu, "Effect of salvianic acid a on lipid peroxidation and membrane permeability in mitochondria," *Journal of Ethnopharmacology*, vol. 97, no. 3, pp. 441–445, 2005.

[34] H. Zhang, Y.-y. Liu, Q. Jiang et al., "Salvianolic acid a protects RPE cells against oxidative stress through activation of Nrf2/HO-1 signaling," *Free Radical Biology and Medicine*, vol. 69, pp. 219–228, 2014.

[35] L. R. Klei, D. Hu, R. Panek et al., "MALT1 protease activation triggers acute disruption of endothelial barrier integrity via CYLD cleavage," *Cell Reports*, vol. 17, no. 1, pp. 221–232, 2016.

[36] S. Liu, J. Lv, L. Han et al., "A pro-inflammatory role of deubiquitinating enzyme cylindromatosis (CYLD) in vascular smooth muscle cells," *Biochemical and Biophysical Research Communications*, vol. 420, no. 1, pp. 78–83, 2012.

[37] K. C. Chen, W. Y. Lee, H. Y. Chen, and C. Y. Chen, "In silico investigation of potential TRAF6 inhibitor from traditional Chinese medicine against cancers," *BioMed Research International*, vol. 2014, Article ID 429486, 14 pages, 2014.

[38] Y. S. Choi, H. J. Choi, J. K. Min et al., "Interleukin-33 induces angiogenesis and vascular permeability through ST2/TRAF6-mediated endothelial nitric oxide production," *Blood*, vol. 114, no. 14, pp. 3117–3126, 2009.

Hindawi
Oxidative Medicine and Cellular Longevity
Volume 2017, Article ID 1703810, 18 pages
https://doi.org/10.1155/2017/1703810

Review Article

Involvement of Nrf2 in Ocular Diseases

Shehzad Batliwala,[1] Christy Xavier,[2] Yang Liu,[2,3] Hongli Wu,[2,3] and Iok-Hou Pang[2,3]

[1]*Texas College of Osteopathic Medicine, University of North Texas Health Science Center, Fort Worth, TX 76107, USA*
[2]*Department of Pharmaceutical Sciences, University of North Texas Health Science Center, Fort Worth, TX 76107, USA*
[3]*North Texas Eye Research Institute, University of North Texas Health Science Center, Fort Worth, TX 76107, USA*

Correspondence should be addressed to Hongli Wu; hongli.wu@unthsc.edu and Iok-Hou Pang; iok-hou.pang@unthsc.edu

Received 5 January 2017; Accepted 14 March 2017; Published 3 April 2017

Academic Editor: Marialaura Amadio

The human body harbors within it an intricate and delicate balance between oxidants and antioxidants. Any disruption in this checks-and-balances system can lead to harmful consequences in various organs and tissues, such as the eye. This review focuses on the effects of oxidative stress and the role of a particular antioxidant system—the Keap1-Nrf2-ARE pathway—on ocular diseases, specifically age-related macular degeneration, cataracts, diabetic retinopathy, and glaucoma. Together, they are the major causes of blindness in the world.

1. Introduction

Free radicals such as reactive oxygen species (ROS) are oxidants that are normally produced as a by-product of normal aerobic metabolism [1]. In addition to endogenous and metabolic production of ROS, environmental sources such as light, smoke, and heavy metals also contribute to increased ROS burden [2–7]. An excessive level of ROS damages many cellular and tissue components. In the eye, these can adversely affect vision. Antioxidants are molecules that reduce ROS and keep the oxidative damage at a minimum. In the human cell, antioxidant molecules include both nonenzymatic compounds such as glutathione (GSH), thioredoxin (Trx), ascorbate, α-tocopherol, β-carotene, and coenzyme Q10 and enzymes such as catalase, glutathione peroxidase, and superoxide dismutase (SOD) [8]. Antioxidant systems in the cell can be categorized into two consecutive phase reactions: phase I and phase II reactions [9–11]. Phase I reactions are reduction-oxidation (redox) reactions carried out via the cytochrome P450 enzyme system. Phase I products are then conjugated with hydrophilic molecules such as GSH in the phase II reactions. The molecules that catalyze phase II reactions can be further classified as "direct" or "indirect." "Direct" antioxidants include SOD1 and GSH, which directly quench ROS. "Indirect" antioxidants serve to synthesize and recycle GSH and Trx, which are the two most important ROS quenchers. Imbalance between oxidants and antioxidants in favor of oxidants leads to oxidative stress. This imbalance has at least two direct consequences: damage to individual components of the living cell and induction of inflammatory pathways that further perpetuate the damage. Oxidative stress can denature lipids and proteins [10, 12–14], as well as induce DNA and RNA fragmentation [15–17], leading to cell dysfunction, injury, and death. In addition, an excess of oxidative free radicals also increases the expression of proinflammatory genes and activates the inflammation process [18, 19]. Inflammation often exacerbates the oxidative stress, creating a self-perpetuating, vicious cycle of oxidation and inflammation [20, 21].

The Keap1-Nrf2-ARE pathway plays a critical role in the regulation of a comprehensive and protective antioxidant response [22]. Nuclear factor erythroid-2-related factor 2 (Nrf2) is a transcription factor that is upregulated in times of oxidative stress. It puts in place a sequence of events that ultimately protect the cell from oxidative injury. Nrf2 activates transcription of antioxidant enzymes by binding to the antioxidant response element (ARE) in the promoter regions of its target genes [23, 24]. As shown in Figure 1, in the absence of oxidative stress, Kelch-like ECH-associated protein 1 (Keap1) keeps Nrf2 sequestered in the cytosol,

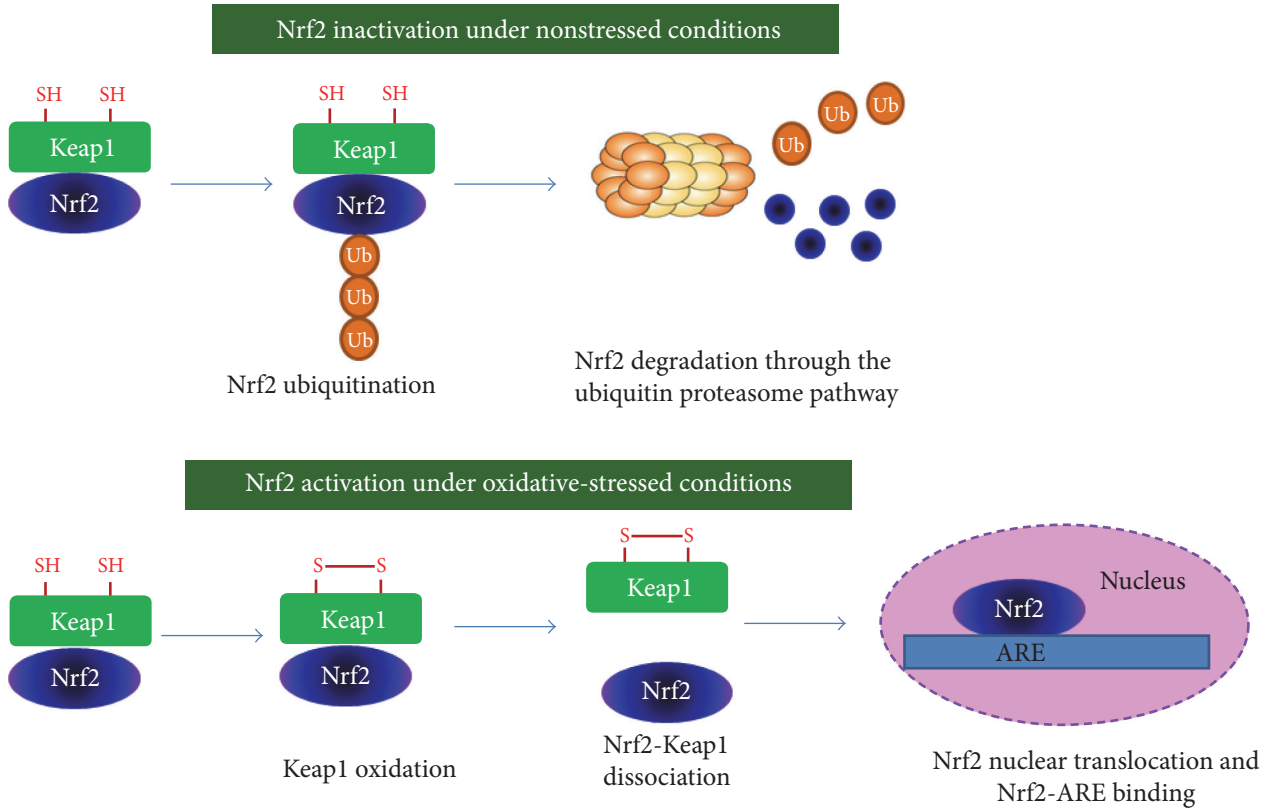

Figure 1: Proposed molecular mechanisms of oxidative stress-induced Nrf2 activation. Under nonstressed conditions, Keap1 keeps Nrf2 sequestered in the cytosol, where it mediates proteasomal degradation of Nrf2. Under oxidative-stressed conditions, cysteine residues of Keap1 are oxidized, forming a disulfide bridge. Oxidized Keap1 dissociates from Nrf2, allowing Nrf2 to translocate to the nucleus, bind to the ARE region, and initiate transcription of target genes.

where it mediates proteasomal degradation of Nrf2 [25–27]. Upon exposure to ROS, Keap1 undergoes a conformational change that allows Nrf2 to translocate to the nucleus, bind to the ARE region, and initiate transcription of target genes [24].

Both "direct" and "indirect" antioxidant enzymes are regulated by Nrf2. "Direct" enzymes that are directly regulated by Nrf2 include catalase and SOD1, and the "indirect" enzymes include GSH- and Trx-generating enzymes and heme oxygenase- (HO-) 1 [28–30]. It is important to note that the baseline expression of many antioxidant enzymes is not significantly upregulated by Nrf2. Rather, the main function of Nrf2 is to induce the antioxidant response [28–30]. This antioxidant response induced by Nrf2 has an early acute phase mediated by the "direct" enzymes and a late chronic phase mediated through maintenance of GSH and Trx. Since the depletion of GSH is directly correlated to oxidative injury and cell death via apoptosis, Nrf2 thus serves as an important link between cell survival and antioxidant gene expression [28–30].

2. Oxidative Stress and Nrf2 in Ocular Diseases

The eye is a prominent target of oxidative stress. It is continuously exposed to various oxidative conditions, such as photo-oxidation, ionizing radiation, smoke, and various forms of pollutants. The retina in particular, because of its high metabolic activities, is a highly perfused and oxygenated tissue. It also contains higher concentrations of polyunsaturated fatty acids than other tissues in the human body [31]. The combination of these factors renders it vulnerable to injurious actions of oxidants such as ROS. Thus, oxidative stress has been associated with many ocular disorders, notably age-related macular degeneration (AMD), cataract, diabetic retinopathy (DR), and glaucoma [32–34]. This review summarizes the current understanding of contributions of oxidation and the Keap1-Nrf2-ARE signaling system in these diseases.

2.1. Age-Related Macular Degeneration

2.1.1. Age-Related Macular Degeneration: Leading Cause of Irreversible Blindness. Age-related macular degeneration is the leading cause of irreversible blindness in individuals aged 60 years and over in developed countries [35]. Due to the increase in the aging population, AMD has become a major healthcare concern, affecting nearly 25 million people worldwide [35]. AMD is often linked to deterioration of central vision, blurriness, and in advanced cases, permanent vision loss. Drusen are extracellular deposits of debris that accumulate between RPE and Bruch's membrane. The appearance of drusen is considered as the clinical hallmark of AMD.

Although the drusen deposits may not initially cause vision loss, individuals with drusen are associated with a greater risk of developing the advanced forms of AMD [36]. Crabb et al. developed a method for isolating drusen for proteome analysis. The authors identified many forms of protein oxidative modifications, including cross-linked species of tissue metalloproteinase inhibitor 3 and vitronectin, and carboxyethyl pyrrole protein adducts in drusen [37, 38]. These observations suggest that protein oxidative modifications may contribute to drusen formation. Another hallmark of AMD is the accumulation of lipofuscin in RPE cells. Lipofuscin, also called "age pigment," is often considered as a symbol of aging [39, 40]. Lipofuscin granules in the RPE are autofluorescent aggregates which are caused by the lifelong accumulation of the nondegradable end products from the phagocytosis of photoreceptor outer segments. Age-dependent accumulation of lipofuscin may cause RPE damage and thereby is associated with AMD pathogenesis.

AMD has two distinct forms: dry (nonexudative) and wet (exudative) forms. The wet form, which is characterized by choroidal neovascularization (CNV)—an abnormal, vascular endothelial growth factor- (VEGF-) dependent development of defective blood vessels below the retina, affects approximately 10% of AMD cases in the US. The use of anti-VEGF antibodies or VEGF-binding peptides is a recently developed therapy; this approach reduces the proliferation of new blood vessels and alleviates the symptoms of the disease [41]. The dry form, characterized by geographic atrophy, is more prevalent, affecting 90% of AMD patients [42]. Its pathogenesis is relatively unknown, and currently, there is no known cure. Interestingly, the Age-Related Eye Disease Study has shown that an antioxidant and mineral cocktail containing β-carotene, vitamin C, vitamin E, and zinc is effective in slowing down the progression of dry AMD by 25%–30% over a 5-year period [43]. This therapeutic breakthrough highlights years of research on oxidative stress as an important contributor and risk factor for AMD pathology.

2.1.2. Contribution of Oxidative Stress in AMD Pathology. Because aging is a major risk factor for AMD, chronic oxidative stress is believed to be an important player in promoting the pathogenesis and progression of AMD. It has been reported that sunlight, UV exposure, cigarette smoke, complement H polymorphisms, high-fat diet, and lack of an antioxidant-rich diet can heighten the risk for individuals to develop AMD [35, 44–46]. The macula, an oval-shaped area of approximately 5.5 mm in diameter, is located at the posterior pole of the retina. In the center of the macula is the foveola (also termed fovea centralis), an area of 1.5 mm in diameter. It comprises a high density of closely packed cone photoreceptors, which provides high-acuity central vision. The retinal pigment epithelium (RPE) is a pigmented cell layer, which at the apical surface, interacts with photoreceptor outer segments of the interphotoreceptor matrix and at the basal surface, connects to the underlying choroid via the acellular Bruch's membrane [47]. RPE is involved in many functions of the retina including vitamin A metabolism, choriocapillaris maintenance, immunity, heat exchange, and forming part of the outer blood-retina barrier (BRB). Most importantly, RPE is primarily responsible for the phagocytosis of photoreceptor outer segments, thereby promoting photoreceptor health [47, 48]. Because light can be damaging and can cause oxidative stress, the photoreceptors are constantly broken down and removed by the RPE. Thus, the RPE's role in the maintenance of the macula and photoreceptors makes it a tissue heavily involved and affected by AMD pathology. Several studies have correlated AMD with chronic oxidative stress, as donor eyes have shown higher oxidative modifications of protein sulfhydryl groups, DNA, lipids, and other molecules [49]. Compared to other tissues, the retina has high metabolic rate, and as a consequence, ROS are leaked as a by-product of metabolism. The combination of a high metabolic rate and its high quantity of polyunsaturated fatty acids makes the retina more prone to ROS accumulation. Moreover, the macula receives a significant amount of blood supply, which makes it more susceptible to endogenous oxygen and oxidative stress [35, 50, 51]. However, in small amounts, ROS are vital for RPE cell signaling and function. As a homeostatic mechanism, the RPE performs continuous phagocytosis of the photoreceptor outer segments, a process that is induced by H_2O_2 production. Signal transduction processes are also driven by ROS signaling and may allow for downstream events that lead to the transcription and translation of proteins. Normally, the endogenous antioxidant enzymes critically reduce the total amount of ROS by directly scavenging free radicals, repairing cell damage, and restoring the redox status of the cell. For example, catalase is increased in healthy RPE cells during phagocytosis to directly scavenge H_2O_2 and prevent unnecessary increases in ROS. Therefore, a critical balance of ROS production and antioxidants is essential to allow for the unhindered functioning of RPE cells. As individuals age, the expression and effectiveness of their antioxidant enzymes decrease, leading to an overwhelming oxidative stress environment in the cell. When the level of ROS exceeds the capacity of the antioxidant enzymes to handle the burden, cell death can be excessive, leading to retinal degeneration. Even though the retina is equipped with numerous antioxidant enzymes, the tissue becomes highly vulnerable with age, as well as various exogenous oxidative stresses like UV light and cigarette smoke. Cigarette smoke contributes numerous pro-oxidants and is predicted to generate about 10^{15} free radicals with every puff [52]. Smoking induces inflammation and encourages the oxidation of proteins, lipids, and DNA due to the reduction of antioxidants like ascorbic acid. Furthermore, smoking has been shown to directly target RPE in a dose-dependent manner and is linked with geographic atrophy, a hallmark of the untreatable dry form of AMD [53]. In summary, with aging and chronic oxidative stress due to UV light or cigarette smoke and impaired antioxidant enzyme function, photoreceptor damage and death accelerate, drusen deposits form, and inflammation increases [54]. Because mitochondria are the primary organelles that produce ROS and free radicals as a by-product of metabolism, mitochondrial dysfunction is often linked to AMD progression [55]. This is significant because mitochondria play key roles in promoting cell survival and ATP production. Therefore, antioxidants that can quench free radicals are of particular

interest due to their potential in treating oxidative stress-induced ocular diseases like AMD.

2.1.3. Involvement of Nrf2 Pathway in AMD. Because of its ability to regulate multiple antioxidant enzymes, the Nrf2 pathway has been hypothesized to be involved in AMD. In multiple studies, aging has been corroborated with many oxidative stress-induced diseases, especially age-related ocular diseases [44, 54, 55]. Lenox et al. determined that the increased activation of the unfolded protein response (UPR) in the aged retinas leads to a severe decline of Nrf2 and its downstream protein HO-1. Due to the compromised antioxidant activity, proinflammatory markers such as RANTES increased, which denotes how aging plays a major role in age-related retinopathies like AMD and diabetic retinopathy [56]. A recent study by Sachdeva et al. showed that the RPE of aging mice displays higher levels of Nrf2, HO-1, and NAD(P)H:quinone oxidoreductase 1 (NQO1). However, when challenged with sodium iodate, the Nrf2 pathway fails to activate. Aged RPE also displays general signs of oxidative damage including increased malondialdehyde (MDA) and superoxide accumulation. Only by using a conditional knockout of *Keap1*, the inhibitor of Nrf2, did aged RPE have some restoration of Nrf2 signaling [57].

Mutations in Nrf2 have been associated with a higher risk of AMD development. Identified from DNA extracted from peripheral blood lymphocytes of wet and dry AMD patients, one mutation of Nrf2 at 25129A>C increases the risk for AMD. The C/C genotype showed a predilection for dry AMD, whereas having an A/C genotype decreased the likelihood of having AMD. The C/C genotype was found to be particularly detrimental when linked with age, bad dietary habits, smoking habits, and an apparent family history [58].

Autophagy, literally defined as "self-eating," is a critical cellular self-protective mechanism that involves the lysosomal-mediated degradation of misfolded proteins, protein aggregates, and damaged organelles like the endoplasmic reticulum, mitochondria, and ribosomes. Autophagy-related proteins are found to be highly expressed and functionally active in the human retina [59, 60]. Both basic and clinical studies have revealed the connection between dysregulated autophagy and AMD. For example, Wang et al. found that drusen in AMD donor eyes contain markers for autophagy and exosomes [61, 62]. Their in vitro autophagy model also indicated that when RPE cells were stressed by mitochondrial oxidative damage, autophagy markers and exosome markers are both upregulated. They proposed that increased autophagy and the release of intracellular proteins via exosomes by aged RPE might contribute to the formation of drusen. Recently, researchers have found autophagy and the Nrf2 pathway are closely linked by the direct binding between p62 (a selective substrate for autophagy) and Keap1 [63, 64]. Both Yamamoto and Zhang's research teams reported that a deficiency in autophagy-sequestered Keap1 into aggregates through direct p62 and Keap1 binding, resulting in Nrf2-Keap1 dissociation and transcriptional activation of Nrf2 target genes. Interestingly, in aged *Nrf2* KO mice, intermediate structures of autophagy, such as the autophagosome and autolysosome, were accumulated in RPE and Bruch's membrane. This accumulation may be due to increased autophagic flux or decreased final degradation by the lysosome [65]. These data strongly suggest that Nrf2-Keap1 and autophagy act in concert to ensure protein quality control and maintain metabolic homeostasis, thereby protecting aging RPE from oxidative stress-induced degeneration.

HO-1 (*HMOX1*) and HO-2 (*HMOX2*), both downstream targets of Nrf2 that are involved in toxic heme catabolism to the antioxidant biliverdin, also have associated polymorphisms that have shown to increase the likelihood of AMD in certain individuals [66]. Similarly, Synoweic et al. have shown that G/A genotype transition of the *HMOX2* gene translates to an increased risk of dry AMD, whereas the A/G genotype is protective [67]. The 19th nucleotide position of the *HMOX1* gene is also correlated with reduced risk of AMD. The G/C transversion genotype of the 19th position of the *HMOX1* gene explains the switch from the dry to the wet form of AMD. The 19G>C-*HMOX1* and the −42 + 1444A>G-*HMOX2* mutations are overall considered to aid in the progression of AMD in AMD patients [67]. The reduced protein levels of HO-1 and HO-2 in exudative AMD patients indicate HO-1- and HO-2-targeted degradation. Both HO-1 and HO-2 were found to be more highly concentrated in the lysosome than their usual position in the cytoplasm, indicating the high turnover rate of HO-1 and HO-2 in the oxidatively stressed retinal environment [68]. Young healthy individuals show the opposite: HO-1 and HO-2 display much higher levels in the cytoplasm. Interestingly, glutathione peroxidase, another downstream Nrf2 phase II antioxidant, does not have any apparent activity in the RPE of AMD patients [68].

Furthermore, polymorphisms in the mitochondrial isomer SOD2 have been associated with AMD prevalence. Kimura et al. analyzed the *SOD2* gene from 102 Japanese wet AMD patients and discovered a valine to alanine switch that translates to a ten times higher risk of developing wet AMD. Although glutathione S-transferases (GST) and microsomal epoxide hydrolase exon-4 show possible polymorphisms, the genotype frequency distributions are not as significant [69]. While these results are more indicative of the Japanese AMD population and distribution, and non-Japanese populations are thought to not have these specific *SOD2* polymorphisms associated with AMD [70], the general consensus is that reduced SOD2 levels are associated with AMD progression [57]. New research suggests that epigenetic control of the *SOD2* gene may accelerate AMD progression because mitochondrial dysfunction and H_2O_2 accumulation are known to increase oxidative damage and death of RPE cells [71, 72]. Overall, these data in particular supported the generation of multiple Nrf2 pathway knockout animal disease models to further study AMD.

Another study by Huang et al. examined how cigarette smoke, a major risk factor for AMD, induced a UPR response injurious to RPE cells. Although cigarette smoke extract activates the apoptotic pathway, Nrf2 upregulation decreases CHOP, a proapoptotic protein, and confers RPE protection [5].

2.1.4. Nrf2 Pathway-Deficient Animal Models of AMD. Because the Nrf2 pathway is considered to be severely

impaired in AMD patients, several disease models involving the knockout of *Nrf2* (*NFE2L2*) and its downstream genes have been proposed and evaluated. *Nrf2* knockout mice display many of the classical signs of AMD pathology, such as soft, large, and yellow drusen-like deposits with distinctly irregular borders [65]. In the peripheral retina, geographic atrophy visible through lesions was found in the RPE. RPE degeneration was also prominent in 12-month *Nrf2* knockout mice, as knockout mice had RPE deficiency, extensive vacuoles, hypopigmentation, and hyperpigmentation. Thickening of the Bruch's membrane was also seen in histological analysis, and staining showed drusen deposition between the RPE and Bruch's membrane. CNV, indicative of the wet form of AMD, was found in nearly 20% of the knockout eyes examined. Considered to be the age pigment, lipofuscin autofluorescence was also found in knockout mice. Zhao et al. further examined the lysosomal degradation pathway to investigate whether RPE cells were capable of phagocytizing the photoreceptor outer segment. Autophagy vacuoles were aberrant and prominent, as enlarged mitochondria were close to autophagy vacuoles [65]. Defects in the lysosomal pathway in *Nrf2* knockout mice show the compromised phagocytic ability of the RPE and also support the idea that cellular homeostasis is breached.

The *SOD1* knockout mouse has also been shown to develop AMD symptoms, with white to yellow drusen-like deposits evident by 10 months of age in 86% of the knockout mice examined [73]. Constant light exposure for 24 h induces drusen formation in young 5-month-old *SOD1* knockout mice, and drusen accumulates with increased exposure time. RPE and Bruch's membrane histology changes are evident, and tight junctions are also lost. Tight junction loss decreases RPE integrity and leads to abnormal RPE morphology, including the loss of its typical hexagonal shape. Additionally, 10% of the *SOD1* knockout mice older than 10 months had observable CNV [73].

Mitochondrial dysfunction has been hypothesized to translate to severe oxidative stress and retinopathy [55, 74]. Because *SOD2* knockout mice do not live beyond 2.5 weeks post birth, the mitochondrial SOD isomer *SOD2*-deficient mice were induced using an AAV-ribozyme-conjugated gene specific for SOD2. The AAV-SOD2 ribozyme particle was injected into the retinas of adult C57BL/6 mice. By four months after injection, *SOD2*-deficient mice had abnormal electroretinograms with 33% and 44% decreases in a- and b-waves, respectively [75]. Hypopigmentation was evident by one month post injection, and outer and inner photoreceptor segments started thinning by 2 months. Extensive vacuoles and RPE atrophy were found to dominate between 2 and 4 months of injection. Electron microscopy further characterized RPE degeneration and thickening of the Bruch's membrane. Also, lipofuscin aggregation was seen by 4.5 months of injection [75].

Although other Nrf2 pathway genes have not been used to define additional AMD animal models, other studies have emphasized that knockout or knockdown of the Nrf2 pathway results in oxidative stress and inflammatory symptoms. For example, *HO-2* knockout mice show abnormal inflammatory processes, impaired corneal healing, ulceration, and choroidal neovascularization [76]. *HO-1* knockout animals have early inflammation and are immunosuppressed [77, 78]. Considering that polymorphisms in several Nrf2 pathway genes are associated with higher AMD risk, more research on antioxidant-deficient models is necessary to uncover the relationship between aging, oxidative stress, and AMD pathogenesis.

2.1.5. Therapeutic Potential of Nrf2 Activation in AMD Treatment

(1) Small Molecule Nrf2 Activators. Many studies have used Nrf2 pathway activating drugs to evaluate the cytoprotective role of Nrf2 in retinal tissues and particularly in rescuing oxidation-induced RPE cell damage and death. By conjugating quercetin and phospholipid together to improve bioavailability, Xu et al. were able to increase RPE proliferation by nearly 80%, reduce ROS and MDA levels, and prevent apoptosis by increasing Nrf2 translocation and upregulating Nrf2 downstream proteins such as HO-1 and NQO1 [79]. Using both synthetic and natural flavonoids, Hanneken et al. demonstrated that pretreatment of flavonoids in low concentrations protected against H_2O_2-induced oxidative injury by restoring RPE cell viability to about 80–100% [80]. The main protective mechanism involved induction of the Nrf2 pathway and its downstream detoxification proteins.

Certain antioxidant natural products and their analogs can be efficacious in stimulating the Nrf2 pathway. Liu et al. analyzed the potential of a natural product drug, RTA 408, in protecting RPE cells. RTA 408, in nanomolar concentrations, has been previously used to treat multiple cancers and mitochondrial myopathies. The mechanism behind RTA 408's efficacy in increasing cell viability in an H_2O_2-stressed environment and restoring redox balance is through the activation of the Nrf2 pathway [81]. With *Nrf2* gene knockdown, RTA 408 cannot exert full RPE protection. Another study by Wang et al. highlights escin, a natural triterpene saponin, as a potential drug to prevent H_2O_2-induced RPE damage and death by activation of the Nrf2-AKT signaling pathway. Escin's ability to reduce ROS and increase cell viability was shown by increasing Nrf2 phosphorylation and leading to higher expression of HO-1, NQO1, and SRXN-1 [82]. P13 kinase/AKT pathway can be used to induce Nrf2 activation through phosphorylation [83], yet other studies have evidenced that alternative posttranslational modifications can also regulate Nrf2 stimulation [84]. Liu et al. showed that glutaredoxin 1 (Grx1), a Nrf2-regulated antioxidant enzyme, can deglutathionylate AKT, which in turn can be activated and can reduce oxidative damage in RPE cells [85]. Pinosylvin is another natural product-derived polyphenol from bark that can protect against oxidative damage induced by hydroquinone by upregulating a downstream enzyme in the Nrf2 pathway, HO-1. At 5–10 μM, pinosylvin has antioxidative, anti-inflammatory, and immunomodulatory properties by stimulation of HO-1 [86]. Likewise, salvianolic acid A in RPE cells was shown to phosphorylate and activate Nrf2 and HO-1 via activating AKT/mTORC1 signaling, thus inhibiting H_2O_2-induced oxidative

stress damage and death [87]. Curcumin, a compound found in turmeric, has also shown multiple antioxidative and anti-inflammatory properties in RPE cells. It protects against both acrolein- and light-induced damages [88, 89]. Interestingly, in other studies, curcumin is controversially thought to be an antiproliferative and possibly cytotoxic agent in RPE cells [90, 91].

α-Tocopherol, the most biologically active form of vitamin E, is protective against RPE oxidative injuries. The molecular mechanism behind its RPE protection was examined using acrolein, a lipid peroxidation by-product and constituent of cigarette smoke, as an oxidative stressor. Acrolein causes severe oxidative damage to the RPE cells. However, α-tocopherol pretreatment accelerates Nrf2 activation and increases the expression of multiple other antioxidant enzymes, such as GST, HO-1, NQO1, and SOD1. Overall, the Nrf2 pathway proteins exerted cytoprotective effects. Moreover, α-tocopherol repairs mitochondrial dysfunction, a contributor to AMD pathogenesis, and restores redox balance in RPE cells [92]. Zinc is also an established vitamin that has antioxidative properties. Zinc reestablishes GSH levels in the RPE to 70% of preinjury level by activating Nrf2, which in turn promotes de novo GSH synthesis [93]. A zinc transporter protein, Zip2, is responsible for transporting zinc into the cell so that the Nrf2 and GSH synthesis pathway could be stimulated [94]. GSH is a crucial small molecule antioxidant that can directly scavenge free radicals. In oxidative stress environments, GSH can conjugate proteins, causing the formation of glutathionylated proteins (PSSG). High PSSG accumulation is often indicative of a deviant redox state and can cause cell damage and death [95, 96]. Hence, chemicals and drugs capable of enhancing GSH levels and restoring redox balance are of key importance to preventing and reducing RPE oxidative injury. In a model of photo-oxidative damage, Gao et al. examined the capability of isothiocyanate sulforaphane in promoting resistance to damaging UV light. Their research highlighted that when Nrf2 pathway is amplified either by *Nrf2* overexpression or by *Keap1* knockdown, GSH and NQO1 levels were boosted in mouse embryonic fibroblasts and conferred protection against UV light damage [97]. Nrf2's capability of promoting cell survival via its antioxidant downstream pathway is due to the scavenging of free radicals and the reinstatement of a good redox balance in the cell.

Other compounds, such as E330 and the NSAID bromfenac, exhibit oxidative stress protection and antiangiogenic properties by stimulating the Nrf2/HO-1 axis. E330 is effective in reducing laser-induced RPE oxidative damage in vivo. This includes preventing CNV and reducing damage to the RPE-Bruch's membrane complex [98]. Bromfenac promotes Nrf2 translocation and upregulates HO-1 expression, which ultimately leads to a decrease in CNV [99].

(2) Nrf2 Gene Therapy. Gene therapy is an innovative method to correct or repair faulty or devoid genes. Ildefonso et al. used an AAV vector to introduce a cell-permeable Nrf2-derived peptide (TatNrf2mer) capable of binding Keap1 in the cell. In stably transfected RPE cells, TatNrf2mer restores cell viability by nearly 20% in H_2O_2-stressed RPE cells and 50% in paraquat-stressed cells. Moreover, GST, NQO1, and catalase expressions are increased by nearly three-fold in these transfected cells [100]. Intravitreal injection of AAV-TatNrf2mer partially protects photoreceptor function based on ERG responses and optical coherence tomography evaluations in the sodium iodate-induced RPE oxidative mouse model [100]. Moreover, Nrf2 induction showed much lower levels of proinflammatory markers like IL-6 and MCP-1 in a mouse model of uveitis [100]. Inflammation plays a key role in complement deposition and drusen formation [101]. Thus, Nrf2's ability to reduce inflammation and oxidation makes it a potential drug target for treating and preventing AMD.

2.2. Cataracts

2.2.1. Cataracts: A Primary Cause of Vision Loss in the World. Cataracts are a form of blurred vision that results from the cloudiness of the lens. Because the light pathway is obstructed, vision loss and blurriness result. It is the most common cause of vision loss in people over the age of 40 around the world, including nearly 20.5 million Americans [102]. Fifty percent of individuals over 80 years old have had or will have cataracts in their lifetime. There are three main types of cataracts: subcapsular, cortical, and nuclear cataracts. Subcapsular cataracts usually involve the breakdown of lens fibers and the accumulation of granular or fibrillary material. Cortical cataracts involve radial or wedge-like opacification, particularly in the cortex area. Nuclear cataracts are the most common type of cataracts and involve the yellowing of the lens nucleus. Along with various mechanisms, each type of cataract has different associated risk factors [102]. Nonetheless, aging and oxidative stress (such as UV irradiation) are the common denominators. However, use of corticosteroids, diabetes, and lifestyle choices such as malnutrition, sunlight exposure, smoking, and alcohol consumption can increase the likelihood of cataract formation [103]. Currently, the only successful treatment for cataracts is surgery, but with a rapidly aging population, there is a growing need to find alternative treatments to prevent and treat cataracts [104].

2.2.2. Maintenance of Transparency in the Lens. In order to keep a clear pathway for light penetration to the retina, the lens must be a flexible, transparent, and biconvex structure [105]. It is composed of the lens capsule, epithelium, and fibers. The transparent lens capsule surrounds the lens and is very elastic with type IV collagen and glycosaminoglycans as its major components. The lens epithelium maintains osmotic volume and forms progenitors for the lens fiber cells. The lens fiber, the bulk of the lens, can stretch anteriorly and posteriorly. To maintain transparency, the lens fiber cells have no organelles or nucleus, and the lens itself has no connective tissue, blood vessels, or nerves [102]. The most common protein found in the lens is crystallins, water-soluble chaperones that aggregate closely together to increase refraction and maintain clarity [106].

2.2.3. Contributions of Oxidative Stress in the Development of Cataracts. Despite chronic exposure to UV light, compared to other tissues, the lens has a competent and efficacious

antioxidant system to combat oxidative stress [107, 108]. Particularly, the lens is rich in proteins with sulfhydryl groups that allow for tight packing for refraction and transparency [109]. It is fully equipped with GSH, an antioxidant that can scavenge free radicals. High amounts of enzymes that carry out de novo GSH synthesis allow for continuous production of GSH [110]. When GSH levels start to deplete with age, especially in the nucleus of the lens, protein oxidation can lead to PSSG, protein aggregation, decreased crystallin, protein solubility abnormalities, and an overall yellowing of the lens [111–113]. The outcome is the eventual development of nuclear cataracts.

Oxidative stress plays a major role in the development of cataracts. In nuclear cataracts, it is predicted that the loss of reduced protein sulfhydryl groups is a major mechanism for cataract growth. More than 90% of cysteine residues and 50% of methionine residues are lost or oxidized [103]. Lou et al. first developed the idea of high amounts of protein-mixed disulfides (PSSP) as the main reason for protein aggregation in the lens [114, 115]. Normally, small amounts of PSSP or PSSG serve multiple normal biological functions such as cell signaling. After all, cysteines are often found in the active site of proteins and can control protein functions. However, continuous oxidation of critical cysteines in proteins can render proteins inactive and eventually lead to their aggregation with other proteins. Lou et al. showed that the increasing yellow discoloration corresponds with an increasing concentration of PSSP and PSSG in the lens nucleus [116]. High levels of PSSP and PSSG are a sign of abundant oxidative stress and damage. With increasing oxidative damage, cell death can occur, and the lens will inevitably develop cataract formation.

Moreover, aggregation in cataracts can be mediated by the abnormal activity and loss of α-crystallin. Normally, α-crystallin works as a chaperone protein that supports lens structure, prevents protein aggregation, and maintains lens protein functionality. Because of increasing protein oxidation and posttranslational modifications like glutathionylation, α-crystallin becomes disabled, causing unrestrained protein aggregation and opacity of the lens [109, 111, 112, 117].

Considering that protein aggregation is heavily involved in lens opacity, it is proposed that restoration of redox balance through reversal of PSSP and PSSG formation can be used as both a preventive measure and a treatment for cataracts. The Trx and Grx antioxidant enzyme systems are fully equipped to reverse posttranslational modifications such as PSSP and PSSG and improve the redox balance in the cells [114, 115, 118]. With the reducing power of NADPH, they act as thioltransferases that reduce protein thiols and reactivate proteins. Moreover, de novo GSH synthesis enzymes, glutathione peroxidase, and other vital antioxidant enzymes can scavenge free radicals to prevent excessive protein oxidation [109, 114, 119]. Nrf2 is the major antioxidant transcriptional regulator that controls the transcription of these specific antioxidant systems and enzymes. Decline of Nrf2 in aging and oxidative stress conditions can translate to lower levels of cytoprotective antioxidant enzymes and may cause cataract formation [103, 111, 120].

2.2.4. Involvement of the Nrf2 Pathway in Cataracts. According to von Otter et al., certain *Nrf2* gene mutations can predict the onset of cataracts but do not necessarily confer higher risk to cataract formation. In one study, 489 cataract cases of European ancestry were analyzed for single nucleotide polymorphism and haplotypes at the *Nrf2* and *Keap1* gene locus. Although none of the single nucleotide polymorphisms for *Nrf2* or *Keap1* gene showed predilection for cataracts, one *Nrf2* haplotype GAAAA did determine the advancement of cataract formation by showing a significant correlation of this haplotype with the onset of cataracts four years earlier [121]. However, having haplotype allele GAAGAGGC in the *Nrf2* gene delayed the need for cataract surgery four more years [121]. Because studies have supported that any delay in the onset of cataracts can save billions of dollars and decrease the incidence of cataracts, these findings may be useful in determining how to prevent or treat cataracts.

Despite the lack of correlation between *Nrf2* haplotypes with cataract risk, epigenetic modifications of the *Nrf2* and *Keap1* genes have been predicted to accelerate cataract pathology. In a study by Gao et al., Nrf2 expression was the lowest in the lens epithelium of the 65–80-year-old individuals, whereas Keap1 expression was significantly increased. Levels of mRNA had correspondingly similar results. When methylation of the *Keap1* gene was examined in 45–90-year-old healthy and cataract lens, gradual demethylation was evident with increasing age, from 16% in the 45–65-year-old group to 39% in the 65–80-year-old group. This is comparable to the 42% demethylation found in cataract lens in the 65–80-year-old group [122]. Demethylation often corresponds with an increase in transcriptional activation of *Keap1* gene, which may explain the lower amount of Nrf2 pathway antioxidant proteins with aging and cataract formation. Aging combined with protein oxidation can increase susceptibility to cataracts. Other studies have supported *Keap1* demethylation in diabetic cataractous lenses. Palsamy et al. have shown that in a study of 21 diabetic cataractous lenses, fragment-1 of cataractous lens consisted of 20 CpG dinucleotides, compared to the fragment-2 of clear lens consisted of 43 CpG dinucleotides. Of those CpG islands in cataractous lens, only 12% of the cytosines were methylated, whereas 64% of the cytosine residues were methylated in clear lens [123]. Clear lens had much higher levels of methylation, indicating less transcription of the *Keap1* genes. Moreover, their study showed that in human lens epithelial cell lines, higher *Keap1* methylation corresponded to increased ROS levels and cell death. Another recent study by the same group revealed that methylglyoxal, a major compound produced as a result of high-sugar diets that cause diabetic complications, can inhibit Nrf2 and DNA methyltransferases and upregulate the demethylation enzyme TET1 [124]. Methylglyoxal functions in altering arginine and lysine residues of lens proteins by causing protein aggregation and leading to the formation of advanced glycation end products [125]. This leads to an increased *Keap1* demethylation, increased proteasomal degradation of Nrf2, an elevated UPR, and consequential endoplasmic reticulum (ER) stress [126]. This group has also attributed

valproic acid, a common antiseizure drug, in stimulating the demethylation of *Keap1* and increasing the incidence of cataracts in epilepsy patients [126].

Research is currently limited in Nrf2 pathway genes and their involvement in cataract development. Chandra et al. showed that in 131 cataract cases of North Indian people, there was an association between the *glutathione S-transferase mu 1* (*GSTM1*) null genotype with cataract formation. The frequency of the *glutathione S-transferase theta 1* (*GSTT1*) gene was also found to be 20% less in cataractous lenses [127].

2.2.5. Nrf2 Pathway-Deficient Animal Models of Cataracts. Although there has not been an established *Nrf2* knockout model for cataracts, there have been models that use pro-oxidants to suppress Nrf2 activation. Palsamy et al. injected sodium selenite into the lenses of rats and observed nuclear cataract formation by the 5th day. Demethylation of the *Keap1* gene was induced by selenite and led to decreased transcription of the Nrf2 antioxidant pathway. Due to diminished calcium homeostasis, low ATP levels, reduced GSH levels from impaired Nrf2 function, ROS overproduction following UPR activation, and ER stress all generated cell damage and death [126].

Phase II antioxidant gene knockout models have also been generated to accelerate cataract formation. Regulated by Nrf2 activation, the Grx family is composed of two specific subsets: the cytoplasmic Grx1 and the primarily mitochondrial Grx2. The Grx family is heavily involved in reversing PSSG and reducing apoptosis in an oxidatively stressed environment. It is concentrated throughout ocular tissue and is thought to reduce light-induced oxidative damage particularly in the lens [128, 129]. Considering the part that PSSG plays in aggravating oxidative stress, protein aggregation, and opacity in the lens, Lou et al. developed two cataract models using both *Grx1* and *Grx2* knockout mouse models [107, 130].

Lens epithelial cells cultured from $Grx1^{-/-}$ mice have rounder shape and increased volume compared to the normal elongated form in $Grx1^{+/+}$ mice. Cell migration is severely impaired, which correlates with an increased doubling time for cell proliferation in $Grx1^{-/-}$ mice. Primary lens epithelial cells isolated from $Grx1^{-/-}$ mice were much more sensitive to oxidative stress as compared with normal lens epithelial cells [130].

Wu et al. characterized the $Grx2^{-/-}$ mouse as a potential cataract model. Because mitochondria are heavily involved in ROS production, mitochondria dysfunction is common in oxidative stress-induced diseases such as cataracts [107]. The primary mitochondrial location of Grx2 makes it a protein of interest especially due to recent publications defining Grx2's antiapoptotic abilities, direct peroxidase activity, and protection over key electron transport chain proteins including complexes I and IV [131, 132]. These studies showed that *Grx2* gene deletion accelerates cataract pathogenesis, including augmenting PSSG formation and diminishing mitochondrial function and ATP production. By 11 months of age, 80% of $Grx2^{-/-}$ mice had developed severe cataracts, whereas only 20% of wild-type mice did [133]. By 16 months, GSH level drops to about 33%, and protein sulfhydryl level drops to about 30% in knockout mice. ATP production is completely devoid in 16-month-old knockout mice, which is accompanied by higher glutathionylation of complex I and complex IV [132–134].

2.2.6. Therapeutic Strategies Based on the Nrf2 Pathway for Cataracts. For diabetic patients, chronic inflammation and oxidative stress can progress to diabetic cataracts [103]. A study by Liu et al. examined *Rosa laevigata* Michx. extract as a potential natural product drug to treat high glucose-stressed lens epithelial cells. HO-1 induction via Nrf2/AKT signaling was responsible for its cytoprotective effects by lowering ROS and increasing mitochondrial membrane potential [135]. DL-3-n-butylphthalide (NBP), an anti-inflammatory and antiapoptotic neuroprotective drug, was examined to see its effects in treating cataracts in streptozotocin-injected rats. ROS and lipid peroxidation products like MDA were found to be much lower in drug-treated diabetic rats. Cataract onset without treatment was seen by 3 weeks and mature cataracts by 9 weeks in diabetic rats. With NBP, cataract onset was significantly delayed, only starting by 6 weeks [136]. By 9 weeks, mature cataracts were not present in diabetic rats with NBP treatment. Nrf2, Trx, and catalase were all upregulated with NBP treatment, indicating that Nrf2 activation is partially responsible for the prevention of cataract pathology in diabetic rats [136].

Vitamin deficiency has also been attributed to cataract formation [102]. Homocysteine is a common pro-oxidant that can cause many inflammatory disorders including heart attack and stroke. Yang et al. analyzed the neuroprotectant and dietary supplement acetyl-l-carnitine as a possible candidate to treat homocysteine-induced lens epithelial cell damage. Acetyl-l-carnitine demonstrated antiapoptotic abilities and decreased ER stress by stimulating Nrf2 and several of its phase II antioxidants including GSH, catalase, SOD, and glutathione peroxidase [137]. The isothiocyanate sulforaphane is another dietary supplement found in cruciferous vegetables like cabbage and horseradish. In addition to an anticarcinogenic function, sulforaphane is also known to induce detoxification and antioxidant enzymes. Using H_2O_2 as a stressor, Liu et al. showed that sulforaphane pretreatment in human lens epithelial cell line FHL124 reduced apoptosis and DNA damage by upregulating Nrf2 translocation into the nucleus [138]. Varma et al. further discovered that sulforaphane is capable of inciting Trx activity 18 times as much compared to non-treated mice lens cells [139]. Trx is vital for the reduction of PSSPs and improving the redox balance of the lens.

Because *Keap1* methylation is accredited to inhibiting Nrf2 activation and is found in higher amounts of cataract patients, drugs increasing methylation or decreasing demethylation are being evaluated for their aptitude in restricting cataract pathology [123, 124, 126]. Gene therapy is also being considered and may represent the future in preventing and treating oxidative stress-induced lens abnormalities.

2.3. Diabetic Retinopathy

2.3.1. Epidemiology of Diabetic Retinopathy. Diabetic retinopathy (DR) is the most common retinal vascular disease

and the leading cause of new cases of blindness in adults [140]. The number of people afflicted with this complication of diabetes is expected to reach 15 million by the year 2050 [140]. It is estimated that DR may soon become the leading cause of visual impairment in the world. The retina uses more oxygen than any other tissue in the body on a per unit weight basis, thus making it very susceptible to oxidative stress. Diabetes alters the balance between the oxidant-antioxidant system by increasing ROS as well as compromising the antioxidant defense system [141]. An increase in ROS is critical in the development of diabetic complications, specifically DR [142]. The highly oxygenated environment of the retina combined with the impaired redox homeostasis seen in diabetes is a crucial prerequisite for the development of DR [142].

2.3.2. Contribution of Oxidative Stress in Diabetic Retinopathy. The possible sources of oxidative stress in diabetes include auto-oxidation of glucose, enhanced aldose reductase activity, increased advanced glycation end products, and altered protein kinase C activity [143]. Together, these various pathways culminate in the production of ROS that upsets the body's redox homeostasis [142]. Additionally, hyperglycemia, hyperlipidemia, and inflammation are the three main metabolic abnormalities in diabetes, all of which are able to stimulate generation of ROS and inflict oxidative stress [140]. Studies have shown that oxidative stress develops in the retina of diabetic animals and galactose-fed animals [144]. This is illustrated by the evidence that nondiabetic animals, in which blood hexose concentration is increased with a galactose-rich diet, develop retinal capillary lesions that are identical to those that develop in diabetic humans or animals [144]. These findings indicate that oxidative stress is at least associated with the development of DR.

2.3.3. Involvement of Nrf2 Pathway in Diabetic Retinopathy. The Nrf2-Keap1 system plays an integral role in the multifaceted pathophysiology of DR. On a cellular level, Nrf2 has shown to be localized in multiple cell types within the retina [141]. Immunohistochemistry experiments have disclosed prominent Nrf2 staining in Muller cells [141]. The Muller cell is an important driver of the proinflammatory processes involved in the progression of DR, including the generation of superoxide radicals [141].

In the retina, the role of Nrf2 is to act as a cytoprotective mechanism in response to oxidative stress [141]. Protection from this injury is crucial to avoid ocular damage by ROS generated in the pathogenesis of diabetes. However, the elevated states of glucose in diabetes decrease the protection offered by Nrf2 [141]. This is supported by a study that found a significant increase in retinal superoxide in diabetic mice deficient in Nrf2 compared with wild-type mice after 5 weeks of diabetes [141]. In addition, the level of the intracellular antioxidant GSH is reduced in diabetes [145]. The enzymes responsible for the GSH redox cycle (glutathione peroxidase and glutathione reductase) are also compromised [145]. GSH biosynthesis is an integral part of the protection system against oxidative stress, and glutamate cysteine ligase is the rate-limiting enzyme in this biosynthesis reaction [145]. Nrf2 is considered a key transcription factor for the regulation of the catalytic subunit of glutamate cysteine ligase (GCLC) [145]. The site of histopathology associated with diabetic retinopathy are the retinal endothelial cells (RECs), and quantification of the Nrf2-GCLC pathway in isolated RECs revealed that the nuclear expression of Nrf2- and DNA-binding activity were decreased by 50% to 60% in RECs exposed to high glucose levels [145]. Binding of Nrf2 with GCLC was also decreased by 90% in diabetic rats, resulting in a significant decrease in GCLC expression [145]. This demonstrates that high glucose levels impair Nrf2 activity and result in a blunted expression of the antioxidant gene GCLC. Studies of human donor eyes with DR also showed decreased GCLC levels compared with age-matched nondiabetic controls [145]. Further evidence shows that disturbances in Nrf2-GCLC signaling are a major event in the development of DR as indicated by the observation that diabetic Nrf2 knockout mice exhibited a significantly lower retinal GSH level compared with wild-type diabetic mice [141, 145]. Although the precise mechanism by which diabetes affects Nrf2-mediated regulation of GSH biosynthesis remains to be elucidated, the inverse relationship between glucose levels and GCLC activity is clearly evident by these observations. This is an important conclusion because it explains the pathway that begins with hyperglycemia and leads to a weakened antioxidant defense system, specifically in the retina. A suboptimal antioxidant defense system due to low retinal GSH sets the stage for the development of DR.

Immunofluorescence studies reveal that under high glucose levels, cytosolic expression of Nrf2 was increased along with increased localization of both Nrf2 and Keap1 in the cytosol [141, 145]. As discussed earlier, Keap1 normally sequesters Nrf2 in the cytosol, which blocks the transcription of antioxidant genes. Diabetic rats have been shown to express increased mRNA and protein levels of Keap1 compared to those from normal control rats [145]. To confirm these in vivo findings, RECs were transfected with Keap1-siRNA, which prevented a glucose-induced decrease in Nrf2 accumulation in the nucleus [145]. These observations illustrate that the hyperglycemic environment results in increased expression of Keap1, thereby leading to increased cytosolic sequestration of Nrf2. This study also suggests that Keap1 knockdown can play a role in allowing Nrf2 to translocate to the nucleus and initiate transcription of antioxidant genes.

The findings reported here concerning the Nrf2-Keap1 system in DR suggest that increased oxidative stress created by the diabetic environment prevents Nrf2 from reaching the nucleus to enhance the transcription apparatus. A redox reaction of the Cys-151 cysteine residue of Keap1 is a key modification required for Nrf2 to dissociate from Keap1 and enter the nucleus [146]. It is possible that the oxidative stress in diabetes alters the redox-sending capacity of Keap1, thereby preventing the dissociation of Nrf2 from Nrf2-Keap1 complex [146]. Another explanation of the altered binding between Nrf2 and Keap1 in diabetes includes diabetes-induced posttranslational or epigenetic modifications of retinal proteins, including Keap1 [147–149]. In fact, nitration, ribosylation, and other posttranslational modifications of retinal proteins have been shown to occur in diabetes [123].

In addition, epigenetic modification of lens Keap1 has also been shown in diabetes [123].

The protective role of Nrf2 is further exemplified by evidence that Nrf2 knockout mice show an increase in inflammatory mediators regardless of blood glucose level [143]. Inflammation is independently associated with an increase in vascular damage in DR and also BRB breakdown [150]. Accumulating evidence shows that inflammation is the key mediator of the endothelial cell injury and BRB dysfunction [150]. TNFα (tumor necrosis factor-α) is an inflammatory cytokine that plays an important role in DR, including BRB dysfunction [150]. Xu et al. have shown a significantly greater amount of TNFα protein in diabetic mice deficient in Nrf2 compared to wild-type diabetic mice [141]. Since an increase in TNFα is associated with breakdown of the BRB, it follows that Nrf2 knockout mice exhibited a significant increase in retinal vascular leakage after 8 weeks of diabetes compared with wild-type diabetic mice [141]. Retinal edema and loss of vision are the direct results of retinal vascular leakage; this pathology is a major end point of DR [141]. These findings indicate the integral role Nrf2 plays in mitigating proinflammatory cytokines, regardless of blood glucose levels.

Visual impairment is a well-regarded end point of diabetes due to the adverse effects on neuronal function caused by hyperglycemia [151]. Since Nrf2 has neuroprotective effects in the retina, Xu et al. measured the effects of Nrf2 on diabetes-induced visual dysfunction in mice using the parameters of spatial frequency and contrast sensitivity [141]. They found that after 8 weeks of diabetes, Nrf2 knockout mice had significant visual deficits in both spatial frequency and contrast sensitivity as compared to nondiabetic Nrf2 knockout controls and diabetic wild-type mice [141]. This finding suggests that Nrf2 deficiency exacerbates diabetes-induced visual impairment in mice.

Diabetes skews the balance between oxidative stress and the antioxidant system. A hyperglycemic environment creates a state of increased oxidative stress in tissues of both humans and animals, and increased oxidative stress might play a role in the development of diabetic complications. Increase in ROS is one of the major retinal metabolic abnormalities associated with the development of DR. The studies presented earlier demonstrate a common theme: the Nrf2-Keap1 signaling pathway plays an important role in the pathogenesis of diabetic retinopathy. A hyperglycemic environment and subsequent oxidative stress adversely affect the binding between Nrf2 and Keap1 and Nrf2 and GCLC, and these also contribute to visual dysfunction. Visual dysfunction is not only caused by a hyperglycemic state, but it is also exacerbated by a loss of Nrf2 due to hyperglycemia. This discussion suggests that Nrf2 is protective against both oxidative stress and inflammation, and hyperglycemia leads to loss of cytoprotection offered by Nrf2.

2.3.4. Therapeutic Strategies Based on the Nrf2 Pathway for DR. At this time, we did not find any published study showing the use of Nrf2-related compounds as a therapeutic approach to treat DR. A recent study by Nakagami et al., however, succeeded in showing that a novel activator of Nrf2 known as RS9 delayed retinal degeneration by inhibiting inflammatory responses and increasing intrinsic antioxidant enzymes [152]. Increase in inflammation and oxidative stress are the cornerstones of the pathophysiology of DR. Thus, this study supports Nrf2 activators' role as possible therapeutic agents for DR.

2.4. Glaucoma

2.4.1. Glaucoma Pathophysiology. Glaucoma is a group of diseases characterized by optic neuropathy and retinopathy. Although the pathogenesis of glaucoma remains uncertain, elevated intraocular pressure (IOP) due to impaired outflow of the aqueous humor is considered the most important risk factor for the disease. The aqueous humor is produced by the ciliary body and drained through the trabecular meshwork (TM). The TM failure reduces outflow of the aqueous humor and increases IOP [153]. Visual loss in glaucoma, characterized by a specific pattern of visual field defects, results from retinal ganglion cell (RGC) apoptosis which appears to be initiated at the optic nerve head where RGC axons pass through.

2.4.2. Involvement of Oxidative Stress in Glaucoma. Increasing clinical evidence suggests that oxidative stress contributes to the pathogenesis of glaucomatous neurodegeneration. Oxidative DNA damage, demonstrated by increased level of 8-hydroxy-2′-deoxyguanosine, has been found in TM tissues from patients with glaucoma [154]. Further study showed the correlation between TM DNA oxidative damage and mean IOP as well as visual field defects in glaucoma patients [155]. Additional evidence supporting the role of oxidative damage in TM degeneration includes significantly decreased total reactive antioxidant potential and increased activities of antioxidant enzymes such as SOD and glutathione peroxidase in the aqueous humor from glaucoma patients [156]. Oxidative stress is demonstrated not only in TM but also in the retina. Upregulation of hypoxic stress-induced proteins, such as hypoxia-inducible factor-1α and heat shock proteins, have been shown in the glaucomatous human retina and optic nerve head [157, 158]. These findings highlight the importance of oxidative stress, the cause or consequence of the glaucomatous neurodegeneration, in the pathogenic cascade of the disease.

Genetic factors contribute to the development of glaucoma. Mutations of genes associated with oxidative stress have been correlated with glaucoma. For example, mutations of *CYP1B1*, a member of cytochromes P450 superfamily, have been identified in primary congenital glaucoma [159–161]. The *GSTM1* null genotype appears more frequent in glaucoma patients than in controls in the Mediterranean region [154, 162]. The GSTM1 enzyme is one of the major polymorphisms of GST. These data further support the possible role of oxidative stress in the pathogenesis of glaucoma.

2.4.3. Involvement of Nrf2 Pathway in Glaucoma. The Nrf2 antioxidant response element pathway-mediated neuroprotection has been shown in animal models mimicking certain aspects of glaucoma pathology. Depletion of *Nrf2* aggravates RGC death induced by optic nerve injury [163]. Similar results have been reported in mice following retinal ischemia/reperfusion insult. Compared to wild-type controls,

Nrf2 knockout mice exhibit an exacerbation of oxidative stress, and capillary and neuronal degeneration [164].

2.4.4. Therapeutic Strategies Based on the Nrf2 Pathway for Glaucoma. Consistent with the findings that Nrf2 is potentially involved in glaucoma, activation of endogenous Nrf2 pathway in the retinas using triterpenoid 2-cyano-3,12-dioxooleana-1,9-dien-28-imidazolide, a Nrf2 activator, promotes neuronal survival in both the retinal ischemia/reperfusion and the optic nerve injury models [163, 165]. The Nrf2 pathway appears to be a promising target for glaucoma neuroprotection.

3. Therapeutic Outlook

3.1. Strategies to Augment Nrf2 Activity. Increase in Nrf2 activity is expected to be protective against oxidative and inflammatory injuries. To achieve that, various approaches have been tried to modulate components of the Nrf2-Keap1 pathway. As mentioned above, compounds that increase Nrf2 activity were evaluated for their therapeutic effects in some of these ocular diseases. For example, quercetin analog, RTA 408, escin, pinosylvin, salvianolic acid A, and curcumin were tested in AMD models; *Rosa laevigata* Michx. extract, NBP, acetyl-l-carnitine, and sulforaphane were assessed in cataract models. Similarly, many natural and synthetic compounds have been assessed in other biological systems for their potential to activate Nrf2 [66, 166, 167]. Discoveries in these biological systems may guide the development of useful drugs for ophthalmology.

In addition to chemical Nrf2 activators, overexpression of Nrf2 is another efficacious means to protect against oxidative stress. Selective overexpression of Nrf2 in the appropriate cells may prevent or reverse ROS-mediated toxicity. This approach has been investigated in various systems [66, 167]; it is likely useful for ocular uses. Similarly, since Keap1 is a negative regulator of Nrf2, interfering with Keap1 activity is a reasonable approach to increase Nrf2 activity, especially in the hyperglycemic environment of the cell. This could be achieved by using siRNA or shRNA directed against Keap1. Keap1 knockdown confers persistent Nrf2 activation and protection against oxidative damage in astrocytes [168], cortical neurons [169], and hepatocytes [170]. It is interesting to note that a number of natural products such as synthetic triterpenoids [171], salvianolic acids [87], and sulforaphane [166] have been identified as potent Nrf2 activators. Instead of directly enhancing the expression level of Nrf2, these compounds inactivate Keap1 by covalently modifying reactive cysteine residues in Keap1, thereby activating the Nrf2 signaling pathway and its downstream target genes. Consequently, activated Nrf2 bypasses Keap1 and then Nrf2 translocates into the nucleus. These results suggest that Keap1 knockdown may be meaningful therapeutic approaches in the future.

In addition to being potential therapeutic means, we speculate that Nrf2-targeted approaches can be useful as disease prevention. By directly stimulating phase II enzyme expression, thereby making cells more resistant to oxidative stress-induced cell injury, preventing ROS overproduction, and inhibiting protein oxidation, Nrf2 activators may be a novel approach for the prevention of a wide variety of oxidative stress-related human diseases and should be used in early or presymptomatic stages of diseases when restoring homeostasis is critical.

3.2. Word of Caution: The Potential Dark Side of Nrf2. Nrf2 has many antioxidative and anti-inflammatory functions, which are typically considered to be beneficial for cell survival and proliferation. However, evidence also indicates that small amounts of ROS are essential to induce cell signaling events including insulin and growth factor signaling [96, 172]. Due to the cytoprotective nature of the Nrf2 pathway, it is not surprising that Nrf2 deficiency may make cells more vulnerable to carcinogens. However, a recent study by DeNicola et al. showed that the expression of classic oncogenes, such as *Kras*, *Braf*, and *Myc*, reduced ROS levels by activating Nrf2 pathway and thereby promoting tumorigenesis [173]. In the eye, Pan et al. showed that a small amount of H_2O_2 enhances rabbit corneal epithelial cell viability, migration, adhesion, and attachment to the extracellular matrix, as well as improves cornea wound closure in an ex vivo porcine model and an in vivo mouse model [174]. Furthermore, Zucker et al. demonstrated that in NIH3T3 cells, an excessive oxidative stress environment can lead to Nrf2-dependent activation of Kruppel-like factor 9 (Klf9), a ubiquitously expressed protein that regulates cell differentiation and promotes oxidative stress-induced cell death [175]. When ROS exceeds a critical threshold, Nrf2 binds to AREs of the *Klf9* gene and upregulates Klf9 expression. Klf9 in turn suppresses expression of Trx reductase 2, amplifies ROS production cascade, and eventually causes cell death [175]. Therefore, although ROS is generally considered to be detrimental to tissues and beneficial to Nrf2, their roles can be complex. Consequently, it is important to define the boundary between beneficial and potentially damaging effects of Nrf2 activation and determine the appropriate redox balance to maintain healthy cellular homeostasis.

4. Concluding Remarks

Inflammation and oxidative stress are important parameters in the pathophysiology of the major ocular diseases. Nrf2 has been shown to have both antioxidant as well as anti-inflammatory properties. These protective effects can be augmented by pharmacologic or molecular modulations. Augmentation of the antioxidant properties and anti-inflammatory properties can provide novel and useful therapeutic targets for these devastatingly blinding diseases.

Abbreviations

AMD: Age-related macular degeneration
ARE: Antioxidant response element
BRB: Blood-retina barrier
CNV: Choroidal neovascularization
DR: Cataract, diabetic retinopathy
ER: Endoplasmic reticulum
GCLC: Catalytic subunit of glutamate cysteine ligase

Grx: Glutaredoxin
GSH: Glutathione
GST: Glutathione S-transferase
HO: Heme oxygenase
IOP: Intraocular pressure
Keap1: Kelch-like ECH-associated protein 1
Klf9: Kruppel-like factor 9
MDA: Malondialdehyde
NBP: DL-3-n-butylphthalide
NQO1: NAD(P)H:quinone oxidoreductase 1
Nrf2: Nuclear factor erythroid-2-related factor 2
PSSG: Glutathionylated protein
PSSP: Protein-mixed disulfide
REC: Retinal endothelial cell
RGC: Retinal ganglion cell
ROS: Reactive oxygen species
RPE: Retinal pigment epithelium
SOD: Superoxide dismutase
TM: Trabecular meshwork
TNFα: Tumor necrosis factor-α
Trx: Thioredoxin
UPR: Unfolded protein response
VEGF: Vascular endothelial growth factor.

Conflicts of Interest

The authors declare that there is no conflict of interest regarding the publication of this paper.

Acknowledgments

This research is supported by the National Eye Institute (R21EY024635; Iok-Hou Pang) and by the BrightFocus Foundation for Macular Degeneration (M2015180; Hongli Wu).

References

[1] B. Chance, H. Sies, and A. Boveris, "Hydroperoxide metabolism in mammalian organs," *Physiological Reviews*, vol. 59, no. 3, pp. 527–605, 1979.

[2] A. E. Fletcher, "Free radicals, antioxidants and eye diseases: evidence from epidemiological studies on cataract and age-related macular degeneration," *Ophthalmic Research*, vol. 44, no. 3, pp. 191–198, 2010.

[3] A. Higuchi, K. Ito, M. Dogru et al., "Corneal damage and lacrimal gland dysfunction in a smoking rat model," *Free Radical Biology & Medicine*, vol. 51, no. 12, pp. 2210–2216, 2011.

[4] S. C. Sacca, A. M. Roszkowska, and A. Izzotti, "Environmental light and endogenous antioxidants as the main determinants of non-cancer ocular diseases," *Mutation Research*, vol. 752, no. 2, pp. 153–171, 2013.

[5] C. Huang, J. J. Wang, J. H. Ma, C. Jin, Q. Yu, and S. X. Zhang, "Activation of the UPR protects against cigarette smoke-induced RPE apoptosis through up-regulation of Nrf2," *The Journal of Biological Chemistry*, vol. 290, no. 9, pp. 5367–5380, 2015.

[6] C. M. Chan, C. H. Huang, H. J. Li et al., "Protective effects of resveratrol against UVA-induced damage in ARPE19 cells," *International Journal of Molecular Sciences*, vol. 16, no. 3, pp. 5789–5802, 2015.

[7] X. Wu, S. J. Cobbina, G. Mao, H. Xu, Z. Zhang, and L. Yang, "A review of toxicity and mechanisms of individual and mixtures of heavy metals in the environment," *Environmental Science and Pollution Research International*, vol. 23, no. 9, pp. 8244–8259, 2016.

[8] T. M. Florence, "The role of free radicals in disease," *Australian and New Zealand Journal of Ophthalmology*, vol. 23, no. 1, pp. 3–7, 1995.

[9] K. A. Jung and M. K. Kwak, "The Nrf2 system as a potential target for the development of indirect antioxidants," *Molecules (Basel, Switzerland)*, vol. 15, no. 10, pp. 7266–7291, 2010.

[10] D. A. Butterfield, M. Perluigi, T. Reed et al., "Redox proteomics in selected neurodegenerative disorders: from its infancy to future applications," *Antioxidants & Redox Signaling*, vol. 17, no. 11, pp. 1610–1655, 2012.

[11] C. Espinosa-Diez, V. Miguel, D. Mennerich et al., "Antioxidant responses and cellular adjustments to oxidative stress," *Redox Biology*, vol. 6, pp. 183–197, 2015.

[12] M. F. Beal, "Oxidatively modified proteins in aging and disease," *Free Radical Biology & Medicine*, vol. 32, no. 9, pp. 797–803, 2002.

[13] T. J. Montine, M. D. Neely, J. F. Quinn et al., "Lipid peroxidation in aging brain and Alzheimer's disease," *Free Radical Biology & Medicine*, vol. 33, no. 5, pp. 620–626, 2002.

[14] C. M. Spickett and A. R. Pitt, "Oxidative lipidomics coming of age: advances in analysis of oxidized phospholipids in physiology and pathology," *Antioxidants & Redox Signaling*, vol. 22, no. 18, pp. 1646–1666, 2015.

[15] Y. Higuchi, "Chromosomal DNA fragmentation in apoptosis and necrosis induced by oxidative stress," *Biochemical Pharmacology*, vol. 66, no. 8, pp. 1527–1535, 2003.

[16] Y. Higuchi, "Glutathione depletion-induced chromosomal DNA fragmentation associated with apoptosis and necrosis," *Journal of Cellular and Molecular Medicine*, vol. 8, no. 4, pp. 455–464, 2004.

[17] E. Radi, P. Formichi, C. Battisti, and A. Federico, "Apoptosis and oxidative stress in neurodegenerative diseases," *Journal of Alzheimer's Disease : JAD*, vol. 42, Supplement 3, pp. S125–S152, 2014.

[18] K. Hensley, M. Mhatre, S. Mou et al., "On the relation of oxidative stress to neuroinflammation: lessons learned from the G93A-SOD1 mouse model of amyotrophic lateral sclerosis," *Antioxidants & Redox Signaling*, vol. 8, no. 11-12, pp. 2075–2087, 2006.

[19] O. Gorelenkova Miller and J. J. Mieyal, "Sulfhydryl-mediated redox signaling in inflammation: role in neurodegenerative diseases," *Archives of Toxicology*, vol. 89, no. 9, pp. 1439–1467, 2015.

[20] I. Rahman, F. Antonicelli, and W. MacNee, "Molecular mechanism of the regulation of glutathione synthesis by tumor necrosis factor-alpha and dexamethasone in human alveolar epithelial cells," *The Journal of Biological Chemistry*, vol. 274, no. 8, pp. 5088–5096, 1999.

[21] A. V. Bakin, N. V. Stourman, K. R. Sekhar et al., "Smad3-ATF3 signaling mediates TGF-beta suppression of genes encoding phase II detoxifying proteins," *Free Radical Biology & Medicine*, vol. 38, no. 3, pp. 375–387, 2005.

[22] T. W. Kensler, N. Wakabayashi, and S. Biswal, "Cell survival responses to environmental stresses via the Keap1-Nrf2-ARE

pathway," *Annual Review of Pharmacology and Toxicology*, vol. 47, pp. 89–116, 2007.

[23] T. H. Rushmore, M. R. Morton, and C. B. Pickett, "The antioxidant responsive element. Activation by oxidative stress and identification of the DNA consensus sequence required for functional activity," *The Journal of Biological Chemistry*, vol. 266, no. 18, pp. 11632–11639, 1991.

[24] D. D. Zhang, "Mechanistic studies of the Nrf2-Keap1 signaling pathway," *Drug Metabolism Reviews*, vol. 38, no. 4, pp. 769–789, 2006.

[25] K. Itoh, N. Wakabayashi, Y. Katoh et al., "Keap1 represses nuclear activation of antioxidant responsive elements by Nrf2 through binding to the amino-terminal Neh2 domain," *Genes & Development*, vol. 13, no. 1, pp. 76–86, 1999.

[26] L. M. Zipper and R. T. Mulcahy, "The Keap1 BTB/POZ dimerization function is required to sequester Nrf2 in cytoplasm," *The Journal of Biological Chemistry*, vol. 277, no. 39, pp. 36544–36552, 2002.

[27] M. McMahon, K. Itoh, M. Yamamoto, and J. D. Hayes, "Keap1-dependent proteasomal degradation of transcription factor Nrf2 contributes to the negative regulation of antioxidant response element-driven gene expression," *The Journal of Biological Chemistry*, vol. 278, no. 24, pp. 21592–21600, 2003.

[28] T. Suzuki and M. Yamamoto, "Molecular basis of the Keap1-Nrf2 system," *Free Radical Biology & Medicine*, vol. 88, no. Part B, pp. 93–100, 2015.

[29] H. Zhang, K. J. Davies, and H. J. Forman, "Oxidative stress response and Nrf2 signaling in aging," *Free Radical Biology & Medicine*, vol. 88, no. Pt B, pp. 314–336, 2015.

[30] K. N. Prasad, "Simultaneous activation of Nrf2 and elevation of antioxidant compounds for reducing oxidative stress and chronic inflammation in human Alzheimer's disease," *Mechanisms of Ageing and Development*, vol. 153, pp. 41–47, 2016.

[31] J. Nourooz-Zadeh and P. Pereira, "Age-related accumulation of free polyunsaturated fatty acids in human retina," *Ophthalmic Research*, vol. 31, no. 4, pp. 273–279, 1999.

[32] G. Pagano, A. A. Talamanca, G. Castello et al., "Oxidative stress and mitochondrial dysfunction across broad-ranging pathologies: toward mitochondria-targeted clinical strategies," *Oxidative Medicine and Cellular Longevity*, vol. 2014, Article ID 541230, p. 27, 2014.

[33] M. D. Pinazo-Duran, R. Gallego-Pinazo, J. J. Garcia-Medina et al., "Oxidative stress and its downstream signaling in aging eyes," *Clinical Interventions in Aging*, vol. 9, pp. 637–652, 2014.

[34] M. Nita and A. Grzybowski, "The role of the reactive oxygen species and oxidative stress in the pathomechanism of the age-related ocular diseases and other pathologies of the anterior and posterior eye segments in adults," *Oxidative Medicine and Cellular Longevity*, vol. 2016, Article ID 3164734, p. 23, 2016.

[35] J. T. Handa, "How does the macula protect itself from oxidative stress?" *Molecular Aspects of Medicine*, vol. 33, no. 4, pp. 418–435, 2012.

[36] D. M. Moshfeghi and H. Lewis, "Age-related macular degeneration: evaluation and treatment," *Cleveland Clinic Journal of Medicine*, vol. 70, no. 12, pp. 1017–1018, 2003, 1020, 1023-1015 passim.

[37] J. W. Crabb, "The proteomics of drusen," *Cold Spring Harbor Perspectives in Medicine*, vol. 4, no. 7, article a017194, 2014.

[38] J. W. Crabb, M. Miyagi, X. Gu et al., "Drusen proteome analysis: an approach to the etiology of age-related macular degeneration," *Proceedings of the National Academy of Sciences of the United States of America*, vol. 99, no. 23, pp. 14682–14687, 2002.

[39] L. S. Murdaugh, L. B. Avalle, S. Mandal et al., "Compositional studies of human RPE lipofuscin," *Journal of Mass Spectrometry*, vol. 45, no. 10, pp. 1139–1147, 2010.

[40] L. S. Murdaugh, S. Mandal, A. E. Dill, J. Dillon, J. D. Simon, and E. R. Gaillard, "Compositional studies of human RPE lipofuscin: mechanisms of molecular modifications," *Journal of Mass Spectrometry*, vol. 46, no. 1, pp. 90–95, 2011.

[41] J. J. Arnold, "Age-related macular degeneration: anti-vascular endothelial growth factor treatment. Systematic review 701," *BMJ Clinical Evidence*, 2016, http://clinicalevidence.bmj.com/x/systematic-review/0701/overview.html.

[42] S. Khandhadia and A. Lotery, "Oxidation and age-related macular degeneration: insights from molecular biology," *Expert Reviews in Molecular Medicine*, vol. 12, article e34, 2010.

[43] AREDS-Study-Group, "A randomized, placebo-controlled, clinical trial of high-dose supplementation with vitamins C and E, beta carotene, and zinc for age-related macular degeneration and vision loss: AREDS report no. 8," *Archives of Ophthalmology*, vol. 119, no. 10, pp. 1417–1436, 2001.

[44] K. M. Bertram, C. J. Baglole, R. P. Phipps, and R. T. Libby, "Molecular regulation of cigarette smoke induced-oxidative stress in human retinal pigment epithelial cells: implications for age-related macular degeneration," *American Journal of Physiology Cell Physiology*, vol. 297, no. 5, pp. C1200–C1210, 2009.

[45] U. Chakravarthy, T. Y. Wong, A. Fletcher et al., "Clinical risk factors for age-related macular degeneration: a systematic review and meta-analysis," *BMC Ophthalmology*, vol. 10, p. 31, 2010.

[46] G. Y. Sui, G. C. Liu, G. Y. Liu et al., "Is sunlight exposure a risk factor for age-related macular degeneration? A systematic review and meta-analysis," *The British Journal of Ophthalmology*, vol. 97, no. 4, pp. 389–394, 2013.

[47] H. E. Grossniklaus, E. E. Geisert, and J. M. Nickerson, "Introduction to the retina," *Progress in Molecular Biology and Translational Science*, vol. 134, pp. 383–396, 2015.

[48] O. Strauss, "The retinal pigment epithelium in visual function," *Physiological Reviews*, vol. 85, no. 3, pp. 845–881, 2005.

[49] M. P. Cabrera and R. H. Chihuailaf, "Antioxidants and the integrity of ocular tissues," *Veterinary Medicine International*, vol. 2011, Article ID 905153, p. 8, 2011.

[50] B. S. Winkler, M. E. Boulton, J. D. Gottsch, and P. Sternberg, "Oxidative damage and age-related macular degeneration," *Molecular Vision*, vol. 5, p. 32, 1999.

[51] S. Beatty, H. Koh, M. Phil, D. Henson, and M. Boulton, "The role of oxidative stress in the pathogenesis of age-related macular degeneration," *Survey of Ophthalmology*, vol. 45, no. 2, pp. 115–134, 2000.

[52] A. Valavanidis, T. Vlachogianni, and K. Fiotakis, "Tobacco smoke: involvement of reactive oxygen species and stable free radicals in mechanisms of oxidative damage, carcinogenesis and synergistic effects with other respirable particles," *International Journal of Environmental Research and Public Health*, vol. 6, no. 2, pp. 445–462, 2009.

[53] R. Klein, M. D. Knudtson, K. J. Cruickshanks, and B. E. Klein, "Further observations on the association between smoking

and the long-term incidence and progression of age-related macular degeneration: the Beaver Dam Eye Study," *Archives of Ophthalmology*, vol. 126, no. 1, pp. 115–121, 2008.

[54] M. D. Marquioni-Ramella and A. M. Suburo, "Photodamage, photo-protection and age-related macular degeneration," *Photochemical & Photobiological Sciences: Official Journal of the European Photochemistry Association and the European Society for Photobiology*, vol. 14, no. 9, pp. 1560–1577, 2015.

[55] H. Mao, S. J. Seo, M. R. Biswal et al., "Mitochondrial oxidative stress in the retinal pigment epithelium leads to localized retinal degeneration," *Investigative Ophthalmology & Visual Science*, vol. 55, no. 7, pp. 4613–4627, 2014.

[56] A. R. Lenox, Y. Bhootada, O. Gorbatyuk, R. Fullard, and M. Gorbatyuk, "Unfolded protein response is activated in aged retinas," *Neuroscience Letters*, vol. 609, pp. 30–35, 2015.

[57] M. M. Sachdeva, M. Cano, and J. T. Handa, "Nrf2 signaling is impaired in the aging RPE given an oxidative insult," *Experimental Eye Research*, vol. 119, pp. 111–114, 2014.

[58] T. Sliwinski, U. Kolodziejska, J. P. Szaflik, J. Blasiak, and J. Szaflik, "Association between the 25129A > C polymorphism of the nuclear respiratory factor 2 gene and age-related macular degeneration," *Klinika Oczna*, vol. 115, no. 2, pp. 96–102, 2013.

[59] S. G. Jarrett, A. S. Lewin, and M. E. Boulton, "The importance of mitochondria in age-related and inherited eye disorders," *Ophthalmic Research*, vol. 44, no. 3, pp. 179–190, 2010.

[60] A. L. Wang, M. E. Boulton, W. A. Dunn Jr. et al., "Using LC3 to monitor autophagy flux in the retinal pigment epithelium," *Autophagy*, vol. 5, no. 8, pp. 1190–1193, 2009.

[61] A. L. Wang, T. J. Lukas, M. Yuan, N. Du, M. O. Tso, and A. H. Neufeld, "Autophagy and exosomes in the aged retinal pigment epithelium: possible relevance to drusen formation and age-related macular degeneration," *PLoS One*, vol. 4, no. 1, artcle e4160, 2009.

[62] S. K. Mitter, H. V. Rao, X. Qi et al., "Autophagy in the retina: a potential role in age-related macular degeneration," *Advances in Experimental Medicine and Biology*, vol. 723, pp. 83–90, 2012.

[63] M. Komatsu, H. Kurokawa, S. Waguri et al., "The selective autophagy substrate p62 activates the stress responsive transcription factor Nrf2 through inactivation of Keap1," *Nature Cell Biology*, vol. 12, no. 3, pp. 213–223, 2010.

[64] A. Lau, X. J. Wang, F. Zhao et al., "A noncanonical mechanism of Nrf2 activation by autophagy deficiency: direct interaction between Keap1 and p62," *Molecular and Cellular Biology*, vol. 30, no. 13, pp. 3275–3285, 2010.

[65] Z. Zhao, Y. Chen, J. Wang et al., "Age-related retinopathy in NRF2-deficient mice," *PLoS One*, vol. 6, no. 4, article e19456, 2011.

[66] M. A. O'Connell and J. D. Hayes, "The Keap1/Nrf2 pathway in health and disease: from the bench to the clinic," *Biochemical Society Transactions*, vol. 43, no. 4, pp. 687–689, 2015.

[67] E. Synowiec, J. Szaflik, M. Chmielewska et al., "An association between polymorphism of the heme oxygenase-1 and -2 genes and age-related macular degeneration," *Molecular Biology Reports*, vol. 39, no. 3, pp. 2081–2087, 2012.

[68] R. N. Frank, R. H. Amin, and J. E. Puklin, "Antioxidant enzymes in the macular retinal pigment epithelium of eyes with neovascular age-related macular degeneration1," *American Journal of Ophthalmology*, vol. 127, no. 1, pp. 694–709, 1999.

[69] K. Kimura, Y. Isashiki, S. Sonoda, T. Kakiuchi-Matsumoto, and N. Ohba, "Genetic association of manganese superoxide dismutase with exudative age-related macular degeneration," *American Journal of Ophthalmology*, vol. 130, no. 6, pp. 769–773, 2000.

[70] H. Esfandiary, U. Chakravarthy, C. Patterson, I. Young, and A. E. Hughes, "Association study of detoxification genes in age related macular degeneration," *British Journal of Ophthalmology*, vol. 89, no. 4, pp. 470–474, 2005.

[71] P. Tokarz, K. Kaarniranta, and J. Blasiak, "Inhibition of DNA methyltransferase or histone deacetylase protects retinal pigment epithelial cells from DNA damage induced by oxidative stress by the stimulation of antioxidant enzymes," *European Journal of Pharmacology*, vol. 776, pp. 167–175, 2016.

[72] Q. Zhong and R. A. Kowluru, "Epigenetic modification of Sod2 in the development of diabetic retinopathy and in the metabolic memory: role of histone methylation," *Investigative Ophthalmology & Visual Science*, vol. 54, no. 1, pp. 244–250, 2013.

[73] Y. Imamura, S. Noda, K. Hashizume et al., "Drusen, choroidal neovascularization, and retinal pigment epithelium dysfunction in SOD1-deficient mice: a model of age-related macular degeneration," *Proceedings of the National Academy of Sciences of the United States of America*, vol. 103, no. 30, pp. 11282–11287, 2006.

[74] M. R. Terluk, R. J. Kapphahn, L. M. Soukup et al., "Investigating mitochondria as a target for treating age-related macular degeneration," *The Journal of Neuroscience*, vol. 35, no. 18, pp. 7304–7311, 2015.

[75] V. Justilien, J.-J. Pang, K. Renganathan et al., "SOD2 knockdown mouse model of early AMD," *Investigative Ophthalmology & Visual Science*, vol. 48, no. 10, pp. 4407–4420, 2007.

[76] L. Bellner, G. Marrazzo, N. van Rooijen, M. W. Dunn, N. G. Abraham, and M. L. Schwartzman, "Heme oxygenase-2 deletion impairs macrophage function: implication in wound healing," *The FASEB Journal*, vol. 29, no. 1, pp. 105–115, 2015.

[77] Y. A. Cao, A. J. Wagers, H. Karsunky et al., "Heme oxygenase-1 deficiency leads to disrupted response to acute stress in stem cells and progenitors," *Blood*, vol. 112, no. 12, pp. 4494–4502, 2008.

[78] A. M. Mitterstiller, D. Haschka, S. Dichtl et al., "Heme oxygenase 1 controls early innate immune response of macrophages to Salmonella typhimurium infection," *Cellular Microbiology*, vol. 18, no. 10, pp. 1374–1389, 2016.

[79] X. R. Xu, H. T. Yu, Y. Yang, L. Hang, X. W. Yang, and S. H. Ding, "Quercetin phospholipid complex significantly protects against oxidative injury in ARPE-19 cells associated with activation of Nrf2 pathway," *European Journal of Pharmacology*, vol. 770, pp. 1–8, 2016.

[80] A. Hanneken, F. F. Lin, J. Johnson, and P. Maher, "Flavonoids protect human retinal pigment epithelial cells from oxidative-stress-induced death," *Investigative Ophthalmology & Visual Science*, vol. 47, no. 7, pp. 3164–3177, 2006.

[81] X. Liu, K. Ward, C. Xavier et al., "The novel triterpenoid RTA 408 protects human retinal pigment epithelial cells against HO-induced cell injury via NF-E2-related factor 2 (Nrf2) activation," *Redox Biology*, vol. 8, pp. 98–109, 2015.

[82] K. Wang, Y. Jiang, W. Wang, J. Ma, and M. Chen, "Escin activates AKT-Nrf2 signaling to protect retinal pigment

epithelium cells from oxidative stress," *Biochemical and Biophysical Research Communications*, vol. 468, no. 4, pp. 541–547, 2015.

[83] L. Wang, Y. Chen, P. Sternberg, and J. Cai, "Essential roles of the PI3 kinase/Akt pathway in regulating Nrf2-dependent antioxidant functions in the RPE," *Investigative Ophthalmology & Visual Science*, vol. 49, no. 4, pp. 1671–1678, 2008.

[84] X. He and Q. Ma, "NRF2 cysteine residues are critical for oxidant/electrophile-sensing, Kelch-like ECH-associated protein-1-dependent ubiquitination-proteasomal degradation, and transcription activation," *Molecular Pharmacology*, vol. 76, no. 6, pp. 1265–1278, 2009.

[85] X. Liu, J. Jann, C. Xavier, and H. Wu, "Glutaredoxin 1 (Grx1) protects human retinal pigment epithelial cells from oxidative damage by preventing AKT glutathionylation," *Investigative Ophthalmology & Visual Science*, vol. 56, no. 5, pp. 2821–2832, 2015.

[86] A. Koskela, M. Reinisalo, J. M. Hyttinen, K. Kaarniranta, and R. O. Karjalainen, "Pinosylvin-mediated protection against oxidative stress in human retinal pigment epithelial cells," *Molecular Vision*, vol. 20, pp. 760–769, 2014.

[87] H. Zhang, Y. Y. Liu, Q. Jiang et al., "Salvianolic acid A protects RPE cells against oxidative stress through activation of Nrf2/HO-1 signaling," *Free Radical Biology & Medicine*, vol. 69, pp. 219–228, 2014.

[88] Y. C. Chang, W. C. Chang, K. H. Hung et al., "The generation of induced pluripotent stem cells for macular degeneration as a drug screening platform: identification of curcumin as a protective agent for retinal pigment epithelial cells against oxidative stress," *Frontiers in Aging Neuroscience*, vol. 6, p. 191, 2014.

[89] W. Zhu, Y. Wu, Y. F. Meng et al., "Effect of curcumin on aging retinal pigment epithelial cells," *Drug Design, Development and Therapy*, vol. 9, pp. 5337–5344, 2015.

[90] M. Hollborn, R. Chen, P. Wiedemann, A. Reichenbach, A. Bringmann, and L. Kohen, "Cytotoxic effects of curcumin in human retinal pigment epithelial cells," *PLoS One*, vol. 8, no. 3, article e59603, 2013.

[91] Y. Sun and Z. P. You, "Curcumin inhibits human retinal pigment epithelial cell proliferation," *International Journal of Molecular Medicine*, vol. 34, no. 4, pp. 1013–1019, 2014.

[92] Z. Feng, Z. Liu, X. Li et al., "Alpha-tocopherol is an effective phase II enzyme inducer: protective effects on acrolein-induced oxidative stress and mitochondrial dysfunction in human retinal pigment epithelial cells," *The Journal of Nutritional Biochemistry*, vol. 21, no. 12, pp. 1222–1231, 2010.

[93] K. N. Ha, Y. Chen, J. Cai, and P. Sternberg Jr., "Increased glutathione synthesis through an ARE-Nrf2-dependent pathway by zinc in the RPE: implication for protection against oxidative stress," *Investigative Ophthalmology & Visual Science*, vol. 47, no. 6, pp. 2709–2715, 2006.

[94] K. A. Rezaei, Y. Chen, J. Cai, and P. Sternberg, "Modulation of Nrf2-dependent antioxidant functions in the RPE by Zip2, a zinc transporter protein," *Investigative Ophthalmology & Visual Science*, vol. 49, no. 4, pp. 1665–1670, 2008.

[95] N. Couto, J. Wood, and J. Barber, "The role of glutathione reductase and related enzymes on cellular redox homoeostasis network," *Free Radical Biology & Medicine*, vol. 95, pp. 27–42, 2016.

[96] J. J. Mieyal and P. B. Chock, "Posttranslational modification of cysteine in redox signaling and oxidative stress: focus on s-glutathionylation," *Antioxidants & Redox Signaling*, vol. 16, no. 6, pp. 471–475, 2012.

[97] X. Gao and P. Talalay, "Induction of phase 2 genes by sulforaphane protects retinal pigment epithelial cells against photooxidative damage," *Proceedings of the National Academy of Sciences of the United States of America*, vol. 101, no. 28, pp. 10446–10451, 2004.

[98] Y. Li, X. Liu, T. Zhou et al., "Inhibition of APE1/Ref-1 redox activity rescues human retinal pigment epithelial cells from oxidative stress and reduces choroidal neovascularization," *Redox Biology*, vol. 2, pp. 485–494, 2014.

[99] N. Yoshinaga, N. Arimura, H. Otsuka et al., "NSAIDs inhibit neovascularization of choroid through HO-1-dependent pathway," *Laboratory Investigation; A Journal of Technical Methods and Pathology*, vol. 91, no. 9, pp. 1277–1290, 2011.

[100] C. J. Ildefonso, H. Jaime, E. E. Brown et al., "Targeting the Nrf2 signaling pathway in the retina with a gene-delivered secretable and cell-penetrating peptide," *Investigative Ophthalmology & Visual Science*, vol. 57, no. 2, pp. 372–386, 2016.

[101] A. Kauppinen, J. J. Paterno, J. Blasiak, A. Salminen, and K. Kaarniranta, "Inflammation and its role in age-related macular degeneration," *Cellular and Molecular Life Sciences: CMLS*, vol. 73, no. 9, pp. 1765–1786, 2016.

[102] J. C. Lim, A. Umapathy, and P. J. Donaldson, "Tools to fight the cataract epidemic: a review of experimental animal models that mimic age related nuclear cataract," *Experimental Eye Research*, vol. 145, pp. 432–443, 2016.

[103] J. A. Vinson, "Oxidative stress in cataracts," *Pathophysiology: The Official Journal of the International Society for Pathophysiology/ISP*, vol. 13, no. 3, pp. 151–162, 2006.

[104] S. Aboobaker and P. Courtright, "Barriers to cataract surgery in Africa: a systematic review," *Middle East African Journal of Ophthalmology*, vol. 23, no. 1, pp. 145–149, 2016.

[105] J. F. Hejtmancik, S. A. Riazuddin, R. McGreal, W. Liu, A. Cvekl, and A. Shiels, "Lens biology and biochemistry," *Progress in Molecular Biology and Translational Science*, vol. 134, pp. 169–201, 2015.

[106] A. Cvekl, R. McGreal, and W. Liu, "Lens development and crystallin gene expression," *Progress in Molecular Biology and Translational Science*, vol. 134, pp. 129–167, 2015.

[107] Y. Ji, L. Cai, T. Zheng et al., "The mechanism of UVB irradiation induced-apoptosis in cataract," *Molecular and Cellular Biochemistry*, vol. 401, no. 1-2, pp. 87–95, 2015.

[108] J. Zhang, H. Yan, S. Lofgren, X. Tian, and M. F. Lou, "Ultraviolet radiation-induced cataract in mice: the effect of age and the potential biochemical mechanism," *Investigative Ophthalmology & Visual Science*, vol. 53, no. 11, pp. 7276–7285, 2012.

[109] M. F. Lou, "Thiol regulation in the lens," *Journal of Ocular Pharmacology and Therapeutics: The Official Journal of the Association for Ocular Pharmacology and Therapeutics*, vol. 16, no. 2, pp. 137–148, 2000.

[110] M. F. Lou, "Redox regulation in the lens," *Progress in Retinal and Eye Research*, vol. 22, no. 5, pp. 657–682, 2003.

[111] J. I. Clark, "Self-assembly of protein aggregates in ageing disorders: the lens and cataract model," *Philosophical Transactions of the Royal Society of London. Series B, Biological Sciences*, vol. 368, no. 1617, p. 20120104, 2013.

[112] R. Yousefi, S. Javadi, S. Amirghofran, A. Oryan, and A. A. Moosavi-Movahedi, "Assessment of structure, stability and aggregation of soluble lens proteins and alpha-crystallin upon

non-enzymatic glycation: the pathomechanisms underlying cataract development in diabetic patients," *International Journal of Biological Macromolecules*, vol. 82, pp. 328–338, 2016.

[113] M. F. Lou, Q. L. Huang, and J. S. Zigler Jr., "Effect of opacification and pigmentation on human lens protein thiol/disulfide and solubility," *Current Eye Research*, vol. 8, no. 9, pp. 883–890, 1989.

[114] G. M. Wang, N. Raghavachari, and M. F. Lou, "Relationship of protein-glutathione mixed disulfide and thioltransferase in H2O2-induced cataract in cultured pig lens," *Experimental Eye Research*, vol. 64, no. 5, pp. 693–700, 1997.

[115] M. Wei, K. Y. Xing, Y. C. Fan, T. Libondi, and M. F. Lou, "Loss of thiol repair systems in human cataractous lenses," *Investigative Ophthalmology & Visual Science*, vol. 56, no. 1, pp. 598–605, 2015.

[116] M. F. Lou, J. E. Dickerson Jr., W. H. Tung, J. K. Wolfe, and L. T. Chylack Jr., "Correlation of nuclear color and opalescence with protein S-thiolation in human lenses," *Experimental Eye Research*, vol. 68, no. 5, pp. 547–552, 1999.

[117] S. R. Hanson, A. A. Chen, J. B. Smith, and M. F. Lou, "Thiolation of the gammaB-crystallins in intact bovine lens exposed to hydrogen peroxide," *The Journal of Biological Chemistry*, vol. 274, no. 8, pp. 4735–4742, 1999.

[118] M. F. Lou, G. T. Xu, and X. L. Cui, "Further studies on the dynamic changes of glutathione and protein-thiol mixed disulfides in H2O2 induced cataract in rat lenses: distributions and effect of aging," *Current Eye Research*, vol. 14, no. 10, pp. 951–958, 1995.

[119] N. Raghavachari, F. Qiao, and M. F. Lou, "Does glutathione-S-transferase dethiolate lens protein-thiol mixed disulfides?-a comparative study with thioltransferase," *Experimental Eye Research*, vol. 68, no. 6, pp. 715–724, 1999.

[120] G. F. Vrensen, C. Otto, A. Lenferink et al., "Protein profiles in cortical and nuclear regions of aged human donor lenses: a confocal Raman microspectroscopic and imaging study," *Experimental Eye Research*, vol. 145, pp. 100–109, 2015.

[121] M. von Otter, S. Landgren, S. Nilsson et al., "Nrf2-encoding NFE2L2 haplotypes influence disease progression but not risk in Alzheimer's disease and age-related cataract," *Mechanisms of Ageing and Development*, vol. 131, no. 2, pp. 105–110, 2010.

[122] Y. Gao, Y. Yan, and T. Huang, "Human age-related cataracts: epigenetic suppression of the nuclear factor erythroid 2-related factor 2-mediated antioxidant system," *Molecular Medicine Reports*, vol. 11, no. 2, pp. 1442–1447, 2015.

[123] P. Palsamy, M. Ayaki, R. Elanchezhian, and T. Shinohara, "Promoter demethylation of Keap1 gene in human diabetic cataractous lenses," *Biochemical and Biophysical Research Communications*, vol. 423, no. 3, pp. 542–548, 2012.

[124] P. Palsamy, K. R. Bidasee, M. Ayaki, R. C. Augusteyn, J. Y. Chan, and T. Shinohara, "Methylglyoxal induces endoplasmic reticulum stress and DNA demethylation in the Keap1 promoter of human lens epithelial cells and age-related cataracts," *Free Radical Biology and Medicine*, vol. 72, pp. 134–148, 2014.

[125] D. E. Maessen, C. D. Stehouwer, and C. G. Schalkwijk, "The role of methylglyoxal and the glyoxalase system in diabetes and other age-related diseases," *Clinical Science (London, England: 1979)*, vol. 128, no. 12, pp. 839–861, 2015.

[126] P. Palsamy, K. R. Bidasee, and T. Shinohara, "Valproic acid suppresses Nrf2/Keap1 dependent antioxidant protection through induction of endoplasmic reticulum stress and Keap1 promoter DNA demethylation in human lens epithelial cells," *Experimental Eye Research*, vol. 121, pp. 26–34, 2014.

[127] A. Chandra, S. T. Raza, S. Abbas et al., "Polymorphism of GST and FTO genes in risk prediction of cataract among a North Indian population," *Ophthalmic Genetics*, vol. 37, no. 1, pp. 19–24, 2016.

[128] L. M. Meyer, S. Lofgren, Y. S. Ho et al., "Absence of glutaredoxin1 increases lens susceptibility to oxidative stress induced by UVR-B," *Experimental Eye Research*, vol. 89, no. 6, pp. 833–839, 2009.

[129] B. Upadhyaya, X. Tian, H. Wu, and M. F. Lou, "Expression and distribution of thiol-regulating enzyme glutaredoxin 2 (GRX2) in porcine ocular tissues," *Experimental Eye Research*, vol. 130, pp. 58–65, 2015.

[130] M. Kronschlager, K. Galichanin, J. Ekstrom, M. F. Lou, and P. G. Soderberg, "Protective effect of the thioltransferase gene on in vivo UVR-300 nm-induced cataract," *Investigative Ophthalmology & Visual Science*, vol. 53, no. 1, pp. 248–252, 2012.

[131] M. R. Fernando, J. M. Lechner, S. Lofgren, V. N. Gladyshev, and M. F. Lou, "Mitochondrial thioltransferase (glutaredoxin 2) has GSH-dependent and thioredoxin reductase-dependent peroxidase activities in vitro and in lens epithelial cells," *The FASEB Journal*, vol. 20, no. 14, pp. 2645–2647, 2006.

[132] H. Wu, K. Xing, and M. F. Lou, "Glutaredoxin 2 prevents H(2)O(2)-induced cell apoptosis by protecting complex I activity in the mitochondria," *Biochimica et Biophysica Acta*, vol. 1797, no. 10, pp. 1705–1715, 2010.

[133] H. Wu, Y. Yu, L. David, Y. S. Ho, and M. F. Lou, "Glutaredoxin 2 (Grx2) gene deletion induces early onset of age-dependent cataracts in mice," *The Journal of Biological Chemistry*, vol. 289, no. 52, pp. 36125–36139, 2014.

[134] H. Wu, L. Lin, F. Giblin, Y. S. Ho, and M. F. Lou, "Glutaredoxin 2 knockout increases sensitivity to oxidative stress in mouse lens epithelial cells," *Free Radical Biology & Medicine*, vol. 51, no. 11, pp. 2108–2117, 2011.

[135] Y. Liu, W. Luo, X. Luo, Z. Yong, and X. Zhong, "Effects of *Rosa laevigata* Michx. extract on reactive oxygen species production and mitochondrial membrane potential in lens epithelial cells cultured under high glucose," *International Journal of Clinical and Experimental Medicine*, vol. 8, no. 9, pp. 15759–15765, 2015.

[136] F. Wang, J. Ma, F. Han et al., "DL-3-n-butylphthalide delays the onset and progression of diabetic cataract by inhibiting oxidative stress in rat diabetic model," *Scientific Reports*, vol. 6, p. 19396, 2016.

[137] S. P. Yang, X. Z. Yang, and G. P. Cao, "Acetyl-l-carnitine prevents homocysteine-induced suppression of Nrf2/Keap1 mediated antioxidation in human lens epithelial cells," *Molecular Medicine Reports*, vol. 12, no. 1, pp. 1145–1150, 2015.

[138] H. Liu, A. J. O. Smith, M. C. Lott et al., "Sulforaphane can protect lens cells against oxidative stress: implications for cataract prevention sulforaphane can protect the lens," *Investigative Ophthalmology & Visual Science*, vol. 54, no. 8, pp. 5236–5248, 2013.

[139] S. D. Varma, K. Chandrasekaran, and S. Kovtun, "Sulforaphane-induced transcription of thioredoxin reductase in lens: possible significance against cataract formation," *Clinical Ophthalmology (Auckland, N.Z.)*, vol. 7, pp. 2091–2098, 2013.

[140] A. D. Deshpande, M. Harris-Hayes, and M. Schootman, "Epidemiology of diabetes and diabetes-related complications," *Physical Therapy*, vol. 88, no. 11, pp. 1254–1264, 2008.

[141] Z. Xu, Y. Wei, J. Gong et al., "NRF2 plays a protective role in diabetic retinopathy in mice," *Diabetologia*, vol. 57, no. 1, pp. 204–213, 2014.

[142] H. Zong, M. Ward, and A. W. Stitt, "AGEs, RAGE, and diabetic retinopathy," *Current Diabetes Reports*, vol. 11, no. 4, pp. 244–252, 2011.

[143] G. Negi, A. Kumar, R. P. Joshi, and S. S. Sharma, "Oxidative stress and Nrf2 in the pathophysiology of diabetic neuropathy: old perspective with a new angle," *Biochemical and Biophysical Research Communications*, vol. 408, no. 1, pp. 1–5, 2011.

[144] R. A. Kowluru, J. Tang, and T. S. Kern, "Abnormalities of retinal metabolism in diabetes and experimental galactosemia. VII. Effect of long-term administration of antioxidants on the development of retinopathy," *Diabetes*, vol. 50, no. 8, pp. 1938–1942, 2001.

[145] Q. Zhong, M. Mishra, and R. A. Kowluru, "Transcription factor Nrf2-mediated antioxidant defense system in the development of diabetic retinopathy," *Investigative Ophthalmology & Visual Science*, vol. 54, no. 6, pp. 3941–3948, 2013.

[146] S. K. Niture, A. K. Jain, and A. K. Jaiswal, "Antioxidant-induced modification of INrf2 cysteine 151 and PKC-delta-mediated phosphorylation of Nrf2 serine 40 are both required for stabilization and nuclear translocation of Nrf2 and increased drug resistance," *Journal of Cell Science*, vol. 122, no. Part 24, pp. 4452–4464, 2009.

[147] A. El-Osta, D. Brasacchio, D. Yao et al., "Transient high glucose causes persistent epigenetic changes and altered gene expression during subsequent normoglycemia," *The Journal of Experimental Medicine*, vol. 205, no. 10, pp. 2409–2417, 2008.

[148] Q. Zhong and R. A. Kowluru, "Epigenetic changes in mitochondrial superoxide dismutase in the retina and the development of diabetic retinopathy," *Diabetes*, vol. 60, no. 4, pp. 1304–1313, 2011.

[149] M. Mishra, Q. Zhong, and R. A. Kowluru, "Epigenetic modifications of Keap1 regulate its interaction with the protective factor Nrf2 in the development of diabetic retinopathy," *Investigative Ophthalmology & Visual Science*, vol. 55, no. 11, pp. 7256–7265, 2014.

[150] H. Huang, J. K. Gandhi, X. Zhong et al., "TNFalpha is required for late BRB breakdown in diabetic retinopathy, and its inhibition prevents leukostasis and protects vessels and neurons from apoptosis," *Investigative Ophthalmology & Visual Science*, vol. 52, no. 3, pp. 1336–1344, 2011.

[151] Y. Shirao and K. Kawasaki, "Electrical responses from diabetic retina," *Progress in Retinal and Eye Research*, vol. 17, no. 1, pp. 59–76, 1998.

[152] Y. Nakagami, E. Hatano, T. Inoue, K. Yoshida, M. Kondo, and H. Terasaki, "Cytoprotective effects of a novel Nrf2 activator, RS9, in rhodopsin Pro347Leu rabbits," *Current Eye Research*, vol. 41, no. 8, pp. 1123–1126, 2016.

[153] S. C. Sacca, S. Gandolfi, A. Bagnis et al., "The outflow pathway: a tissue with morphological and functional unity," *Journal of Cellular Physiology*, vol. 231, no. 9, pp. 1876–1893, 2016.

[154] A. Izzotti, S. C. Sacca, C. Cartiglia, and S. De Flora, "Oxidative deoxyribonucleic acid damage in the eyes of glaucoma patients," *The American Journal of Medicine*, vol. 114, no. 8, pp. 638–646, 2003.

[155] S. C. Sacca, A. Pascotto, P. Camicione, P. Capris, and A. Izzotti, "Oxidative DNA damage in the human trabecular meshwork: clinical correlation in patients with primary open-angle glaucoma," *Archives of Ophthalmology*, vol. 123, no. 4, pp. 458–463, 2005.

[156] S. M. Ferreira, S. F. Lerner, R. Brunzini, P. A. Evelson, and S. F. Llesuy, "Oxidative stress markers in aqueous humor of glaucoma patients," *American Journal of Ophthalmology*, vol. 137, no. 1, pp. 62–69, 2004.

[157] G. Tezel and M. B. Wax, "Hypoxia-inducible factor 1alpha in the glaucomatous retina and optic nerve head," *Archives of Ophthalmology*, vol. 122, no. 9, pp. 1348–1356, 2004.

[158] G. Tezel, R. Hernandez, and M. B. Wax, "Immunostaining of heat shock proteins in the retina and optic nerve head of normal and glaucomatous eyes," *Archives of Ophthalmology*, vol. 118, no. 4, pp. 511–518, 2000.

[159] S. G. Panicker, A. B. Reddy, A. K. Mandal et al., "Identification of novel mutations causing familial primary congenital glaucoma in Indian pedigrees," *Investigative Ophthalmology & Visual Science*, vol. 43, no. 5, pp. 1358–1366, 2002.

[160] G. C. Soley, K. A. Bosse, D. Flikier et al., "Primary congenital glaucoma: a novel single-nucleotide deletion and varying phenotypic expression for the 1,546-1,555dup mutation in the GLC3A (CYP1B1) gene in 2 families of different ethnic origin," *Journal of Glaucoma*, vol. 12, no. 1, pp. 27–30, 2003.

[161] A. L. Vincent, G. Billingsley, Y. Buys et al., "Digenic inheritance of early-onset glaucoma: CYP1B1, a potential modifier gene," *American Journal of Human Genetics*, vol. 70, no. 2, pp. 448–460, 2002.

[162] O. Yildirim, N. A. Ates, L. Tamer et al., "May glutathione S-transferase M1 positive genotype afford protection against primary open-angle glaucoma?" *Graefe's Archive for Clinical and Experimental Ophthalmology = Albrecht von Graefes Archiv fur Klinische und Experimentelle Ophthalmologie*, vol. 243, no. 4, pp. 327–333, 2005.

[163] N. Himori, K. Yamamoto, K. Maruyama et al., "Critical role of Nrf2 in oxidative stress-induced retinal ganglion cell death," *Journal of Neurochemistry*, vol. 127, no. 5, pp. 669–680, 2013.

[164] Y. Wei, J. Gong, T. Yoshida et al., "Nrf2 has a protective role against neuronal and capillary degeneration in retinal ischemia-reperfusion injury," *Free Radical Biology & Medicine*, vol. 51, no. 1, pp. 216–224, 2011.

[165] Z. Xu, H. Cho, M. J. Hartsock et al., "Neuroprotective role of Nrf2 for retinal ganglion cells in ischemia-reperfusion," *Journal of Neurochemistry*, vol. 133, no. 2, pp. 233–241, 2015.

[166] C. E. Guerrero-Beltran, M. Calderon-Oliver, J. Pedraza-Chaverri, and Y. I. Chirino, "Protective effect of sulforaphane against oxidative stress: recent advances," *Experimental and Toxicologic Pathology: Official Journal of the Gesellschaft fur Toxikologische Pathologie*, vol. 64, no. 5, pp. 503–508, 2012.

[167] D. A. Johnson and J. A. Johnson, "Nrf2—a therapeutic target for the treatment of neurodegenerative diseases," *Free Radical Biology & Medicine*, vol. 88, no. Pt B, pp. 253–267, 2015.

[168] T. P. Williamson, D. A. Johnson, and J. A. Johnson, "Activation of the Nrf2-ARE pathway by siRNA knockdown of Keap1 reduces oxidative stress and provides partial

protection from MPTP-mediated neurotoxicity," *Neurotoxicology*, vol. 33, no. 3, pp. 272–279, 2012.

[169] T. Satoh, N. Harada, T. Hosoya, K. Tohyama, M. Yamamoto, and K. Itoh, "Keap1/Nrf2 system regulates neuronal survival as revealed through study of keap1 gene-knockout mice," *Biochemical and Biophysical Research Communications*, vol. 380, no. 2, pp. 298–302, 2009.

[170] S. A. Reisman, R. L. Yeager, M. Yamamoto, and C. D. Klaassen, "Increased Nrf2 activation in livers from Keap1-knockdown mice increases expression of cytoprotective genes that detoxify electrophiles more than those that detoxify reactive oxygen species," *Toxicological Sciences: An Official Journal of the Society of Toxicology*, vol. 108, no. 1, pp. 35–47, 2009.

[171] X. Liu, K. Ward, C. Xavier et al., "The novel triterpenoid RTA 408 protects human retinal pigment epithelial cells against H2O2-induced cell injury via NF-E2-related factor 2 (Nrf2) activation," *Redox Biology*, vol. 8, pp. 98–109, 2016.

[172] R. J. Mailloux and W. G. Willmore, "S-glutathionylation reactions in mitochondrial function and disease," *Frontiers in Cell and Developmental Biology*, vol. 2, p. 68, 2014.

[173] G. M. DeNicola, F. A. Karreth, T. J. Humpton et al., "Oncogene-induced Nrf2 transcription promotes ROS detoxification and tumorigenesis," *Nature*, vol. 475, no. 7354, pp. 106–109, 2011.

[174] Q. Pan, W.-Y. Qiu, Y.-N. Huo, Y.-F. Yao, and M. F. Lou, "Low levels of hydrogen peroxide stimulate corneal epithelial cell adhesion, migration, and wound healing," *Investigative Ophthalmology & Visual Science*, vol. 52, no. 3, pp. 1723–1734, 2011.

[175] S. N. Zucker, E. E. Fink, A. Bagati et al., "Nrf2 amplifies oxidative stress via induction of Klf9," *Molecular Cell*, vol. 53, no. 6, pp. 916–928, 2014.